

Defining Handling Qualities of Unmanned Aerial Systems: Phase II Final Report

*David H. Klyde, Chase P. Schulze, Justin P. Miller,
Jose A. Manriquez, and Aditya Kotikalpudi
Systems Technology Inc., Hawthorne, California*

*David G. Mitchell
Mitchell Aerospace Research, Long Beach, California*

*Peter J. Seiler, Christopher Regan, Brian Taylor, and Curt Olson
University of Minnesota, Minneapolis, Minnesota*

NASA STI Program . . . in Profile

Since its founding, NASA has been dedicated to the advancement of aeronautics and space science. The NASA scientific and technical information (STI) program plays a key part in helping NASA maintain this important role.

The NASA STI program operates under the auspices of the Agency Chief Information Officer. It collects, organizes, provides for archiving, and disseminates NASA's STI. The NASA STI program provides access to the NTRS Registered and its public interface, the NASA Technical Reports Server, thus providing one of the largest collections of aeronautical and space science STI in the world. Results are published in both non-NASA channels and by NASA in the NASA STI Report Series, which includes the following report types:

- **TECHNICAL PUBLICATION.** Reports of completed research or a major significant phase of research that present the results of NASA Programs and include extensive data or theoretical analysis. Includes compilations of significant scientific and technical data and information deemed to be of continuing reference value. NASA counter-part of peer-reviewed formal professional papers but has less stringent limitations on manuscript length and extent of graphic presentations.
- **TECHNICAL MEMORANDUM.** Scientific and technical findings that are preliminary or of specialized interest, e.g., quick release reports, working papers, and bibliographies that contain minimal annotation. Does not contain extensive analysis.
- **CONTRACTOR REPORT.** Scientific and technical findings by NASA-sponsored contractors and grantees.

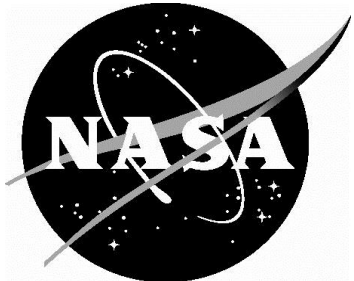
- **CONFERENCE PUBLICATION.** Collected papers from scientific and technical conferences, symposia, seminars, or other meetings sponsored or co-sponsored by NASA.
- **SPECIAL PUBLICATION.** Scientific, technical, or historical information from NASA programs, projects, and missions, often concerned with subjects having substantial public interest.
- **TECHNICAL TRANSLATION.** English-language translations of foreign scientific and technical material pertinent to NASA's mission.

Specialized services also include organizing and publishing research results, distributing specialized research announcements and feeds, providing information desk and personal search support, and enabling data exchange services.

For more information about the NASA STI program, see the following:

- Access the NASA STI program home page at <http://www.sti.nasa.gov>
- E-mail your question to help@sti.nasa.gov
- Phone the NASA STI Information Desk at 757-864-9658
- Write to:
NASA STI Information Desk
Mail Stop 148
NASA Langley Research Center
Hampton, VA 23681-2199

NASA/CR-2020-220564



Defining Handling Qualities of Unmanned Aerial Systems: Phase II Final Report

*David H. Klyde, Chase P. Schulze, Justin P. Miller,
Jose A. Manriquez, and Aditya Kotikalpudi
Systems Technology Inc., Hawthorne, California*

*David G. Mitchell
Mitchell Aerospace Research, Long Beach, California*

*Peter J. Seiler, Christopher Regan, Brian Taylor, and Curt Olson
University of Minnesota, Minneapolis, Minnesota*

National Aeronautics and
Space Administration

Langley Research Center
Hampton, Virginia 23681-2199

Prepared for Langley Research Center
under Contract NNX17CL13C

February 2020

The use of trademarks or names of manufacturers in this report is for accurate reporting and does not constitute an official endorsement, either expressed or implied, of such products or manufacturers by the National Aeronautics and Space Administration.

Available from:

NASA STI Program/Mail Stop 148
NASA Langley Research Center
Hampton, Virginia 23681-2199
Fax: 757-864-6500

TABLE OF CONTENTS

List of Figures.....	vii
List of Tables.....	xi
A. Project Summary	1
1. Identification and Significance of Innovation.....	1
2. Technical Objectives and Work Plan.....	1
3. Technical Accomplishments.....	2
4. NASA Application(s)	3
5. Non-NASA Commercial Application(s).....	3
B. Introduction	4
1. Program Overview.....	4
2. Barriers to UAS Certification	5
3. UAS Classification	5
4. Lessons Learned from Manned Aircraft Requirements	6
5. Autonomy and Handling Qualities	7
6. UAS Stakeholders Engagement.....	7
7. Report Outline	7
C. The Mission-Oriented Approach	9
1. Old School – Sorting by Class and Flight Phase	9
2. Eliminating Classifications	9
3. Mission Task Elements (MTEs)	11
a. Non-Precision, Non-Aggressive	11
b. Non-Precision, Aggressive	11
c. Precision, Non-Aggressive	12
d. Precision, Aggressive	12
e. MTE Categories and Candidate UAS Handling Qualities Requirements	12
4. Classification	13
a. Background.....	13
b. Consideration of Class and the Pilot/Operator.....	14
5. Selected sUAS Mission Task Elements	15
D. Requirements in a UAS Handling Qualities Specification	17
1. Assumptions	17
a. Breadth of Application.....	17
b. Mode of Operation.....	17
c. Configuration.....	17
d. Operating Airspace	18
e. Focus of the Requirements	18
f. Limitations to the Current Specification.....	18
2. Format of the Draft Specification	18
3. Stakeholder Involvement	19
4. Dynamic Scaling.....	19
5. Overview of Uncertainty Analysis Methods Applied to Handling Qualities	20
a. Traditional Stochastic Monte Carlo Methods	20
b. Design of Experiments and Response Surface Methods (DOE/RSM)	21
c. μ -analysis Methods.....	21
E. UAS Handling Qualities Process Demonstration	23
1. Fixed Wing UAS	23
a. University of Minnesota Laboratory and Flight Test Facilities	23
b. Model-based Prediction of Handling Qualities.....	26
c. System Identification Flight Tests	30
d. Model Revisions Based on Flight Test Results	33
e. Mission Task Element Flight Tests.....	39
2. Multirotor UAS MTE Flight Test Evaluations	47
a. Introduction	47
b. Lateral Sidestep	48

c. Pilot Evaluations of the MTEs.....	53
3. Additional Multirotor sUAS Flight Test Activities	55
a. Multirotor UAS MTEs in the Presence of Steady Winds	55
b. UMN System Identification Flights.....	55
F. Phase II Summary and Conclusions	57
1. Summary.....	57
2. Process Success Criteria	57
3. Conclusions and Next Steps	58
References	60
Appendix A – Emerging Handling Qualities Specification.....	62
A. Introduction	63
B. Table of Draft Requirements	63
C. Recommended Requirements	67
D. Rationale for Requirements	77
E. References	86
Appendix B – Mission Task Element Catalog.....	88
A. Introduction	89
B. Fixed Wing	89
1. Evaluations Conducted by the University of Minnesota UAV Lab.....	89
a. Flightpath Regulation in the presence of a Discrete Gust (Non-precision, Non-aggressive or Non-Precision, Aggressive depending on gust input magnitude)	89
b. Flightpath Regulation in the presence of a Sum-of-Sines Disturbance (Precision, Aggressive)	91
c. Waypoint Following (Non-Precision, Non-Aggressive and Precision, Non-Aggressive depending task requirements)	93
d. Precision Lateral Offset Landing (Precision, Non-Aggressive).....	93
2. Unusual Attitude Recovery, Nose-High (Non-Precision, Aggressive).....	95
C. Rotary Wing Mission Task Elements	96
1. Evaluations Conducted in the NASA LaRC Autonomy Incubator.....	96
a. Precision Hover (Precision, Non-Aggressive)	96
b. Lateral Sidestep (Precision, Non-Aggressive)	97
c. Vertical Reposition (Precision, Non-Aggressive).....	98
d. Landing (Non-Precision, Non-Aggressive)	99
2. Scaled Autonomous ADS-33E-PRF Mission Task Elements	100
3. Hover MTE under First Person View Cueing (Precision, Non-Aggressive)	104
References	106
Appendix C – Fixed Wing System Identification Flight Test Data.....	107
A. Flight Test Campaign	108
1. Test Objectives	108
2. Test Description.....	108
a. Vehicle Configurations	108
b. Airspeeds	108
c. Altitudes.....	108
d. Flight Patterns	108
e. Pilot.....	108
3. Test Inputs	109
a. Multi-Sine	109
b. Frequency Sweep.....	109
c. Doublet	110
d. Pulse	110
e. 3-2-1-1	110
4. UltraStick120.....	111
B. Flight 03.....	114
1. Longitudinal Survey	114
2. Lateral Survey.....	117
3. Directional Survey	120
C. Flight 04.....	123

1.	Longitudinal Survey	123
2.	Lateral Survey.....	126
3.	Directional Survey	129
D.	Flight 05.....	132
1.	Longitudinal Survey	133
a.	MOI Method 1	134
b.	MOI Method 2	137
2.	Lateral Survey.....	139
a.	MOI Method 1	140
b.	MOI Method 2	143
3.	Directional Survey	145
a.	MOI Method 1	146
b.	MOI Method 2	149
E.	Flight 06.....	151
1.	Longitudinal Survey	152
a.	MOI Method 1	153
b.	MOI Method 2	156
2.	Lateral Survey.....	158
a.	MOI Method 1	159
b.	MOI Method 2	162
3.	Directional Survey	164
a.	MOI Method 1	165
b.	MOI Method 2	168
F.	Flight 10.....	171
1.	Longitudinal Survey	171
2.	Lateral Survey.....	174
3.	Directional Survey	177
G.	Flight 11.....	181
1.	Longitudinal Survey	181
2.	Lateral Survey.....	184
3.	Directional Survey	187
H.	Short Duration Model Response Evaluation.....	191
1.	Flight 03.....	191
a.	Longitudinal Survey	191
b.	Lateral Survey.....	193
c.	Directional Survey	195
2.	FLT 04	197
a.	Longitudinal Survey	197
b.	Lateral Survey.....	199
c.	Directional Survey	202
3.	Select Model Responses	204
a.	FLT 05: Aft CG Longitudinal Survey	204
b.	FLT 10: Time Delay Lateral Survey.....	207
	References	210
	Appendix D – Multirotor Flight Test Data	211
A.	Introduction	212
B.	Flight Test Summary	212
C.	Flight Test Results	212
1.	Run Logs.....	212
2.	Performance Metrics.....	215
3.	Analysis	218
a.	Precision Hover MTE	218
b.	Lateral Sidestep MTE	223
c.	Vertical Reposition MTE.....	233
d.	Landing MTE.....	241
e.	Heading Performance	246

4. Pilot Responses.....	248
D. Conclusions	248
References	250
Appendix E – Exploration of Dynamic Scaling	251
A. Introduction	252
B. Froude Scaling for Dynamic Similitude	252
C. Froude-Scaled Dynamics.....	254
1. Longitudinal Dynamics	254
a. Longitudinal Modes Comparison	254
2. Modal Flying Qualities Requirements (CAP).....	255
3. Lateral-Directional Dynamics.....	256
D. Scaling Up Analysis for Ultrastick Aircraft.....	256
1. Longitudinal Dynamics	257
2. CAP Specifications.....	258
3. Lateral-Directional Dynamics.....	259
a. Roll Subsidence	259
b. Spiral Mode	260
c. Dutch Roll Mode	260
4. Aircraft Bandwidth Specifications.....	260
E. Conclusions / Future Work.....	261
References	262

LIST OF FIGURES

Figure 1: The Proposed UAS Handling Qualities Assessment Process	4
Figure 2: Relationship between MTE Categories and Specification Boundaries for Aircraft Bandwidth Criterion (Ref. 9) as Defined by Phase Delay (τ_p , sec) versus Bandwidth Frequency (ω_{BW} , rad/s).....	12
Figure 3: Example UAS	13
Figure 4: Closed-Loop Feedback System of Stable Operators	22
Figure 5: UltraStick120 (center) and UltraStick25e Aircraft.....	23
Figure 6: Avionics Functional Diagram, Based on UltraStick25e Installation.....	24
Figure 7: System Architecture	25
Figure 8: UAS Flight Test Facilities at the University of Minnesota	26
Figure 9: Predicted Handling Qualities	26
Figure 10: Pitch Attitude Tracker	27
Figure 11: Representative Tracker Block	27
Figure 12: UltraStick120 Model Pitch Attitude to Attitude Command (θ/θ_c) Frequency Responses	28
Figure 13: Parameters for Attitude Bandwidth and Phase Delay	29
Figure 14: Pitch Rate Overshoot Parameter.....	29
Figure 15: Aircraft Bandwidth Model Parameters for the UltraStick120	30
Figure 16: Predicted Handling Qualities from Models Revised from Flight Test	30
Figure 17: Example Orthogonal Multi-Sine Input and Resulting Aircraft Output	32
Figure 18: Example Frequency Sweep Input and Resulting Aircraft Output	32
Figure 19: Example Doublet Input and Resulting Aircraft Output	33
Figure 20: Example Pulse Input and Resulting Aircraft Output	33
Figure 21: Example 3-2-1-1 Input and Resulting Aircraft Output.....	33
Figure 22: Original and Updated Elevator Actuator Models Compared with Flight Test	34
Figure 23: Original and Updated q/δ_e Responses Compared with Flight Test	35
Figure 24: Time Response Comparisons	36
Figure 25: Comparison of UltraStick120 Model versus Flight Cruise (23 m/s) Frequency Responses	37
Figure 26: Comparison of UltraStick120 Model versus Flight Approach (17 m/s) Frequency Responses	38
Figure 27: Aircraft Bandwidth Parameters for the UltraStick120 Model and Flight	39
Figure 28: Flight 14 Flighthpath Regulation in the Presence of a Discrete Gust MTE	41
Figure 29: Flight 14 Flighthpath Regulation in the Presence of a Sum-of-Sines Altitude Disturbance MTE	42
Figure 30: Flight 16 Example Sum-of-Sines Attitude Disturbance	43
Figure 31: Flight 16 Flighthpath Regulation in the Presence of a SOS Attitude Disturbance MTE, No Delay	43
Figure 32: Flight 16 Waypoint Following	44
Figure 33: Flight 16 Precision Lateral Offset Landing Ground Tracks	45
Figure 34: Head-Up Display (HUD) for the Research Pilot Depicting Virtual Runway (Ref. 32).....	46
Figure 35: Bank Angle Performance for Example AirSTARS Runs	46
Figure 36: Lateral and Longitudinal Offset Performance, Runs 1-3, Flight 44, Card 86	47
Figure 37: Multirotor Test Vehicles	48
Figure 38: Lateral Reposition (mini course)	49
Figure 39: Tarot 650 Sport Lateral Sidestep MTE, Pilot 1, Batch 1 – Inertial Position	50
Figure 40: Debrief Questionnaire Results	54
Figure 41: UMN Multicopter.....	55
Figure 42: Definitions of Aircraft Attitude Bandwidth and Phase Delay	71
Figure 43: Definition of Pitch Rate Overshoot	71
Figure 44: Definition of Vertical-Axis Bandwidth and Phase Delay	74
Figure 45: “1 – cosine” Shape for Discrete Gust	76
Figure 46: “1 – cosine” Shape for Discrete Gust.....	90
Figure 47: Sum-of-Sines Disturbance (Gain = 1.5 deg)	92
Figure 48: Precision Offset Landing Course at the UMore Park Test Range	94
Figure 49: Precision Hover	97
Figure 50: Lateral Reposition (mini course)	98
Figure 51: Bob-up/Down (Vertical Altitude Change)	99
Figure 52: Landing	100
Figure 53: Lateral Reposition MTE Full Scale Trajectory	103

Figure 54: Depart Abort Full Scale MTE Full Scale Trajectory.....	103
Figure 55: Pirouette Full Scale MTE Trajectory	104
Figure 56: Example Orthogonal Multi-Sine Input and Resulting Aircraft Output	109
Figure 57: Example Frequency sweep Input and Resulting Aircraft Output	109
Figure 58: Example Doublet Input and Resulting Aircraft Output	110
Figure 59: Example Pulse Input and Resulting Aircraft Output	110
Figure 60: Example 3-2-1-1 Input and Resulting Aircraft Output.....	111
Figure 61: FLT03 - q/δ_{ec} Identification – All Methods.....	115
Figure 62: FLT03 - q/δ_{ec} Identification – OMS	116
Figure 63: FLT03 - q/δ_{ec} Identification – Frequency sweep	116
Figure 64: FLT03 - q/δ_{ec} Identification – Short Duration Inputs	117
Figure 65: FLT03 - p/δ_{ac} Identification – All Methods.....	118
Figure 66: FLT03 - p/δ_{ac} Identification – OMS	119
Figure 67: FLT03 - p/δ_{ac} Identification – Frequency sweep	119
Figure 68: FLT03 - p/δ_{ac} Identification – Short Duration Inputs	120
Figure 69: FLT03 - r/δ_{rc} Identification – All Methods.....	121
Figure 70: FLT03 - r/δ_{rc} Identification – OMS	122
Figure 71: FLT03 - r/δ_{rc} Identification – Frequency Sweep	122
Figure 72: FLT03 - r/δ_{rc} Identification – Short Duration Inputs	123
Figure 73: FLT04 - q/δ_{ec} Identification – All Methods.....	124
Figure 74: FLT04 - q/δ_{ec} Identification – OMS	125
Figure 75: FLT04 - q/δ_{ec} Identification – Frequency sweep	125
Figure 76: FLT04 - q/δ_{ec} Identification – Short Duration Inputs	126
Figure 77: FLT04 - p/δ_{ac} Identification – All Methods.....	127
Figure 78: FLT04 - p/δ_{ac} Identification – OMS	128
Figure 79: FLT04 - p/δ_{ac} Identification – Frequency sweep	128
Figure 80: FLT04 - p/δ_{ac} Identification – Short Duration Inputs	129
Figure 81: FLT04 - r/δ_{rc} Identification – All Methods.....	130
Figure 82: FLT04 - r/δ_{rc} Identification – OMS	131
Figure 83: FLT04 - r/δ_{rc} Identification – Frequency sweep	131
Figure 84: FLT04 - r/δ_{rc} Identification – Short Duration Inputs	132
Figure 85: FLT05-MOI Method 1 - q/δ_{ec} Identification – All Methods	134
Figure 86: FLT05-MOI Method 1 - q/δ_{ec} Identification – OMS.....	135
Figure 87: FLT05-MOI Method 1 - q/δ_{ec} Identification – Frequency sweep.....	135
Figure 88: FLT05-MOI Method 1 - q/δ_{ec} Identification – Short Duration Inputs.....	136
Figure 89: FLT05-MOI Method 2 - q/δ_{ec} Identification – All Methods	137
Figure 90: FLT05-MOI Method 2 - q/δ_{ec} Identification – OMS.....	138
Figure 91: FLT05-MOI Method 2 - q/δ_{ec} Identification – Frequency sweep.....	138
Figure 92: FLT05-MOI Method 2 - q/δ_{ec} Identification – Short Duration Inputs.....	139
Figure 93: FLT05-MOI Method 1 - p/δ_{ac} Identification – All Methods	140
Figure 94: FLT05-MOI Method 1 - p/δ_{ac} Identification – OMS.....	141
Figure 95: FLT05-MOI Method 1 - p/δ_{ac} Identification – Frequency sweep.....	141
Figure 96: FLT05-MOI Method 1 - p/δ_{ac} Identification – Short Duration Inputs.....	142
Figure 97: FLT05-MOI Method 2 - p/δ_{ac} Identification – All Methods	143
Figure 98: FLT05-MOI Method 2 - p/δ_{ac} Identification – OMS.....	144
Figure 99: FLT05-MOI Method 2 - p/δ_{ac} Identification – Frequency sweep.....	144
Figure 100: FLT05-MOI Method 2 - p/δ_{ac} Identification – Short Duration Inputs.....	145
Figure 101: FLT05-MOI Method 1 - r/δ_{rc} Identification – All Methods	146
Figure 102: FLT05-MOI Method 1 - r/δ_{rc} Identification – OMS.....	147
Figure 103: FLT05-MOI Method 1 - r/δ_{rc} Identification – Frequency sweep.....	147
Figure 104: FLT05-MOI Method 1 - r/δ_{rc} Identification – Short Duration Inputs.....	148
Figure 105: FLT05-MOI Method 2 - r/δ_{rc} Identification – All Methods	149
Figure 106: FLT05-MOI Method 2 - r/δ_{rc} Identification – OMS.....	150
Figure 107: FLT05-MOI Method 2 - r/δ_{rc} Identification – Frequency sweep.....	150
Figure 108: FLT05-MOI Method 2 - r/δ_{rc} Identification – Short Duration Inputs.....	151
Figure 109: FLT06-MOI Method 1 - q/δ_{ec} Identification – All Methods	153

Figure 110: FLT06-MOI Method 1 - q/δ_{ec} Identification – OMS.....	154
Figure 111: FLT06-MOI Method 1 - q/δ_{ec} Identification – Frequency sweep.....	154
Figure 112: FLT06-MOI Method 1 - q/δ_{ec} Identification – Short Duration Inputs.....	155
Figure 113: FLT06-MOI Method 2 - q/δ_{ec} Identification – All Methods	156
Figure 114: FLT06-MOI Method 2 - q/δ_{ec} Identification – OMS.....	157
Figure 115: FLT06-MOI Method 2 - q/δ_{ec} Identification – Frequency sweep.....	157
Figure 116: FLT06-MOI Method 2 - q/δ_{ec} Identification – Short Duration Inputs.....	158
Figure 117: FLT06-MOI Method 1 - p/δ_{ac} Identification – All Methods	159
Figure 118: FLT06-MOI Method 1 - p/δ_{ac} Identification – OMS.....	160
Figure 119: FLT06-MOI Method 1 - p/δ_{ac} Identification – Frequency sweep.....	160
Figure 120: FLT06-MOI Method 1 - p/δ_{ac} Identification – Short Duration Inputs.....	161
Figure 121: FLT06-MOI Method 2 - p/δ_{ac} Identification – All Methods	162
Figure 122: FLT06-MOI Method 2 - p/δ_{ac} Identification – OMS.....	163
Figure 123: FLT06-MOI Method 2 - p/δ_{ac} Identification – Frequency sweep.....	163
Figure 124: FLT06-MOI Method 2 - p/δ_{ac} Identification – Short Duration Inputs.....	164
Figure 125: FLT06-MOI Method 1 - r/δ_{rc} Identification – All Methods	165
Figure 126: FLT06-MOI Method 1 - r/δ_{rc} Identification - OMS	166
Figure 127: FLT06-MOI Method 1 - r/δ_{rc} Identification - Frequency sweep	167
Figure 128: FLT06-MOI Method 1 - r/δ_{rc} Identification - Short Duration	167
Figure 129: FLT06-MOI Method 2 - r/δ_{rc} Identification - All Methods	168
Figure 130: FLT06-MOI Method 2 - r/δ_{rc} Identification - OMS	169
Figure 131: FLT06-MOI Method 2 - r/δ_{rc} Identification - Frequency sweep	169
Figure 132: FLT06-MOI Method 2 - r/δ_{rc} Identification - Short Duration	170
Figure 133: FLT10 - q/δ_{ec} Identification - All Methods	172
Figure 134: FLT10 - q/δ_{ec} Identification – OMS	173
Figure 135: FLT10 - q/δ_{ec} Identification - Frequency sweep.....	173
Figure 136: FLT10 - q/δ_{ec} Identification - Short Duration.....	174
Figure 137: FLT10 - p/δ_{ac} Identification - All Methods	175
Figure 138: FLT10 - p/δ_{ac} Identification - OMS.....	176
Figure 139: FLT10 - p/δ_{ac} Identification - Frequency sweep.....	176
Figure 140: FLT10 - p/δ_{ac} Identification - Short Duration.....	177
Figure 141: FLT10 - r/δ_{rc} Identification - All Methods	178
Figure 142: FLT10 - r/δ_{rc} Identification - OMS.....	179
Figure 143: FLT10 - r/δ_{rc} Identification - Frequency Sweep	179
Figure 144: FLT10 - r/δ_{rc} Identification - Short Duration.....	180
Figure 145: FLT11 - q/δ_{ec} Identification - All Methods	182
Figure 146: FLT11 - q/δ_{ec} Identification - OMS	183
Figure 147: FLT11 - q/δ_{ec} Identification - Frequency sweep.....	183
Figure 148: FLT11 - q/δ_{ec} Identification - Short Duration.....	184
Figure 149: FLT11 - p/δ_{ac} Identification - All Methods	185
Figure 150: FLT11 - p/δ_{ac} Identification - OMS.....	186
Figure 151: FLT11 - p/δ_{ac} Identification - Frequency Sweep	186
Figure 152: FLT11 - p/δ_{ac} Identification - Short Duration.....	187
Figure 153: FLT11 - r/δ_{rc} Identification - All Methods	188
Figure 154: FLT11 - r/δ_{rc} Identification - OMS.....	189
Figure 155: FLT11 - r/δ_{rc} Identification - Frequency sweep.....	189
Figure 156: FLT11 - r/δ_{rc} Identification - Short Duration.....	190
Figure 157: FLT03 - Doublet Response	191
Figure 158: FLT03 - Pulse Response	192
Figure 159: FLT03 - 3-2-1-1 Response	192
Figure 160: FLT03 - Doublet Response	193
Figure 161: FLT03 - Pulse Response	194
Figure 162: FLT03 - Wider Pulse Response	194
Figure 163: FLT03 - 3-2-1-1 Response	195
Figure 164: FLT03 - Doublet Response	196
Figure 165: FLT03 - Pulse Response	196

Figure 166: FLT03 - 3-2-1-1 Response	197
Figure 167: FLT04 - Doublet Response	198
Figure 168: FLT04 - Pulse Response	198
Figure 169: FLT04 - 3-2-1-1 Response	199
Figure 170: FLT04 - Doublet Response	200
Figure 171: FLT04 - Pulse Response	200
Figure 172: FLT04 - Wider Pulse Response	201
Figure 173: FLT04 - 3-2-1-1 Response	201
Figure 174: FLT04 - Doublet Response	202
Figure 175: FLT04 - Pulse Response	203
Figure 176: FLT04 - 3-2-1-1 Response	203
Figure 177: FLT05-MOI Method 1 - Doublet Response	204
Figure 178: FLT05-MOI Method 1 - Pulse Response	205
Figure 179: FLT05-MOI Method 1 - 3-2-1-1 Response	205
Figure 180: FLT05-MOI Method 2 - Doublet Response	206
Figure 181: FLT05-MOI Method 2 - Pulse Response	206
Figure 182: FLT05-MOI Method 2 - 3-2-1-1 Response	207
Figure 183: FLT10 - Doublet Response	208
Figure 184: FLT10 - Pulse Response	208
Figure 185: FLT10 - Wider Pulse Response	209
Figure 186: FLT10 - 3-2-1-1 Response	209
Figure 187: Multirotor Test Vehicles	212
Figure 188: Tarot 650 Sport Precision Hover MTE, Pilot 1, Run 1 – Positions	215
Figure 189: Tarot 650 Sport Precision Hover MTE, Pilot 1, Run 1 – Attitudes	216
Figure 190: Tarot 650 Sport Precision Hover MTE, Pilot 1, Run 1 – Velocities	217
Figure 191: Tarot 650 Sport Precision Hover MTE, Pilot 1, Batch 1 – Inertial Position	218
Figure 192: Tarot 650 Sport Precision Hover MTE, Pilot 1, Batch 1 – Inertial Position	219
Figure 193: Tarot 650 Sport Lateral Sidestep MTE, Pilot 1, Batch 1 – Inertial Position	223
Figure 194: Tarot 650 Sport Vertical Reposition MTE, Pilot 1, Batch 1 – Inertial Position	234
Figure 195: Tarot 650 Sport Landing MTE, Pilot 1, Batch 1 – Inertial Position	242
Figure 196: Juxtaposition of Heading Angle and Lateral Position	247
Figure 197: Debrief Questionnaire Results	249
Figure 198: Short period frequency specifications	258
Figure 199: CAP vs ζ_{sp} requirements short period mode	259
Figure 200: Dutch Roll Mode Damping and Frequency Specifications	260
Figure 201: Pitch Attitude Bandwidth and Phase Delay Specifications	261
Figure 202: Roll Attitude Bandwidth and Phase Delay Specifications	261

LIST OF TABLES

Table 1: UltraStick120 Aircraft Parameters	23
Table 2: Actuator Models	27
Table 3: UltraStick120 System Identification Flight Test Run Log	31
Table 4: UltraStick120 MTE Flight Test Run Log	39
Table 5: Performance Requirements for Offset Landing Task (Ref. 32).....	46
Table 6: Lateral Sidestep MTE Pilot Performance Averages	51
Table 7: Left/Right Hover Performance Averages	52
Table 8: UMN Multicopter Parameters	55
Table 9. Proposed Requirements and Current Status.....	63
Table 10: Pitch Aircraft Attitude Bandwidth and Phase Delay Limits	70
Table 11: Roll Aircraft Attitude Bandwidth and Phase Delay Limits	72
Table 12: Yaw Aircraft Attitude Bandwidth and Phase Delay Limits.....	73
Table 13: Vertical Response Bandwidth and Phase Delay Limits.....	73
Table 14: Minimum Achievable Flight Path Angle Change.....	74
Table 15: Example SOS Input Forcing Function Parameters for Lower Frequency Identification	91
Table 16: Scoring Parameters for IRIS+.....	102
Table 17: Performance Levels, Gentle Maneuvering Mission	102
Table 18: Performance Levels, Aggressive Maneuvering Mission	102
Table 19: Flight Conditions	111
Table 20: Flight Test Card	111
Table 21: Model Gains for FLT 03.....	114
Table 22: FLT 03 – Longitudinal Aircraft and Elevator Actuator Models	114
Table 23: FLT 03 – Lateral Aircraft and Aileron Actuator Model	117
Table 24: FLT 03 - Directional Aircraft and Rudder Actuator Model.....	120
Table 25: Model Gains for FLT 04.....	123
Table 26: FLT 04 - Longitudinal Aircraft and Elevator Actuator Models.....	123
Table 27: FLT 04 - Lateral Aircraft and Aileron Actuator Model.....	126
Table 28: FLT 04 - Directional Aircraft and Rudder Actuator Model.....	129
Table 29: Moment of Inertia Results for Aft-CG	133
Table 30: Model Gains for FLT 05.....	133
Table 31: FLT05 - Longitudinal Aircraft and Elevator Actuator Models.....	133
Table 32: FLT05 - Lateral Aircraft and Aileron Actuator Model.....	139
Table 33: FLT05 - Directional Aircraft and Rudder Actuator Model.....	145
Table 34: Model Gains for FLT 06.....	151
Table 35: FLT 06 - Longitudinal Aircraft and Elevator Actuator Models.....	152
Table 36: FLT 06 - Lateral Aircraft and Aileron Actuator Model.....	158
Table 37: FLT 06 - Directional Aircraft and Rudder Actuator Model.....	164
Table 38: Model Gains for FLT 10.....	171
Table 39: FLT 10 – Longitudinal Aircraft and Elevator Actuator Models	171
Table 40: FLT 10 – Lateral Aircraft and Aileron Actuator Model	174
Table 41: FLT 03 - Directional Aircraft and Rudder Actuator Model.....	177
Table 42: Model Gains for FLT 11.....	181
Table 43: FLT 11 – Longitudinal Aircraft and Elevator Actuator Models	181
Table 44: FLT 11 – Lateral Aircraft and Aileron Actuator Model	184
Table 45: FLT 11 - Directional Aircraft and Rudder Actuator Model.....	187
Table 46: Vicon Data Run Logs	213
Table 47: Precision Hover MTE Performance – Pilot 1, Tarot 650 Sport	220
Table 48: Precision Hover MTE Performance – Pilot 2, Tarot 650 Sport	220
Table 49: Precision Hover MTE Performance – Pilot 3, Tarot 650 Sport	221
Table 50: Precision Hover MTE Performance – Pilot 2, Tarot X6-2	221
Table 51: Precision Hover MTE Pilot Performance Averages	222
Table 52: Lateral Sidestep MTE Performance – Pilot 1, Tarot 650 Sport	225
Table 53: Lateral Sidestep MTE Performance – Pilot 2, Tarot 650 Sport	227
Table 54: Lateral Sidestep MTE Performance – Pilot 3, Tarot 650 Sport	229

Table 55: Lateral Sidestep MTE Performance – Pilot 2, Tarot X6-2	230
Table 56: Lateral Sidestep MTE Performance – Pilot 3, Tarot X6-2	231
Table 57: Lateral Sidestep MTE Pilot Performance Averages	232
Table 58: Left/Right Hover Performance Averages	233
Table 59: Vertical Reposition MTE Performance – Pilot 1, Tarot 650 Sport.....	235
Table 60: Vertical Reposition MTE Performance – Pilot 2, Tarot 650 Sport.....	237
Table 61: Vertical Reposition MTE Performance – Pilot 3, Tarot 650 Sport.....	238
Table 62: Vertical Reposition MTE Performance – Pilot 2, Tarot X6-2	239
Table 63: Vertical Reposition MTE Performance – Pilot 3, Tarot X6-2	240
Table 64: Vertical Reposition MTE Pilot Performance Averages	241
Table 65: Landing MTE Performance – Pilot 1, Tarot 650 Sport	244
Table 66: Landing MTE Performance – Pilot 3, Tarot 650 Sport	244
Table 67: Landing MTE Performance – Pilot 2, Tarot X6-2	245
Table 68: Landing MTE Performance – Pilot 3, Tarot X6-2	245
Table 69: Landing MTE Pilot Performance Average	246
Table 70: Heading Angle Performance Averages.....	246
Table 71: Froude Scaling Factors for Scaled Models	253
Table 72: Comparison of UltraStick120 to the Froude-Scaled Cessna 172.....	253
Table 73: Mass properties comparison between UltraStick120 and 25e	254
Table 74: Modal Frequencies and Damping Comparison (Long.)	254
Table 75: Modal Frequencies and Damping Comparison (Long.), 120 & 25e.....	255
Table 76: CAP Value Comparison	255
Table 77: CAP Value Comparison (120 & 25e)	255
Table 78: Modal Frequencies and Damping Comparison (Lateral-Directional)	256
Table 79: Modal Frequencies and Damping Comparison (Lateral-Directional), 120 & 25e.....	256
Table 80: Longitudinal Modal Damping and Frequencies	257
Table 81: Roll Time Constant.....	259
Table 82: Dutch Roll Mode Damping and Frequencies	260

A. PROJECT SUMMARY

1. Identification and Significance of Innovation

Unmanned Air Systems (UAS) are no longer coming, they are here, and operators from first responders to Google and Amazon are demanding access to the National Airspace System (NAS) for a wide variety of missions. This includes a proliferation of small UAS or sUAS that will operate beyond line of sight at altitudes of 500 ft and below. A myriad of issues continues to slow the development of verification, validation, and certification methods that will enable the safe introduction of UAS to the NAS. These issues include the lack of both a consensus in UAS categorization process and quantitative certification requirements, including the definition of handling qualities. Because of the wide variety of UAS types (fixed wing, rotary wing from traditional helicopters to multirotor configurations, ducted fans, airships, etc.) and vehicle size from micro vehicles to the Global Hawk with a wing span similar to that of a Boeing 737, there cannot be a one-size-fits-all set of requirements.

To address these issues, Systems Technology Inc. (STI) has developed the UAS Handling Qualities Assessment (UAS-HQ) process and corresponding draft specification that will guide UAS stakeholders through a systematic evaluation process. The work described herein builds on the existing, highly successful, military rotorcraft handling qualities specifications that features a mission-oriented approach, a concept that originated at STI. The vehicle is first identified by a simple weight-based classification and then the associated vehicle mission task elements are considered. These missions have specific tasks inclusive to them that then dictate the criteria and demonstration maneuvers necessary to evaluate the UAS handling qualities. An assessment of both modeled responses and flight test data can then be conducted to examine the predicted versus actual handling qualities and, if required, design modifications can then be made.

Mr. David Klyde, Vice President and Technical Director, Engineering Services, served as Principal Investigator, while Dr. Natalia Alexandrov served as the NASA LaRC technical representative. In the Phase II program, STI was joined by David Mitchell of Mitchell Aerospace Research and the University of Minnesota. Mr. Mitchell led the draft specification development effort, while the University of Minnesota UAV Lab conducted sUAS flight tests under the direction of Dr. Peter Seiler.

2. Technical Objectives and Work Plan

The technical objectives for the Phase II program were as follows:

- Continuing and expanding upon the processes established in Phase I, engage government, industry, and academic stakeholders at regular intervals in Phase II to build support from potential end users, respond to relevant questions, and identify means to expand UAS data sources to enhance the requirement definition process.
- Identify and/or define UAS handling qualities metrics/criteria to support each MTE category (i.e., precision/aggressiveness levels) and define associated MTE performance requirements that will ultimately result in a draft specification.
- Conduct fixed wing full envelope flight tests with a representative sUAS. Flight tests will include system identification at various flight conditions as well as the evaluation of MTEs at various levels of precision/aggressiveness.
- Conduct limited envelope multirotor flight tests with a representative sUAS. Flight test will include system identification and the evaluation of MTEs at select hover/low speed flight conditions.
- Using the flight test data acquired in the fixed wing and multi-rotor flight tests, the UAS-HQ evaluation process will be assessed against defined success criteria.

All work plan tasks were conducted at STI's facility in Hawthorne, CA, except for those activities associated with subcontractors, Mitchell Aerospace Research and the University of Minnesota. Mr. David Mitchell conducted his activities in support of this program from his office in Long Beach, CA. The University of Minnesota conducted the UAS flight test program. All flights were conducted from the UMore Test Range that is located south of the main campus. The University of Minnesota UAV lab has obtained the proper Certificates of Authorization (COAs) for legal operation of UAV flights.

The above technical objectives were addressed through the following Phase II tasks:

- Task 1 – Stakeholder Engagement: The objective of this task was to engage government, industry, and academic stakeholders at regular intervals in Phase II to build support from potential end users, respond to relevant questions, and identify means to expand UAS data sources to enhance the requirement definition process.
- Task 2 – UAS handling Qualities Requirements and Draft Specification: The objective of this task was to define a set of UAS handling qualities requirements and mission task elements that can address the range of UAS vehicles in terms of weight/size, type, and mode of operation. The process followed that of current piloted aircraft methods with adjustments for varying levels of pilot interaction/autonomy.
- Task 3 – Fixed Wing UAS Flight Tests: The objective of this task was to conduct a handling qualities evaluation flight test program using a fixed wing UAS operated at two unique flight conditions.
- Task 4 – Multi-Rotor Hover/Low Speed Flight Tests: The objective of this task was to conduct a limited envelope handling qualities evaluation using a multi-rotor UAS.
- Task 5 –Process Assessment: The objective of this task was to exercise and evaluate the UAS-HQ process with the UAS vehicle models and flight test data from Tasks 3 and 4. Available models and data provided a means to demonstrate the effectiveness of the predicted and flight verified handling qualities pathways. While the situation is improving, the lack of data across vehicle types, whether flight or model generated, remains a limitation of this work. Thus, the Phase II analysis conducted in this program represents the first systematic attempt to fully address UAS handling qualities. It is important to note that this is a start to the process and not an end as more data will be needed to address all MTEs in all UAS weight classes.

3. Technical Accomplishments

The specific technical accomplishments in this Phase II program are as follows:

- UAS Handling Qualities Stakeholders from industry, academia, and government agencies were engaged throughout the two-year program. Highlights of this engagement include the three UAS Handling Qualities Workshops that were conducted; one at NASA LaRC and two as part of the AIAA SciTech conference. All the workshop presentations have been made available to the Stakeholders via an easily accessible website hosted by the University of Minnesota. There are no restrictions regarding access to this website.
- A process to define UAS handling qualities was defined, demonstrated, and validated through analysis and flight tests. Process validation has also been demonstrated by UAS Handling Qualities Stakeholders that conducted their own work in parallel with this program.
 - While it was beyond the scope of this program to quantify new UAS handling qualities requirements because of a significant lack of data, there has been a significant growth in the data that are now available in the public record.

- The use of end-to-end system identification was used to demonstrate UAS model validation methods in both the frequency and time domains using both long and short duration command inputs. Furthermore, the frequency responses generated from the system identification tests were used to extract parameters that are used to predict handling qualities.
- UAS handling qualities verification flight tests were conducted using a set of mission task elements defined for both fixed wing and rotary wing mission task elements.

4. NASA Application(s)

First, this program directly supports the NASA Air Vehicle Technology topic that “solicits tools, technologies and capabilities to facilitate assessment of new vehicle designs and their potential performance characteristics” and as specifically called out under Topic A1.05 Physics-Based Computational Tools - Stability and Control/High Lift Design Tools, the “definition of handling qualities for unmanned aerial systems.” Beyond these specific NASA goals, NASA issued in 2014 a new strategic vision for the Aeronautics Research Mission Directorate (ARMD). From this effort came six new strategic thrusts. Of these thrusts, several involve the safe expansion of global air operations and are therefore directly related to the safe integration of UAS into the air space. The specific thrusts include “safe, efficient growth in global operations,” “real-time, system-wide safety assurance,” and “assured autonomy for aviation transformation.” This proposal therefore supports NASA’s Integrated Aviation Systems Program (IASP) of which the UAS Integration in the National Airspace System (NAS) Project is another direct application. In this arena, the Phase II team has supported the UAS Traffic Management (UTM) Safety/Risk Analysis Technical Lead from the NASA LaRC Dynamic Systems and Control Branch. The support has focused on the definition of UAS hazards and potential mitigations as well as the development of mission task elements to assess UAS performance in the presence of hazards.

5. Non-NASA Commercial Application(s)

In describing the growing UAS market, Teal Group reported that the worldwide UAS market spending will increase from \$6.4 billion in 2014 to \$11.5 billion in 2024 (Ref. 1). The Teal Group article also states that “Our 2014 UAV study calculates the UAV market at 89% military, 11% civil cumulative for the decade, with the numbers shifting to 86% military and 14% civil by the end of the 10-year forecast.” There is a strong demand for the advancement of UAS handling qualities capability on the military side where the Air Force and Navy have long been looking for a path forward in this area. This assertion is supported by the active participation of Army Aviation Development Directorate, Naval Air Systems Command (NAVAIR), and Air Force Research Laboratory (AFRL) personnel in the three workshops conducted in Phase II that included invited stakeholders.

The team also sees this demand expanding to the growing commercial market, particularly on the sUAS side, as the FAA continues to grant access to the NAS to new UAS applications over the coming months and years. Note that the proposed team also received feedback from FAA personnel from the Small Airplanes Standards Branch/Policy and Innovation Division.

Outside of the government, this work is generating strong interest from traditional airframers, UAS manufacturers, and academia and the UAS Stakeholders participants list now includes over 160 members. Further details regarding UAS Stakeholders engagement is covered elsewhere in this report.

B. INTRODUCTION

1. Program Overview

Unmanned Air Systems (UAS) are no longer coming, they are here, and operators from first responders to Google and Amazon are demanding access to the National Airspace System (NAS) for a wide variety of missions. This includes a proliferation of small UAS or sUAS that will operate beyond line of sight at altitudes of 500 ft and below. A myriad of issues continues to slow the development of verification, validation, and certification methods that will enable the safe introduction of UAS to the NAS. These issues include the lack of both a consensus UAS categorization process and quantitative certification requirements including the definition of handling qualities. The “how to” of safely integrating UAS in the NAS raises many questions, and to date, there have been few answers. Perhaps the problem is too big. Because of a lack of quantitative data, attempts to address core problems thus far have failed to achieve consensus support. A prominent figure at a major UAS manufacturer referred to the current landscape as “the new wild west.” That is, many are coming looking for riches, but there is limited law and order to be found. Currently this arena includes traditional airframers, established UAS manufacturers, academic institutions, and many newcomers such as Amazon, Google, and Facebook that see UAS as a means to other commercial ends. The program described herein does not propose to tame the entire verification, validation, and certification problem, but instead to address the important need to define UAS handling qualities in both piloted and autonomous operations with an end product being the UAS Handling Qualities Assessment Process (UAS-HQ), illustrated in Figure 1.

Figure 1 begins with UAS classification. Because of the wide variety of UAS types (fixed wing, rotary wing from traditional helicopters to multirotor configurations, ducted fans, airships, etc.) and vehicle size from micro vehicles to the Global Hawk with a wing span like that of a Boeing 737, there cannot be a one-size-fits-all set of requirements. Given an appropriate classification, a mission in the form of mission task elements (MTEs) (Ref. 2) is next considered. Missions may be as varied as the vehicle types. Examples include air-to-air and/or air-to-ground sensor tracking for surveillance, terrain surveying for pipelines or agriculture, entertainment or real estate filming, weather monitoring, package delivery, and WiFi access. Missions are then broken down into specific task elements that include those elements that will be a part of any mission (e.g., takeoff and landing) to those that are mission specific (e.g. precision target tracking, high altitude loiter, obstacle avoidance, etc.). These mission task elements are used to identify specific criteria that predict handling qualities analytically and test demonstration maneuvers that verify handling qualities in flight.

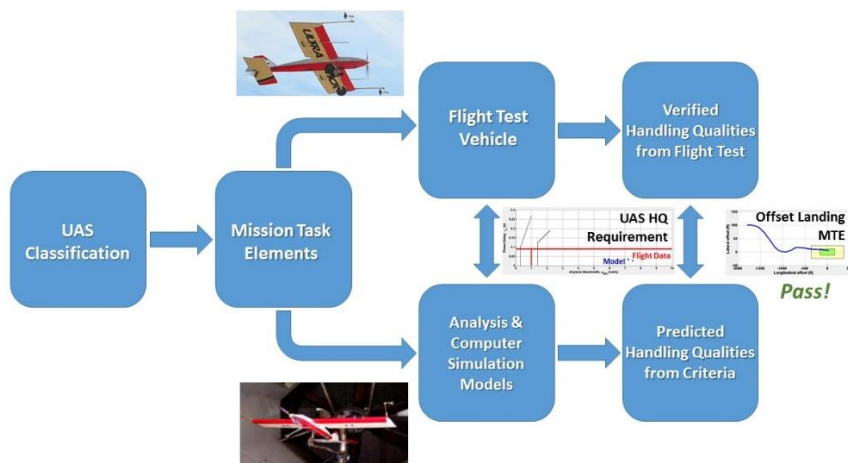


Figure 1: The Proposed UAS Handling Qualities Assessment Process

2. Barriers to UAS Certification

“A drone crashes in the middle of a Capitol Hill hearing on drones,” the Washington Post headline reads in a January 21, 2015 on-line article (Ref. 3). Only in passing does the article mention that NASA and FAA officials also testified in front of the House Science, Space and Technology Committee, and there is no description of the content of this testimony. Even though this “crash” was a non-event, this article does reflect the public skepticism regarding UAS integration and use in the NAS.

Other recent government reports and media articles have highlighted more troubling issues. “FAA Faces Significant Barriers to Safely Integrate Unmanned Aircraft Systems into the National Airspace System.” This title is taken from a report (Ref. 4) generated by the FAA Office of Inspector General that was released on June 24, 2014. The FAA Modernization and Reform Act of 2012 mandated a goal of safe integration of unmanned aircraft systems (UAS) into the NAS by 30 September 2015. The report identifies “significant technological, regulatory, and management barriers” that will prevent the FAA from meeting this rapidly approaching deadline. Of the many shortcomings indicated in the report, two related areas are a lack of certification requirements and an identification of safety risks. Perhaps the media is addressing the latter as a series of high profile articles from the Washington Post in June 2014 exposed to the general public the high number of military drone crashes around the world and the growing number of crashes here in the US. Many of these crashes resulted from aircraft departures from controlled flight that often took the operators by surprise. Below are recorded comments from two operators that appeared in the June 23, 2014 Washington Post article by Whitlock (Ref. 5):

“Drone just pitched up. Drone’s pitching over. Drone is uh, crashed and destructed, at uh, the end of the runway.”

“This thing’s kind of climbing like a pig. Climb, you pig. . . . Boy, this is going to be tight. . . . Okay, interesting. We are falling out of the sky.”

Piloted fixed wing and rotary wing aircraft must demonstrate appropriate handling qualities through a well-defined certification process before access to the NAS is granted. No such process or proven requirements yet exist for UAS. Again applying the piloted aircraft analogy, decades of research with dedicated variable stability aircraft were undertaken to create the databases necessary to define handling qualities requirements. For UAS that as mentioned above range in size from a hand-launched micro air vehicle to the Global Hawk with a wingspan akin to a B-737, no such database exists. In fact, it is difficult to find consensus for what “handling qualities” of a UAS means. Indeed, in similar fashion, data upon which to design flight control systems to meet specified handling qualities, define the ‘safe’ envelope in which they are expected to operate, and regulate how the aircraft should respond if those bounds are crossed and departure from controlled flight occurs is sparse for UAS, especially so in those flight regimes where the vehicle dynamics are nonlinear and sometimes ill-behaved. These are well-recognized issues, but to date, no focused research efforts have been funded to define UAS handling qualities. Instead, piloted aircraft requirements, which may or, more likely, may not be appropriate, are often proposed. Even though the FAA has been granting more commercial UAS exemptions in recent months, the end result is that validation, verification, and certification of UAS systems including the definition of UAS handling qualities remain elusive.

3. UAS Classification

To define UAS handling qualities, there must first be an effective classification scheme. Unfortunately, this goal also remains elusive, despite past and ongoing efforts. The Navy has been particularly concerned with the classification of UAS as part of a larger goal to define quantitative requirements (Ref. 6). The Navy approach thus far has been to base classification on those defined in the fixed wing flying qualities specifications for piloted aircraft, which classifies based on aircraft size and weight. What’s missing from this approach is a consideration of airspeed, a critical factor with regards to assessing safety. Cotting, as part of his doctoral dissertation, proposed an approach that classifies by Reynolds number, Mach number, and weight (Ref. 7). A more recent NASA-funded study led by Embry-Riddle Aeronautical University

used an expert system approach to map UAS characteristics with operational requirements to derive their classification scheme (Ref. 8). Based on this approach, the top three weighted system parameters were maximum kinetic energy, weight, and wingspan. Given a mission-oriented approach as addressed later in this report, UAS classification can be simplified as the mission addresses many of these considerations.

4. Lessons Learned from Manned Aircraft Requirements

All of the issues discussed thus far add up to one primary concern – airworthiness of the UAS. That is, the UAS must demonstrate through an approved verification, validation, and certification process an equivalent level of safety to those other aircraft operating in the NAS. NATO has been evolving airworthiness requirements for UAS via its STANAG 4671, “UAV Systems Airworthiness Requirements (USAR) for North Atlantic Treaty Organization (NATO) Military UAV Systems.” While there is still a lack of supporting data to quantify many of the requirements and the emphasis is on military operations, it does provide a roadmap for civilian certification in many ways. Foremost, it defines the broad areas of airworthiness disciplines that must be addressed as part of the certification process including flight, structures, design and construction, powerplant, equipment, operating limitations and information, command and control data link, and control station. It is beyond the scope of this effort to address all of these important areas. Instead, the focus herein is on defining UAS handling qualities.

There is a wealth of literature available regarding the development and application of fixed wing flying and handling qualities metrics and criteria. As first described in Ref. 9, there has been a tendency, historically, to use the terms “flying qualities” and “handling qualities” interchangeably. For the engineering community, there is often no recognized difference between these phrases. To some, however, the terms have begun to take on different meanings, and this difference has been reflected, where possible, in this work. The terms are interpreted as follows.

“Flying qualities” is taken to mean those analytical and empirical parameters or criteria that can be measured for a given airplane. All such parameters or criteria can be related to the demands the pilot places on the airplane to achieve desired performance. That is, they are *open-loop* metrics describing *pilot-in-the-loop* operations.

By contrast, “handling qualities” is meant to describe operations while the pilot is actively in the loop. This includes the definition put forth by Cooper and Harper (Ref. 10): “Those qualities or characteristics of an aircraft that govern the ease and precision with which a pilot is able to perform the tasks required in support of an aircraft role.” For UAS, consideration is also given to the ability of the autonomous system to perform the task.

In this context, the “flying qualities” criteria are open-loop measures by which one attempts to quantify the “handling qualities” of the airplane. The most prominent criteria have been included in the several incarnations of the military specifications and design standards, including the most recent release of MIL-STD-1797B *Flying Qualities of Piloted Aircraft* (Ref. 11), while the rotorcraft criteria can be found in ADS-33E-PRF *Handling Qualities Requirements for Military Rotorcraft* (Ref. 12). A more detailed look at the evolution of aircraft flying qualities can be found in Ref. 13.

For military rotorcraft, handling qualities are specified using a highly successful mission-oriented approach. The foundation of the mission-oriented approach (Ref. 2) is that requirements are based on realistic MTEs, not Flight Phases. As described in Ref. 9, the goal has been to tie specific flight test demonstration maneuvers to these MTEs. Ultimately, a truly mission-oriented specification will have all quantitative requirements tied directly to realistic MTEs, and for every MTE, there will be a corresponding demonstration maneuver as is done with the rotorcraft design standard. The MTE will be what is expected of the aircraft; the demonstration maneuver will be an explicit way of testing suitability for performing the corresponding MTE. This is perhaps the most significant “mission-oriented” concept and, as such, led to the research reported in Ref. 2. In a sense this is what the FARs and the Flight Test

Guide do for the FAA; however, the applicability of the approach is for key requirements limited to the traditional aircraft response type, else special conditions must be defined.

A mission-oriented approach provides for the possibility of different dynamic response characteristics or response-types. One shortcoming of several of the requirements of MIL-STD-1797B is that they are not applicable to all response-types. As mentioned above, a further significant feature of the mission-oriented approach is the inclusion of demonstration maneuvers as an integral part of the standard. It is recognized that the quantitative requirements defined by predictive criteria are not comprehensive. Meeting these requirements does not guarantee desirable handling qualities or mission performance. Conversely, failing one or more of the requirements is not necessarily a guarantee of less than desirable handling qualities (although it is highly probable). For this reason, qualitative flight test evaluations by experienced test pilots are the fundamental element of the FAA certification process regarding commercial transport flying qualities. For UAS operations, a process in which system performance is quantified via flight evaluations will be an essential component to defining UAS handling qualities.

5. Autonomy and Handling Qualities

Historically, handling qualities are defined for piloted aircraft. UAS operations may be piloted, pilot monitored, autonomous, or a combination of the three. It is often asked, how can handling qualities be defined for vehicles not directly controlled by a human pilot? When actively engaged in flying an aircraft, the pilot provides guidance, navigation, and control functions. Autopilots can provide regulation of some of these functions, e.g., speed and altitude hold modes thereby reducing pilot workload, but they are not autonomous functions. Autonomous functions feature a decision making capability that attempts to replicate or even improve upon piloted operations. Thus, if a UAS mission is to, for example, station keep over a given location it matters not in terms of handling qualities whether it is remotely piloted or autonomous, the mission requirements will be the same. Of course, some consideration of the autonomous systems must be made in the analysis just as consideration is given to the pilot in traditional handling qualities.

6. UAS Stakeholders Engagement

A key objective of this program was to engage government, industry, and academic stakeholders at regular intervals in Phase II to build support from potential end users, respond to relevant questions, and identify means to expand UAS data sources to enhance the requirement definition process. This engagement process began in Phase I with stakeholders participating in kickoff, midterm, and final briefings over the six-month program. In Phase II this engagement continued through a series of UAS Handling Qualities Workshops, a growing Stakeholders mailing list, and document sharing via a publicly accessible website hosted by the University of Minnesota (<https://www.uav.aem.umn.edu/workshops>).

During the Phase II period of performance, three UAS Handling Qualities Workshops were held. The first was held as a program kickoff event at NASA LaRC. The next two were held in conjunction with the American Institute of Aeronautics and Astronautics (AIAA) SciTech Conferences that were held in Kissimmee, FL in 2018 and San Diego, CA in 2019. The workshops were invited sessions sponsored by the Atmospheric Flight Mechanics Technical Committee. All three workshops featured presentations from the program team and UAS Stakeholders. Based on the engagement activities, the UAS Stakeholders participants list now includes over 160 members.

7. Report Outline

The report continues in Section C with a discussion of the mission-oriented approach and addresses both the mission task element framework and classification considerations. Section D details the process of defining candidate requirements including the governing assumptions, introduces a proposed specification template, details the stakeholder involvement, and addresses both dynamic scaling and uncertainty analysis. The UAS handling qualities process demonstration is described in Section E including details on the flight test activities with fixed wing and multirotor vehicles. The program summary and conclusions

are provided in Section F including next steps. Appendix A contains the draft specification that is intended to serve as a preliminary specification and point of discussion for future evolutions of the document. The mission task element catalog developed in this effort is provided in Appendix B along with contributions from UAS Stakeholders. Appendix C contains a description of the fixed wing system identification flight tests. Similar information for the multirotor flight testing is given in Appendix D. Finally, Appendix E contains a study concerning the use of dynamic scaling on vehicles to apply existing manned vehicle requirements to smaller UAS.

C. THE MISSION-ORIENTED APPROACH

1. Old School – Sorting by Class and Flight Phase

For decades through the incarnations of the military flying qualities specifications MIL-F-8785 and MIL-STD-1797, fixed wing requirements for piloted airplanes have been defined by specific classifiers – size, weight, and flight phase. The public release of MIL-STD-1797, Version A, defines four fixed wing air vehicle classes as follows:

- Class I: Small, light air vehicles such as light utility, primary trainer, or light observation.
- Class II: Medium weight, low-to-medium maneuverability air vehicles such as heavy utility/search and rescue; light or medium transport/cargo/tanker; early warning/electronic countermeasures/airborne command, control, or communications relay; antisubmarine; assault transport; reconnaissance; tactical bomber; heavy attack; or trainer for Class II.
- Class III: Large, heavy, low-to-medium maneuverability air vehicles such as heavy transport/cargo/tanker; heavy bomber; patrol/early warning/electronic countermeasures/airborne command, control, or communications relay; or trainer for Class III.
- Class IV: High-maneuverability air vehicles such as fighter/interceptor; attack; tactical reconnaissance; observation; or trainer for Class IV.

Given an identified air vehicle class, requirements are further classified by Flight Phase. MIL-STD-1797A defines three Flight Phases:

- Category A: Those nonterminal Flight Phases that require rapid maneuvering, precision tracking, or precise flight-path control. Examples include air-to-air combat, reconnaissance, terrain following, in-flight refueling (receiver), and close formation flying.
- Category B: Those nonterminal Flight Phases that are normally accomplished using gradual maneuvers and without precision tracking, although accurate flight-path control may be required. Examples include climb, cruise, loiter, in-flight refueling (tanker), and aerial delivery.
- Category C: Terminal Flight Phases are normally accomplished using gradual maneuvers and usually require accurate flight-path control. Examples include takeoff, power approach, landing, carrier approach, carrier landing, and ground handling.

On the surface, this appears to be a “tortoise and hare” approach to requirements. That is, the big and slow tortoise will naturally have unique requirements from the small and fast hare. Is this always the case? Consider the AC-130 gunship and the C-130J transport, both considered Class III aircraft. While the airframes are in many ways the same, their missions could not be more different. Does the AC-130’s ground attack mission have more in common with the A-10, a much smaller and lighter Class IV aircraft? If the answer to this question is “yes,” then should not the handling qualities requirements for the AC-130 be more akin to the A-10? If the answer is again “yes,” then an approach to defining handling qualities based on mission can be more appropriate than an approach based on Class or Flight Phase. This may be especially true for UAS where the number of potential classes and flight phases is expansive.

2. Eliminating Classifications

The material in this section has been updated from *Handling Qualities Demonstration Maneuvers for Fixed wing Aircraft, Volume I: Maneuver Development Process* (Ref. 9), a project for the USAF Flight Dynamics Directorate that was jointly conducted by Systems Technology, Inc. and Hoh Aeronautics, Inc.

For handling qualities flight test evaluations, it is desirable to categorize segments of the missions into handling qualities evaluation tasks. The ability of the aircraft to accomplish these tasks is predicted according to the appropriate criteria. Parameters for these requirements are generated first analytically,

then via simulation, and finally via flight test. It is not practical, or necessary, to derive a separate set of criteria for every defined task. Instead, the tasks are grouped in terms of the criteria boundaries that apply to them. The task definitions included specific desired and adequate performance requirements to facilitate evaluation test pilot use of the Cooper-Harper handling qualities rating scale (Ref. 10). In a mission-oriented approach to aircraft handling qualities (Ref. 2), requirements are based on realistic MTEs, not the general Flight Phases identified above that define the current and long standing approach to piloted fixed wing aircraft flying qualities. An MTE therefore defines a specific flight test demonstration maneuver.

Ultimately, a truly mission-oriented UAS specification will have all quantitative requirements tied directly to realistic MTEs. The associated MTE requirement will be what is expected of the UAS; the MTE itself will be an explicit method of test to verify handling qualities in piloted simulation and flight test. This is perhaps the most significant “mission-oriented” concept, and, as such, led to the research effort reported in Ref. 9. This fixed wing research was based on the mission-oriented approach to handling qualities that was successfully established for military rotorcraft via ADS-33.

In the mission-oriented approach, references to Class are removed. A number of the requirements in MIL-STD-1797A have different values depending upon aircraft size, defined in terms of four the Classes of aircraft, particularly the modal requirements that were defined in MIL-F-8785 and that have remained through the current version of the fixed wing standard. This division is actually somewhat arbitrary, and is sometimes irrelevant. For example, if a particular mission requires a high level of aggressiveness and precision, it should not matter if the airplane proposed for that mission is small or large. Only the mission requirements should set handling qualities. It is recognized that, in some cases, this may lead to unreasonable demands on very large airplanes. Returning to the previous transport example, if the AC-130 is required to perform ground attack, then the Level 1 roll performance limits stated for Class IV fighters may be unachievable without the use of extremely fast actuators and the possible introduction of very high lateral accelerations at the pilot’s station. In this case, it should be obvious that either (1) a new MTE, such as *transport ground attack*, with relaxed mission demands needs to be defined, or (2) it is simply not possible to build a Level 1 transport for the ground attack task. Because the AC-130 has been highly successful in the ground attack mission, the former is the more likely scenario.

A mission-oriented approach provides for the possibility of different dynamic response characteristics or flight control system response-types. One shortcoming of several of the requirements of MIL-STD-1797A is that they are not applicable to all response-types. For example, aircraft with an attitude response-type such as pitch attitude command/attitude hold dynamics should not be evaluated using the control anticipation parameter (CAP) criteria for short-term response. The number of different response types possible for fixed wing airplanes is not extensive, so this amounts, in essence, to simply amplifying the guidance to the user. For UAS that can feature many unique response types and levels of autonomy, requirements that are not specific to these elements of the design are needed.

Finally, one of the most significant features of the mission-oriented approach is the inclusion of MTEs as an integral part of the standard. This was done for rotorcraft in ADS-33 and an initial fixed wing catalog of maneuvers (Ref. 14), but these maneuvers have not yet been incorporated into the fixed wing standard. It is recognized that the quantitative requirements of MIL-STD-1797A are not now, and can never hope to be, completely comprehensive. Meeting the diverse requirements of the fixed wing standard does not guarantee desirable handling qualities. Conversely, failing one or more of the requirements is not necessarily a guarantee of less than desirable handling qualities (although it is highly probable). Therefore, qualitative flight test evaluations by trained evaluators that are familiar with the handling qualities rating process as established by Cooper and Harper (Ref. 10) should be made an integral part of the handling qualities assessment process. For the evaluation of UAS handling qualities it is recognized that modifications to the rating process including alternate rating scale versions will be required based on the role of the pilot/operator.

The addition of MTEs allows for two separate methods for assessing the Levels of UAS handling qualities:

- *Predicted Levels based on handling qualities parameters.* Here, comparisons are made with quantitative boundaries of handling qualities parameters. When establishing compliance, the parameters of the UAS are determined and compared with the boundaries appropriate to the MTE requirements. These criteria are inherently single-axis. A Level 1 UAS must meet the Level 1 standards for all of the criteria. The quantitative criteria are based on previous experiments and analyses, and hence result in predicted Levels of handling qualities. When using a given requirement, users should have a good understanding of the theory behind a particular requirement and the supporting data that were used to define the quantitative requirements.
- *Assigned Levels based on flight test maneuvers.* The second method of establishing Levels is to perform a set of well-defined flight test maneuvers (i.e., the defined MTEs) using a team of at least three test pilot/operator evaluators. These evaluators assign Cooper-Harper Handling Qualities Ratings or HQRs (Ref. 10) to the aircraft for each maneuver. The collective HQR determines the Level for each maneuver and a Level 1 aircraft must be rated Level 1 for all of the maneuvers designated as appropriate to its operational requirements. As mentioned above, evolutions of this rating process will be needed for UAS evaluations. The flight test maneuvers may be either single- or multi-axis by design, though it may be appropriate to evaluate the aircraft one axis at a time first before moving to multi-axis evaluations. Compliance with the flight test maneuvers is based on piloted evaluations, and therefore results in assigned Levels of handling qualities. These pilot/operator evaluations will provide the ultimate check of UAS handling qualities.

3. Mission Task Elements (MTEs)

It is desirable to categorize segments of the mission into specific tasks. The ability of the aircraft to accomplish these tasks is measured according to the appropriate requirements. The mission tasks in the mission-oriented specification are more formally defined as “Mission Task Elements” or MTEs. It is intended that the MTEs be specified in detail, including performance requirements. Furthermore, flight phase categories are defined in terms of the level of *precision* and *aggressiveness* required of the UAS. Four MTE categories are defined as follows:

a. Non-Precision, Non-Aggressive

Non-precision tasks that require only a moderate amount of remote pilot or autonomous system control fall in this category. Example tasks from this category include:

- Heading and altitude changes to optimize on-board sensor performance; and
- Non-precision station keeping (e.g., weather monitoring, wildfire monitoring, internet access provider, etc.).

b. Non-Precision, Aggressive

This category is intended to include the large amplitude maneuvering MTEs that emphasize control power over crisp dynamics. It is true, however, that a reasonably good dynamic response is inherently necessary to effectively utilize a large amount of control authority, i.e., to stop and start the large amplitude maneuvers with some precision (recall the old control power vs. damping plots). The moderate- and large-amplitude maneuvering requirements will be of primary interest for these MTEs. This category will invoke some of the existing control power criteria, as well as other agility criteria. Example tasks from this category include:

- Ground-based or air-based obstacle avoidance; and

- Gross acquisition of air or ground targets.

c. Precision, Non-Aggressive

This category includes tasks where considerable precision is required, but without the aggressive control activity. The dynamic response requirements for these tasks are expected to be less stringent than for *Precision, Aggressive*, but significantly greater than for *Non-Precision, Non-Aggressive*. Example tasks from this category include:

- Precision landings;
- Precision path following at altitude (e.g., border patrol, highway/roadway/railway monitoring, etc.);
- Precision station keeping;
- Precision hover;
- Precise pitch attitude and bank angle captures; and
- Final approach and landing for package delivery.

d. Precision, Aggressive

This category includes precision tasks, where an extremely crisp and predictable response to control inputs is required. The results of not achieving the required precision are usually significant in terms of accomplishing the mission or safety of flight. Example tasks in this category include:

- Air-to-air and air-to-ground fine tracking, and
- Low altitude precision path following (e.g., crop dusting/monitoring, pipeline scanning, etc.).

e. MTE Categories and Candidate UAS Handling Qualities Requirements

The intent of the MTE categories is that the requirements in a given category are sufficiently similar so that a single criterion boundary will apply. For example, the Bandwidth criterion (Ref. 13) should have a form similar to that shown in Figure 2. As described elsewhere in this paper, data are required to properly define these boundaries for UAS applications.

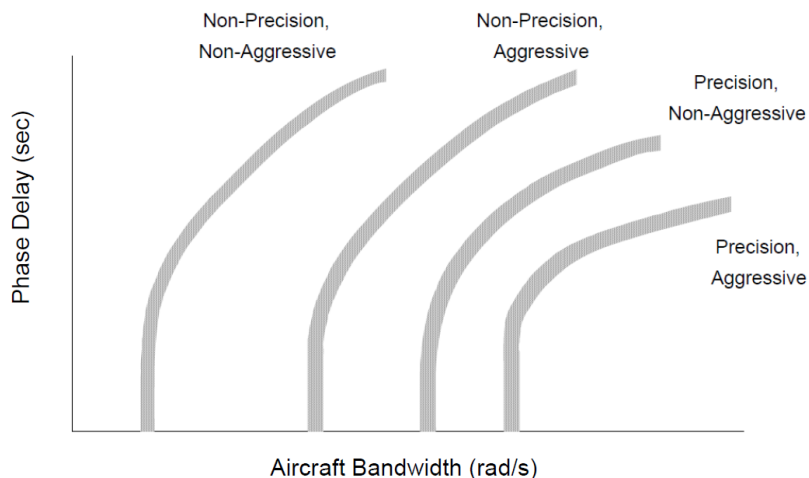


Figure 2: Relationship between MTE Categories and Specification Boundaries for Aircraft Bandwidth Criterion (Ref. 9) as Defined by Phase Delay (τ_p , sec) versus Bandwidth Frequency (ω_{BW} , rad/s)

4. Classification

a. Background

Building on the material in the Introduction, the common denominator in all of the past classification approaches is size, weight, and airspeed. Clearly size and weight are tied together, although examples of very large but lightweight and very small but dense UAS examples can be identified. Neglecting the fringe examples, however, a combined weight (or mass) and speed classifier is attractive. Such an approach can be applied to vehicles defined as sUAS or small UAS that are designed to fly at relatively low speeds and low altitudes (i.e., < 500 ft) and weigh less than 55 pounds and UAS that are designed to operate at higher altitudes assigned to the NAS and weigh more than 55 pounds though they currently typically operate in restricted airspace. A small sampling of the wide variety of UAS is shown in Figure 3.



a) WASP III ~1 lbs (USAF Photo)



b) FASER ~19.72 lbs (NASA Photo)



c) AirSTAR ~49.6 lbs (NASA Photo)



d) MQ-8B Fire Scout ~3,150 lbs (USN Photo)



e) Ikhana Predator B, ~10,500 lbs (NASA Photo)



f) Global Hawk, ~25,600 lbs (NASA Photo)

Figure 3: Example UAS

b. Consideration of Class and the Pilot/Operator

Throughout 2016, the FAA has been moving more rapidly to develop rulemaking for UAS. The focus thus far has been on those small UAS that weigh 55 pounds or less and are designed to operate primarily at altitudes below 500 feet. Rules for operating vehicles in this class were released on June 21, 2016 (Ref. 15). Operational limitations include the following:

- Visual line-of-sight operations only;
- Daylight-only operations;
- Maximum groundspeed of 100 mph (87 knots) and a maximum altitude of 400 feet AGL; and

Operator must hold or be under the direct supervision of someone who holds a remote pilot certificate.

Above this UAS class, the sizes and weights of current vehicles including those exemplified in Figure 3 are significantly larger and significantly heavier. Furthermore, these vehicles are designed to operate at much higher altitudes and much greater speeds than the under 55 pound vehicles. While the majority of these vehicles only operate in restricted airspace, the FAA has recently awarded the General Atomics Aeronautical Systems Predator C Avenger an Experimental Certificate (EC) that enables this vehicle to perform “routine operations” within the NAS. This is the first jet-powered remotely piloted aircraft to receive an FAA EC.

A unique group of UAS vehicles that falls below the under 55 pound weight is the micro UAS. The FAA is currently considering rules for this weight class that is defined as 250 grams (0.55 pounds) or less (Ref. 16). These vehicles are small enough to operate indoors as well as outdoors. With configurations that can vary significantly (e.g., flapping wing designs, vehicles with perching capabilities, etc.) and feature unique dynamic modes, it is beyond the scope of this Phase I project to address these vehicles, but they will be considered in Phase II.

While one can consider further weight classifications, the following weight classifiers will be used herein as a starting point:

- UAS (Weight > 55 pounds);
- sUAS ($0.55 < \text{Weight} < 55$ pounds); and
- μ UAS (Weight < 0.55 pounds).

Other classifiers such as speed, type (e.g., fixed wing, rotary wing, ducted fan, etc.) will be captured by vehicle mission as discussed next.

The role of the pilot is an important factor in defining UAS handling qualities. For a remote pilot that is actively engaged in flying the vehicle, issues such as latency in pilot inceptor to vehicle response may be an important factor and must be reflected in the requirements. On the other hand, an autonomous system can be considered an on-board “pilot” where the impact of the guidance, navigation, and control functions of the software must be considered in the handling qualities assessments. Thus, the role of the pilot/operator will be reflected in the requirements that are linked to a given MTE.

Historically, handling qualities are defined for piloted aircraft. UAS operations may be:

- Remotely Piloted;
- Remote Pilot Assisted (delegated or supervised);
- Fully Autonomous; or
- A combination of the three.

The above correspond with the four levels of autonomy as defined in the DoD Unmanned Systems Integrated Roadmap (Ref. 17). These definitions are repeated below:

- Level 1 – Human Operated: The human operator makes all decisions. The system has no autonomous control of its environment although it may have information-only responses to sensed data.
- Level 2 – Human Delegated: The vehicle can perform many functions independently of human control when delegated to do so (e.g., autopilot functions). This level encompasses automatic controls, engine controls, and other low-level automation that must be activated or deactivated by human input and must act in mutual exclusion of human operation.
- Level 3 – Human Supervised: The system can perform a wide variety of activities when given top-level permissions or direction by a human. Both the human and the system can initiate behaviors based on sensed data, but the system can do so only if within the scope of its currently directed tasks.
- Level 4 – Fully Autonomous: The system receives goals from humans and translates them into tasks to be performed without human interaction. A human could still enter the loop in an emergency or change the goals, although in practice there may be significant time delays before human intervention occurs.

When actively engaged in flying, the pilot provides GNC functions. Autopilots can provide regulation of some of these functions, but they are not autonomous functions, they are regulators. Autonomous functions feature a decision making capability that attempts to replicate or even improve upon piloted operations. If a UAS mission is to, for example, station keep over a given location it matters not in terms of handling qualities whether it is remotely piloted or autonomous, the mission requirements will be the same.

As introduced herein, a number of classification techniques of varying complexity were considered. Because UAS handling qualities was defined using the mission-oriented approach, a simple classification technique based on FAA weight classifications was employed. Further classifications will come naturally from the MTE selection that will then identify handling qualities requirements or flight test procedures that will be used to predict handling qualities via the analysis path and verify handling qualities via test.

5. Selected sUAS Mission Task Elements

To demonstrate the Figure 1 process, example mission task elements (MTEs) were defined for the fixed wing and multirotor flight tests that were conducted by the University of Minnesota and at NASA LaRC. Detailed descriptions of these MTEs and those provided by UAS Stakeholders are in Appendix B. The format for the MTEs is as shown below:

MTE Name (Precision/Aggressiveness Level)

Autonomy Level

- Should specify expected operator intervention.
- If MTE can be flown with differing amounts of intervention, and any part of the MTE changes as a result, consider creating separate MTEs for the different levels of autonomy.

Task Objectives

- Approximately two to four high-level bulleted items that will help the user determine why this MTE should be used, and the expected outcomes.

Task Description

Brief but explicit description of the task, including test course layout and specialized equipment/displays needed. Keep the MTE simple in operation. If it becomes too elaborate, consider breaking it into two (or more) MTEs. Be careful setting time as a task parameter. Consider whether time is a part of the task description (meaning it must be met) or a performance limit (meaning it is a measure of goodness).

Desired Performance

- Bullet list of the expected level of task performance for a UAS that is satisfactory without improvement.
- List those parameters you think are important, even if the limits for now are just listed as “TBD.”

Adequate Performance

- Bullet list of the expected level of task performance for a UAS that has deficiencies that warrant improvement.
- List those parameters you think are important, even if the limits for now are just listed as “TBD.”

Notes for developing this MTE:

1. Any additional comments are provided here.

Included in Appendix C are the following fixed wing MTEs:

- Flightpath Regulation in the Presence of a Discrete Gust
- Flightpath Regulation in the Presence of a SOS Disturbance
 - Altitude Disturbance
 - Attitude Disturbance
- Waypoint Following
- Precision Offset Landing

Also included in Appendix C are the following rotary wing MTEs:

- Precision Hover
- Lateral Reposition
- Vertical Reposition
- Landing.

MTEs provided by UAS Stakeholders include the following:

- Unusual Attitude Recovery, Nose-High provided by Dr. Nate Richards of Barron Associates, Inc.
- Scaled ADS-33E-PRF Rotary Wing MTEs provided by Dr. Christina M. Ivler, University of Portland, and Chad Goerzen, U.S. Army
- Hover MTE under First Person View Cueing provided by William Geyer, US Navy Test Pilot School

D. REQUIREMENTS IN A UAS HANDLING QUALITIES SPECIFICATION

A significant portion of this technical effort has been devoted to the development of a specification for UAS that can be used for design, verification, validation, and airworthiness. It was recognized from the outset that the quantitative documentation to finalize such a specification simply does not exist, so the version included in Appendix A is a proposed format for the final specification. While it has been extensively improved and modified over the duration of the contract, it is still lacking in many details.

1. Assumptions

Several assumptions were made before the specification development work even began. The most important of these are as follows.

a. Breadth of Application

An “Unmanned Aircraft System” can consist of multiple elements: the air vehicle, the ground control (or monitoring) station, and the operator (or observer). The degree of autonomy determines the details of each of these elements. It was recognized from the start that the creation of a specification to cover requirements for both the air vehicle and the ground station would be an overwhelming task, so the specification limited in scope to the air vehicle alone.

For this reason, the subject of the draft specification is limited to the Unmanned Aircraft, abbreviated UA. The “UA” designation is not common in practice, but is in keeping with a military-based flight control systems document issued by the SAE, Aerospace Recommended Practice ARP94910, titled “Aerospace - Vehicle Management Systems - Flight Control Design, Installation and Test of, Military Unmanned Aircraft, Specification Guide For” (Ref. 18).

The abbreviations “UAS” and “UAV” are also used in the draft specification, but in the following context: UA refers only to the Unmanned Aircraft, the airborne element of a larger Unmanned Aircraft System. In this usage, UA is synonymous with the abbreviation UAV, Unmanned Aerial Vehicle. UAS can include a Control Station (CS) and other elements. Some requirements in the draft specification have an implicit impact on the CS for manually controlled UA; time delay in response to manual control commands is one example. Work must be performed to fully define the requirements for the CS, but that work is not in the scope of this effort.

b. Mode of Operation

UA for which this draft specification is intended are likely to be operated autonomously for at least part of their intended missions. This is considered to be the biggest challenge to setting “handling qualities” requirements, as those requirements must of necessity look unlike most that are used in military and civil specifications for flying qualities or airworthiness of piloted aircraft. Instead of focusing on inner-loop, angular attitude/rate/acceleration control, the emphasis is more on outer-loop flight path control and regulation, areas not commonly considered to be high-priority for pilot-in-the-loop handling qualities. These areas are, however, critical for the completion of an autonomous mission.

c. Configuration

Most commercial UA, at least in the near future, are likely to be powered-lift for at least a portion of their normal operation. For missions as envisioned by commercial operators such as Amazon and Google, fixed wing airplanes will not do the job: package delivery or loitering in confined spaces requires the ability to hover and maneuver in those spaces. Variable-configuration platforms such as tilt-rotor or tilt-wing designs are not going to be needed if travel distances are kept reasonably small: there will be no advantage to converting between vertical-takeoff-and-landing (VTOL) and airplane modes if forward flight speed is not a priority. Longer distances will dictate wing-borne lift for speed and efficiency, so while the focus here is on VTOL UA, some provision has also been made for conventional aircraft, and for variable-configuration aircraft.

d. Operating Airspace

Small commercial UA may be expected to operate within the National Airspace System (NAS), but will most likely spend their lifetimes operating below NAS (≤ 500 ft), in urban, suburban, or rural environments. The consequence of this assumption is that much tighter control of position will be required to fly around obstacles (e.g., foliage, buildings, power lines, birds, other UA, etc.), and for more of the flight time in a typical mission, than is required to cruise at altitude with only a fraction of the flight spent near the ground.

e. Focus of the Requirements

Focus is limited to dynamic response, as opposed to design guidance or performance. The intent of this specification is verification of satisfactory flight characteristics of UA. In deference to the myriad of UA types already in operation, or in final design stages, we have made a conscious effort to avoid, to the extent possible, the adoption of any requirements that will inhibit or favor one design over another. While we intend this specification to be adopted and applied at the start of any new design process, we do not wish to direct the course of the design.

As UA handling qualities requirements are defined they should meet the following three criteria:

- 1) Validity – Validity implies that the metrics are associated with properties and characteristics that define the environment of interest. Specifically, in this application, valid metrics will differentiate between desirable, acceptable, and unacceptable handling qualities.
- 2) Selectivity - Selectivity demands that the metric differentiate sharply between “desirable” systems and those that are merely “acceptable.” This assures that there will be no question at all about selecting between “desirable” and “unacceptable” per se.
- 3) Ready Applicability – Ready applicability simply requires that the metric be easily and conveniently applied. Its expression in terms of readily available system parameters should be compact; procedures for its analytical evaluation should be convenient; and it should be easily measured in terms of either simulation models and/or empirical operations on the actual airplane and its systems.

f. Limitations to the Current Specification

There are two clear limitations to the content of the draft specification.

- 1) It deals almost entirely with quantitative requirements; development of Mission Task Elements (MTEs) has been a separate effort. Integration of the quantitative requirements with relevant MTEs will be done once both areas are better defined. Placeholders for tentative MTEs have been included to allow integration when they are available.
- 2) There are no values stated for any of the quantitative requirements. While the contract has provided for the assembly of a limited set of dynamic response characteristics, the data base required to set any of the limiting values defined in the specification simply does not yet exist. The hope is that, as this draft specification is disseminated among the user community, the necessary data will become available, and in the not-too-distant future a realistic and useful set of criterion values will be incorporated.

2. Format of the Draft Specification

There are two published and accepted flying qualities specifications in use today. Both, however, are written specifically for piloted aircraft, assuming the pilot is actually onboard the aircraft. Those specifications are:

- 1) MIL-STD-1797B, “Department of Defense Interface Standard, Flying Qualities of Piloted Aircraft” (Ref. 11), released in 2006. This document has a limited distribution, and while it is intended for almost any aircraft – including fixed wing airplanes, V/STOLs, and rotorcraft – the contents are geared almost

entirely toward fixed wings, and in particular fighter airplanes. In addition, the detailed requirements are now twenty years old, or more, and lack coverage for very highly-augmented or highly-automated airplanes. So the fact that access to MIL-STD-1797B is limited has had little impact on its application here; more, it is that the requirements are simply not very relevant.

2) ADS-33E-PRF, “Aeronautical Design Standard, Performance Specification, Handling Qualities Requirements for Military Rotorcraft” (Ref. 12), is a US Army-developed document for rotorcraft. This specification is much more aligned with the intent of the UA specification, and the format of the specification and of many of the detailed requirements meshes with the UA specification. In particular, ADS-33E-PRF incorporates both quantitative requirements and qualitative flight tasks (mission task elements, MTEs) and gives them equal weighting in the determination of handling qualities. We have adopted this philosophy in the development of the Appendix A specification – with the obvious exception that our MTEs will of necessity be more quantitative than qualitative in form, since there may not be a pilot in the loop to assess handling qualities. Unlike MIL-STD-1797B, the quantitative requirements in ADS-33E-PRF are suited for both unaugmented and highly-augmented aircraft, meaning they are amenable to the range of operation we wish to cover in the final UA specification. It is for these reasons that we have in general structured our draft UA specification in the format of ADS-33E-PRF.

In addition, it is recognized that many UAVs, and perhaps in the not-too-distant future, all UAVs, will be controlled entirely by onboard sensing and command systems. The implications for overall airworthiness – the ability, for example, to safely operate in civil airspace and execute guidance and navigation commands that comply with FAA requirements – are that more than just dynamic response requirements are needed. Fortunately, there is a document that has been beneficial in drafting airworthiness requirements into the draft UA specification. That document is SAE Aerospace Recommended Practice ARP94910, “Aerospace - Vehicle Management Systems - Flight Control Design, Installation and Test of, Military Unmanned Aircraft, Specification Guide For,” mentioned above (Ref. 18). A number of the proposed requirements in the draft UA specification are based on similar statements in ARP94910.

3. Stakeholder Involvement

Several versions of the draft specification were distributed to UAV stakeholders and interested parties. Comments and critiques were solicited; to the extent possible, all suggestions for improvement have been incorporated into the specification in Appendix A. Where the changes were deemed to be less relevant, mention of the suggested changes is included in the background discussion in the appendix.

The variety and detail of suggested changes that were received reflects the intense interest in this topic. Because the draft specification is just a start, and real data are needed to formalize the requirements, it was not possible to incorporate every suggested change or addition proposed by the reviewers. Those changes have not been discarded, by any means, and it is the intent of the authors of this report that the collected stakeholder comments be retained and revisited when sufficient real data, and sufficient funding, can be obtained.

Successful development of the final specification depends entirely on continued interaction with members of the UAV community. It is hoped that the draft specification will continue to evolve, and as it does, more inputs will be received from the user community.

4. Dynamic Scaling

Decades of criterial development based on piloted simulation and flight test evaluations were used to create the piloted handling qualities specifications and standards described herein. Thus, there is a strong desire to use this foundational work as a basis for establishing UA requirements. To this end, work is underway, including by UAS Stakeholders that have presented results at the workshops hosted as part of this program and elsewhere, to explore the use of dynamic scaling with existing handling qualities criteria

and mission task elements. Use of scaling methods was briefly explored as part of this program the results of which can be found in Appendix F.

The overall conclusion from these analyses is that the dynamics of UltraStick family of UAS, flown in this program as described in later sections of this report, is qualitatively very similar to the Cessna 172 aircraft. The mass properties scale well between the aircraft, and subsequently, modal frequencies and damping are shown to be qualitatively close under appropriate flight conditions. The Froude scaling process is also validated by scaling the UltraStick120 down by 66% and compared to the known dynamics of UltraStick25e. The second part of the analysis involved scaling in the opposite direction, where the dynamics of both UltraStick vehicles are scaled up to the dimensions of the Cessna 172 aircraft. This analysis was primarily carried out in order to evaluate the flying/handling qualities of UltraStick120 and 25e using standards and requirements established for Cessna-sized (Class I as described in Ref. 11) aircraft. The analysis shows that the UltraStick vehicles met or exceeded all Level 1 requirements in the longitudinal as well as lateral-directional axes.

This analysis (carried out for cruise – Category B as described in Ref. 11) can be extended to Category C flight conditions that include terminal flight conditions, landing and take-off. Further research using data from different UAS and manned aircraft can help establish Froude-scaling based analysis as an important step for evaluating handling qualities for small UAS.

5. Overview of Uncertainty Analysis Methods Applied to Handling Qualities

The entirety of this section is derived directly from Ref. 19, which documents previous work conducted by STI for NASA regarding the analysis of robust flutter boundaries.

Traditional handling qualities prediction uses a deterministic rigid body simulation model with parameters representing the “as designed” aircraft to calculate metrics such as Aircraft Bandwidth as a function of mission task (i.e., levels of precision and aggressiveness) to predict handling qualities. While not incorrect, outside of the simulation environment, nothing is exactly “as designed.” Flight control system command path and feedback path elements including nonlinearities all add uncertainty to the predicted handling qualities. Thus, handling qualities level boundaries become a confidence interval, rather than an absolute bound.

At its most basic level, the purpose of uncertainty analysis is the estimation of the “degree-of-confidence” of the output of a system or model based on known uncertainties in the inputs and system characteristics or model parameters. Input and parameter uncertainties are propagated through a model and the distribution of the model outputs constitute the uncertainty.

Traditional stochastic uncertainty analysis techniques require making multiple, and often many simulation runs. The number of required runs typically scales by a power law based on the number of inputs and parameters with defined uncertainty. Analysis quickly becomes time prohibitive for all but the shortest simulation runs. Therefore, goals are to produce efficient, yet still accurate, models and to reduce the number of required simulation runs. This is accomplished with the use of Design of Experiments/Response Surface Methods and Robust Stability/ μ -analysis. The widely accepted Monte Carlo approach is also utilized as an effective, but brute force method. Overview descriptions of each uncertainty analysis method follow.

a. Traditional Stochastic Monte Carlo Methods

Monte Carlo methods describe a class of computational algorithms that use repeated random sampling to compute results. These methods primarily involve simulating a physical system repeatedly while randomly changing parameters that the system is dependent on for each simulation. Results are collected and can be analyzed statistically to determine means, standard deviations, maxima, minima and other statistical parameters. With several simulation runs, the results of Monte Carlo approach a continuous

surface. The optimal number of runs is that which is a minimum number but produces relatively identical statistical results if more runs are made. By this manner, that minimal amount of runs represents the results as if infinite runs were made. Monte Carlo analysis is used when it is impossible or infeasible to compute exact results with a deterministic approach.

Monte Carlo methods provide a reliable means to analyze problems that are concerned with uncertainty. Uncertain parameters of a physical system are randomly sampled over several runs and the results represent system behavior subject to these uncertainties. Sensitivity to the uncertain parameters is realized by the statistical analysis of the Monte Carlo results. The drawback of these methods is the large amount of runs can be computationally burdensome. If the physical system being modeled is complex and takes a relatively large amount of computational time to run, this burden is amplified by the large amount of simulation runs required to obtain meaningful statistical results.

b. Design of Experiments and Response Surface Methods (DOE/RSM)

Any system can be described as an input/output relationship. The outputs of a system are dependent on the system inputs and independent parameters. With highly complex or empirical systems that feature large amounts of uncertainty, the input/output relationship of the system in question may be difficult to determine. Response Surface Methods (RSM) are used as an accurate approximation to characterize a system's outputs based on variations of the system's inputs and parameters. The Design of Experiments (DOE) /RSM technique is used to determine an accurate approximate model of a system with minimal sets of input required. The resulting analytical model described by the Response Surface Equation (RSE) is, in most cases, in a simpler form (usually a polynomial) than the original model and is thus more efficient while retaining a level of accuracy.

DOE (Ref. 20) and RSM (Ref. 21) are used to significantly reduce the number of full model simulation runs. While Monte Carlo generates random values within the range of input and parameter values, DOE is used to purposely select input and parameter values in order to maximize the information available from the output.

RSEs are used to characterize a system's outputs (referred to as "targets") based on variations in its inputs and parameters (referred to as "factors"). The DOE/RSM technique chooses a RSE that is appropriate for characterizing a particular system, and then designs a set of experiments that will yield maximal information for the regression analysis to fit the RSE to the data. This is the fundamental difference between DOE/RSM and Monte Carlo: Monte Carlo makes no assumption about the relationship between the model output and its inputs/parameters, while DOE/RSM does. The down side for DOE/RSM is when the form of the RSE is poorly selected, it yields poor or misleading information. The advantage is that, with the properly selected RSE, the number of full model runs required is cut by an order of magnitude or more.

c. μ -analysis Methods

μ -analysis can be used to determine a mathematically guaranteed robust stability point (e.g., handling qualities boundary) subject to a specified bounded uncertainty. Robust stability and μ -analysis deal with the stability of the interconnections of stable operators. The *Small Gain Theorem* serves as a basis for the determination of stability of the interconnections of stable operators. The small gain theorem states that a closed-loop feedback system of stable operators (Figure 4) is internally stable if the loop gain of those operators is stable and bounded by unity (Ref. 22).

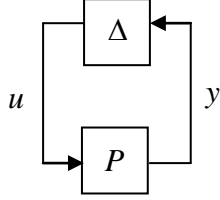


Figure 4: Closed-Loop Feedback System of Stable Operators

In Figure 4, the operators P and Δ can be represented by stable transfer function operators. By direct use of the small gain theorem and properties of the norm it can be shown that the interconnection is robustly stable if Eq. (1) is satisfied.

$$\|P\|_\infty < \|\Delta\|_\infty^{-1} \quad (1)$$

In the above equation, $\|\cdot\|_\infty$ denotes the infinity norm. Robust stability is analyzed with respect to a set of perturbations. The stability of the interconnection involves a known nominal plant and unknown bounded perturbations (or uncertainties) to that plant. Figure 4 represents a general feedback interconnection of stable operators. Without loss of generality, the known nominal plant dynamics can be represented by P and the unknown perturbations to that plant can be represented by Δ . The true plant is assumed to be a known nominal plant value with perturbations that represent the plant's uncertainty. The small gain theorem can be used to analyze the stability of the interconnection if the operators are stable and bounded by unity. Although the small gain theorem guarantees stability of the system, it is overly restrictive since the structure of the uncertainty is not considered. The Δ block, representing the uncertainty in the nominal plant, has a known structure and given this knowledge of the uncertainty structure, a less conservative measure of the robust stability of the system, which is based on the small gain theorem, can be formulated. This referred to as μ : the structured singular value (Eq. (2)).

$$\mu(P) = \frac{1}{\min_{\Delta \in \Delta} \{\bar{\sigma}(\Delta) : \det(I - P\Delta) = 0\}} \quad (2)$$

In the above equation, $\bar{\sigma}$ represents the maximum singular value and I is the identity matrix. Equation (2) is an exact measure of robust stability for any system with a known structured uncertainty since it only considers uncertainty of the form defined by Δ , which represents the bounded space of all possible uncertainty descriptions under the known structure. Given the system in Figure 4, the plant P is robustly stable with respect to the set Δ if and only if Eq. (3) is satisfied.

$$\mu(P) < \|\Delta\|_\infty^{-1} \quad (3)$$

μ (Eq. (3)) is equivalent to the small gain theorem (Eq. (1)) if the uncertainty is unstructured. One problem with μ is that it is often difficult to compute. Closed form solutions exist for only a small number of uncertainty structures. Due to this, upper and lower bounds are computed to represent worst and best case μ values for generalized uncertainty structures.

It is necessary to utilize the upper bound on μ as a basis for analyzing the smallest Δ matrix that drives the interconnection unstable since the upper bound is guaranteed. The lower bound is not guaranteed and may produce a Δ matrix that drives the plant unstable. In practice, computing upper and lower μ bounds is an optimization problem and is described extensively in public domain literature (Refs. 23, 24, and 25).

E. UAS HANDLING QUALITIES PROCESS DEMONSTRATION

1. Fixed Wing UAS

a. University of Minnesota Laboratory and Flight Test Facilities

1. Aircraft Description

The UAS laboratory at UMN maintains the UltraStick series of fixed wing UAS to serve as testbeds in several ongoing research projects such as control law design, navigation and guidance and fault detection, isolation and reconfiguration (Ref. 26). The series consists of the UltraStick120, UltraStick25e and the UltraStick mini. The laboratory also supports UAS related research of other organizations by providing flight-testing services on these testbeds. Two vehicles were flown as a part of this test campaign, the UltraStick25e and the UltraStick120 and are shown in Figure 5. The flight data shown and discussed here are from the UltraStick120 only. While only the UltraStick120 results are reported on here, this vehicle's design is widely used in the sUAS industry and is representative of a broad category of vehicles.



Figure 5: UltraStick120 (center) and UltraStick25e Aircraft

The UltraStick120 was a commercially available, RC hobbyist airframe. The UMN UAS Lab converts these airframes into UAS platforms for research. Relevant size and performance values for the UltraStick120 are included in Table 1.

Table 1: UltraStick120 Aircraft Parameters

Wingspan	1.92 m
Chord	0.43 m
Length	1.73 m
Airframe Weight	6.0 kg
Max Weight	10.0 kg
Cruise speed	23 m/s (typical)
Stall speed at Max Weight	13 m/s
Airspeed range	10-41 m/s

The aircraft is equipped with a commercial RC hobbyist control system (propulsion system, batteries, receiver, and servos) for manual control as well as additional systems for data collection and autonomous flight modes. A system-level design has been implemented that allows the pilot to take manual control of

the aircraft. Further, the manual control system failsafe defaults to a descending, power-off spiral to keep the aircraft contained within the test range.

It is powered by an electric motor and has removable wings for transport. The UltraStick120 has a conventional horizontal and vertical tail with rudder and elevator control surfaces. The aircraft has a symmetric airfoil wing with aileron and flap control surfaces. The rudder and elevator are actuated by Hitec HS5245MG servos. The flaps and ailerons use Hitec HS5625MG servos. The aircraft is propelled by a 1900W Actro 40-4 brushless electric motor with a Graupner 14 x 9.5 folding propeller. Power for the motor comes from two 5000mAh 5-cell lithium polymer batteries connected in series. The servos are powered by a separate 1350 mAh 3-cell lithium polymer battery. The main internal payload bay is located in the fuselage, directly under the wing; additional payloads may be accommodated in the aft fuselage or externally. The UltraStick120 aircraft has space aft of the avionics bay for additional sensors or payloads. sUAS with these general specifications and configuration are typical of the sUAS community at large

2. Goldy3 Flight Control System

The Goldy3 flight control system was designed to integrate with a RC hobbyist control system and allow complete autopilot functionality. The system was developed in house by the UMN UAV Lab. The system allows for data collection and autonomous flight modes. A system-level design has been implemented that allows the pilot to take manual control of the aircraft via a programmed micro-controller. A functional diagram of this system is in Figure 6.

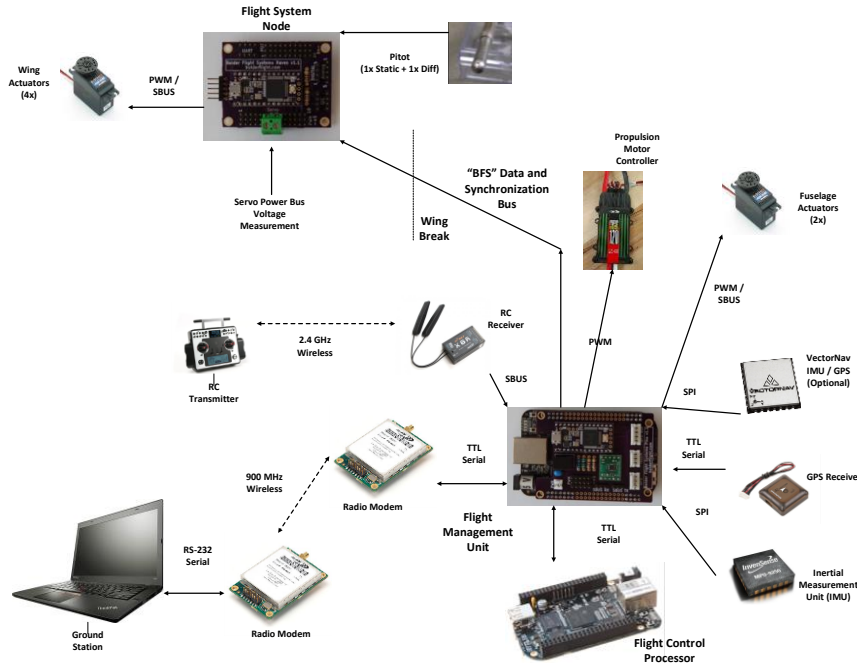


Figure 6: Avionics Functional Diagram, Based on UltraStick25e Installation

Commands are sent to the aircraft via a hobbyist RC transmitter and receiver. The receiver sends commands and communicates with the FMU via a SBUS-2 protocol. The FMU controls the “safety/auto” switch; in “safety” mode, commands from the receiver are forwarded to the servo actuators. In “auto” mode, commands from the flight computer are sent to the servo actuators. The flight computer receives flight data from sensors including GPS, Inertial Measurement Unit (IMU), and pressure transducers. Data from the flight computer is downlinked through a radio modem to a ground control station where researchers can monitor its operation.

At any time, the pilot can revert to the “safety” mode via the “safety/auto” switch. Additionally, failsafe commands are set in the RC receiver and FMU such that in the event of a lost link, the receiver switches the aircraft to “safety” mode, cuts power to the motor, and puts the aircraft in the previously mentioned descending spiral.

3. System Architecture

For system identification analysis, the system architecture shown in Figure 7 was used. The bare-airframe (or plant) is noted by A/C, the actuators are identified by ACT, and any flight control system or feedback compensators are defined by C and FB respectively. Each of A/C, ACT, C, and FB are in general multi-input-multi-output systems. The pilot commands are defined by the vector r and denote commanded aircraft states (e.g., pitch-command or roll-command). In some cases, the computer may command some of the r inputs (e.g., for velocity or speed-command inputs). The commands to the actuators are defined by the vector u . The vector δ defines the bare-airframe control surface deflections. Both u and δ also include the throttle command and input. The u_{ex} signal is the location where computer-commanded input excitations are applied.

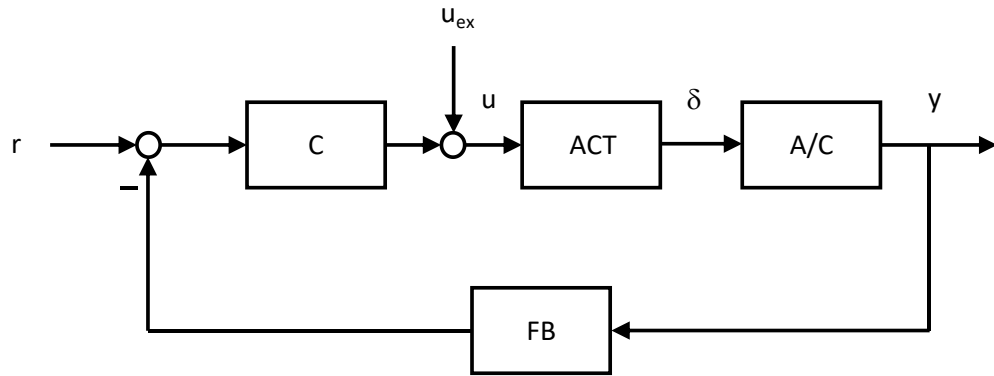


Figure 7: System Architecture

4. University of Minnesota Flight Test Facilities

The flight test facilities, shown in Figure 8, consist of the UAV laboratory on the UMN campus and the airfield located at the UMore Park Test Range. The aircraft maintenance and pre-flight checkouts (simulation-in-the-loop, hardware-in-the-loop, etc.) occur in the UAV laboratory. The flight tests took place at the UMore Park Test Range near Rosemount, MN. The Test Range is located on sparsely populated agriculture fields owned by the UMN. Flights are conducted year-round. A winter flight is shown in Figure 8.

The UMore Park Test Range is located within Class G airspace. The test aircraft must remain within the area centered at $44^{\circ} 43'32.71''N$ and $93^{\circ} 4'44.49''W$, with a radius of 0.28 NM and a ceiling of 400 feet Above Ground Level (AGL). All flights are coordinated with the Rosemount Research and Outreach Center Manager. In addition, the University of Minnesota UAV lab has obtained the proper Certificates of Authorization (COAs) for legal operation of UAS flights at the UMore Test Range. Non-participants are kept clear of this zone during operations. The dimensions comply with the 1-mile lateral and 400 foot ceiling limits and were created to avoid structures and major roadways while staying within direct line of sight of the operations crew. Restriction to the flight research zone minimizes risk to non-participants. The Operations Lead, Pilot, and Observer ensure that the aircraft remains within the flight research zone and will abort the mission if there is a risk of exiting the area. Failsafes on the aircraft ensure that the aircraft will remain in the test area in the event of link loss. Launch and recovery are conducted from a 900 foot by 60 foot turf runway aligned in an East-West direction. A right pattern is used when

launching/recovering in an east-bound direction and a left pattern is used when launching/recovering in a west-bound direction. These patterns are used to avoid overflying the operations crew.



Figure 8: UAS Flight Test Facilities at the University of Minnesota

b. Model-based Prediction of Handling Qualities

Dynamic models that can provide complete system output to command input responses are used to predict handling qualities as illustrated in Figure 9. A description of the UltraStick120 model provided by UMN is included next.

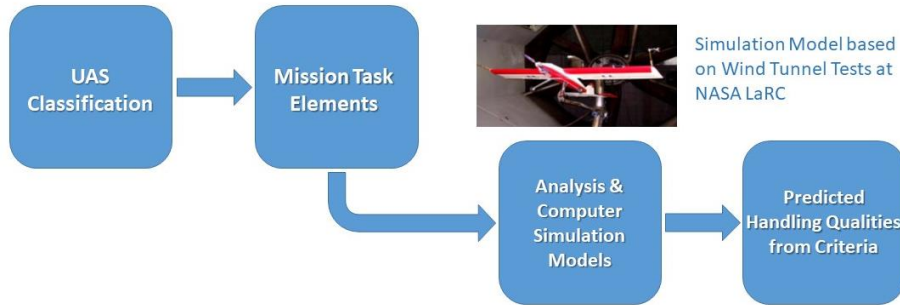


Figure 9: Predicted Handling Qualities

1. UltraStick120 Model

The UMN laboratory provided MATLAB/Simulink-based (Ref. 27) simulation models for the UltraStick series. These models are typically used to obtain linear state-space models at different trim conditions, to enable control/navigation and other function software design, and to carry out simulations in closed loop with the developed software before actual flight-testing. Depending on the UltraStick UAS simulated, these models have nonlinear rigid body dynamics coupled with either a linear, coefficient-based aerodynamic model or a look-up-table-based nonlinear aerodynamic model. Data for the look-up table have been obtained from a wind tunnel test of the UltraStick mini and other additional and extensive testing of the UltraStick120.

The Matlab/Simulink UAS simulation package provided by UMN is capable of modeling 3 different airframes: 1) UltraStick120, 2) UltraStick25e and 3) miniMUTT (flex wing UAS). The simulation package consists of different Simulink models and accompanying Matlab scripts, .mat files and Simulink Library blocks. The Library blocks are key to maintaining consistency across the different models and making it easier to modify or swap different blocks.

The UltraStick120 bare airframe models feature standard aircraft inputs, states, and outputs. The inputs include throttle, elevator, rudder, left/right aileron, and left/right flaps. The states include the attitudes, rates, velocities of the vehicle, and Earth relative position. The outputs include the body attitudes, rates, accelerations, airspeed, angle of attack, flight path angle, sideslip, and altitude.

A simple first-order model is used for the elevator, aileron, rudder, and flap actuator control surfaces. The throttle is non-dimensional and limited to 0-1. The original actuators models for each control surface are given in Table 2.

Table 2: Actuator Models

Elevator	Aileron	Rudder
$\frac{\delta_e}{\delta_{ec}} = \frac{50.27}{s + 50.27} e^{-0.05s}$	$\frac{\delta_a}{\delta_{ac}} = \frac{50.27}{s + 50.27} e^{-0.05s}$	$\frac{\delta_r}{\delta_{rc}} = \frac{50.27}{s + 50.27} e^{-0.05s}$

The aircraft controller implements a simple pitch and bank attitude tracker. The pitch attitude tracker is shown in Figure 10. The internals of the Pitch Tracker block are shown in Figure 11. The Roll Tracker block is an exact duplicate, but with unique gains. A yaw damper was included as a simple washout filter in the yaw rate to rudder feedback loop. As flown with the UltraStick120, the pitch axis featured an attitude command system with speed hold, while the roll axis featured an attitude command, and the yaw axis featured a rate command system.

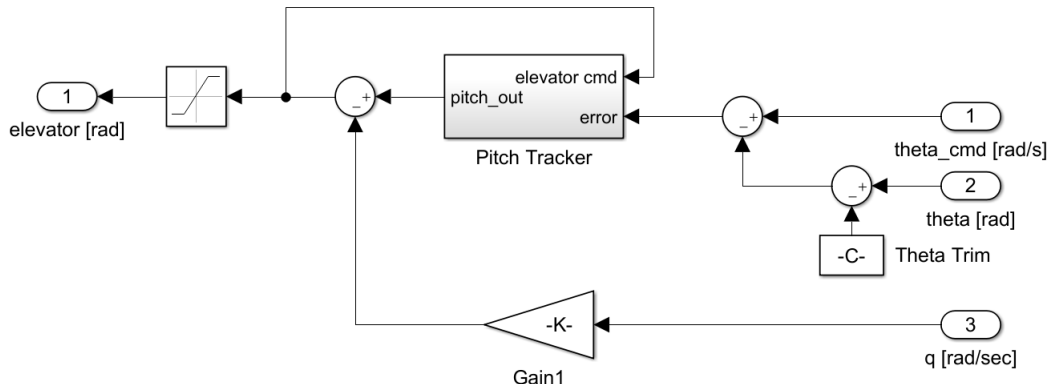


Figure 10: Pitch Attitude Tracker

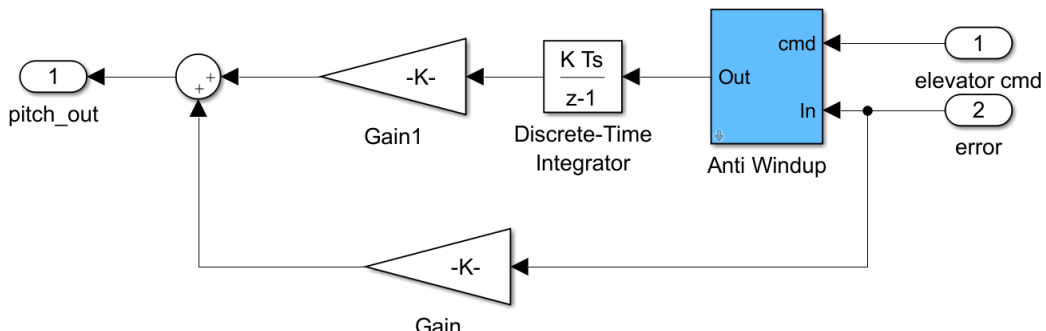


Figure 11: Representative Tracker Block

2. Exemplar Model Frequency Responses

The UltraStick120 model provided by the University of Minnesota was exercised to generate the pitch attitude to pitch attitude command frequency responses shown in Figure 12 for both the cruise and approach flight conditions. In the figure the solid lines represent the magnitude response, while the dashed lines represent the phase response with colors selected to match the Nominal case (blue), Aft CG case (black), and Added Time Delay case (red) as indicated in the plot legend. The magnitude responses of all three cases indicate the signature of an attitude command system with zero dB magnitude at low frequencies. The added time delay cruise case indicates reduced closed-loop stability via the lightly damped magnitude response peak and the dramatic phase roll off. This characteristic is present, but less pronounced in the approach case.

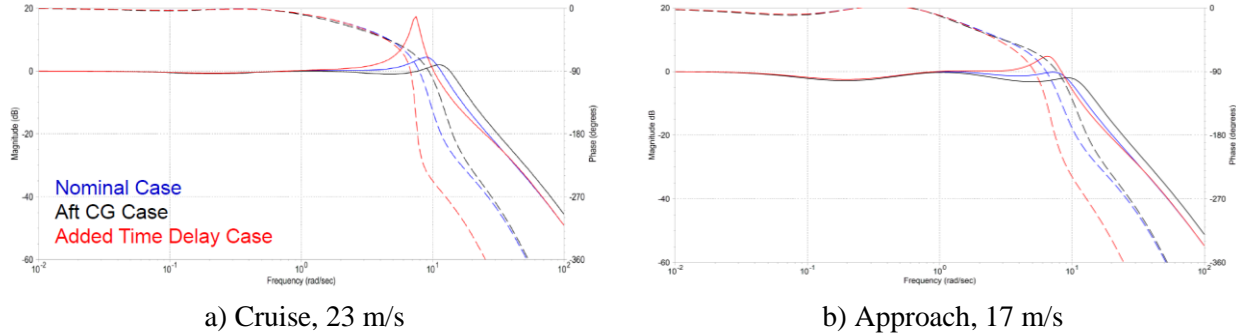


Figure 12: UltraStick120 Model Pitch Attitude to Attitude Command (θ/θ_c) Frequency Responses

3. Exemplar Handling Qualities Metric – Aircraft Bandwidth

The Aircraft Bandwidth criteria, measured from a frequency response (Bode plot) of attitude to control input (position or force), were developed for the evaluation of handling qualities of highly-augmented airplanes where more conventional criteria could not be easily applied (Ref. 28). These criteria are included in MIL-STD-1797A and formed the basis of the US Army's rotorcraft airworthiness standard ADS-33E-PRF. The fixed wing requirements for handling qualities levels as published in MIL-STD-1797A have been found to be much too stringent and have been adjusted significantly, especially given the addition of a requirement on pitch rate overshoot. Furthermore, the requirements have also been adapted to the prediction of PIO susceptibility (Ref. 29), as will be documented shortly.

The fundamental theory behind “Aircraft Bandwidth” – which is not the “classic bandwidth” that is used in other control systems applications – is that the principal stability characteristics of the aircraft can be described by the frequency response of angular attitude for control inputs. This is true, at least, for continuous closed-loop control of attitude by the pilot, and when attitude is used as an inner loop to generate changes in load factor or flight path. The concept is that the aircraft should have good inherent stability, whether from basic design or by augmentation with a SAS. The lower this inherent stability, the more stability the pilot must provide to perform required tasks, resulting in increasing workload, degraded performance, poor flying qualities, and ultimately, PIO.

There are three measures in the criteria that capture the basic pitch attitude characteristics of the aircraft (Figure 13). The first is the “phase margin Bandwidth frequency,” the lowest frequency for which there is a phase margin of 45 degrees. The higher this frequency, the better attitude follows control inputs: if phase margin is 180 degrees, that is, phase angle is zero, then output follows input exactly. At the frequency for 0 degrees phase margin – the “neutral-stability” or 180-degree frequency – attitude is exactly out of phase with inputs. If the phase margin Bandwidth frequency is very low, the pilot must generate lead to improve the overall response of the pilot-plus-aircraft system in order to do a task.

The second measure is the “gain margin Bandwidth frequency,” and it is basically the same type of measure, except it determines the change in effective-aircraft dynamics the pilot will encounter if closed-loop gain is increased by a factor of 2 (6 decibels).

The third measure, inappropriately named “Phase Delay,” is really a measure of how rapidly the phase angle of attitude/control inputs degrades at high frequencies. The assumption is that, if the pilot should find it necessary to operate at higher frequencies – which can be done with closed-loop stability only if the pilot generates lead compensation – a gradually-degrading phase curve is much better than a rapidly-degrading one.

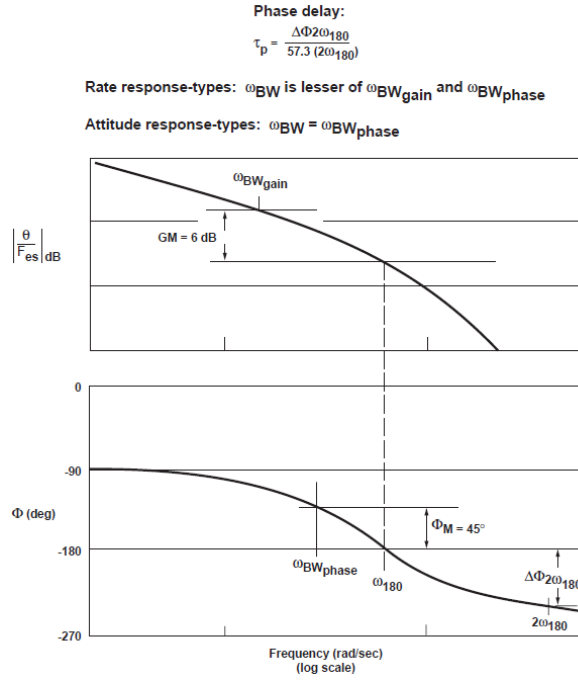


Figure 13: Parameters for Attitude Bandwidth and Phase Delay

There are aircraft where PIO is unlikely on the basis of the attitude Bandwidth characteristics alone. In some instances, high pitch rate overshoot is a contributor, and limits are placed on the frequency-domain-based metric, $\Delta G(q)$ (Figure 14). In others inadequate flight path control is the culprit, so limits are placed on flight path Bandwidth frequency, $\omega_{BW\gamma}$.

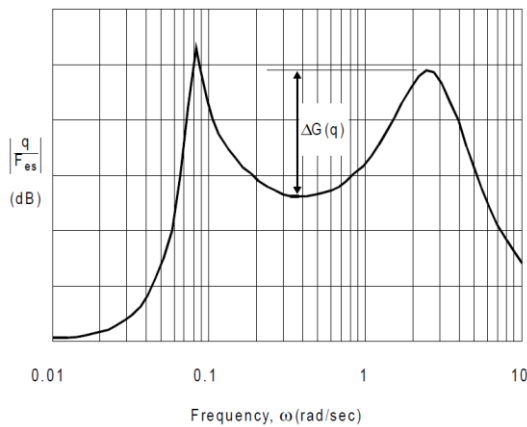
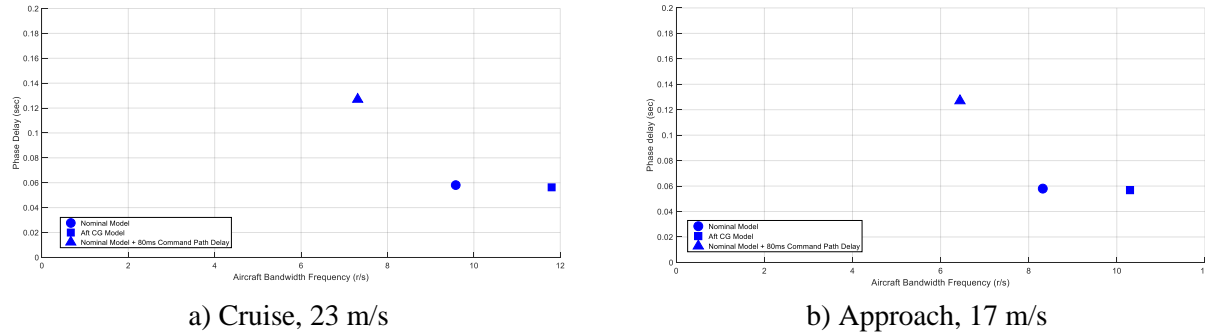


Figure 14. Pitch Rate Overshoot Parameter

4. Predicted Aircraft Bandwidth Parameters from UltraStick120 Model

The UltraStick120 model frequency responses were used to identify the Aircraft Bandwidth parameters for the three configurations. The resulting phase delay versus bandwidth frequency plots are shown in Figure 15. As indicated in Figure 13, for an attitude command system, the bandwidth frequency is the measured phase bandwidth frequency. All three configurations feature higher bandwidth frequencies than traditionally seen with piloted aircraft – a dynamic scaling effect as discussed in Appendix F. The phase delay of the Added Time Delay case at both flight conditions is approaching a region where impact on mission performance could be a concern. There is an overall decrease in bandwidth frequencies for all three cases in the approach flight condition.



a) Cruise, 23 m/s

b) Approach, 17 m/s

Figure 15: Aircraft Bandwidth Model Parameters for the UltraStick120

c. System Identification Flight Tests

A series of system identification flights were conducted to revise the vehicle models based on flight test data. As illustrated in Figure 16, this also provides the means to update the predicted handling qualities using the revised vehicle models.

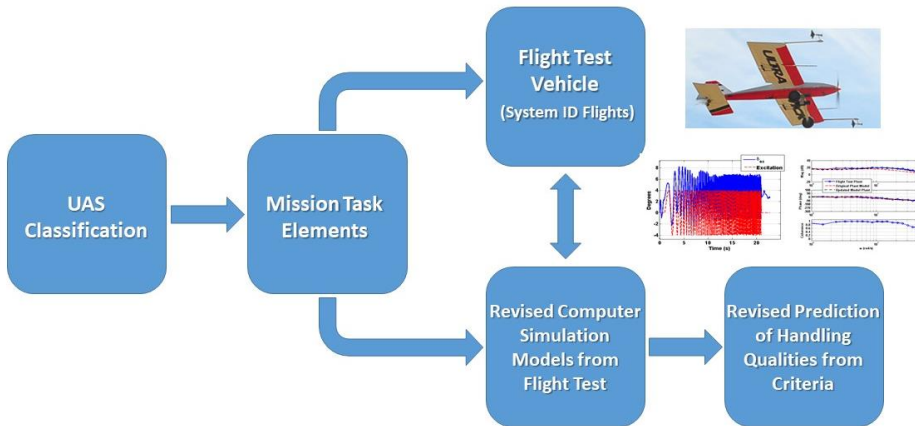


Figure 16: Predicted Handling Qualities from Models Revised from Flight Test

1. Test Description

A nominal baseline configuration and two additional off-nominal configurations were flown. All configurations included the same flight control system feedback augmentation response types as identified above. The off-nominal configurations were: 1) added delay and 2) a configuration with an unfavorable c.g. shift. Two airspeed flight conditions were flown. The primary cruise airspeed for all evaluation tasks was 23 m/s and the primary approach airspeed for all evaluation tasks was 17 m/s. The primary altitude for all cruise and approach evaluation tasks was approximately 50 m. The defined

“approach” condition is not a true approach condition because it was flown at a constant altitude, but at a lower airspeed, with 50% flap deflections to reflect a true approach condition. Maintaining a constant altitude for the defined approach condition was done to simplify and minimize risk for system identification flight test points and to preserve the desired test conditions. No specific flight patterns were required, other than to remain in visual line of sight. The vehicle was flown in circuits around the test area with 700 m straight legs and 45° turns at the constant 50 m altitude. All evaluated test conditions were flown by the on-board flight computer, emulating an autonomous or semi-autonomous system. The test inputs were preprogrammed into the flight computer and initiated by the remote UAS operator. The operator limited his inputs to small, low frequency commands that were intended to maintain the test condition. A summary of the system identification flights is provided in Table 3.

Table 3: UltraStick120 System Identification Flight Test Run Log

Flight	Flight Type	Speed	Condition		
03	SysID	23 m/s	Cruise	Normal CG	No Added Delay
04	SysID	17 m/s	Approach	Normal CG	No Added Delay
05	SysID	23 m/s	Cruise	Aft CG	No Added Delay
06	SysID	17 m/s	Approach	Aft CG	No Added Delay
07	SysID	23 m/s	Cruise	Normal	Added Delay*
08	SysID	23 m/s	Cruise	Normal	Added Delay*
09	SysID	23 m/s	Cruise	Normal	Added Delay*
10	SysID	23 m/s	Cruise	Normal CG	Extra Delay 80ms
11	SysID	17 m/s	Approach	Normal CG	Extra Delay 80ms

***Added Delay** – In these flights, the added delay was placed in the feedback path rather than command path.

All system identification (SysID) flights flew the same test card, which can be seen in detail in Table 20 of Appendix D, but generally the test excitation signals described next were used.

2. Excitation Signals

This section provides descriptions of each of the input profiles and includes sample time histories of both the excitation command, the shaped command that was sent to the actuator, and the attitude responses. The profiles were uniform across each axis. Here, pitch axis examples are shown. These examples represent the computer-generated inputs and the resulting vehicle responses. Each of the sample commands includes both a plot of the original excitation command u_{ex} (red dashed line), and the resultant shaped surface command u (solid blue line).

Multi-Sine: The orthogonal multi-sine (OMS) (Ref. 30) input profiles are mutually orthogonal in the time and frequency domains and completely uncorrelated. These OMS were applied to each axis independently, the elevator and aileron in combination, and all three axes in combination, elevator, aileron and rudder. Each OMS was 20 seconds long, had a 4 deg amplitude and covered a frequency range from 1-50 rad/s. Example pitch command and attitude responses are provided in Figure 17.

Frequency Sweep: The frequency sweep input excitation was designed to be 20 seconds in duration, have an amplitude of 4 deg, and cover a frequency range of 1 to 50 rad/s. This was applied to each axis independently, and the aileron and elevator in combination. For the input to the elevator and aileron in combination, the pitch excitation had increasing frequencies over time, while the roll excitation started at

high frequency and decreased to the lower frequency limit over time. This provided separation in the frequencies between the axes. Example pitch command and attitude responses are given in Figure 18.

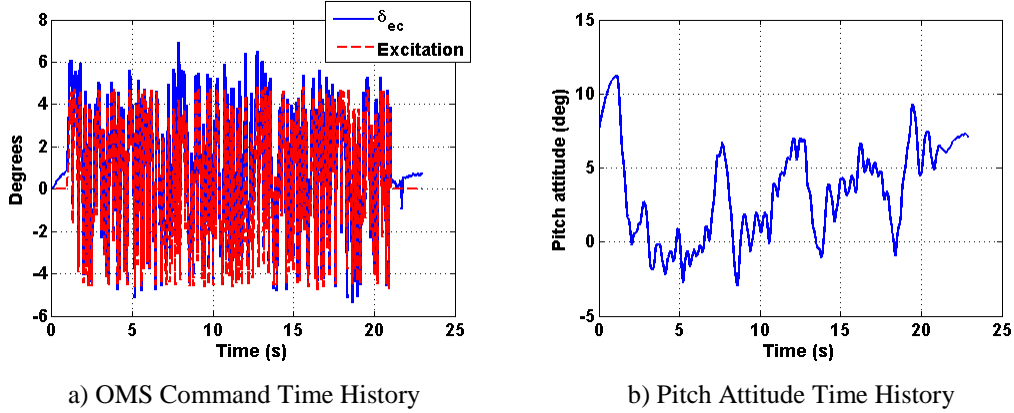


Figure 17: Example Orthogonal Multi-Sine Input and Resulting Aircraft Output

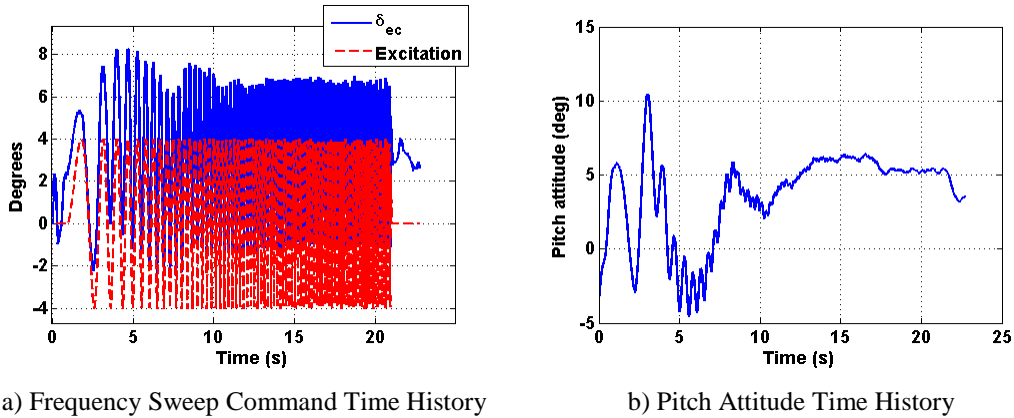
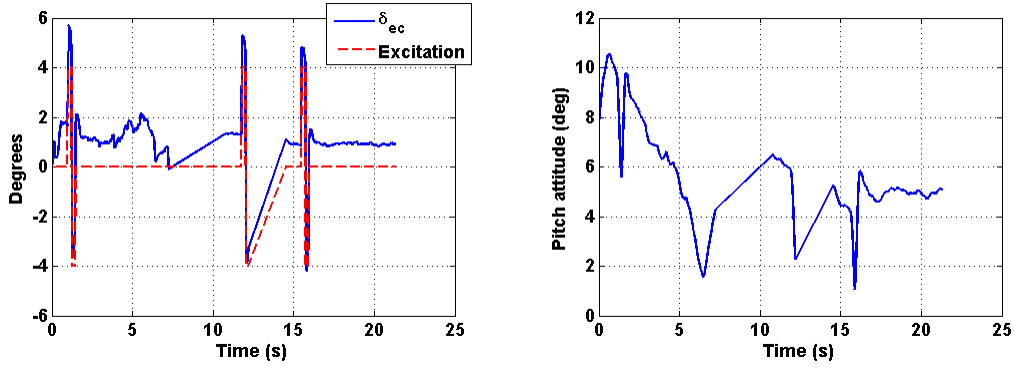


Figure 18: Example Frequency Sweep Input and Resulting Aircraft Output

Doublet: The doublet excitation profile was designed to have a 4 deg amplitude. The pulse width varied based upon the axis of the input. For every axis, the pulse width (half of the total doublet width) was designed to target a particular frequency through the following relation: $0.7/(2*\text{target frequency})$. The target frequency is in Hz. For pitch, the target frequency was the short period mode, estimated at 1.51 Hz. For the aileron and rudder doublet, the Dutch roll frequency was targeted and estimated to be 0.65 Hz. Example pitch command and attitude responses are given in Figure 19.

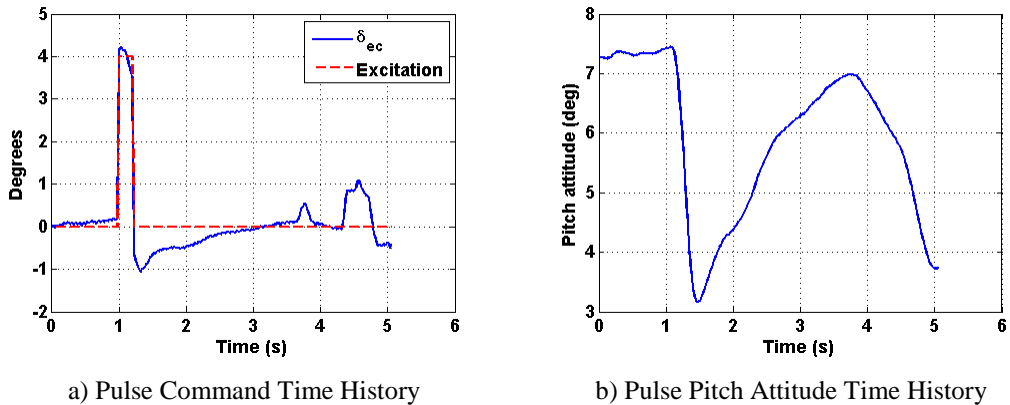
Pulse: The pulse input was designed to have a 4 deg amplitude. The pulse width was defined in the same manner as the doublet. Example pitch command and attitude responses are given in Figure 20.

3-2-1-1: The 3-2-1-1 input is a set of pulses of varied widths. A base width, the “1” in 3-2-1-1, is defined in the same manner as the pulse and doublet widths, based on the short period and Dutch roll frequencies for the pitch and roll axis, respectively. The “2” and “3” are then double and triple the base width pulses. For example, if the base width was 1 second, the first pulse would be 3 seconds wide, the next 2 seconds wide, followed by two pulses of 1 second each. Each new pulse reverses direction from the prior one. Example pitch command and attitude responses are given in Figure 21.



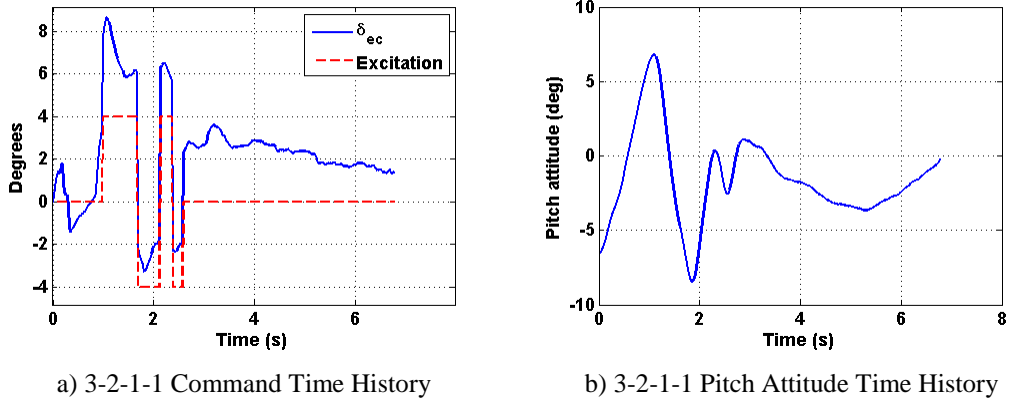
a) Doublet Command Time History

b) Doublet Pitch Attitude Time History

Figure 19: Example Doublet Input and Resulting Aircraft Output

a) Pulse Command Time History

b) Pulse Pitch Attitude Time History

Figure 20: Example Pulse Input and Resulting Aircraft Output

a) 3-2-1-1 Command Time History

b) 3-2-1-1 Pitch Attitude Time History

Figure 21: Example 3-2-1-1 Input and Resulting Aircraft Output

d. Model Revisions Based on Flight Test Results

The model update process is a key component of any handling qualities assessment program, manned or otherwise. As accurate as models can be, they are only representations of the true flight vehicle. The process defined below was conducted to both validate and update, if required, the existing analytical models, based upon the newly collected data. The identification of each set of data was performed using STI's FREquency Domain Analysis (FREDA) software (Ref. 31). The flight test data in this section are

from a baseline configuration flight test conducted in straight and level flight, 23 m/s airspeed and 100m altitude. The UltraStick120 model used in the comparison was trimmed at these flight conditions. Using the system identification flight test results, the revised models based on the analysis described above were used to update the handling qualities parameter predictions as illustrated in Figure 15.

1. Revised Control Surface Actuator Models

The following process was used to modify and update the actuator dynamic models:

- Compare the frequency response identified from the flight test data of the actuator (actuator command to actuator position) with the frequency response of the actuator model, a 1st order transfer function with added delay. The magnitude response was matched first by modifying the inverse time constant of the actuator model until a suitable overlay of the identified data was found. This also included adjustments to the actuator gain as well.
- The phase response was then modified by adding delay to the transfer function in the form of e^{-st} where t is the added delay. With the phase response matched, the flight data and the actuator model were compared once again to ensure a desired fit was found.

The adjustments to the elevator actuator model are shown in Figure 22. The updated elevator transfer function is also shown.

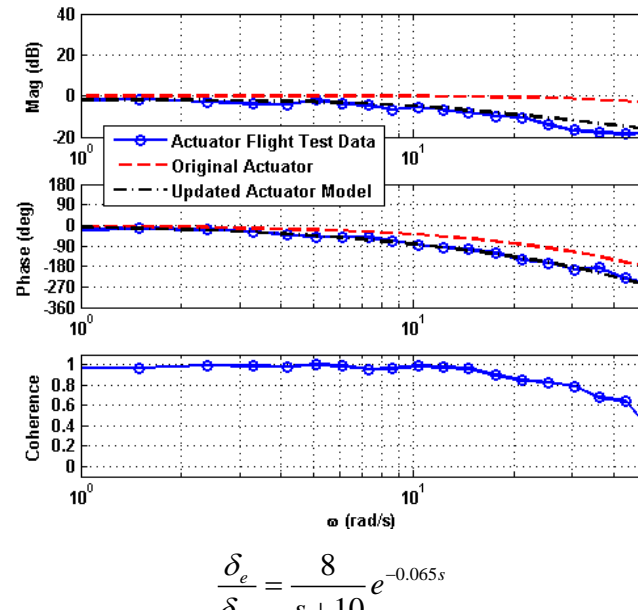


Figure 22: Original and Updated Elevator Actuator Models Compared with Flight Test

2. Revised Bare Airframe Dynamics

The process for updating the bare airframe dynamics of the UltraStick120 was as follows:

- Compare the frequency response identified from the flight test data with the original UltraStick120 model.
- The bare airframe dynamics were identified from the flight test data using the following input/output time histories:
 - Pitch: Input – Measured elevator actuator position; Output – Measured pitch rate

- Roll: Input – Measured aileron actuator position; Output – Measured roll rate
- Yaw: Input – Measured rudder actuator position; Output – Measured yaw rate
- Identify any model discrepancies relative to the flight test data and adjust the modal parameters in each axis as appropriate to achieve an improved match to the flight test data. Adjust the model gain as required. The relevant modal parameters are discussed below.

For the longitudinal axis, the phugoid and short period frequency and damping ratio were considered for adjustment though most conditions only required adjustments to the short period. For the lateral-directional axis, the roll mode and the Dutch roll frequency and damping were considered for adjustment. Most lateral-directional cases only required adjustments to the roll mode.

The changes in the bare airframe model were made to the pitch rate to elevator (q/δ_e) transfer function. A comparison of the original plant model, new plant model, and the flight test frequency response generated from a chirp input is shown in Figure 23a. Note that the gain of new model represents an increase of 1.5 times the original model value. Only the short period dynamics were altered, increasing the frequency slightly, while reducing the damping. The response of the longitudinal system, including aircraft and actuator dynamics is shown in Figure 23b.

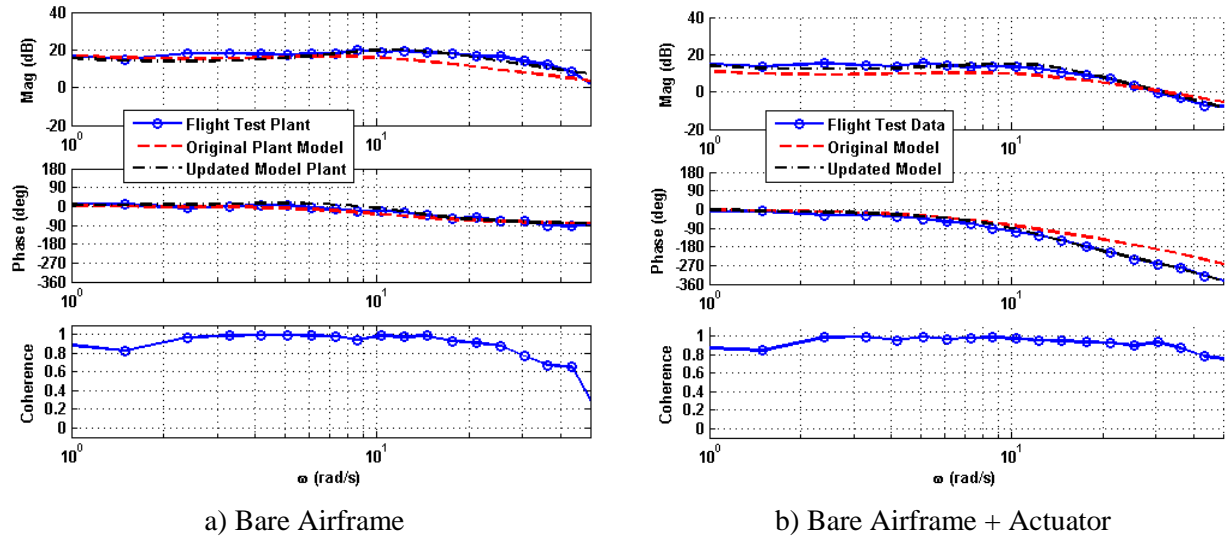


Figure 23: Original and Updated q/δ_e Responses Compared with Flight Test

To validate the updated model, simulated time history responses of the model were compared against flight test responses generated from short duration inputs for the same test condition. These short duration inputs were the same doublets, pulses, and 3-2-1-1s described above. The actual flight test inputs were used to generate the model responses, so a true one-to-one comparison could be performed.

The short duration responses are shown in Figure 24. Two sets of data dropouts from ~7-11 seconds and ~12-15 seconds region affected the later portion of the doublet maneuver, Figure 24a. Even in the presence of these dropouts, the model response for the doublet excitation exhibited a close match to the excitation flight data. The pulse and 3-2-1-1 excitation response demonstrated a good model fit as well; however, there is a modest amount of amplitude mismatch. This mismatch, which occurs for the lower frequency inputs, is likely due to system nonlinearities, such as actuator free play. As a whole, these responses validate the model updates made above and the process used to generate the model revisions.

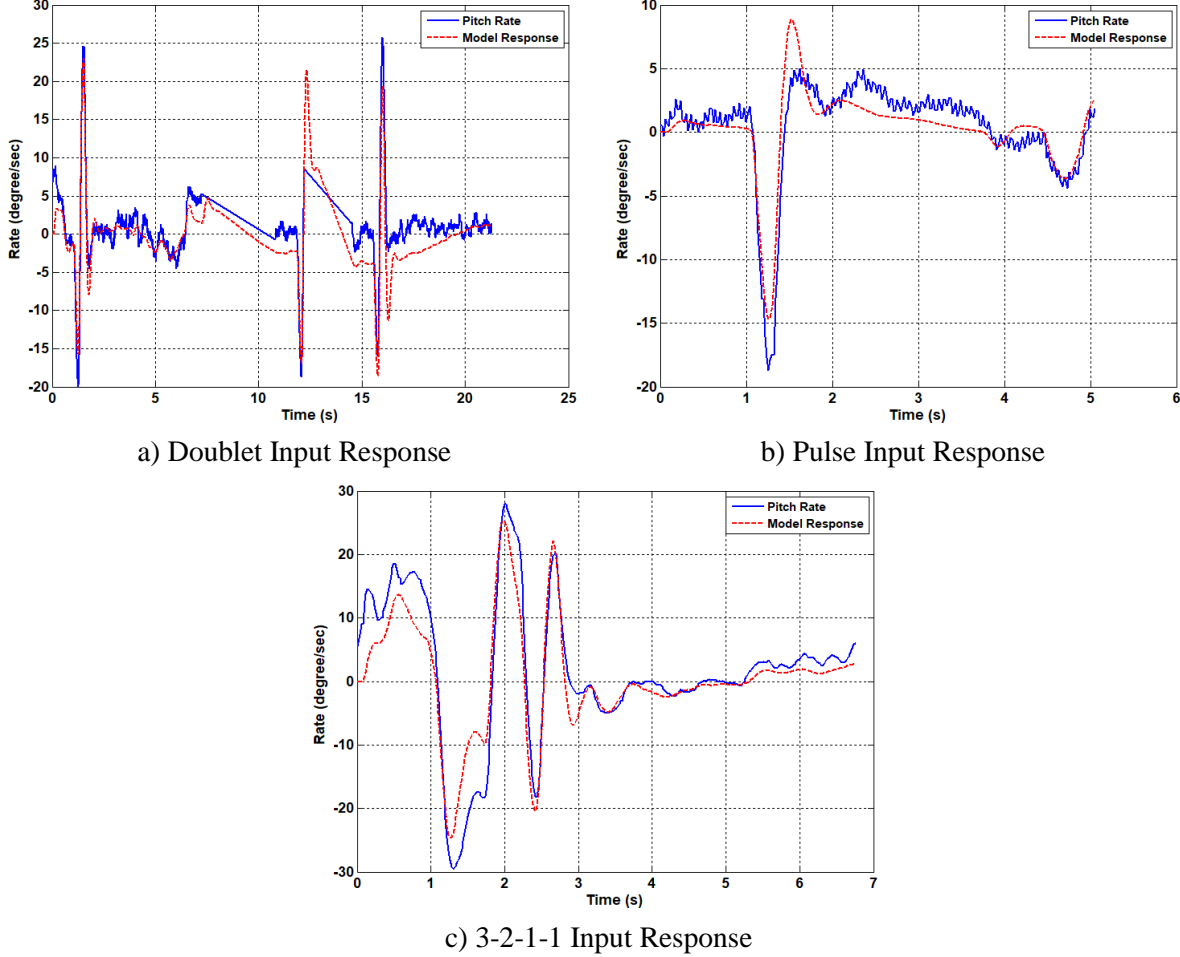


Figure 24: Time Response Comparisons

3. Revised Handling Qualities Predictions

As described above, the data generated from the system identification flight tests were used to revise the vehicle models. Using the pitch axis as an example, the revised frequency responses for the three test conditions (i.e., Nominal, Aft CG, and Added Time Delay) were compared with the original models for both the cruise and approach flight conditions as shown in Figure 22 and Figure 23, respectively. The key observations are that the Nominal and Aft CG cases were actually quite similar in flight and both displayed reduced closed-loop damping when compared the original model. The time delay cases, on the other hand, displayed more closed-loop damping in flight. All cases display added phase lag due to the revised actuator model.

In Figure 27, the updated pitch attitude Aircraft Bandwidth parameters as derived from the flight revised vehicle models are compared with the original model parameters. Here, the revised actuator model results in a significant increase in phase delay for all cases. As planned, the Added Time Delay cases display a further increase in phase delay. This also results in a further drop in bandwidth frequency. Finally, as observed with the frequency responses, the Nominal and Aft CG cases were effectively equivalent cases in flight. Hence, one would anticipate that the handling qualities would be similar for these cases when assessed via a given mission task element.

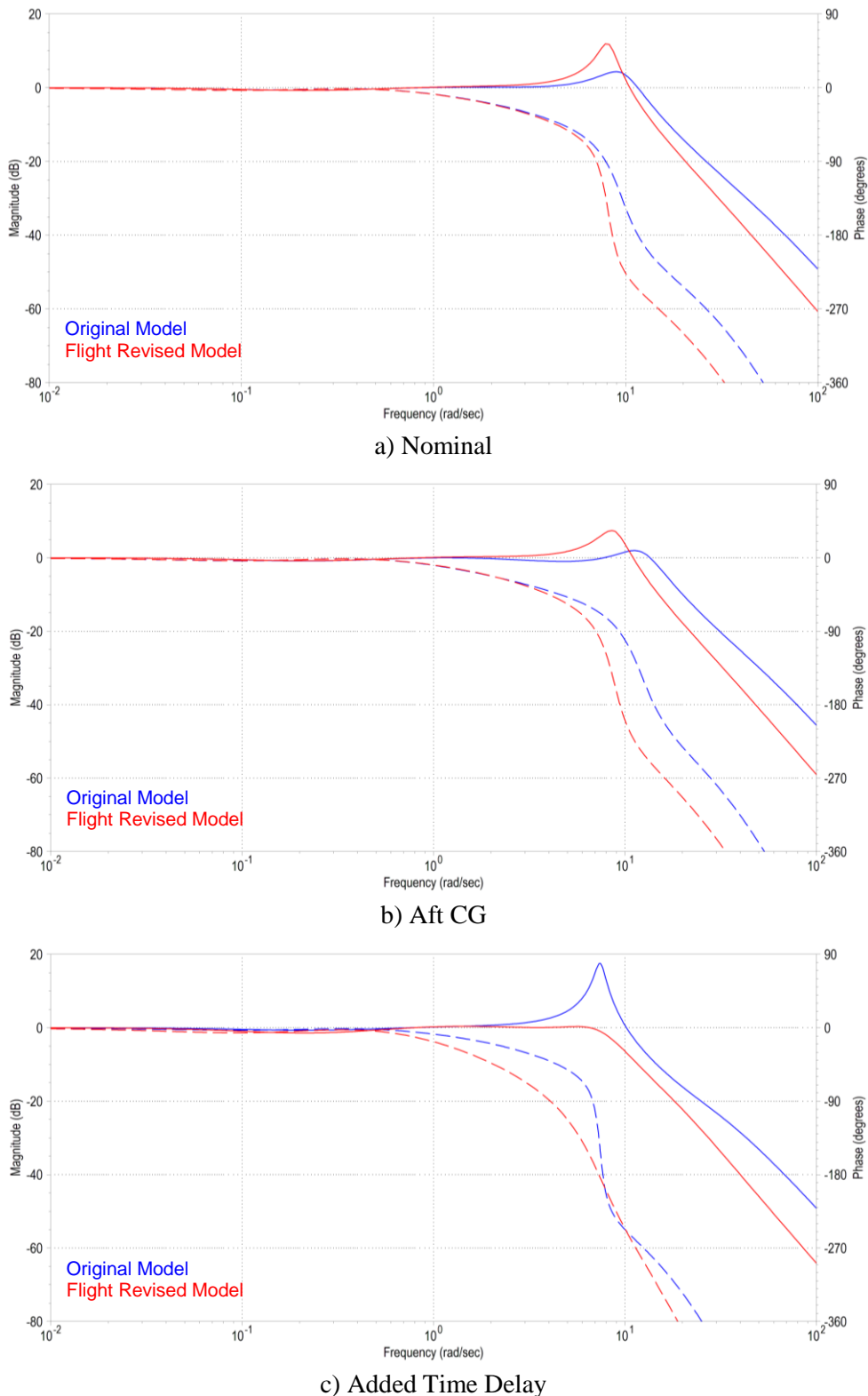


Figure 25: Comparison of UltraStick120 Model versus Flight Cruise (23 m/s) Frequency Responses

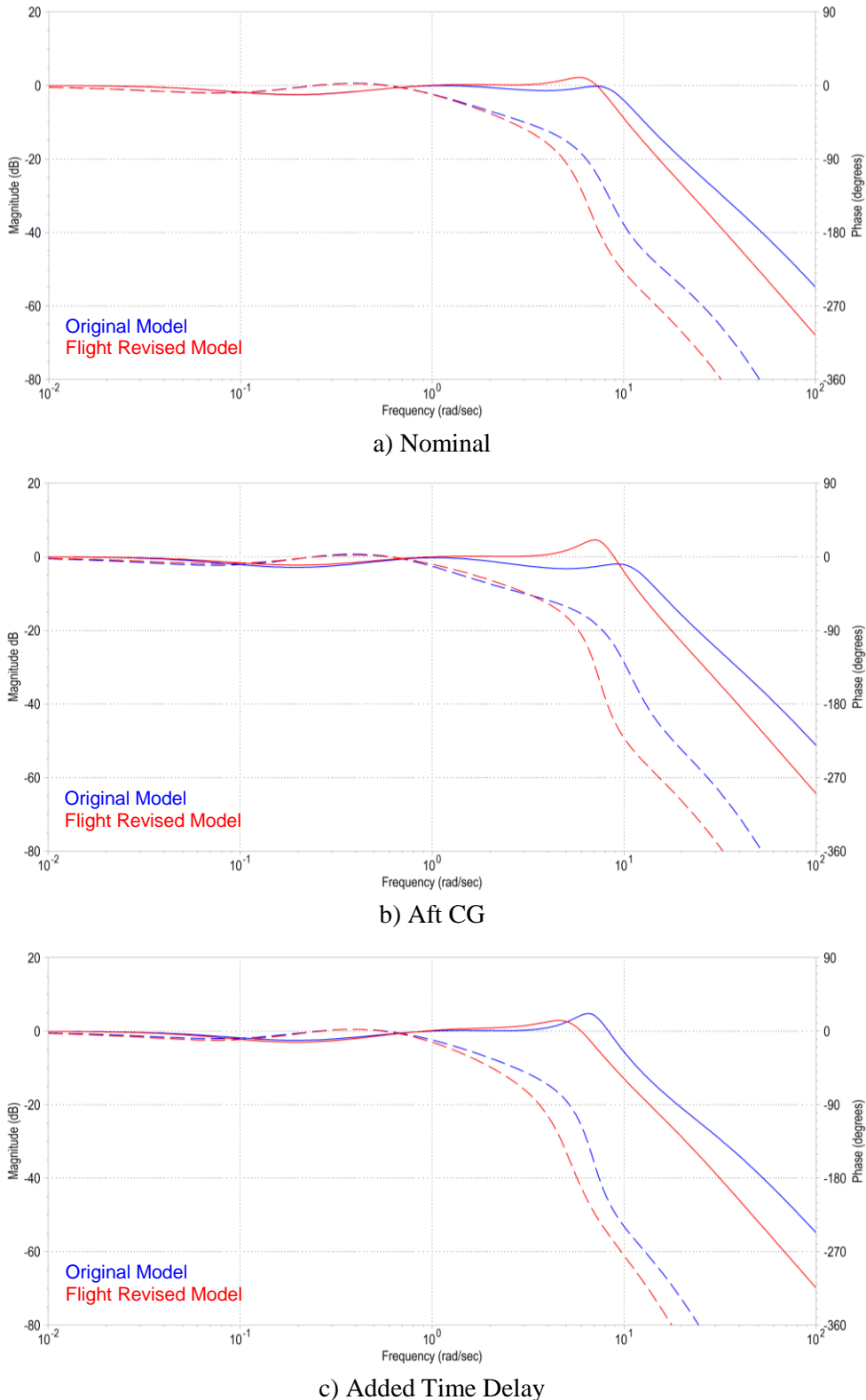


Figure 26: Comparison of UltraStick120 Model versus Flight Approach (17 m/s) Frequency Responses

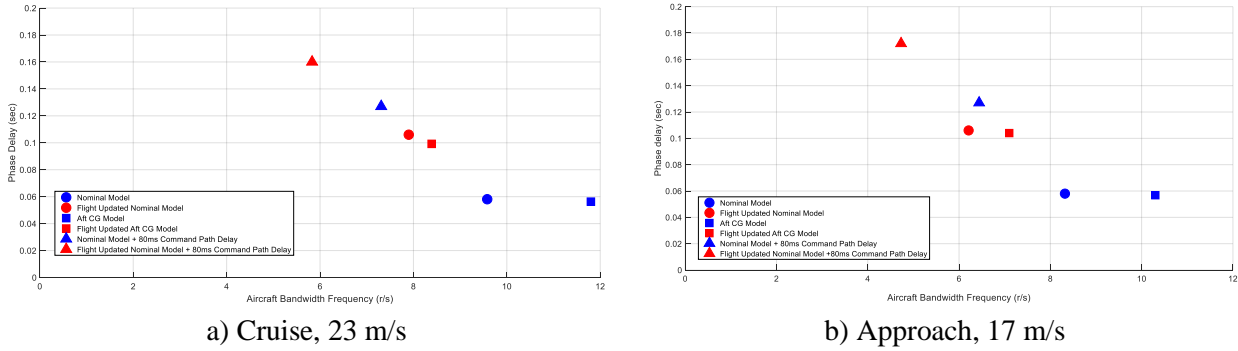


Figure 27: Aircraft Bandwidth Parameters for the UltraStick120 Model and Flight

e. Mission Task Element Flight Tests

1. Overview

Using the fixed wing MTEs described in Appendix B, a series of MTE evaluation flights were conducted by the University of Minnesota from November 2018 through March 2019 using the UltraStick120. A run log for the four evaluation flights is provided in Table 4.

Table 4: UltraStick120 MTE Flight Test Run Log

Flight	Flight Type	Speed	Condition		
12	MTE	23/17 m/s	Cruise/Approach	Normal CG	No Delay/Added Delay
13	MTE	23/17 m/s	Cruise/Approach	Normal CG	No Delay/Added Delay
14	MTE	23/17 m/s	Cruise/Approach	Normal CG	No Delay/Added Delay
16	MTE	23/17 m/s	Cruise/Approach	Normal CG	No Delay/Added Delay

All four MTE flights flew a combination of 4 MTEs:

- Flightpath Regulation in the Presence of a Discrete Gust
- Flightpath Regulation in the Presence of a Sum-of-Sines Disturbance
 - Altitude Disturbance (non-precision, non-aggressive)
 - Attitude Disturbance (precision, non-aggressive)
- Waypoint Tracking
- Precision Lateral Offset Landing

Below is the list of MTE flights and the tasks that were flown:

- Flight 12
 - Flightpath Regulation in the Presence of a Discrete Gust
 - (1-Cosine) excitation to pitch rate
 - Flightpath Regulation in the Presence of a Sum-of-Sines Disturbance
 - Non-Precision, Non-Aggressive (Altitude)
 - Precision Lateral Offset Landing

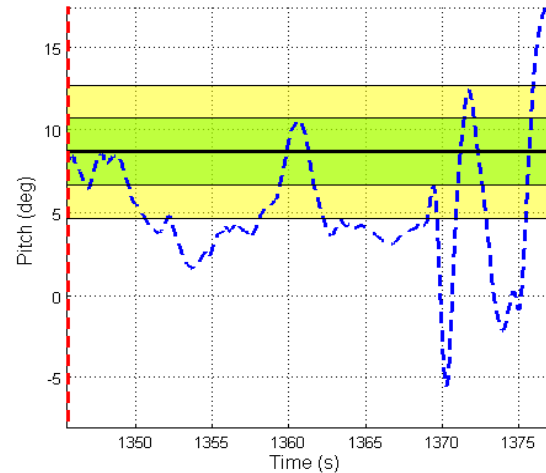
- Flight 13
 - Flightpath Regulation in the Presence of a Discrete Gust
 - (1-Cosine) excitation to pitch rate
 - Flightpath Regulation in the Presence of a Sum-of-Sines Disturbance
 - Non-Precision, Non-Aggressive (Altitude)
 - Precision Lateral Offset Landing
- Flight 14
 - Flightpath Regulation in the Presence of a Discrete Gust
 - (1-Cosine) excitation to pitch rate
 - Flightpath Regulation in the Presence of a Sum-of-Sines Disturbance
 - Non-Precision, Non-Aggressive (Altitude)
 - Waypoint Following
 - Precision Lateral Offset Landing
- Flight 16
 - Flightpath Regulation in the Presence of a Sum-of-Sines Disturbance
 - Precision, Non-Aggressive (Attitude)
 - Waypoint Following
 - Precision Lateral Offset Landing

2. Flightpath Regulation Tasks

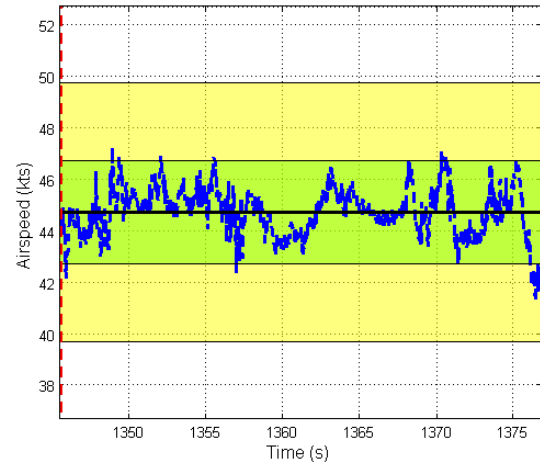
Flightpath Regulation in the Presence of a Discrete Gust: An example flightpath regulation task is shown in Figure 28. These tasks were flown in a “pseudo” autonomous mode where in the remote pilot placed the vehicle on condition, while the on-board controller responded to the disturbance. The aggressiveness of the task can be adjusted based on the size of the input. For this example, the aggressiveness level was set by a 1-Cosine gust disturbance based on a 2 r/s pitch rate disturbance for the 23 m/s cruise flight condition. Note that a turn is initiated just prior to the 1370 second time index as seen in the heading response (Figure 28d). Desired and adequate performance requirements are indicated by the green and yellow bands, respectively. Prior to the turn, the vehicle maintains airspeed and altitude within desired tolerances, however, the pitch attitude response often falls out of the adequate bounds. The UltraStick120 attitude flight control system was known to have a low-bandwidth control response, so this result was not unexpected. With this limitation in mind, the MTE was successful in exposing the handling qualities deficiencies associated with the aircraft controller. More work is needed with other fixed wing vehicles to properly size inputs and refine performance requirements, but this MTE shows promise for inclusion in a UAS handling qualities specification.

Flightpath Regulation in the Presence of a Sum-of-Sines Disturbance (Altitude): Two sum-of-sines disturbance regulation tasks were considered in this program. Both feature the same Fibonacci-based sum-of-sines signal as defined in Appendix C. The first was introduced as an altitude disturbance of ± 10 meters. The aggressiveness of the task can be adjusted by sizing the input. Example flight test results from Flight 14 are shown in Figure 29. Because of the flight test course visual line of sight limitations, many of the runs were cut short due to the need to remain within the test area as was the case here (see Figure 29d). Before the turn is initiated, the vehicle was able to maintain altitude and airspeed within mostly the desired performance bounds. There were more issues with the pitch attitude performance, however, the current requirements on this parameter may be too stringent for a non-precision, non-aggressive task. Again, more work is needed with other fixed wing vehicles to properly size inputs and refine performance requirements, but this MTE shows promise for inclusion in a UAS handling qualities specification. With a more consistent MTE set (i.e., fewer heading changes while responding to the

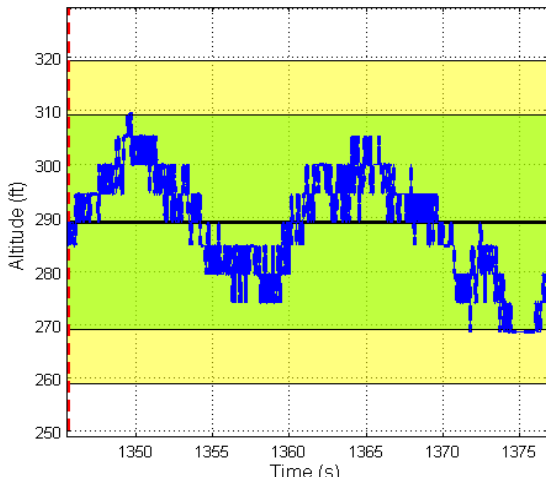
disturbance), a complete controller-vehicle system analysis can be conducted because of the known disturbance input.



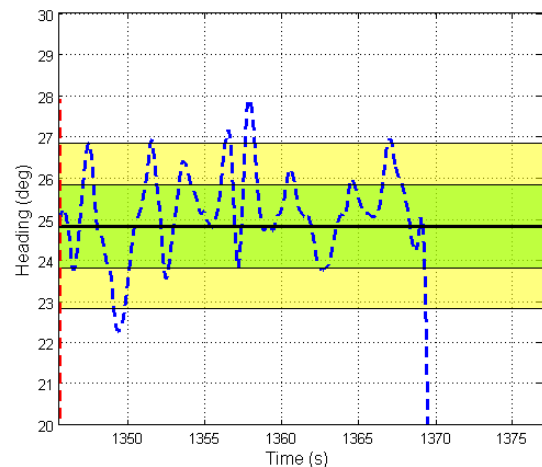
a) Pitch Attitude



b) Airspeed



c) Altitude



d) Heading

Figure 28: Flight 14 Flighthpath Regulation in the Presence of a Discrete Gust MTE

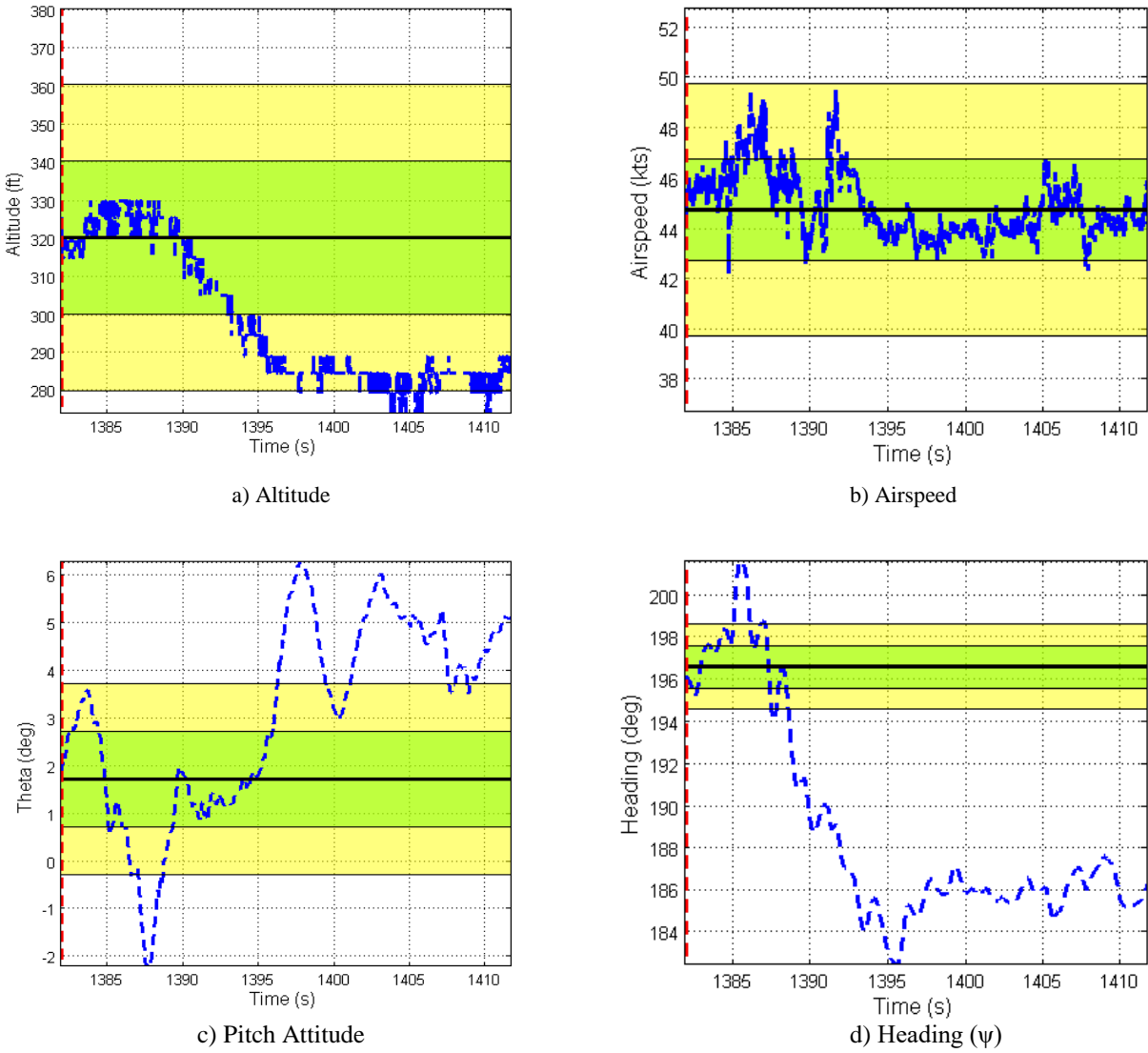
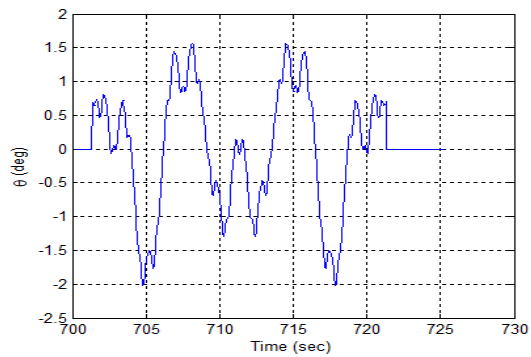
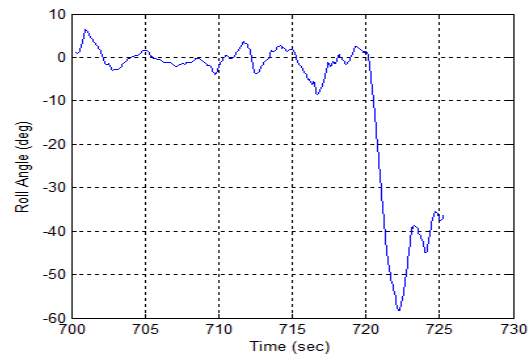


Figure 29: Flight 14 Flighthpath Regulation in the Presence of a Sum-of-Sines Altitude Disturbance MTE

Sum-of-Sines Attitude Disturbance: The attitude sum-of-sines disturbance signal, seen in Figure 30a, is added to the reference signal of the attitude controller (see Figure 7). This task was also flown as a “pseudo” autonomous task. Unlike the altitude disturbance task, this MTE is intended to be a precision, non-aggressive task. For the example case included herein, the aircraft is flying straight and level for the beginning portions of the maneuver, and then the aircraft banks, e.g., see Figure 30b, to initiate a turn to remain within the desired test area. MTE performance plots are shown in Figure 30. During the section of the maneuver where the aircraft is straight and level, the altitude performance generally meets desired performance requirements, while airspeed meets adequate performance requirements. Because of the turn, it is difficult to assess the key performance indicator – pitch attitude, but it does seem likely that at least adequate performance may have been attainable. As with the previous examples, this fixed wing MTE shows promise, but further refinements are likely needed before it is ready for inclusion in the UAS handling qualities specification.

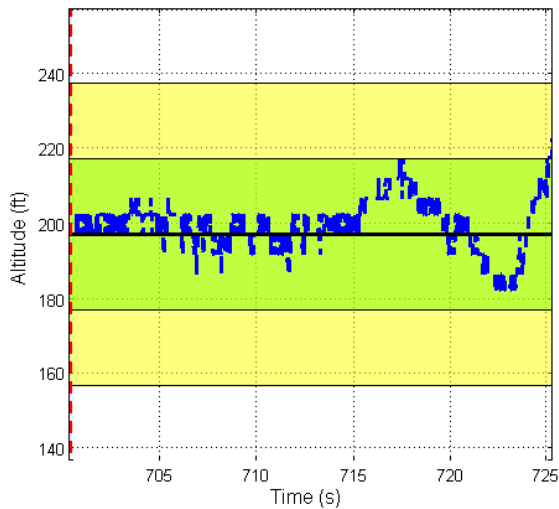


a) Pitch Attitude Disturbance

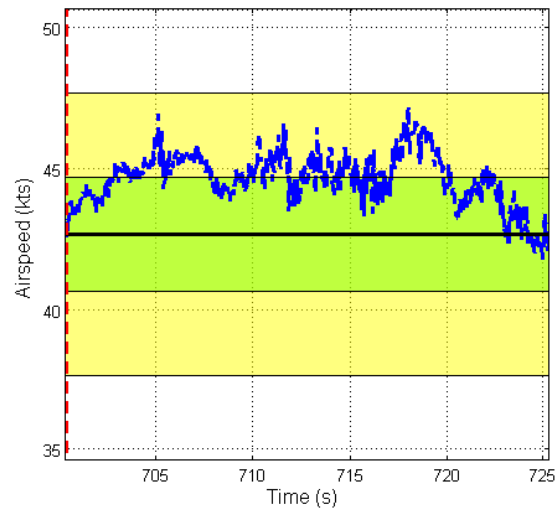


b) Bank Angle

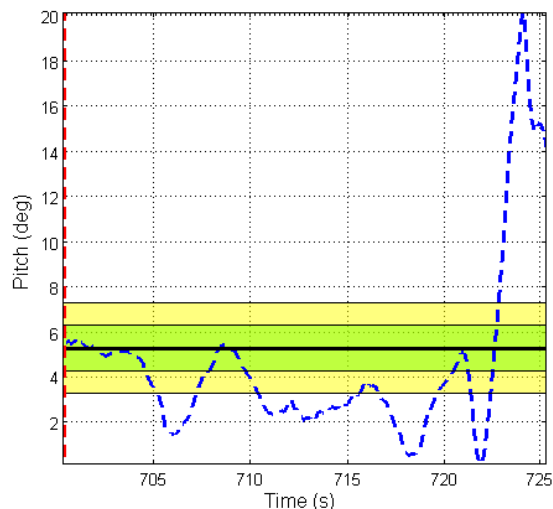
Figure 30: Flight 16 Example Sum-of-Sines Attitude Disturbance



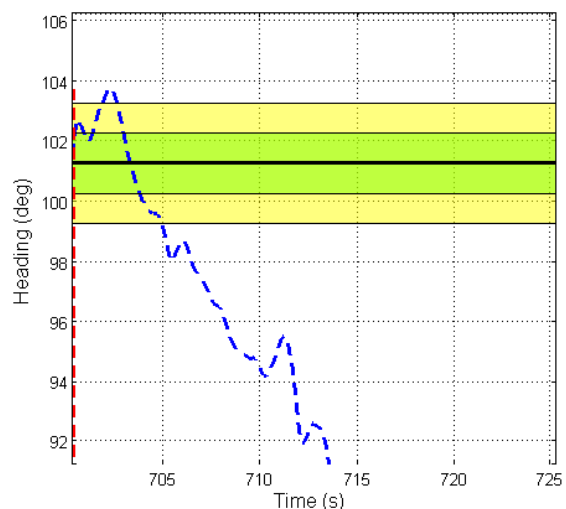
a) Altitude



b) Airspeed



a) Pitch Attitude



b) Heading

Figure 31: Flight 16 Flighthpath Regulation in the Presence of a SOS Attitude Disturbance MTE, No Delay

3. Waypoint Following

The Waypoint Following task was flown as a completely autonomous MTE. A description of the MTE is provided in Appendix C. The MTE featured a square x-y course with altitude changes. Example x-y trajectories are shown in Figure 32 for the Nominal (blue trajectory) and Added Delay (red trajectory) configurations. Note that there is little difference between the two cases. Furthermore, the vehicle does not meet even a generous set of performance requirements, ± 50 ft/ ± 100 ft, though in this case the waypoints are generally met within adequate bounds. No refinements to the controller were made to improve upon this performance and as discussed earlier, there were known limitations. An important question regarding the performance requirements will ultimately determine precision and aggressiveness levels. Specifically, is the vehicle required to meet the performance requirements throughout its trajectory or only in the vicinity of the waypoints? Despite these questions, this MTE also shows great promise. With refinements, this MTE will likely be a good discriminator of UAS handling qualities.

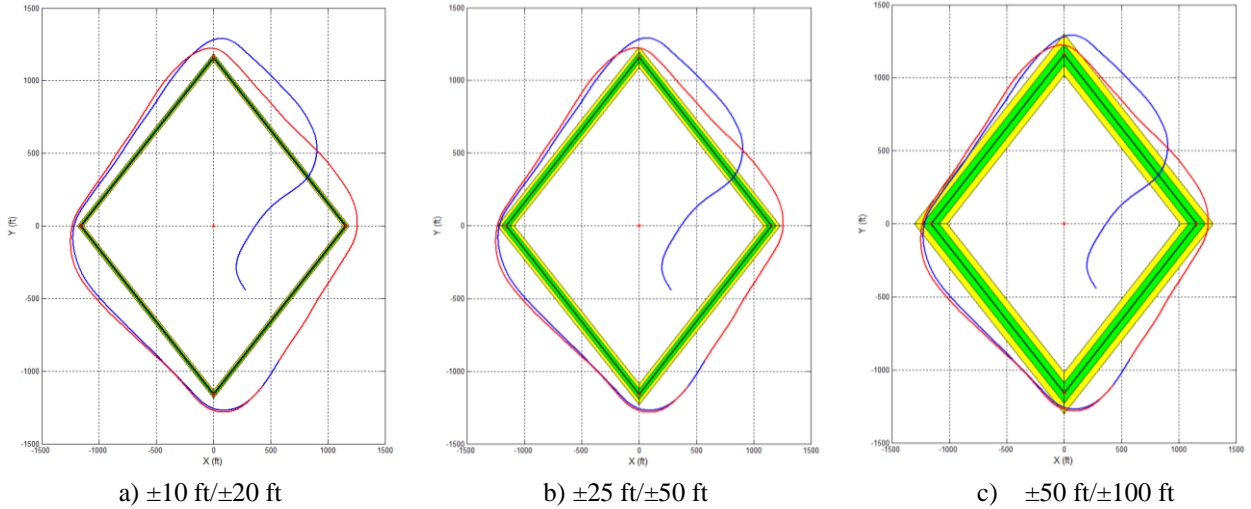


Figure 32: Flight 16 Waypoint Following

4. Precision Lateral Offset Landing

Line of Sight MTE: As defined in Appendix C, the Precision Lateral Offset Landing task was executed as a pilot line of sight task. Figure 33 shows all Flight 16 runs of the offset landing. In total, there were 4 offset landing attempts flown. Most of the runs missed the adequate box where the center of the desired and adequate boxes is 50ft to the left and 10 ft back of the operator's position (runway). The centerline of the adequate and desired boxes was marked with one or two cones in the middle of the field. The Pilot noted that it was difficult to setup the offset landing task with the snow bank and 24 inches of snow on the ground. Furthermore, the pilot also mentioned that he did not have a great sight line to establish an initial approach. He also noted that the case with 160 ms of added delay was flyable, and the landing task was feasible with this delay present.

The results from all four MTE evaluation flights showed similar results. That is, without adequate cueing present, and this may not be feasible to consistently attain in a line of sight task, the task performance was effectively random. A “good” handling configuration may miss the mark, while a “poor” handling configuration ends up in the box. Thus, when flown in this manner, the MTE will not properly expose UAS handling qualities. There may still be value in an offset landing task if an aircraft point of view display is available with proper cueing such as was used in the AirSTARS flight test program. This is discussed further below.

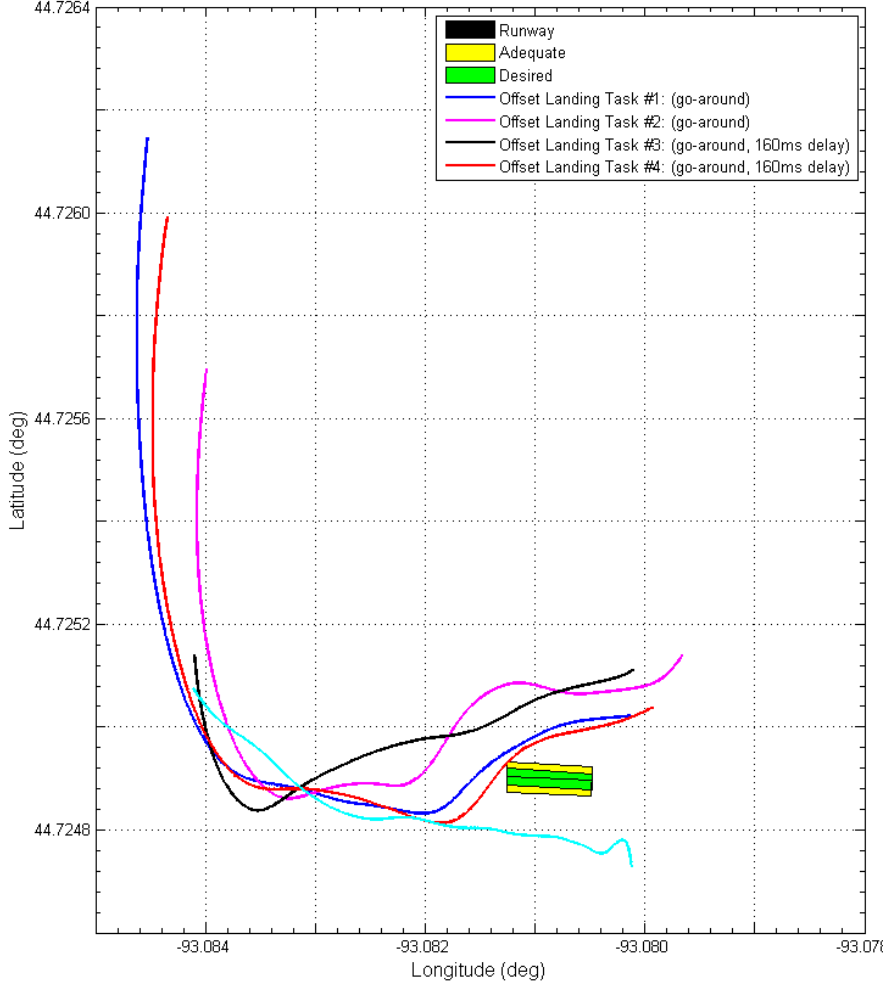


Figure 33: Flight 16 Precision Lateral Offset Landing Ground Tracks

Point of View MTE: While the UltraStick120 test results with the precision lateral offset landing task clearly exposed the limitations of the MTE as a visual line of sight task, previous work at NASA Langley with the AirSTARS vehicle was more successful. In this case, the task was flown as pilot point-of-view (POV) task from a ground station using a synthetic head-up display. In this application, the MTE was successfully executed and did expose handling qualities variations between aircraft configurations.

The maneuver is conducted at a nominal altitude of 1000 feet to avoid any damage to the aircraft and provide the safety pilot with ample window to recover the aircraft from any unexpected situation (e.g., a loss of control departure). The runway is ‘simulated’ 100 feet below the aircraft, at a longitudinal distance of 1800 feet and a lateral offset of 100 feet towards starboard side of the aircraft. The simulated landing is carried out by projecting a virtual runway on the head-up display (HUD) of the research pilot. A screenshot of the HUD, taken from Ref. 32, is provided in Figure 34 for reference.

The task was to land within a target touchdown reference location on the runway after performing an ‘S’ maneuver to align with the runway centerline. Performance of the pilot-vehicle system was evaluated using a set of desired and adequate performance requirements. Performance analysis is discussed next for all the three runs.

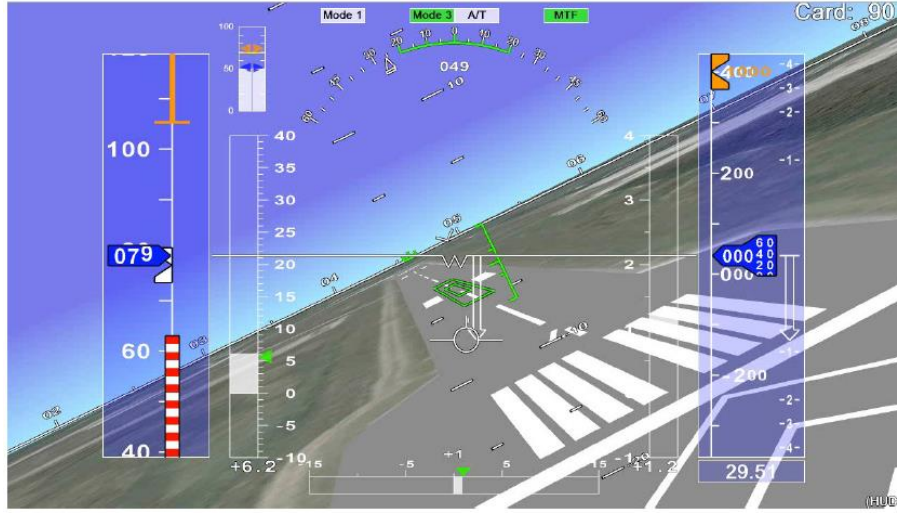


Figure 34: Head-Up Display (HUD) for the Research Pilot Depicting Virtual Runway (Ref. 32)

The desired and adequate performance requirements for the offset landing task are provided in Ref. 32 and are reproduced in Table 5 for convenience.

Table 5: Performance Requirements for Offset Landing Task (Ref. 32)

Parameter	Target	Desired	Adequate
Bank Angle (deg)	0	$\pm 10^\circ$	$\pm 20^\circ$
Flightpath Angle (deg)	-3	$\pm 1^\circ$	$\pm 3^\circ$
Lateral Offset (feet)	0	± 12	± 24
Longitudinal Offset (feet)	0	± 164	± 363

The task is to touchdown within a pre-defined target touchdown zone. To begin the maneuver, the UAS is located at a lateral offset position with respect to the runway. To meet performance requirements, the touchdown should occur with bank angle, longitudinal offset, and lateral offset within the bounds specified in Table 5. The bank angle in mode 1 for runs 1-3 is shown in Figure 35. The run-to-run signals were adjusted to be plotted on the same time axis. Since all the three runs have a duration between 13.86s-14.2s, the signals were shortened to the same duration without any significant loss of data.

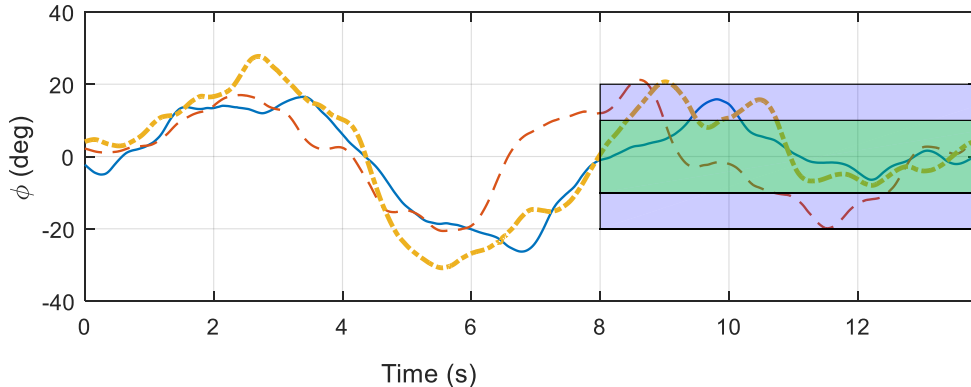


Figure 35: Bank Angle Performance for Example AirSTARS Runs

From Figure 35 the bank angle performance is largely in the adequate range across the entire time interval, with run 3 showing the largest overshoots beyond the desired bounds. It should be noted that since an ‘S’ maneuver is required to align the aircraft with the runway centerline, thus the bank angle requirement is applied from the centerline capture to touchdown. Beyond 12s, all three runs have bank angles that fall within the desired range.

Next, the longitudinal and lateral offset performance is considered. All of the runs start with the virtual target touchdown point located at a lateral right shift of 100 feet and 1800 feet in front of the aircraft. Lateral and longitudinal offset specifications are provided to illustrate the performance at touchdown. The objective is to land as close to the reference touchdown point as possible. Figure 36 shows the lateral and longitudinal performance of the aircraft for runs 1-3 during the offset landing maneuver.

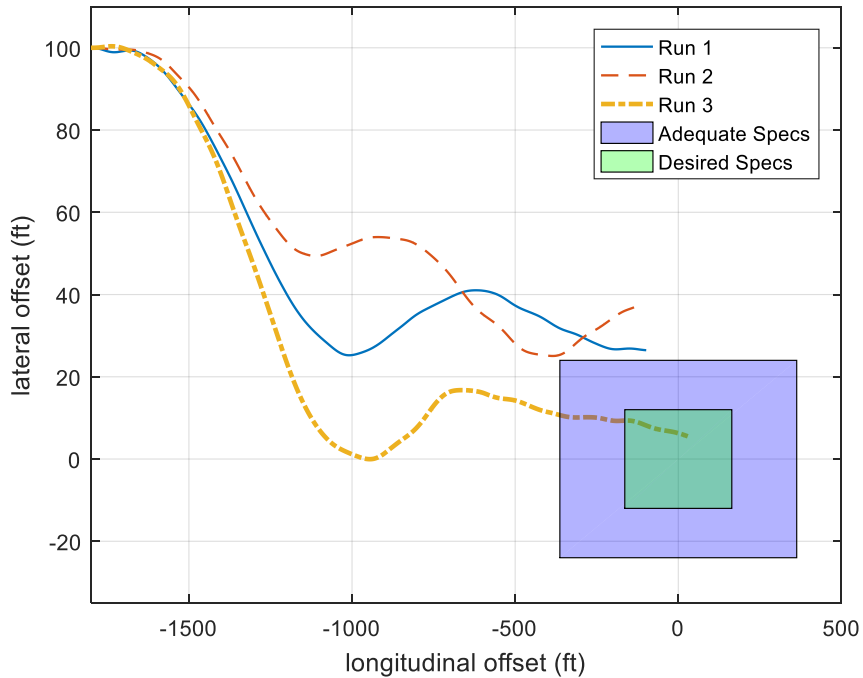


Figure 36: Lateral and Longitudinal Offset Performance, Runs 1-3, Flight 44, Card 86

The position of the aircraft with respect to the runway is not directly available as a data signal. Therefore, the lateral and longitudinal positions were computed using heading angle data and airspeed data available during the run. From heading angle and airspeed, lateral and longitudinal components of aircraft velocity are found. Positions can then be determined by integrating the velocities in a discrete manner. Figure 36 shows that of the three runs, only run 3 meets the performance requirements; in fact, run 3 meets the desired specifications very well. Run 2 is the possibly the most interesting in this regard, since the aircraft goes off-course just as it approaches the target touchdown area. In general, the AirSTARS results indicate a POV Precision Lateral Offset Landing MTE can be an appropriate discriminator of UAS handling qualities.

2. Multirotor UAS MTE Flight Test Evaluations

a. Introduction

Four low speed multirotor MTEs were tested at the Autonomy Incubator (AI) at NASA Langley Research Center in April 2018. Four remotely piloted visual line-of-sight MTEs were evaluated: Precision Hover, Lateral Sidestep, Vertical Reposition, and Landing. Complete descriptions of the four MTEs are provided in Appendix B. The flight tests were conducted at the AI on a course defined by hover boards positioned

according to each MTE description. Three pilots participated in the flight evaluations. Pilot 1 was an expert sUAS pilot, Pilot 2 was an experienced sUAS test pilot, and Pilot 3 was a sUAS pilot with limited test experience. Two multirotors, shown in Figure 188, were used in the evaluations: a Tarot X6 hexacopter and a Tarot 650 Sport quadcopter.



a) Tarot X6



b) Tarot 650 Sport

Figure 37: Multirotor Test Vehicles

Two sets of data and video were generated for each set of flight test evaluation runs. The video consists of a stationary video that captures the entire test range and an over-the-shoulder video of the pilot to capture pilot perception and line-of-sight. The AI is equipped with a Vicon system that provides precision position tracking of vehicles. Both multirotors were outfitted with Vicon tracking nodes. These data in concert with the over-the-shoulder video can and will be used to calculate performance metrics for these tests. In addition, the aircraft carry Pixhawk autopilots that record GPS, IMU, pilot command, and control deflection data. The GPS data are not accurate in the indoor AI environment and cannot be used for measuring performance, but the IMU, pilot command, and control deflection data will be valuable in understanding the pilot-vehicle system and how that affects performance.

A complete analysis summary for all four MTEs is provided in Appendix D. The Lateral Sidestep MTE is used here to exemplify the analysis process.

b. Lateral Sidestep

1. MTE Description

Autonomy Level

- Remotely piloted with visual line-of-sight.
- Autonomous variations are possible.

Objectives

- Assess roll axis and heave axis response during moderately aggressive maneuvering.
- Identify undesirable coupling between the roll controller and the other axes.

Description

From a stabilized hover at an altitude of 5 ft with the longitudinal axis of the multi-rotor sUAS oriented 90 degrees to a reference line marked on the ground, initiate a lateral acceleration to approximately 5 kts groundspeed followed by a deceleration to laterally reposition the vehicle to a stabilized hover 12.5 ft left of the starting point as indicated by another ground marker all while maintaining the initial heading throughout the maneuver. The acceleration and deceleration phases shall be accomplished as single smooth maneuvers. The reposition capture is complete when a stabilized hover is achieved as indicated by the vehicle position in front of the hover boards, left or right depending on course position.

The center of the (left and right) hover boards will be placed 5 ft above ground and approximately 25 ft apart laterally, equally spaced left and right of the starting point. (In the NASA LaRC Autonomy Incubator, the starting point was 20 ft aft of the precision hover board.) The hover board will have distinct boundaries indicating desired and adequate performance requirements.

Desired Performance

- ± 1 vertical deviation from hover board center at each capture point.
- ± 1 ft lateral deviation as indicated by the hover board center at each capture point.
- ± 1 ft longitudinal (fore/aft) deviation from ground marker.
- $\pm 5^\circ$ heading deviation from reference heading.

Adequate Performance

- ± 2 vertical deviation from hover board center at each capture point.
- ± 2 ft lateral deviation as indicated by the hover board center at each capture point.
- ± 2 ft longitudinal (fore/aft) deviation from ground marker.
- $\pm 10^\circ$ heading deviation from reference heading.

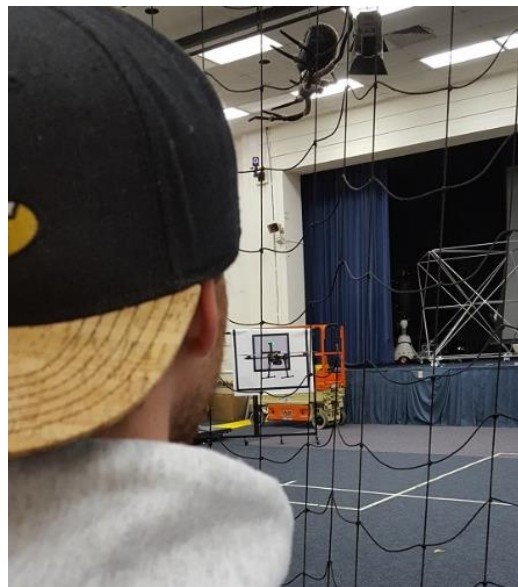


Figure 38: Lateral Reposition (mini course)

2. Lateral Sidestep Test Overview

For the Lateral Sidestep MTE, the pilots were instructed to fly the vehicle laterally in one direction, capture and hold a static position, then sidestep in the other direction to capture and hold the original position. In most cases, the pilot first flew the aircraft to a hover board approximately 6.5 feet to the right of the takeoff point and then sidestepped towards a hover board about 15 feet to the left of the takeoff point. The lateral sidestep was then repeated several times (see example in Figure 194). Most flights consisted of 5 or 6 sidesteps with Pilot 1 performing 8. The time spent hovering in position after completing the lateral movement was short, lasting 10-25 seconds depending on the preference of the pilot. In general, the pilots had a higher degree of success with the right sidestep.

The pilots were effective at maintaining desired performance during the right lateral maneuver. They also performed the left sidestep well, though they were prone to under- or overshooting the target. This under- and overshooting the target can be attributed to depth perception and line-of-sight issues. The right sidestep end position was much closer to the pilot making it easier to judge vehicle's position relative to the hover board and adequate/desired bounds. In terms of maintaining altitude, the pilots had moderate success with small dips when beginning the sidestep.

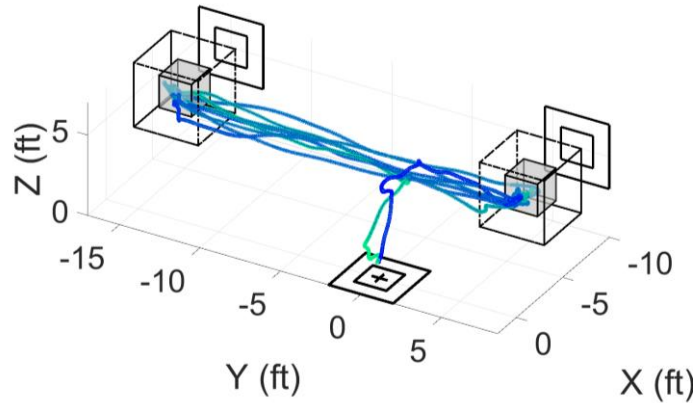


Figure 39: Tarot 650 Sport Lateral Sidestep MTE, Pilot 1, Batch 1 – Inertial Position

3. Qualitative Individual Pilot Assessment

Pilot 1 performed very well during each individual sidestep maneuver. He completed 8 different lateral repositions, starting by sidestepping to the right. Aside from the first left sidestep, he finished the entire run in the desired area. In the altitude portion of the task, he remained in the desired zone for the duration of the run but deviated by a few inches every time a lateral reposition was initiated. This deviation was then corrected during each quick hover at the sidestep point. For the longitudinal position, Pilot 1 was unable to complete the aft reposition 5 feet behind the origin, and instead held a very unsteady position 3-4 feet behind. He was, however, able to return the vehicle to landing zone at the conclusion of the task.

Pilot 2 faced some difficulty in performing sections of the sidestep maneuver. While piloting the Tarot 650 Sport he made multiple altitude overcorrections and was unable to achieve a steady hover during any left lateral repositions. He found more success in the right sidestep maneuver, consistently achieving a desired position. He also attempted to perform a 5 foot aft reposition that was unsuccessful and resulted in erratic longitudinal position changes between 2 and 5 feet behind the origin. While piloting the Tarot X6-2, he encountered many similar problems as he did with the Tarot 650 Sport, but with the additional variable of increased air circulation. There was a glass panel near the right hoverboard which allowed the air circulation from the powerful hex rotors to bounce off it, disturbing the air around it causing fluctuations in altitude and lateral position.

Pilot 3 proved to be adept at maintaining lateral positioning of each of his vehicles. Additionally, unlike the other two pilots, he was able to successfully perform the aft reposition five feet behind the origin. Despite the correct repositioning of the vehicle, Pilot 3 still exhibited similar oscillatory behavior in the longitudinal axis to Pilot 2, although his perturbations mostly fell within the desired and adequate areas. His performance piloting the Tarot 650 Sport and the Tarot X6-2 were very comparable, but understandably, the were more jarring and frequent movements during the Tarot X6-2 runs due to its bulkier size.

4. Performance

Summary performance scores are shown in Table 6. Pilots excelled at staying in the desired region for altitude with a desired performance of 94.33% and an adequate performance of 99.94%. Holding altitude between hover positions was an easy task for the pilots with an average of 87% desired performance score with a near 100% adequate score. Lateral position was relatively easy for the pilots to control with a desired performance of 85.21% and an adequate performance of 96.95%. Average heading angle performance was 65.52% desired and 97.47% adequate. Longitudinal position performance was just 39.08% desired and 70.87% adequate.

Comparing the two vehicles, there are small differences in performance measures. In altitude during hover, the Tarot 650 Sport has a desired performance over 12% higher at 97.64% than the Tarot X6-2 at 85.35%. In lateral position, the pilots achieved a higher desired performance with the Tarot X6-2 at 87.83%, 10% higher than with the Tarot 650 Sport. However, this can be explained by Pilot 2's poor performance flying the Tarot 650 Sport while Pilot 3 performed slightly worse with the Tarot X6-2. Heading angle performance was nearly identical between the two vehicles. This lack of consistency in one vehicle performing better than the other means that a claim cannot be made for an evidence-based difference in vehicle performance.

Table 6: Lateral Sidestep MTE Pilot Performance Averages

Average Pilot Performance for Lateral Sidestep MTE								
	Altitude		Fore/Aft Position		Lateral Position		Heading Angle	
Pilot #	Desired	Adequate	Desired	Adequate	Desired	Adequate	Desired	Adequate
1	100.00	100.00	43.85	78.32	90.28	99.34	27.26	94.58
2	97.62	99.81	15.62	39.72	72.75	91.52	92.03	99.67
3	85.38	100.00	57.76	94.57	92.60	100.00	77.27	98.16
AVG	94.33	99.94	39.08	70.87	85.21	96.95	65.52	97.47

Average Pilot Performance for Lateral Sidestep MTE Using Tarot 650 Sport								
	Altitude		Fore/Aft Position		Lateral Position		Heading Angle	
Pilot #	Desired	Adequate	Desired	Adequate	Desired	Adequate	Desired	Adequate
1	100.00	100.00	43.85	78.32	90.28	99.34	27.26	94.58
2	96.78	99.63	8.82	30.36	56.24	84.27	88.62	99.35
3	98.51	100.00	69.54	98.58	98.80	100.00	77.20	98.58
AVG	98.43	99.88	40.74	69.09	81.78	94.53	64.36	97.50

Average Pilot Performance for Lateral Sidestep MTE Using Tarot 650 Sport without Pilot 1								
	Altitude		Fore/Aft Position		Lateral Position		Heading Angle	
Pilot #	Desired	Adequate	Desired	Adequate	Desired	Adequate	Desired	Adequate
1								
2	96.78	99.63	8.82	30.36	56.24	84.27	88.62	99.35
3	98.51	100.00	69.54	98.58	98.80	100.00	77.20	98.58
AVG	97.64	99.81	39.18	64.47	77.52	92.13	82.91	98.97

Average Pilot Performance for Lateral Sidestep MTE Using Tarot X6-2									
	Altitude		Fore/Aft Position		Lateral Position		Heading Angle		
Pilot #	Desired	Adequate	Desired	Adequate	Desired	Adequate	Desired	Adequate	
1									
2	98.46	100.00	22.42	49.08	89.25	98.77	95.45	100.00	
3	72.24	100.00	45.97	90.56	86.40	100.00	77.33	97.74	
AVG	85.35	100.00	34.20	69.82	87.83	99.38	86.39	98.87	

Average Pilot Performance for Altitude Hold Translation		
Vehicle	Desired (%)	Adequate (%)
Tarot 650 Sport	87.66	100.00
Tarot X6-2	85.51	99.91
Average	87.02	99.97

5. Left/Right Hover Performance

When capturing and hovering at the left and right hover boards at the ends of the Lateral Sidestep MTE course, there is a noticeable difference in performance as listed in Table 58, though it is not consistent between aircraft. This is surprising since the left hover board is 15 ft from the pilot and the right hover board is only 5 ft from the pilot, which one would think would make the left more difficult to cue from. However, when flying the Tarot X6-2, there is a 10% difference in the average performance of hovering at the left hover board as compared to the right, which reflects the perceived difficulty in precisely capturing and hovering this aircraft at a distance. There is only a 3% difference when flying the Tarot 650 Sport with capturing and hovering near the left hover having higher performance. This could be due to visual feedback and the faster dynamics of the smaller vehicle at close range compared to long range, but more data for more multi-rotor vehicles are needed to draw a confident conclusion.

Table 7: Left/Right Hover Performance Averages

Pilot Lateral Sidestep Direction Comparison Tarot 650 Sport		
	Desired (%)	Adequate (%)
AVG Right	70.40	88.71
AVG Left	73.36	92.34

Pilot Lateral Sidestep Direction Comparison Tarot X6-2		
	Desired (%)	Adequate (%)
AVG Right	78.40	91.59
AVG Left	68.49	92.45

Pilot Lateral Sidestep Direction Comparison		
	Desired (%)	Adequate (%)
AVG Right	73.60	89.86
AVG Left	71.41	92.38

c. Pilot Evaluations of the MTEs

1. Pilot Questionnaire

The questionnaire developed for the Lateral Sidestep MTE is shown below. Similar questionnaires were created for the other three MTEs. Each evaluation pilot completed a set of questionnaires as part of the flight test debrief process.

	Strongly Disagree	Disagree	Neither Agree Nor Disagree	Agree	Strongly Agree
The Remote Piloted Lateral Sidestep MTE is representative of an operational task element.	<input type="radio"/>	<input type="radio"/>	<input type="radio"/>	<input type="radio"/>	<input type="radio"/>
The MTE is well defined.	<input type="radio"/>	<input type="radio"/>	<input type="radio"/>	<input type="radio"/>	<input type="radio"/>
The MTE is repeatable and easy to perform.	<input type="radio"/>	<input type="radio"/>	<input type="radio"/>	<input type="radio"/>	<input type="radio"/>
Entry/exit conditions for the MTE were easy to establish.	<input type="radio"/>	<input type="radio"/>	<input type="radio"/>	<input type="radio"/>	<input type="radio"/>
The course markers used were easy to follow and provided all the information required to perform the MTE.	<input type="radio"/>	<input type="radio"/>	<input type="radio"/>	<input type="radio"/>	<input type="radio"/>
The MTE is able to effectively expose the aircraft characteristics identified in the task objectives.	<input type="radio"/>	<input type="radio"/>	<input type="radio"/>	<input type="radio"/>	<input type="radio"/>
The MTE is valid for defining nominal UAS performance.	<input type="radio"/>	<input type="radio"/>	<input type="radio"/>	<input type="radio"/>	<input type="radio"/>

What changes if any would you recommend to the MTE objectives or description?

What changes if any would you recommend for the desired and adequate performance requirements?

What changes if any would you make to the course markers to aid your task performance (sketches are welcome)?

2. Summary of Questionnaire Results for all Four MTEs

After completing all four MTEs with the checkout vehicle, each piloted answered a debrief questionnaire the results of which are presented in Figure 198. The three pilots all agreed or strongly agreed that the MTEs were representative of an operational task element, well defined, and repeatable and easy to perform. They also agreed or strongly agreed that the MTEs had entry/exit conditions that were easy to establish and had course markers that were easy to follow. All agreed or strongly agreed that the MTEs effectively exposed aircraft characteristics and that the MTEs were valid for defining nominal performance. Note that one exception was that Pilot 3 neither agreed nor disagreed that the precision hover task was valid for defining nominal performance.

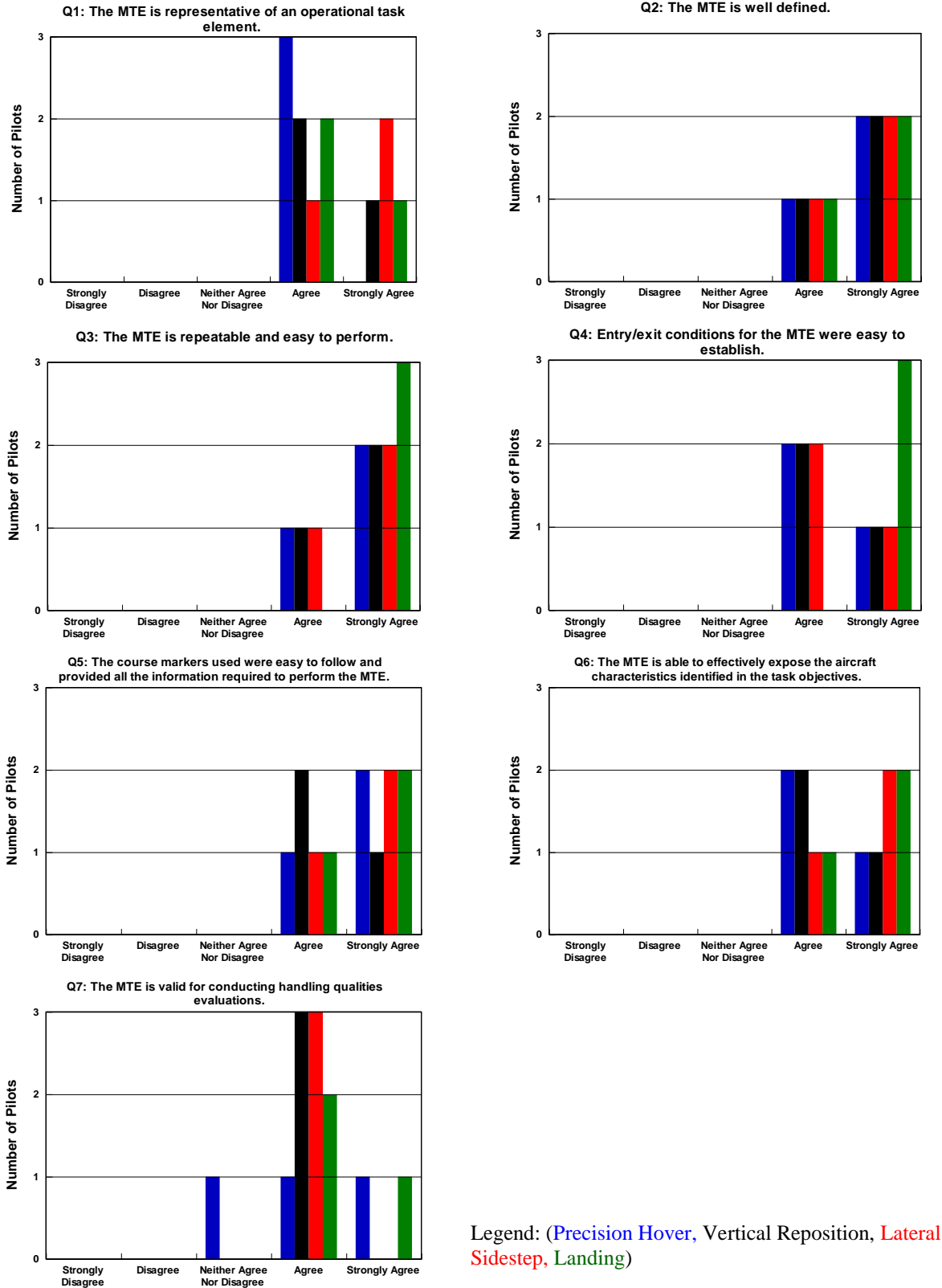


Figure 40: Debrief Questionnaire Results

3. Additional Multirotor sUAS Flight Test Activities

a. Multirotor UAS MTEs in the Presence of Steady Winds

At the end of March 2019, the four multicopter MTEs originally flown in the AI were evaluated in the NASA LaRC 14 foot by 22 foot wind tunnel. The MTEs were conducted in steady winds from 0 to 25 mph. When available, analysis results will be made available to NASA via the technical point of contact for this program.

b. UMN System Identification Flights

1. Vehicle Description

The UMN multicopter is shown in Figure 41 with key parameters defined in Table 8.

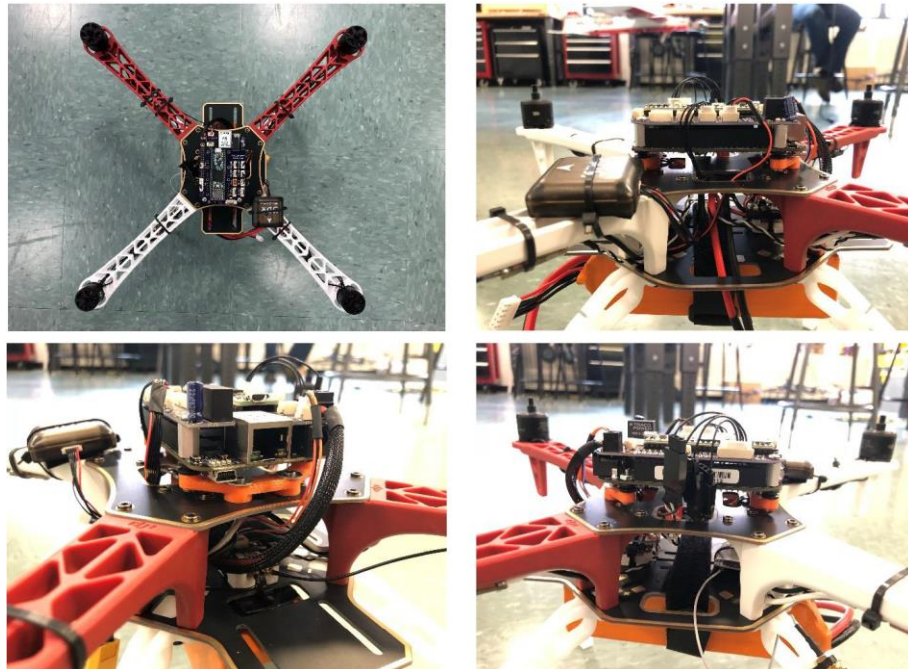


Figure 41: UMN Multic平

Table 8: UMN Multic平 Parameters

Parameter	Value
Length	14.5 inches
Width	14.5 inches
Height	9.0 inches
Weight with Battery	1280 g
Weight without Battery	800 g
Battery Type	5100mAh 4s 35c
Motors	DJI 2312E 960 kv
ESC	DJI 430 LITE 4S 30 A

2. Status of Flight Tests

The UAV lab personnel at UMN have been upgrading the multirotor flight control laws, so that they can better execute the system identification test plan. While not available to include in this report, the test plan will be conducted, and the analysis results will be made available to NASA via the technical point of contact for this program when available.

F. PHASE II SUMMARY AND CONCLUSIONS

1. Summary

The program described herein addressed the important need to define UAS handling qualities in both piloted and autonomous operations. The overall objective was to validate a UAS handling qualities assessment process via analysis to predict handling qualities and flight test to verify handling qualities. An end product of this program was the UAS Handling Qualities Assessment Process (UAS-HQ) and corresponding draft specification that is intended to guide UAS stakeholders through the systematic evaluation process defined herein.

The specific technical accomplishments, as repeated from the Project Summary, were as follows:

- UAS Handling Qualities Stakeholders from industry, academia, and government agencies were engaged throughout the two-year program. Highlights of this engagement include the three UAS Handling Qualities Workshops that were conducted; one at NASA LaRC and two as part of the AIAA SciTech conference. All the workshop presentations have been made available to the Stakeholders via an easily accessible website hosted by the University of Minnesota. There are no restrictions regarding access to this website.
- A process to define UAS handling qualities was defined, demonstrated, and validated through analysis and flight tests. Process validation has also been demonstrated by UAS Handling Qualities Stakeholders that conducted their own work in parallel with this program.
 - While it was beyond the scope of this program to quantify new UAS handling qualities requirements because of a significant lack of data, there has been a significant growth in the data that are now available in the public record.
 - The use of end-to-end system identification was used to demonstrate UAS model validation methods in both the frequency and time domains using both long and short duration command inputs. Furthermore, the frequency responses generated from the system identification tests were used to extract parameters that are used to predict handling qualities.
 - UAS handling qualities verification flight tests were conducted using a set of mission task elements defined for both fixed wing and rotary wing mission task elements.
 - Dynamic scaling methods show promise to preserve use of appropriate handling qualities criteria and mission task elements from piloted handling qualities specifications and standards.

2. Process Success Criteria

The following success criteria were used to evaluate the approach, methods, and process for defining UAS handling qualities:

- A simplified classification system and mission descriptions appropriately guide the user to the analytical requirements and analysis steps necessary to define predicted handling qualities and the mission task elements with defined performance requirements to establish flight-verified handling qualities.
- The candidate handling qualities metrics included in the toolbox and draft specification (e.g., aircraft bandwidth) satisfied the three prerequisites; validity, selectivity, and ready applicability.
- UAS flight test evaluations were conducted with fixed wing and multirotor exemplar aircraft to expand the available database, explore system identification methods as a means to update

predicted handling qualities, and define and evaluate mission task elements as a means to characterize UAS handling qualities in flight.

3. Conclusions and Next Steps

Based on the results of this Phase II program, the following conclusions are made:

- The extensive UAS Stakeholder outreach including three workshops with invited presentations from government, industry, and academic representatives achieved the desired “buy-in” of the community to the proposed evaluation process. Of significant importance was the complimentary work conducted by the Army Aviation Development Directorate as presented at all three workshops and in other published works.
- The handling qualities assessment process defined in this program provides the means to analytically predict UAS handling qualities using appropriate vehicle models and verify handling qualities via well-defined mission task elements.
- Established handling qualities metrics such as Aircraft Bandwidth that are response-type agnostic are well-suited for UAS applications as demonstrated in this program. Significantly more data are needed, however, to firmly establish desired/adequate, pass/fail, etc. requirements. Aircraft Bandwidth was also found to meet the requirements of validity, selectivity, and ready applicability.
- While more work is needed to refine descriptions and performance requirements, the fixed wing and rotary wing MTEs evaluated in this program provide an effective means to assess UAS handling qualities. The one exception was the visual line of sight precision lateral offset landing task that was not found to be an easily repeatable with the given the cueing environment. A pilot point of view precision lateral offset landing task, however, is a feasible MTE.
- Use of dynamic scaling should be explored further to more quickly establish handling qualities requirements and mission task elements for all categories of UAS.

Based on the results of this Phase II program, the following conclusions are made regarding the mission task elements attempted:

- Fixed Wing MTEs flown under remote pilot control, semi-autonomous control, and fully autonomous control.
 - The flightpath regulation in the presence of a discrete gust or SOS disturbance MTEs show promise. The limitations of the relatively low bandwidth attitude command loop closure of the UltraStick120 was clearly exposed by the tasks. This was a positive result as it clearly showed that the MTEs can expose handling qualities deficiencies. More work is also needed to properly size disturbance inputs and to more concretely define desired and adequate performance requirements.
 - The waypoint following task worked well as a fully autonomous MTE. Furthermore, this task also exposed the limitations of the UltraStick120 controller bandwidth. Because of these limitations, however, specific desired and adequate performance requirements remain a work in progress.
 - As a piloted task the precision offset landing requires more clearly defined reference points that may be difficult to create in a repeatable manner using standard visual line of sight references.
- Multirotor MTEs flown as piloted visual line of sight tasks.

- All four low speed piloted tasks worked well as evaluated in the NASA LaRC Autonomy Incubator. The low speed tasks are well suited to visual line of sight operations.
 - The hover boards provided well-defined performance requirement references.
 - The tasks can be readily applied to autonomous operations.

Given these technical accomplishments, the next steps in defining UAS handling qualities are as follows:

- Increase the available handling qualities flight test database beyond the limited sUAS data generated in this program. It will not be possible to accurately define predictive handling qualities requirements without a much larger flight test database.
- As the available database expands, address the “to be determined” elements of the draft specification with quantitative requirements.
- Expand the catalog of mission task elements to cover a wider design space of vehicle types and missions.
- Continue to explore dynamically scaling as a means to use existing requirements and mission task elements to a wider range of UAS weight classes.

REFERENCES

1. <http://www.tealgroup.com/index.php/about-teal-group-corporation/press-releases/118-2014-uav-press-release>, published on July 17, 2014, retrieved Jan 26, 2015.
2. Mitchell, D. G., R. H. Hoh, B. L. Aponso, and D. H. Klyde, *Proposed Incorporation of Mission-Oriented Flying Qualities into MIL-STD-1797A*, WL-TR-94-3162, Oct. 1994.
3. <http://www.washingtonpost.com/news/checkpoint/wp/2015/01/21/a-drone-crashes-in-the-middle-of-a-capitol-hill-hearing-about-drones/>, retrieved Jan. 22, 2015.
4. Anon., *FAA Faces Significant Barriers to Safely Integrate Unmanned Aircraft Systems into the National Airspace System*, AV-2014-061, Federal Aviation Administration, Washington, DC, 24 June 2014.
5. <http://www.washingtonpost.com/news/checkpoint/wp/2014/06/23/stop-saying-uh-oh-while-youre-flying-drone-crash-pilot-quotes-unveiled/>, retrieved June 23, 2014.
6. Holmberg, J. A., D. J. King, J. R. Leonard, and M. C. Cotting, “Flying Qualities Specifications and Design Standards for Unmanned Air Vehicles,” AIAA 2008-6555, presented at the *Atmospheric Flight Mechanics Conference*, Honolulu, HI, 18-21 Aug. 2008.
7. Cotting, M. C., “An Initial Study to Characterize Unmanned Aerial Vehicles for Flying Qualities Evaluation,” AIAA 2009-307 presented at the *47th Aerospace Sciences Meeting*, Orlando, FL, 5-8 Jan. 2009.
8. Stansbury, R. S., K. Rigby, J. Clifford, and D. Rudolph, “An Alternative UAS Classification and Analysis Approach for Integration into the National Airspace System,” AIAA 2015-1197 presented at *Infotech @ Aerospace*, Kissimmee, FL, 5-9 Jan. 2015.
9. Klyde, D. H., B. L. Aponso, and D. G. Mitchell, *Handling Qualities Demonstration Maneuvers for Fixed wing Aircraft, Volume I: Maneuver Development Process*, WL-TR-97-3099, Oct. 1997.
10. Cooper, G. E., and R. P. Harper, Jr., *The Use of Pilot Rating in the Evaluation of Aircraft Handling Qualities*, NASA TN D-5153, April 1969.
11. Anon., *Department of Defense Interface Standard, Flying Qualities of Piloted Aircraft*,” MIL-STD-1797B, Feb. 2006 [Distribution Statement D: Distribution authorized to the Department of Defense and U.S. DoD contractors only; contains critical technology (3 November 2005)].
12. Anon., Aeronautical Design Standard, Performance Specification: Handling Qualities Requirements for Military Rotorcraft, US Army Aviation and Missile Command, Redstone Arsenal, AL, ADS-33E-PRF, Mar. 2000.
13. Mitchell, D. G., D. B. Doman, D. L. Key, D. H. Klyde, D. B. Leggett, D. J. Moorhouse, D. H. Mason, D. L. Raney, and D. K. Schmidt, “Evolution, Revolution, and Challenges of Handling Qualities,” *J. Guidance, Control, and Dynamics*, Vol. 27, No. 1, Jan.-Feb. 2004, pp. 12-28.
14. Klyde, D. H., and D. G. Mitchell, *Handling Qualities Demonstration Maneuvers for Fixed wing Aircraft, Volume II: Maneuver Catalog*, WL-TR-97-3100, Oct. 1997.
15. Anon., “Summary of Small Unmanned Aircraft Rule (Part 107),” Federal Aviation Administration, Washington, D.C., June 21, 2016.
16. Anon., *ARC Recommendations Final Report*, Micro Unmanned Aircraft Systems Aviation Rulemaking Committee, April 1, 2016.
17. Anon., *Unmanned System Integrated Roadmap FY2011-2036*, Reference Number 11-S-3613, Department of Defense, September 2010.

18. Anon, *Aerospace - Vehicle Management Systems - Flight Control Design, Installation and Test of, Military Unmanned Aircraft, Specification Guide For*, SAE ARP94910, Society of Automotive Engineers, issued Dec. 2012.
19. Danowsky, B., P. Chrstos, J. R., Klyde, D. H., Farhat, C. and Brenner, M., "Evaluation of Aeroelastic Uncertainty Analysis Methods," *Journal of Aircraft*, Vol. 47, No. 4, July-August 2010, pp. 1266-1273.
20. Montgomery, D. C., Design and Analysis of Experiments, 5th Edition, John Wiley & Sons, Inc., New York, 2001.
21. Myers, R. H. and Montgomery, D. C., Response Surface Methodology: Process and Product Optimization using Designed Experiments, 2nd Edition, John Wiley and Sons, Inc., New York, 2002.
22. Lind, R. and M. J. Brenner, "Robust Flutter Margin Analysis That Incorporates Flight Data," NASA TP-1998-206543, March, 1998.
23. Lind, R. and M. Brenner, Robust Aerostervoelastic Stability Analysis, Springer-Verlag London Limited, Great Britain, 1999.
24. Zhou, K., J. C. Doyle, and K. Glover, Robust and Optimal Control, Prentice Hall, New Jersey, 1996.
25. Zhou, K. and J. C. Doyle, Essentials of Robust Control, Prentice Hall, New Jersey, 1998.
26. Dorobantu, A., W. Johnson, A. Lie, B. Taylor, A. Murch, Y. C. Paw, D. Gebre-Egziabher, and G. Balas, "An Airborne Experimental Test Platform: From Theory to Flight," *1st American Control Conference*, Washington D.C., June 2013.
27. MATLAB and Simulink Release 2012b, The MathWorks, Inc., Natick, MA, United States.
28. Hoh, R. H., D. G. Mitchell, and J. Hodgkinson, "Bandwidth — A Criterion for Highly Augmented Airplanes," *Criteria for Handling Qualities of Military Aircraft*, AGARD-CP-333, Apr. 1982, pp. 9-1 – 9-11.
29. Mitchell, D. G., and Hoh, R. H., *Development of Methods and Devices to Predict and Prevent Pilot-Induced Oscillations*, AFRL-VA-WP-TR-2000-3046, Jan. 2000.
30. Morelli, E.A., "Multiple Input Design for Real-Time Parameter Estimation in the Frequency Domain," Paper REG-360, *13th IFAC Symposium on System Identification, Rotterdam*, The Netherlands, August 2003.
31. Myers, T. T., B. L. Aponso, D. H. Klyde, T. J. Rosenthal, R. E Magdaleno, *FREDA, Frequency Domain Analysis Program User's Guide*, STI-WP-433-2, Systems Technology, Inc., 1988.
32. Cunningham, K., D. E. Cox, D. G. Murri, and S. E. Riddick, "A Piloted Evaluation of Damage Accommodating Flight Control Using a Remotely Piloted Vehicle," AIAA-2011-6451 presented at the *AIAA Guidance, Navigation, and Control Conference*, Portland Oregon, 8-11 Aug. 2011.

Appendix A – Emerging Handling Qualities Specification

A. INTRODUCTION

This appendix contains initial recommendations for establishing flying characteristics for Unmanned Aircraft (UA). It is intended to be a very preliminary specification that will promote discussion, eventually leading to a set of requirements that is accepted and applied throughout the UAS community.

Requirements proposed here follow the structure documented in Table 1 of the Phase I final technical report (Ref. 33). Some minor modifications have been made to that structure, but in general the format is as defined in the Phase I work.

Requirements are structured to follow the format of the SAE Aerospace Recommended Practices (ARP) 94910 (Ref. 34), “Aerospace - Vehicle Management Systems - Flight Control Design, Installation and Test of, Military Unmanned Aircraft, Specification Guide For.” It is not necessarily meant to suggest that we will use that structure, but for now it helps assure that we do not overlook any critical requirements for the proposed specification. For the most part, the requirements have been based on ARP94910, ADS-33E-PRF for piloted military rotorcraft (Ref. 35), MIL-STD-1797B for piloted military airplanes (Ref. 36), and FAA Title 14 Code of Federal Regulations (CFR) Parts 23 through 29 (the “FARs”) and related Advisory Circulars. Sources are listed for the requirements; additional explanations are included, especially in cases where the requirements have been modified from their source document.

Because MIL-STD-1797B is a limited-distribution document (Distribution Statement D, DoD and DoD Contractors Only), requirements will not be quoted verbatim here. Supporting graphics have been taken from reports with unlimited distribution.

B. TABLE OF DRAFT REQUIREMENTS

A list of the draft quantitative requirements is given in Table 9. A status of “Complete” is not meant to imply that no further input is desired. It simply reflects the subjective level of maturity for the proposed requirement, at this time, given our best assessment.

Table 9. Proposed Requirements and Current Status

Requirement	Rationale	Source Ref(s)	Status
1. Scope	States scope of the specification.	Based on Ref. 34	Complete
2. References and Definitions: 2.1 Applicable Documents; 2.2 Abbreviations, Acronyms, Symbols and Their Definitions	Required information for a formal spec; will be filled in as the spec is developed.	Only later parts of 2.3 (Definitions) have details at this time (see specific entries below)	Most TBD, major emphasis in current SBIR Phase II research work; 2.3 in relatively good shape
2.3.1.1 Flight Phase Categories	Currently a placeholder that will be replaced by a logical MTE-based structure	TBD	TBD – prefer to delete
2.3.1.2 Classification	Class depends upon mission more than any other factor; will be set with MTEs.	Weight classification from ref. 33	Tentative; may be able to add more details
2.3.1.3 Modes of Operation	Follows established definitions.	Ref. 34	Complete
2.3.1.4 Human Operator	Specifies what is meant by “operator.”	Ref. 34	Complete
2.3.1.5 Flight Envelopes	Divisions used in military specs, adopted by the FAA to allow for degradations in Flight Characteristics for uncommon wind, turbulence, and failure conditions.	Ref. 36	Complete
2.3.1.6 Flight Characteristics	Meant to encompass Stability & Control, Flying Qualities, Handling Qualities, Automatic Control, in concise terms.	Ref. 36	Complete
2.3.1.7 Levels of Flight Characteristics	Defines Levels 1, 2, and 3.	Ref. 36	Complete
2.3.1.8 Predicted and	Overall handling qualities requires both	Ref. 35	Confirm wording

Requirement	Rationale	Source Ref(s)	Status
Demonstrated Levels	analytical and practical evaluations		
2.3.1.8.1 Predicted Levels	Checks against the quantitative requirements of Section 3	Ref. 35	Might need tweaking
2.3.1.8.2 Demonstrated Levels	Checks against the MTEs of Section 3	Ref. 3	Might need tweaking
2.3.1.9 UA Control Systems and Functions	Definitions to help with interpretation of the requirements of the spec. Might prove unnecessary, but a placeholder for now.	TBD	TBD
3. Requirements	Detailed response requirements, separated by axis		
3.1 Trim and Stability	Trimmability is essential for safe flight; basic stability margin limits must be specified.	Based on Refs. 34, 35, and 36	Consider more detailed stability margin limits
3.1.5 Residual Oscillations	Need some upper limit on frequency and amplitude of residual oscillations, especially for ops near obstacles or people: can't have a LCO that endangers property.	Ref. 35	Needed more for confidence in stability than for controllability; deserves investigation
3.2 Pitch Axis Requirements			
3.2.1 Pitch Axis Dynamic Response to Control Inputs (Bandwidth)	The primary short-term requirement to assure good stability; for Manual ops, it will be a measure of the attitude response to manual control inputs; for others, it will be the response to onboard control commands	Appears in Refs. 35 and 36; limits for conventional UA from Refs. 37 and 40	Need considerable research to establish limits; TBD for now
3.2.2 Pitch Axis Damping	Bandwidth and Stability Margin should provide good damping; this is needed for instances where one or the other of those requirements is relaxed	Damping value from Ref. 35; pitch rate overshoot from Ref. 40	Complete
3.2.3 Pitch Axis Control Power	Verify that UA is capable of operating throughout its expected flight regime when pitch is the primary axis of control	Based on Ref. 35	Complete
3.2.4 Pitch Attitude Hold	Sets limits on pitch control if pitch attitude is a primary control method	Ref. 34	Need to verify limits
3.3 Roll Axis Requirements			
3.3.1 Roll Axis Dynamic Response to Control Inputs (Bandwidth)	The primary short-term requirement to assure good stability; for Manual ops, it will be a measure of the attitude response to manual control inputs; for others, it will be the response to onboard control commands	Ref. 35; proposed limits for conventional UA in Ref. 37	For piloted aircraft, roll BW is higher than pitch; we don't expect this to be true for autonomous UA: probably symmetrical
3.3.2 Roll Axis Damping	Same rationale as for pitch axis (3.2.2)	Damping value from Ref. 35	Complete
3.3.3 Roll Axis Control Power	Verify that UA is capable of operating throughout its expected flight regime when attitude is the primary control method	Based on Ref. 35	Complete
3.3.4 Roll Attitude Hold	Sets limits on roll control if roll attitude is a primary control method	Ref. 34	Need to verify limits
3.4 Yaw Axis Requirements			
3.4.1 Yaw Axis Dynamic Response to Control Inputs (Bandwidth)	Yaw control will be important for hovering UA, not so much for UA that fly like conventional airplanes	Ref. 35 provides numbers that are much too high for any aircraft	Detailed limits TBD
3.4.2 Yaw Damping	Precise nose pointing is required for some ops;	Similar to pitch	

Requirement	Rationale	Source Ref(s)	Status
	may be a very limited application	and roll	
3.4.3 Yaw Control Power	Similar in format to the pitch and roll requirements, with added wording for crosswind operations	Refs. 34 and 36 for conventional aircraft	Basic wording in place; need limits, MTEs
3.4.4 Heading Hold	Wording similar to pitch and roll paragraphs	Same as pitch and roll (for now)	First draft
3.5 Vertical (Heave) Axis Requirements			
3.5.1 Dynamic Response to Control Inputs	Two requirements depending upon primary vertical-axis control method		
3.5.1.1 When a Direct Vertical Control Effector is Provided	This is a version of the helicopter vertical control requirements: need to assure rapid and precise vertical-axis control		
3.5.1.1.1 Short-Term Response (Bandwidth)	Heave-axis Bandwidth and Phase Delay are a direct counterpart to requirements in other axes	Tentative limits in a study for piloted V/STOL ³⁸	Flight testing needed to define limits
3.5.1.1.2 Vertical-Axis Control Power	Some form of control power is justified, but details are still TBD	Using hover requirement from ADS-33	Limits from ADS-33 may be sufficient
3.5.1.2 When a Direct Vertical Control Effector is Not Provided	Flight path response for conventional aircraft: control h with elevator		
3.5.1.2.1 Short-Term Response (Bandwidth)	Assure rapid flightpath control with attitude changes	Concept based on requirement in 1797B ³⁶	Need to confirm limits from MIL standard
3.5.1.2.2 Vertical-Axis Control Power	Ability to arrest sink rate, and to climb if needed, is essential for normal operations of any UA	Studied in Air Force report for powered-lift STOLs ⁴⁴	Format is reasonable; confirm numbers from MTE tests
3.6 Transition Between Powered-Lift and Wing-Borne Flight	Studies with piloted V/STOLs have shown that there are stability and control power issues during transitions between vertical powered lift and purely wing-borne lift	Piloted-aircraft requirements developed in simulations ³⁹	Some research required just to determine scope of the issue for UA
3.6.1 Pitch Stability During Transition	Rapid shift in CG and CP during thrust rotation can create momentary instability; combined with large power changes, control margins can also be lost (V-22 experiences)		
3.6.1.1 Transition to STOL	This should be a very brief, but highly dynamic, portion of a typical flight profile	Ref. 39 allows momentary instability for Levels 2 & 3	Based on piloted VSTOL study; ³⁹ may be unnecessary for augmented UA
3.6.1.2 Transition to Hover	For a typical UA mission, hover will be a critical phase of flight; there should not be a loss of stability during the transition	Ref. 39 suggests stability be maintained through the hover	May end up with different pitch requirements (3.1) for hover; will need to reword this to reflect it
3.6.1.3 Coupling Between Pitch Attitude and Power	Pitch/power coupling is a common issue with some V/STOL designs; need to ensure no loss of control		
3.7 Transients Between Command Sources	UA that can be both manually and autonomously controlled should not exhibit undesirable dynamic responses during the transition in Modes of Operation; similarly, changes in waypoints should not cause undesirable responses		
3.7.1 Mode Switching	Switching between Manual, Assisted, and	ARP94910 ³⁴	Taken with

Requirement	Rationale	Source Ref(s)	Status
	Autonomous Modes should not result in large transients		modification from Ref. 34; needs verification
3.7.2 Guidance and Navigation Commands	Generation of new waypoints, switching from a Hold mode to waypoint tracking, or vice versa, should be relatively seamless	New requirement	Needs verification
3.8 Response to Turbulence and Gusts	Need to assure that the UA is stable in presence of gusts; for high turbulence, a performance degradation is allowed as long as control can be retained		
3.8.1 Dynamic Response to Turbulence	With no pilot onboard, the concern is more loss of control than ride qualities	Qualitative statement only at this time	Need flight data and detailed study of models of turbulence
3.8.2 Response to a Unit Gust	Flight path deviations and ability to recover to initial course will be paramount	Gust based on that defined in MIL-STD-1797B ³⁶	Needs mod to be time-based, not distance-based
3.9 Response to Failures	This will be a substantial effort to undertake; considerable insight can be gained from SAE ARP-94910 ³⁴ , ADS-33E-PRF ³⁵ , and MIL-STD-1797B ³⁶	Qualitative statement only at this time	Need flight data
4. Mission Task Elements	Practical demonstration of capability, using well-defined maneuvers that represent small portions of a typical mission, will carry equal importance to the requirements in section 3.	TBD	Flight testing is ongoing to define suitable MTEs

C. RECOMMENDED REQUIREMENTS

1. SCOPE

This document establishes recommended practices for the specification of general performance, design, test, development, and quality assurance requirements for the flying and handling qualities of Unmanned Aircraft (UA), the airborne element of Unmanned Aircraft Systems (UAS). The document is written for unmanned aircraft intended for use primarily in civilian operational areas. The document also provides a foundation for considerations applicable to safe flight in all classes of airspace.

2. REFERENCES

2.1 Applicable Documents

2.2 Abbreviations, Acronyms, Symbols and Their Definitions

[To be assembled.]

2.3 Definitions

2.3.1 UA Design and Operational Categorization Schemes

2.3.1.1 Flight Phase Categories

[To be developed.]

2.3.1.2 Classification

UA shall be classified according to weight, mission, and modes of operation (2.3.1.4). The UA shall be classified according to the following weight ranges:

Weight Class I: weight \leq 0.55 pounds (μ UA)

Weight Class II: $0.55 < \text{weight} < 55$ pounds (sUA)

Weight Class III: weight ≥ 55 pounds (UA)

For this classification, “weight” refers to the heaviest expected weight of the vehicle during its normal flight operation.

2.3.1.3 Modes of Operation

MANUAL: Those modes of operation wherein the operator provides, in at least one phase of flight, direct and continuous control of the UA, acting as an element of the UA control inner loop by directly manipulating control force effectors and engine power setting and employing visual cues, video feedback or other sensory feedback, in combination or individually. The onboard UA control system may still be augmenting stability but the trajectory of the vehicle is completely dependent upon continuous control inputs from the operator.

ASSISTED: Those modes of operation wherein the operator periodically adjusts UA outer loop controlled states such as airspeed, altitude, heading, climb/descent rate, etc., and determines or adjusts the waypoints the vehicle should fly to. In the absence of new inputs, the UA control system maintains the last controlled states.

AUTONOMOUS: Those modes of operation wherein the UA executes a pre-planned mission and the operator plays no part in the UA control outer loop but may provide decision-making, supervisory or initiation and termination inputs. In this mode of operation, the UA may also generate waypoints independently of the mission plan or otherwise alter trajectory autonomously based on decisions made aboard the vehicle.

NOTE: At the time of writing, competing schemes exist defining Levels of Autonomy (LOA) and no single standard has been generally adopted. The higher levels of mission autonomy, when defined and employed, are not expected to require levels of VMS capability beyond those presently defined by this specification.

2.3.1.4 Human Operator

The human being responsible for controlling, directing or supervising the operation of the UA from a remote CS. The operator is responsible for the safe, orderly flight of one or more UA, as related to this physical control capability. The operator is often trained and identified by a government agency as a pilot. In the civil field the term is often used for the organization responsible for the UA but it is never used in this manner in this document. The term Operator is analogous to the term Pilot in Command, for a manned aircraft.

2.3.1.5 Flight Envelopes

For the purpose of this specification, the flight envelopes are defined as follows:

Operational Flight Envelopes: The Operational Flight Envelopes define the boundaries in terms of speed, altitude, and normal acceleration within which the aircraft must be capable of operating in order to accomplish the required missions. Envelopes for each applicable Flight Phase are defined by the prime contractor in the UA Detail Specification.

Service Flight Envelopes: For each Aircraft Normal State, the prime contractor defines, in the Aircraft Detail Specification, Service Flight Envelopes showing the combinations of speed, altitude, and normal acceleration derived from aircraft limits, as distinguished from the mission requirements. For each applicable Flight Phase and Aircraft Normal State, the boundaries of the Service Flight Envelopes can be coincident with or lie outside the corresponding Operational Flight Envelopes, but in no case do they fall inside those Operational Boundaries.

Permissible Flight Envelope: The prime contractor defines Permissible Flight Envelopes, which encompass all regions in which operation of the aircraft is both allowed and possible. These envelopes define boundaries in terms of speed, altitude, and normal acceleration. From all points in the permissible flight envelope, it should be possible to consistently return to the service flight envelope.

2.3.1.6 Flight Characteristics

Defined in terms of measures based upon the expected response to human operator control inputs. For operations in all three modes, flight characteristics consist of Flying Qualities metrics; for manual control, and in some conditions assisted control, additional requirements are based on Handling Qualities evaluations by a trained operator.

FLYING QUALITIES are defined as the stability and control characteristics that have an important bearing on the safety of flight and on the ease of operation of the air vehicle in steady flight and in maneuvers. They are defined in terms of measurable analytical and empirical parameters or criteria that can be measured for a given UA.

HANDLING QUALITIES are those qualities or characteristics of a UA that govern the ease and precision with which an operator or autonomous system is able to perform the tasks required in support of the UA's role.

2.3.1.7 Levels of Flight Characteristics

Three levels of UA flight characteristics are defined. The levels are as follows:

Level 1: Flight characteristics clearly adequate for the Mission Task Element.

Level 2: Flight characteristics adequate to accomplish the Mission Task Element, but some degradation in mission effectiveness exists.

Level 3: Flight characteristics such that the aircraft can be controlled safely, but mission effectiveness is inadequate. Category A Mission Task Elements can be terminated safely, and Category B and C Mission Task Elements can be completed.

2.3.1.8 Predicted and Demonstrated Levels

The overall UA Level of handling qualities shall be a combination of the two distinct methods of assessment, Predicted Levels and Demonstrated Levels.

2.3.1.8.1 Predicted Levels

To obtain the Predicted Levels of handling qualities, the UA's handling qualities parameters shall be determined and compared with the criteria limits appropriate to the UA's operational requirements. For the predicted Level of handling qualities to be Level 1, the UA shall meet the Level 1 standards for all of the criteria. Violation of any one requirement is expected to degrade handling qualities. Violation of several individual requirements (e.g., to Level 2) could have a synergistic effect so that, overall, the handling qualities degrade to Level 3, or worse.

2.3.1.8.2 Demonstrated Levels

To determine the Demonstrated Level of handling qualities, the UA shall perform all designated MTEs. Meeting or exceeding the Desired performance limits for all designated MTEs shall be considered to demonstrate Level 1 handling qualities. Meeting or exceeding the Adequate performance limits for any designated MTE shall demonstrate Level 2 handling qualities. Failure to achieve at least Adequate performance for any designated MTE shall be considered Level 3 handling qualities.

2.3.1.9 UA Control Systems and Functions

[To be defined.]

3. REQUIREMENTS

3.1 Trim and Stability

3.1.1 Trim for Hovering UA

It shall be possible to achieve a stable hover in calm air, and in a steady wind of up to 15 kt from the most critical direction.

3.1.2 Trim for Manually Controlled UA

It shall be possible to trim all operator effector forces to zero for any airspeed in the Operational Flight Envelope.

3.1.3 Stability

All transients from trimmed flight shall be stable for any airspeed expected to be encountered in flight.

3.1.4 Aerodynamic Closed-Loop Stability Margins

An aerodynamic loop is one which relies on aerodynamics and/or thrust vectoring for loop closure such as stability augmentation. For automatic modes, the stability requirement applies only to the airspeed range of operation of these modes. In multiple loop systems, variations should be made with all feedback paths held at their nominal values except for the path under investigation. A path is defined to include those elements connecting feedback sensors to a force or moment effector. The loop breaks for analysis should be made at the input to the mixer or control allocation.

For all flight conditions within the Operational and Service Flight Envelopes, aerodynamic closed-loop stability margins shall be at least 6.0 dB gain margin and 45 degrees phase margin. These margins may be relaxed for failure cases and for flight in the Permissible Flight Envelopes provided the closed-loop system meets the requirement of 3.1.3.

3.1.5 Residual Oscillations

Any sustained oscillations in any axis in calm air shall not interfere with the UA's ability to perform the specified Mission-Task-Elements. For Level 1, oscillations in attitude and in acceleration greater than 0.5 degrees and 0.05g shall be considered excessive for any Response-Type and Mission-Task-Element. Residual motions that are classified as a vibration shall be excluded from this requirement. Residual motions that are to be classified as vibrations shall be subject to Government approval.

3.2 Pitch Axis Requirements

3.2.1 Pitch Axis Dynamic Response to Control Inputs (Bandwidth)

If angular attitude is used as a primary controller, the pitch attitude response to longitudinal control inputs shall meet the limits specified in Table 10. The Aircraft Attitude Bandwidth (ω_{BW}) and Phase Delay (τ_p) parameters shall be obtained from frequency responses as defined in Figure 42.

Table 10: Pitch Aircraft Attitude Bandwidth and Phase Delay Limits

Flying Qualities Level	Minimum Bandwidth, ω_{BW} (rad/s)	Maximum Phase Delay, τ_p (s)
Level 1	TBD	TBD
Level 2	TBD	TBD

3.2.2 Pitch Axis Damping

All oscillatory modes resulting from aerodynamics or flight control system functions shall have a damping ratio of at least 0.3. For UA where precise nose pointing is required, the limit is increased to 0.7. In addition, the pitch rate overshoot parameter $\Delta G(q)$, defined in Figure 43, shall be less than TBD dB for Level 1 and TBD dB for Level 2.

3.2.3 Pitch Axis Control Power

The effectiveness of the pitch control shall not affect performance of any of the required tasks of the UA. Further, if angular attitude is used as a primary controller, pitch control power shall be sufficient to achieve the range of airspeeds required for normal operation, with sufficient control margin to counter gusts and upsets that might be encountered in normal operation.

3.2.4 Pitch Attitude Hold

If pitch Attitude Hold is provided as an operator workload relief function, or as a normal operational state for Assisted or Autonomous UA, pitch attitude shall be maintained in smooth air with a static accuracy of ± 1.0 degree pitch attitude with respect to the reference attitude. Accuracy requirements shall be achieved and maintained within 5 s of mode engagement for a 5 degree attitude disturbance. Upon completion of an operator-controlled maneuver, the aircraft attitude maintained by the VMS shall be the aircraft attitude at the time the commanded forces were removed, if this attitude is within the limits of the Attitude Hold mode.

Phase delay:

$$\tau_p = \frac{\Delta\Phi_{2\omega_{180}}}{57.3(2\omega_{180})}$$

Note: If phase is nonlinear between ω_{180} and $2\omega_{180}$, τ_p shall be determined from a linear least squares fit to phase curve between ω_{180} and $2\omega_{180}$

Caution:

For ACAH, if $\omega_{BWgain} < \omega_{BWphase}$ or if ω_{BWgain} is indeterminate, the rotorcraft may be PIO prone for super-precision tasks or aggressive pilot technique.

Rate response-types:

ω_{BW} is lesser of ω_{BWgain} and $\omega_{BWphase}$

Attitude Command/Attitude Hold Response-Types (ACAH):

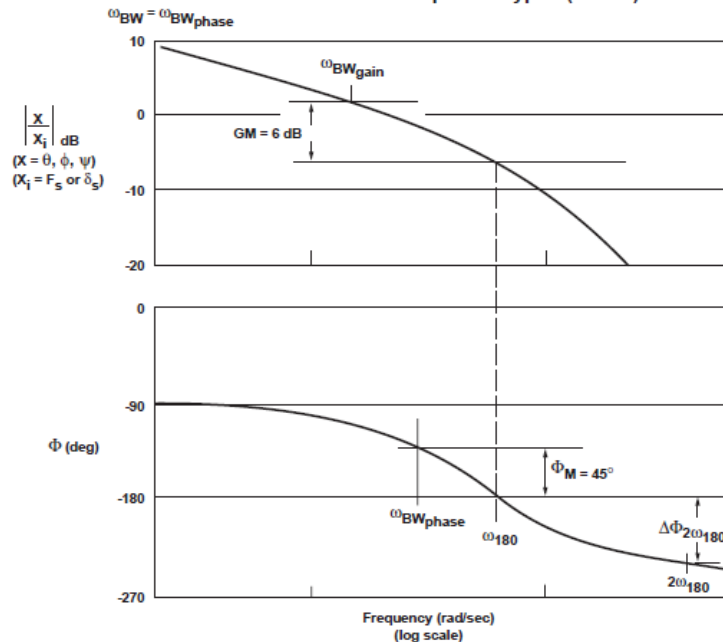


Figure 42: Definitions of Aircraft Attitude Bandwidth and Phase Delay

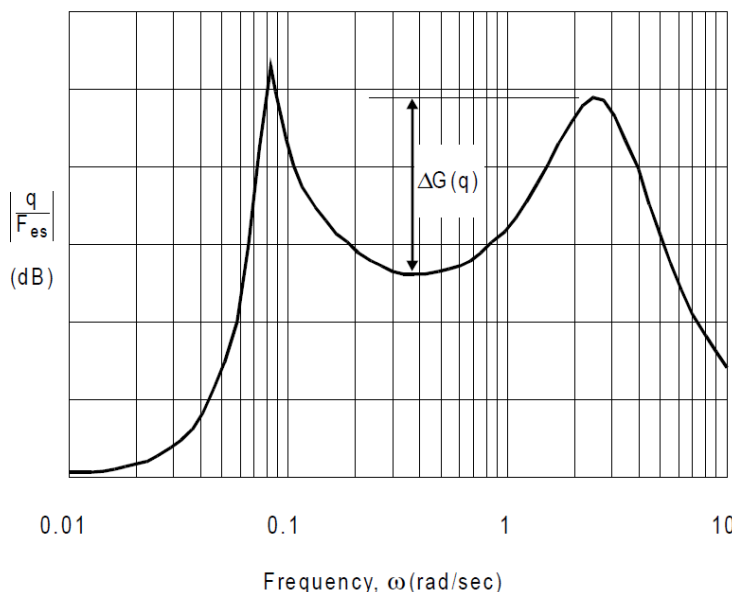


Figure 43: Definition of Pitch Rate Overshoot

3.2.5 Pitch Responses to Turbulence and Gusts

To be developed.

3.2.6 Pitch Response to Failures

TBD.

3.3 Roll Axis Requirements

3.3.1 Roll Axis Dynamic Response to Control Inputs (Bandwidth)

If angular attitude is used as a primary controller, the roll attitude response to lateral control inputs shall meet the limits specified in Table 11. The Aircraft Attitude Bandwidth (ω_{BW}) and Phase Delay (τ_p) parameters shall be obtained from frequency responses as defined in Figure 42.

Table 11: Roll Aircraft Attitude Bandwidth and Phase Delay Limits

Flying Qualities Level	Minimum Bandwidth, ω_{BW} (rad/s)	Maximum Phase Delay, τ_p (s)
Level 1	TBD	TBD
Level 2	TBD	TBD

3.3.2 Roll Axis Damping

All oscillatory modes resulting from aerodynamics or flight control system functions shall have a damping ratio of at least 0.3. For UA where precise nose pointing is required, the limit is increased to 0.7.

3.3.3 Roll Axis Control Power

The effectiveness of the roll control shall not affect performance of any of the required tasks of the UA. Further, if angular attitude is used as a primary controller, roll control power shall be sufficient to achieve the range of airspeeds required for normal operation, with sufficient control margin to counter gusts and upsets that might be encountered in normal operation.

3.3.4 Roll Attitude Hold

If roll Attitude Hold is provided as an operator workload relief function, or as a normal operational state for Assisted or Autonomous UA, roll attitude shall be maintained in smooth air with a static accuracy of ± 1.0 degree roll attitude with respect to the reference attitude. Accuracy requirements shall be achieved and maintained within 5 s of mode engagement for a 5 degree attitude disturbance. Upon completion of an operator-controlled maneuver, the aircraft attitude maintained by the VMS shall be the aircraft attitude at the time the commanded forces were removed, if this attitude is within the limits of the Attitude Hold mode.

3.3.5 Roll Response to Turbulence and Gusts

To be developed.

3.3.6 Roll Response to Failures

TBD.

3.4 Yaw Axis Requirements

3.4.1 Yaw Axis Dynamic Response to Control Inputs (Bandwidth)

If angular attitude is used as a primary controller, the yaw attitude response to directional control inputs shall meet the limits specified in Table 12. The Aircraft Attitude Bandwidth (ω_{BW}) and Phase Delay (τ_p) parameters shall be obtained from frequency responses as defined in Figure 42.

Table 12: Yaw Aircraft Attitude Bandwidth and Phase Delay Limits

Flying Qualities Level	Minimum Bandwidth, ω_{BW} (rad/s)	Maximum Phase Delay, τ_p (s)
Level 1	TBD	TBD
Level 2	TBD	TBD

3.4.2 Yaw (Heading) Axis Damping

All oscillatory modes resulting from aerodynamics or flight control system functions shall have a damping ratio of at least 0.3. For UA where precise nose pointing is required, the limit is increased to 0.7.

3.4.3 Yaw Control Power

The effectiveness of the yaw control shall not affect performance of any of the required tasks of the UA. Further, yaw control power shall be sufficient to achieve the range of airspeeds required for normal operation, with sufficient control margin to counter gusts and upsets that might be encountered in normal operation. Takeoff, approach, and landing in crosswinds up to TBD knots shall not be limited by yaw control power.

3.4.4 Heading Hold

If Heading Hold is provided as an operator workload relief function, or as a normal operational state for Assisted or Autonomous UA, heading shall be maintained in smooth air with a static accuracy of ± 1.0 degree heading error with respect to the reference heading. Accuracy requirements shall be achieved and maintained within 5 s of mode engagement for a 5 degree heading disturbance. Upon completion of an operator-controlled maneuver, the aircraft heading maintained by the VMS shall be the aircraft heading at the time the commanded forces were removed.

3.5 Vertical (Heave) Axis Requirements

3.5.1 Vertical (Heave) Axis Dynamic Response to Control Inputs

3.5.1.1 When a Direct Vertical Control Effector is Provided

3.5.1.1.1 Short-Term Response (Bandwidth)

Short-term heave response to vertical control inputs shall meet the limits specified in Table 13. The Aircraft Vertical-Axis Bandwidth (ω_{BW}) and Phase Delay (τ_p) shall be obtained from frequency responses as defined in Figure 44.

Table 13: Vertical Response Bandwidth and Phase Delay Limits

Flying Qualities Level	Minimum Bandwidth, ω_{BW} (rad/s)	Maximum Phase Delay, τ_p (s)
Level 1	TBD	TBD
Level 2	TBD	TBD

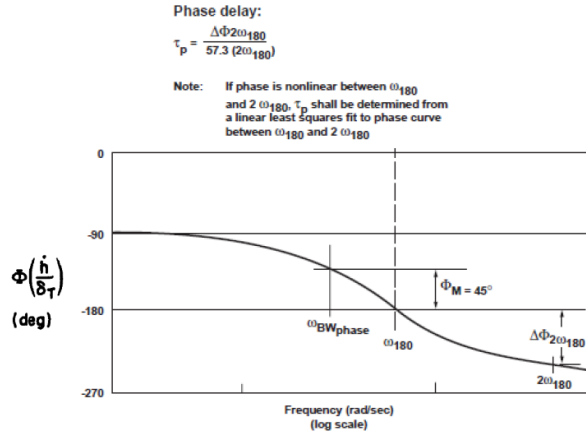


Figure 44: Definition of Vertical-Axis Bandwidth and Phase Delay

3.5.1.1.2 Vertical-Axis Control Power

From a spot hover with the wind vector from the most critical speed and direction at a velocity of up to 35 knots, and with the most critical loading and density altitude, for Level 1 it shall be possible to achieve a vertical rate of at least TBD ft/min, 1.5 seconds after initiation of a rapid displacement of the collective control from trim. The minimum vertical rates shall be TBD ft/min for Level 2 and TBD ft/min for Level 3. Pitch, roll, and heading shall be maintained essentially constant.

3.5.1.2 When a Direct Vertical Control Effector is Not Provided

3.5.1.2.1 Short-Term Response (Bandwidth)

The relation of flight path response to changes in pitch attitude following control inputs shall be such that the flight path Bandwidth frequency is greater than TBD rad/sec but less than TBD rad/sec for Level 1. These limits are TBD rad/sec and TBD rad/sec, respectively, for Level 2. Flight path Bandwidth is defined as the frequency at which the response of flight path angle, measured at the center of gravity, lags control inputs by 135 degrees.

3.5.1.2.2 Vertical-Axis Control Power

It shall be possible to achieve a steady-state flight path angle change as specified in Table 14 without reconfiguring the UA.

Table 14: Minimum Achievable Flight Path Angle Change

MTE	Level	Minimum Flight Path Angle Change (from Trim) (deg)	
		Up $\Delta\gamma$	Down $\Delta\gamma$
Landing Approach	1	TBD	TBD
	2	TBD	TBD
Offset Landing	1	Level Flight + TBD deg	TBD
	2	Level Flight + TBD deg	TBD

3.6 Transition Between Powered-Lift and Wing-Borne Flight

3.6.1 Pitch Stability During Transition

3.6.1.1 Transition to STOL

For Level 1, the requirements of 3.2 shall be met during the transition from forward flight to STOL. For Levels 2 and 3, any loss of pitch stability in this flight regime shall not result in a time to double pitch attitude of less than TBD seconds for Level 2 and TBD seconds for Level 3.

3.6.1.2 Transition to Hover

There shall be no degradation in pitch stability in the transition from STOL to hover.

3.6.1.3 Coupling Between Pitch Attitude and Power

Changes in power (thrust level) shall not result in excessive changes in pitch attitude. The maximum coupling between power and pitch attitude shall be less than TBD deg change in peak pitch attitude per change in percent thrust for Level 1. For Levels 2 and 3, changes in power shall not result in unrecoverable changes in pitch attitude.

3.7 Transients Between Command Sources

3.7.1 Mode Switching

With the UA in trimmed, level flight, switching between Modes shall not result in exceedance of the Operational Flight Envelope. In addition, transients resulting from Mode switching during Precision, Aggressive MTES shall not be greater than ± 0.05 g and ± 1 degree bank. For all other MTEs, transients shall not be greater than ± 0.5 g and ± 10 degrees bank angle.

3.7.2 Guidance and Navigation Commands

Switching between waypoints or Hold modes shall not result in exceedance of the Operational Flight Envelope. This includes introduction of new waypoints, whether from a manual operator or from onboard guidance, and switching to or from Heading or Altitude Hold and waypoint navigation.

3.8 Response to Turbulence and Gusts

3.8.1 Dynamic Response to Turbulence

When flying in the Operational Flight Envelope, the UA shall be capable of countering any turbulence that may be encountered in normal maneuvering. Turbulence that results in a momentary incursion out of the OFE shall not result in loss of positive control, and return to the OFE shall always be achievable following the excursion.

3.8.2 Response to a Unit Gust

The UA shall be capable of safely responding to a unit gust applied in the most critical direction.

The gust shall have a “1 – cosine” shape as shown in Figure 46. The gust shall be applied to the most direct controller for vertical flight path (e.g., elevator for a conventional UA or rotor RPM/collective for a VTOL UA), with magnitude v_m selected to provide an altitude change of at least 10 ft in one second after application, determined for the UA with outer-loop hold modes (or pilot intervention, for manually controlled) inactive. The distance d_m shall be tuned to the estimated rigid-body short-term response mode of interest. It is acceptable to replace the “1 – cosine” shape with a discrete gust.

The “1 – cosine” gust has the following shape:

$$\begin{aligned}
 v &= 0 && \text{for } x < 0 \\
 v &= v_m [1 - \cos(\pi x/d_m)]/2 && \text{for } 0 \leq x \leq d_m \\
 v &= v_m && \text{for } x > d_m
 \end{aligned}$$

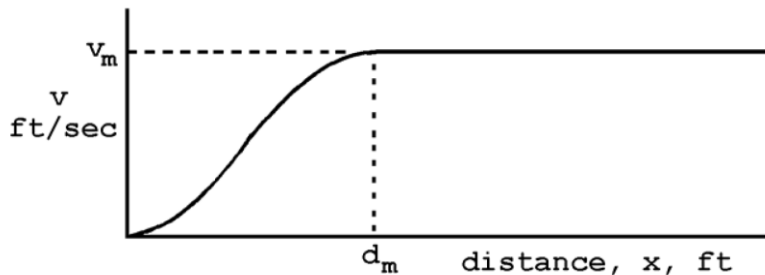


Figure 45: “1 – cosine” Shape for Discrete Gust

3.9 Response to Failures

For flight in the Operational Flight Envelope, no single failure of the flight control system, including propulsion and powered lift components, shall result in loss of control. Momentary excursions outside the OFE are permitted, provided the UA returns to stable flight within the OFE within a reasonable time.

Occurrence of more than one failure shall not result in loss of control of the UA; it is acceptable, however, that the handling qualities degrade outside the OFE for the duration of the flight, provided the limits of the Permissible Flight Envelope are not exceeded.

4. MISSION TASK ELEMENTS

TBD.

D. RATIONALE FOR REQUIREMENTS

1. SCOPE

This overarching statement, adopted from Ref. 34, will set the breadth – and define the limitations – of the document as it evolves. ARP94910 specifically calls out military aircraft; in this case we are directing the requirements toward civil aircraft, but many of the requirements are applicable in either case.

2. REFERENCES AND DEFINITIONS

2.1 Applicable Documents

2.2 Abbreviations, Acronyms, Symbols and Their Definitions

To be assembled.

2.3 Definitions

2.3.1 UA Design and Operational Categorization Schemes

2.3.1.1 Flight Phase Categories

This designation may not be applied to the specification at all. As discussed in the Phase I final report (Ref. 33), the intent is to move to MTEs as the driving force instead of Flight Phases and Categories. This paragraph is a placeholder in the event that it is discovered during the Phase II research that some definition is still justified.

2.3.1.2 Classification

Another definition that may be eliminated in an MTE-driven specification. What should matter most is the intended use of the UA, but there is a precedent for keeping some other classification for operation in civil airspace, so a weight-based classification is currently proposed.

2.3.1.3 Modes of Operation

Specification requirements – especially those dictated by MTEs – must acknowledge the degree of operator interactions in the performance of vehicle missions. This set of definitions comes from ARP94910 and provides a method for specifying that degree of interactions.

As the note in this paragraph states, “[a]t the time of writing, competing schemes exist defining Levels of Autonomy (LOA) and no single standard has been generally adopted.” Various documents divide LOA into four – and up to as many as 11 – different autonomy levels. For specification of UA handling qualities, the proposed levels in ARP94910 seem sufficient; there is no “fully-autonomous” mode in this document as it is felt that UA that operate entirely autonomously must have equivalent dynamic response characteristics of those that may receive operator-based waypoint guidance. Inner-loop stabilization and outer-loop guidance responses should be generated onboard and not from a ground operator.

There is an obvious challenge, of course: many UA are intended to be autonomous for a portion of their missions, with some degree of operator interaction at other times. It is incumbent on the procuring activity and the designer to come to agreement on the specific modes of operation to be applied for specific MTEs. Such an agreement should be set in advance of initial design.

2.3.1.4 Human Operator

In concert with the Modes of Operation, this paragraph, taken from ARP94910, clarifies what is meant by “human operator.”

2.3.1.5 Flight Envelopes

Commensurate with levels of flight characteristics, envelopes where the UA could operate must also be specified. There is no reason to demand the same response characteristics in calm winds and in winds at the limit of control for the UA.

2.3.1.6 Flight Characteristics

These are the MIL-STD-1797B (Ref. 36) definitions of flying qualities and handling qualities. They are as applicable for unpiloted aircraft as for piloted ones.

2.3.1.7 Levels of Flight Characteristics

Unlike requirements that dictate airworthiness, where the goal is to insure a reasonable level of flight safety, the requirements on flight characteristics must have a wider application. It is possible that the UA will be entirely “safe” (to a well-established probability), but may not be able to fully perform its intended mission; or it may be suitable to complete a mission, but with heightened attention on the part of the operator. Levels of flight characteristics allow for degraded operations with some loss of efficiency or performance, or an increase in risk of failure for completing the mission entirely, without simply applying “go” or “no go” criteria.

Conditions of failed states, increased turbulence or winds, etc., can lead to degraded task performance even if the aircraft itself is functioning as intended. These external variables can also cause a reduction in the level of flight characteristics.

The Levels stated are taken directly from MIL-STD-1797B,³⁶ but we have replaced “mission flight phase” with “Mission Task Element,” in keeping with our objective of using MTE as the mission driver.

2.3.1.8 Predicted and Demonstrated Levels

2.3.1.8.1 Predicted Levels

2.3.1.8.2 Demonstrated Levels

Assessment of handling qualities is not limited to analysis, nor to flight testing. Analysis is critically important, of course, and with a validated simulation model, it is possible to quickly check compliance with the quantitative requirements in Section 3 for a myriad of flight conditions and configurations.

Flight demonstration, by contrast, is much more challenging and, or necessity, limited in scope. The MTEs in Section 4 are intended to be methods of test for demonstrating handling qualities, but the range of conditions and configurations will be much more narrow than is possible for analytical study.

This set of definitions is taken, with slight modification, from ADS-33E-PRF (Ref. 35). That specification for rotorcraft is the first attempt to acknowledge that neither analysis nor flight test is a complete method for compliance, and that overall assessment of handling qualities is a logical combination of the two methods. The most significant changes are renaming “Assigned Levels” to “Demonstrated Levels,” and removal of any mention of pilot-assigned handling qualities ratings. In the UA specification, consistent demonstration of MTEs is sufficient to confirm Levels of handling qualities.

2.3.1.9 UA Control Systems and Functions

2.3.2 Flight Control Functional Classifications

Appearing in ARP94910 (Ref. 34), these sections define the Mission and Vehicle Management Systems and the Utility and Propulsion Control Systems; and the functions of the flight control system. All the material in these sections is very useful, and if we need the material, we may simply cross-reference the ARP.

3. REQUIREMENTS

3.1 Trim and Stability

3.1.1 Trim for Hovering UA

There is an obvious need for trimmability, and this paragraph serves as an example of what is expected to appear in the specification. There will be additional requirements for trim in fixed wing UAs.

3.1.2 Trim for Manually Controlled UA

Some statement requiring trim for manually-controlled aircraft is needed. This paragraph may very well evolve as the Phase II research is conducted.

3.1.3 Stability

A sweeping statement for “stability” in general, as reflected in response to external forces.

3.1.4 Aerodynamic Closed-Loop Stability Margins

This requirement is taken from SAE ARP94910 (Ref. 34) with some simplification. Since the aerodynamic loops are more critical than ever on highly-augmented (and especially autonomous) aircraft, this paragraph is almost certain to expand as the Phase II research is performed. Extension of the stability margins to flexible aircraft, as is done in the ARP, is a topic for future research.

3.1.5 Residual Oscillations

This requirement is meant as a placeholder for now; the numbers are reasonable for piloted aircraft, and may be suitable for any UA on which there is a human occupant, but more work is needed to set limits for smaller UA. In any case, a clear delineation between “residual oscillations” and vibration must be made, and a method devised to separate the two: tolerance for very high-frequency vibrations may be lower – or perhaps in some cases higher – than the limits for low-frequency residual oscillations. A future version of the specification will probably contain a very different set of requirements for limits on residual oscillations, including methods to determine just what those oscillations might be.

3.2 Pitch Axis Requirements

3.2.1 Pitch Axis Dynamic Response to Control Inputs (Bandwidth)

Aircraft Attitude Bandwidth is a fundamental measure of the quality of angular responses to control inputs. The specific requirements and definition are taken from ADS-33E-PRF and AFWAL-VA-WP-TR-2000-3046 (Ref. 40), but similar requirements – with different limits – appear in MIL-STD-1797B as well. The intent is to place response limits on any controller that commands pitch attitude changes to translate over the earth, or to increase or decrease speed or altitude; we will have separate requirements for aircraft that use direct force control, rather than by tilting the airframe, for those purposes.

Values in Table 10 are obviously a major focus of the Phase II research effort. The table is intended purely as a placeholder for now.

While there is a vast database for piloted fixed- and rotary-wing aircraft, there is no documentation at all of the possible requirements for UAs. In fact, based on an assessment of Bandwidth for UAs, we expect that most small vehicles will meet the numbers easily, especially for autonomous operation; Bandwidth frequencies as high as 10 rad/s are possible for such aircraft (Ref. 41). On the other end of the spectrum, operator-controlled aircraft such as Predator and Reaper exhibit very high Phase Delay, as total throughput delay for beyond-line-of-sight operations is close to 2 s. Pilots are not required to perform precision tracking operations with such UAs, and in fact, some relief is provided by the incorporation of gimballed sensors, so that the demands on the system are shared with the sensor. The impact on handling

qualities on this combination of aircraft-plus-sensor has yet to be fully explored; initial concepts are available in a PhD dissertation that investigates a unified set of criteria for the entire system (Ref. 42).

3.2.2 Pitch Axis Damping

The damping ratio limit of 0.3 comes from ARP94910 and the pitch rate overshoot parameter from AFWAL-VA-WP-TR-2000-3046. As discussed in the latter reference, Aircraft Bandwidth reduces the chance for low damping, but does not prevent it. This requirement prevents low damping in the pitch axis. For UA, system damping must be reasonably high to begin with. Whether “reasonably high” corresponds to a damping ratio of 0.3 may be a matter for future debate, but it is certain that anything much lower will result in an aircraft that is too easily excited to oscillate in pitch without direct suppression of the oscillations.

If the UA is to provide precise attitude control – surveillance with a fixed optical sensor, for instance – a damping ratio of 0.3 is simply too low. We have increased the lower limit to 0.7, and there may be justification for even higher values of damping.

3.2.3 Pitch Axis Control Power

There are very specific requirements on pitch control power in the piloted specification MIL-STD-1797B, but they are obviously intended to provide the pilot with sufficient power to perform tasks such as takeoffs and landings, stall recovery, etc. Those requirements, while important for pilot-in-the-loop operations, are of lesser importance for UAs, especially those that operate autonomously.

We may find it prudent to incorporate a subset of the piloted-airplane requirements for fully Manual flight, and for Assisted flight when the pilot is in the loop. In addition, just what constitutes “sufficient” control power, and the level of gusts and upsets to be applied, should be defined and included in the specification. At this time, the general statements given here are considered guidance to the designer.

3.2.4 Pitch Attitude Hold

Some form of pitch Attitude Hold (AH) will be essential on all but the most rudimentary manually controlled UAs. The technology to achieve a reasonable level of AH can be achieved with very low cost, but some low-cost attitude sensor and control systems are prone to limit-cycle oscillations (LCO) or reference drift over time. This requirement, taken with some modification from ARP94910, assures long-term AH. The biggest change from ARP94910 is opening the pitch static accuracy requirement from ± 0.5 degree to ± 1.0 degree. For a vehicle such as a hovering aircraft carrying an external load, the tightness of the AH is of secondary importance to the ability to stabilize the load. We have also removed a line specifying rms accuracy in disturbances – important, but in need of research that will be a focus in Phase II.

3.2.5 Pitch Axis Response to Turbulence and Gusts

This requirement is TBD. There are very detailed requirements in MIL-STD-1797B, but they may be excessive when applied to UAs. There is no question that the ability to operate in high winds and turbulence is a critical need for UAs.

A viable requirement for testing gust rejection is application of a 1-cosine gust as defined in MIL-STD-1797B. This form of gust is amenable to analysis, is simple in its design and implementation, and is highly modifiable. On the other hand, it is not testable in flight, and it does not exercise the overall system’s gust rejection capabilities.

There is a critical need for turbulence rejection testing; this was a major effort in the development of MIL-STD-1797B and remains a high priority today. Just how to specify testing, without over- or under-specifying, will require some research and development effort. Much more research is needed.

3.2.6 Pitch Response to Failures

There will be several critical issues to be addressed when it comes to failure control in UA. These will include the intended use, operational area, phase of flight, and consequences of the failure, among other challenges. As an example, loss of a pitching actuator on a fixed wing UA in high-altitude cruise may be tolerable, if the following are true: the transients are not sufficiently large to lead to further damage to, or loss of, the airframe; transients in flight path do not put the UA into conflicting airspace; recovery to safe, controlled flight is possible; the primary mission can be continued, or at least diversion to an emergency landing can be safely performed. By contrast, loss of a rotor on a multi-rotor hovering package delivery aircraft – even if there is still excess thrust and pitch control power from the working rotor – could be catastrophic, depending upon proximity to the ground or other objects.

Specification of failure transients is a complicated process, and for the latter case described above we can glean guidance from requirements in ADS-33E-PRF for a start, but there is much to be done to try to develop a comprehensive set of failure requirements for UA. This is an area deserving of considerable research work, beyond the scope of the current effort.

3.3 Roll Axis Requirements

3.3.1 Roll Axis Dynamic Response to Control Inputs (Bandwidth)

The structure of this requirement is identical to that for 3.2.1 in pitch. For piloted aircraft, extensive testing has shown that acceptable limits of Bandwidth and Phase Delay differ between pitch and roll. For helicopters, for instance, the ratio of allowable pitch Bandwidth to roll Bandwidth in hover is about 1-to-2 (Ref. 35). Theories abound to attempt to explain this difference, ranging from the physiological: binocular vision makes humans more sensitive to roll than pitch, therefore tolerance to errors is lower – to the physical: most helicopters are inertially slender, and the human has adapted to expect better control in roll.

The latter theory breaks down for fixed wings, however, where the (admittedly very sparse) available evidence suggests the opposite (Ref. 37); yet airplanes are, in general, even more inertially slender than helicopters.

At this time, we are providing for a separate set of attitude Bandwidth requirements for roll as opposed to pitch, even though there is an expectation that the limits will be identical for some UA. This will allow us to make a distinction if the need for one is identified, and we can coalesce the requirements in the future if appropriate.

3.3.2 Roll Axis Damping

The damping ratio limit comes from ARP94910. Aircraft Bandwidth reduces the chance for low damping but does not prevent it. This requirement prevents low damping in the roll axis.

For UA that exhibit Dutch-roll-like oscillations in the roll axis, this limit might be viewed as being a bit excessive. Much lower values of Dutch roll damping are allowed in the fixed wing specifications for piloted airplanes, for instance. But the assumption for piloted airplanes is that the pilot can easily suppress Dutch roll oscillations, whether in roll or yaw. For UA, system damping must be reasonably high to begin with. Whether “reasonably high” corresponds to a damping ratio of 0.3 may be a matter for future debate, but it is certain that anything much lower will result in an aircraft that is too easily excited to roll without direct suppression of the oscillations.

If the UA is to provide precise attitude control – surveillance with a fixed optical sensor, for instance – a damping ratio of 0.3 is simply too low. We have increased the lower limit to 0.7, and there may be justification for even higher values of damping.

3.3.3 Roll Axis Control Power

There are very specific requirements on control power in the piloted specification MIL-STD-1797B, but they are obviously intended to provide the pilot with sufficient power to perform tasks such as takeoffs and landings, rolling maneuvers, etc. Those requirements, while important for pilot-in-the-loop operations, are of lesser importance for UAs, especially those that operate autonomously.

We may find it prudent to incorporate a subset of the piloted-airplane requirements for fully Manual flight, and for Assisted flight when the pilot is in the loop. At this time, the general statements given here are considered sufficient as guidance to the designer.

3.3.4 Roll Attitude Hold

For now, it is assumed that the ability for the UA to hold attitude should be the same in pitch or roll, and hence the two requirements are identical. The rationale and source for this requirement are as discussed under 3.2.4 for Pitch Attitude Hold.

3.3.5 Roll Axis Response to Turbulence and Gusts

See discussion for 3.2.5.

3.3.6 Roll Response to Failures

See discussion for 3.2.6.

3.4 Yaw Axis Requirements

3.4.1 Yaw Axis Dynamic Response to Control Inputs (Bandwidth)

Precise heading (or yaw) control is typically required of aircraft that operate at very low speeds, down to hover. Piloted conventional airplanes must demonstrate turn coordination and Dutch roll damping; for fixed wing UA, neither is as critical, though some level of yaw damping is desirable for performance and for public confidence. It is expected that this requirement will end up being restricted explicitly to very-low-speed operation only, with a separate requirement for damping of the Dutch roll mode. We have chosen to not apply such a restriction at this time.

For piloted helicopters, the yaw Bandwidth limits of ADS-33E-PRF are regarded as too stringent. Research will be required to determine the limits on yaw Bandwidth for hovering UA.

3.4.2 Yaw Axis Damping

This requirement is identical to that in roll, but it is possible that it will eventually differ. For instance, lower damping might be allowable for fixed wing UA in cruise flight, perhaps reflective of Dutch roll requirements for piloted airplanes. We will reevaluate when appropriate MTEs are defined and data become available to confirm limits on Dutch roll damping.

3.4.3 Yaw Control Power

A direct rewording of the requirements for pitch and roll, with an additional statement for crosswind operations. The additional statement is reflective of requirements in MIL-STD-1797B (Ref. 36) and will be updated to reflect specific MTEs once those MTEs are defined. Both the MIL Standard and ARP94910 mention crosswinds up to 20 knots, but for now we have left the limits TBD.

An additional use of yaw control for conventional airplanes is recovery from, and trimming out of, asymmetric flight, usually due to engine failure in multi-engine airplanes. Such a requirement is needed, but flight in failed conditions is an entire topic that has yet to be undertaken.

3.5 Vertical (Heave) Axis Requirements

3.5.1 Vertical (Heave) Axis Dynamic Response to Control Inputs

3.5.1.1 When a Direct Vertical Control Effector is Provided

3.5.1.1.1 Short-Term Response (Bandwidth)

Past attempts to define Bandwidth requirements for heave control have not been fully successful. Perhaps the most thorough, and most promising, work on this topic was done in the mid-1980s and documented in a Navy report (Ref. 38). The criterion proposed in that effort was based entirely on the frequency where phase angle of the vertical-rate-to controller was -135 degrees. We have added an option to also specify a Phase Delay parameter, should research prove such a metric is justified.

As work shifted from powered-lift V/STOLs to rotorcraft, the Bandwidth approach in Ref. 38 was abandoned for a time-domain metric, as is used in ADS-33E-PRF (Ref. 35) and described in detail in an earlier background document (Ref. 43). The time-domain metric is a bit clumsy to apply but was considered necessary to capture throttle-governor dynamics effects on some vertical-lift aircraft.

We would hope that, as a result of future research, if not from the current effort, we will be able to revisit this topic and generate Bandwidth-based requirements. Such requirements will be much simpler to apply and will share philosophies with the dynamic response requirements for other axes.

At this time there is no reason to expect that the short-term dynamic response requirements will vary with airspeed or groundspeed; ADS-33E-PRF makes no such distinction for piloted rotorcraft, and in keeping with the spirit of this draft specification the determining factor should be mission-based, not speed-based. The table of allowable Bandwidth and Phase Delay may very well increase in size as limits are defined for differing missions, but not for differing speeds.

Separate requirements are justified for aircraft that are not powered-lift, i.e., that generate flight path changes through attitude changes, as described later in this report.

3.5.1.1.2 Vertical-Axis Control Power

This is a challenging subject: should a handling-qualities specification set control power requirements? It was a topic of discussion for the pilot rotorcraft standard ADS-33E-PRF, with two competing philosophies: 1) control power for vertical-lift aircraft is a fundamental design decision, and setting limits will effectively dictate design – this is not the purpose of a compliance specification; and 2) control power has a direct impact on mission effectiveness, and to the degree that a handling-qualities specification is intended to help assure mission effectiveness, inclusion of a direct control power requirement is warranted.

In the development process for ADS-33, it was decided that vertical-axis control power for handling qualities is not simply a question of maximum achievable climb rate, but an issue of how rapidly a minimum climb rate can be achieved.

The words proposed in this requirement are taken almost verbatim from the hover paragraph in ADS-33E-PRF. We have replaced the limits in ADS-33E-PRF – 160 ft/min, 55 ft/min, and 40 ft/min for Levels 1, 2, and 3, respectively – with TBD, and removed reference to “OGE” (out-of-ground-effect) hover. For small UAVs, hover height for ground effect will be very small, and specifying OGE seems unnecessarily complicated. If this document is extended to cover autonomous, large-sized VTOLs, the wording change should be revisited. Similarly, while we have retained the wind speed limit for compliance of up to 35 kts, this limit can be reconsidered as data become available.

3.5.1.2 When a Direct Vertical Control Effector is Not Provided

3.5.1.2.1 Short-Term Response (Bandwidth)

Pitch attitude is the primary short-term controller for flight path in winged aircraft. This requirement is intended to assure that flight path change occurs sufficiently rapidly in response to attitude changes. There are plots published in MIL-STD-1797B (Ref. 36), taken from Ref. 37, that impose an absolute minimum Bandwidth, and suggest an upper limit that is a function of pitch attitude Bandwidth. We are hopeful that single numbers can be determined for both upper and lower limits, but it is possible that this requirement will resemble that in the referenced documents.

This requirement does not assure sufficient flight path control power: it is possible that flight path response to pitch is sufficiently rapid, but of too low magnitude to provide essential flight path control.

An alternative flight path response criterion was proposed in the early 1980's for STOL operations (Ref. 44) based on the frequency response of flight path to attitude. The “ $(1/T_{\theta 2})_{\text{eff}}$ ” parameter was a direct measure of the consonance between the two states. While data correlation with the parameter showed promise, its implementation added a level of complication that is felt to be unnecessary. Flight path Bandwidth frequency is a more direct metric, and if it should prove to be related to pitch attitude Bandwidth (as is the case for piloted airplanes), requirements like those in the MIL standard can be developed.

3.5.1.2.2 Vertical-Axis Control Power

For conventional UA, the critical measures of flight path control power will be in collision avoidance and landing. It is assumed at this time that, if the aircraft can generate sufficient flight path change to go around during the approach and landing tasks, there will be ample flight-path control power for higher-speed operations.

The requirement proposed here is taken from a study of STOL requirements (Ref. 44) performed for the US Air Force in the early 1980's. The numbers proposed there were all quite small – between 1.5 and 4 deg flight path change from trim – and those values may be suitable for UA as well. A possible simple process for populating this requirement is to simply note the climb capabilities of typical fixed winged UAs while executing go-arounds.

MIL-STD-1797B also addresses flight path control power, but in the more traditional sense for piloted airplanes: the degree of “backsidedness” in power approach, expressed through the parameter dy/dV . While dy/dV is a critically important measure of speed stability – it relates directly to the value of a “non-minimum-phase” zero in the frequency response of altitude rate to elevator (Ref. 44) – it is of much less consequence for fixed wing UAs that are likely to operate with full-time, full-authority speed control systems. It might be a factor for unpowered approaches and landings, but that is likely to be more a failed-state operation than normal procedure for UA. We may find it necessary to incorporate limits on dy/dV in a future iteration of the specification, but it is felt that such a requirement is not justified as this time.

3.6 Transition Between Powered-Lift and Wing-Borne Flight

This set of requirements is intended to build a foundation for variable-configuration UAs. There is no documented requirement, much less guidance, for the transitional operation of such UAs. Nevertheless, the limited number of proposed requirements introduced in this draft reflects a concern about possible loss of stability and controllability during the transition from wing-borne to powered-lift flight.

3.6.1 Pitch Stability During Transition

3.6.1.1 Transition to STOL

A simulation study of transition requirements for piloted V/STOL aircraft (Ref. 39) found that some level of instability was tolerable, but not desired. That study suggested times to double in pitch attitude of 4.5 seconds for Level 2 and 2.2 seconds for Level 3. The experiment was quite limited in scope, so these

numbers are not ready for application to a UA. The intent of the requirement, however, is to allow some loss of pitch stability during the transition.

3.6.1.2 Transition to Hover

There is no formal support for this requirement. It is recommended in Ref. 39 as an “intuitive conclusion,” given the criticality of the transition to hover, as it usually occurs near the ground or other objects.

If data become available, some degradation might be allowable for UAs, but such degradation may very well be driven more by public perception than by any concern over flight dynamics: assuming the UA will operate in populated areas, an appearance of loss-of-control – even if there is no risk of actual loss of control – could lead to public distrust of the UA.

3.6.1.3 Coupling Between Pitch Attitude and Power

In the simulations reported in Ref. 39, cross-coupling between pitch and power was a large factor in degraded handling qualities. While the concern is lessened with the removal of a pilot, it is still necessary to assure that power changes do not lead to excessive pitching. In Ref. 39, this coupling was expressed as the ratio of peak pitch attitude change (in degrees) divided by thrust lever movement (in percent). For UA, the focus will be on total thrust, so it is recommended that the parameter be change in percent thrust, where thrust is scaled from 0 (idle) to 100 (full) percent.

The simulation proposed a Level 1 limit of 0.30 (deg/%) in the transition to STOL and 0.20 (deg/%) in the transition to hover. There was no clear Level 2 or 3 limit. In this case, we simply recommend that the coupling for Levels 2 and 3 not lead to a dangerous flight condition.

3.7 Transients Between Command Sources

3.7.1 Mode Switching

Operator intervention in an otherwise autonomously-controlled UA should not cause unusual transients in dynamic response. Likewise, operator disengagement from manual control should be relatively seamless.

It is carefully worded to specifically reference *trimmed, level flight*: the inference is that, for an emergency takeover by an operator, or emergency reversion to autonomous control, the limits as stated can be exceeded. It may be appropriate in the future to add a specific requirement covering mode switching in emergency operation, but much more needs to be learned about such operations before an explicit requirement can be developed,

This requirement is taken, with some modification, from SAE ARP-94910 (Ref. 34) and is meant to apply to any type of UA, whether powered-lift or wing-lift. There will be a need to confirm and update it when MTEs have been formally developed.

3.7.2 Guidance and Navigation Commands

Changes in guidance and navigation commands should never cause exceedance of the OFE. This new requirement is intended to prevent such transients. The user is advised to consult similar requirements in SAE ARP-94910 (Ref. 34) that deal with waypoint navigation. Because that specification has more to do with the operation of the system, rather than the dynamic response from operation of the system, we have chosen to go with the current statement.

3.8 Response to Turbulence and Gusts

3.8.1 Dynamic Response to Turbulence

For small UAs that are built to operate at low altitudes, turbulence from diurnal heating, combined with perturbations in winds resulting from buildings, trees, and other obstacles, means a good portion of their operation is almost certainly going to be in unsteady air.

There is a temptation to simply reiterate the multitude of turbulence requirements and models that exist in the specifications for manned airplanes, V/STOLs, and helicopters, but with no flight data, we have chosen to ignore that temptation. SAE ARP-94910 (Ref. 34) provides requirements on response to turbulence, but once again, those requirements relate either indirectly or directly to the turbulence models for manned aircraft.

The qualitative statements proposed here are placeholders for what will, hopefully, eventually be a well-supported quantitative requirement. At this time, we simply wish to ensure that low levels of turbulence do not result in control issues, and that higher levels do not prevent control entirely.

3.8.2 Response to a Unit Gust

The format of this requirement is taken from MIL-STD-1797B; the details for scaling the gust need to be confirmed in flight test. For a hovering vehicle, the distance parameter d_m used in the requirement becomes irrelevant, so the requirement needs revision to be time-dependent, not distance-dependent.

The intent of this requirement is to make the UA resistant to large shear forces when flying over a building or a sudden change in terrain height or type. Flight testing is needed to confirm and convert the scaling parameters.

A high-feedback SCAS should have no problem suppressing excursions in flight path, but possibly at the expense of very large and violent pitching motions. It might be prudent to de-tune control system gains, and accept some momentary small excursions, rather than try to eliminate them entirely.

3.9 Response to Failures

In handling qualities specifications for piloted aircraft, failure response is usually stated in terms of maximum aircraft excursion and pilot recovery. Eventually, it is hoped that similar requirements will be available for UAs, and certainly the piloted-aircraft specs are a good start.

For lack of real data, we have chosen to make a rather generic statement in this document. When flight data become available, there should be a whole new set of requirements based on failure probabilities and severity.

4. MISSION TASK ELEMENTS

Work is currently ongoing to develop a candidate set of MTEs. These MTEs will be incorporated into a future draft of this specification.

E. REFERENCES

33. Klyde, D. H., P. C. Schulze, A. Kotikalpudi, and D. G. Mitchell, *Defining Handling Qualities of Unmanned Aerial Systems: Phase I Final Report*, Systems Technology, Inc., TR-1488-1, Nov. 2016.
34. Anon., *Aerospace - Vehicle Management Systems - Flight Control Design, Installation and Test of Military Unmanned Aircraft, Specification Guide For*, SAE ARP94910, Society of Automotive Engineers, issued Dec. 2012.

35. Anon., *Aeronautical Design Standard, Performance Specification, Handling Qualities Requirements for Military Rotorcraft*, US Army Aviation and Missile Command, Redstone Arsenal, AL, ADS-33E-PRF, 2000.
36. Anon., *Department of Defense Interface Standard, Flying Qualities of Piloted Aircraft*, MIL-STD-1797B, Feb. 2006 [Distribution Statement D: Distribution authorized to the Department of Defense and U.S. DoD contractors only; contains critical technology (3 November 2005)].
37. Mitchell, D. G., R. H. Hoh, B. L. Aponso, and D. H. Klyde, *Proposed Incorporation of Mission-Oriented Flying Qualities into MIL-STD-1797A*, WL-TR-94-3162, Oct. 1994.
38. Hoh, R. H., and D. G. Mitchell, *Proposed Revisions to MIL-F-83300 V/STOL Flying Qualities Specification*, NADC-82146-60, Jan. 1986 [Distribution Limited to U.S. Government Agencies and their Contractors; Critical Technology; 17 January 1986].
39. Hoh, R. H., and D. G. Mitchell, *Proposed Revisions to VSTOL Transition Requirements in MIL-F-83300*, NADC-80066-60, Oct. 1984 [Distribution Limited to U.S. Government Agencies and their Contractors; Critical Technology; 18 October 1984].
40. Mitchell, D. G., and R. H. Hoh, *Development of Methods and Devices to Predict and Prevent Pilot-Induced Oscillations*, AFRL-VA-WP-TR-2000-3046, Jan. 2000.
41. Mitchell, D. G., and T. K. Nicoll, *UAV Flying Characteristics Design Requirements*, Hoh Aeronautics, Inc., Technical Report No. 1169-1, Feb. 2011.
42. Cotting, M. C., *Evolution of Flying Qualities Analysis: Problems for a New Generation of Aircraft*, PhD Dissertation, Virginia Tech, Mar. 2010.
43. Hoh, R. H., D. G. Mitchell, B. L. Aponso, D. L. Key, and C. L. Blanken, *Background Information and User's Guide for Handling Qualities Requirements for Military Rotorcraft*, USAAVSCOM TR-89-A-008, Dec. 1989 [originally released with Limited Distribution, Distribution authorized to U.S. Government agencies and their contractors; re-issued, with unlimited distribution, as the following: Key, David L., Chris L. Blanken, Roger H. Hoh, David G. Mitchell, and Bimal L. Aponso, *Background Information and User's Guide (BIUG) for Handling Qualities Requirements for Military Rotorcraft*, U.S Army SR-RDMR-AD-16-0, Dec. 2015].
44. Hoh, R. H., and D. G. Mitchell, *Tentative STOL Flying Qualities Criteria for MIL Standard and Handbook*, AFWAL-TR-83-3059, June 1983.

Appendix B – Mission Task Element Catalog

A. INTRODUCTION

This appendix provides an initial Mission Task Element (MTE) catalog based on the flight test evaluations conducted as part of this Phase II program as described in the main text and on the MTE submittals made by UAS Handling Qualities Stakeholders.

B. FIXED WING

1. Evaluations Conducted by the University of Minnesota UAV Lab

a. Flightpath Regulation in the presence of a Discrete Gust (Non-precision, Non-aggressive or Non-Precision, Aggressive depending on gust input magnitude)

Autonomy Level

- MTE can be applied to any level of autonomy.
- Intended to be a “surprise” disturbance, so pilot should not be alerted if under manual control.
No assumptions required for delayed pilot response.

Task Objectives

- Assess response to and recovery from a discrete gust.
- Evaluate vehicle control following a perturbation in pitch or flight path.

Task Description

In straight, level flight at constant airspeed, apply a gust to perturb the aircraft vertically. After the aircraft has recovered from the gust, apply a gust of equal amplitude and opposite sign. Assess the ability to reject the gust and return to equilibrium flight at the initial altitude and airspeed.

No specific ground-referenced course is needed. The MTE may be accomplished at any initial altitude and airspeed. With the aircraft trimmed for level, unaccelerated flight, apply the gust documented below in either the up or down direction; once the aircraft has recovered from the gust (defined as meeting either the Adequate or Desired performance standards), apply an equal and opposite gust. The maneuver is complete when the aircraft has returned to equilibrium flight.

The gust has a “1 – cosine” shape as shown in Figure 46. The gust shall be applied to the most direct controller for vertical flight path (e.g., elevator for a conventional UA or rotor RPM/collective for a VTOL UA), with magnitude v_m selected to provide an altitude change of at least 10 ft in one second after application, determined for the UA with outer-loop hold modes (or pilot intervention, for an RPA) inactive. The time d_m shall be tuned to the estimated rigid-body short-term response mode of interest. It is acceptable to replace the “1 – cosine” shape with a discrete gust.

The “1 – cosine” gust has the following shape:

$$v = 0 \quad \text{for } x < 0$$

$$v = v_m [1 - \cos(\pi x/d_m)]/2 \quad \text{for } 0 \leq x \leq d_m$$

$$v = v_m \quad \text{for } x > d_m$$

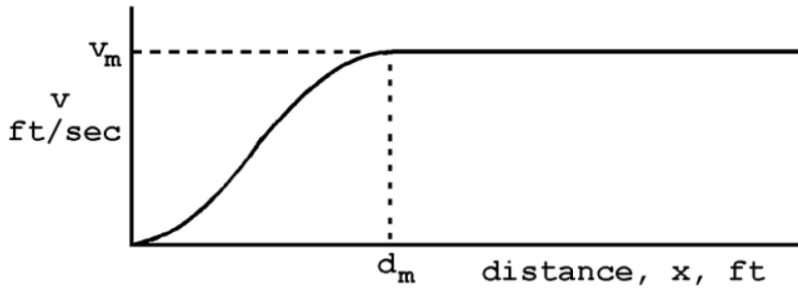


Figure 46: “1 – cosine” Shape for Discrete Gust

Desired Performance

- Maximum altitude deviation following gust, ± 20 ft.
- Recover to initial altitude (for height hold systems) within ± 2 ft.
- Recover to initial trim attitude (for attitude hold systems) within ± 1 deg.
- Recover airspeed to initial trim conditions within ± 2 kt.
- Hold trim conditions following recovery for at least 10 sec.
- Retain initial heading within ± 1 deg.
- Time to recover to within performance standards 10 sec.

Adequate Performance

- Maximum altitude deviation following gust, ± 30 ft.
- Recover to initial altitude (for height hold systems) within ± 5 ft.
- Recover to initial trim attitude (for attitude hold systems) within ± 2 deg.
- Recover airspeed to initial trim conditions within $\pm 10\%$ of trim.
- Hold trim conditions following recovery for at least 5 sec.
- Retain initial heading within ± 2 deg.
- Time to recover to within performance standards 15 sec.

Notes for developing this MTE:

1. The input is based on MIL-STD and FAA gust requirements, but the proper values for UAs is entirely unknown. Suggest running gusts in basic model (no autopilot or manual reactions) varying d_m and v_m including pure discrete gusts.
2. I imagined this to be equivalent to a small UA flying over a low building or changing terrain: how well can the UA handle the upset? Is it trivial, or will the UA get blown into power lines, a tree, etc.?
3. Suggest the first gust be up and the second down; initially probably can get by with just the initial up gust, until there is confidence the down gust is not a safety issue.
4. Want to measure aircraft flight path and pilot control inputs to correct for the gust, with the pilot not knowing the gust is coming; maybe after a few runs with the pilot knowing it is coming, try a few with random application.

b. Flightpath Regulation in the presence of a Sum-of-Sines Disturbance (Precision, Aggressive)

Autonomy Level

- MTE can be applied to any level of autonomy.
- Intended to be a continuous, “random” disturbance that the pilot/autonomous controller must regulate against to maintain flightpath. No assumptions required for delayed pilot response.

Task Objectives

- Assess ability of pilot/autonomous controller to maintain flightpath in the presences of a “random” appearing continuous disturbance.
- Evaluate vehicle control following a continuous perturbation in pitch or flight path.

Task Description

In straight, level flight at constant airspeed, apply a sum-of-sines disturbance input to perturb the aircraft vertically. Continuously regulate desired flightpath in the presence of the disturbance for a minimum of 20 seconds. Assess the ability to reject the disturbance and maintain flightpath at the initial airspeed.

No specific ground-referenced course is needed. The MTE may be accomplished at any initial altitude and airspeed. With the aircraft trimmed for level, unaccelerated flight, apply the disturbance documented below. The maneuver is complete when the aircraft has responded to the continuous disturbance for at least 20 seconds and has returned to equilibrium flight.

The sum-of-sines (SOS) disturbance forcing function is used to drive the flightpath regulation task through which the pilot or autonomous controller attempts to minimize the flightpath error within desired performance constraints. Table 15 presents the parameters for a Fibonacci series-based SOS input that has been designed for the anticipated longitudinal dynamics of a typical fixed wing sUAS. The input is defined for a 20 second scoring time run length. Thus, each sine wave frequency is defined by f_n (Hz) = N_n (cycles/run)/20 (s/run). An example disturbance signal with a Gain of 1.5 deg placed on the nominal signal is shown in Figure 47.

Table 15: Example SOS Input Forcing Function Parameters for Lower Frequency Identification

Frequency No.	1	2	3	4	5	6	7
Cycles/Run, N_n	3	5	8	13	21	34	55
Frequency, f_n (Hz)	0.1500	0.2500	0.4000	0.6500	1.0500	1.7000	2.7500
Frequency, (r/s)	0.9425	1.5708	2.5133	4.0841	6.5973	10.6814	17.2788
Amplitude ($A_i = f_1/f_n$)	+1.0000	-0.6000	+0.3750	-0.2308	+0.1429	-0.0882	+0.0545
Initial Rate $A_n \times \omega_n$	+0.9425	-0.9425	+0.9425	-0.9425	+0.9425	-0.9425	+0.9425

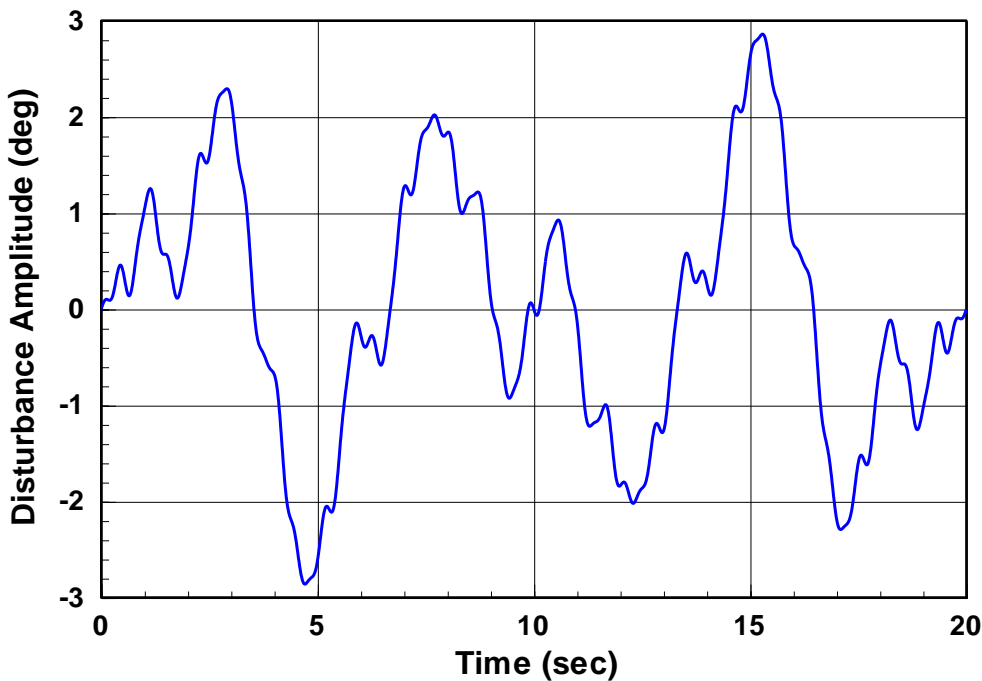


Figure 47: Sum-of-Sines Disturbance (Gain = 1.5 deg)

Desired Performance (Precision Task – Pitch Disturbance)

- Maintain flightpath during disturbance within ± 1 deg for at least 50% of the scoring time.
- Maintain altitude during disturbance through the disturbance, ± 20 ft.
- Maintain airspeed during disturbance to initial trim conditions within ± 2 kt.
- Maintain initial heading during disturbance within ± 1 deg.

Adequate Performance (Precision Task – Pitch Disturbance)

- Maintain flightpath during disturbance within ± 2 deg for at least 75% of the scoring time.
- Maintain altitude during disturbance through the disturbance, ± 40 ft.
- Maintain airspeed during disturbance to initial trim conditions within ± 5 kt.
- Maintain initial heading during disturbance within ± 2 deg.

Desired Performance (Non-Precision Task – Altitude Disturbance)

- Maintain altitude during disturbance through the disturbance, ± 10 ft.
- Maintain airspeed during disturbance to initial trim conditions within ± 2 kt.
- Maintain initial heading during disturbance within ± 1 deg.

Adequate Performance (Non-Precision Task – Altitude Disturbance)

- Maintain altitude during disturbance through the disturbance, ± 20 ft.
- Maintain airspeed during disturbance to initial trim conditions within ± 5 kt.
- Maintain initial heading during disturbance within ± 2 deg.

Notes for developing this MTE:

1. Gain on SoS disturbance and performance requirements will be refined as part of the flight test evaluations.

c. Waypoint Following (Non-Precision, Non-Aggressive and Precision, Non-Aggressive depending task requirements)

Autonomy Level

- Intended to assess autonomous operations.

Task Objectives

- Assess ability of an autonomous controller to follow a waypoint flightpath.

Task Description

In straight, level flight at constant airspeed, initiate a waypoint following autonomous control command sequence. Waypoint legs will feature a minimum of 500 ft (or approximately 150 m). The waypoint sequence will feature at least two turns about a rectangular/square path with an altitude change of at least 50 ft on one of the legs.

Desired Performance (Precision Task)

- Maintain lateral, longitudinal, and vertical flightpath position within ± 2 ft of the defined waypoint path within each leg.
- No undesirable control motions.

Adequate Performance (Precision Task)

- Maintain lateral, longitudinal, and vertical flightpath position within ± 5 ft of the defined waypoint path within each leg.
- No undesirable control oscillations.

Desired Performance (Non-Precision Task)

- Maintain lateral, longitudinal, and vertical flightpath position within ± 10 ft of the defined waypoint path within each leg.
- No undesirable control motions.

Adequate Performance (Non-Precision Task)

- Maintain lateral, longitudinal, and vertical flightpath position within ± 25 ft of the defined waypoint path within each leg.
- No undesirable control oscillations.

Notes for developing this MTE:

1. Specific waypoints and performance requirements will be refined as part of the flight test evaluations.

d. Precision Lateral Offset Landing (Precision, Non-Aggressive)

Autonomy Level

- Typically, this will be a remotely piloted MTE.
- No assumptions required for delayed pilot response. Any response delays will be reflected in MTE performance.

Task Objectives

- Evaluate ability to precisely control horizontal and vertical flightpath and airspeed.
- Evaluate ability to precisely control sink rate and attitude in the flare.
- Evaluate tendency for nose bobble or PIO.
- Evaluate control sensitivity and harmony in landing.

Task Description

The offset landing task consists of a visual approach during which the evaluation pilot aligns the aircraft approximately 50 feet off the runway centerline (see Figure 48). At approximately 65 ft AGL, the EP corrects back to the centerline and attempts to touchdown within the desired parameters. Offsets to the left or right can be used interchangeably; however, the direction of offset may be dictated by pilot line-of-sight.

A Precision Offset Landing test course at the UMore Park Test Range is shown in Figure 48. In the figure, the yellow area is the usable turf runway (approximately 900 x 100 ft). An extended centerline in light blue has been added to the figure. The south edge of the runway adjoins a crop field with a distinct edge. The notional “base” and “final” shown in light green will position the aircraft along that edge. The remote pilot will be positioned along that line in order provide a good perspective for tracking during the turn to final, and during the final approach. The offset start will be based on altitude. Temporary markings for the runway centerline and “touchdown” target markers will be made. A landing “T” and an extended centerline can be painted on the turf.



Figure 48: Precision Offset Landing Course at the UMore Park Test Range

Desired Performance

- Approach airspeed maintained within ± 2 kts.
- Touchdown within 5 feet of centerline (nose wheel on centerline).
- Touchdown within ± 5 feet of aimpoint.
- Sink rate – smooth touchdown.
- No PIO.

Adequate Performance

- Approach airspeed maintained within -2 kts/+5 kts.
- Touchdown within 10 feet of centerline.

- Touchdown within \pm 10 feet of aimpoint.
- No PIO.

Notes for developing this MTE:

1. Correction height (altitude) and performance requirements will be refined as MTE is initially evaluated.

2. Unusual Attitude Recovery, Nose-High (Non-Precision, Aggressive)

This MTE description was provided by Dr. Nate Richards of Barron Associates, Inc.

Autonomy Level

- This task shall be flown at all levels of autonomy under which the vehicle is expected to operate (from Level 1 – Human Operated to Level 4 – Fully Autonomous).

Task Objectives

- Recovery from a set of unusual attitudes at each level of autonomy expected for the vehicle.
- Evaluate the ability of a UAS to recover (return to defined safe flight envelope) from an unusual attitude.
- Evaluate the tendency of a UAS to depart controlled flight following an intentional or unintentional unusual attitude state.

Task Description

Starting at an airspeed of approximately 1.73 times the test article stall speed at the test configuration and weight, slowly advance throttle and raise the nose until it reaches a pitch attitude of at least 40 degrees without inducing a stall. Once at or above 40 degrees pitch up, initiate recovery to a defined safe flight envelope (0 to 5 degrees pitch, -5 to 5 degrees bank, -50 to 50 feet/min vertical speed, a speed of at least 1.3 times the stall speed, and steady). Altitude, pitch attitude, bank angle, and airspeed data shall be collected during task execution.

Repeat this task at each level of autonomy under which the vehicle is expected to operate.

The scenario may be initiated manually or autonomously.

Desired Performance

- Vehicle recovers to defined safe flight envelope (0 to 5 degrees pitch, -5 to 5 degrees bank, -50 to 50 feet/min vertical speed, steady) without further excursion.
- Vehicle recovers to defined safe flight envelope without a loss of more than 400 ft in altitude (from recovery initiation altitude).

Adequate Performance

- Vehicle recovers to defined safe flight envelope (0 to 5 degrees pitch, -5 to 5 degrees bank, -50 to 50 feet/min vertical speed, steady).
- Vehicle recovers to defined safe flight envelope without a loss of more than 800 ft in altitude.

C. ROTARY WING MISSION TASK ELEMENTS

1. Evaluations Conducted in the NASA LaRC Autonomy Incubator

a. Precision Hover (Precision, Non-Aggressive)

Autonomy Level

- Remotely piloted with visual line-of-sight.
- Autonomous variations are possible.

Objectives

- Evaluate ability to transition from translating flight to a stabilized hover over a target hover zone with precision and a reasonable amount of aggressiveness.
- Evaluate ability to maintain precise position, heading, and altitude over the target.

Description

The MTE will start 25 ft aft of the hover board and approximately 15 ft left or right of the hover board center. From this starting point, the vehicle will maneuver at a constant altitude of approximately 5 ft and a speed of approximately 5 kts to the precision hover point that is 25 ft aft of the hover board center. Attain a stabilized hover in the defined target hover zone marked by the hover board. Maintain the stabilized hover at the 25 ft aft location in front of the hover board for the time duration specified in the performance requirements. Repeat as needed.

The center of the hover board will be placed 5 ft above and 25 ft in front of the hover point marker at ground level. The hover board will have distinct boundaries indicating desired and adequate performance requirements.

Desired Performance

- Attain stabilized hover from the lateral sidestep before exiting the desired region of the hover board.
- ≥ 30 sec of stabilized hover in desired region.
- ± 1 ft altitude deviation from hover board center.
- ± 1 ft lateral deviation from hover board center.
- ± 1 ft longitudinal (fore/aft) deviation from hover point.
- $\pm 5^\circ$ heading deviation from target or hover board.
- No undesirable motions (bobble, overshoots/undershoots) that impact task performance during the transition to hover or stabilized hover.

Adequate Performance

- Attain stabilized hover from the lateral sidestep before exiting the adequate region of the target and hover board.
- ≥ 30 sec of stabilized hover in adequate region.
- ± 2 ft altitude deviation from hover board center.
- ± 2 ft lateral deviation from hover board center.
- ± 2 ft longitudinal (fore/aft) deviation from hover point.

- $\pm 10^\circ$ heading deviation from target or hover board.
- No oscillations that impact system stability or safety of flight during the transition to hover or stabilized hover.

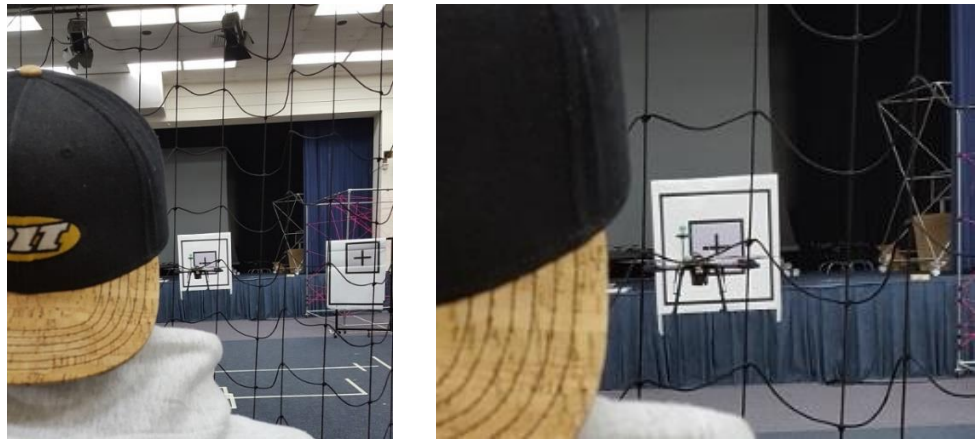


Figure 49: Precision Hover

b. Lateral Sidestep (Precision, Non-Aggressive)

Autonomy Level

- Remotely piloted with visual line-of-sight.
- Autonomous variations are possible.

Objectives

- Assess roll axis and heave axis response during moderately aggressive maneuvering.
- Identify undesirable coupling between the roll controller and the other axes.

Description

From a stabilized hover at an altitude of 5 ft with the longitudinal axis of the multi-rotor sUAS oriented 90 degrees to a reference line marked on the ground, initiate a lateral acceleration to approximately 5 kts groundspeed followed by a deceleration to laterally reposition the vehicle to a stabilized hover 12.5 ft left of the starting point as indicated by another ground marker all while maintaining the initial heading throughout the maneuver. The acceleration and deceleration phases shall be accomplished as single smooth maneuvers. The reposition capture is complete when a stabilized hover is achieved as indicated by the vehicle position in front of the hover boards, left or right depending on course position.

The center of the (left and right) hover boards will be placed 5 ft above ground and approximately 25 ft apart laterally, equally spaced left and right of the starting point. (In the NASA LaRC Autonomy Incubator, the starting point was 20 ft aft of the precision hover board.) The hover board will have distinct boundaries indicating desired and adequate performance requirements.

Desired Performance

- ± 1 vertical deviation from hover board center at each capture point.
- ± 1 ft lateral deviation as indicated by the hover board center at each capture point.
- ± 1 ft longitudinal (fore/aft) deviation from ground marker.
- $\pm 5^\circ$ heading deviation from reference heading.

Adequate Performance

- ± 2 vertical deviation from hover board center at each capture point.
- ± 2 ft lateral deviation as indicated by the hover board center at each capture point.
- ± 2 ft longitudinal (fore/aft) deviation from ground marker.
- $\pm 10^\circ$ heading deviation from reference heading.



Figure 50: Lateral Reposition (mini course)

c. Vertical Reposition (Precision, Non-Aggressive)

Autonomy Level

- Remotely piloted with visual line-of-sight.
- Autonomous variations are possible.

Objectives

- Evaluate heave damping, i.e., the ability to precisely control and stop a vertical rate.
- Evaluate vertical control power.
- Identify undesirable coupling between collective and the pitch, roll, and yaw axes.

Description

From a stabilized hover at an altitude of 5 ft, initiate a vertical ascent of at least 10 ft and stabilize for 5 seconds at an altitude of at least 15 ft using an available landmark to stabilize vertical position. Descend back to the initial hover position in front of the hover board (5 ft altitude and 25 ft aft of the hover board center) and stabilize for at least 5 seconds. Maintain initial heading and longitudinal/lateral position throughout the maneuver. Repeat as needed.

The center of the hover board will be placed 5 ft above and 25 ft in front of the hover point marker at ground level. The hover board will have distinct boundaries indicating desired and adequate performance requirements.

Desired Performance

- ± 1 vertical deviation from start/finish altitude as indicated by the hover board center.
- ± 1 ft lateral deviation as indicated by the hover board center.
- ± 1 ft longitudinal (fore/aft) deviation from ground marker.
- $\pm 5^\circ$ heading deviation from ground marker.

Adequate Performance

- ± 2 vertical deviation from start/finish altitude as indicated by the hover board center.
- ± 2 ft lateral deviation as indicated by the hover board center.
- ± 2 ft longitudinal (fore/aft) deviation from ground marker.
- $\pm 10^\circ$ heading deviation from ground marker.

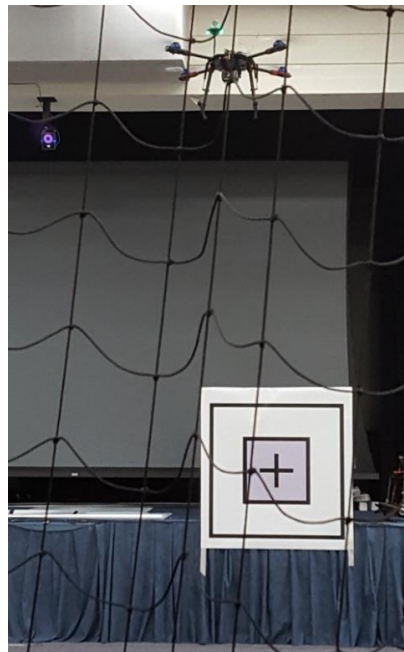


Figure 51: Bob-up/Down (Vertical Altitude Change)

d. Landing (Non-Precision, Non-Aggressive)

Autonomy Level

- Remotely piloted with visual line-of-sight.
- Autonomous variations are possible.

Objectives

- Evaluate precision control of multi-rotor position during final descent to a precision landing point.

Description

From an initial altitude of greater than 10 ft as indicated by a hover board or other appropriate landmark, maintain an essentially steady descent to a prescribed landing point as marked on the ground by a landing

marker while maintaining a reference heading. It is acceptable to arrest the sink rate momentarily to make last-minute corrections before touchdown.

Desired Performance

- ≤ 2 fps vertical speed at touchdown.
- ± 1 ft longitudinal (fore/aft) deviation from landing marker.
- ± 1 ft lateral deviation from landing marker.
- $\pm 5^\circ$ heading deviation from landing marker.
- Smooth, continuous descent with no undesirable motions that may impact task performance.

Adequate Performance

- ≤ 4 fps vertical speed at touchdown.
- ± 2 ft longitudinal (fore/aft) deviation from landing marker.
- ± 2 ft lateral deviation from landing marker.
- $\pm 10^\circ$ heading deviation from landing marker.
- No system oscillations during landing maneuver.



Figure 52: Landing

2. Scaled Autonomous ADS-33E-PRF Mission Task Elements

Authors: Dr. Christina M. Ivler (University of Portland), Chad Goerzen (U.S. Army)

A description of the development of these MTEs is found in Ref. 45.

Autonomy Level

- Fully autonomous.
- Operator will only intervene to knock-off the maneuver for safety reasons.

Task Objectives

- Track velocity and heading trajectories of scaled rotorcraft mission task element maneuvers.

Task Description

- Complete scaled versions of ADS-33E-PRF MTE maneuvers by autonomously tracking velocity/position and heading commands.
- Example full scale maneuver Level 1 performance ADS-33E-PRF trajectories are given in Figs. 1-3. The position commands should be calculated by integration of the velocity commands.
- The velocity scale of maneuver shall be scaled appropriately for the size of the UAS by the ratio of the maximum speed of the UAS relative to the maximum speed of a full-scale aircraft, such as the UH-60. The associated velocity and time scales of the nominal trajectory, where aggressiveness $\alpha = 1$ is given by:

$$V_{\text{scale}} = \alpha \frac{\max(V_{\text{UAS}})}{\max(V_{\text{UH60}})} \quad (1)$$

$$t_{\text{scale}} = \alpha^{-1} \frac{\max(V_{\text{UAS}})}{\max(V_{\text{UH60}})} \quad (2)$$

- For higher required aggressiveness/agility the value of α can be increased.
- Then by integrating the scaled velocity over the scaled time, the associated position scale is:

$$L_{\text{scale}} = \left(\frac{\max(V_{\text{UAS}})}{\max(V_{\text{UH60}})} \right)^2 \quad (3)$$

- The MTE should be completed multiple times to evaluate robustness at the maximum level of desired aggressiveness, as appropriate for the intended mission of the UAS.
- No special equipment is required, but command and measured velocities and positions must be recorded.

Performance Metric

- The maneuver performance is rated with a trajectory tracking and aggressiveness (TTA) score. A weighted sum of the individual objectives for aggressiveness (α), tracking performance (ε), and robustness (R) is used to calculate a trajectory tracking and aggressiveness (TTA) score:

$$L = w_\alpha \frac{\alpha - \alpha_G}{\alpha_B - \alpha_G} + w_\varepsilon \frac{\varepsilon - \varepsilon_G}{\varepsilon_B - \varepsilon_G} + w_R \frac{R - R_G}{R_B - R_G} \quad (4)$$

$$\text{TTA Score} = \frac{200}{1+e} \quad (5)$$

- The weights, w_α , w_ε , and w_R , in Eqn. 4 determine the relative importance of the individual objectives. For each individual objective metric, the conditioning parameter with a subscript B (α_B , for instance) stands for the “bad” or worst possible value for the metric, whereas the conditioning parameter with a subscript G (α_G , for instance) stands for the “good” or best possible value.
- The aggressiveness is used for the trajectory scaling in Eqns. 1-2 and is defined as:

$$\alpha = V_{\text{traj}} / V_{\text{nom}} \quad (6)$$

V_{nom} is the maximum speed of the scaled MTE using the scaling methodology, such that $\alpha = 1$ would be flown such that the UAS is performing at the equivalent aggressiveness of the full-scale maneuver.

- The tracking error term is defined as:

$$\varepsilon = w_{vel} \frac{RMSE(vel)}{V_{max,cmd}} + w_{pos} \frac{RMSE(pos)}{L_{path}} \quad (7)$$

where RMSE stands for the root mean square of the error between the commanded and measured velocity or position. As shown by Eqn. 6, the RMSE for velocity and position are normalized by the maximum velocity command $V_{max,cmd}$, and the length of the commanded path L_{path} , respectively.

- If the operator knocks-off a maneuver for safety reasons or if the vehicle crashes, the maneuver is considered unsuccessful. The robustness term is defined as:

$$R = \frac{\# \text{successful events}}{\# \text{total events}} \quad (8)$$

The scoring parameters for the IRIS+ quadcopter as used in Ref. 1 are given by Table 16. The robustness weighting of zero was chosen given the low number of flights performed, where no unsuccessful flights were recorded. As such, including the robustness parameter in the TTA score would have resulted in an artificially inflated value. For a larger flight test program, it would make sense to include a nonzero robustness weighting as part of the score.

Table 16: Scoring Parameters for IRIS+

Parameter	Value for IRIS+
w_a	0.5
w_ε	0.5
w_R	0
α_G	3
α_B	0
ϵ_G	0
ϵ_B	0.35
w_{vel}	0.7
w_{pos}	0.3

Performance Levels

Table 17: Performance Levels, Gentle Maneuvering Mission

Maneuver	Desired TTA Score (Level 1)	Adequate TTA Score (Level 2)
Lateral Reposition	$\phi_{TTA} \geq 75$	$75 > \phi_{TTA} \geq 70$
Depart Abort	$\phi_{TTA} \geq 75$	$75 > \phi_{TTA} \geq 70$
Pirouette	$\phi_{TTA} \geq 73$	$73 > \phi_{TTA} \geq 68$

Table 18: Performance Levels, Aggressive Maneuvering Mission

Maneuver	Desired TTA Score (Level 1)	Adequate TTA Score (Level 2)
Lateral Reposition	$\phi_{TTA} \geq 82$	$82 > \phi_{TTA} \geq 77$
Depart Abort	$\phi_{TTA} \geq 82$	$82 > \phi_{TTA} \geq 77$
Pirouette	$\phi_{TTA} \geq 80$	$80 > \phi_{TTA} \geq 75$

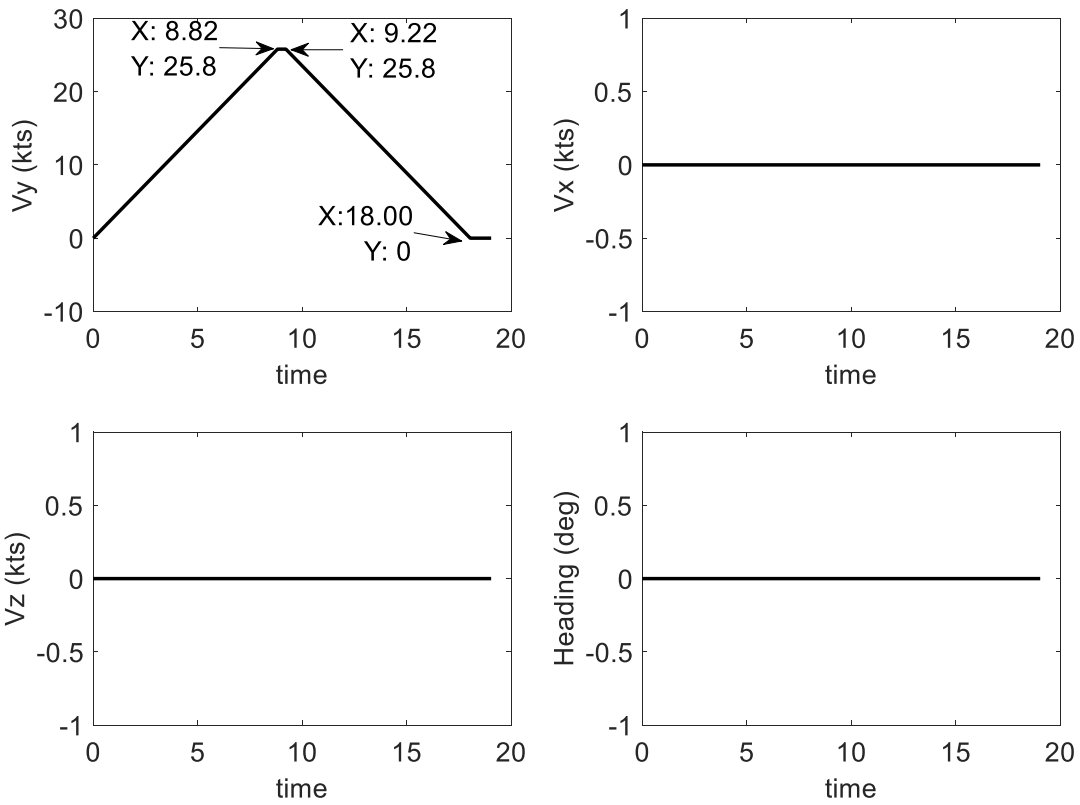


Figure 53: Lateral Reposition MTE Full Scale Trajectory

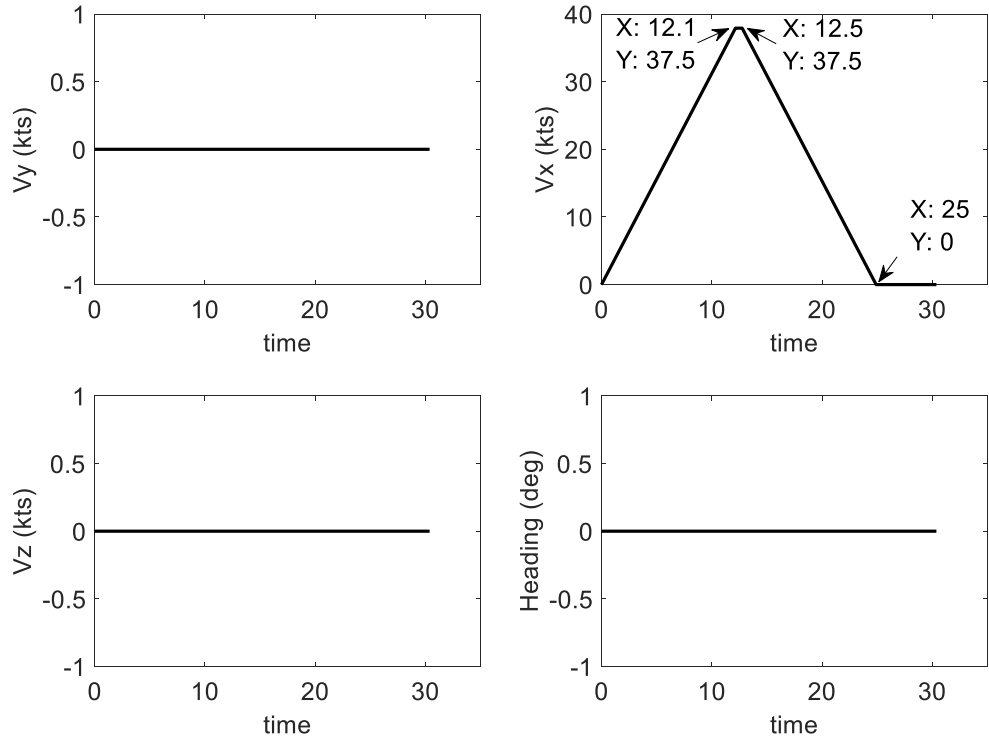


Figure 54: Depart Abort Full Scale MTE Full Scale Trajectory

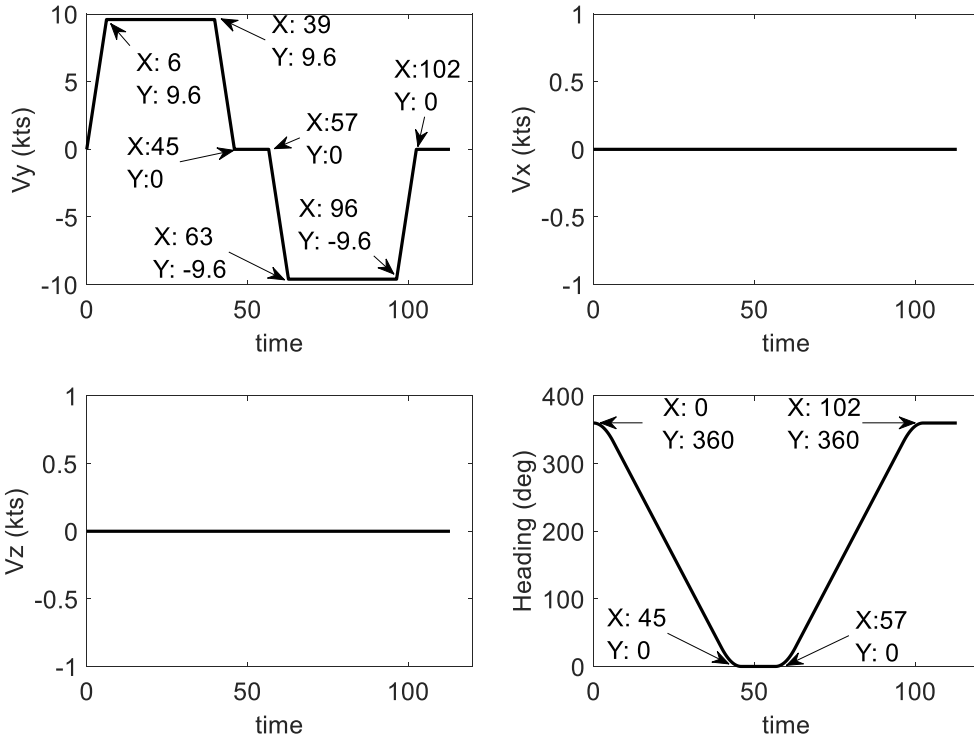


Figure 55: Pirouette Full Scale MTE Trajectory

3. Hover MTE under First Person View Cueing (Precision, Non-Aggressive)

Author: William Geyer, US Navy Test Pilot School

Autonomy Level

- This MTE is flown with pilot-in-the-loop with some level of augmentation from a simple stability augmentation system (SAS) to advanced control modes such as Translational Rate Command (TRC).

Task Objectives

- Check ability to transition from translating flight to a stabilized hover with precision and a reasonable amount of aggressiveness.
- Check ability to maintain precise position, heading, and altitude in the presence of a moderate wind from most critical direction

Task Description

Initiate the maneuver at a ground speed of between 3 and 5 knots, at an altitude less than 5 ft. Target hover point shall be oriented approximately 45 deg relative to the heading of the rotorcraft. More acute angles may be used if FPV camera cannot provide the necessary field-of-view. The target point is a repeatable, ground-referenced point from which rotorcraft deviations are measured. The ground track should be such that the rotorcraft will arrive over the target hover point. The transition to hover should be accomplished in one smooth maneuver. It is not acceptable to accomplish most of the deceleration well before the hover point and then to creep up to the final position. The maneuver shall be accomplished in calm winds and in moderate winds from the most critical direction.

A layout of the course is shown in Figure 56. A 1 in x 1 in black square was used for the reference symbol with an appropriately sized backboard with the desired and adequate performance cues. Pegboards were

used on both 45 deg azimuths to provide for fore/aft cueing as most FPV systems do not have the FOV to enable peripheral cueing at the +/-90 azimuths to the aircraft heading. Pegboards were constructed from 1/4 wood dowels pushed into a Styrofoam board to provide centerline, desired and adequate performance cues.

*Desired Performance**

- Longitudinal/Lateral Position (feet) +/- 3 x L_{scale}
- Altitude (feet) +/- 2 x L_{scale}
- Heading (deg) +/- 5
- Attain a stabilized hover within TBD seconds of initial deceleration
- Maintain a stabilized hover for at least 30 second

*Adequate Performance**

- Longitudinal/Lateral Position (feet) +/- 6 x L_{scale}
- Altitude (feet) +/- 4 x L_{scale}
- Heading (deg) +/- 10
- Attain a stabilized hover within TBD seconds of initial deceleration
- Maintain a stabilized hover for at least 30 second

* Performance measures are scaled based on dynamic scaling factor which is given below for velocity and distance performance measures. V_{max} is the maximum velocity of the vehicle in knots.

$$L_{scale} = (V_{max}/160)^2$$

$$V_{scale} = V_{max}/160$$

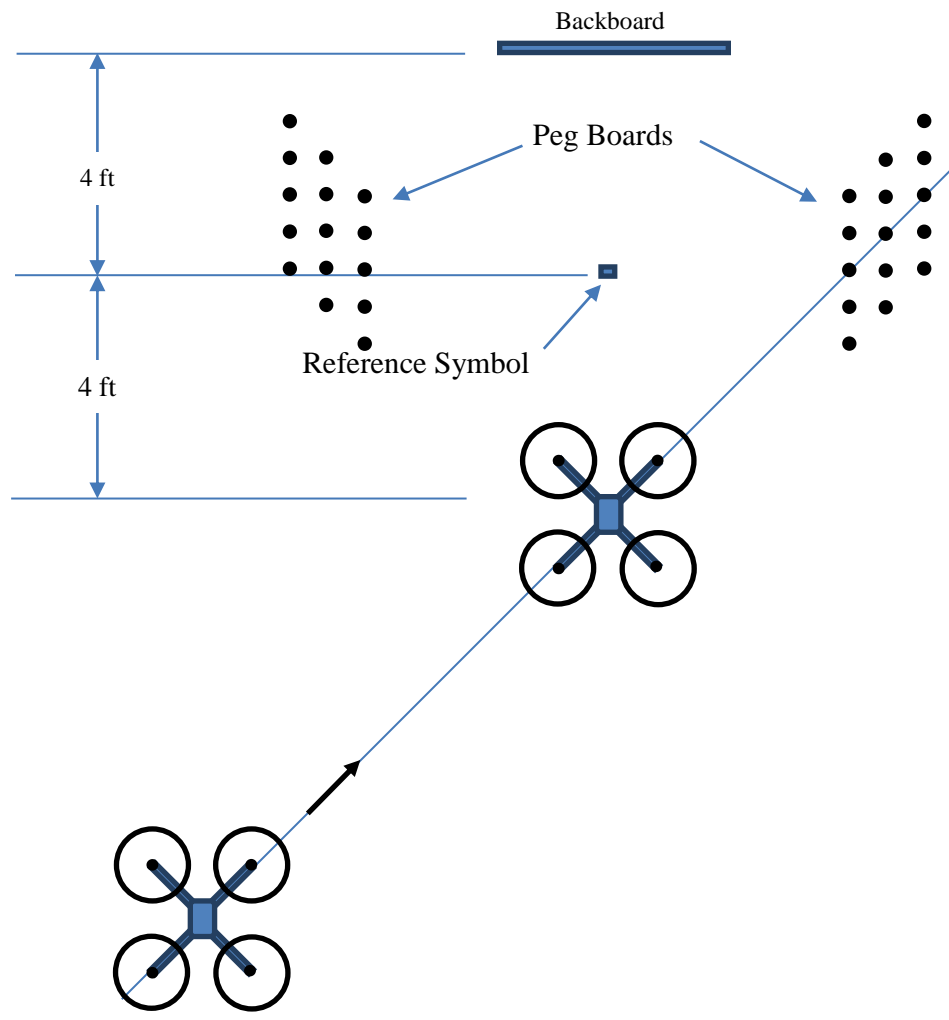


Figure 56: Hover under FPV Cueing MTE Course Layout

REFERENCES

45. Ivler, C. M., C. L. Goerzen, J. A. Wagster IV, F. C. Sanders, K. K. Cheung, and M. B. Tischler, "Control Design for Tracking of Scaled MTE Trajectories on an IRIS+ Quadcopter," presented at the *AHS International 74th Annual Forum & Technology Display*, Phoenix, Arizona, May 14-17, 2018.

Appendix C – Fixed Wing System Identification Flight Test Data

A. FLIGHT TEST CAMPAIGN

1. Test Objectives

The objectives for the fixed wing sUAS system identification flight test program were as follows:

- Generate a flight test database using a variety of flight test inputs for a fixed wing sUAS at multiple flight conditions and aircraft configurations.
 - Collected data will be sufficient to determine aircraft flying and handling qualities metrics at each flight condition and configuration (Ref. 46).
 - The database will include a nominal baseline configuration as well as two off-nominal configurations (e.g., a configuration with added time delay and a configuration with an unfavorable c.g. shift).
- Use several input excitation command types from frequency sweeps to multi-sines to short duration inputs.
 - The database will be used to determine the effectiveness of each command input leading to recommendations that will guide future sUAS tests.
- Demonstrate an efficient process for determining aircraft flying and handling qualities metrics for UAS via flight testing.
- Use the resulting flight test database to compute flight-derived handling qualities parameters and compare with those obtained analytically.

2. Test Description

a. Vehicle Configurations

A nominal baseline configuration and two additional off-nominal configurations were flown. All configurations included the same flight control system feedback augmentation. The off-nominal configurations were: 1) added delay at the feedback sensor and 2) a configuration with an unfavorable c.g. shift.

b. Airspeeds

Two airspeed flight conditions were flown. The primary cruise airspeed for all evaluation tasks was 23 m/s and the primary approach airspeed for all evaluation tasks was 17 m/s.

c. Altitudes

The primary altitude for all cruise and approach evaluation tasks was approximately 50 m. The defined “approach” condition is not a true approach condition as it was flown at a constant altitude, but at a lower airspeed with 50% flap deflections to be reflective of a true approach condition. Maintaining a constant altitude for the defined approach condition was done to simplify and minimize risk for system identification flight test points and to preserve the desired test conditions.

d. Flight Patterns

No specific flight patterns were required, other than to remain in visual line of sight. It flew circuits around the test area with 700 m straight legs and 45° turns at the constant 50 m altitude.

e. Pilot

All evaluated test conditions have been flown by the on-board flight computer, emulating an autonomous or semi-autonomous system. The test inputs were preprogrammed into the flight computer and initiated by the UAS controller on the ground. A subset of these evaluations will also be performed by the UAS controller directly, representative of a remote pilot.

3. Test Inputs

This section provides descriptions of each of the input profiles and includes sample time histories of both the excitation command, the shaped command that was sent to the actuator, and the attitude responses. The profiles were uniform across each axis. Here, pitch axis examples are shown. These examples represent the computer-generated inputs and the resulting vehicle responses. Each of the sample commands include both a plot of the original excitation command u_{ex} (red dashed line), and the resultant shaped surface command u (solid blue line).

a. Multi-Sine

The orthogonal multi-sine (OMS)⁴⁷ input profiles are mutually orthogonal in the time and frequency domains and completely uncorrelated. These OMS were applied to each axis independently, the elevator and aileron in combination, and all three axes in combination, elevator, aileron and rudder. Each OMS was 20 seconds long, had a 4 deg amplitude and covered a frequency range from 1-50 rad/s. Samples of the pitch command and attitude response are provided in Figure 57.

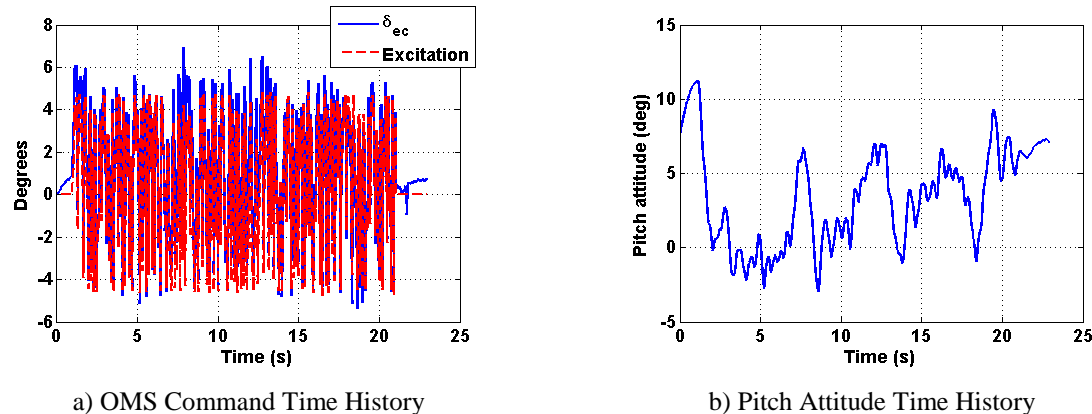


Figure 57: Example Orthogonal Multi-Sine Input and Resulting Aircraft Output

b. Frequency Sweep

The frequency sweep input excitation was designed to be 20 seconds in duration, have an amplitude of 4 deg, and cover a frequency range of 1 to 50 rad/s. This was applied to each axis independently, and the aileron and elevator in combination. When applying this input to the elevator and aileron in combination, the pitch excitation had increasing frequencies over time, while the roll excitation started at high frequency and decreased over time. This provided separation in the frequencies between the axes. Samples of the pitch command and attitude response are given in Figure 58.

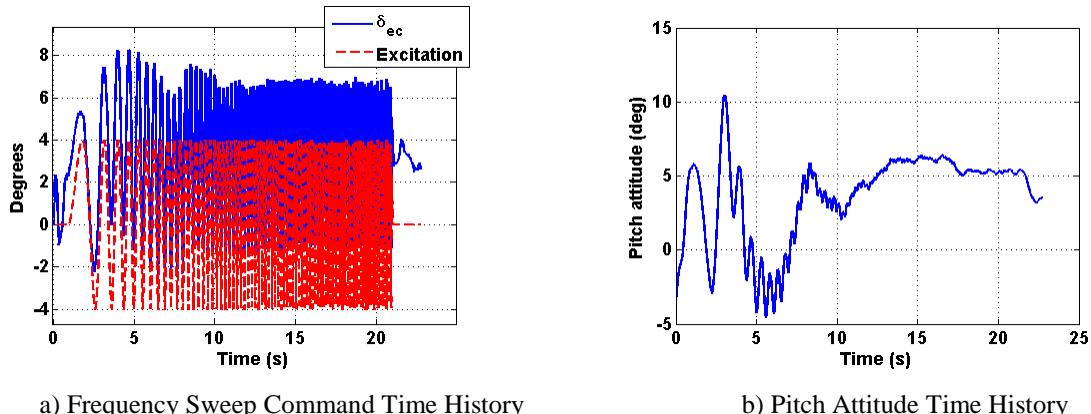
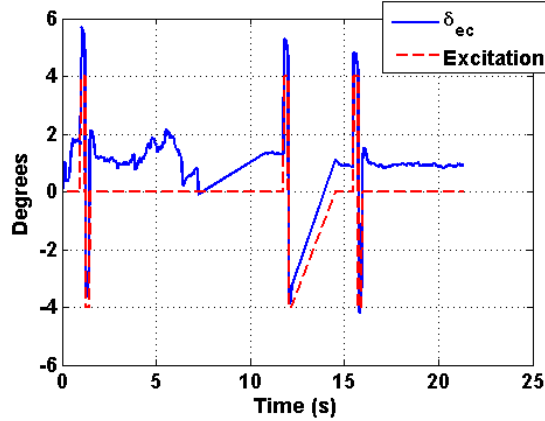


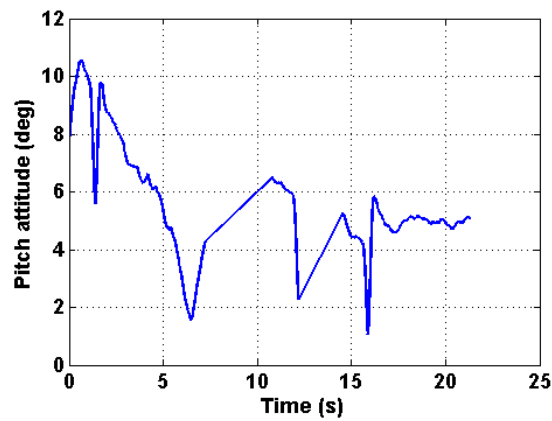
Figure 58: Example Frequency sweep Input and Resulting Aircraft Output

c. Doublet

The doublet excitation profile was designed to have a 4 deg amplitude. The pulse width varied based upon the axis of the input. For every axis, the pulse width (half of the total doublet width) was designed to target a particular frequency through the following relation: $0.7/(2*\text{target frequency})$. The target frequency is in units of Hz. For pitch, the target frequency was the short period mode, estimated as 1.51 Hz. For the aileron and rudder doublet, the Dutch roll frequency was targeted and estimated to be 0.65 Hz. Samples of the pitch command and attitude response are given in Figure 59.



a) Doublet Command Time History

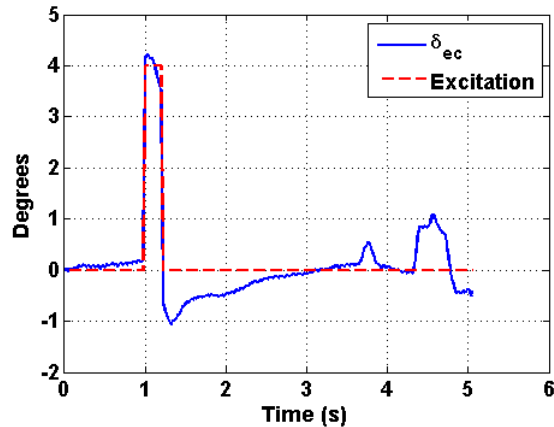


b) Doublet Pitch Attitude Time History

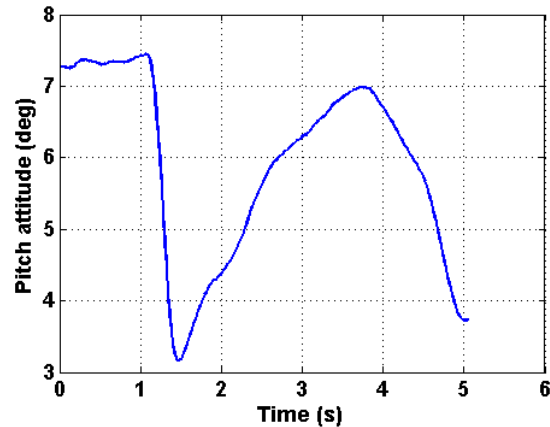
Figure 59: Example Doublet Input and Resulting Aircraft Output

d. Pulse

The pulse input was designed to have a 4 deg amplitude. The pulse width was defined in the same manner as the doublet. A wider aileron input was also defined as an additional input type that was used to determine time to bank values for 30, 50, and 60 degrees. Samples of the pitch command and attitude response are given in Figure 60.



a) Pulse Command Time History



b) Pulse Pitch Attitude Time History

Figure 60: Example Pulse Input and Resulting Aircraft Output

e. 3-2-1-1

The 3-2-1-1 input is a set of pulses of varied widths. A base width is defined, the “1” in 3-2-1-1. This base width is defined in the same manner as the pulse and doublet widths, based on the short period and Dutch roll frequencies for the pitch and roll axis respectively. The “2” and “3” in this is then double and

triple the base width pulses. For example, if the base width was 1 second, the first pulse would be 3 seconds wide, the next 2 seconds wide, followed by two pulses of 1 second each. Each new pulse reverses direction from the prior one. Samples of the pitch command and attitude response are given in Figure 61.

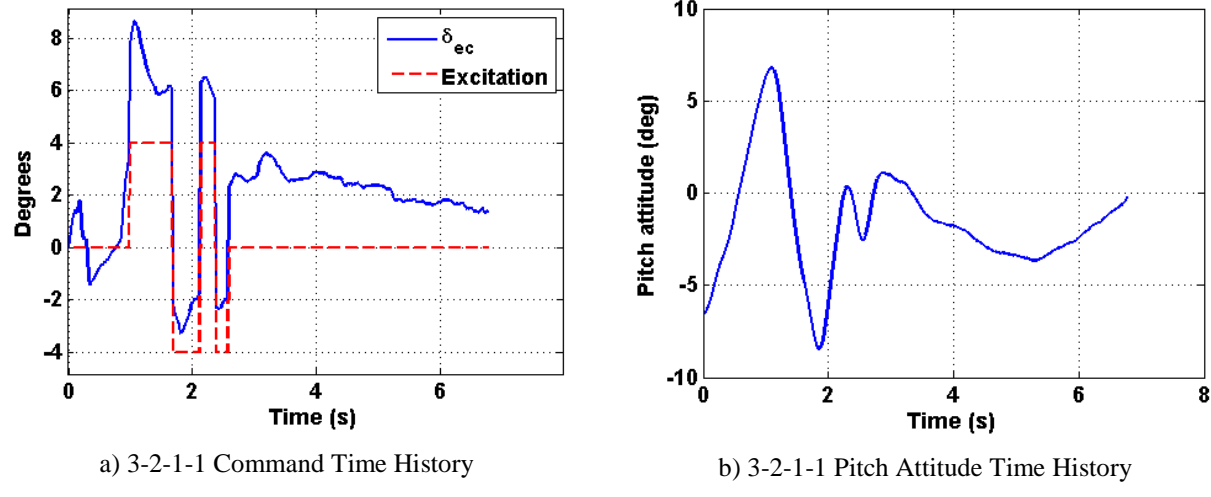


Figure 61: Example 3-2-1-1 Input and Resulting Aircraft Output

4. UltraStick120

UltraStick120 flights 03-06 were flown in late February through mid-March 2018. Flights 10 and 11 were flown in mid-June 2018. The flight vehicle was the UltraStick120. The flight conditions of each flight can be seen in Table 19. Fifty percent flaps were utilized in the Approach Condition. The test card for all 6 flights seen below in Table 20 were flown with computer generated inputs.

Table 19: Flight Conditions

Flight	Speed	Condition		
FLT 03	23 m/s	Cruise	Normal CG	No Added Delay
FLT 04	17 m/s	Approach	Normal CG	No Added Delay
FLT 05	23 m/s	Cruise	Aft CG	No Added Delay
FLT 06	17 m/s	Approach	Aft CG	No Added Delay
FLT 10	23 m/s	Cruise	Normal CG	Extra Delay 80ms
FLT 11	17 m/s	Approach	Normal CG	Extra Delay 80ms

Table 20: Flight Test Card

Leg	Input Name	Description	Duration (sec)	Amplitude (deg)	Start-End Frequency (rad/s)
1	OMS_ele1	Orthogonal multi-sine applied to elevator	20	4	1-50
2	OMS_ail1	Orthogonal multi-sine applied to ailerons	20	4	1-50
3	OMS_rud1	Orthogonal multi-sine applied to rudder	20	4	1-50
4	OMS_elevail1	Orthogonal multi-sine applied to elevator and ailerons in combination	20	4	1-50
5	OMS_3axes1	Orthogonal multi-sine applied to elevator, ailerons and rudder in combination	20	4	1-50
6	frequency sweep_elev1	Frequency sweep to the elevator	20	4	1-50
7	frequency sweep_ail1	Frequency sweep to the ailerons	20	4	1-50
8	frequency	Frequency sweep to the rudder	20	4	1-50

Leg	Input Name	Description	Duration (sec)	Amplitude (deg)	Start-End Frequency (rad/s)
	sweep_rud1				
9	frequency sweep_elevail1	Simultaneous frequency sweep to the elevator and ailerons (ele increasing freq, ail decreasing)	20	4	1-50
Leg	Input Name	Description			
10	doublet_elev	A doublet input to the elevator	20	4	0.23 (half width)
11	doublet_ail	A doublet input to the ailerons	20	4	0.54 (half width)
12	doublet_rud	A doublet input to the rudder	20	4	0.54 (half width)
13	pulse_elev	A pulse input to the elevator	20	4	0.23
14	pulse_ail	A pulse input to the ailerons	20	4	0.54
15	pulse_rud	A pulse input to the rudder	20	4	0.54
16	pulse_ail_wide	A wider pulse input to the aileron	20	25	0.6
17	3211_elev	A combination of 3 width, 2 width, 1 width, 1width elevator pulses in opposing directions for each new input	20	4	0.23 (the “1” width)
18	3211_ail	A combination of 3 width, 2 width, 1 width, 1width aileron pulses in opposing directions for each new input	20	4	0.54 (the “1” width)
19	3211_rud	A combination of 3 width, 2 width, 1 width, 1width rudder pulses in opposing directions for each new input	20	4	0.54 (the “1” width)

In support of the flight test objectives outlined earlier in this document, each input profile was leveraged to identify the flight vehicle from the test data. The excitation input was summed with the compensated feedback signal to generate the actuator input signal “u”, as seen in Figure 7. The output variables were the pitch rate for longitudinal, roll rate for lateral, and yaw rate for directional. This identification returns the actuator and bare airframe dynamics of the vehicle and is not a complete closed-loop identification.

As an initial checkout, every input profile that included an elevator, aileron, or rudder excitation was identified using STI’s FREquency Domain Analysis (FREDA) software (Ref. 48). The overlay of each of these identifications, including the Simulink model frequency response, is shown below in the first figure in each subsequent subsection.

Following the summary figure in each subsection, the individual input types have been broken out. The OMS profile was flown under three configurations: elevator input only, elevator and aileron inputs at the same time, and the elevator, aileron and rudder inputs at the same time.

An encouraging result from this evaluation is the relative uniformity of the identified systems with one another, even in the presence of excitations of the other control surfaces. This result would indicate that the OMS input excitation can be performed in multiple axes without interfering with or contaminating the results of the others, as has been exemplified by Morelli (Ref. 47). This characteristic means that fewer numbers of flights are required to perform the identification of the vehicle, saving on time and cost during the test campaign.

The follow-on figures in each subsection shows the frequency sweep profiles which was flown under four conditions: elevator input only, aileron input only, rudder input only, and elevator and aileron inputs at the same time. Like for the OMS identification, the frequency sweep exhibits the same property: the ability to have multi-axis input excitations not adversely affect the system identification.

The next figure in each subsection show the short duration inputs. Four different signals are shown in this section: doublet, pulse, 3-2-1-1, and for aileron only, wider pulse.

As a side note, all the model responses shown in the subsequent sections are models that were updated to match the flight data using the frequency sweep test run.

B. FLIGHT 03

Flight 03 was flown at cruise condition, that was straight and level flight with computer generated inputs. This flight is the baseline configuration.

In order to match the gain values of the longitudinal, lateral, and directional bare airframe models with the flight data, a series of gains were applied to the bare airframe models which can be seen in Table 21.

Table 21: Model Gains for FLT 03

Longitudinal	Lateral	Directional
1.5	1.0	3.5

1. Longitudinal Survey

All identified responses from the longitudinal excitations can be seen plotted with the updated reference model in Figure 62. Table 22 provides the actuator model and bare airframe dynamics in the longitudinal axis.

Table 22: FLT 03 – Longitudinal Aircraft and Elevator Actuator Models

Elevator Actuator Model	Longitudinal Model
$\frac{\delta_e}{\delta_{ec}} = \frac{8}{s+10} e^{-0.065s}$	$\frac{q}{\delta_e} = \frac{75.03(-0)(0.3977)(5.966)}{[0.3078, 0.5362][0.5, 12.5]}_1$

The identified longitudinal OMS input excitation for flight 03 can be seen in Figure 63. All identified systems provide a close match to the modeled response, with higher levels of coherence except at the highest ($> 40\text{rad/s}$) ends of the frequency region.

The identified longitudinal frequency sweep input excitation for flight 03 can be seen in Figure 64, featuring the elevator only input, and the multi-axis elevator and aileron input. Given that the model was updated to match the elevator only frequency sweep response, the model closely matches this as expected. The multi-axis input frequency sweep also matches well. There was good coherence throughout the range of frequencies shown.

The identified longitudinal short duration input excitation can be seen in Figure 65. The identified systems closely overlaid the model response. Of the three excitations, the 3-2-1-1 input profile maintained the highest level of coherence across the frequency region shown, but all excitations lacked the content to identify the lowest and highest frequencies of interest.

¹. The STI shorthand form of displaying a transfer function is defined by: $a(s+b)[s^2 + 2\zeta\omega s + \omega^2] = a(b)[\zeta, \omega]$

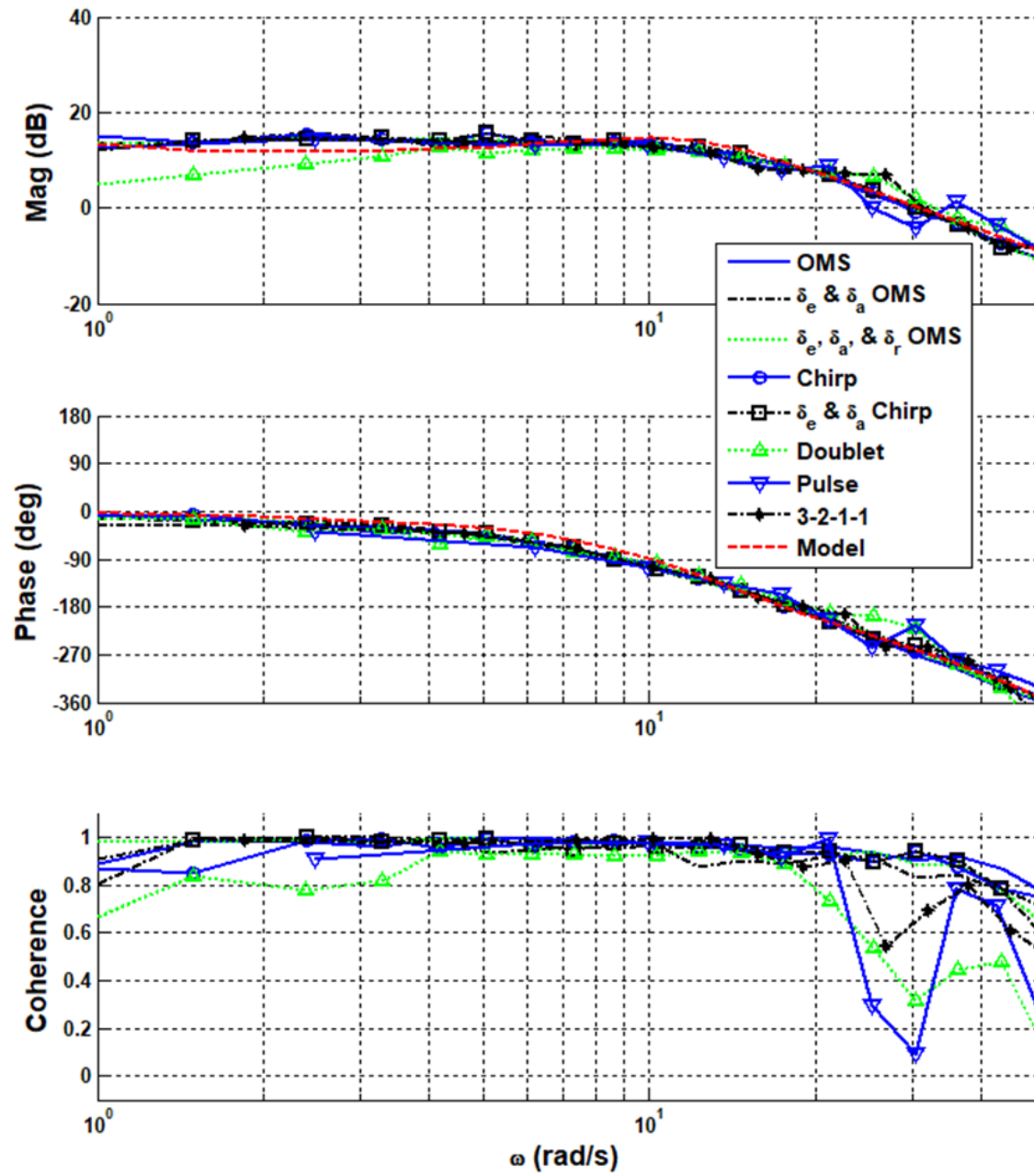


Figure 62: FLT03 - q/δ_{ec} Identification – All Methods

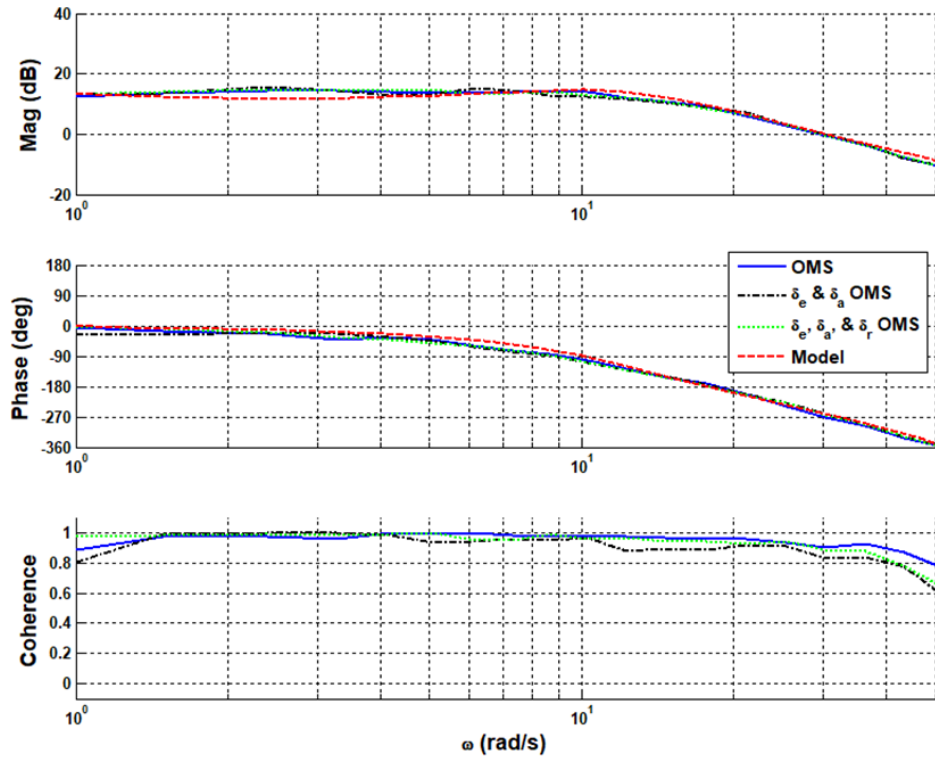


Figure 63: FLT03 - q/δ_{ec} Identification – OMS

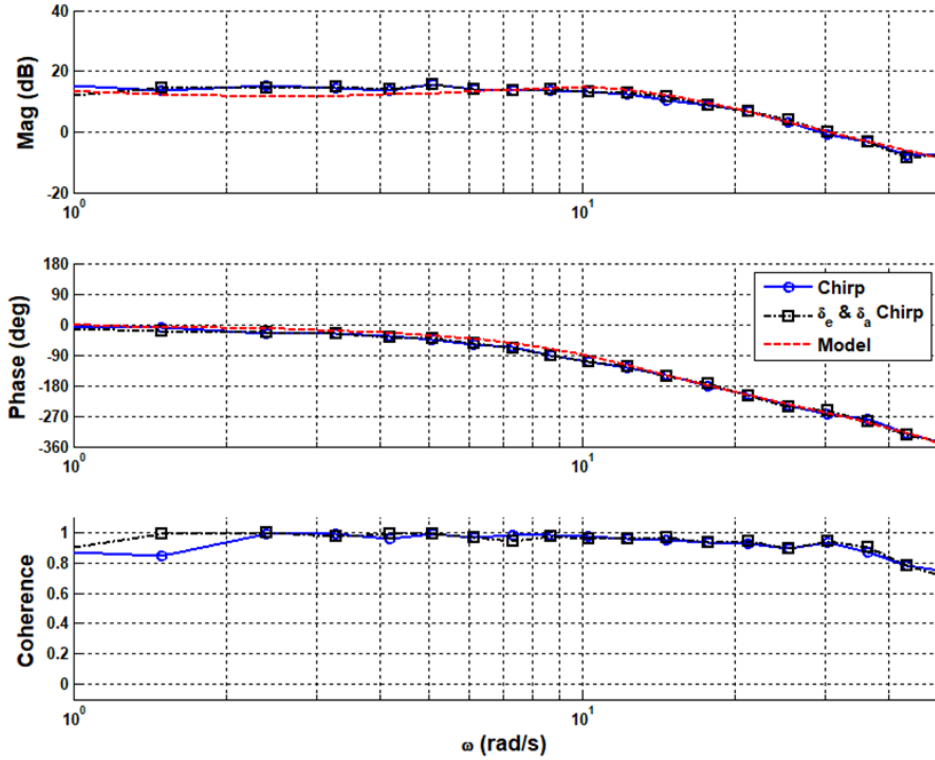


Figure 64: FLT03 - q/δ_{ec} Identification – Frequency sweep

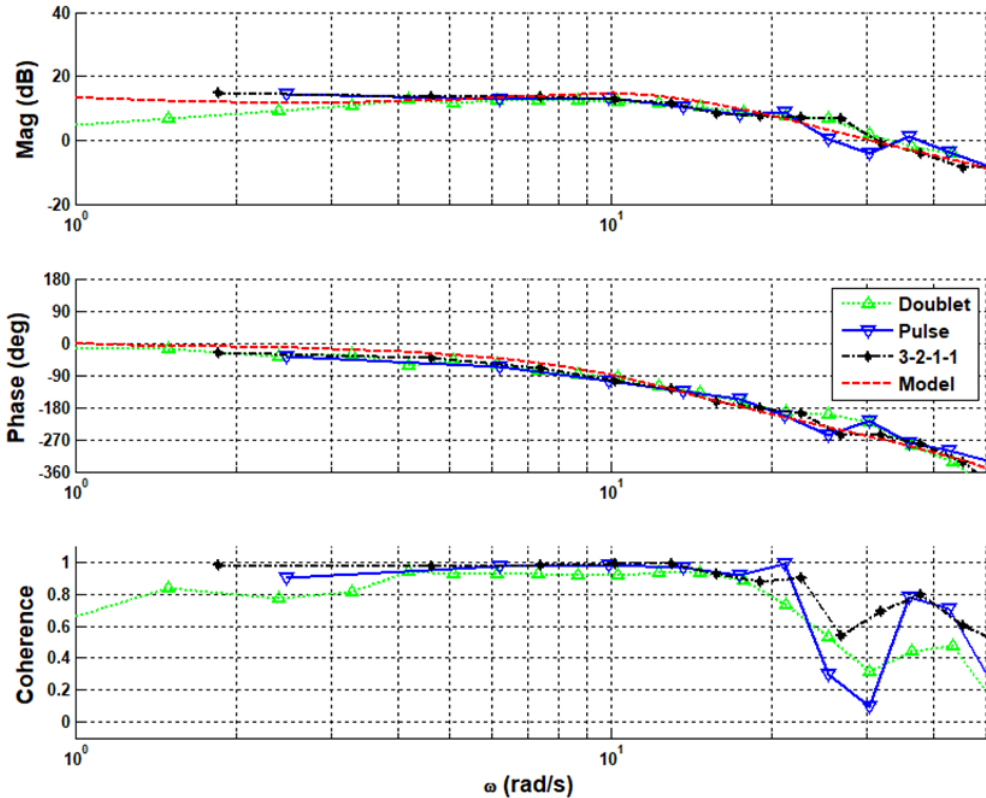


Figure 65: FLT03 - q/δ_{ec} Identification – Short Duration Inputs

2. Lateral Survey

All lateral excitations can be seen plotted with the model in Figure 66. Table 23 provides the aileron actuator model and lateral aircraft model.

Table 23: FLT 03 – Lateral Aircraft and Aileron Actuator Model

Aileron Actuator Model	Lateral Model
$\frac{\delta_a}{\delta_{ac}} = \frac{40}{s+12} e^{-0.060s}$	$\frac{p}{\delta_a} = \frac{48.98(-0.03415)[0.2767, 3.436]}{(0.0456)[0.2961, 3.943](12.5)}$

The identified lateral OMS input excitation for flight 03 can be seen in Figure 67. The magnitude and phase response of the aileron alone, and elevator-aileron multi axis, and the elevator-aileron-rudder multi axis excitations closely match the model. The coherence levels are high in general, with some slight tapering at the highest frequencies and a drop in the 2-3 rad/s region for the elevator-aileron-rudder multi axis input. This did not significantly alter the quality of the fit.

The identified lateral frequency sweep input excitation for flight 03 can be seen in Figure 68 that features the aileron only input, and the multi-axis elevator and aileron excitation. Overall, the magnitude and phase response of both signals closely fit the model. The aileron only excitation generally has a higher coherence relative to the multi-axis input though both are close to 1. In addition, the coherence rolls off at the highest frequency levels for both input profiles.

The identified lateral short duration input excitation can be seen in Figure 69. Of the four excitations, the 3-2-1-1 input profile maintained the highest level of coherence across the frequency region shown, but all

excitations had either major issues with or lacked the content to identify the lowest and highest frequencies of interest.

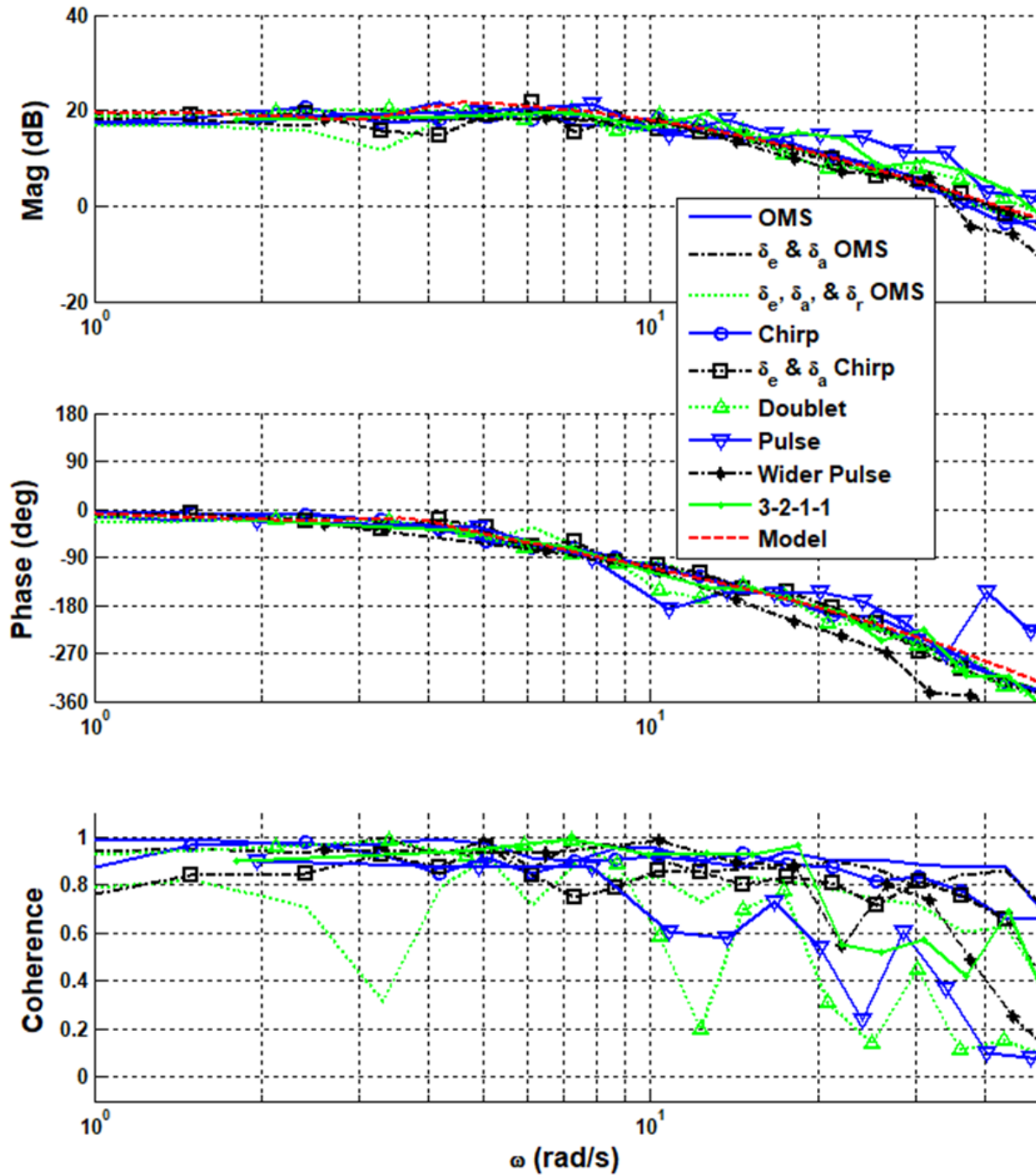


Figure 66: FLT03 - p/δ_{ac} Identification – All Methods

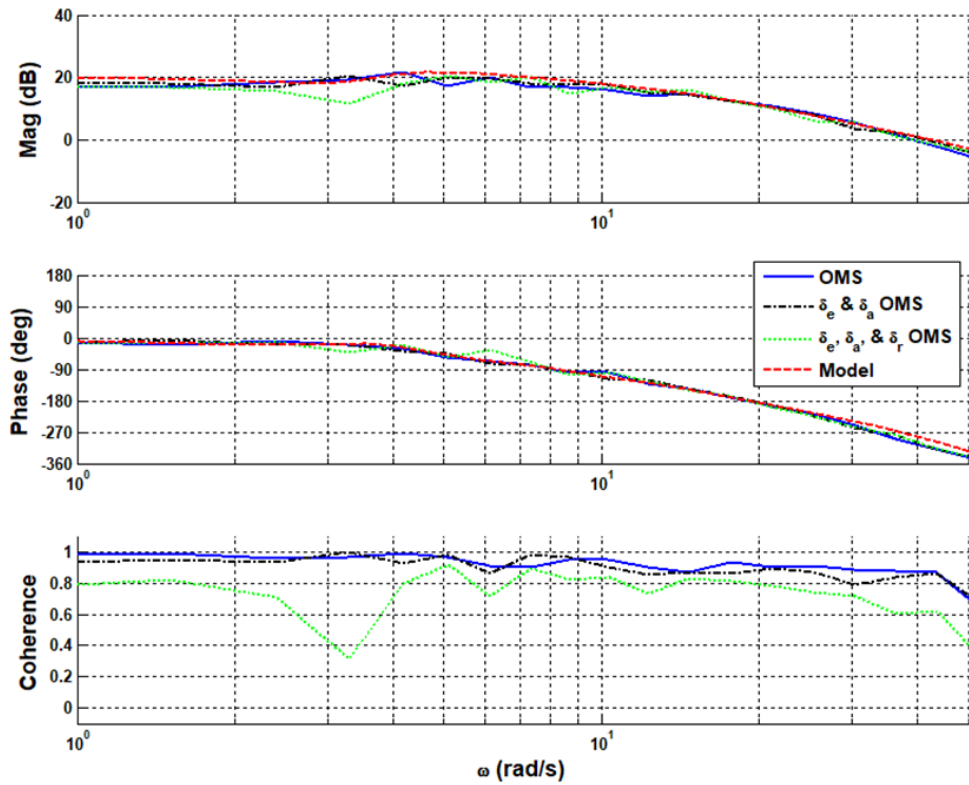


Figure 67: FLT03 - p/δ_{ac} Identification – OMS

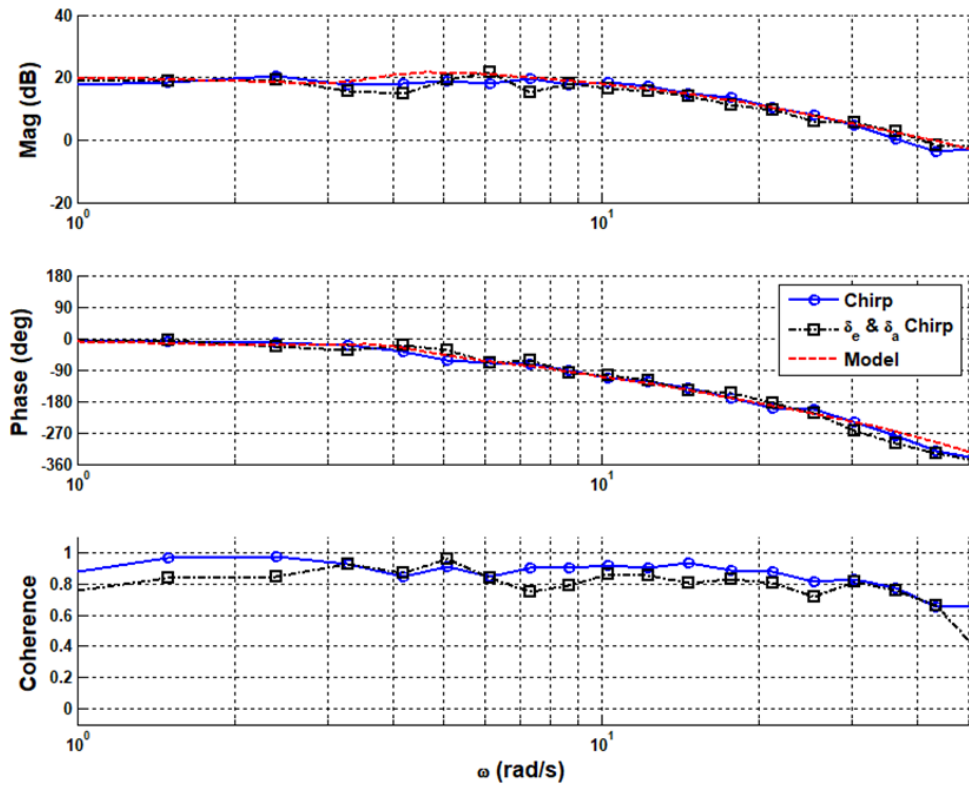


Figure 68: FLT03 - p/δ_{ac} Identification – Frequency sweep

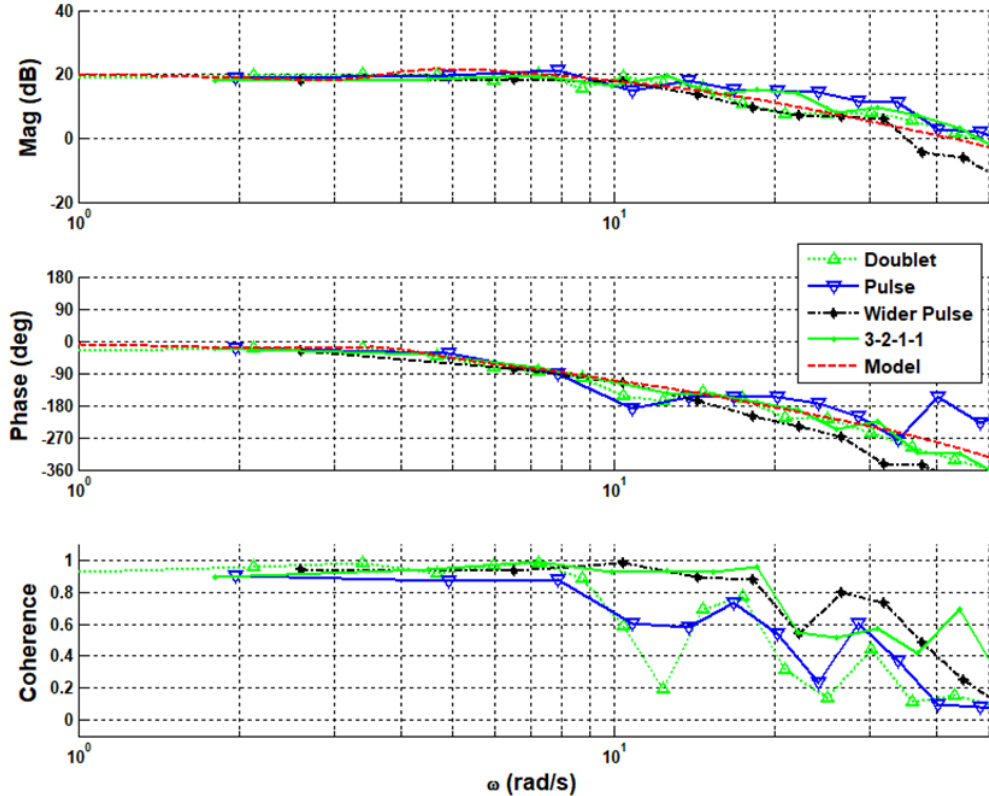


Figure 69: FLT03 - p/ δ_{ac} Identification – Short Duration Inputs

3. Directional Survey

All directional excitations can be seen plotted with the model in Figure 70. Table 24 provides the rudder actuator model and directional aircraft model.

Table 24: FLT 03 - Directional Aircraft and Rudder Actuator Model

Rudder Actuator Model	Directional Model
$\frac{\delta_r}{\delta_{rc}} = \frac{10}{s+10} e^{-0.065s}$	$\frac{r}{\delta_r} = \frac{-7.547[0.245, 1.247](8.928)}{(0.0456)[0.299, 4](12.5)}$

The identified directional OMS input excitation for flight 03 can be seen in Figure 71. The magnitude and phase response of the rudder alone, and the elevator-aileron-rudder multi axis closely match each other and the model at frequencies above 5 rad/s. At the lower frequencies the coherence tended to be less than 0.8. The coherence rolls off at the highest frequencies, though ~10 rad/s sooner than for the pitch and roll evaluations.

The identified directional frequency sweep input excitation for flight 03 can be seen in Figure 72, which features the rudder only input. Overall, the magnitude and phase response of the excitation matches the model above ~2-3 rad/s. The lowest and highest frequency regions have coherence levels below 0.8 and the identified fits reflect that.

The identified directional short duration input excitation can be seen in Figure 73. Of the four excitations, the 3-2-1-1 input profile maintained the highest level of coherence across the frequency region shown, but all excitations either had low coherence or lacked the frequency content to identify the lowest and highest frequencies of interest.

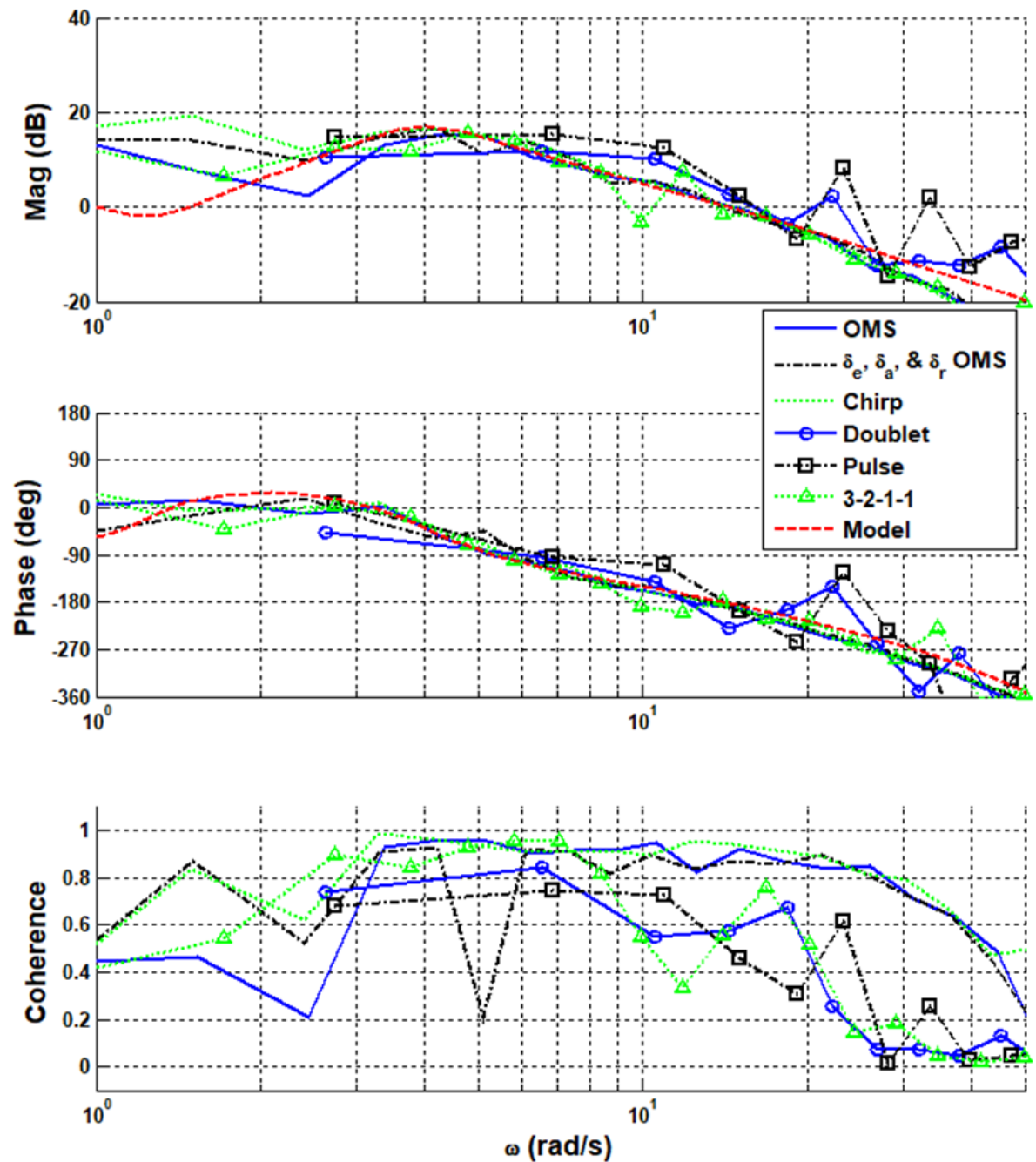


Figure 70: FLT03 - r/ δ_{rc} Identification – All Methods

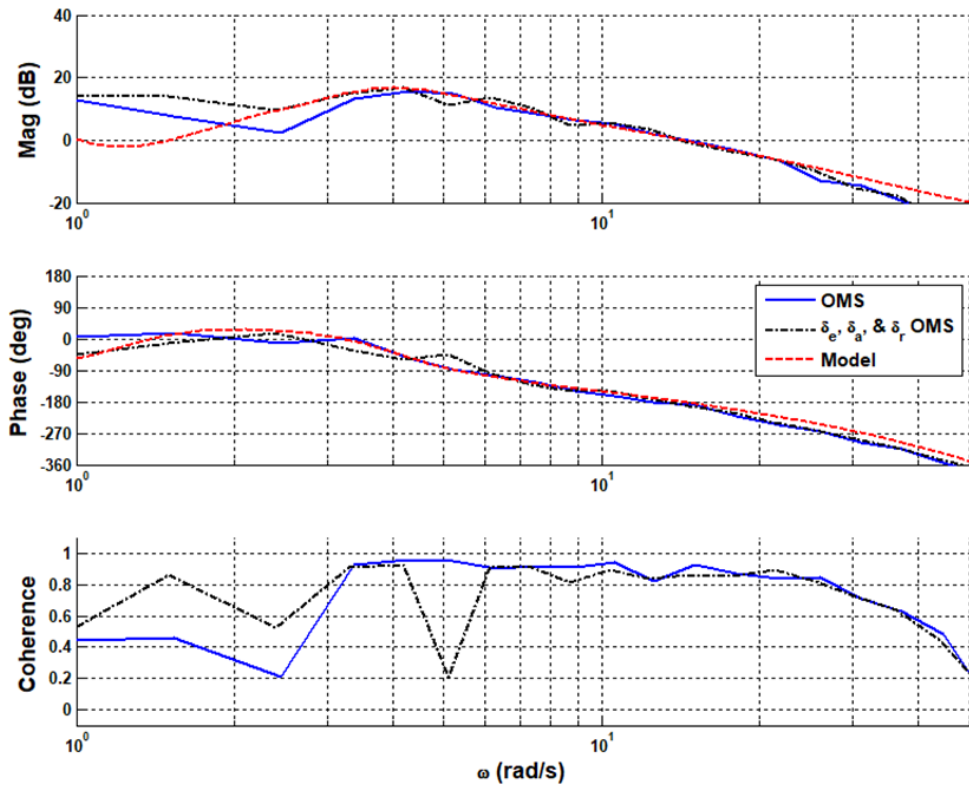


Figure 71: FLT03 - r/δ_{rc} Identification – OMS

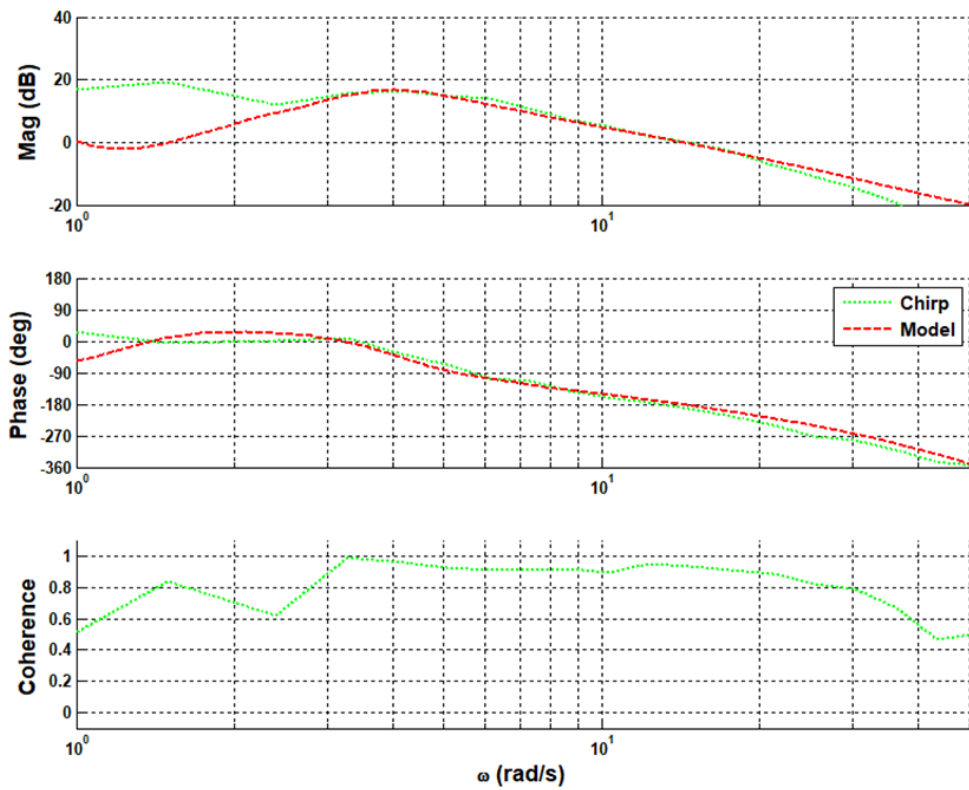


Figure 72: FLT03 - r/δ_{rc} Identification – Frequency Sweep

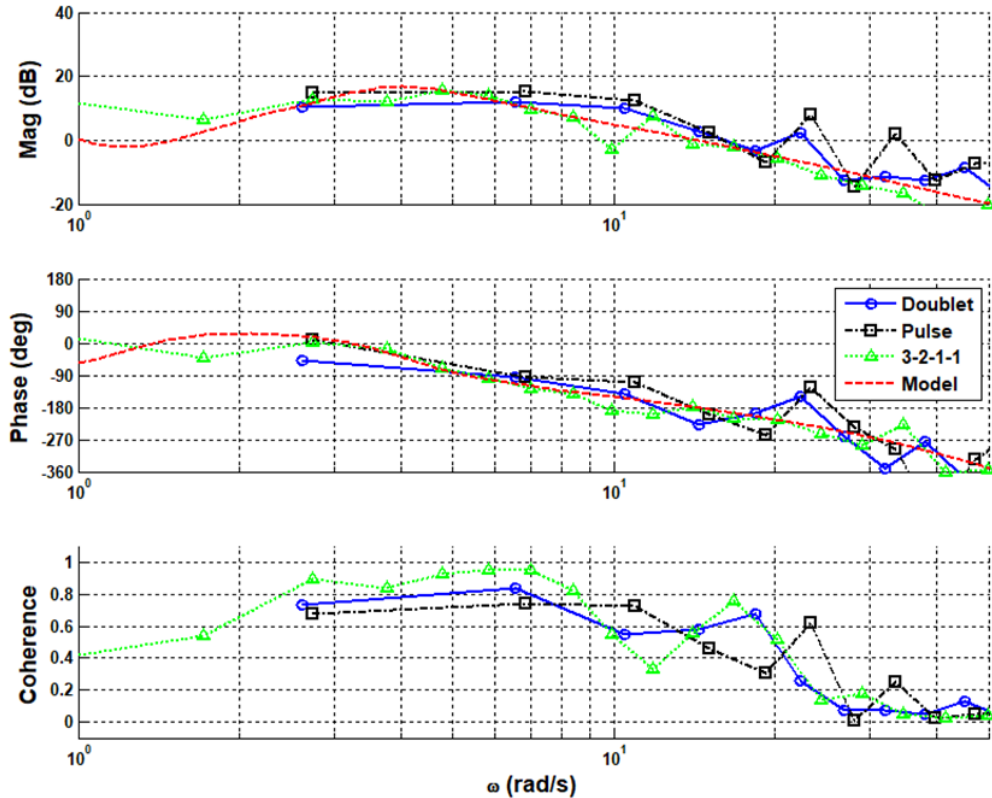


Figure 73: FLT03 - r/δ_{rc} Identification – Short Duration Inputs

C. FLIGHT 04

Flight 04 was flown at the approach condition, essentially a lower airspeed cruise (17m/s) with flaps at 50%. In order to match the gain values of the longitudinal, lateral, and directional bare airframe models with the flight data, a series of gains were applied to the bare airframe models which can be seen in Table 25.

Table 25: Model Gains for FLT 04

Longitudinal	Lateral	Directional
1.25	1.0	4.0

1. Longitudinal Survey

All identified responses from the longitudinal excitations can be seen plotted with the updated reference model in Figure 74. Table 26 provides the actuator model and bare airframe dynamics in the longitudinal axis.

Table 26: FLT 04 - Longitudinal Aircraft and Elevator Actuator Models

Elevator Actuator Model	Longitudinal Model
$\frac{\delta_e}{\delta_{ec}} = \frac{8}{s + 10} e^{-0.065s}$	$\frac{q}{\delta_e} = \frac{40.54(-0)(0.3175)(4.617)}{[0.1748, 0.6876][0.651, 8.18]}$

The identified longitudinal OMS input excitation for flight 04 can be seen in Figure 75. All identified signals match each other and the model with high coherence (near 1) except at the higher frequencies of interest.

The identified longitudinal frequency sweep input excitation for flight 04 can be seen in Figure 76, featuring the elevator only input, the multi-axis elevator and aileron input, and the multi axis elevator-aileron-rudder input. All the frequency sweep input excitations closely match the model. High coherence can be seen throughout the range of frequencies shown.

The identified longitudinal short duration input excitation can be seen in Figure 77. The excitations match the model at lower frequencies. Of the three excitations, the pulse input profile maintained the highest level of coherence across the frequency region shown, but all excitations had either issues with or lacked the content to identify frequencies of interest.

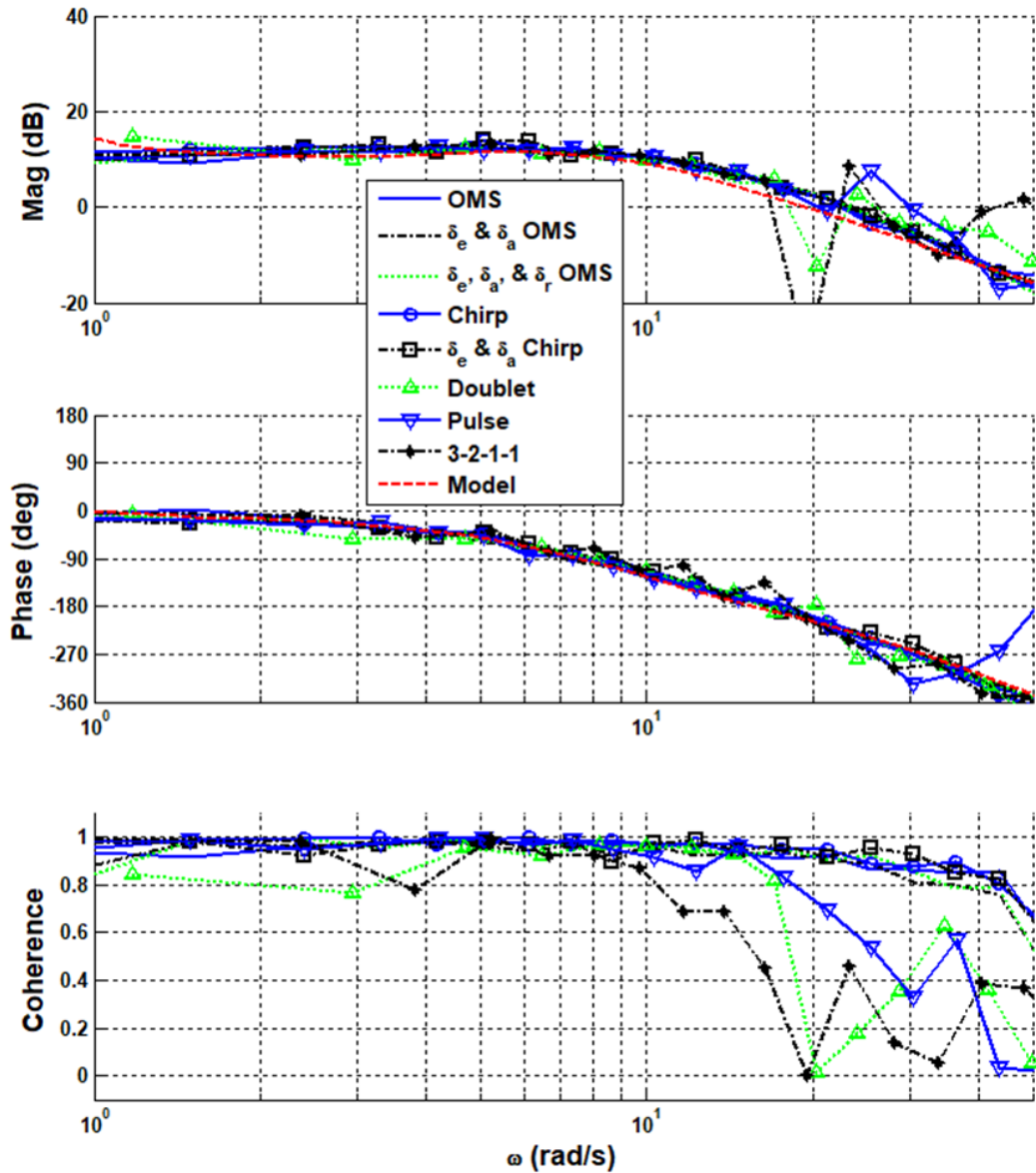


Figure 74: FLT04 - q/δ_{ec} Identification – All Methods

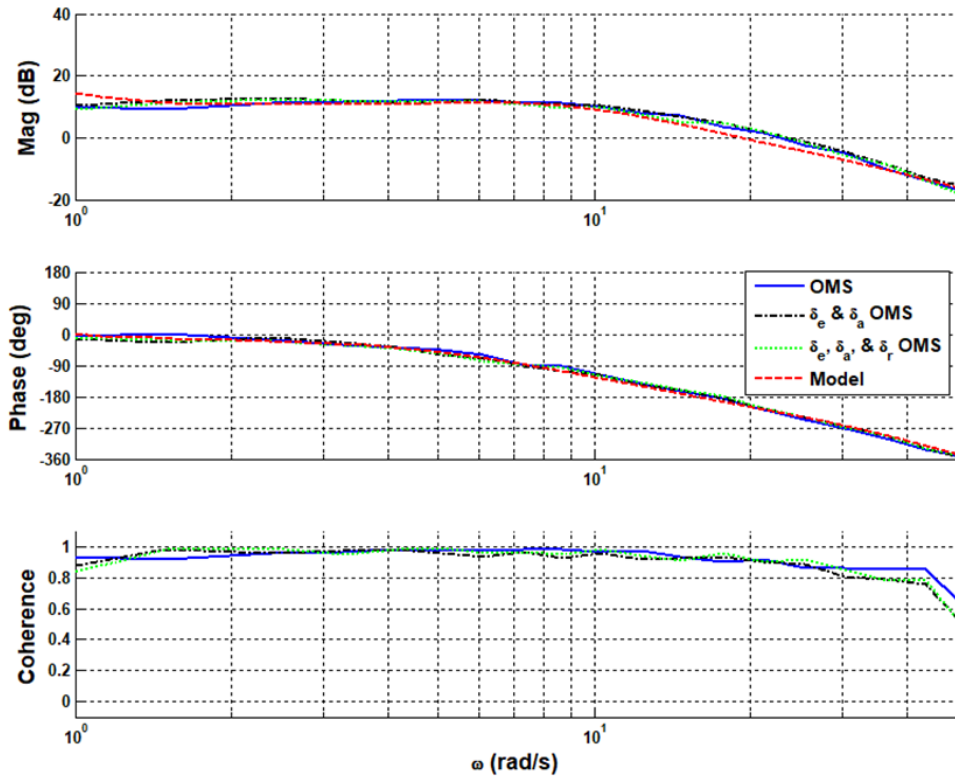


Figure 75: FLT04 - q/δ_{ec} Identification – OMS

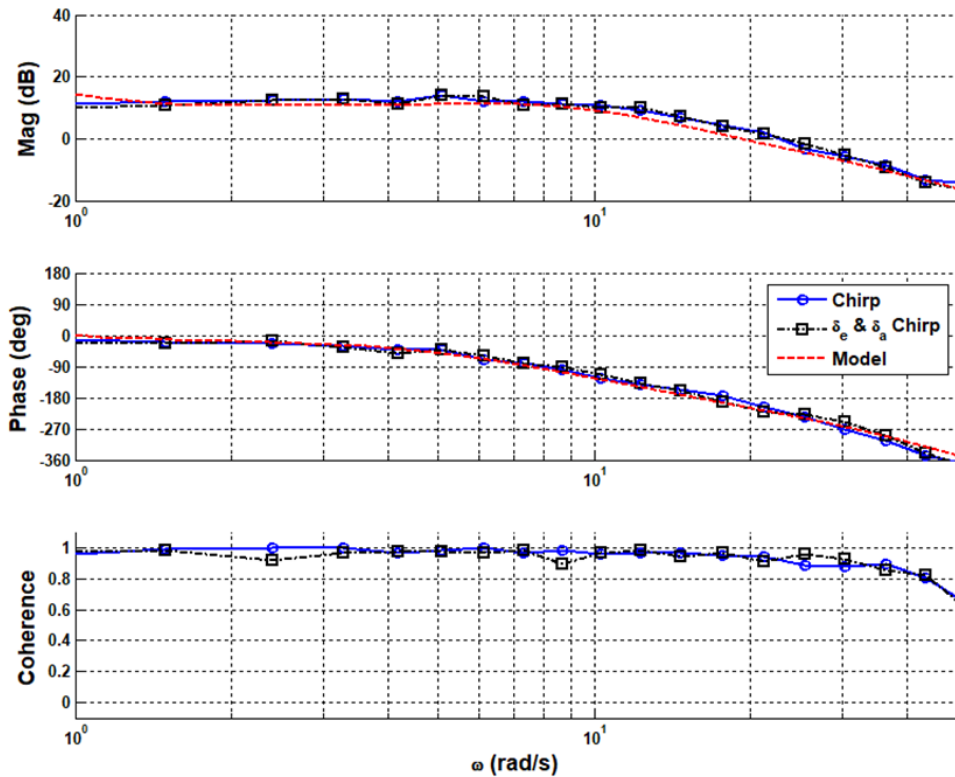


Figure 76: FLT04 - q/δ_{ec} Identification – Frequency sweep

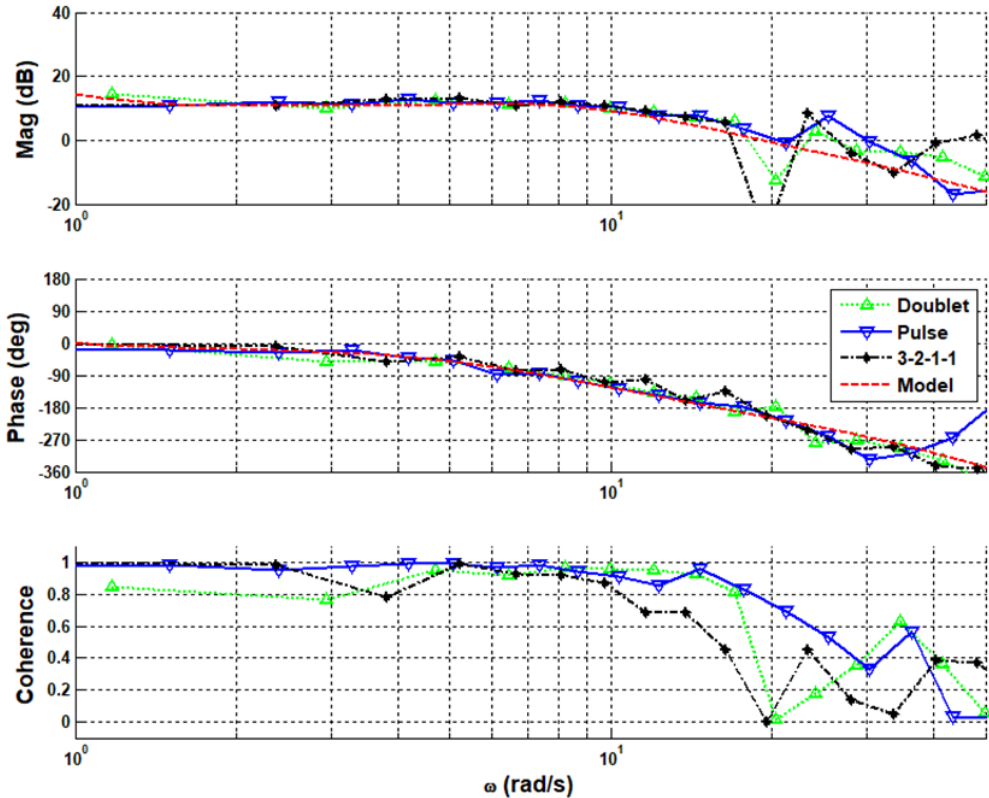


Figure 77: FLT04 - q/δ_{ec} Identification – Short Duration Inputs

2. Lateral Survey

All lateral excitations can be seen plotted against the model in Figure 78. Table 27 provides the aileron actuator model and lateral aircraft model.

Table 27: FLT 04 - Lateral Aircraft and Aileron Actuator Model

Aileron Actuator Model	Lateral Model
$\frac{\delta_a}{\delta_{ac}} = \frac{40}{s+12} e^{-0.060s}$	$\frac{p}{\delta_a} = \frac{30.27(-0.08536)[0.3335, 2.24]}{(0.05395)[0.3226, 3.066](12.5)}$

The identified lateral OMS input excitation for flight 04 can be seen in Figure 79. The magnitude and phase response of the aileron alone, and elevator-aileron multi axis match closely to the model at all frequencies of interest. The elevator-aileron-rudder multi axis excitation matches closely the other OMS input excitations and the model at higher frequencies. However, there is a drop in coherence at frequencies less than 4 rad/s.

The identified lateral frequency sweep input excitation for flight 04 can be seen in Figure 80, which features the aileron only input, and the multi-axis elevator-aileron excitation. Overall, the magnitude and phase response of both excitations match the model, with the aileron only excitation generally having a higher coherence. The elevator and aileron multi axis excitation have high coherence which occasionally drops below 0.8. once again, as the frequency approaches the upper bounds of the test, the coherence drops off.

The identified lateral short duration input excitation can be seen in Figure 81. Of the four excitations, the 3-2-1-1 and the doublet input profiles maintained the highest level of coherence across the frequency

region shown, but all excitations had either issues with or lacked the content to identify the lowest and highest frequencies of interest.

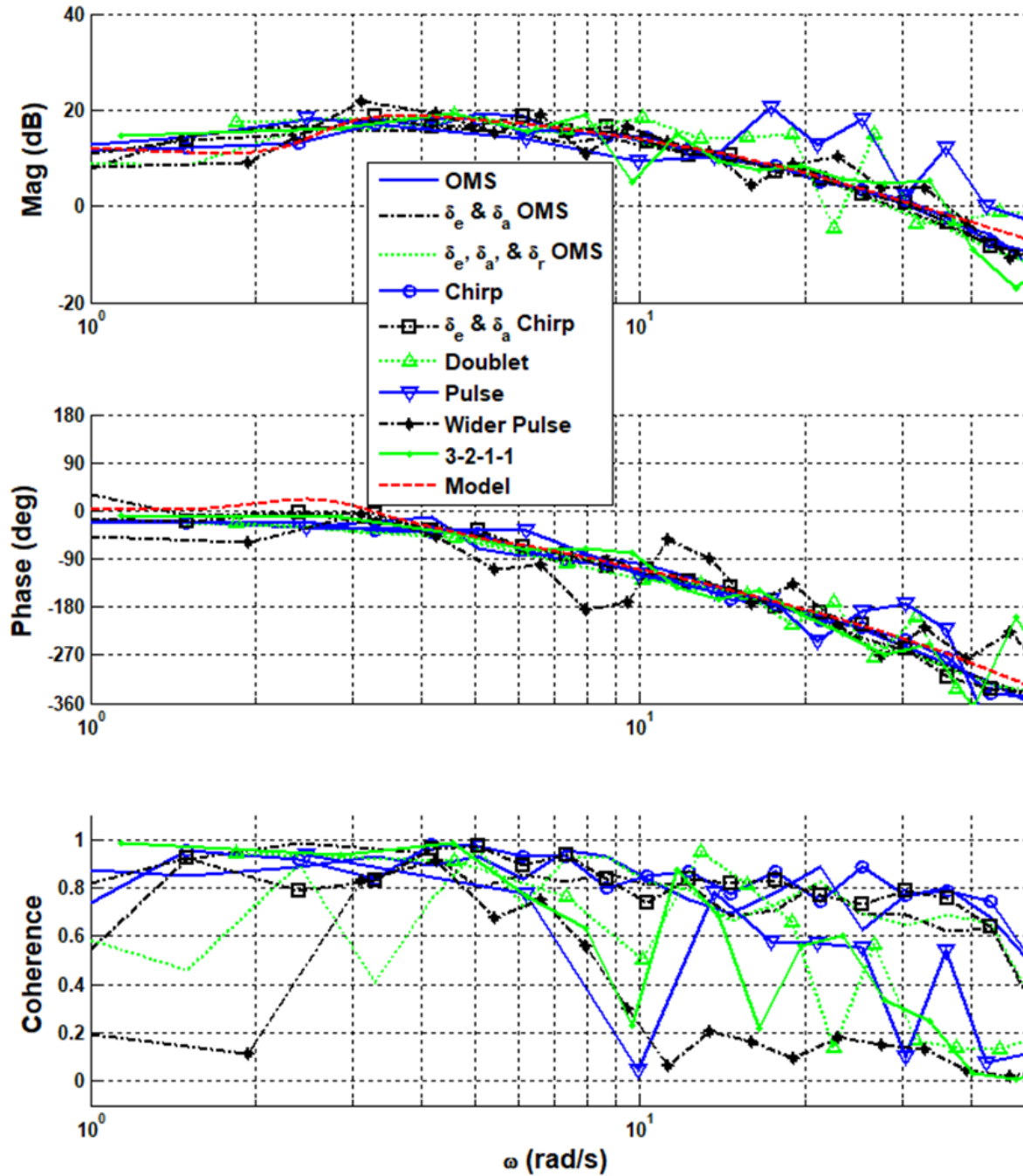


Figure 78: FLT04 - p/δ_{ac} Identification – All Methods

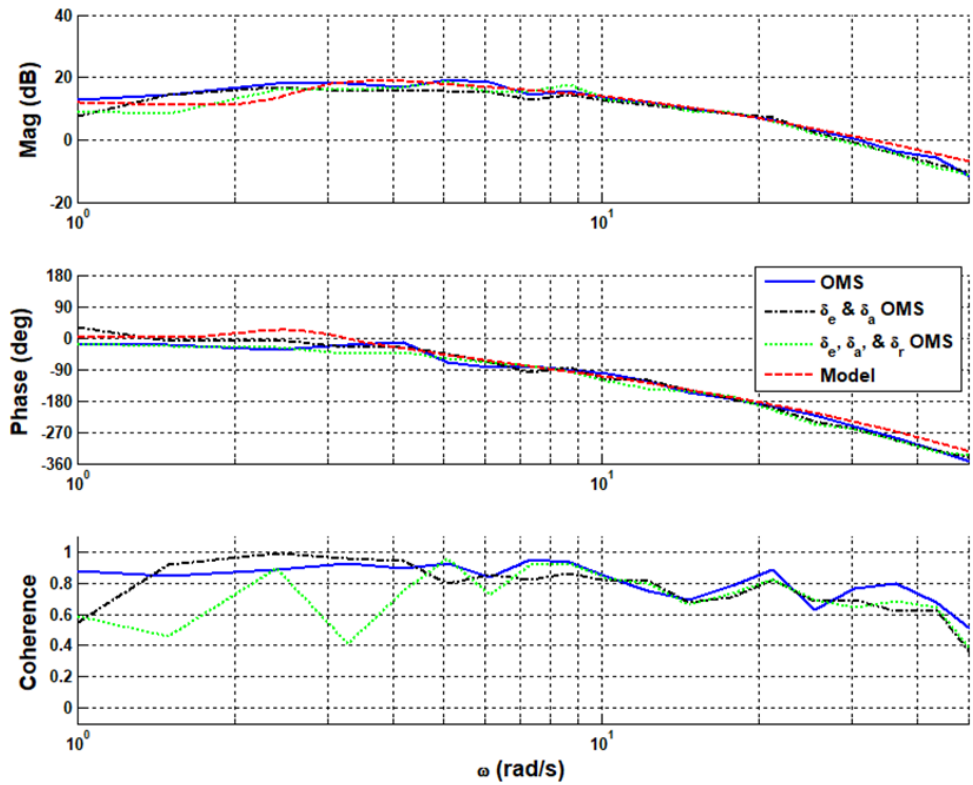


Figure 79: FLT04 - p/δ_{ac} Identification – OMS

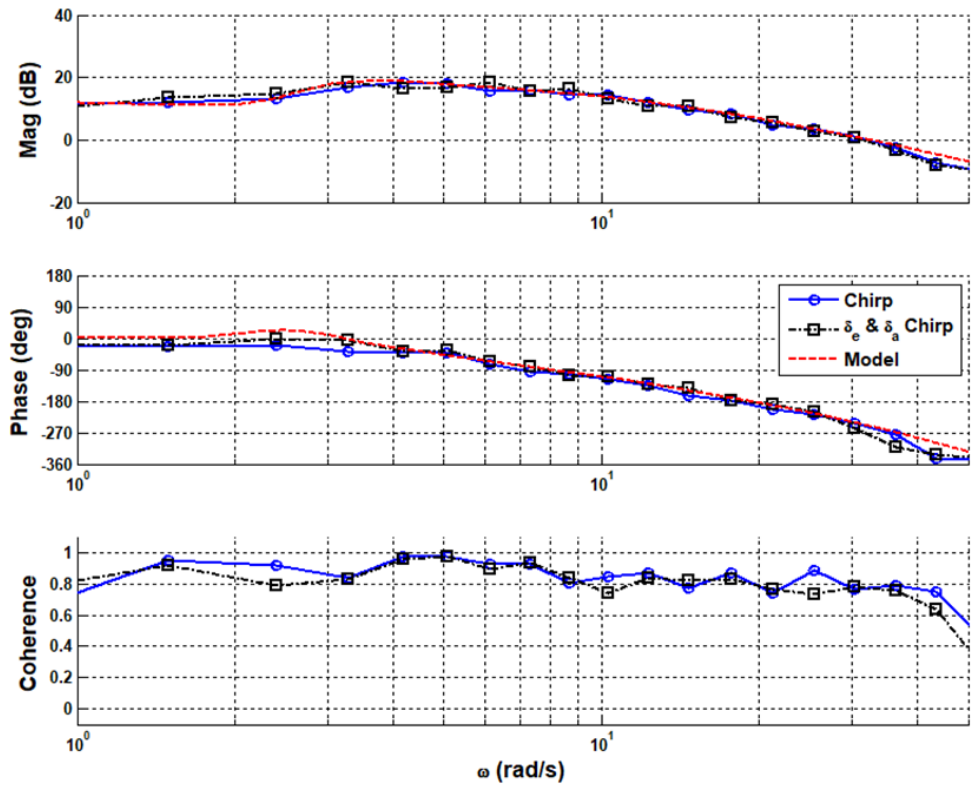


Figure 80: FLT04 - p/δ_{ac} Identification – Frequency sweep

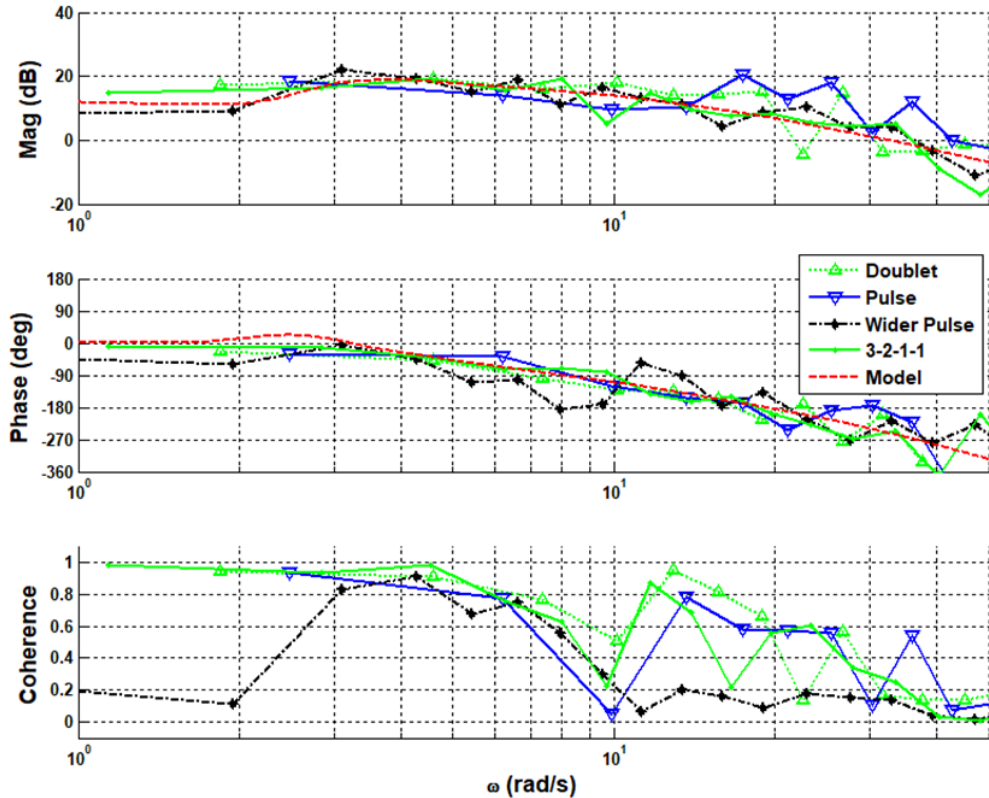


Figure 81: FLT04 - p/ δ_{ac} Identification – Short Duration Inputs

3. Directional Survey

All directional excitations can be seen plotted with the model and modes in Figure 82. Table 28 provides the rudder actuator model and directional aircraft model.

Table 28: FLT 04 - Directional Aircraft and Rudder Actuator Model

Rudder Actuator Model	Directional Model
$\frac{\delta_r}{\delta_{rc}} = \frac{10}{s+10} e^{-0.065s}$	$\frac{r}{\delta_r} = \frac{-3.754[0.2292, 1.387](6.949)}{(0.05395)[0.3, 3.5](12.5)}$

The identified directional OMS input excitation for flight 04 can be seen in Figure 83. The magnitude and phase response of the rudder alone, and the elevator-aileron-rudder multi axis have a fluctuating value of coherence throughout the frequencies of interest. The rudder only excitation is close to 0.8 throughout but the combined OMS generally had coherence values less than 0.8.

The identified directional frequency sweep input excitation for flight 04 can be seen in Figure 84, which features the rudder only input. Overall, the magnitude and phase response of the excitation are a match to the model above $\sim 2\text{-}3$ rad/s.

The identified directional short duration input excitation can be seen in Figure 85. Of the four excitations, the 3-2-1-1 input profile maintained the highest level of coherence across the frequency region shown, but all excitations had either issues with or lacked the content to identify the lowest and highest frequencies of interest.

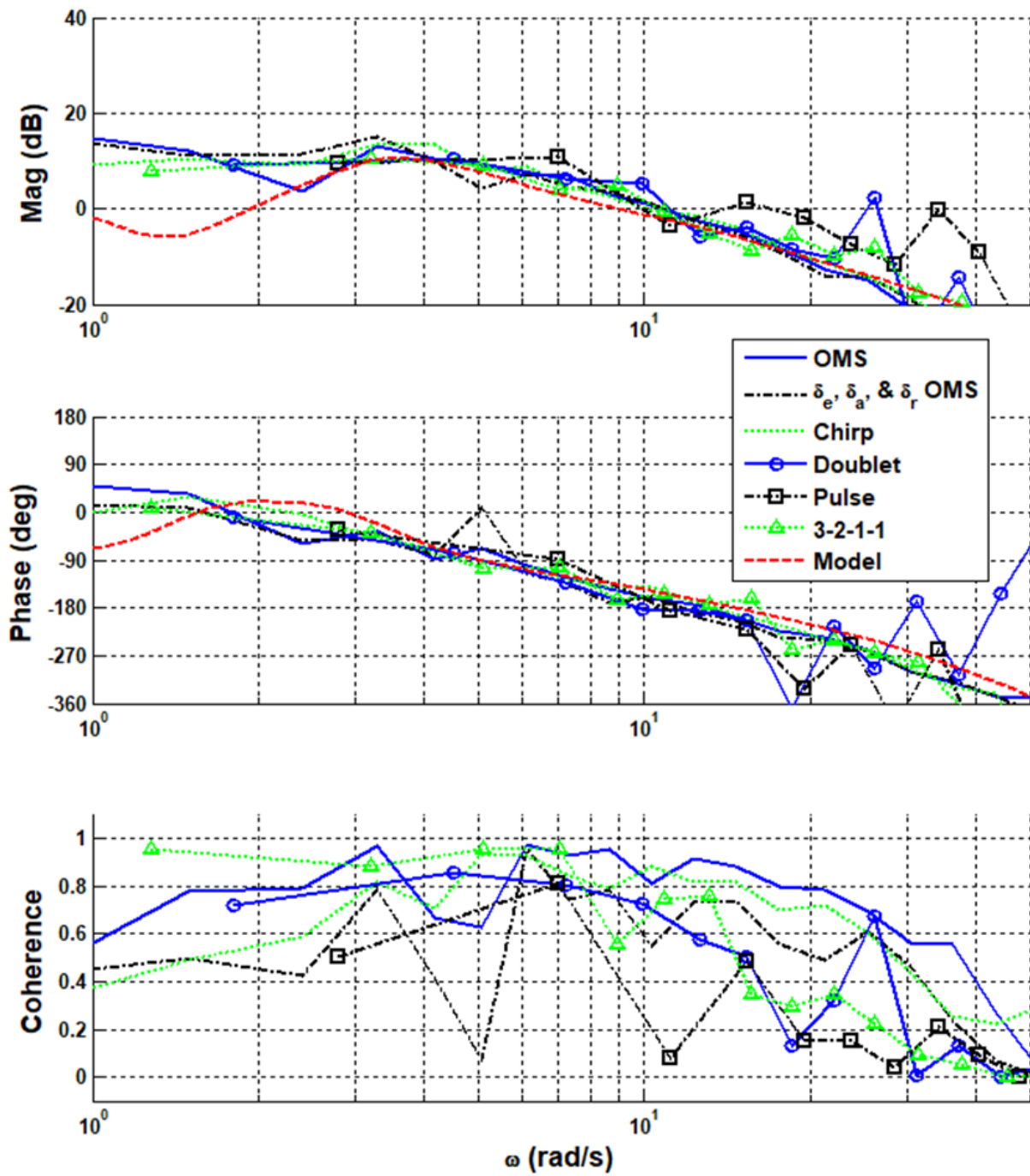


Figure 82: FLT04 - r/δ_{rc} Identification – All Methods

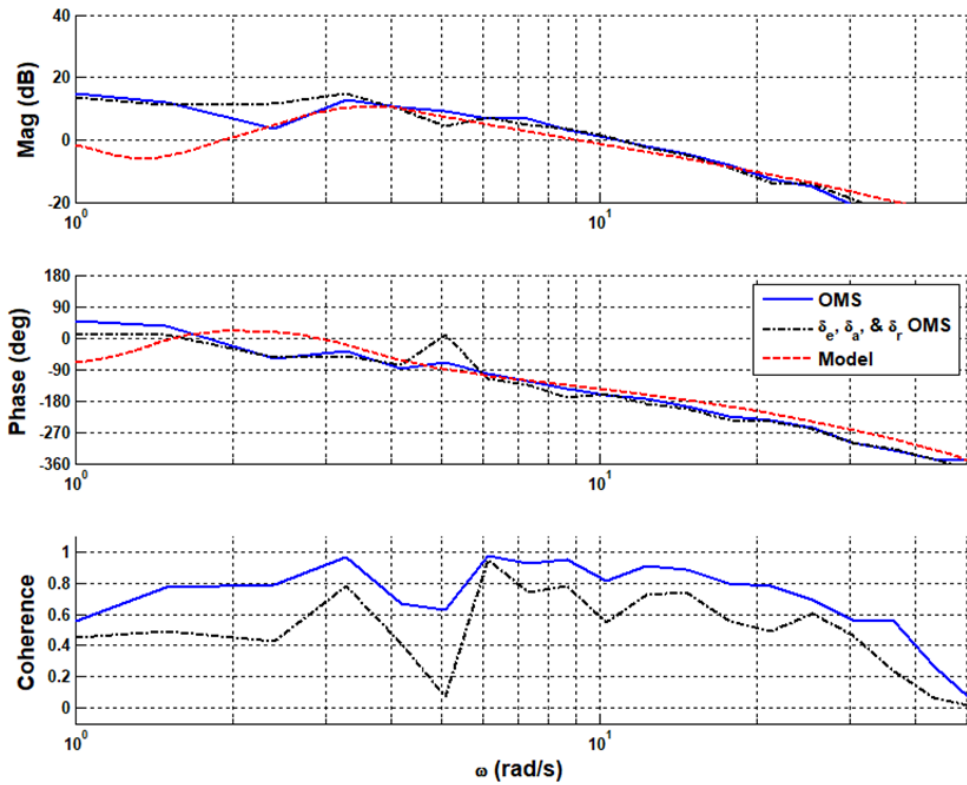


Figure 83: FLT04 - r/δ_{rc} Identification – OMS

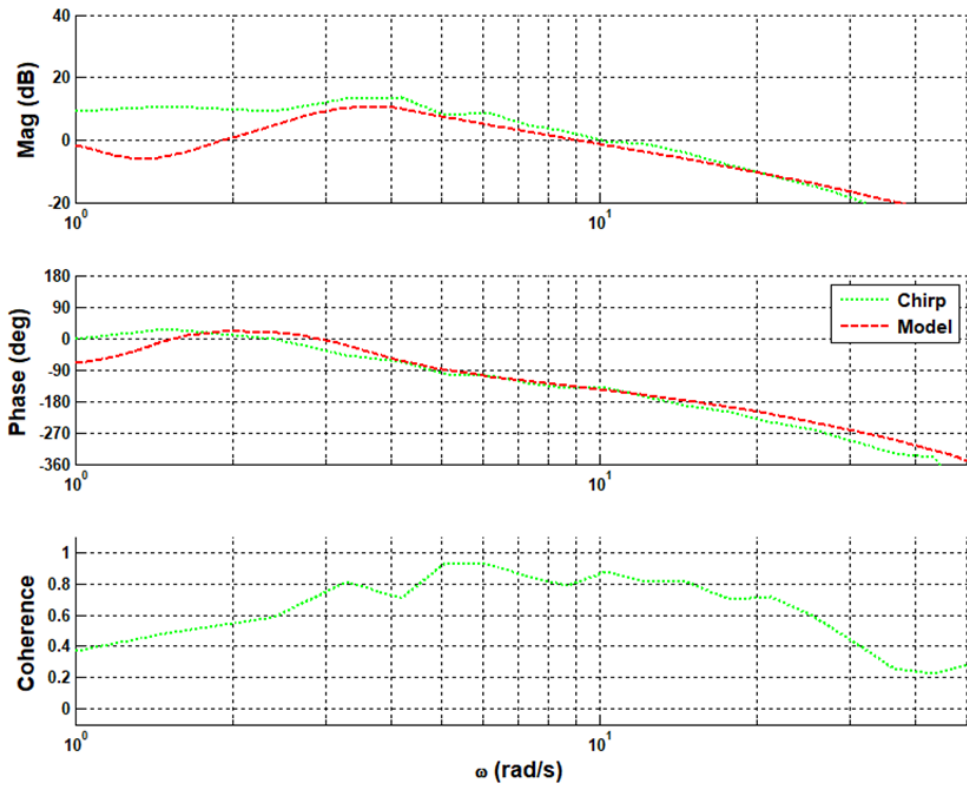


Figure 84: FLT04 - r/δ_{rc} Identification – Frequency sweep

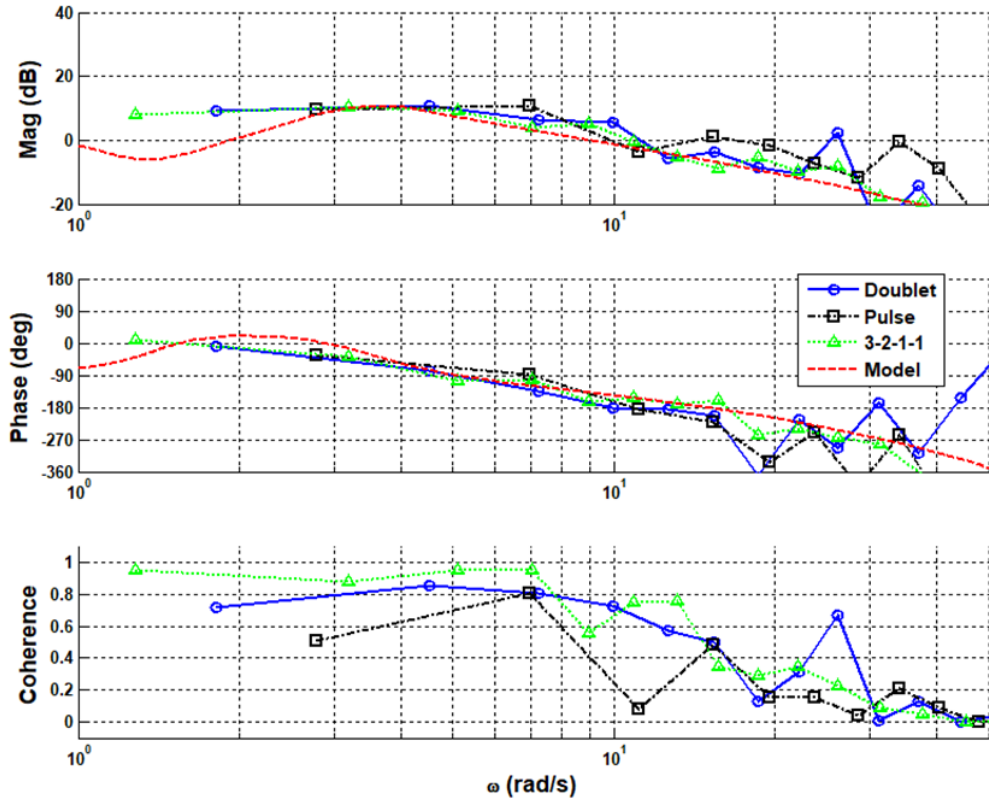


Figure 85: FLT04 - r/δ_{rc} Identification – Short Duration Inputs

D. FLIGHT 05

Flight 05 was flown at cruise condition but with weight added to the aft portion of the vehicle, in order to move the CG back and to create an off-nominal case.

When changing the parameters in the UM model to reflect the aft CG condition, new mass moment of inertia (MOI) values had to be calculated. Two methods were employed to determine the new MOI values.

The first method used a table build up to calculate the components of the MOI values. The first component used was the existing vehicle, with the weight and CG location as inputs. The second component used was the new added mass with the weight of the mass and the location of the mass on the aircraft. This method will be denoted as “MOI Method 1” in the subsequent sections where the data is presented.

The second method used a series of hand calculations. The first step was to uses the parallel axis theorem on the new added mass and the distance from the old CG to the location of the added mass and add this term to the current I_{zz} value. Next use the parallel axis theorem on the vehicle as a whole with the new mass of the vehicle and the distance between the new and old CG values. This method will be denoted as “MOI Method 2” in the subsequent sections where the data is presented. The results of both methods can be seen in Table 29.

In order to match the gain values of the longitudinal, lateral, and directional bare airframe models with the flight data, a series of gains were applied to the bare airframe models which can be seen in Table 30.

Table 29: Moment of Inertia Results for Aft-CG

-	Nominal CG	Method 1	Method 2
I _{xx} (kg-m ²)	0.8568	0.8568	0.8568
I _{yy} (kg-m ²)	1.0095	0.677	0.8791
I _{zz} (kg-m ²)	1.7005	1.534	1.735

Table 30: Model Gains for FLT 05

-	Longitudinal	Lateral	Directional
MOI Method 1	0.75	0.75	2.5
MOI Method 2	1.0	0.75	2.5

1. Longitudinal Survey

All identified responses from the longitudinal excitations can be seen plotted for each MOI method in Figure 86 and Figure 90. Table 31 provides the actuator model and bare airframe dynamics in the longitudinal axis.

Table 31: FLT05 - Longitudinal Aircraft and Elevator Actuator Models

Elevator Actuator Model	Longitudinal Model
$\frac{\delta_e}{\delta_{ec}} = \frac{8}{s+10} e^{-0.065s}$	$\frac{q}{\delta_e} = \frac{89.62(0)(0.4055)(6.045)}{[0.3157, 0.5423][0.716, 10]}$

The identified longitudinal OMS input excitation for flight 05 can be seen in Figure 87 and Figure 91. All input excitations match closely to the model with high coherence (near 1) except at the higher (> 40rad/s) ends of the frequency region shown.

The identified longitudinal frequency sweep input excitation for flight 05 can be seen in Figure 88 and Figure 92 and features the elevator only input, the multi-axis elevator and aileron input, and the multi axis elevator-aileron-rudder input. Overall the frequency sweep input excitations closely match the model response. The coherence drops slightly for each at the highest frequencies considered.

The identified longitudinal short duration input excitation can be seen in Figure 89 and Figure 93. Of the three excitations, the pulse input profile maintained the highest level of coherence across the frequency region shown. There is significant drop-off of coherence at frequencies above 20 rad/s

a. MOI Method 1

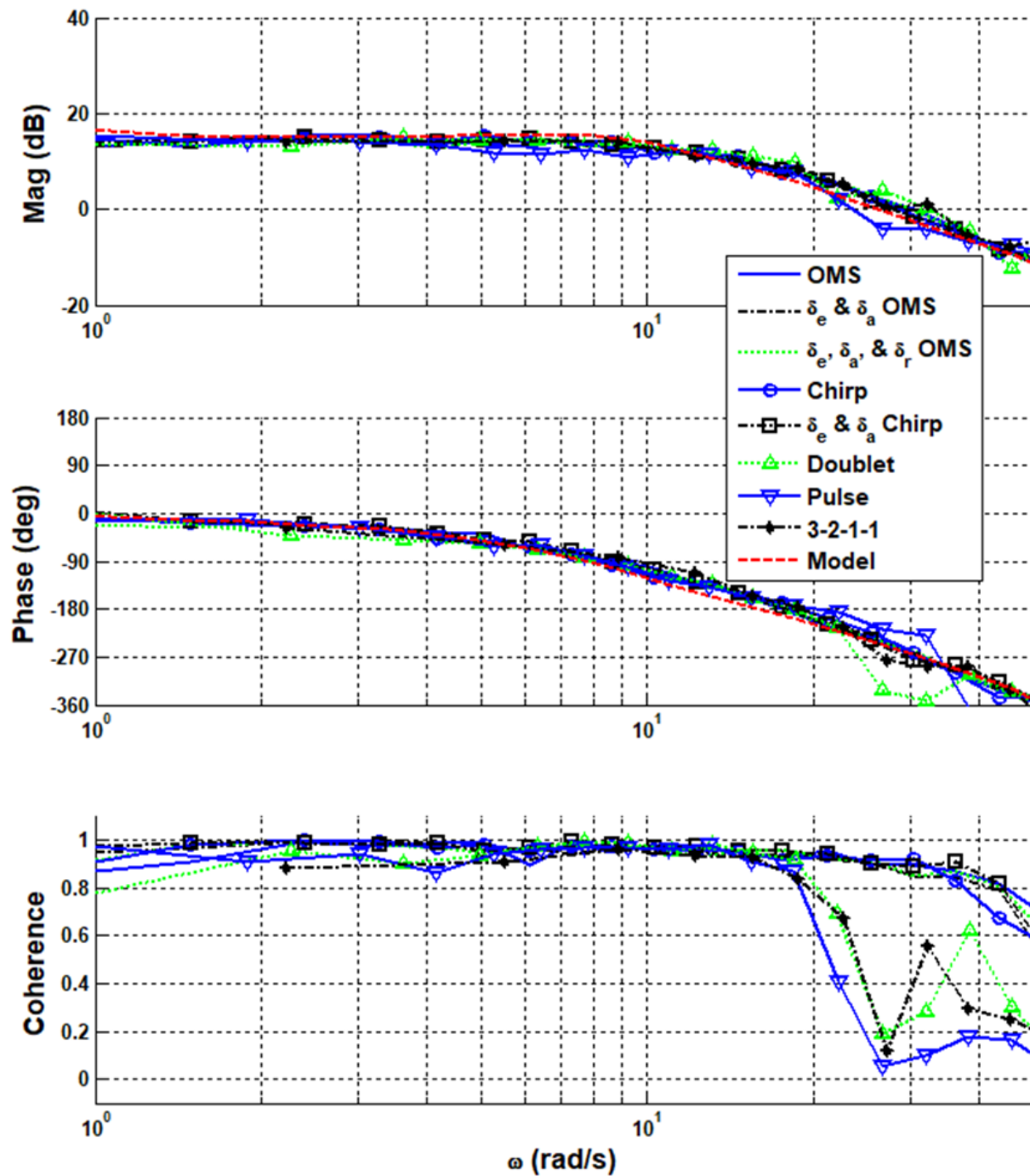


Figure 86: FLT05-MOI Method 1 - q/δ_{ec} Identification – All Methods

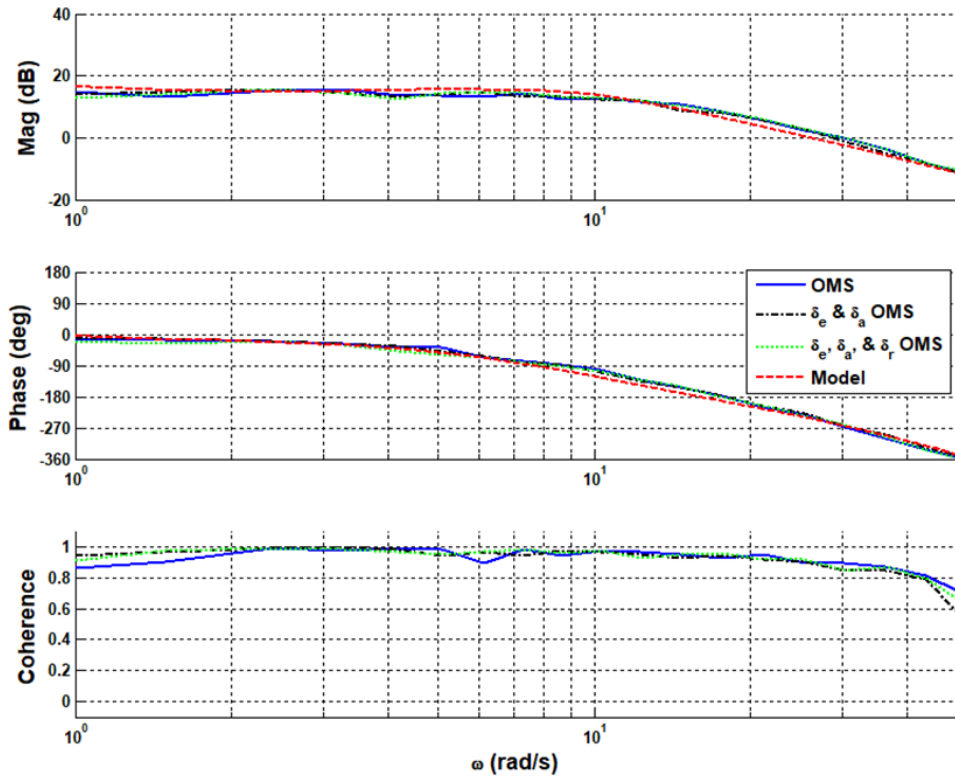


Figure 87: FLT05-MOI Method 1 - q/δ_{ec} Identification – OMS

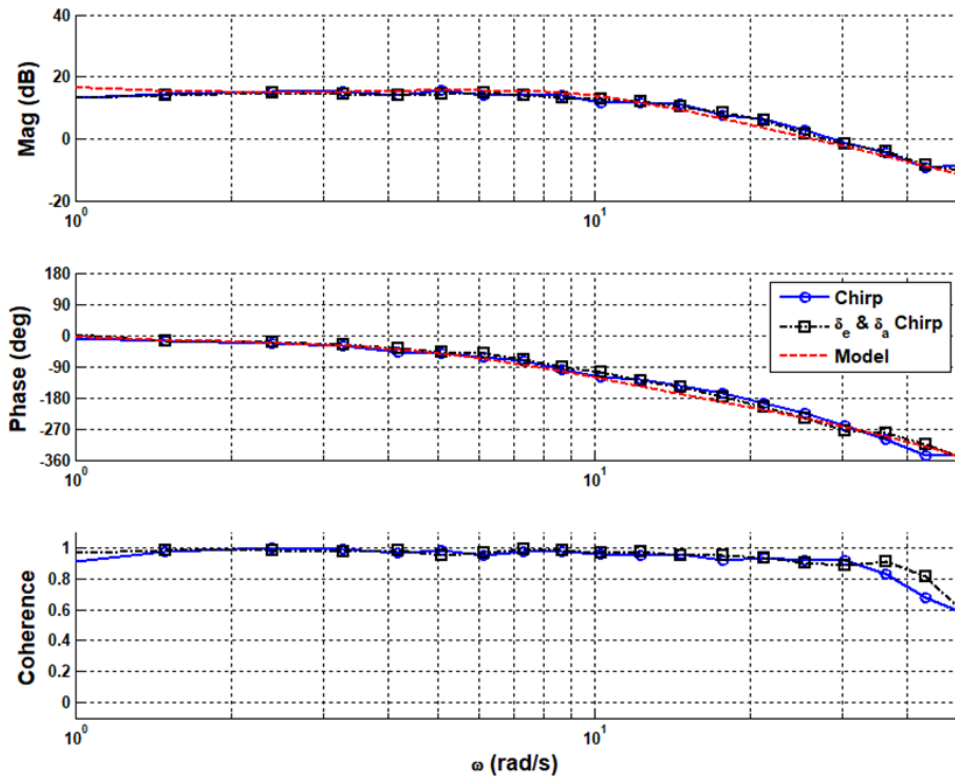


Figure 88: FLT05-MOI Method 1 - q/δ_{ec} Identification – Frequency sweep

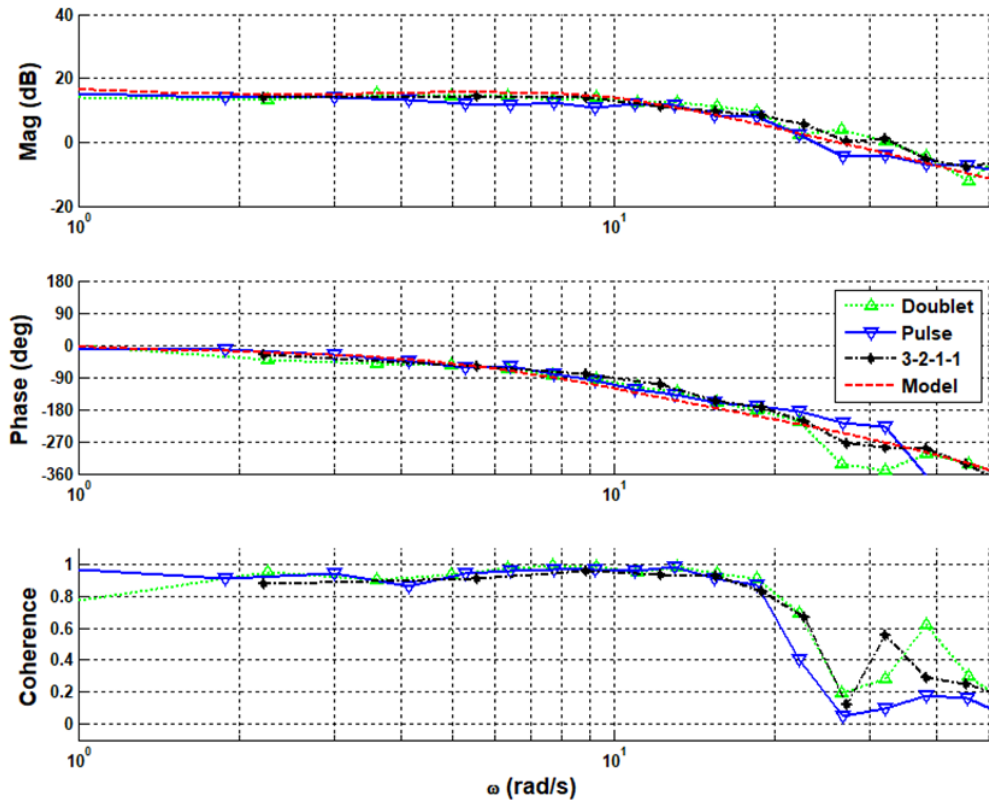


Figure 89: FLT05-MOI Method 1 - q/δ_{ec} Identification – Short Duration Inputs

b. MOI Method 2

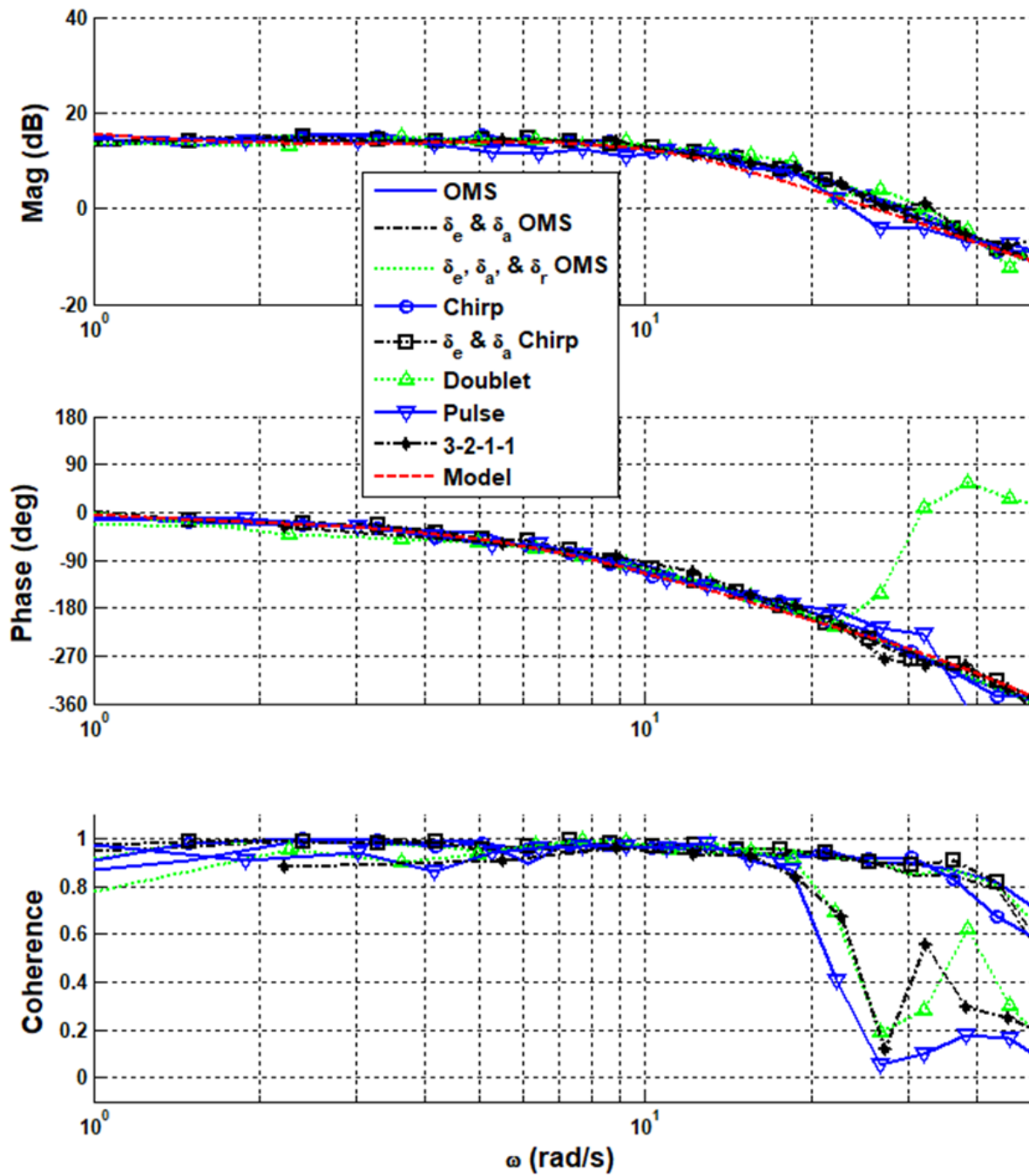


Figure 90: FLT05-MOI Method 2 - q/δ_{ec} Identification – All Methods

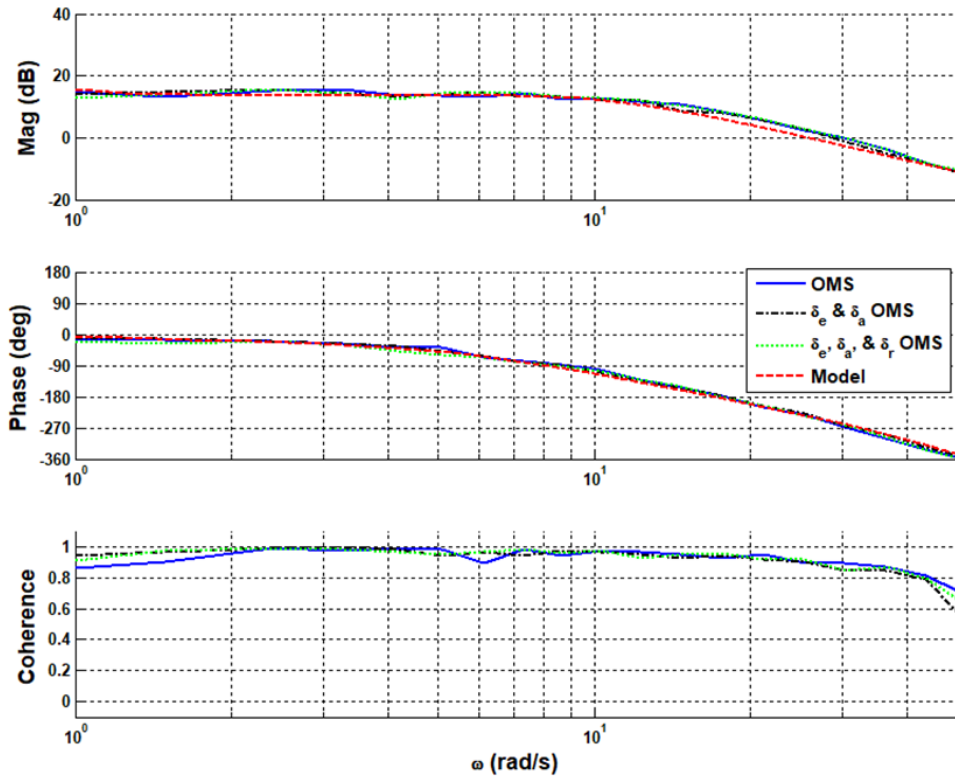


Figure 91: FLT05-MOI Method 2 - q/δ_{ec} Identification – OMS

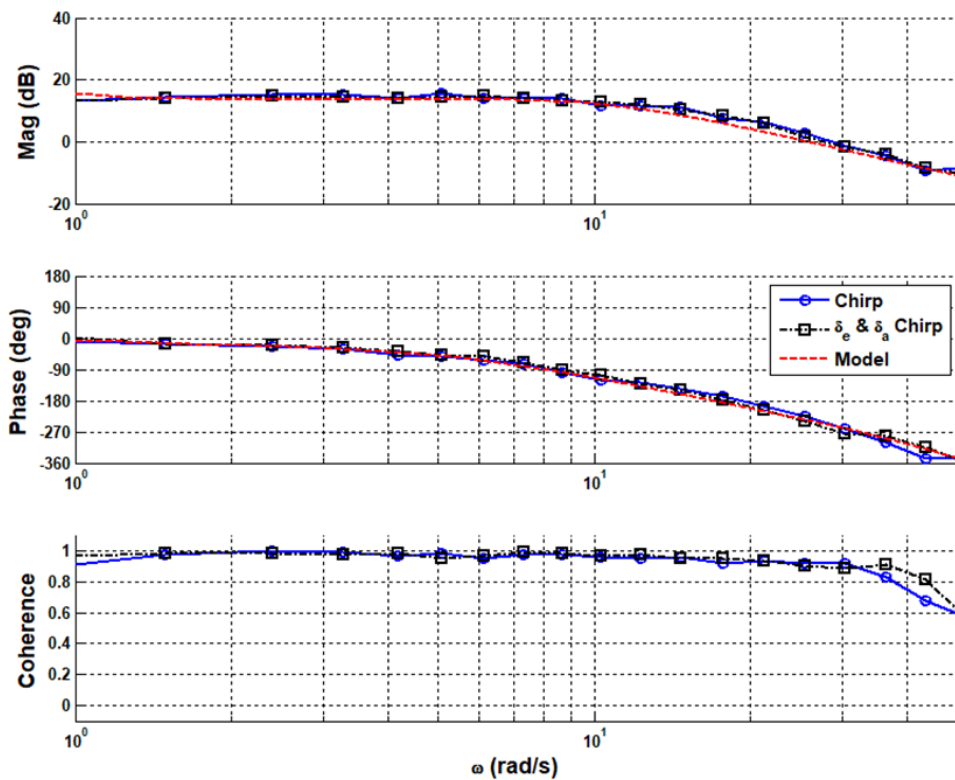


Figure 92: FLT05-MOI Method 2 - q/δ_{ec} Identification – Frequency sweep

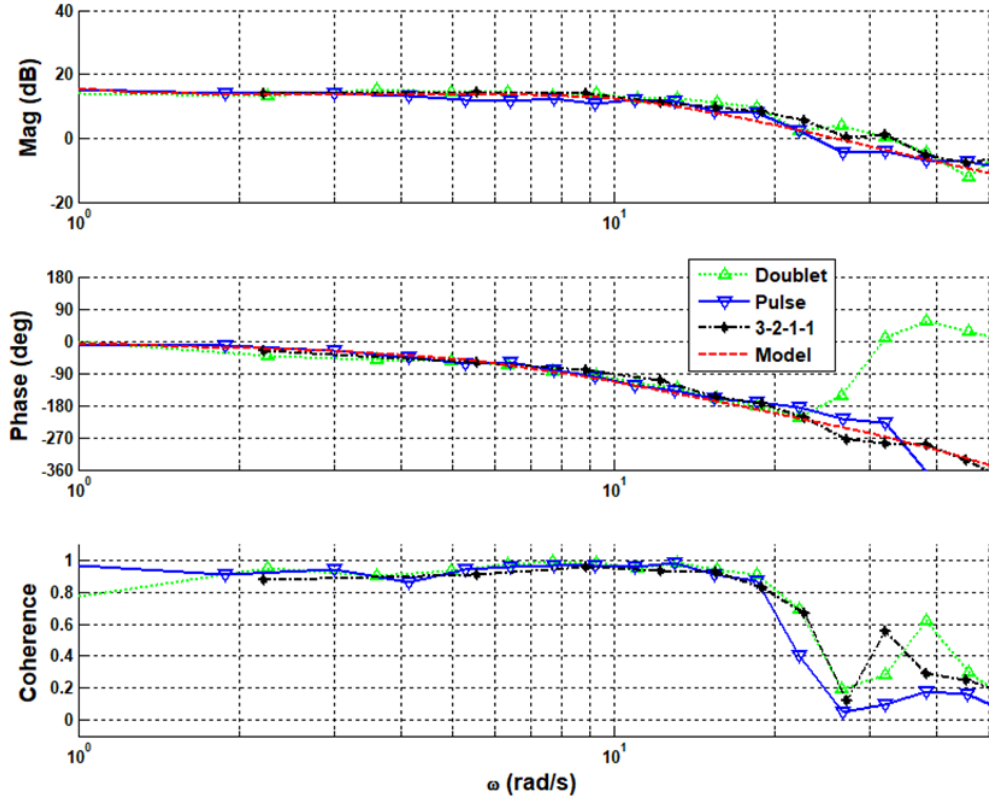


Figure 93: FLT05-MOI Method 2 - q/δ_{ec} Identification – Short Duration Inputs

2. Lateral Survey

All identified responses from the lateral excitations can be seen plotted with the updated reference model in Figure 94 and Figure 98. Table 32 provides the aileron actuator model and lateral aircraft model.

Table 32: FLT05 - Lateral Aircraft and Aileron Actuator Model

Aileron Actuator Model	Lateral Model
$\frac{\delta_a}{\delta_{ac}} = \frac{40}{s+12} e^{-0.060s}$	$\frac{p}{\delta_a} = \frac{50.39(-0.03378)[0.2752, 3.531]}{(0.04175)[0.2952, 4.022](9.2)}$

The identified lateral OMS input excitation for flight 05 can be seen in Figure 95 and Figure 99. The magnitude and phase response of the aileron alone, and elevator-aileron multi axis closely match the model. The elevator-aileron-rudder multi axis excitation follows the same trend as the other two OMS excitations, however, there is a drop in coherence at frequencies between 2-3 rad/s.

The identified lateral frequency sweep input excitation for flight 05 can be seen in Figure 96 and Figure 100, which features the aileron only input, and the multi-axis elevator-aileron excitation. Overall, the magnitude and phase response of both input excitations match the model, with the aileron only excitation generally having a higher coherence throughout. The elevator and aileron multi axis excitation coherence occasionally drops below 0.8 as the frequency approaches the upper bounds of the test.

The identified lateral short duration input excitation can be seen in Figure 97 and Figure 101. Of the four excitations, the 3-2-1-1 and the doublet input profiles maintained the highest level of coherence across the frequency region shown, but all excitations had either issues with or lacked the content to identify the highest frequencies of interest.

a. MOI Method 1

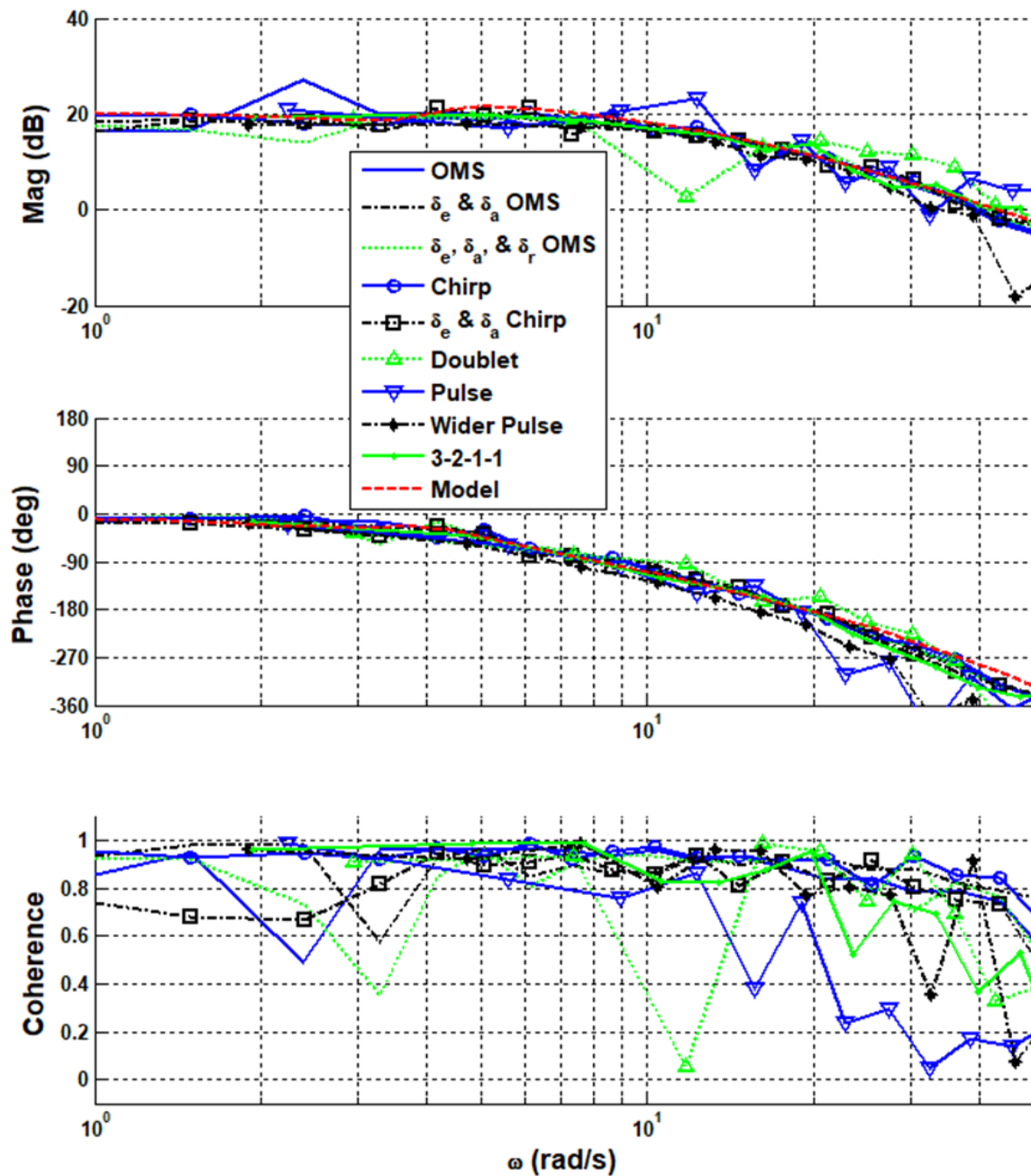


Figure 94: FLT05-MOI Method 1 - p/ δ_{ac} Identification – All Methods

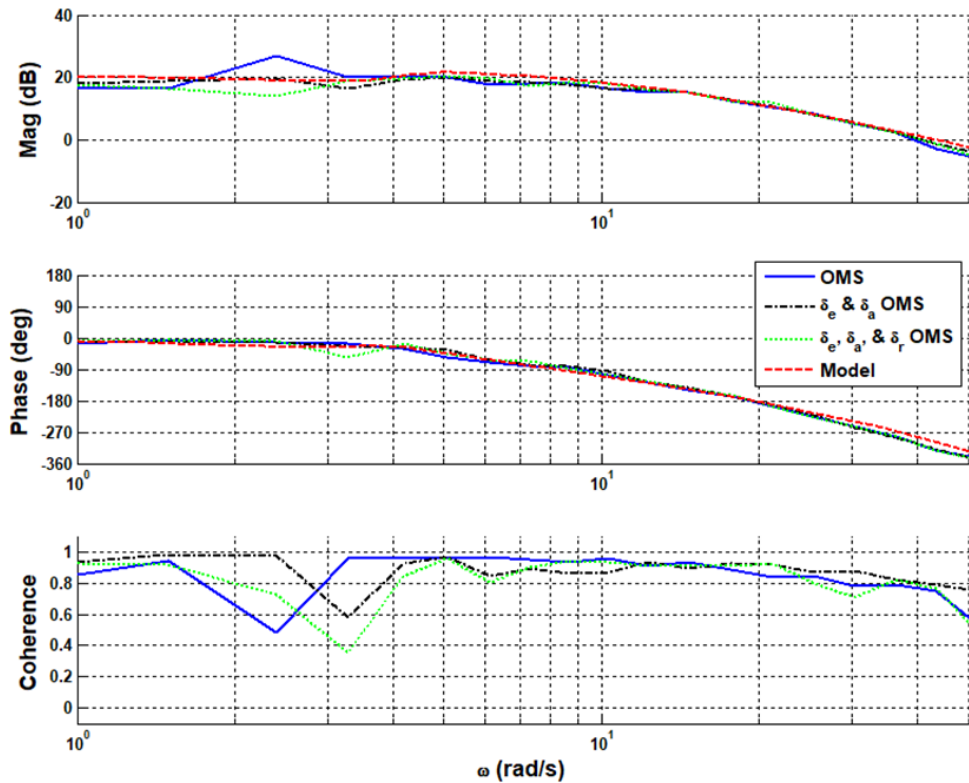


Figure 95: FLT05-MOI Method 1 - p/ δ_{ac} Identification – OMS

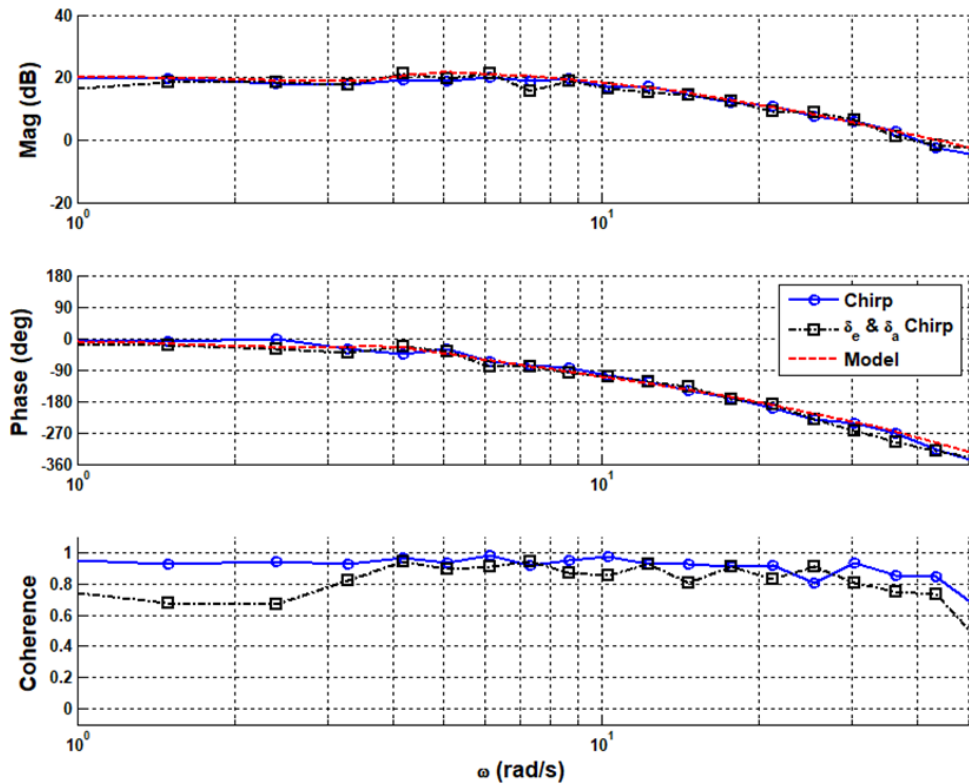


Figure 96: FLT05-MOI Method 1 - p/ δ_{ac} Identification – Frequency sweep

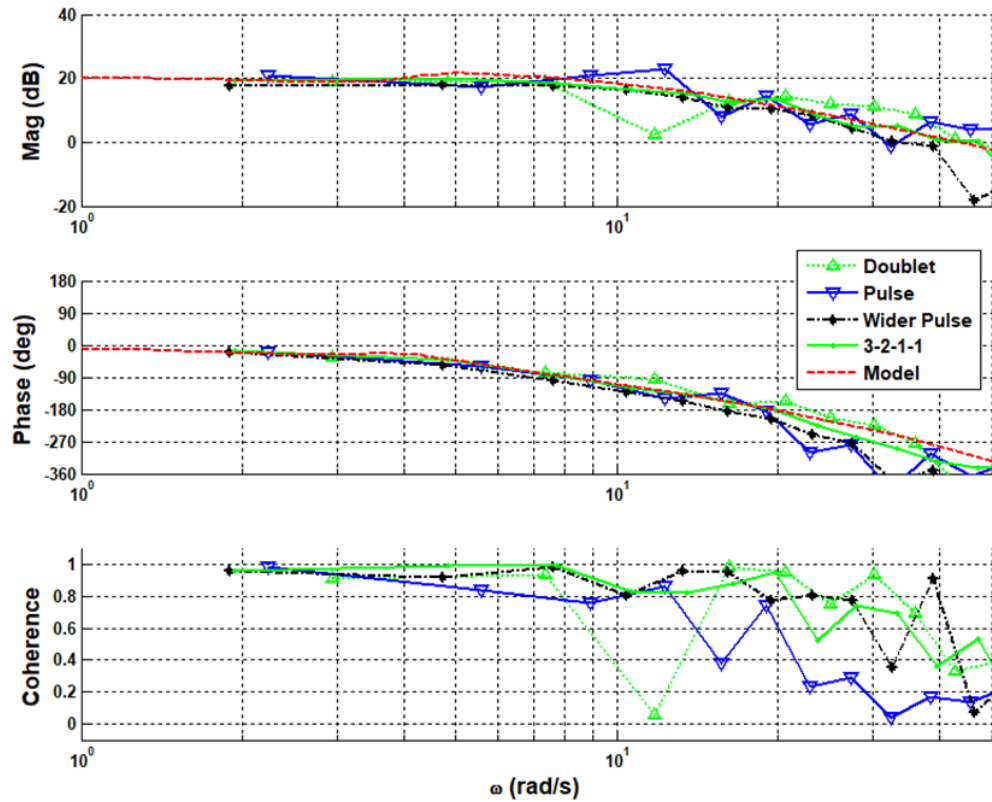


Figure 97: FLT05-MOI Method 1 - p/δ_{ac} Identification – Short Duration Inputs

b. MOI Method 2

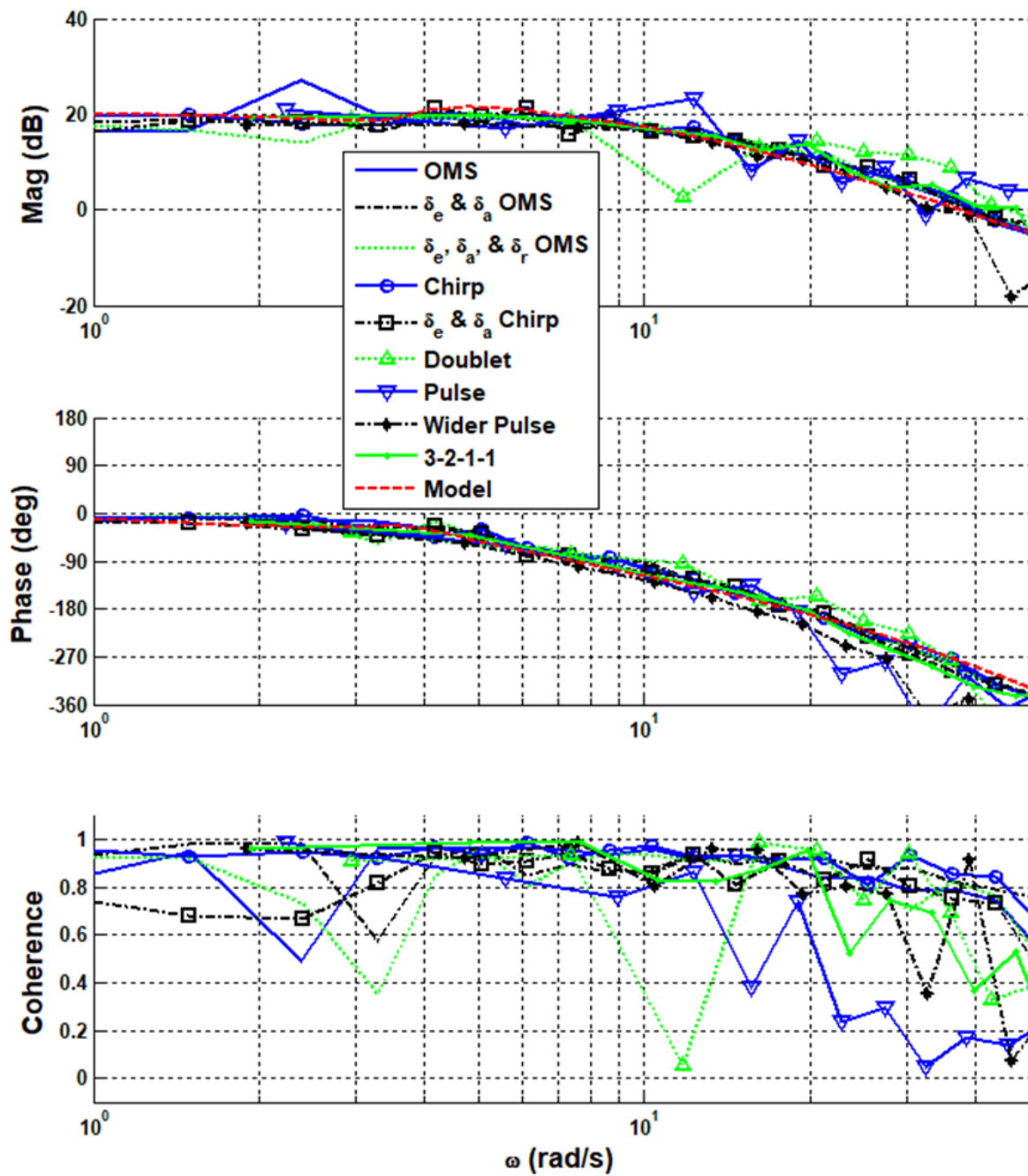


Figure 98: FLT05-MOI Method 2 - p/δ_{ac} Identification – All Methods

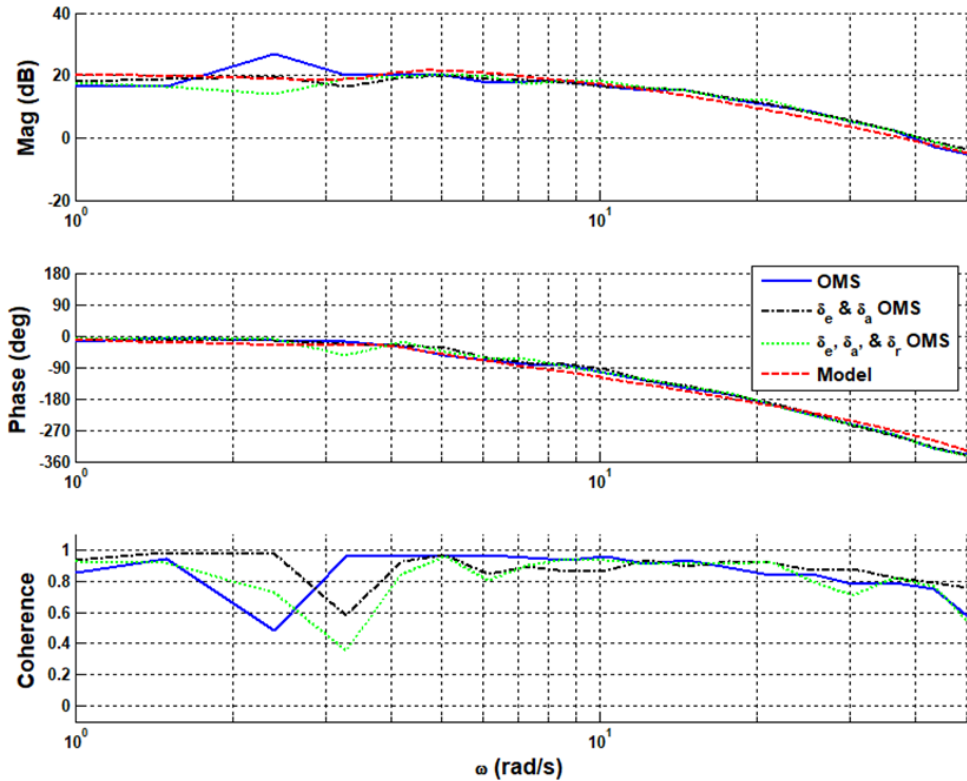


Figure 99: FLT05-MOI Method 2 - p/δ_{ac} Identification – OMS

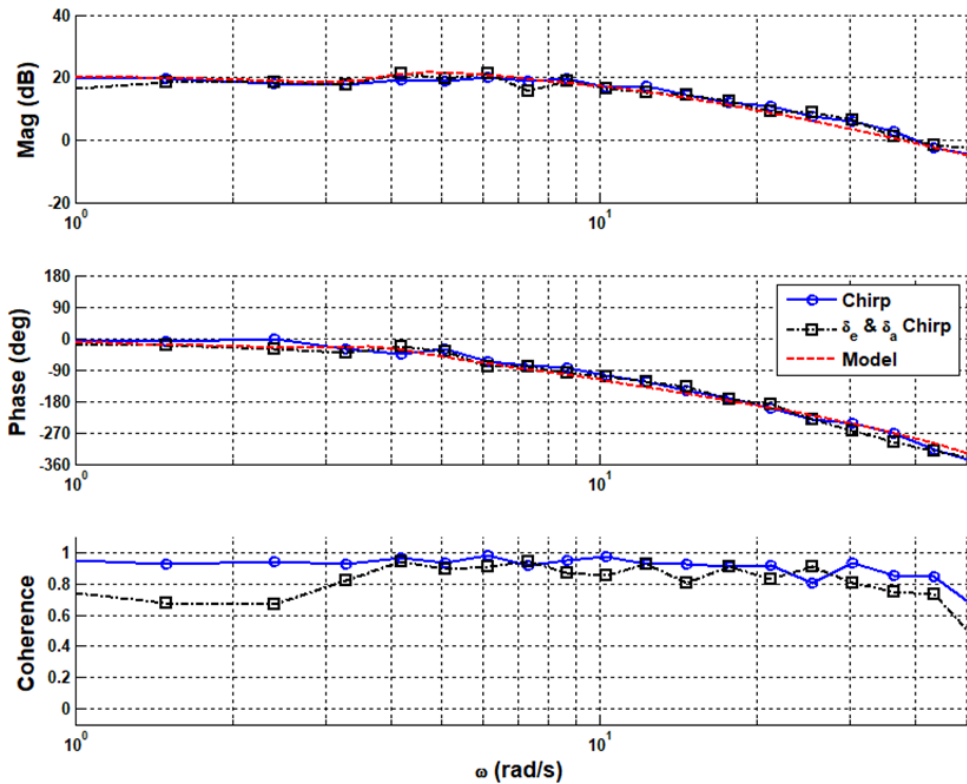


Figure 100: FLT05-MOI Method 2 - p/δ_{ac} Identification – Frequency sweep

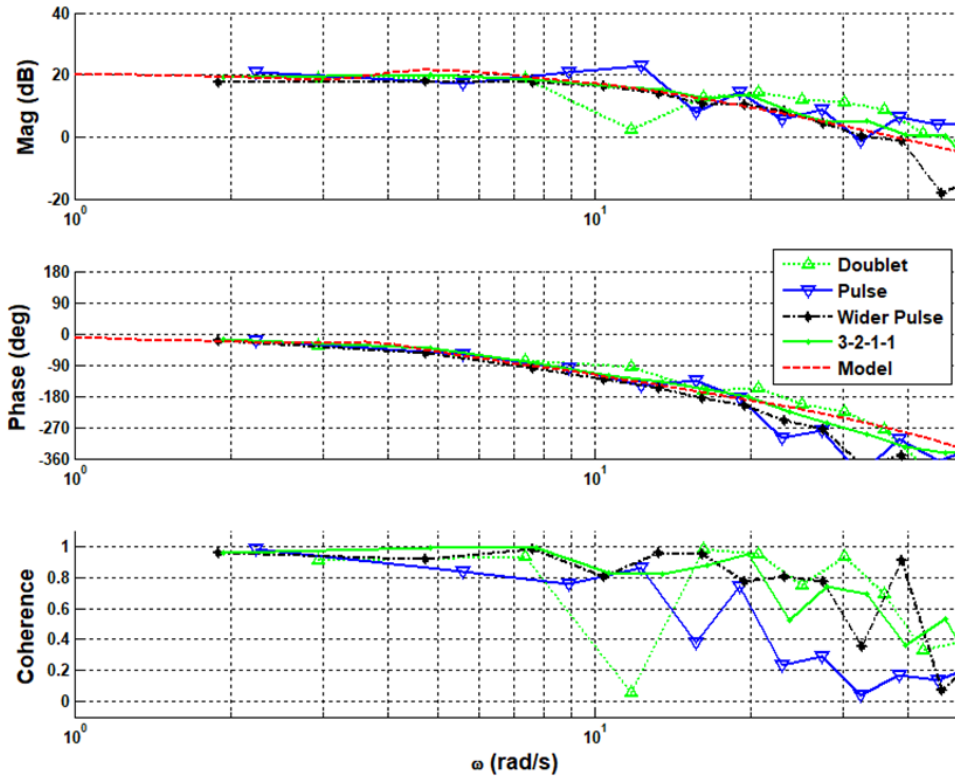


Figure 101: FLT05-MOI Method 2 - p/δ_{ac} Identification – Short Duration Inputs

3. Directional Survey

All directional excitations can be seen plotted with the model in Figure 102 and Figure 106. Table 33 provides the rudder actuator model and directional aircraft model.

Table 33: FLT05 - Directional Aircraft and Rudder Actuator Model

Rudder Actuator Model	Directional Model
$\frac{\delta_r}{\delta_{rc}} = \frac{10}{s+10} e^{-0.065s}$	$\frac{r}{\delta_r} = \frac{-7.623[0.2505, 1.242](9.186)}{(0.04175)[0.305, 3.05](9.2)}$

The identified directional OMS input excitation for flight 05 can be seen in Figure 103 and Figure 107. The magnitude and phase response of the rudder alone, and the elevator-aileron-rudder multi axis match the model at frequencies above 6 rad/s. Both excitations remained above 0.8 coherence at the middle frequencies. A brief spike occurred in the phase of both input excitations at about 5 rad/s.

The identified directional frequency sweep input excitation for flight 05 can be seen in Figure 104 and Figure 108, which features the rudder only input. Overall, the magnitude and phase response of the excitation close match to the model where coherence does not fall below 0.8 until the higher frequencies, which follows the trend of the previous response types.

The identified directional short duration input excitation can be seen in Figure 105 and Figure 109. The identified and model appear to match, however there is significant loss in coherence at all frequencies of interest.

Adjustments were considered to improve the fit, particularly in the 1 to 5 rad/s region, but all alterations had a negative effect on the lateral system fits. As more confidence was placed in the roll identifications, the model dynamics remained unchanged beyond those already performed for the roll fit.

a. MOI Method 1

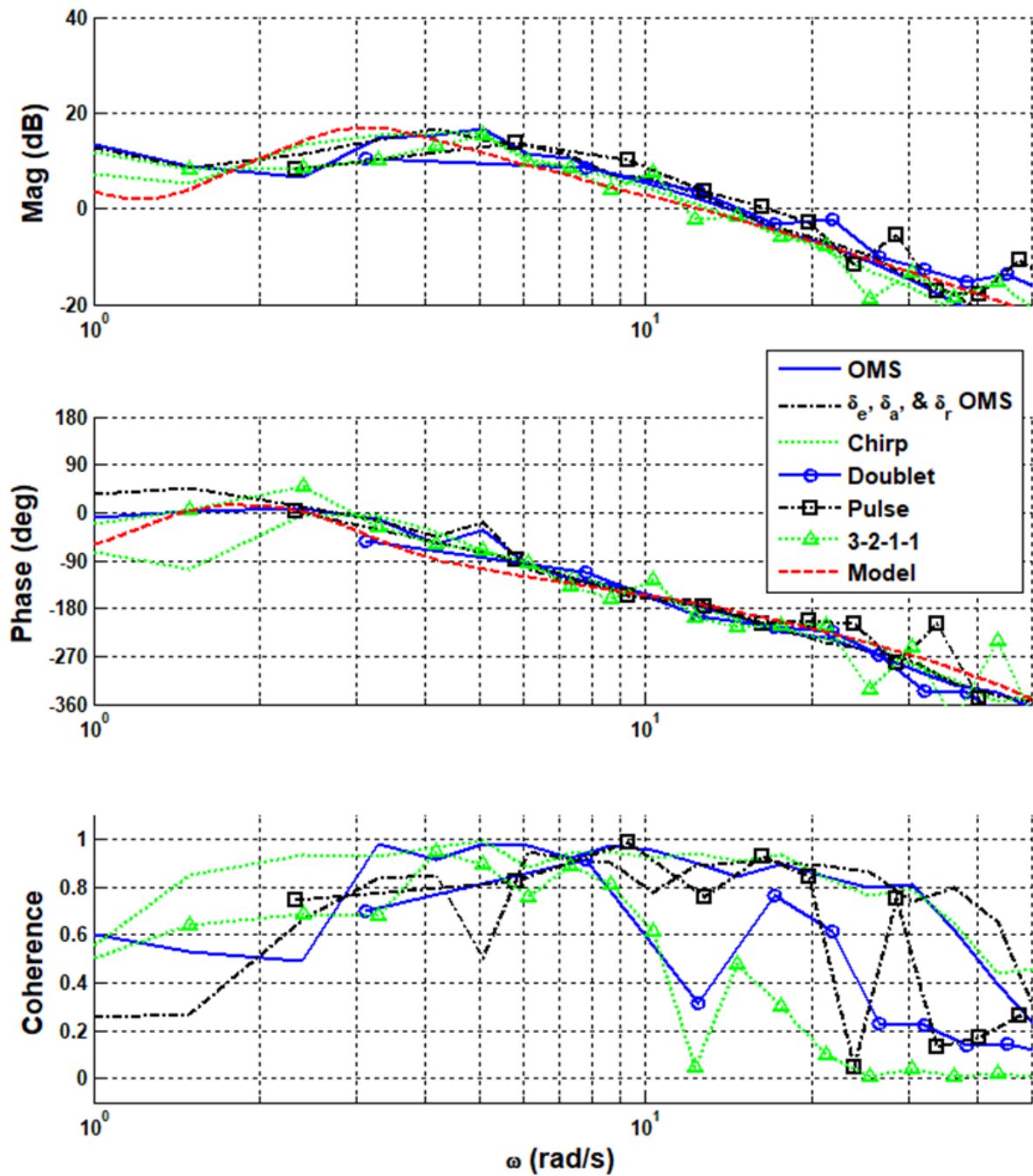


Figure 102: FLT05-MOI Method 1 - r/δ_{rc} Identification – All Methods

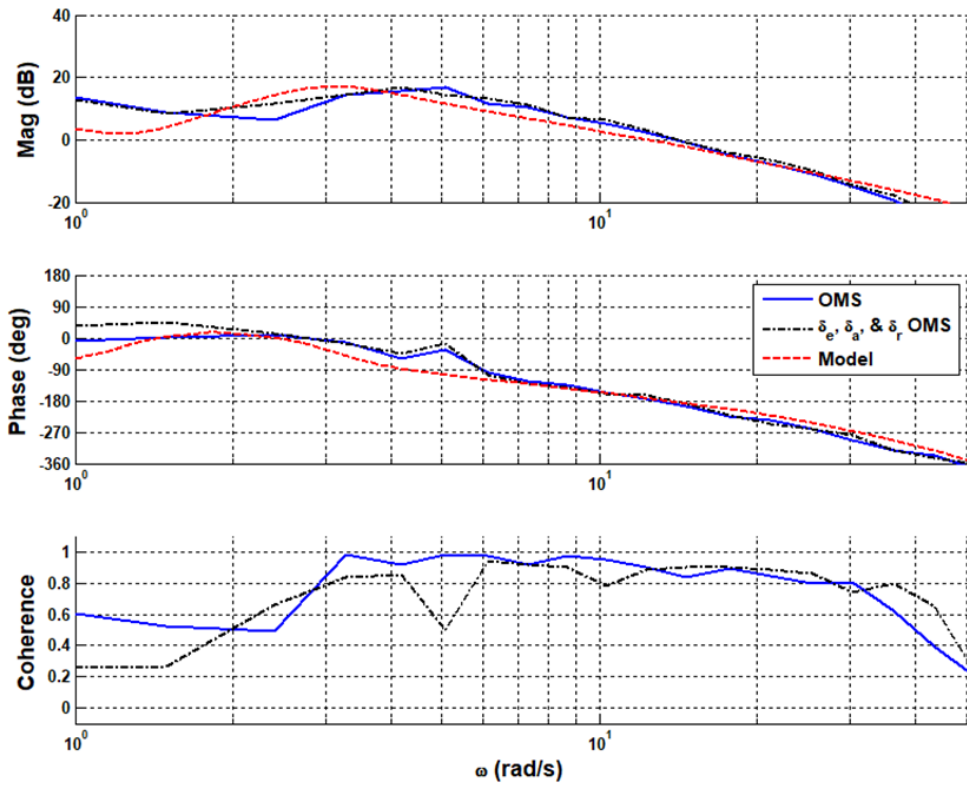


Figure 103: FLT05-MOI Method 1 - r/δ_{rc} Identification – OMS

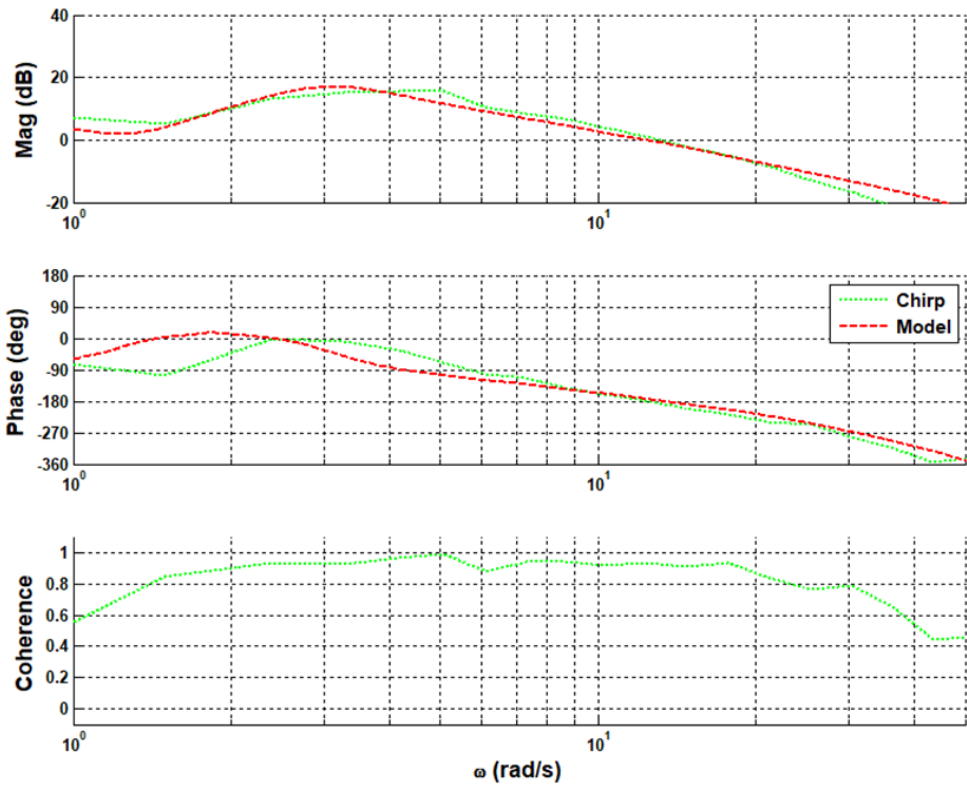


Figure 104: FLT05-MOI Method 1 - r/δ_{rc} Identification – Frequency sweep

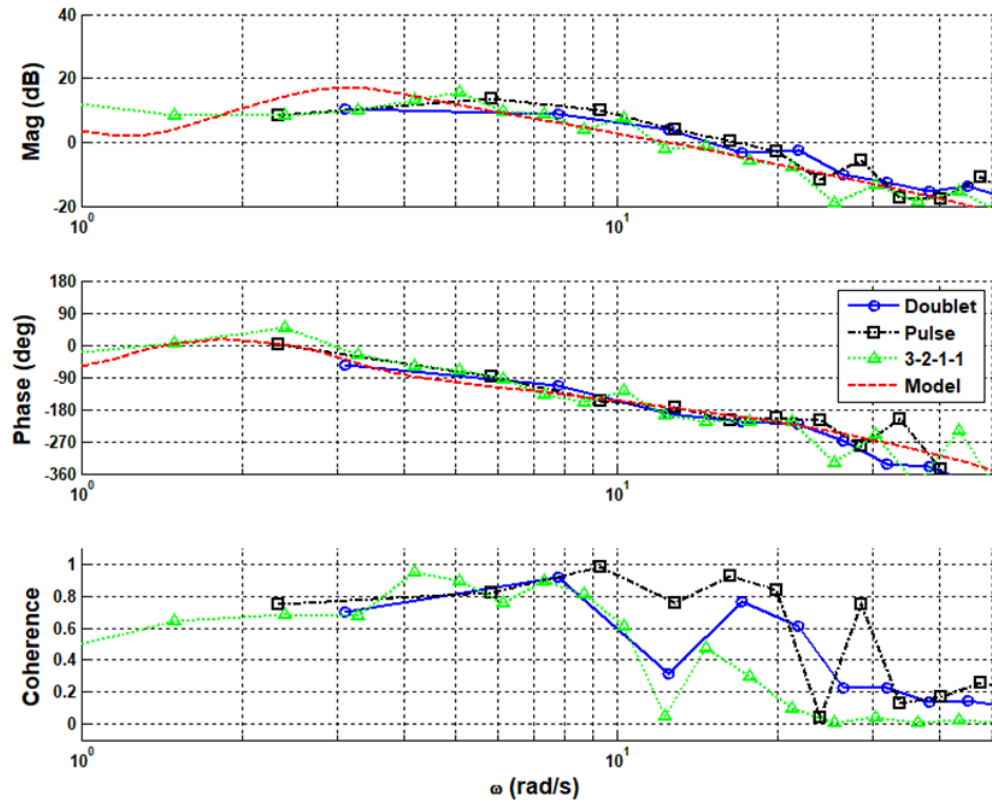


Figure 105: FLT05-MOI Method 1 - r/δ_{rc} Identification – Short Duration Inputs

b. MOI Method 2

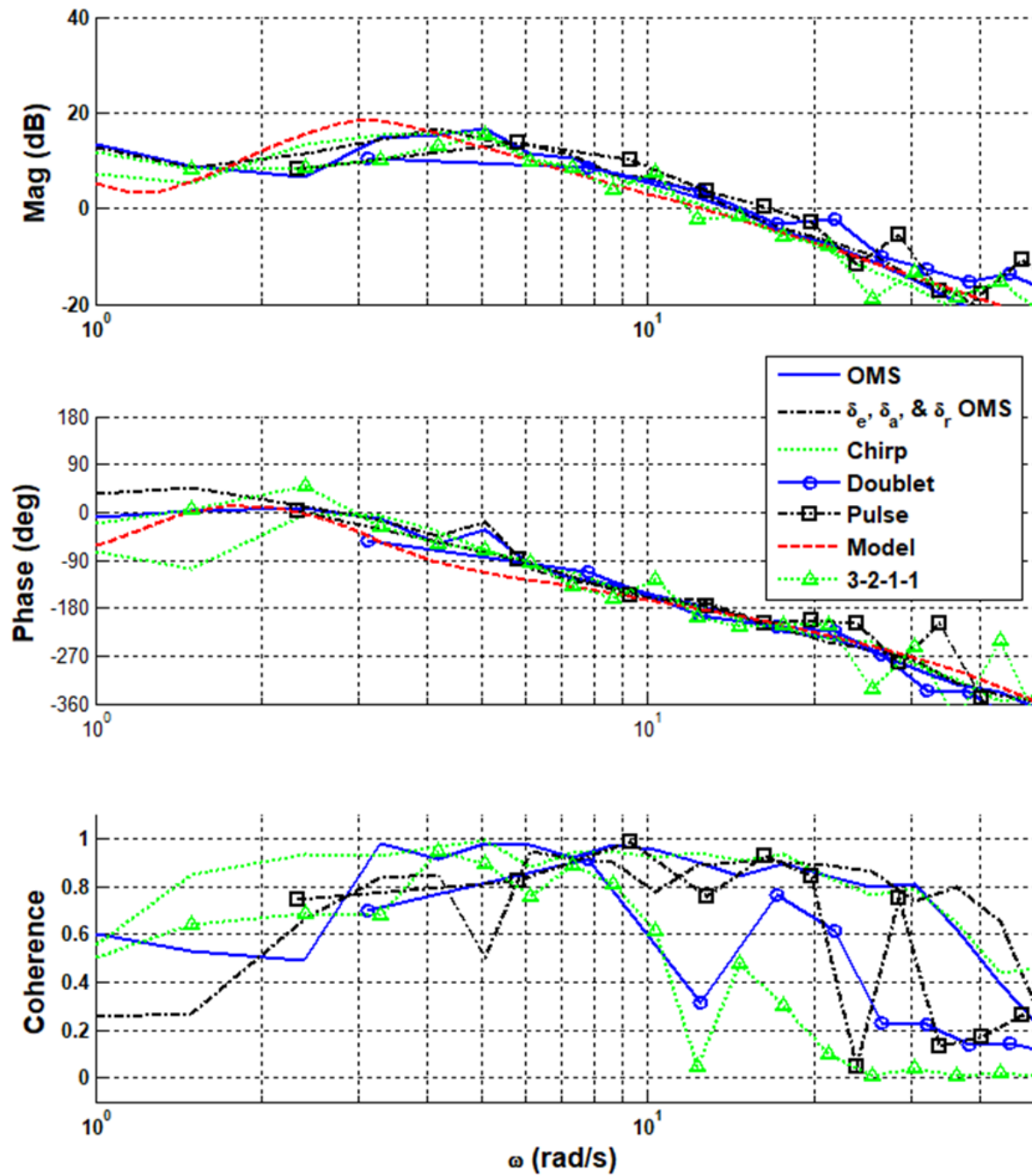


Figure 106: FLT05-MOI Method 2 - r/δ_{rc} Identification – All Methods

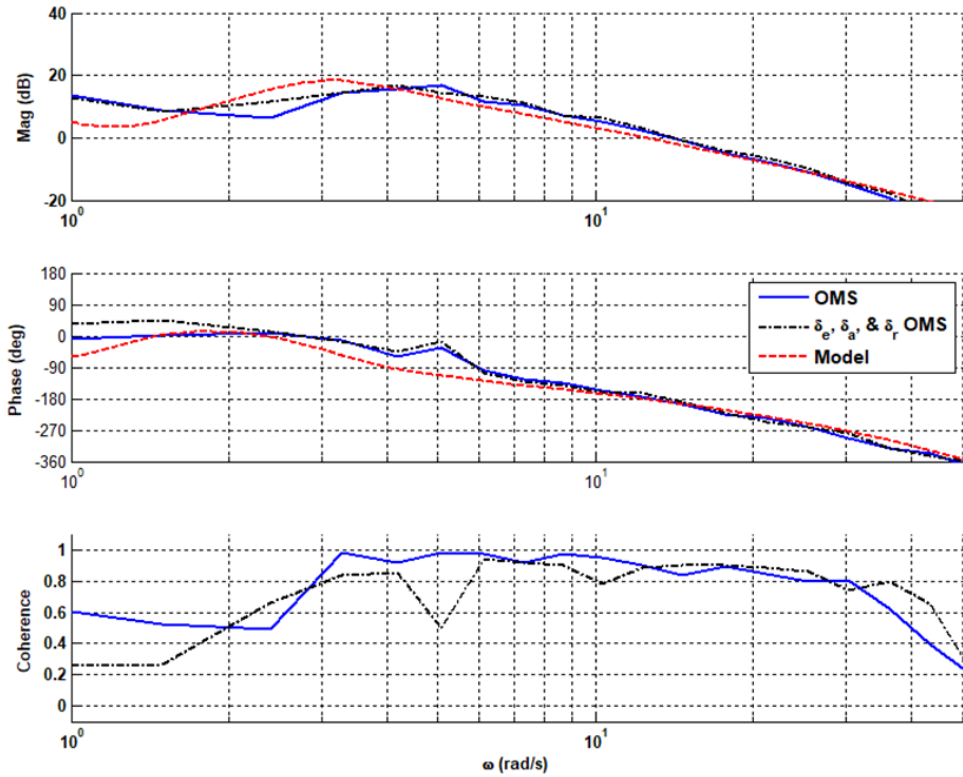


Figure 107: FLT05-MOI Method 2 - r/δ_{rc} Identification – OMS

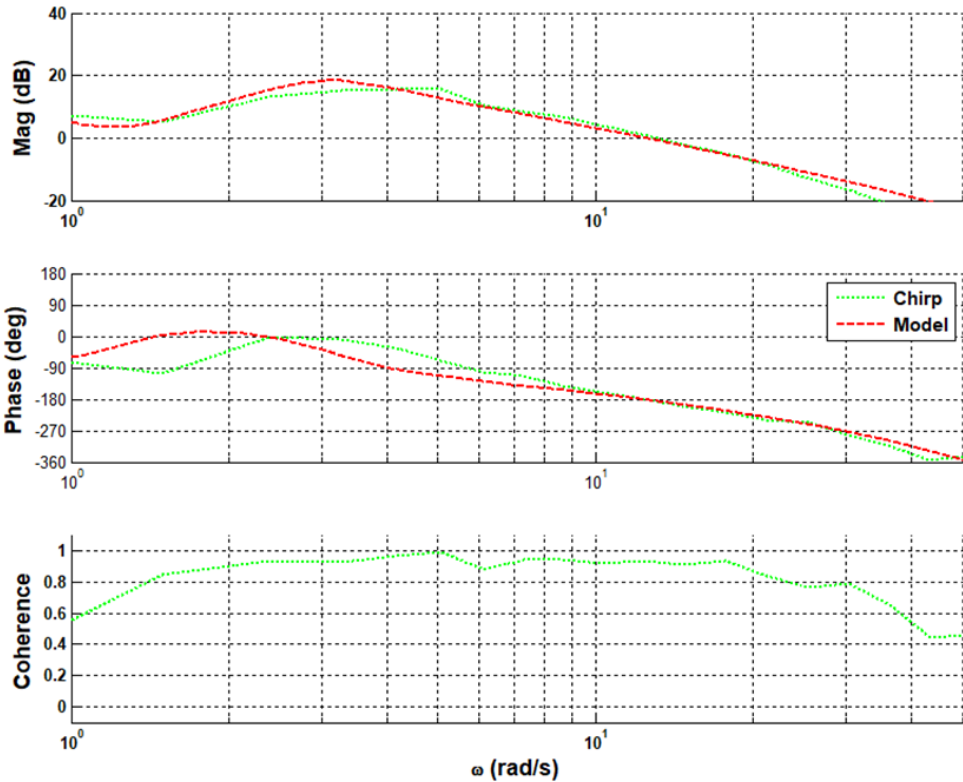


Figure 108: FLT05-MOI Method 2 - r/δ_{rc} Identification – Frequency sweep

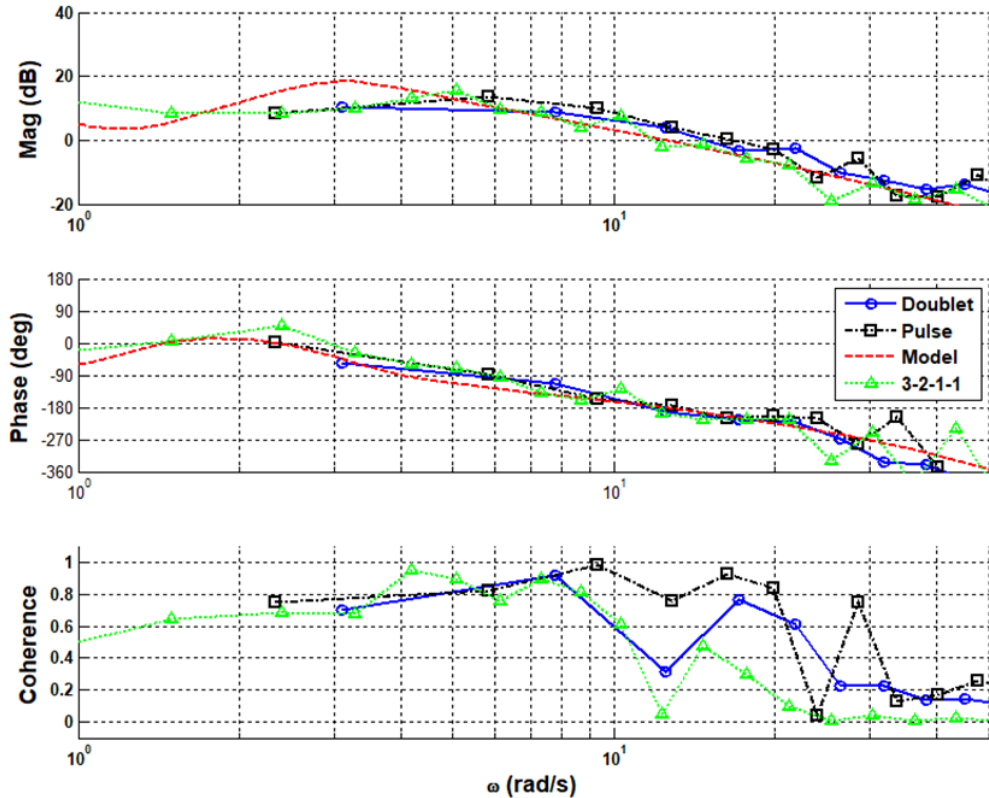


Figure 109: FLT05-MOI Method 2 - r/δ_{rc} Identification – Short Duration Inputs

E. FLIGHT 06

Flight 06 was flown at the approach condition (50% flaps at 17m/s) with the aft CG.

When changing the parameters in the UM model to reflect the aft CG condition, new (MOI) values had to be calculated. The methodologies and naming conventions are mirrored from the flight 05 condition above. To match the gain values of the longitudinal, lateral, and directional bare airframe models with the flight data, a series of gains were applied to the bare airframe models which can be seen in Table 34. The primary difference between the two MOI cases is the longitudinal gains which was due to the additional weight added along the central axis near the rear of the aircraft.

Table 34: Model Gains for FLT 06

-	Longitudinal	Lateral	Directional
MOI Method 1	1.0	1.0	2.5
MOI Method 2	1.25	1.0	2.5

1. Longitudinal Survey

All identified responses from the longitudinal excitations can be seen plotted in Figure 110 and Figure 114. Table 35 provides the actuator model and bare airframe dynamics in the longitudinal axis.

Table 35: FLT 06 - Longitudinal Aircraft and Elevator Actuator Models

Elevator Actuator Model	Longitudinal Model
$\frac{\delta_e}{\delta_{ec}} = \frac{8}{s + 10} e^{-0.065s}$	$\frac{q}{\delta_e} = \frac{46.95(-0)(0.319)(4.579)}{[0.1771, 0.699][0.627, 9.18]}$

The identified longitudinal OMS input excitation for flight 06 can be seen in Figure 111 and Figure 115. All signals have a close match to the model with high coherence (near 1) except at the higher (> 30 rad/s) ends of the frequency region.

The identified longitudinal frequency sweep input excitation for flight 06 can be seen in Figure 112 and Figure 116 features the elevator only input, the multi-axis elevator and aileron input, and the multi axis elevator-aileron-rudder input. Overall the frequency sweep input excitations closely match the model and each other over the range of considered frequencies.

The identified longitudinal short duration input excitation can be seen in Figure 113 and Figure 117. There is significant drop-off of coherence at frequencies above 7-8 rad/s though the magnitude and phase overlays appear to reflect the modeled trend.

a. MOI Method 1

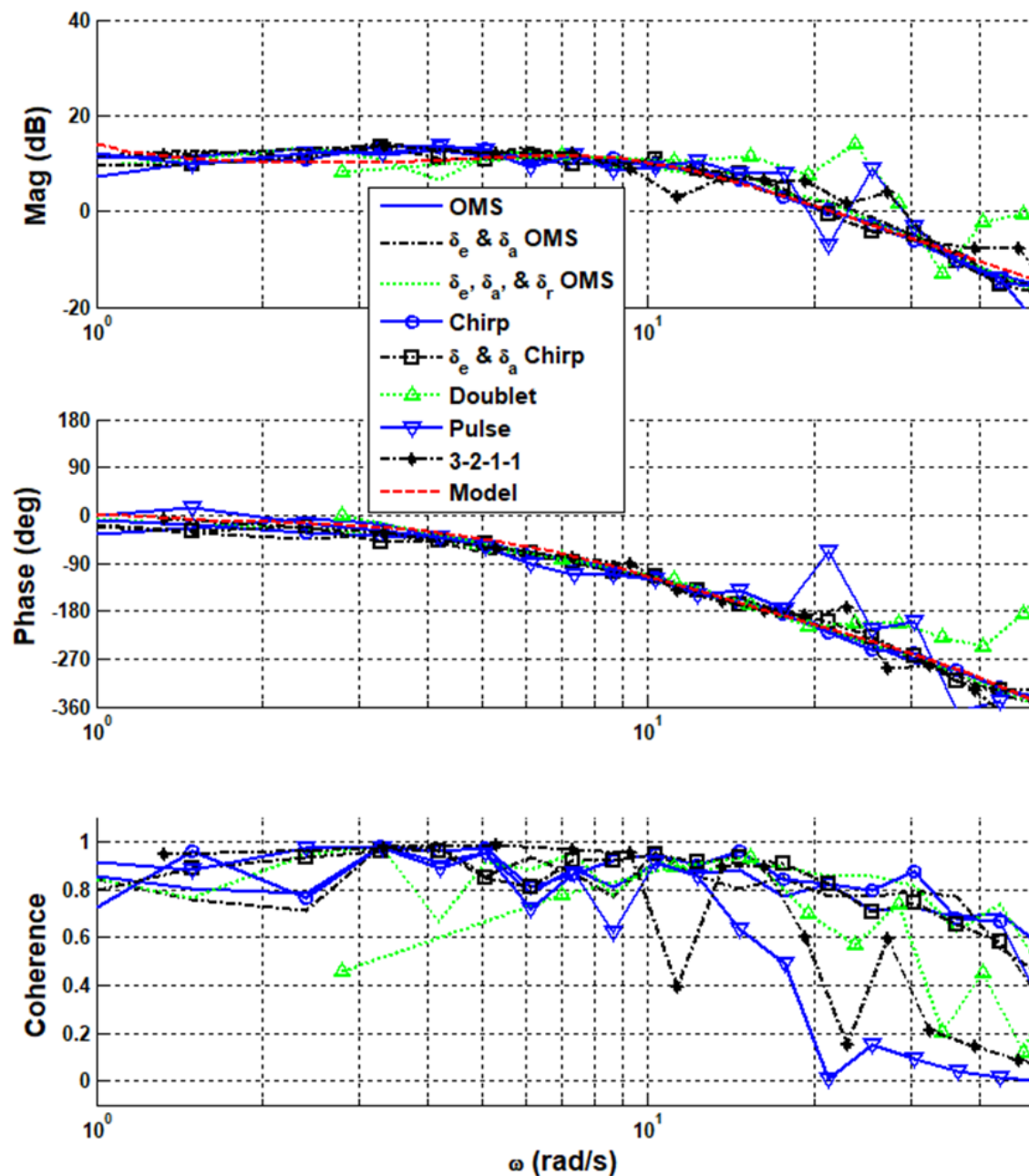


Figure 110: FLT06-MOI Method 1 - q/δ_{ec} Identification – All Methods

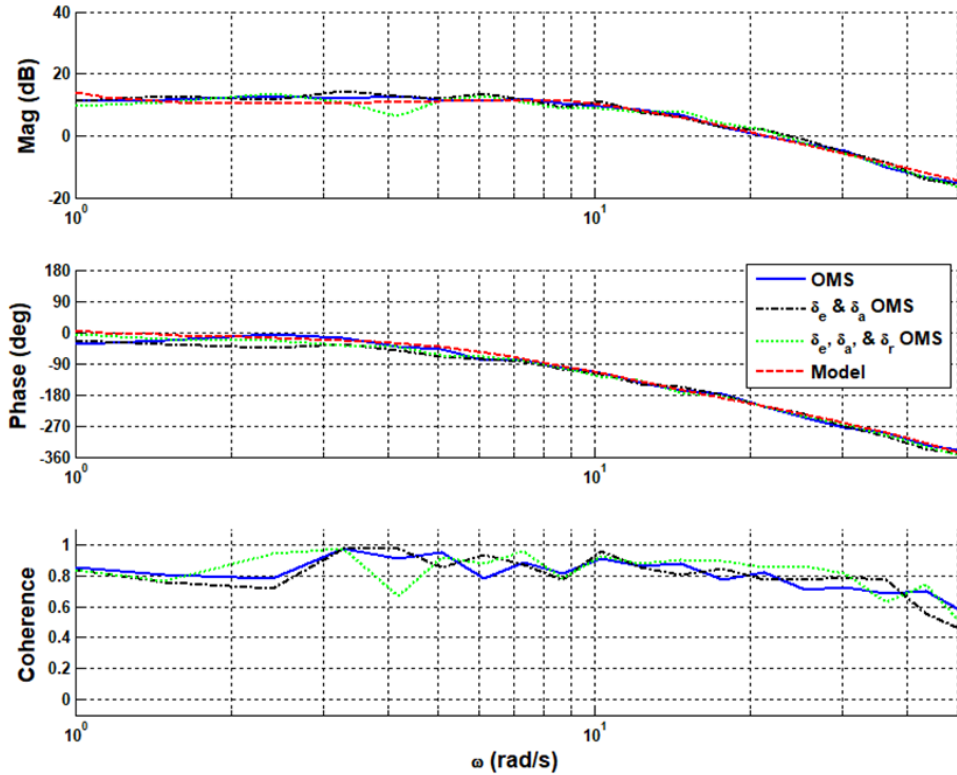


Figure 111: FLT06-MOI Method 1 - q/δ_{ec} Identification – OMS

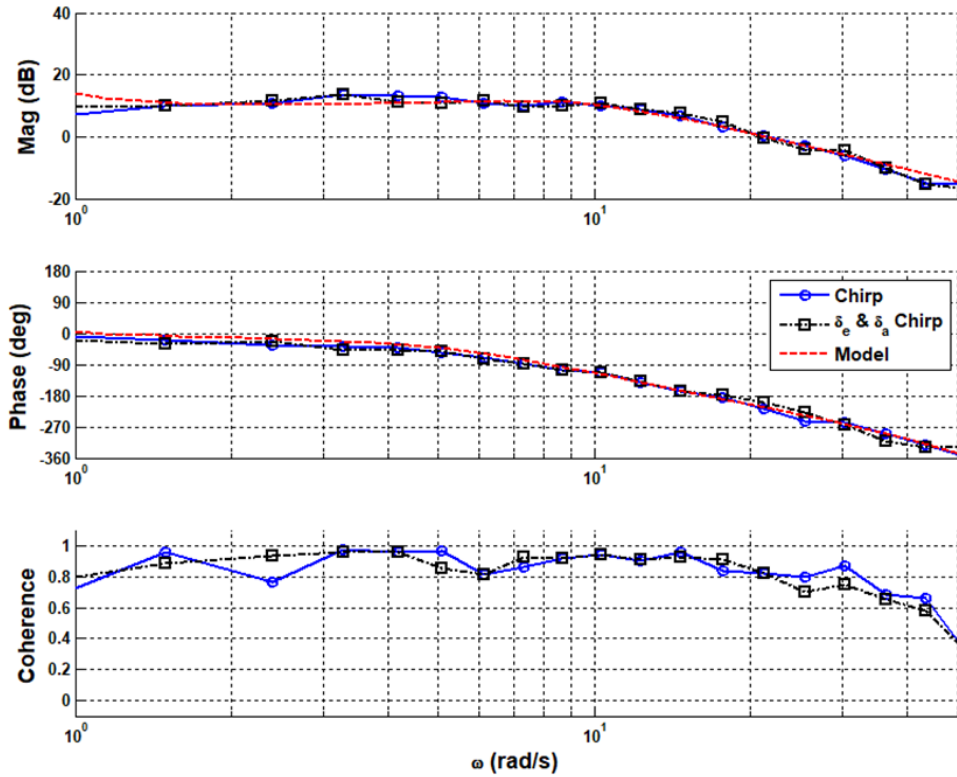


Figure 112: FLT06-MOI Method 1 - q/δ_{ec} Identification – Frequency sweep

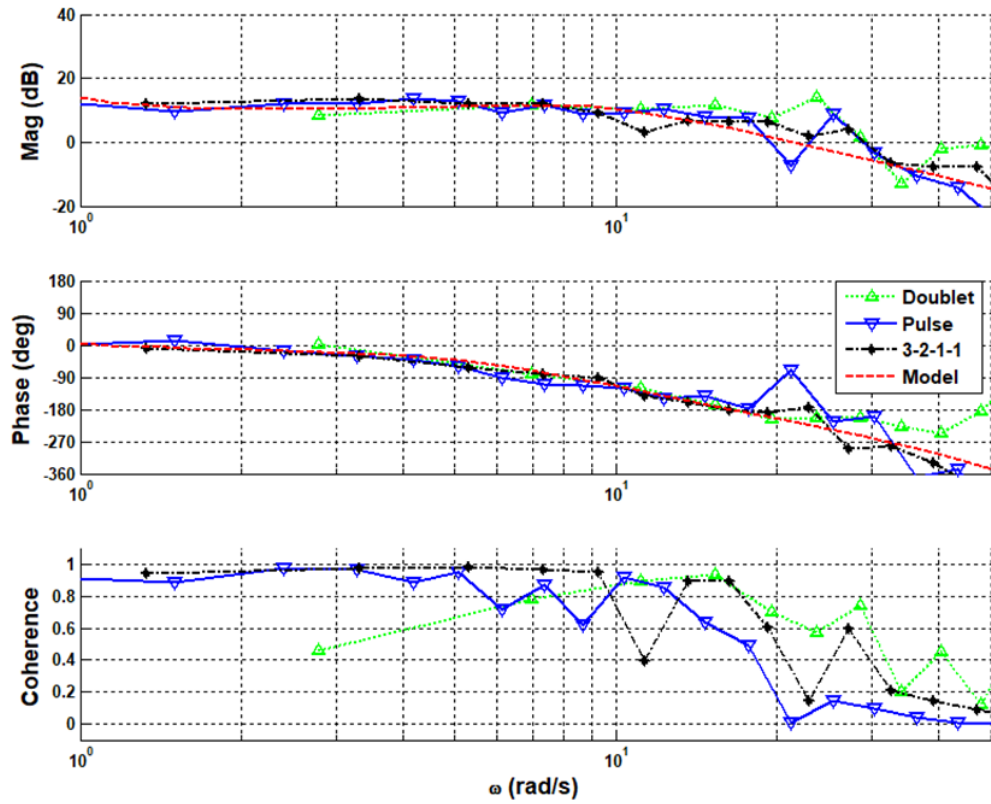


Figure 113: FLT06-MOI Method 1 - q/δ_{ec} Identification – Short Duration Inputs

b. MOI Method 2

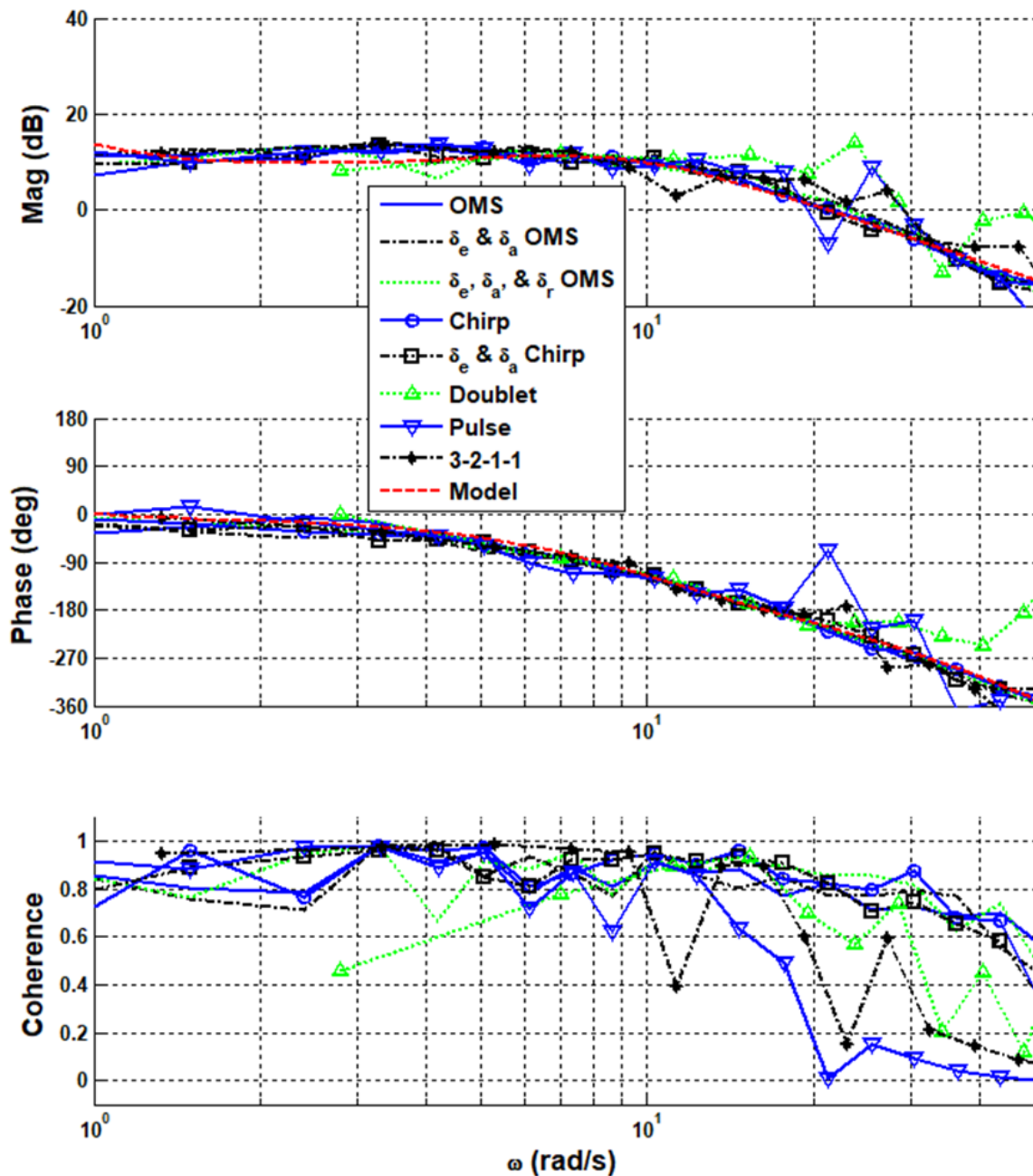


Figure 114: FLT06-MOI Method 2 - q/δ_{ec} Identification – All Methods

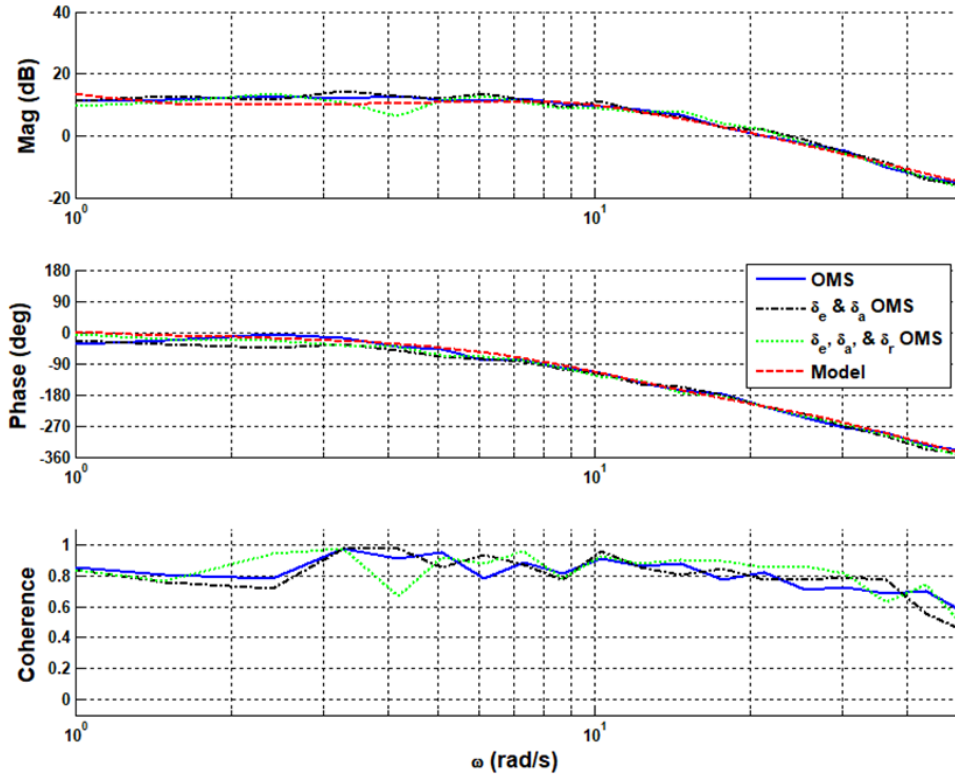


Figure 115: FLT06-MOI Method 2 - q/δ_{ec} Identification – OMS

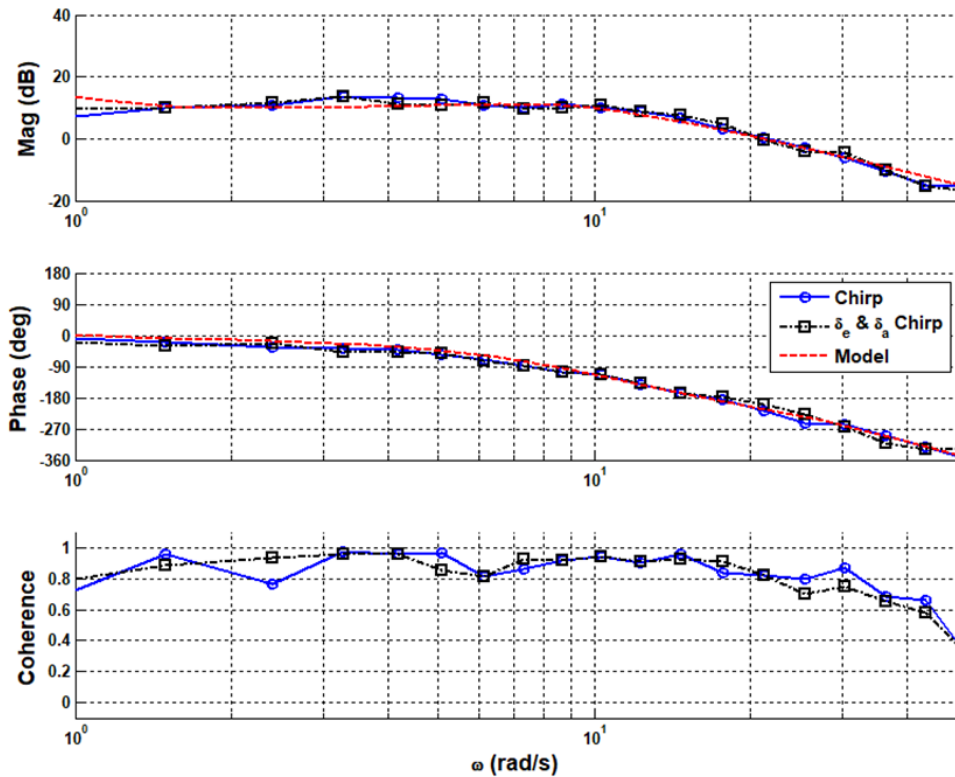


Figure 116: FLT06-MOI Method 2 - q/δ_{ec} Identification – Frequency sweep

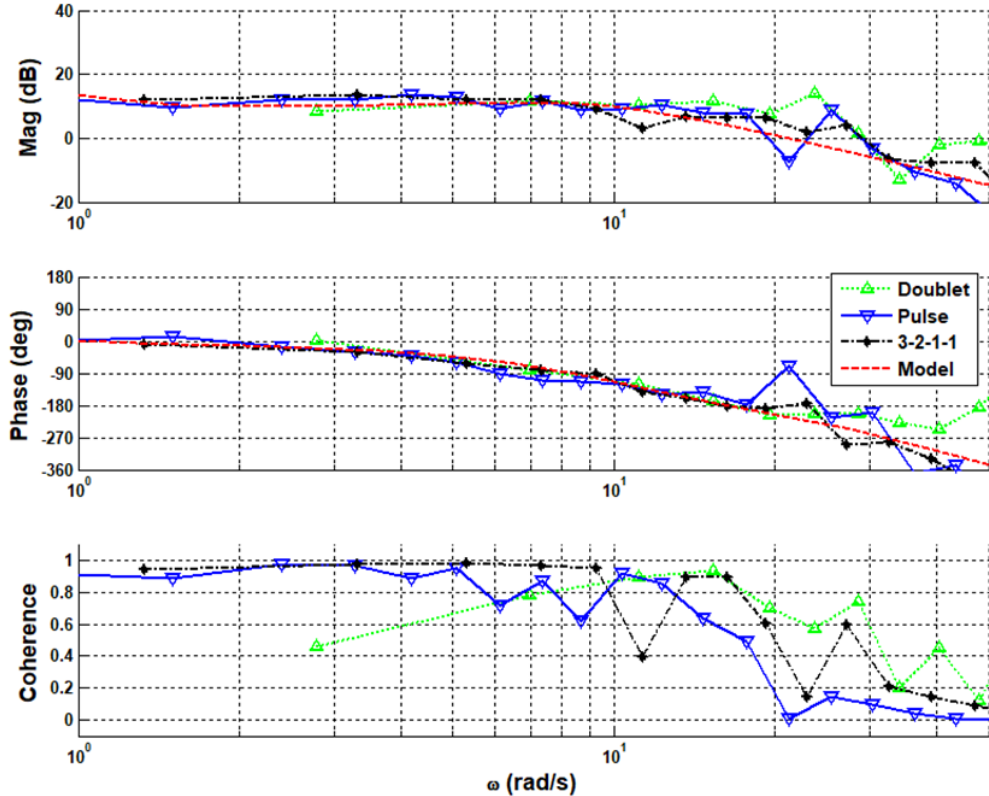


Figure 117: FLT06-MOI Method 2 - q/δ_{ec} Identification – Short Duration Inputs

2. Lateral Survey

All identified responses from the lateral excitations can be seen plotted with the updated reference model in Figure 118 and Figure 122. Table 36 provides the actuator model and bare airframe dynamics in the lateral axis.

Table 36: FLT 06 - Lateral Aircraft and Aileron Actuator Model

Aileron Actuator Model	Lateral Model
$\frac{\delta_a}{\delta_{ac}} = \frac{40}{s+12} e^{-0.060s}$	$\frac{p}{\delta_a} = \frac{30.37(-0.08657)[0.3275, 2.266]}{(0.04581)[0.3201, 3.085](12.5)}$

The identified lateral OMS input excitation for flight 06 can be seen in Figure 119 and Figure 123. The magnitude and phase response of the aileron alone, and elevator-aileron multi axis through all frequencies of interest have highly variable coherence values. The magnitude and phase responses closely match each other and the model, but not as well as previous fits.

The identified lateral frequency sweep input excitation for flight 06 can be seen in Figure 120 and Figure 124 and features the aileron only input, and the multi-axis elevator-aileron excitation. While the fit of the identified systems is close to the model, the coherence is again lower than desired.

The identified lateral short duration input excitation can be seen in Figure 121 and Figure 125. Similarly, the magnitude and phase match with one another and the model, but with regions of poorer fits. Again, the coherence is not as high as desired.

a. MOI Method 1

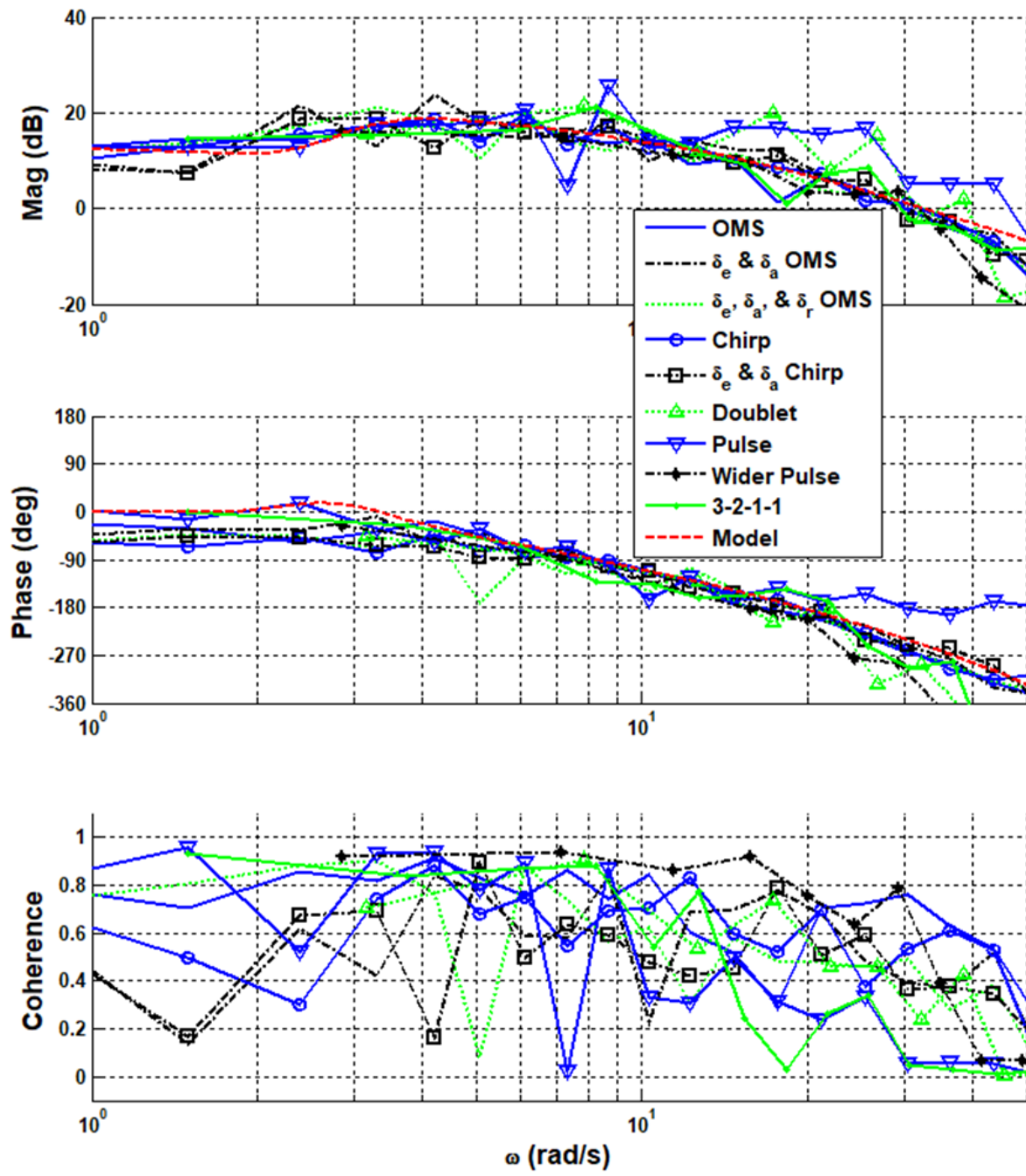


Figure 118: FLT06-MOI Method 1 - p/ δ_{ac} Identification – All Methods

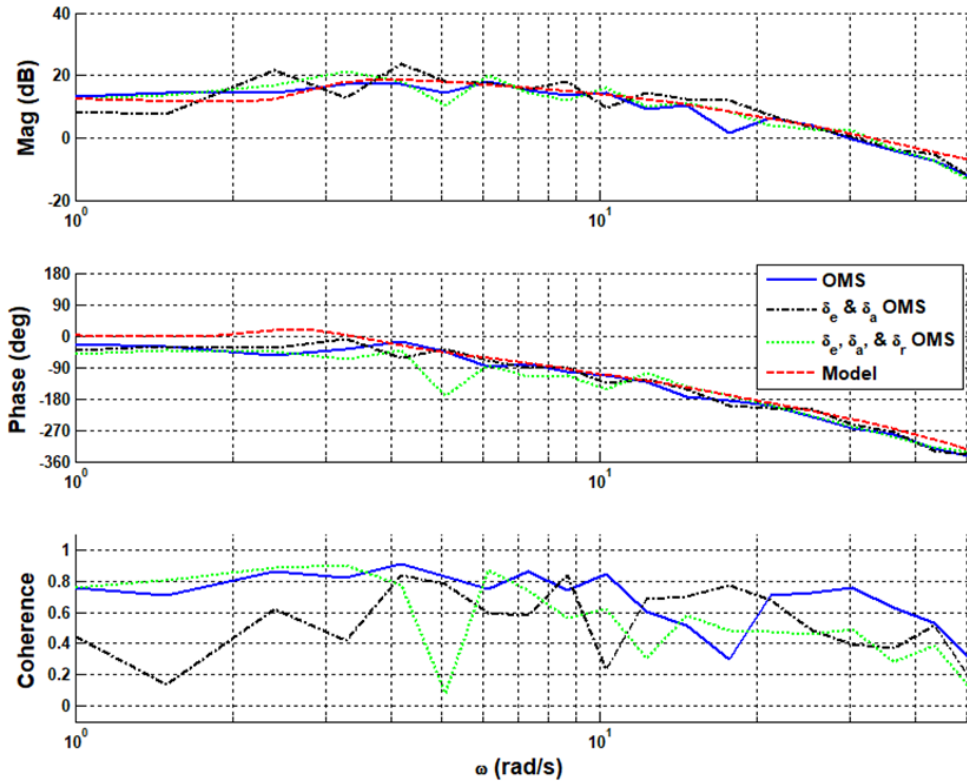


Figure 119: FLT06-MOI Method 1 - p/δ_{ac} Identification – OMS

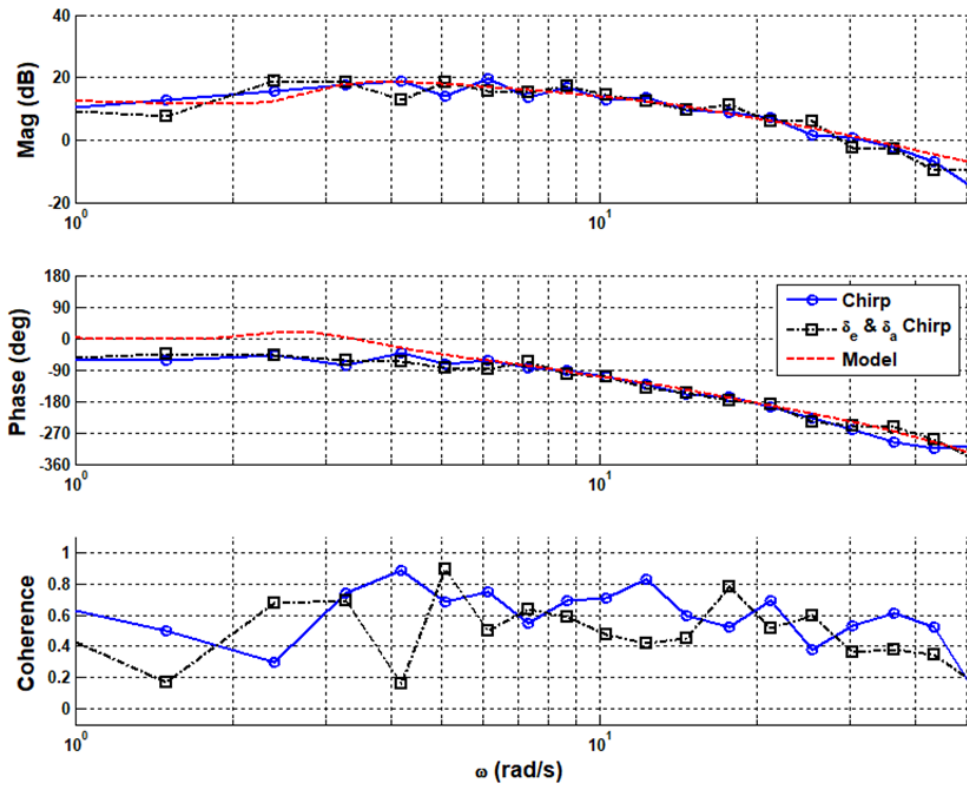


Figure 120: FLT06-MOI Method 1 - p/δ_{ac} Identification – Frequency sweep

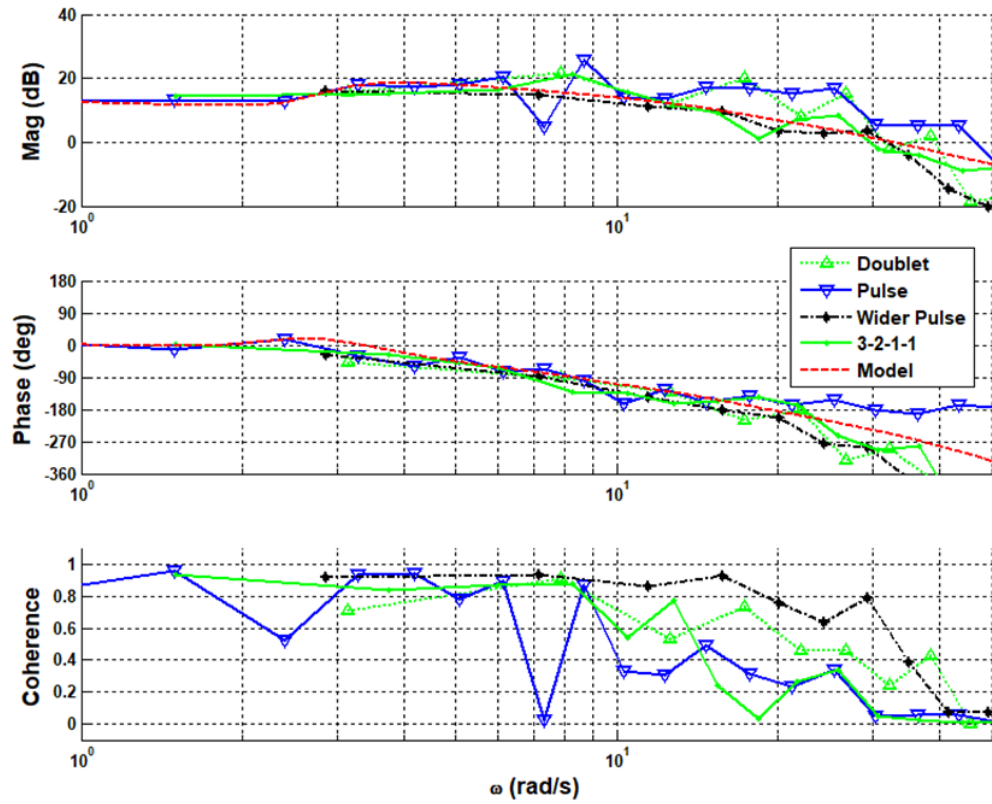


Figure 121: FLT06-MOI Method 1 - p/δ_{ac} Identification – Short Duration Inputs

b. MOI Method 2

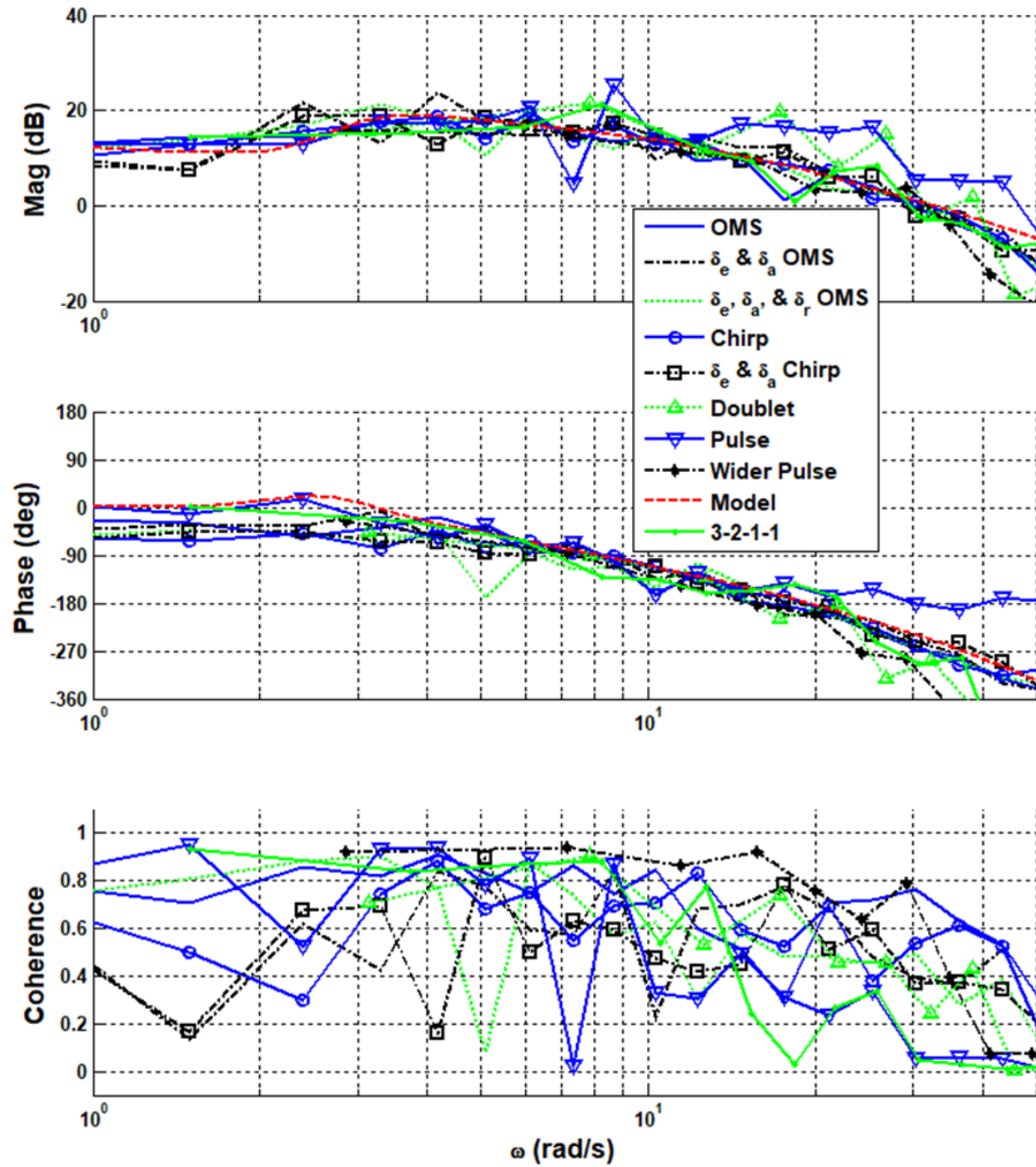


Figure 122: FLT06-MOI Method 2 - p/δ_{ac} Identification – All Methods

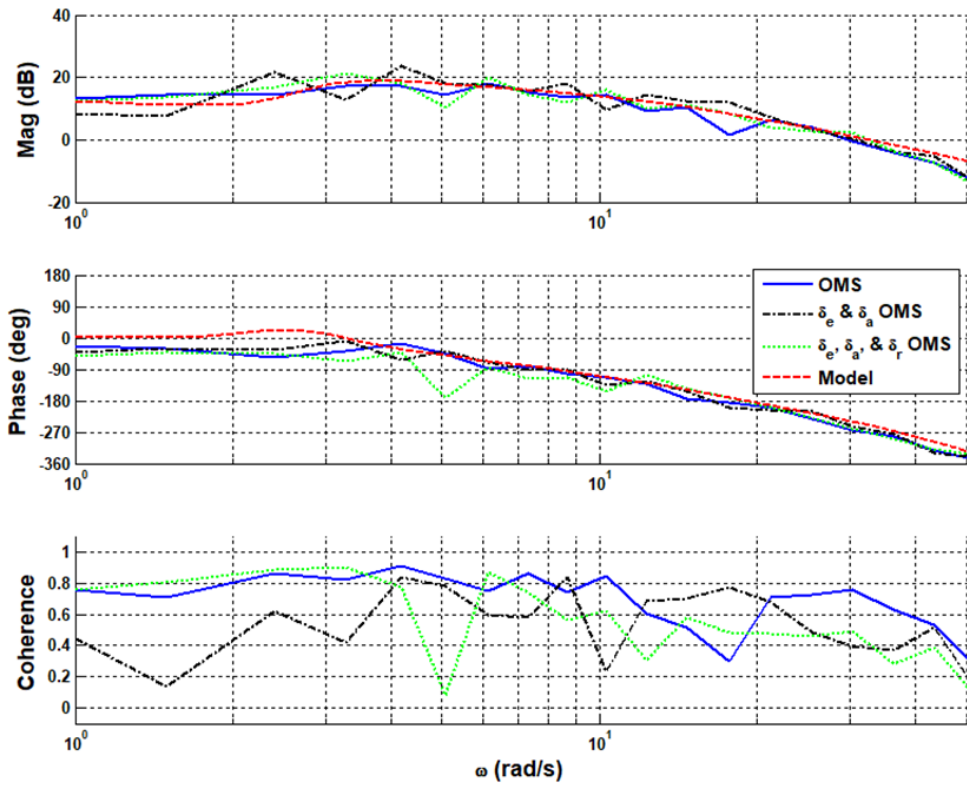


Figure 123: FLT06-MOI Method 2 - p/ δ_{ac} Identification – OMS

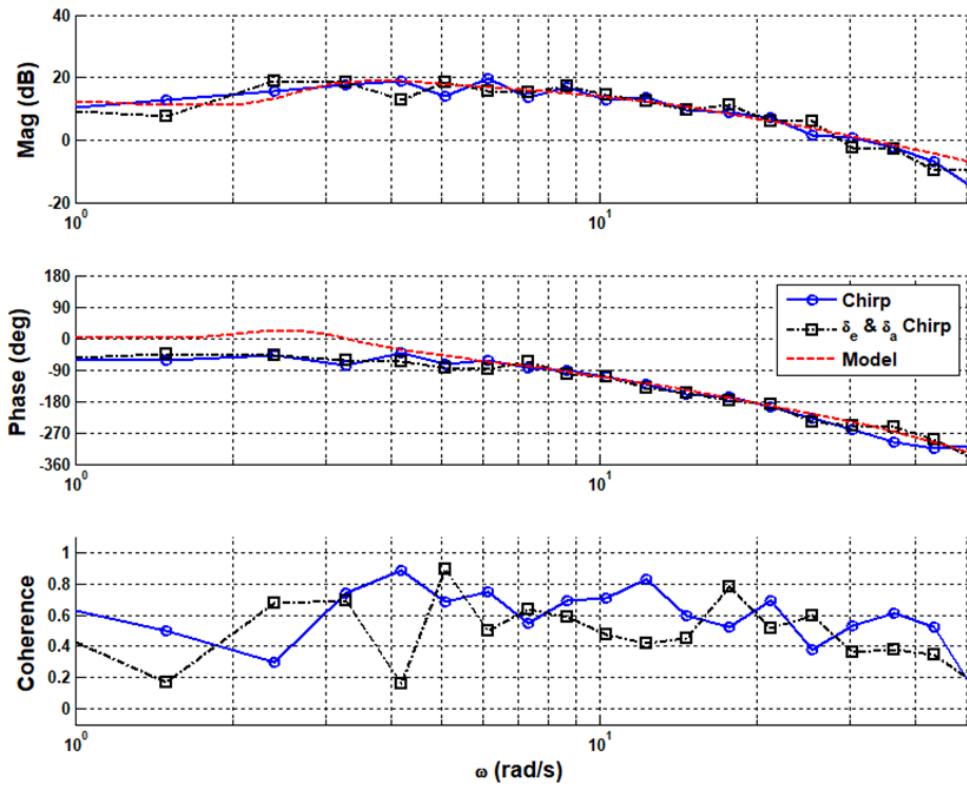


Figure 124: FLT06-MOI Method 2 - p/ δ_{ac} Identification – Frequency sweep

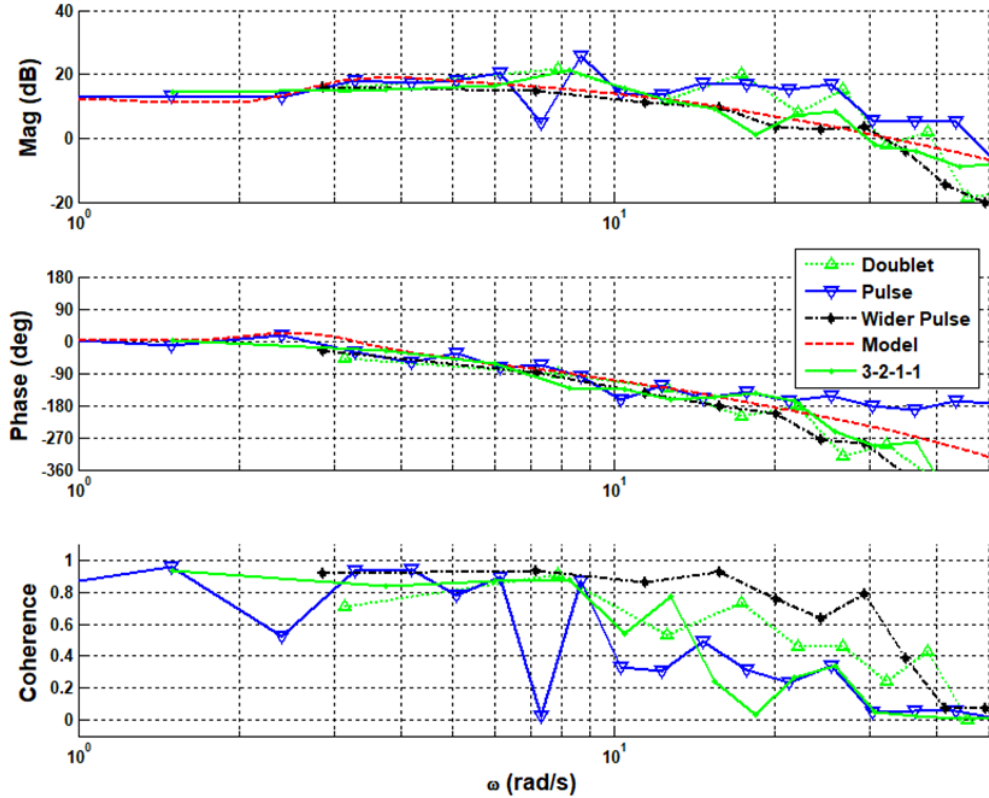


Figure 125: FLT06-MOI Method 2 - p/δ_{ac} Identification – Short Duration Inputs

3. Directional Survey

All identified responses from the directional excitations can be seen plotted with the updated reference model in Figure 126 and Figure 130. Table 37 provides the actuator model and bare airframe dynamics in the directional axis. All excitations had poor coherence levels, resulting in poor matches with the modeled response and each other. Although the directional identifications have not been as clean as the identifications in the other axes, efforts are underway to understand the reason for these poor fits as they are the worst of the considered data sets.

Table 37: FLT 06 - Directional Aircraft and Rudder Actuator Model

Rudder Actuator Model	Directional Model
$\frac{\delta_r}{\delta_{rc}} = \frac{10}{s+10} e^{-0.065s}$	$\frac{r}{\delta_r} = \frac{-3.656[0.2313, 1.386](6.95)}{(0.04581)[0.305, 3.05](12.5)}$

The identified directional OMS input excitation for flight 06 can be seen in and Figure 127 and Figure 131. The magnitude and phase response of the rudder alone and the elevator-aileron-rudder multi axis generally match the model at frequencies above 6 rad/s. Both excitations did not remain in a desired coherence level at any of the frequencies shown. A brief spike occurred in the phase of the elevator-aileron-rudder multi axis input excitation at about 5 rad/s. A ramp up in the phase for the rudder alone input excitation is shown at low frequencies up to about 6 rad/s, the extremely low coherence shows this as well.

The identified directional frequency sweep input excitation for flight 06 can be seen in Figure 128 and Figure 132, which features the rudder only input. Overall, the magnitude and phase response of the

excitation generally match to the model at frequencies above 5rad/s and ~3rad/s, respectively. The coherence was generally unsatisfactory.

The identified directional short duration input excitation can be seen in Figure 129 and Figure 133. Of the four excitations, the 3-2-1-1 input profile maintained the highest level of coherence across the frequency region shown, but all excitations had either issues with or lacked the content to identify the lowest and highest frequencies of interest.

a. MOI Method 1

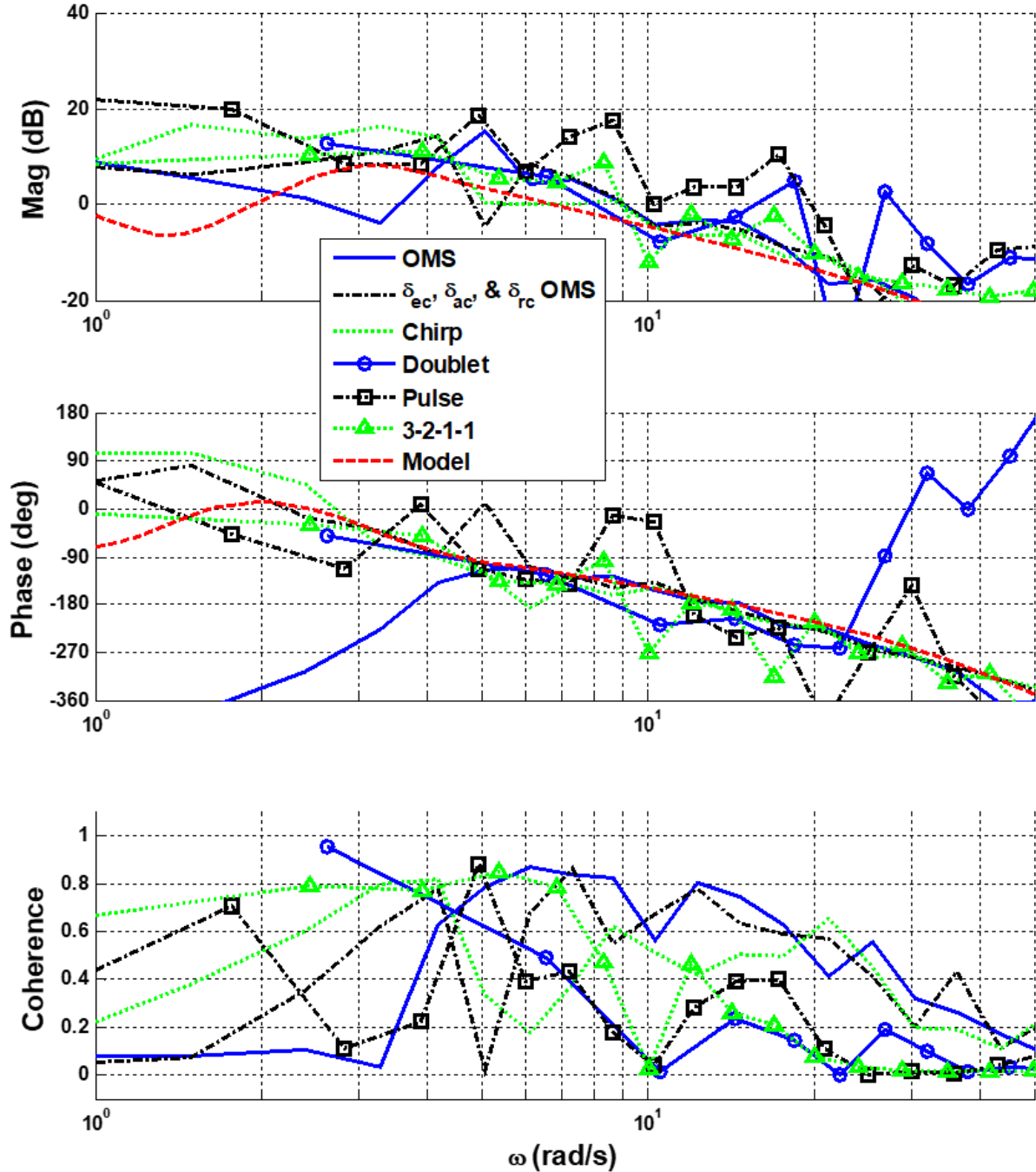


Figure 126: FLT06-MOI Method 1 - r/δ_{rc} Identification – All Methods

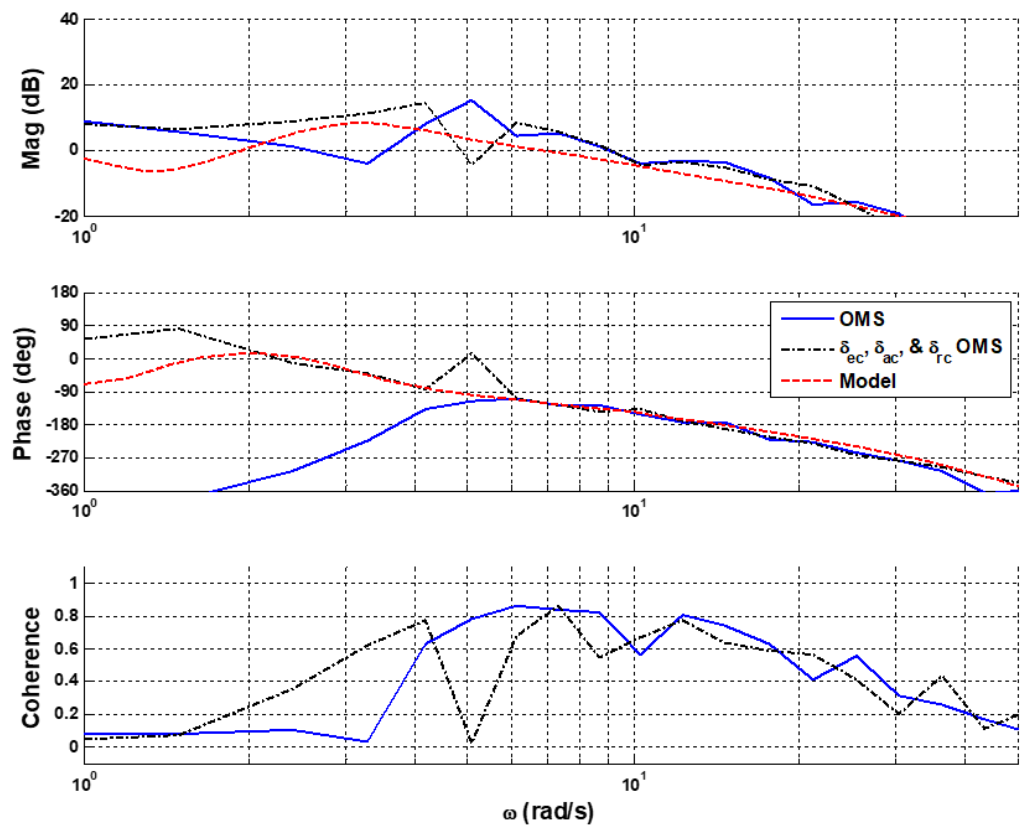


Figure 127: FLT06-MOI Method 1 - r / δ_{rc} Identification - OMS

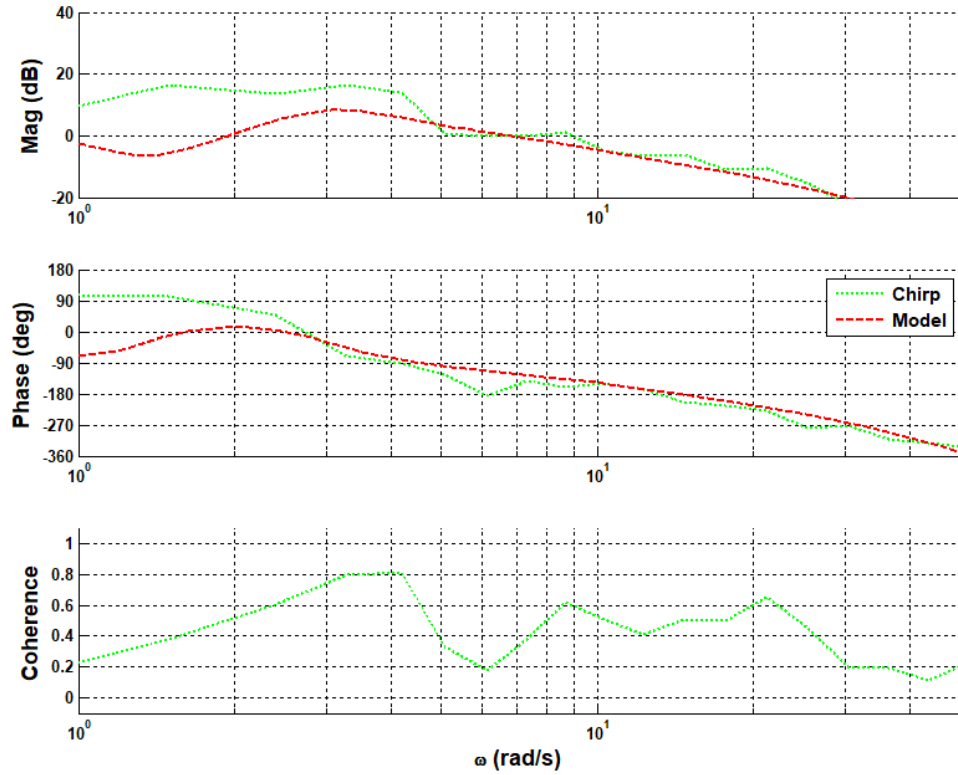


Figure 128: FLT06-MOI Method 1 - r/δ_{rc} Identification - Frequency sweep

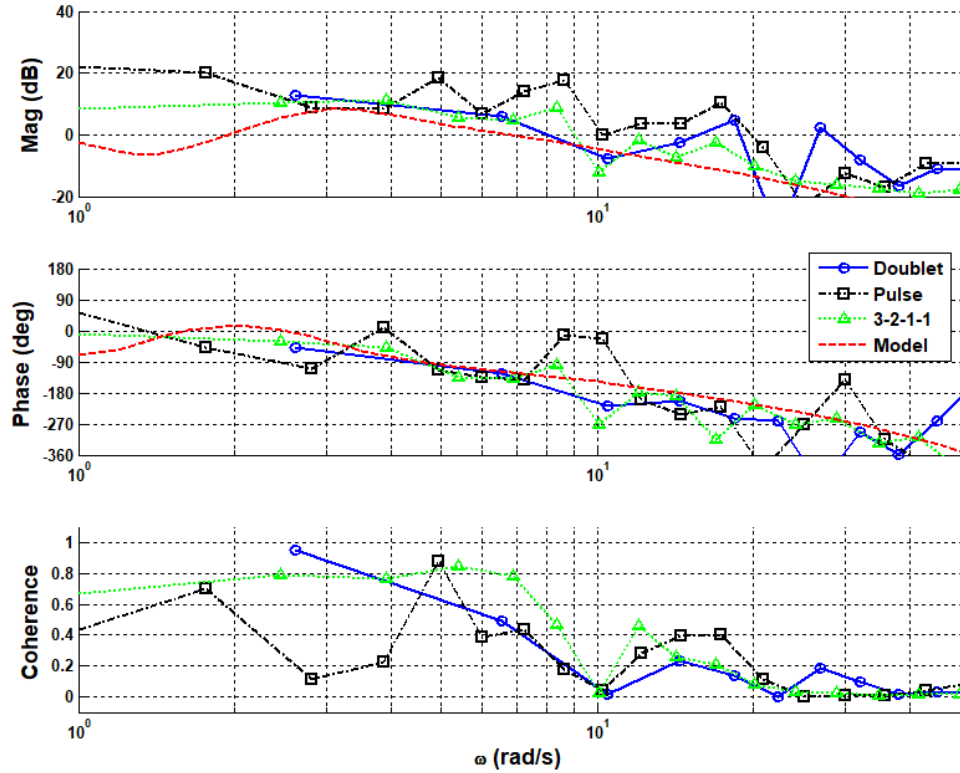


Figure 129: FLT06-MOI Method 1 - r/δ_{rc} Identification - Short Duration

b. MOI Method 2

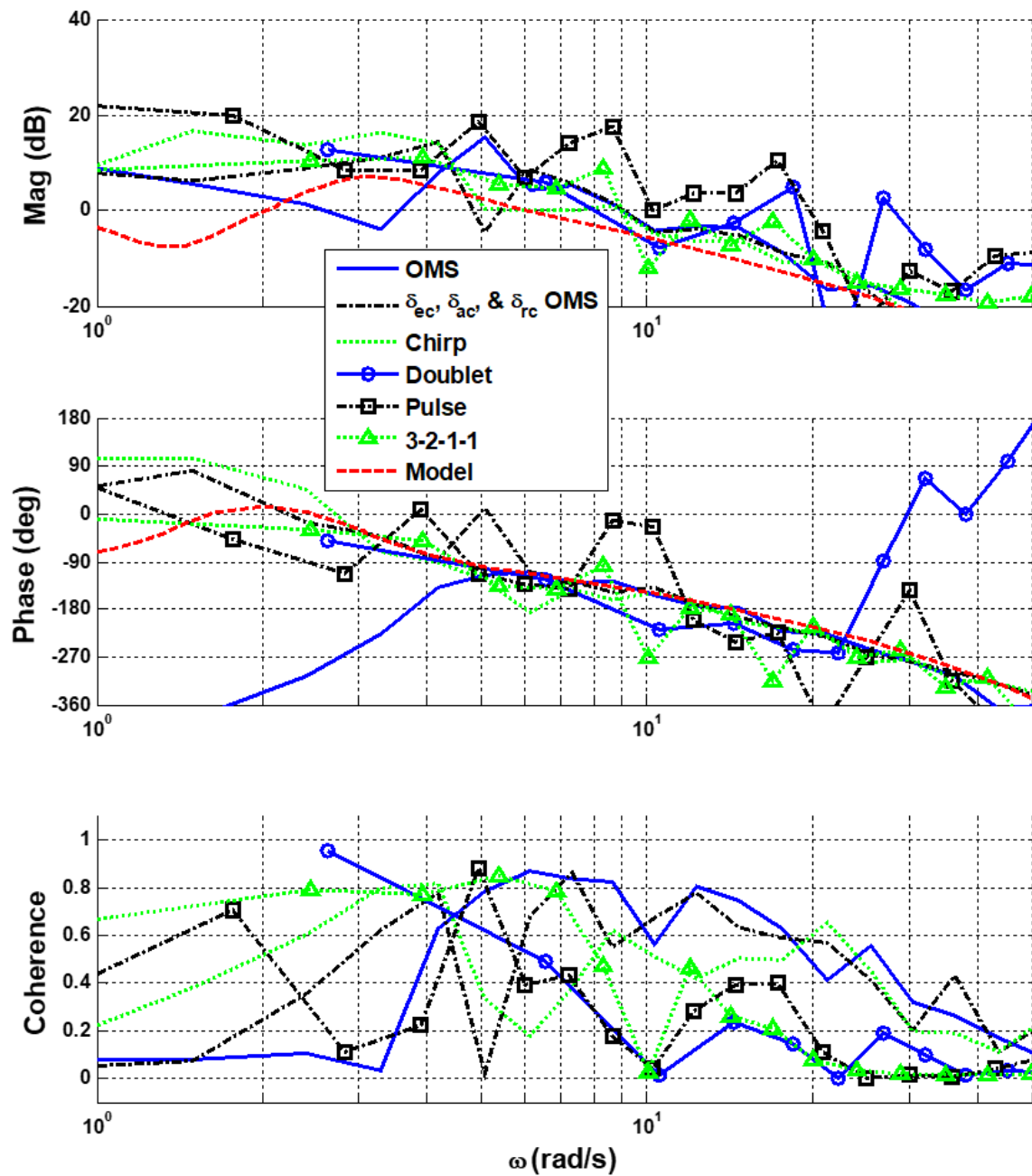


Figure 130: FLT06-MOI Method 2 - r/δ_{rc} Identification - All Methods

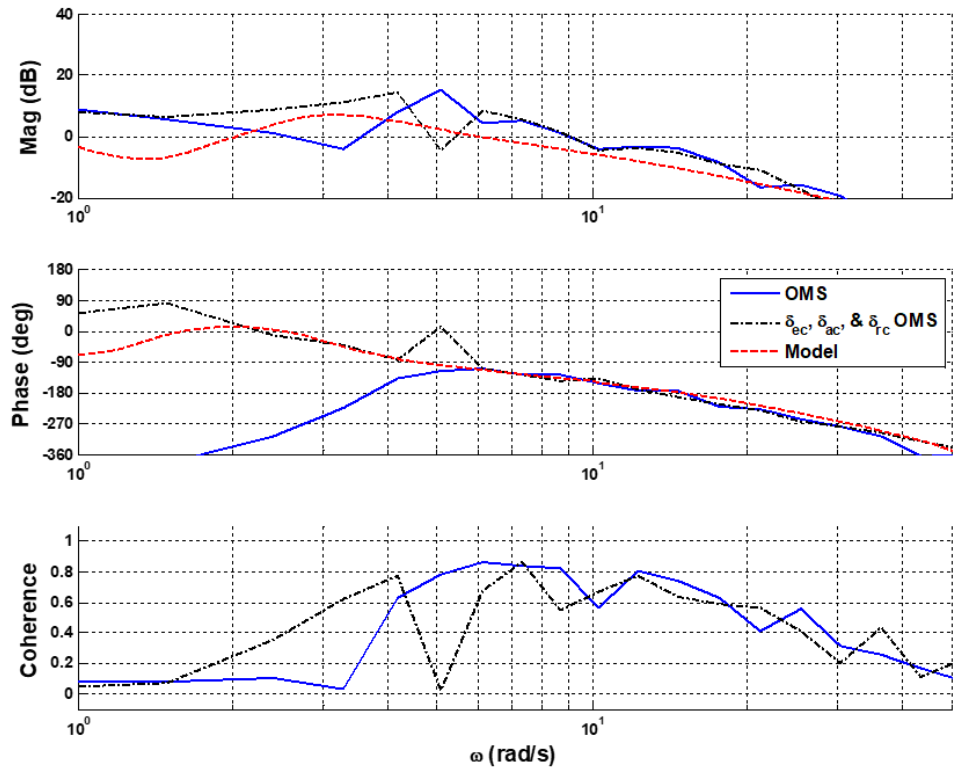


Figure 131: FLT06-MOI Method 2 - r/δ_{rc} Identification - OMS

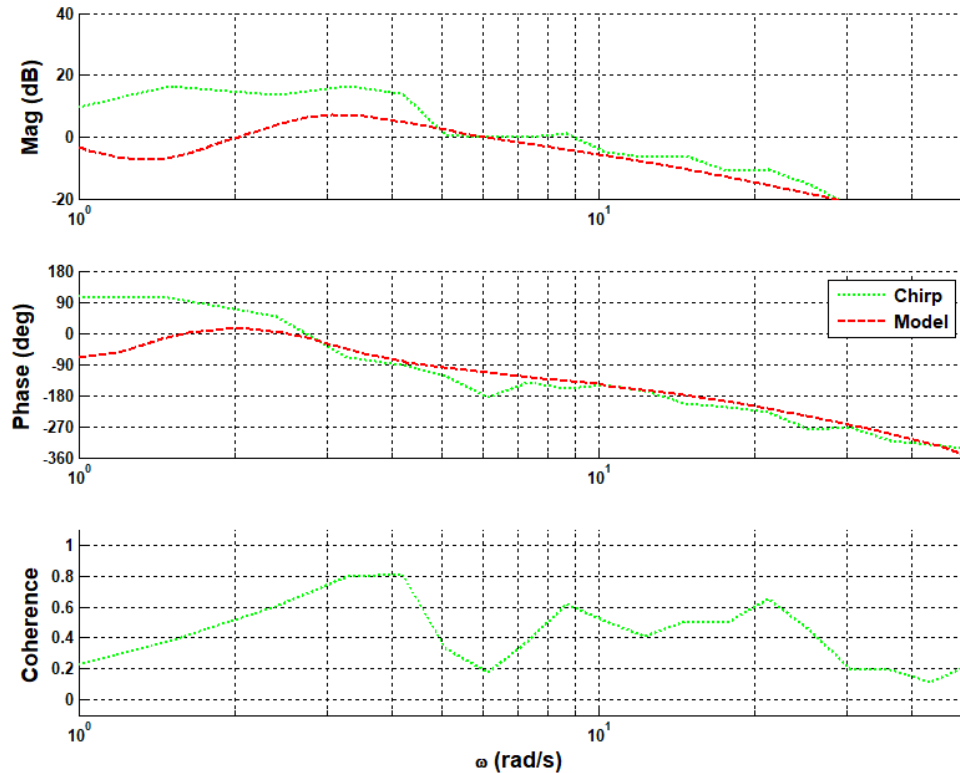


Figure 132: FLT06-MOI Method 2 - r/δ_{rc} Identification - Frequency sweep

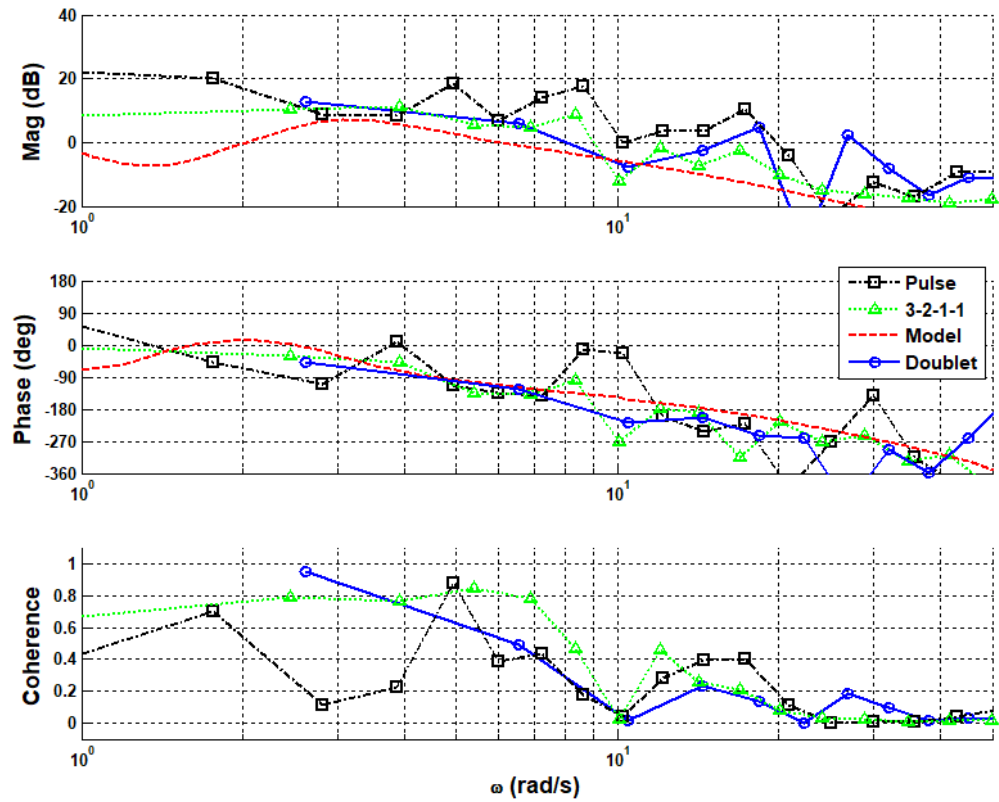


Figure 133: FLT06-MOI Method 2 - r/δ_{rc} Identification - Short Duration

F. FLIGHT 10

Flight 10 was flown at cruise condition, that was straight and level flight with computer generated inputs. An additional time delay of 80ms was added to the system for this flight.

In order to match the gain values of the longitudinal, lateral, and directional bare airframe models with the flight data, a series of gains were applied to the bare airframe models which can be seen in Table 38.

Table 38: Model Gains for FLT 10

Longitudinal	Lateral	Directional
1.2	0.8	4.0

1. Longitudinal Survey

All identified responses from the longitudinal excitations can be seen plotted with the updated reference model in Figure 134. Table 39 provides the actuator model and bare airframe dynamics in the longitudinal axis.

Table 39: FLT 10 – Longitudinal Aircraft and Elevator Actuator Models

Elevator Actuator Model	Longitudinal Model
$\frac{\delta_e}{\delta_{ec}} = \frac{8}{s+10} e^{-0.065s}$	$q = \frac{77.33(0)(0.4055)(6.147)}{[0.3178, 0.5352][0.7533, 9.484]}^2$

The identified longitudinal OMS input excitation for flight 10 can be seen in Figure 135. All identified systems provide a close match to the modeled response. There is a drop in coherence in the 2-3rad/s region with a taper off starting at 10rad/s of the frequency region.

The identified longitudinal frequency sweep input excitation for flight 10 can be seen in Figure 136, featuring the elevator only input, and the multi-axis elevator and aileron input. Overall, the magnitude and phase response of both signals fit the model with a slight offset from 1-6rad/s. There was decent coherence throughout the range of frequencies shown, however it is seen to roll off at 10rad/s.

The identified longitudinal short duration input excitation can be seen in Figure 137. The identified systems closely overlaid the model response. Of the three excitations, the 3-2-1-1 input profile maintained the highest level of coherence across the frequency region shown, but all excitations lacked the content to identify the lowest and highest frequencies of interest.

². The STI shorthand form of displaying a transfer function is defined by: $a(s+b)[s^2 + 2\zeta\omega s + \omega^2] = a(b)[\zeta, \omega]$

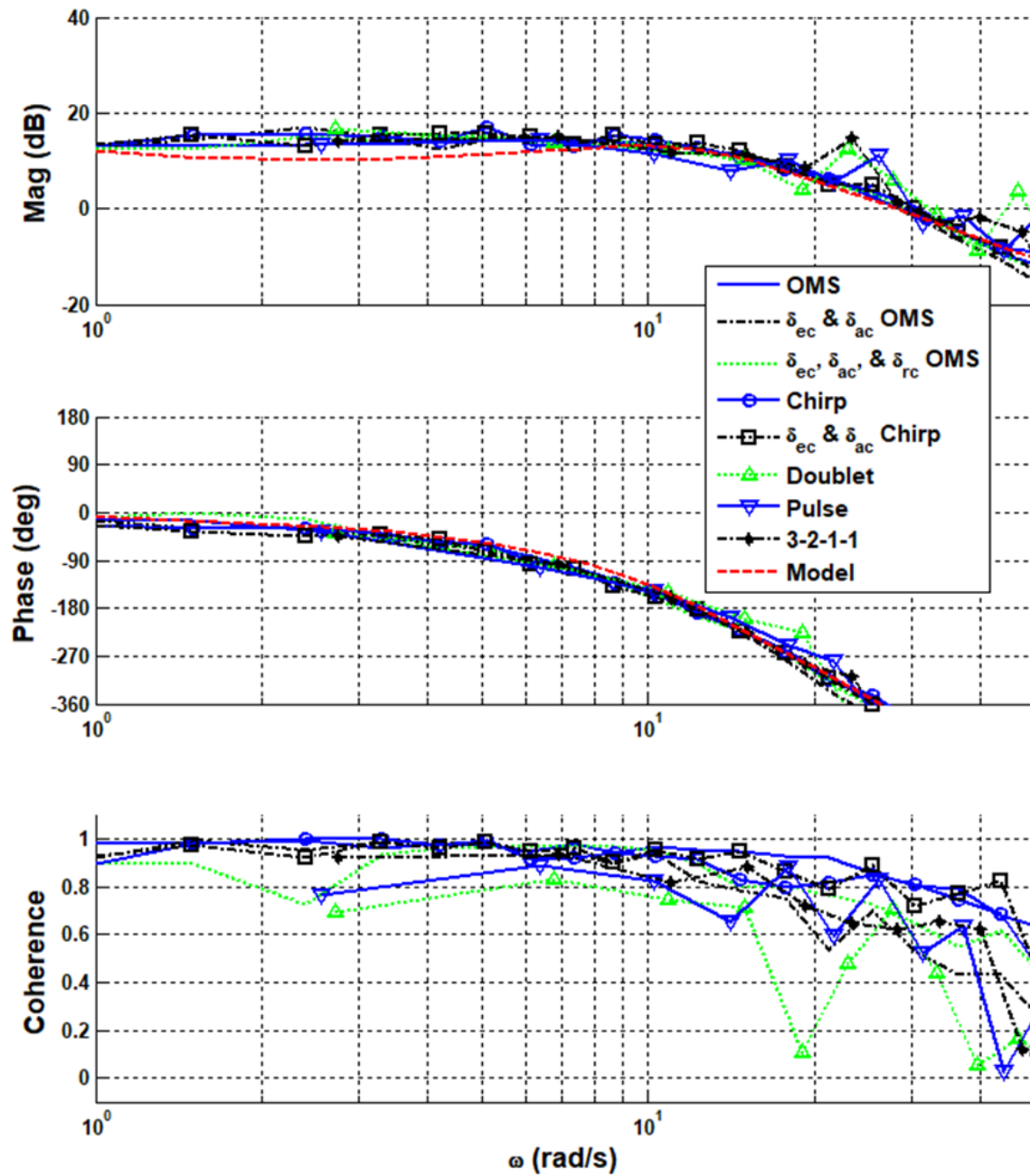


Figure 134: FLT10 - q/δ_{ec} Identification - All Methods

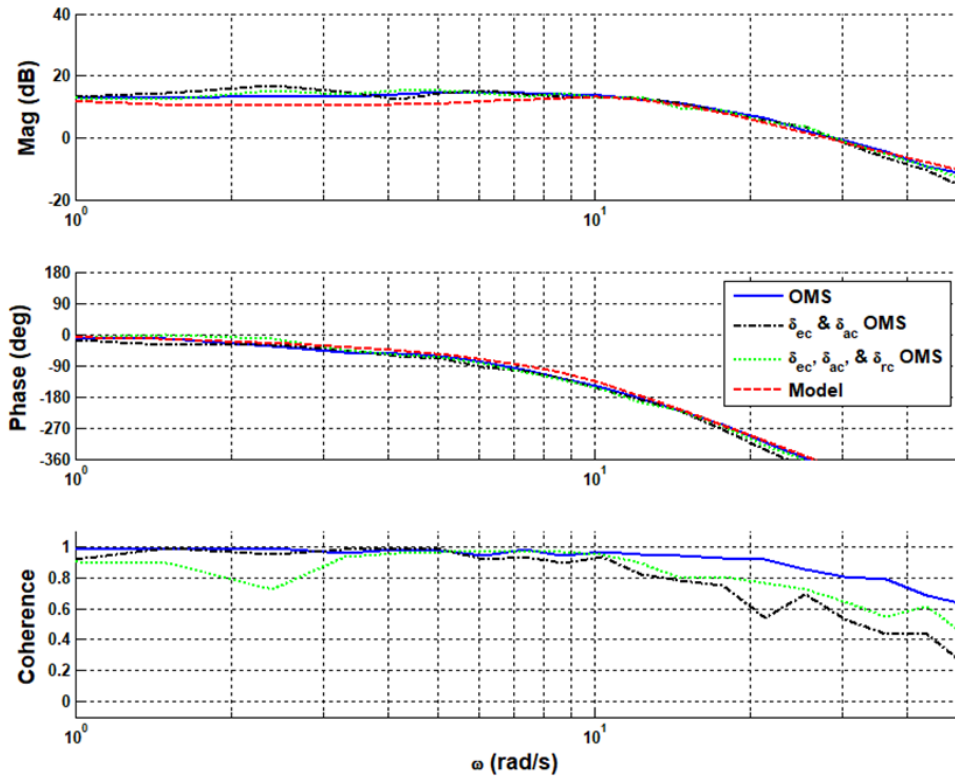


Figure 135: FLT10 - q/δ_{ec} Identification – OMS

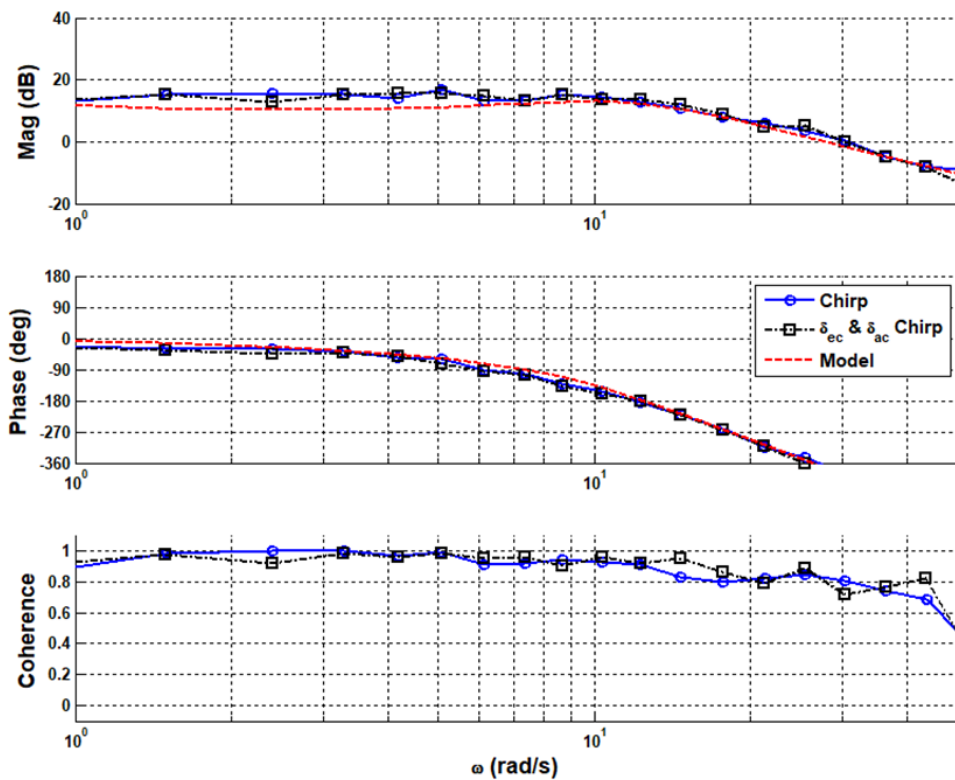


Figure 136: FLT10 - q/δ_{ec} Identification - Frequency sweep

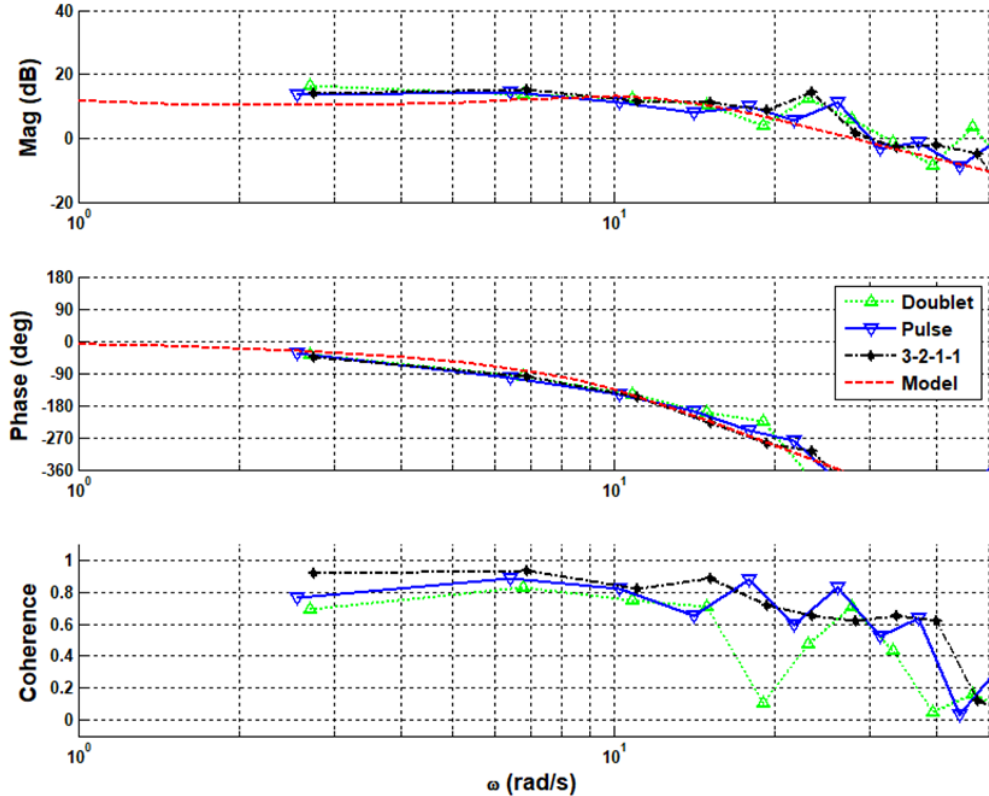


Figure 137: FLT10 - q/δ_{ec} Identification - Short Duration

2. Lateral Survey

All lateral excitations can be seen plotted with the model in Figure 138. Table 40 provides the aileron actuator model and lateral aircraft model.

Table 40: FLT 10 – Lateral Aircraft and Aileron Actuator Model

Aileron Actuator Model	Lateral Model
$\frac{\delta_a}{\delta_{ac}} = \frac{40}{s+12} e^{-0.060s}$	$\frac{p}{\delta_a} = \frac{50.41(-0.0333)[0.2792, 3.505]}{(0.04542)[0.2987, 3.999](9.191)}$

The identified lateral OMS input excitation for flight 10 can be seen in Figure 139. The magnitude and phase response of the aileron alone, elevator-aileron multi axis, and the elevator-aileron-rudder multi axis excitations match the model. The coherence levels are high in general, with coherence rolling off beginning at the ~10rad/s for all inputs. However, this did not significantly alter the quality of the fit.

The identified lateral frequency sweep input excitation for flight 10 can be seen in Figure 140 that features the aileron only input, and the elevator-aileron multi axis. Overall, the magnitude and phase response of both signals closely fit the model. The elevator-aileron multi axis excitation generally had a higher coherence relative to the aileron only input though both taper at about 10rad/s.

The identified lateral short duration input excitation can be seen in Figure 141. Of the four excitations, the 3-2-1-1 input profile maintained the highest level of coherence across the frequency region shown, but all excitations had either major issues with or lacked the content to identify the lowest and highest frequencies of interest. Due to the low coherence levels, the phase for the pulse excitation was left unwrapped.

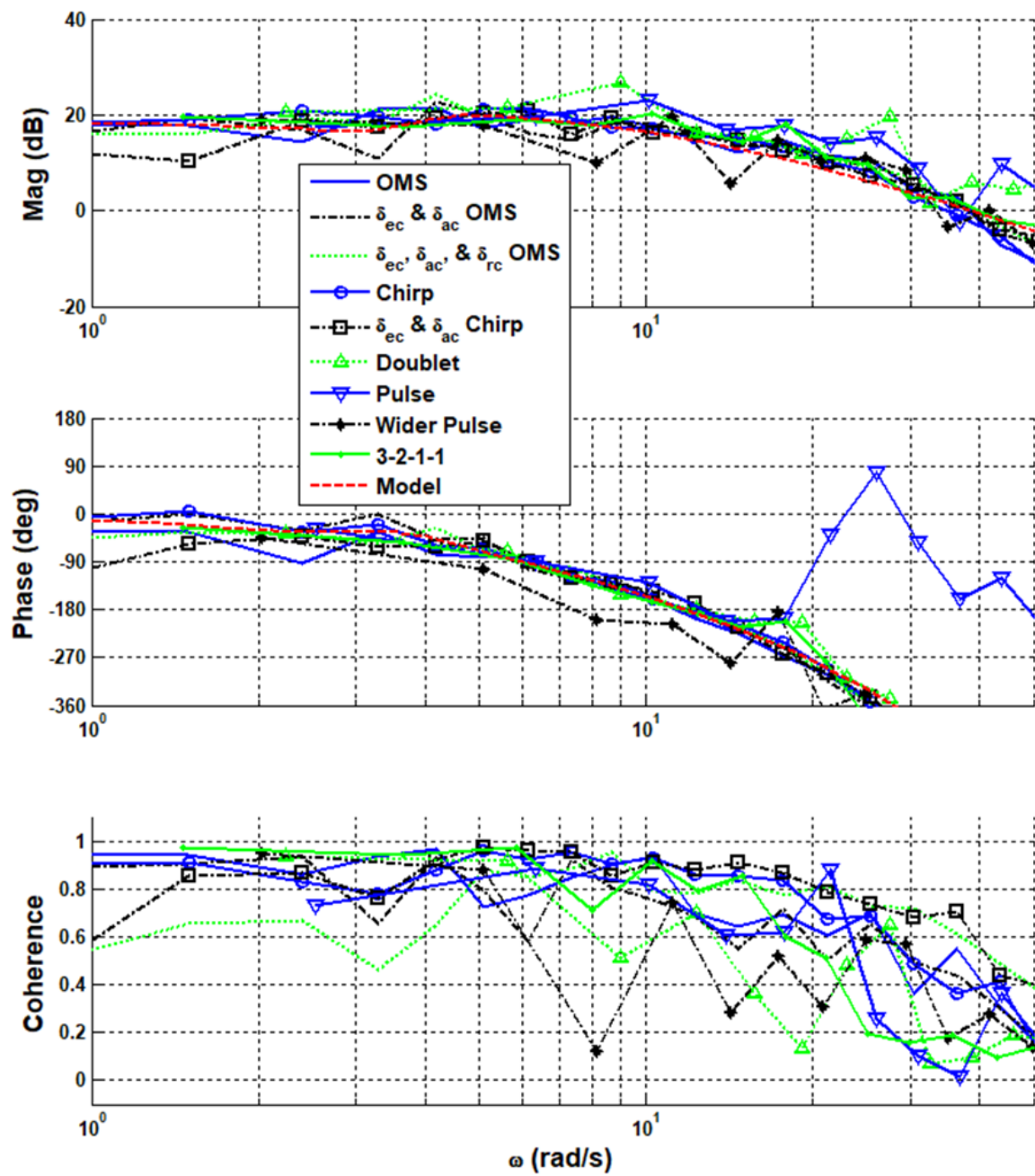


Figure 138: FLT10 - p/ δ_{ac} Identification - All Methods

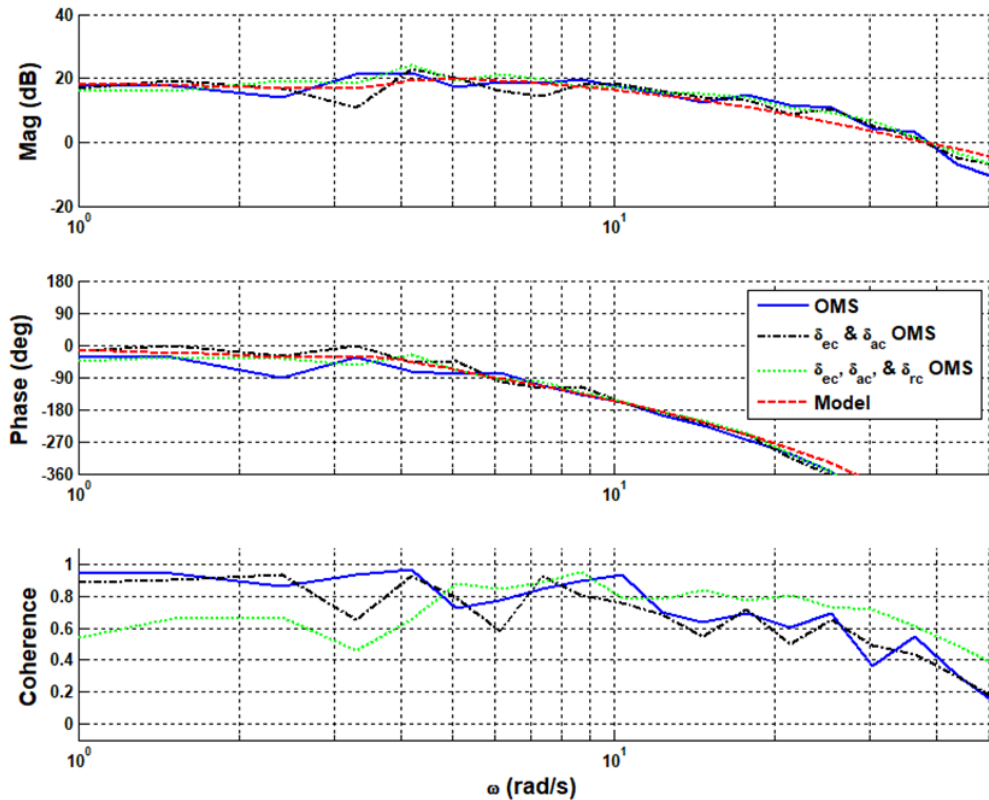


Figure 139: FLT10 - p/ δ_{ac} Identification - OMS

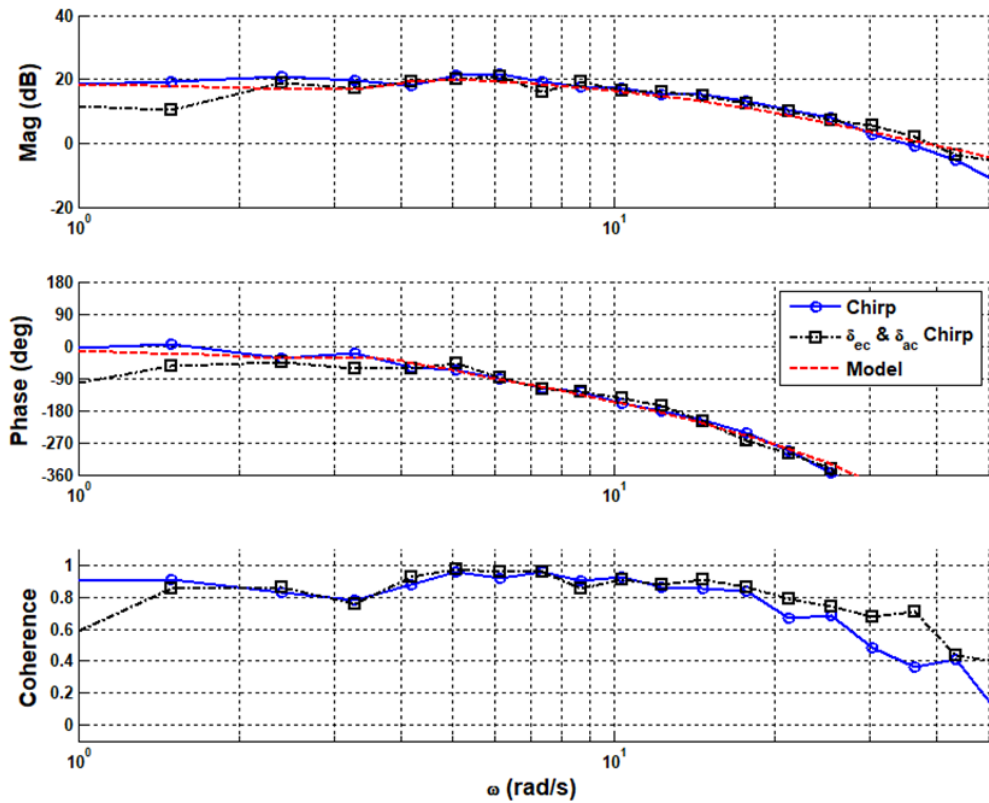


Figure 140: FLT10 - p/ δ_{ac} Identification - Frequency sweep

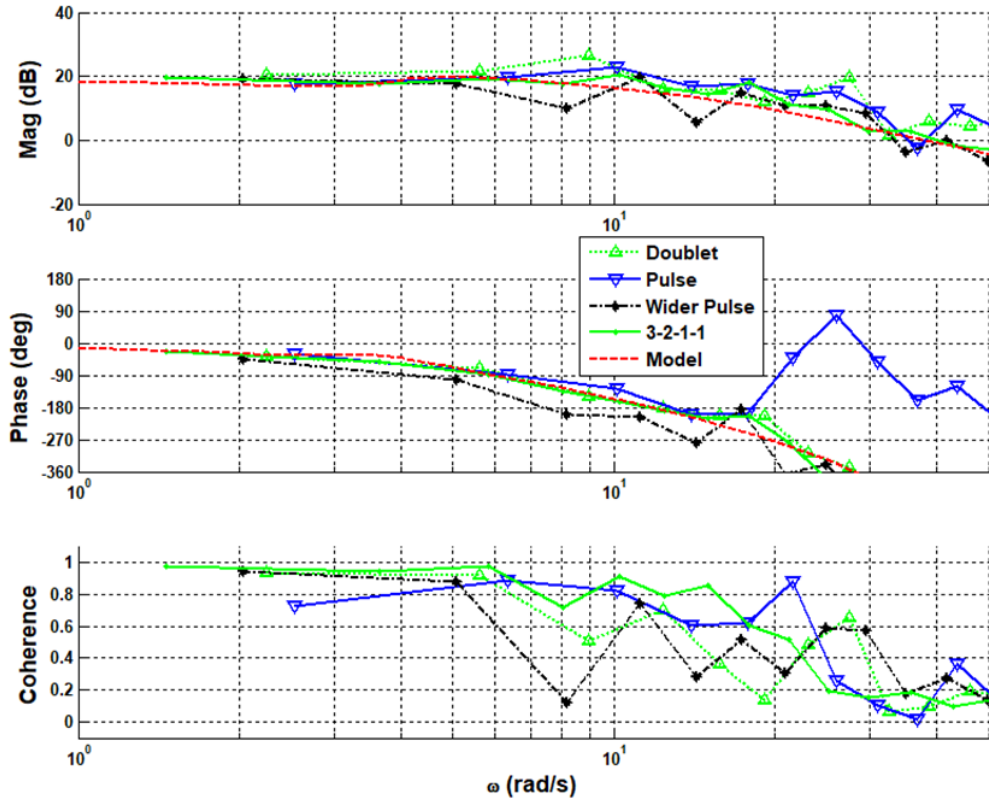


Figure 141: FLT10 - p/δ_{ac} Identification - Short Duration

3. Directional Survey

All directional excitations can be seen plotted with the model in Figure 142. Table 41 provides the rudder actuator model and directional aircraft model.

Table 41: FLT 03 - Directional Aircraft and Rudder Actuator Model

Rudder Actuator Model	Directional Model
$\frac{\delta_r}{\delta_{rc}} = \frac{10}{s+10} e^{-0.065s}$	$\frac{r}{\delta_r} = \frac{7.794[0.2501, 1.241](9.181)}{(0.04542)[0.2987, 3.999](9.191)}$

The identified directional OMS input excitation for flight 10 can be seen in Figure 143. The magnitude and phase response of the rudder alone, and the elevator-aileron-rudder multi axis closely match each other and the model at frequencies above 5 rad/s. At the lower frequencies the coherence tended to be less than 0.8. The coherence rolls off at the highest frequencies.

The identified directional frequency sweep input excitation for flight 10 can be seen in Figure 144, which features the rudder only input. Overall, the magnitude and phase response of the excitation matches the model above ~ 2 rad/s. The lowest and highest frequency regions have coherence levels below 0.8 and the identified fits reflect that.

The identified directional short duration input excitation can be seen in Figure 145. Of the four excitations, the 3-2-1-1 input profile maintained the highest level of coherence across the frequency region shown, but all excitations either had low coherence or lacked the frequency content to identify the lowest and highest frequencies of interest. Due to the low coherence levels, the phase for the doublet excitation was left unwrapped.

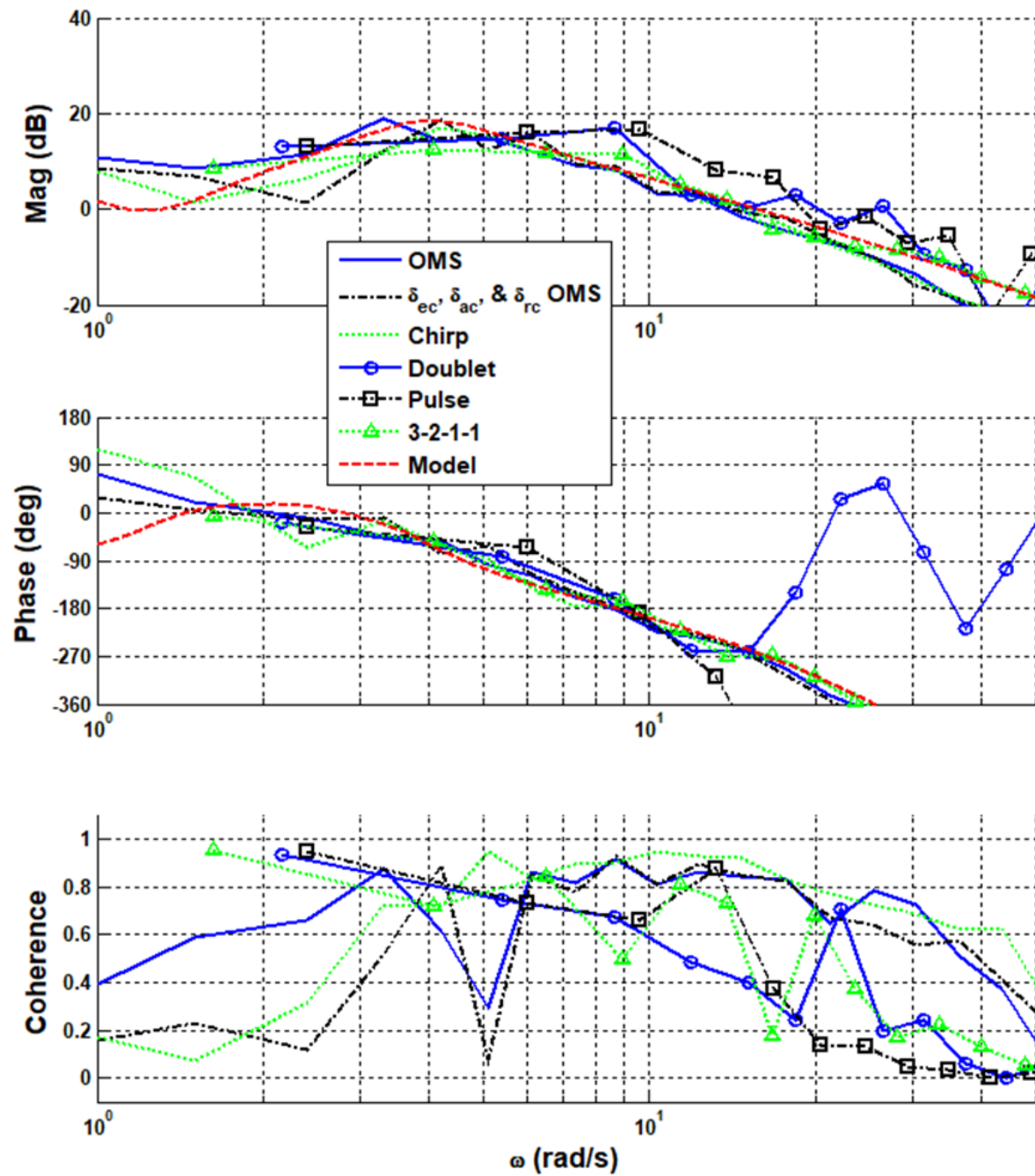


Figure 142: FLT10 - r/δ_{rc} Identification - All Methods

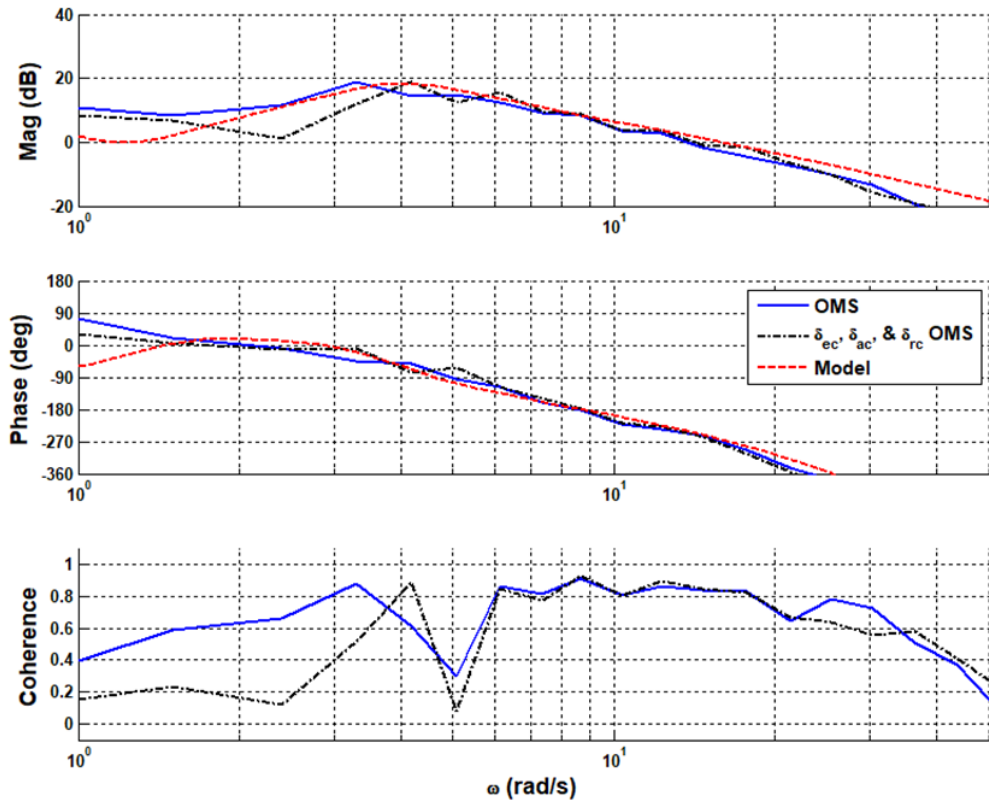


Figure 143: FLT10 - r/δ_{rc} Identification - OMS

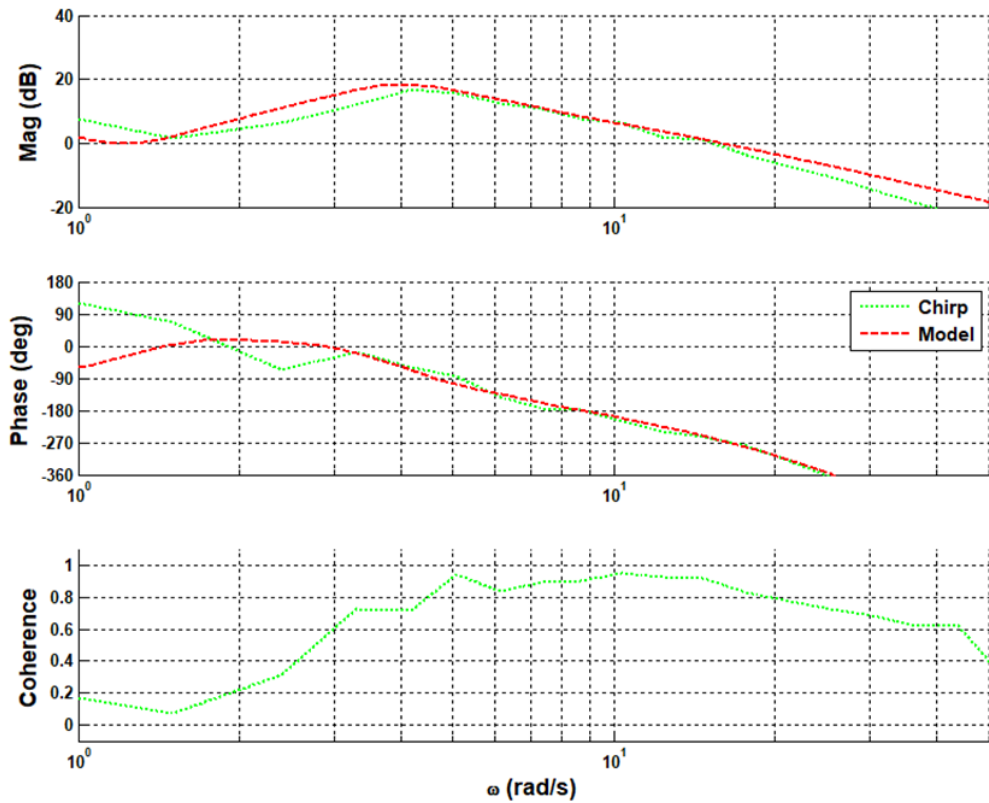


Figure 144: FLT10 - r/δ_{rc} Identification - Frequency Sweep

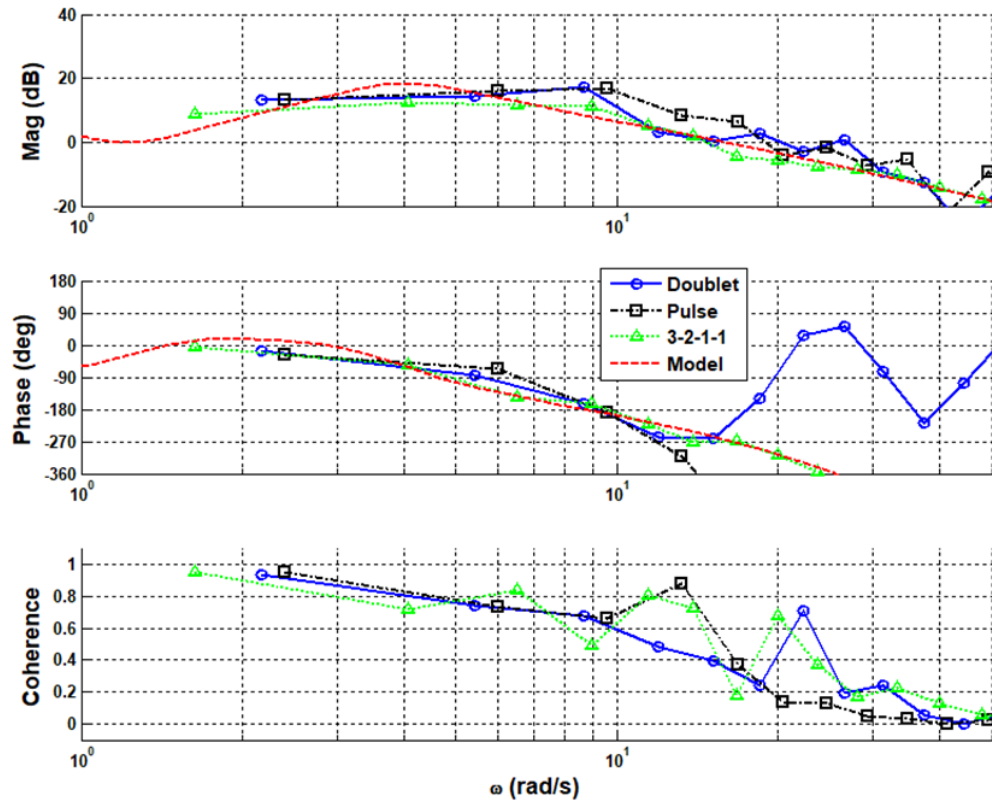


Figure 145: FLT10 - r/δ_{rc} Identification - Short Duration

G. FLIGHT 11

Flight 11 was flown at approach condition (50% flaps at 17 m/s), that was straight and level flight with computer generated inputs. An extra delay of 80ms was added to the system for flight 11.

In order to match the gain values of the longitudinal, lateral, and directional bare airframe models with the flight data, a series of gains were applied to the bare airframe models which can be seen in Table 42.

Table 42: Model Gains for FLT 11

Longitudinal	Lateral	Directional
1.6	1.0	4.5

1. Longitudinal Survey

All identified responses from the longitudinal excitations can be seen plotted with the updated reference model in Figure 146. Table 43 provides the actuator model and bare airframe dynamics in the longitudinal axis.

Table 43: FLT 11 – Longitudinal Aircraft and Elevator Actuator Models

Elevator Actuator Model	Longitudinal Model
$\frac{\delta_e}{\delta_{ec}} = \frac{8}{s+10} e^{-0.065s}$	$q = \frac{40.54(0)(0.3175)(4.617)}{[0.1748, 0.6876][0.6664, 8.077]}^3$

The identified longitudinal OMS input excitation for flight 11 can be seen in Figure 147. All identified systems provide a close match to the modeled response, with higher levels of coherence except there is a taper of coherence at the higher frequency region (~20rad/s).

The identified longitudinal frequency sweep input excitation for flight 11 can be seen in Figure 148 featuring the elevator only input, the multi-axis elevator and aileron input. All identified systems provide a close match to the modeled response. There was good coherence throughout the range of frequencies shown with a slight taper at the higher frequencies (>40rad/s).

The identified longitudinal short duration input excitation can be seen in Figure 149. The identified systems closely overlaid the model response. Of the three excitations, the 3-2-1-1 input profile maintained the highest level of coherence across the frequency region shown, but all excitations lacked the content to identify the lowest and highest frequencies of interest. Due to the low coherence levels, the phase for the doublet excitation was left unwrapped.

³. The STI shorthand form of displaying a transfer function is defined by: $a(s+b)[s^2 + 2\zeta\omega s + \omega^2] = a(b)[\zeta, \omega]$

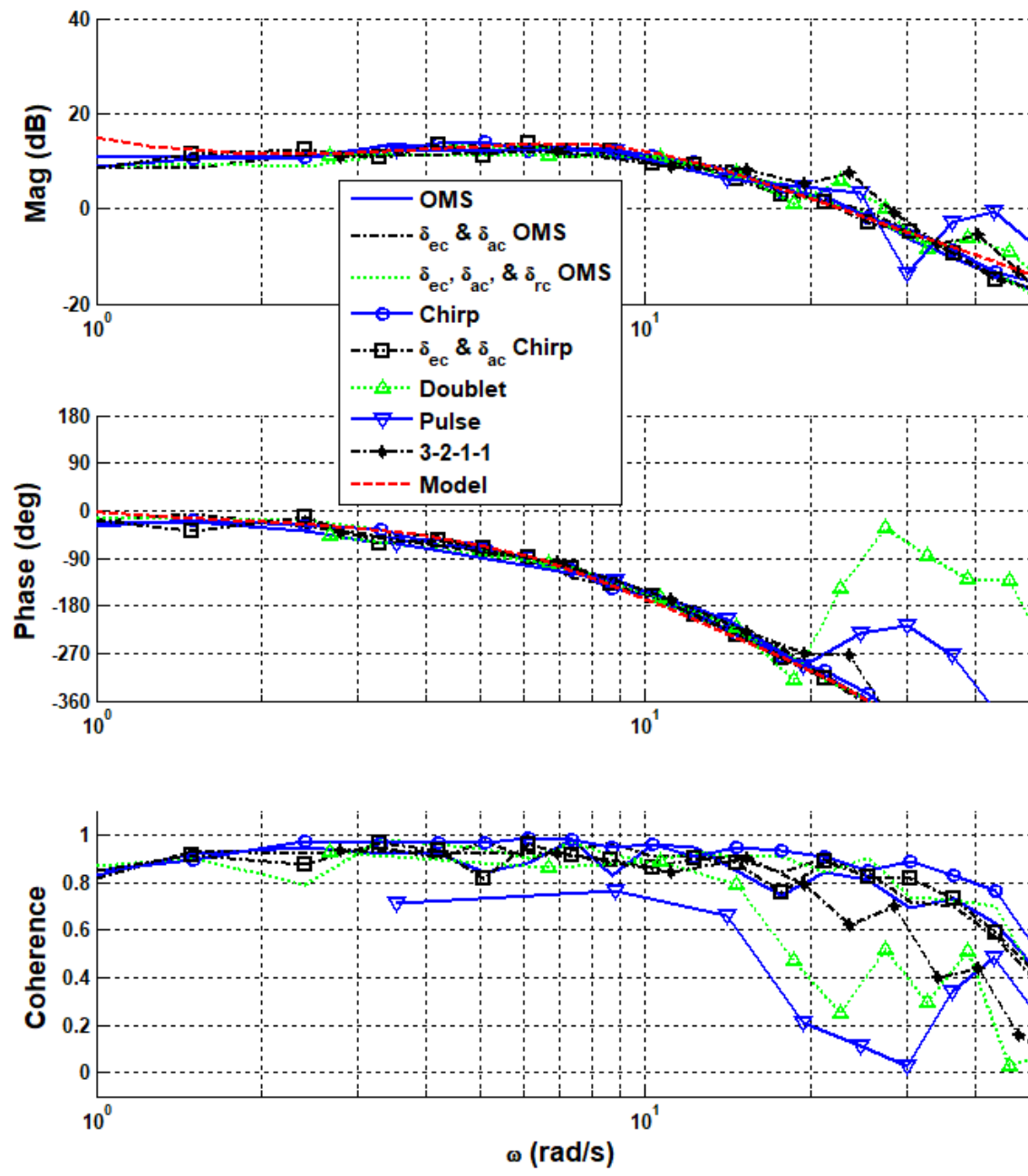


Figure 146: FLT11 - q/δ_{ec} Identification - All Methods

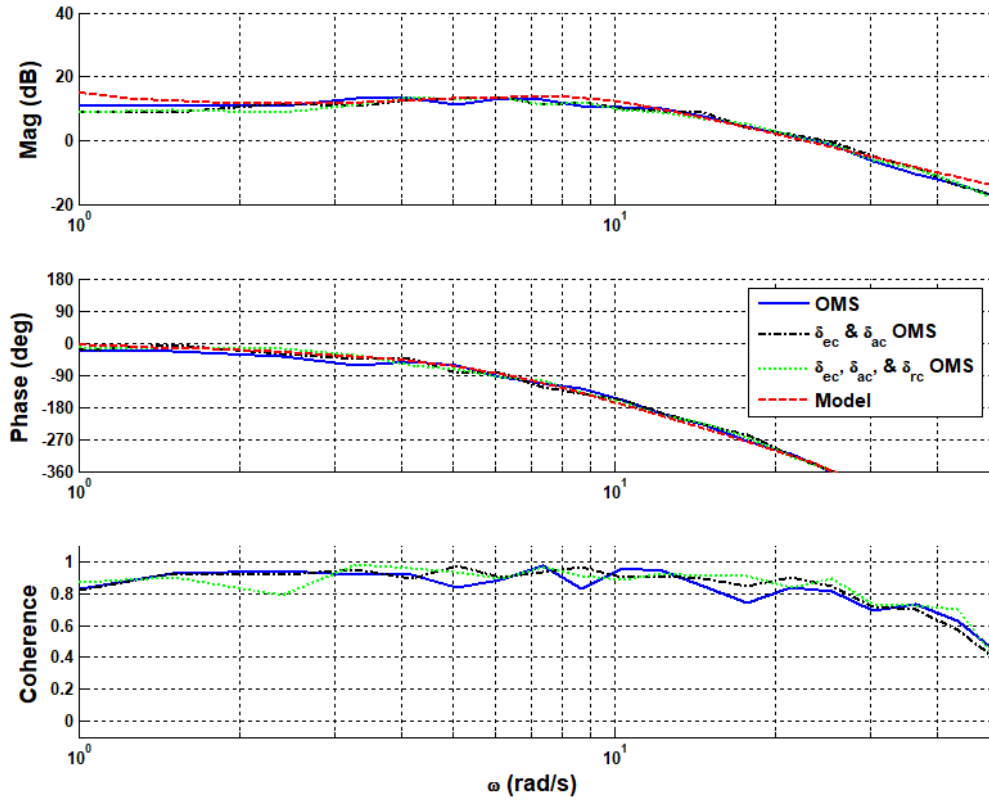


Figure 147: FLT11 - q/ δ_{ec} Identification - OMS

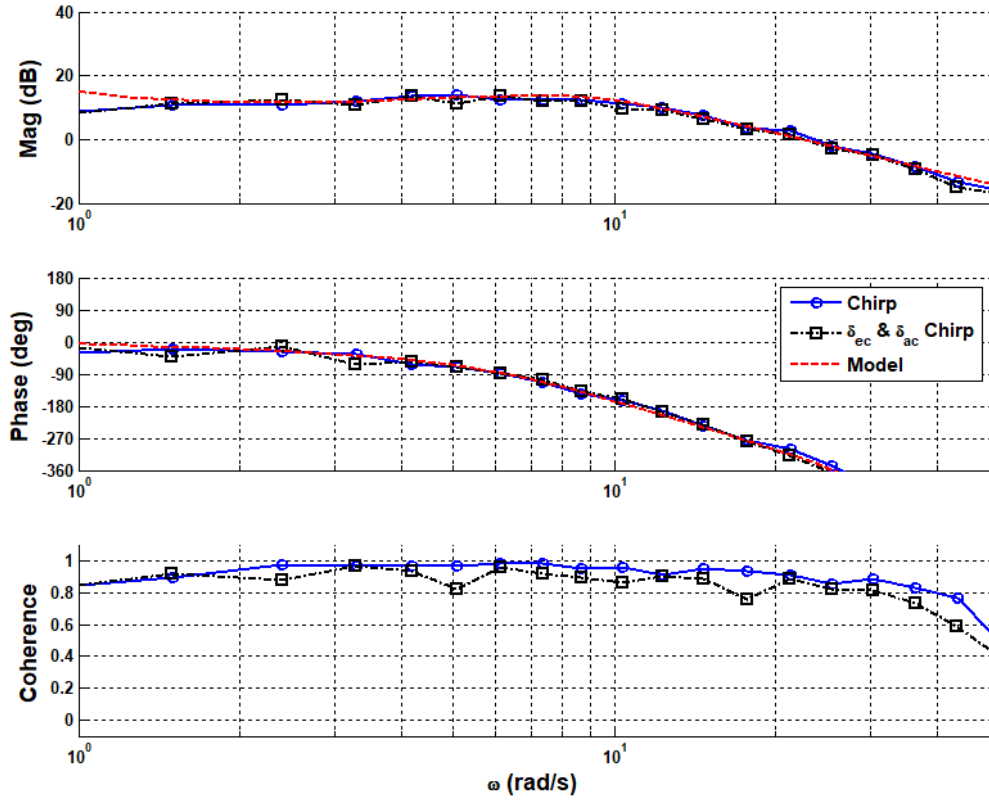


Figure 148: FLT11 - q/ δ_{ec} Identification - Frequency sweep

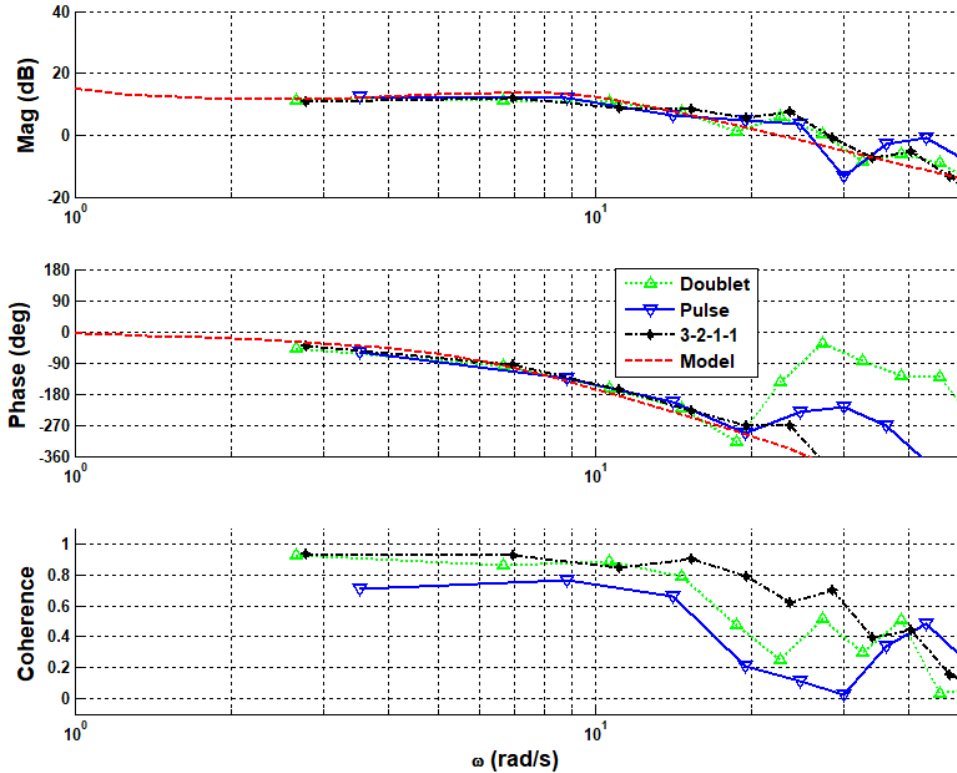


Figure 149: FLT11 - q/δ_{ac} Identification - Short Duration

2. Lateral Survey

All lateral excitations can be seen plotted with the model in Figure 150. Table 44 provides the aileron actuator model and lateral aircraft model.

Table 44: FLT 11 – Lateral Aircraft and Aileron Actuator Model

Aileron Actuator Model	Lateral Model
$\frac{\delta_a}{\delta_{ac}} = \frac{40}{s+12} e^{-0.060s}$	$\frac{p}{\delta_a} = \frac{30.27(-0.08536)[0.3335, 2.24]}{(0.05395)[0.3226, 3.066](6.956)}$

The identified lateral OMS input excitation for flight 11 can be seen in Figure 151. The magnitude and phase response of the aileron alone, elevator-aileron multi axis, and the elevator-aileron-rudder multi axis excitations closely match the model, however there is a slight mismatch with the aileron alone and this is reflected in the coherence. The coherence levels are not ideal, however the elevator-aileron multi axis input profile maintained the highest level of coherence across the frequency region shown.

The identified lateral frequency sweep input excitation for flight 11 can be seen in Figure 152 that features the aileron only input and the elevator-aileron multi axis excitation. Overall, the magnitude and phase response of both signals closely fit the model. The aileron only excitation generally has a higher coherence relative to the elevator-aileron multi axis input though both are close to 1 in the lower frequencies. In addition, the coherence rolls off starting at the 5-6 rad/s frequency levels for both input profiles.

The identified lateral short duration input excitation can be seen in Figure 153. Of the four excitations, the wider pulse input profile maintained the highest level of coherence across the frequency region shown, but all excitations had either major issues with or lacked the content to identify the lowest and highest

frequencies of interest. Due to the low coherence levels, the phase for the pulse excitation was left unwrapped.

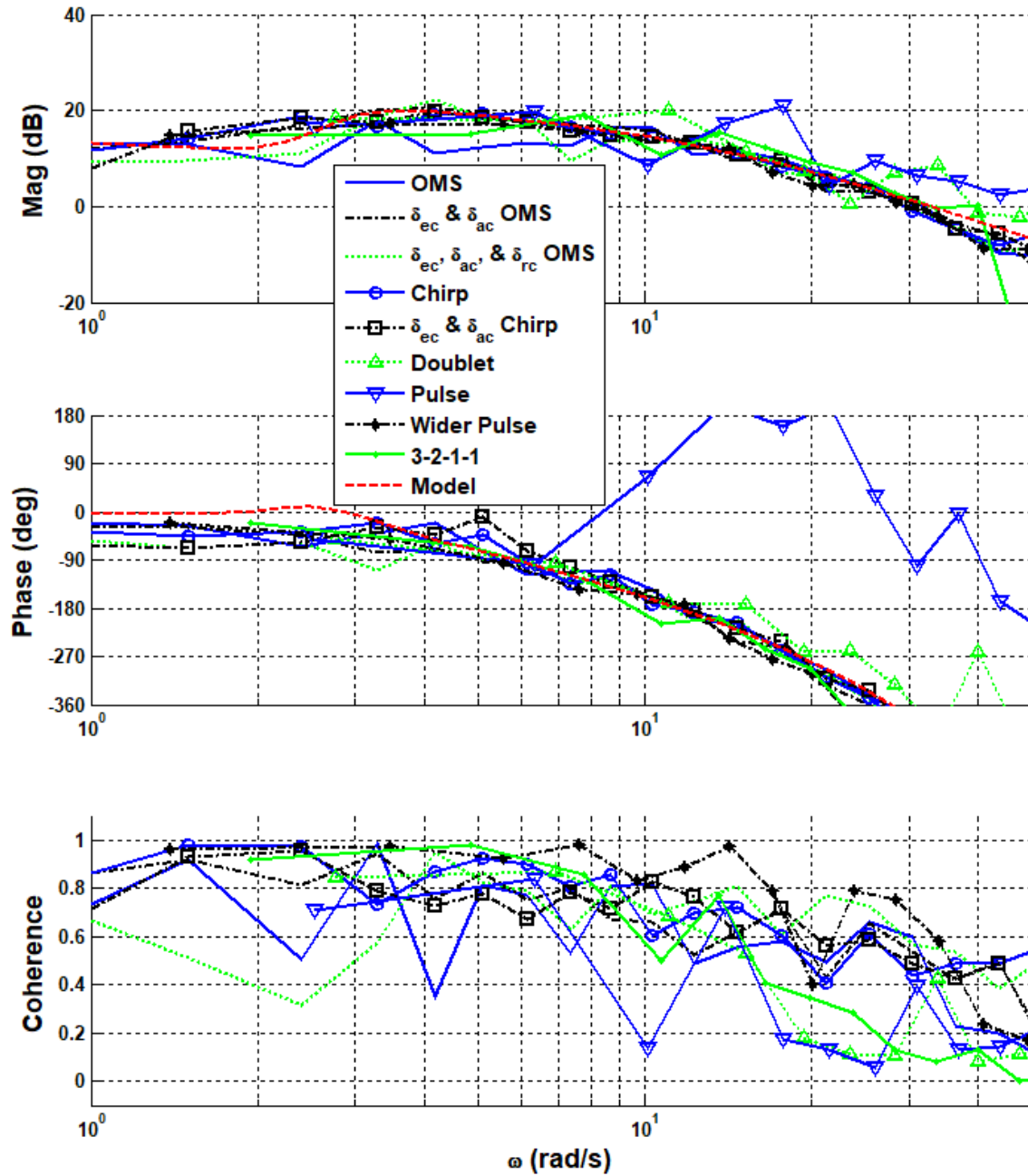


Figure 150: FLT11 - p/ δ_{ac} Identification - All Methods

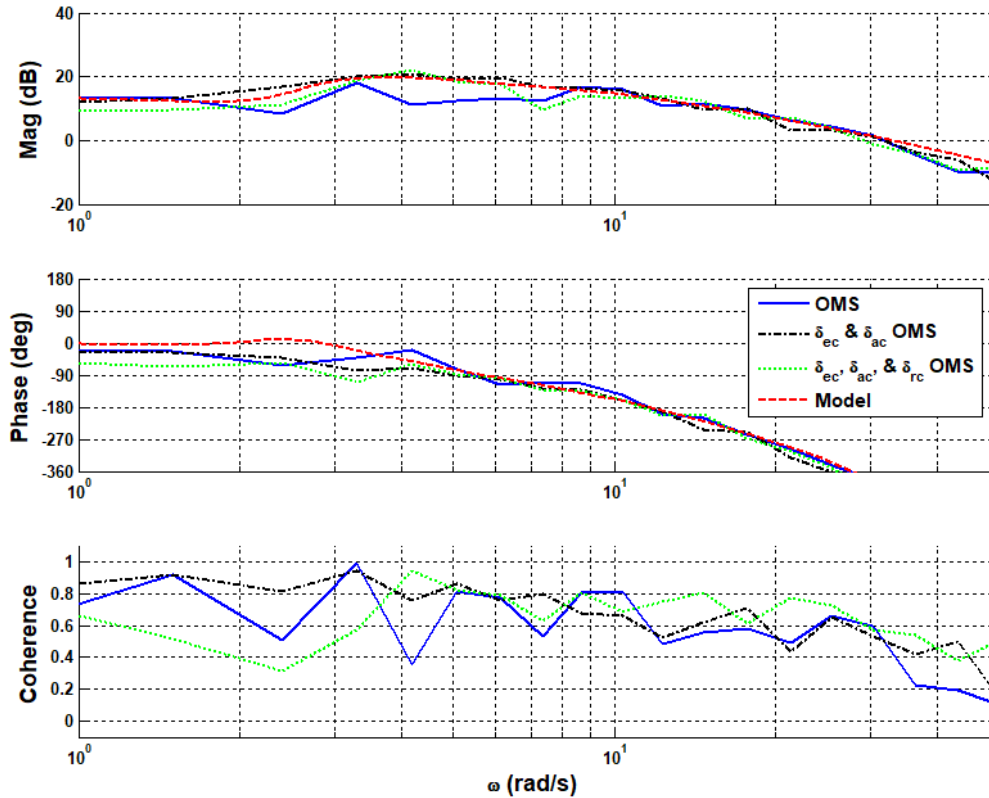


Figure 151: FLT11 - p/ δ_{ac} Identification - OMS

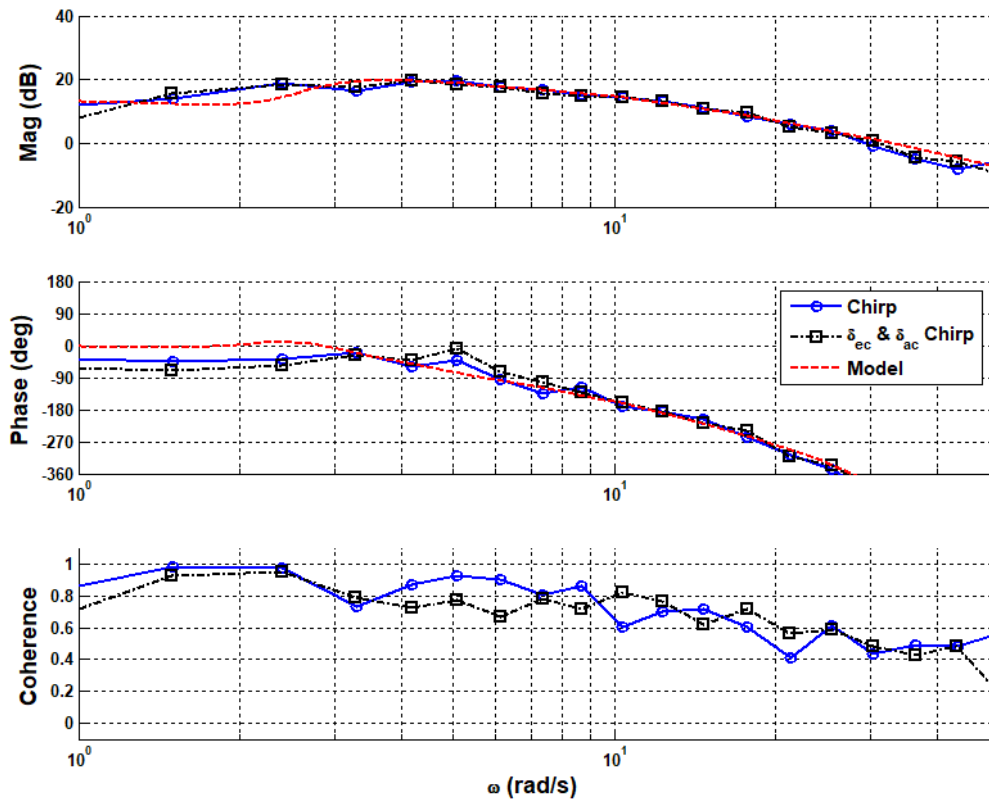


Figure 152: FLT11 - p/ δ_{ac} Identification - Frequency Sweep

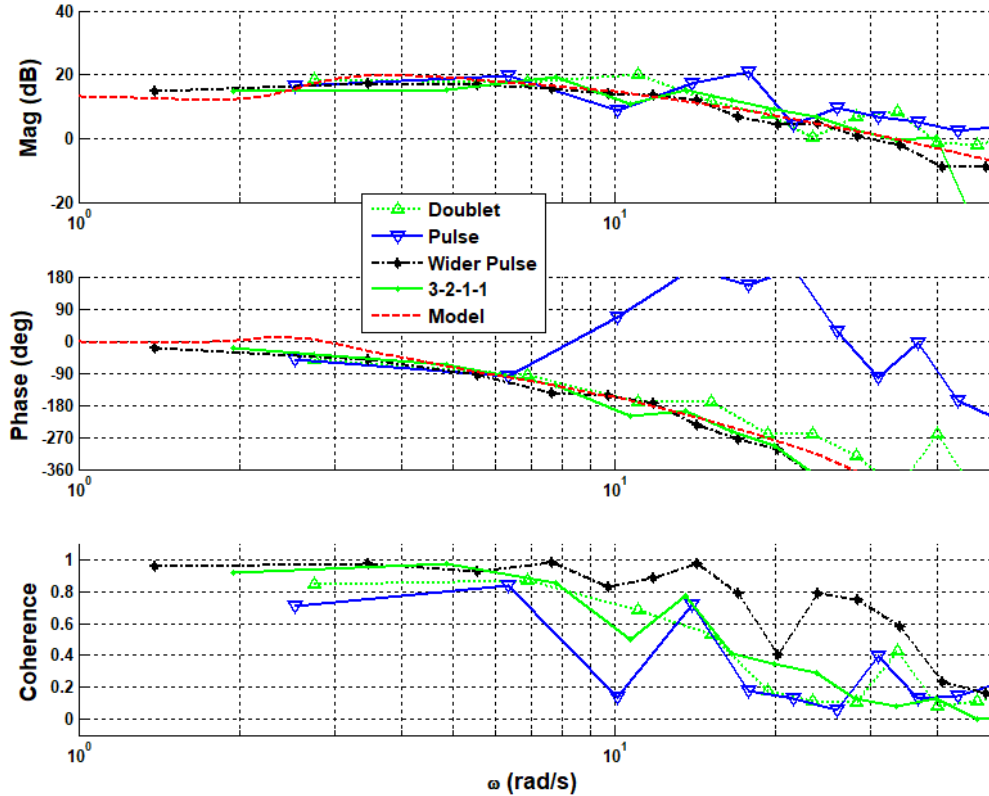


Figure 153: FLT11 - p/δ_{ac} Identification - Short Duration

3. Directional Survey

All directional excitations can be seen plotted with the model in Figure 154. Table 45 provides the rudder actuator model and directional aircraft model.

Table 45: FLT 11 - Directional Aircraft and Rudder Actuator Model

Rudder Actuator Model	Directional Model
$\frac{\delta_r}{\delta_{rc}} = \frac{10}{s+10} e^{-0.065s}$	$\frac{r}{\delta_r} = \frac{3.754[0.2292, 1.387](6.949)}{(0.05395)[0.3226, 3.066](6.956)}$

The identified directional OMS input excitation for flight 11 can be seen in Figure 155. The magnitude and phase response of the rudder alone and the elevator-aileron-rudder multi axis closely match each other and the model at frequencies above 5 rad/s. At the lower frequencies the coherence tended to be less than 0.8. The coherence rolls off at the ~10 rad/s frequency.

The identified directional frequency sweep input excitation for flight 11 can be seen in Figure 156, which features the rudder only input. Overall, the magnitude and phase response of the excitation matches the model above ~2-3 rad/s. The lowest and highest frequency regions have coherence levels below 0.8 and the identified fits reflect that.

The identified directional short duration input excitation can be seen in Figure 157. Of the four excitations, the doublet input profile maintained the highest level of coherence across the frequency region shown, but all excitations either had low coherence or lacked the frequency content to identify the lowest and highest frequencies of interest. Due to the low coherence levels, the phase for the 3-2-1-1 excitation was left unwrapped.

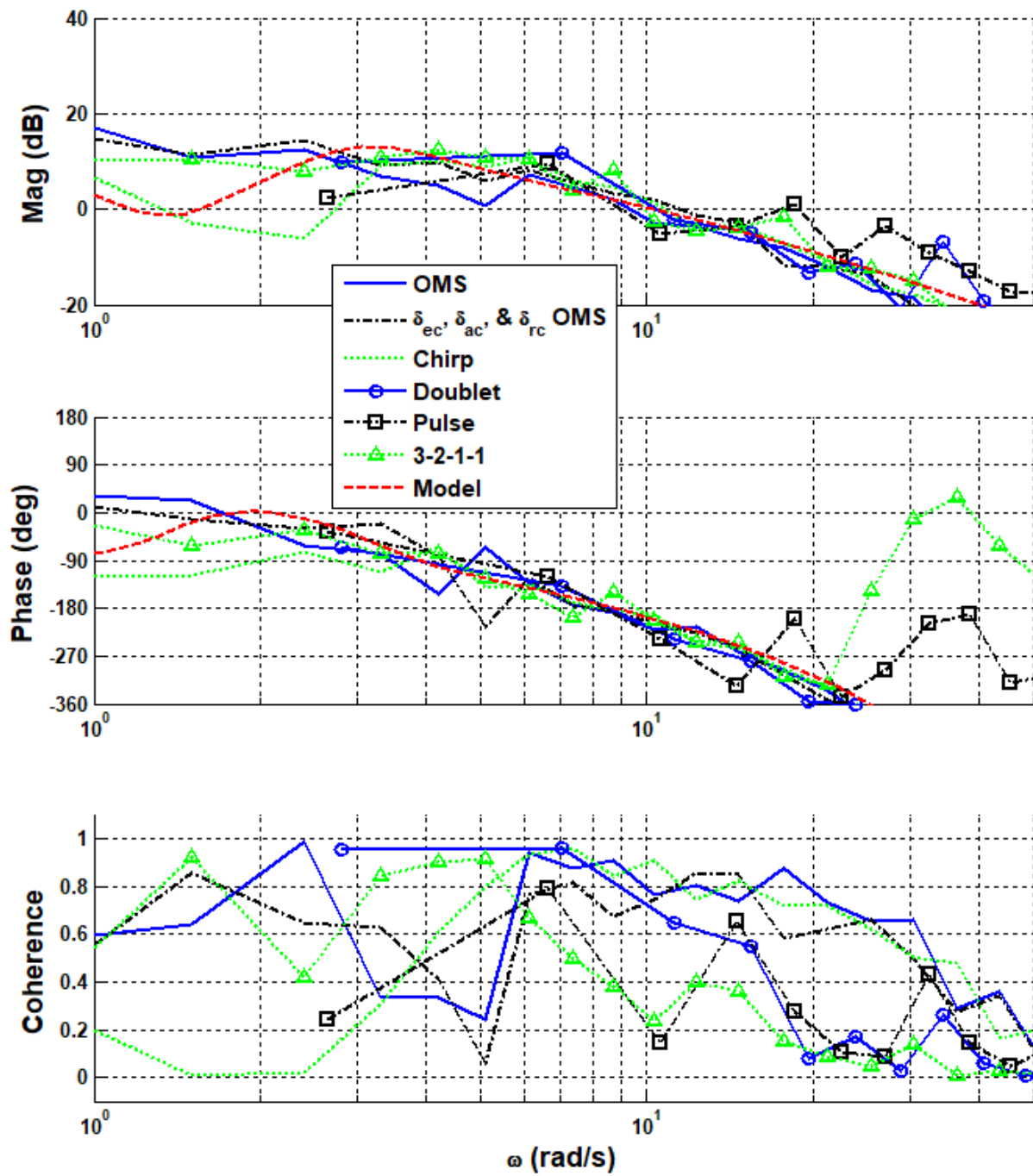


Figure 154: FLT11 - r/ δ_{rc} Identification - All Methods

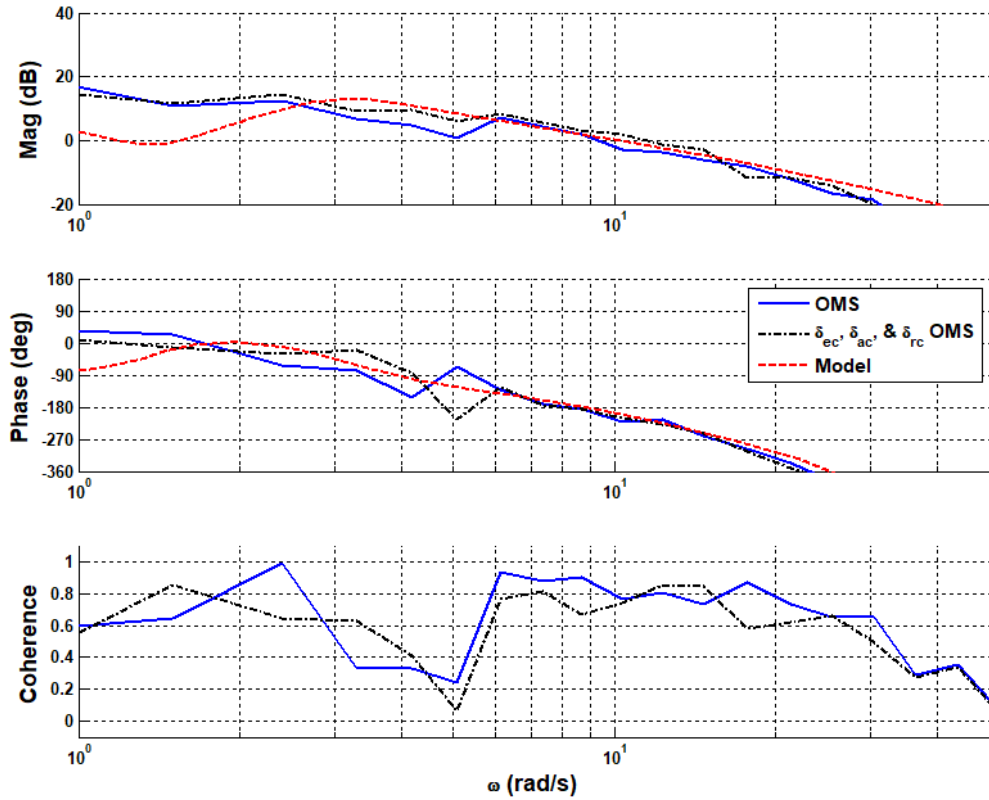


Figure 155: FLT11 - r/δ_{rc} Identification - OMS

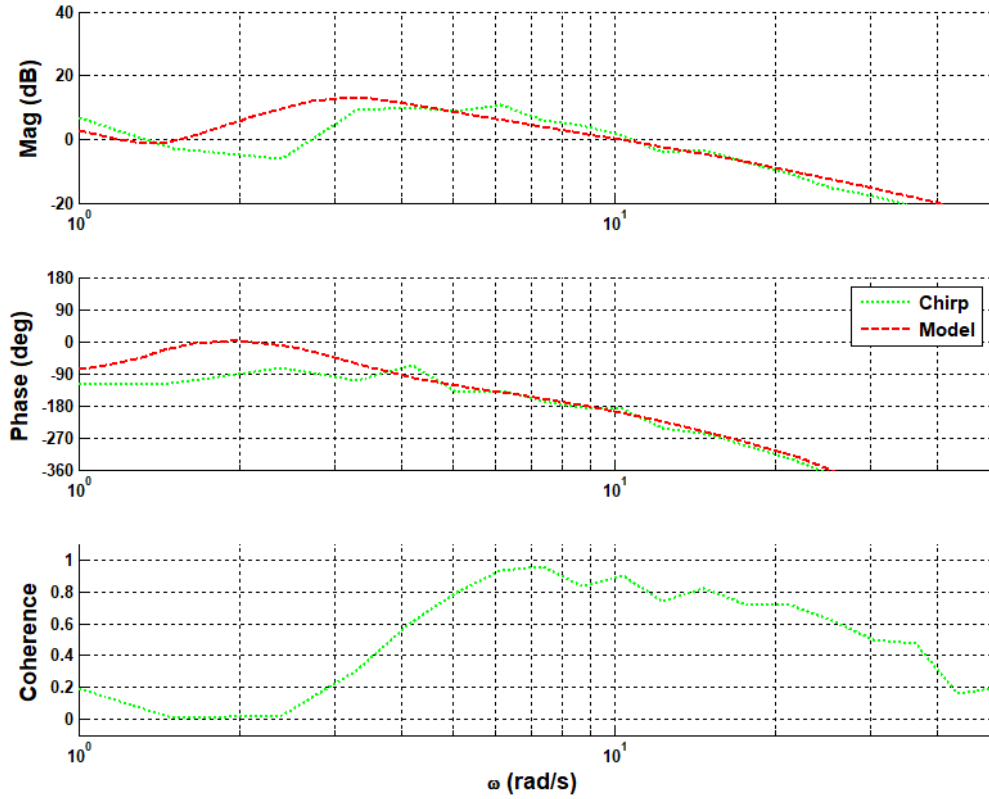


Figure 156: FLT11 - r/δ_{rc} Identification - Frequency sweep

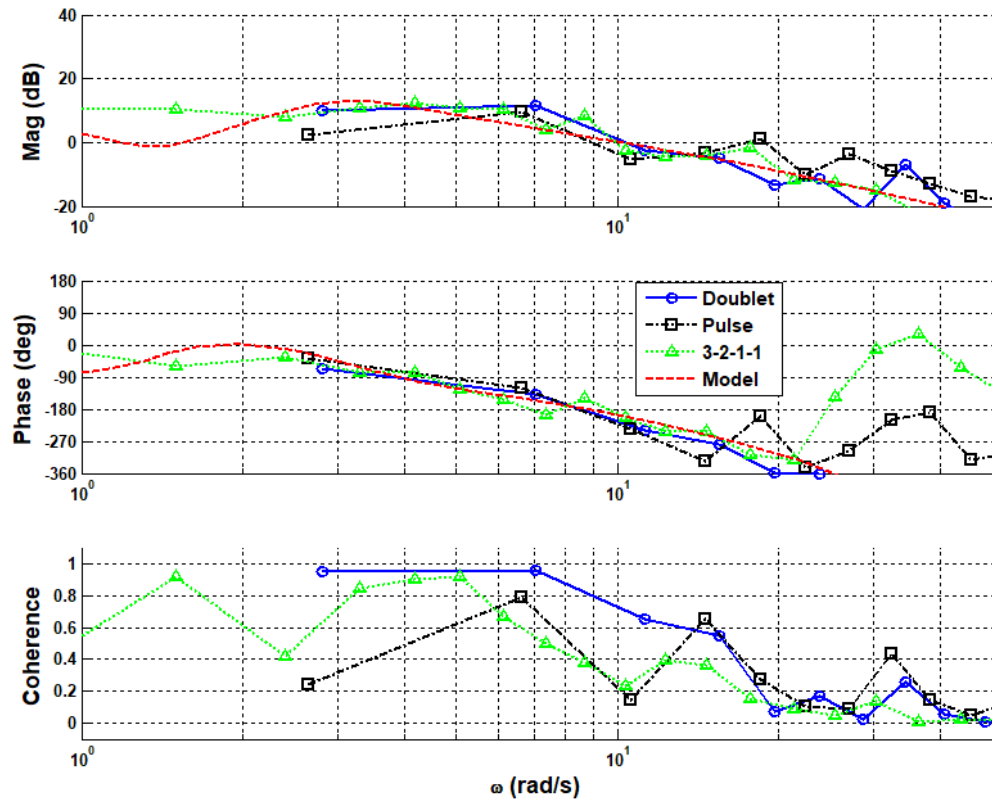


Figure 157: FLT11 - r/δ_{rc} Identification - Short Duration

H. SHORT DURATION MODEL RESPONSE EVALUATION

The following figures in this section demonstrate the response of the previously identified model with a frequency sweep input against short duration inputs. For flights 03 and 04, the test input profiles for the longitudinal and directional axes were doublets, pulses, and 3-2-1-1 pulse sets. The lateral test input profiles were the same as the other two axes, however, there was an additional wider pulse input as well. These test input profiles are described in detail in section 3. Section 5.3 shows some of the short duration off-nominal model responses for select flight conditions and test excitation inputs.

1. Flight 03

Flight 03 was flown at cruise condition, straight and level flight with computer generated inputs. This flight is the baseline configuration. The identified model was simulated with initial conditions set to zero.

a. Longitudinal Survey

The short duration responses for the longitudinal axis can be seen in Figure 158, Figure 159, and Figure 160. The model response for the doublet excitation exhibited a close match to the excitation flight data. The pulse and 3-2-1-1 excitation response demonstrated a good model fit, however there is a modest amount of amplitude mismatch. This mismatch, which occurs for the lower frequency inputs, is likely due to system nonlinearities such as actuator free play. There are two sets of data drop outs from ~7-11 seconds and ~12-15 seconds region that impacted the second doublet maneuver.

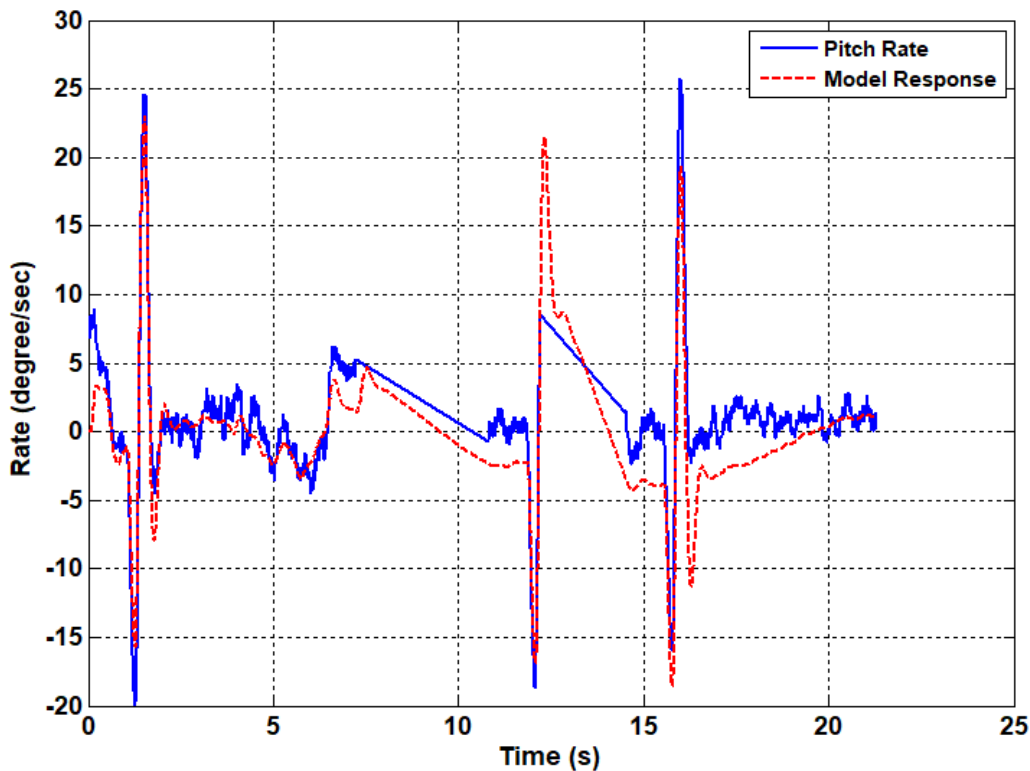


Figure 158: FLT03 - Doublet Response

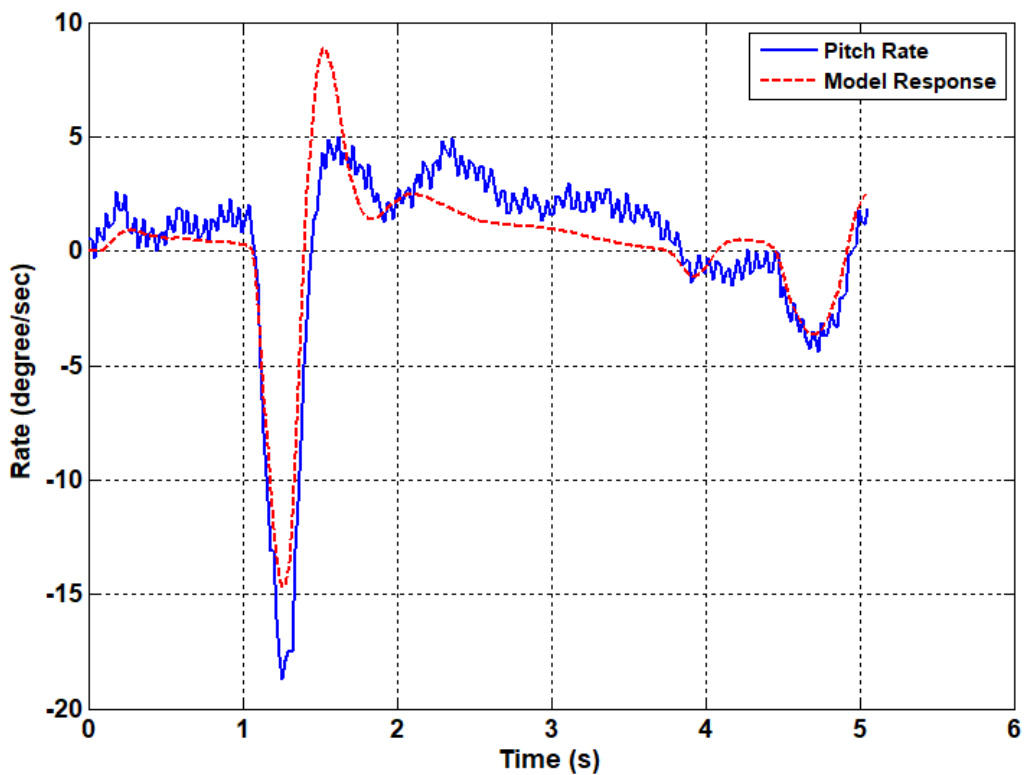


Figure 159: FLT03 - Pulse Response

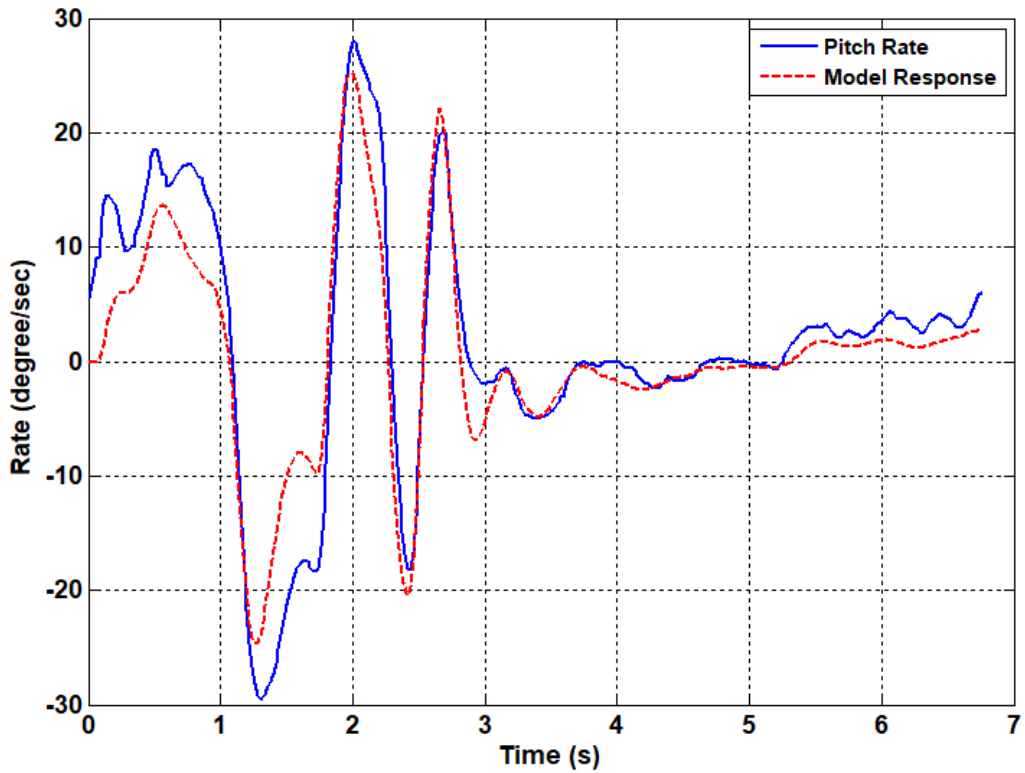


Figure 160: FLT03 - 3-2-1-1 Response

b. Lateral Survey

The short duration responses for the lateral axis can be seen in Figure 161, Figure 162, Figure 163, and Figure 164. The model response for the doublet, wider pulse, and 3-2-1-1 test input excitations exhibited a close match to the excitation flight data with the wider pulse response being the best. However, there is a considerable amount of amplitude offset demonstrated in all model responses except for the wider pulse response. There is one set of data drop out from the ~6-9 seconds region in the doublet maneuver flight data. The wider pulse response also exhibits a minor time delay.

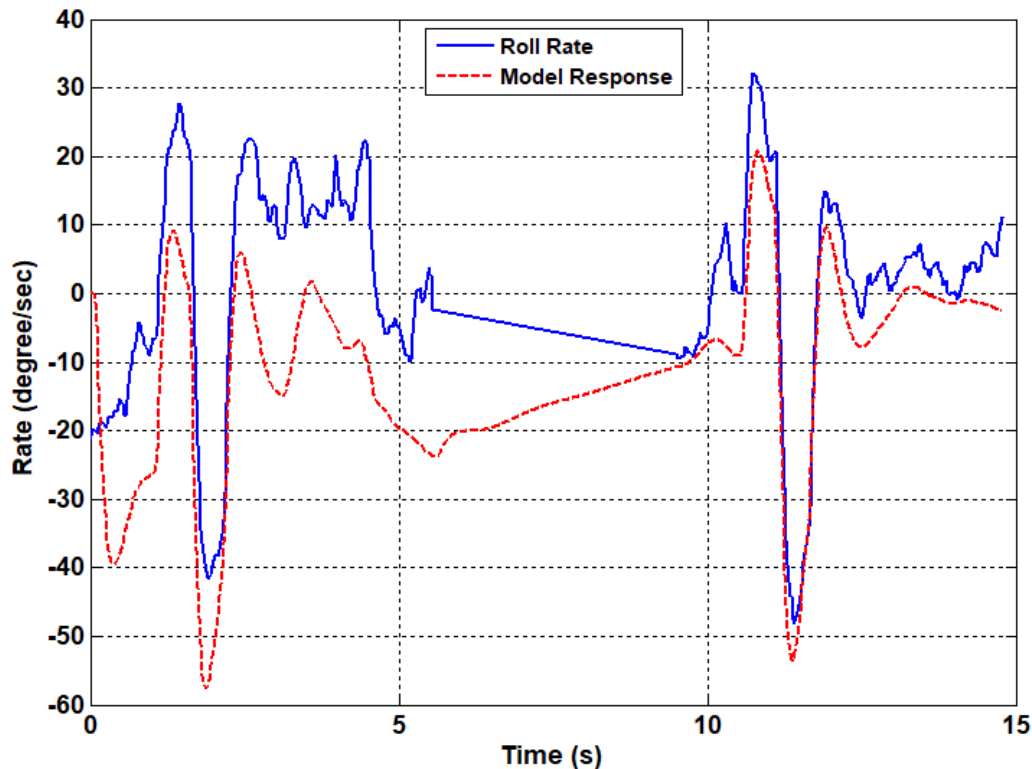


Figure 161: FLT03 - Doublet Response

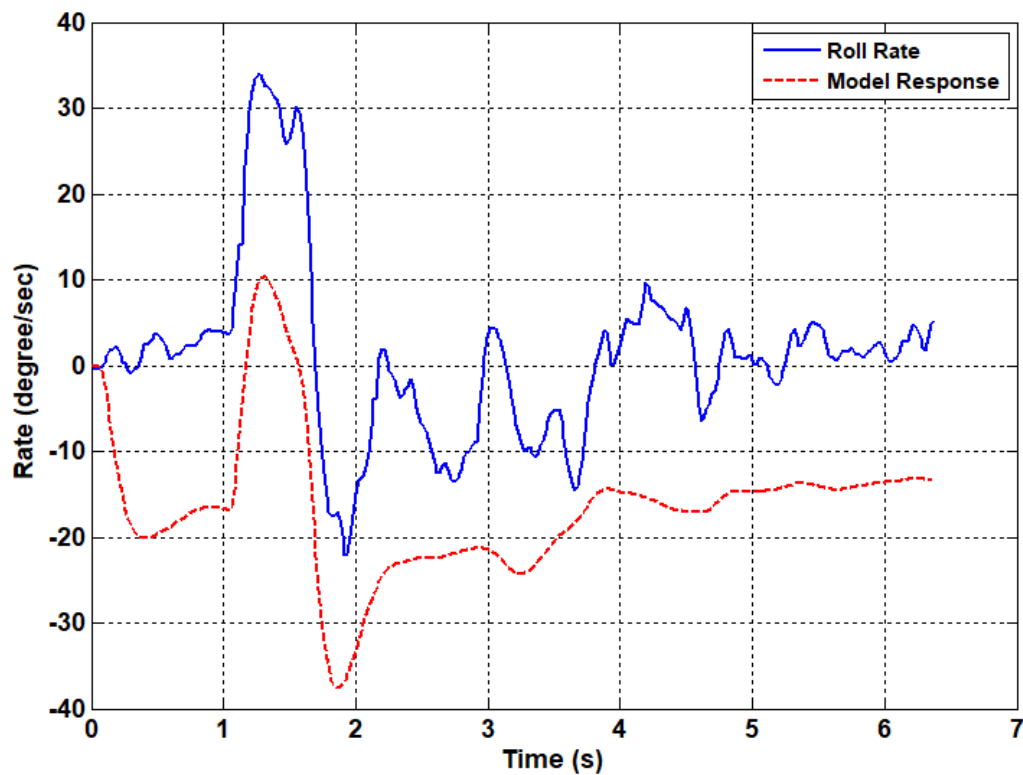


Figure 162: FLT03 - Pulse Response

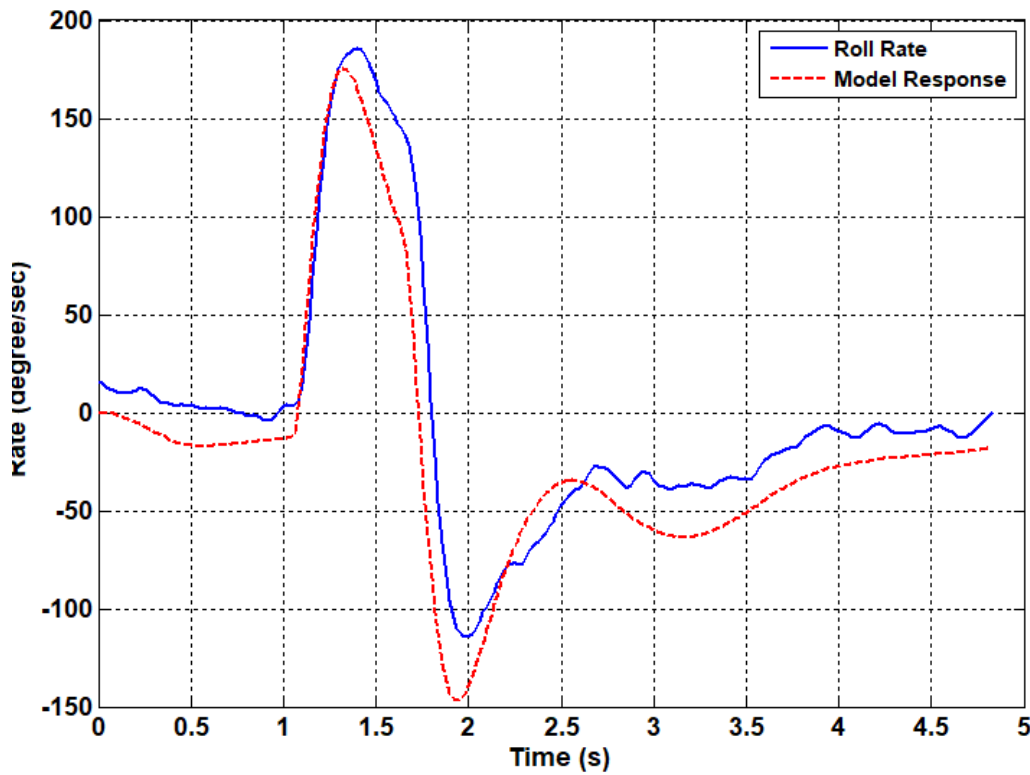


Figure 163: FLT03 - Wider Pulse Response

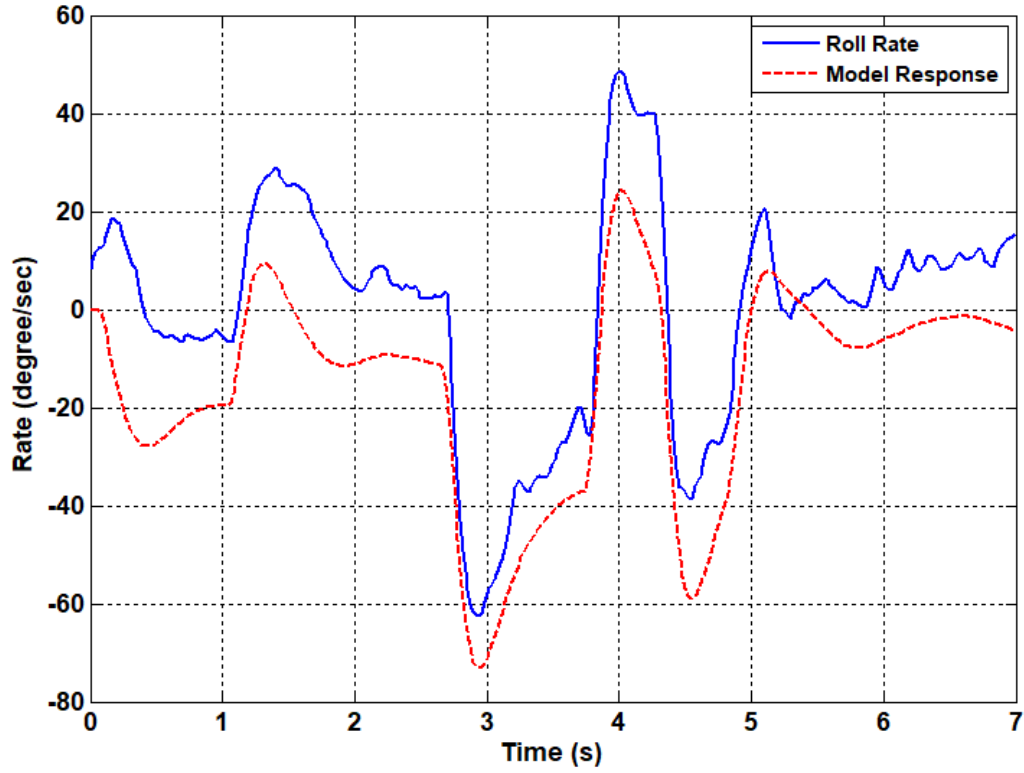


Figure 164: FLT03 - 3-2-1-1 Response

c. Directional Survey

The short duration responses for the directional axis can be seen in Figure 165, Figure 166, and Figure 167. The model response for all test input excitations exhibited a close match to the excitation flight data with the doublet response being the best. However, there is a moderate amount of amplitude offset demonstrated in all model responses.

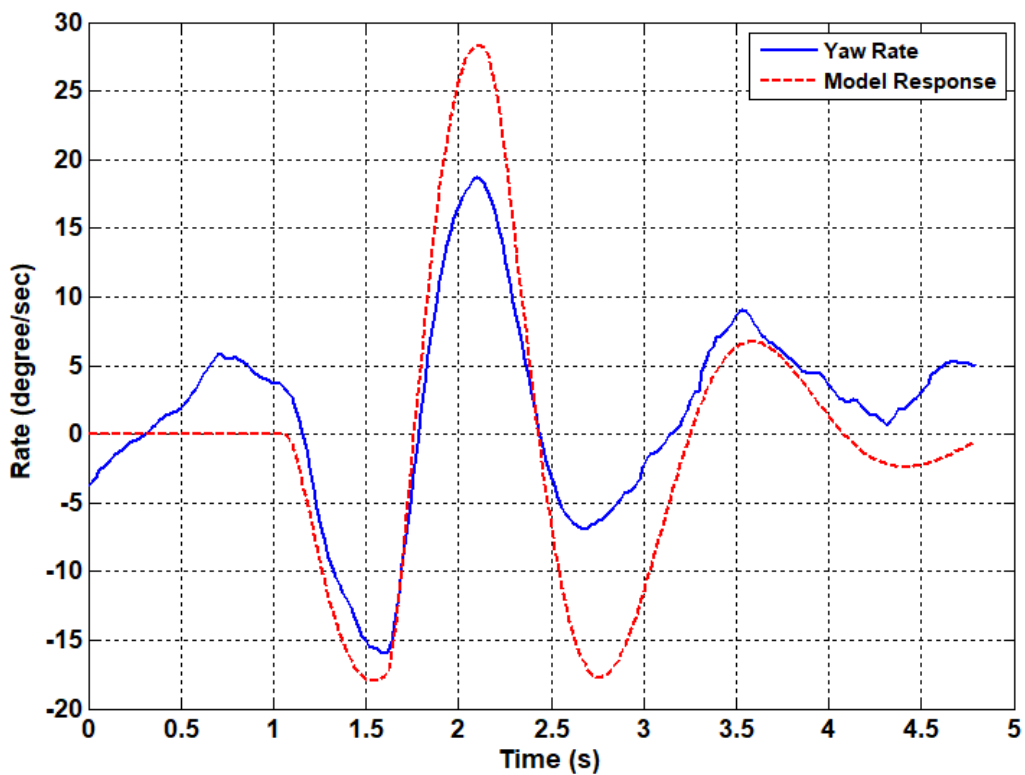


Figure 165: FLT03 - Doublet Response

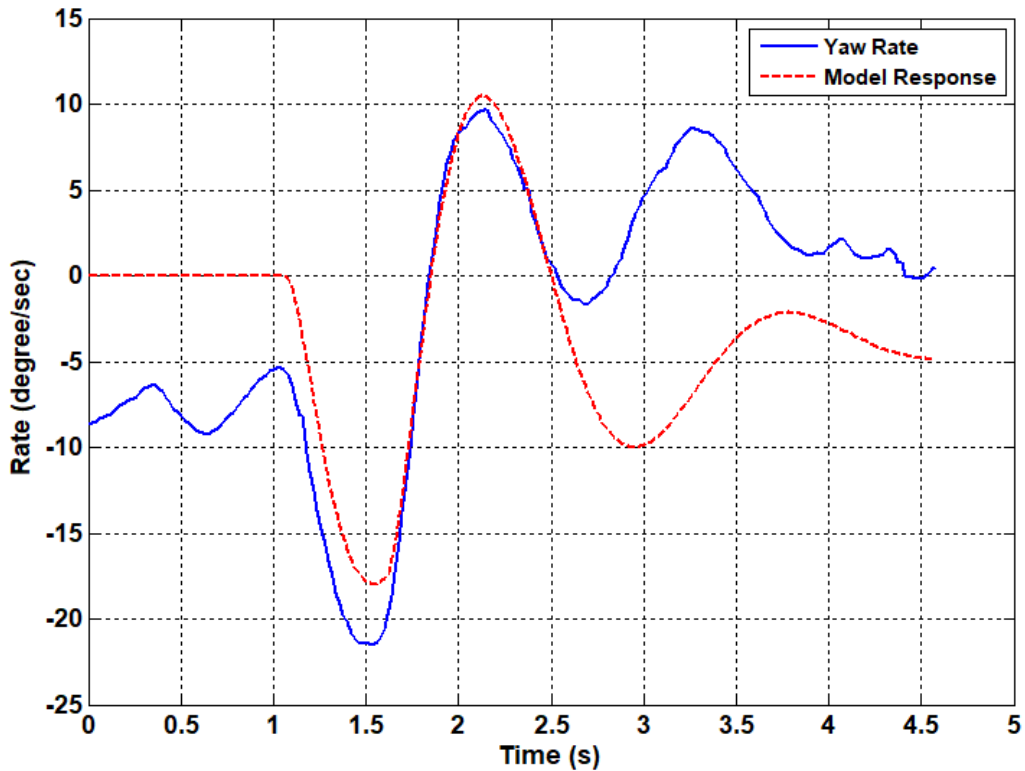


Figure 166: FLT03 - Pulse Response

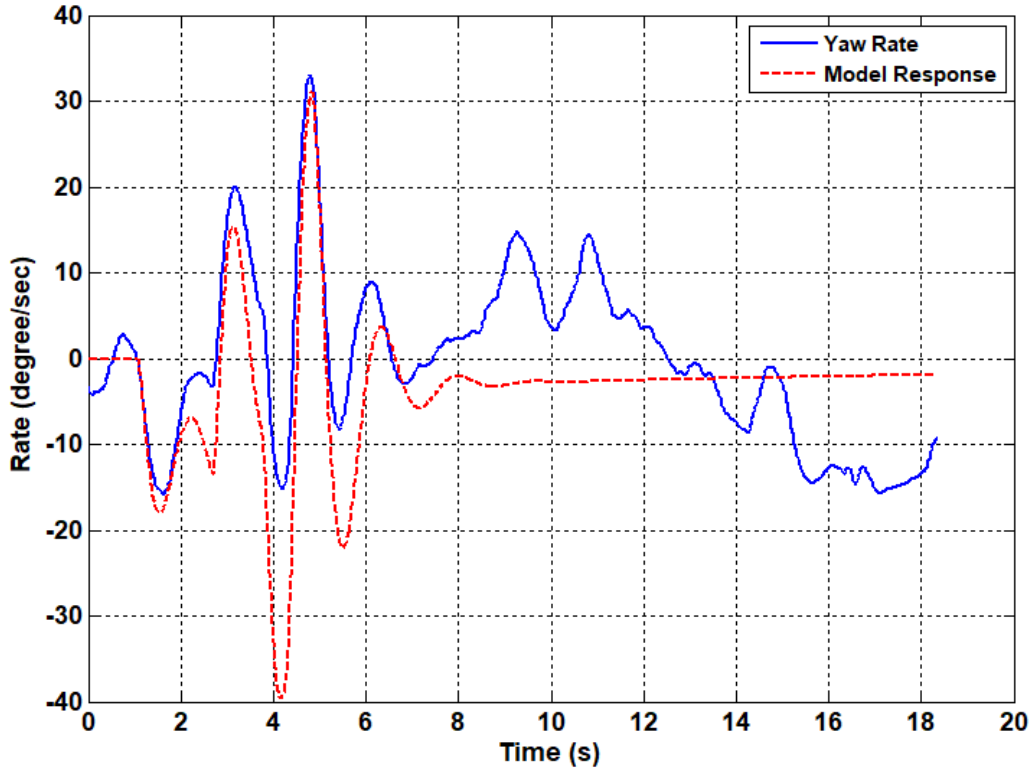


Figure 167: FLT03 - 3-2-1-1 Response

2. **FLT 04**

Flight 04 was flown at the approach condition, essentially a lower airspeed cruise (17m/s) with flaps at 50%. The identified model was simulated with initial conditions set to zero.

a. **Longitudinal Survey**

The short duration responses for the lateral axis can be seen in Figure 168, Figure 169, and Figure 170. The model response for all test input excitations exhibited a close match to the excitation flight data with the last doublet response being the best. There is a moderate amount of amplitude offset demonstrated in all model responses except for the last doublet and pulse excitation responses and the first 3-2-1-1 excitation response. The doublet and pulse maneuver flight data both exhibit one set of data drop out from the ~4-6 seconds and ~7-18 seconds region, respectively.

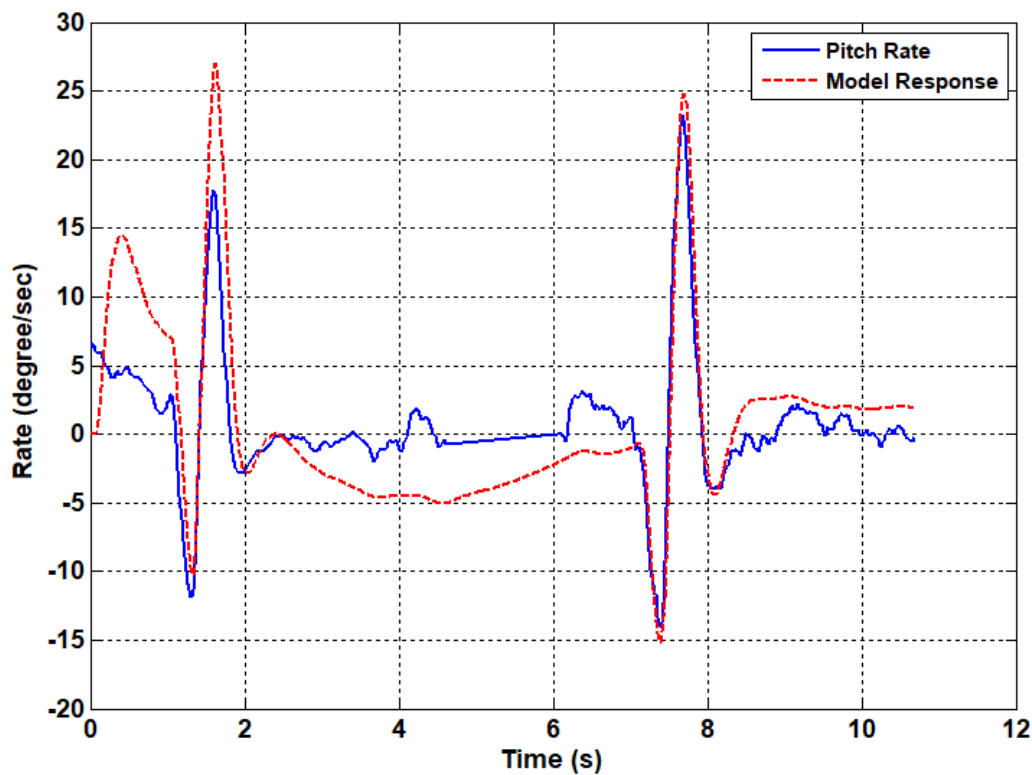


Figure 168: FLT04 - Doublet Response

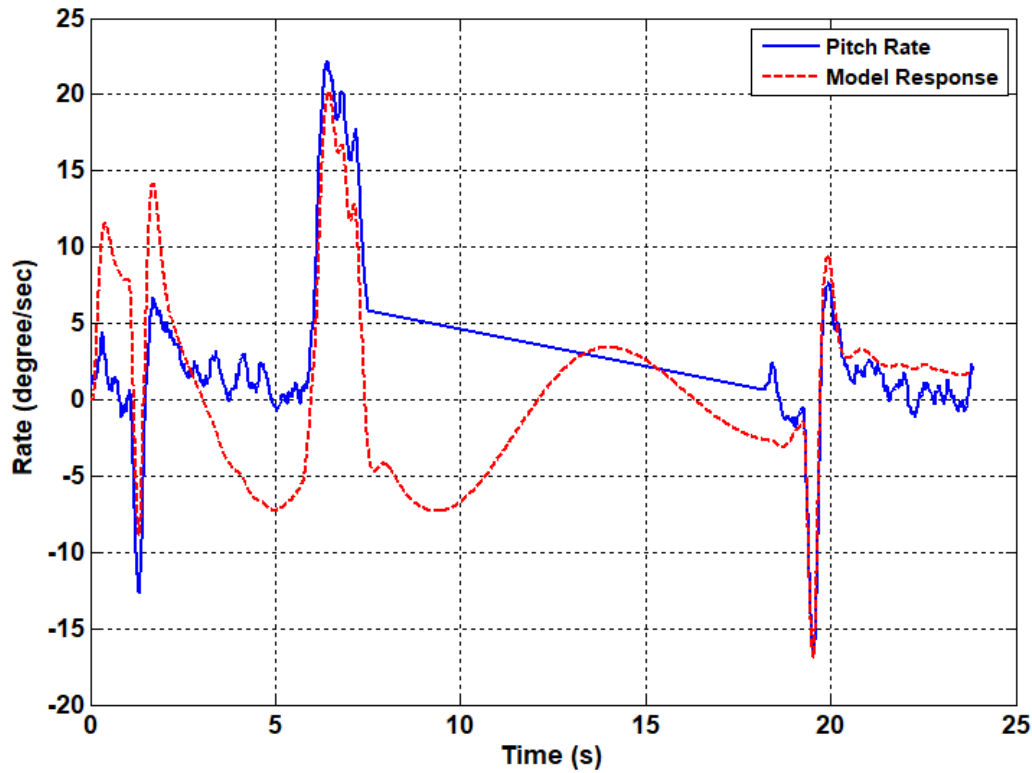


Figure 169: FLT04 - Pulse Response

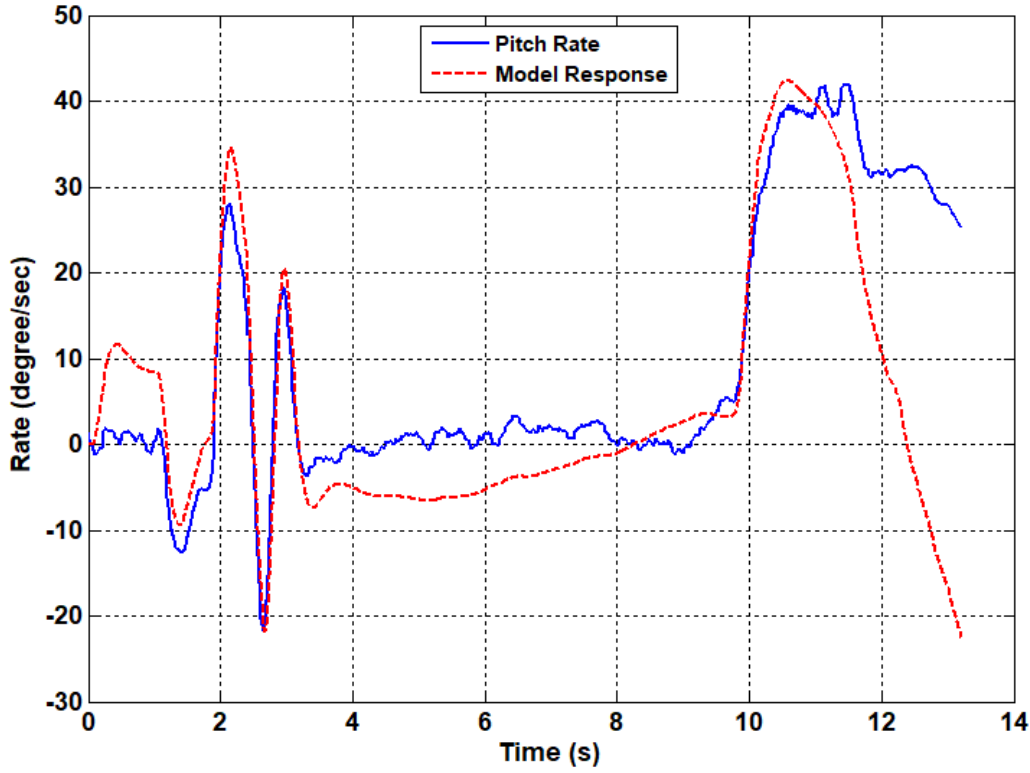


Figure 170: FLT04 - 3-2-1-1 Response

b. Lateral Survey

The short duration responses for the lateral axis can be seen in Figure 171, Figure 172, Figure 173, and Figure 174. The model response for the doublet and 3-2-1-1 test input excitations exhibited a close match to the excitation flight data. The model response for the pulse somewhat matches the test input excitation and there is some resemblance of a model response fit for the wider pulse test input excitation. There is a moderate amount of amplitude offset demonstrated in all model responses. The wider pulse maneuver flight data exhibits two sets of data drop out from the ~9-12 seconds and ~16-31 seconds region.

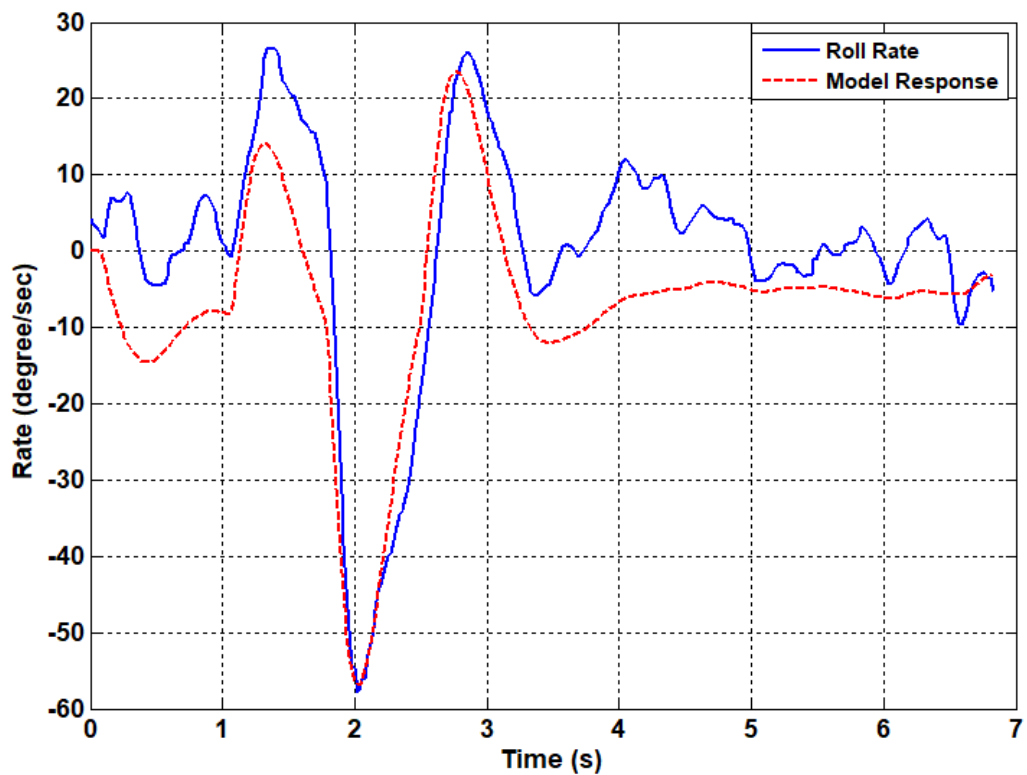


Figure 171: FLT04 - Doublet Response

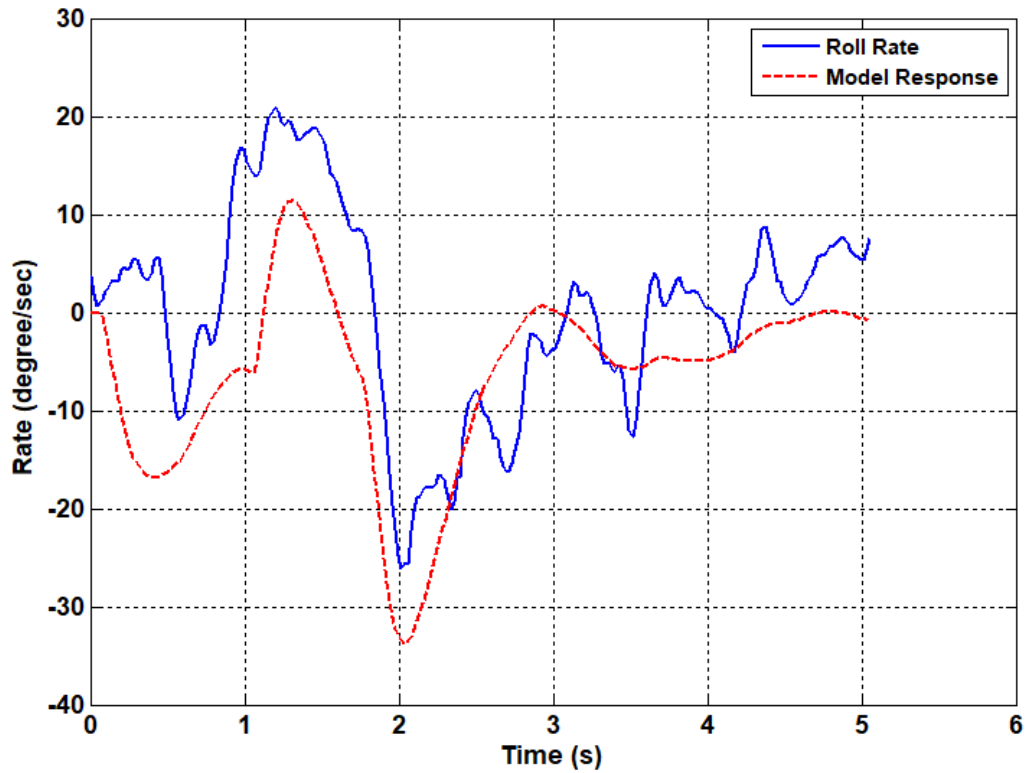


Figure 172: FLT04 - Pulse Response

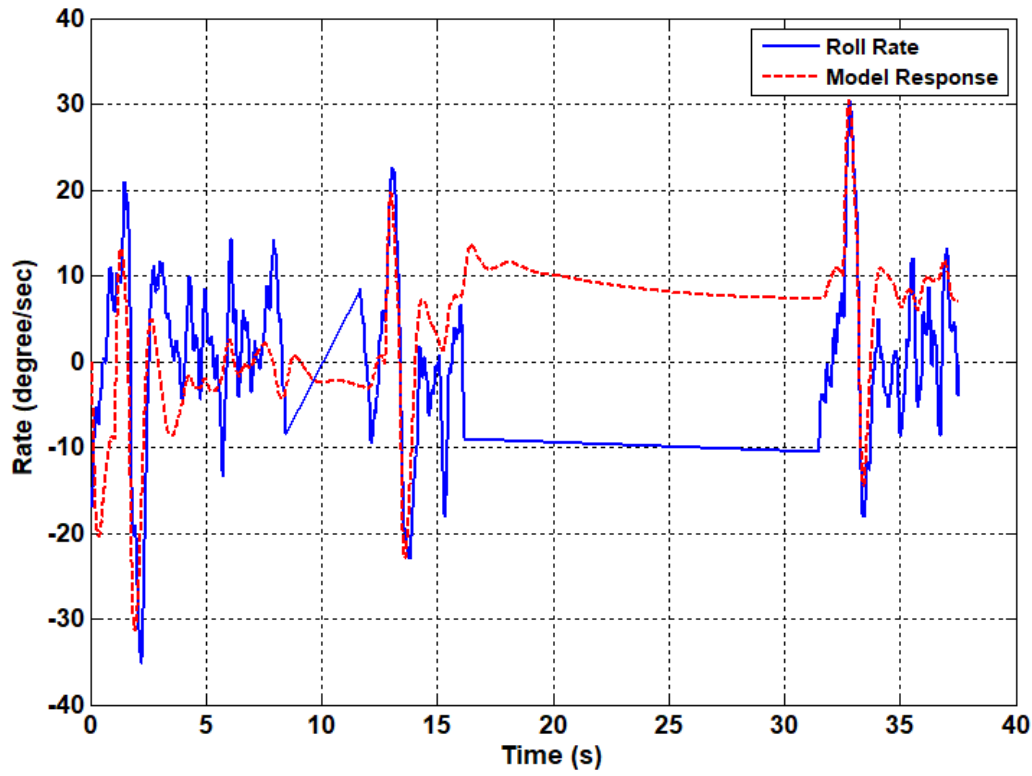


Figure 173: FLT04 - Wider Pulse Response

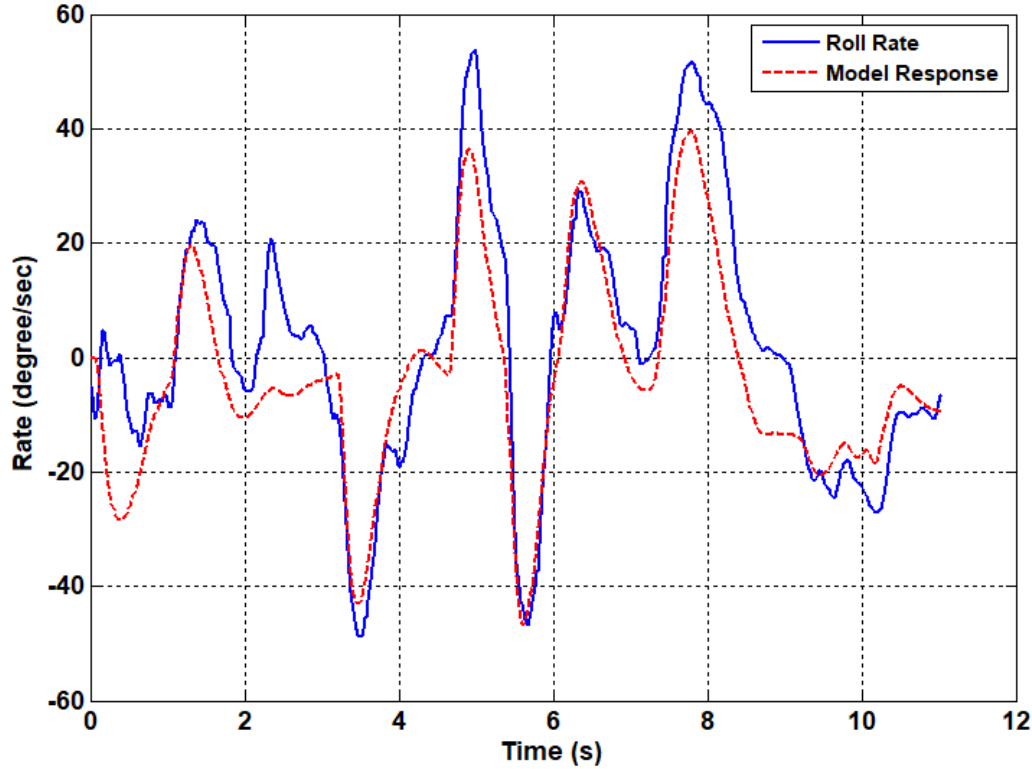


Figure 174: FLT04 - 3-2-1-1 Response

c. Directional Survey

The short duration responses for the directional axis can be seen in Figure 175, Figure 176, and Figure 177. The model response for all test input excitations exhibited a close match to the excitation flight data. There is a moderate amount of amplitude offset demonstrated in the doublet and 3-2-1-1 model responses, however, the pulse model response shows a larger amplitude offset. All model responses exhibit a time delay.

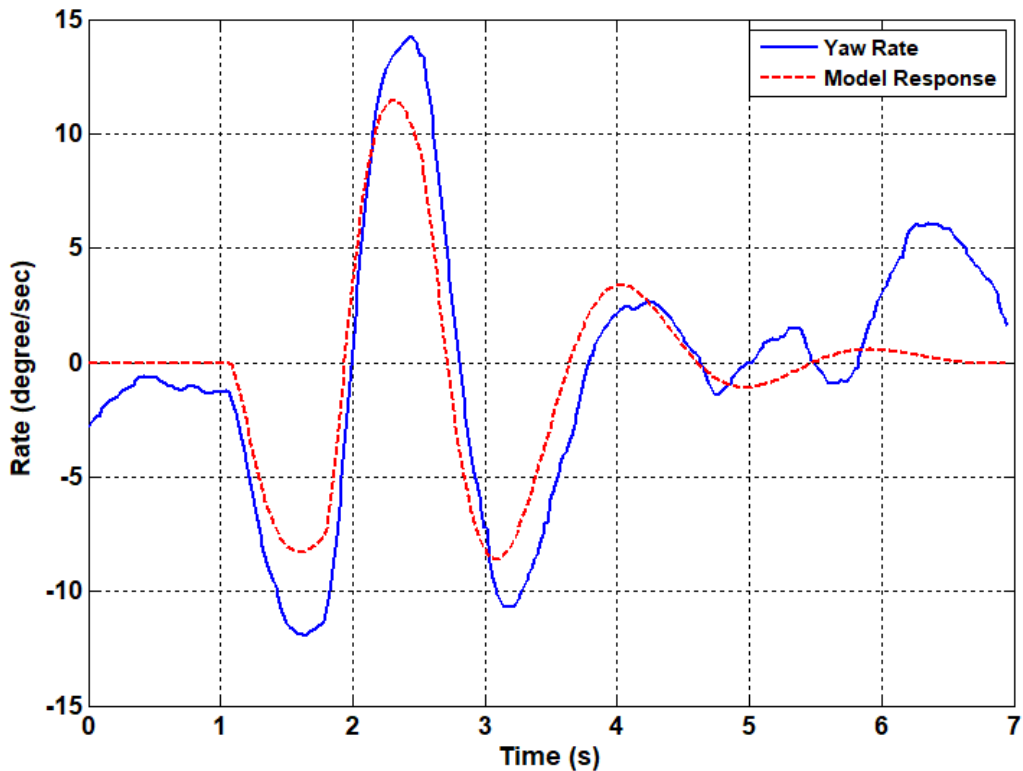


Figure 175: FLT04 - Doublet Response

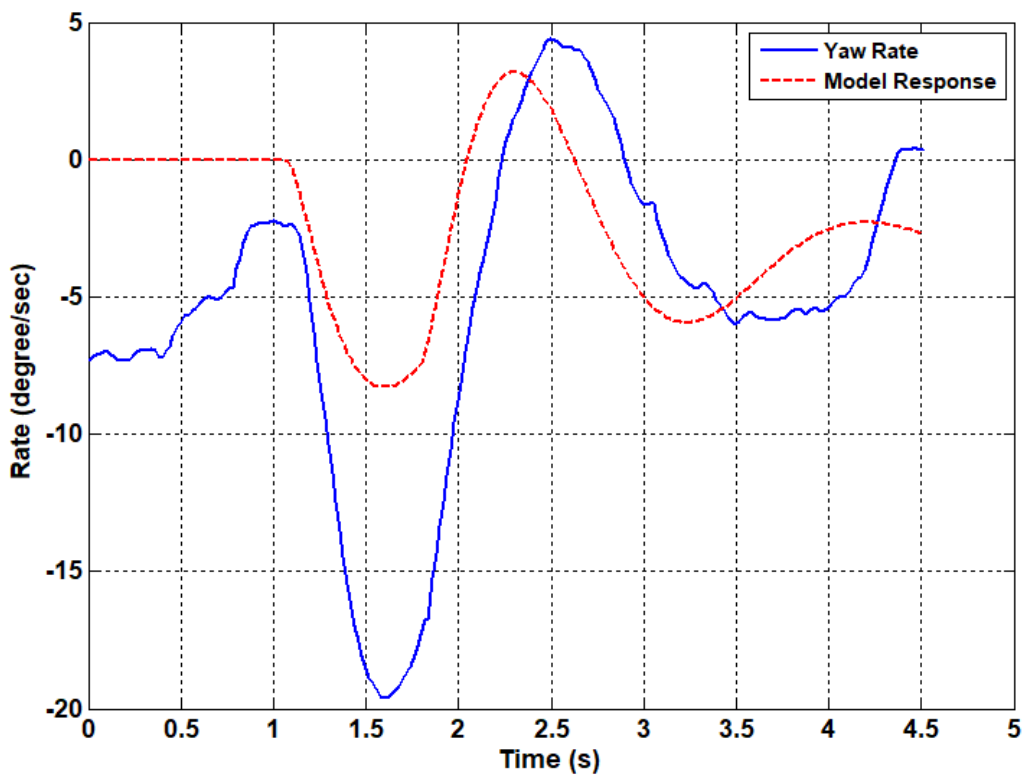


Figure 176: FLT04 - Pulse Response

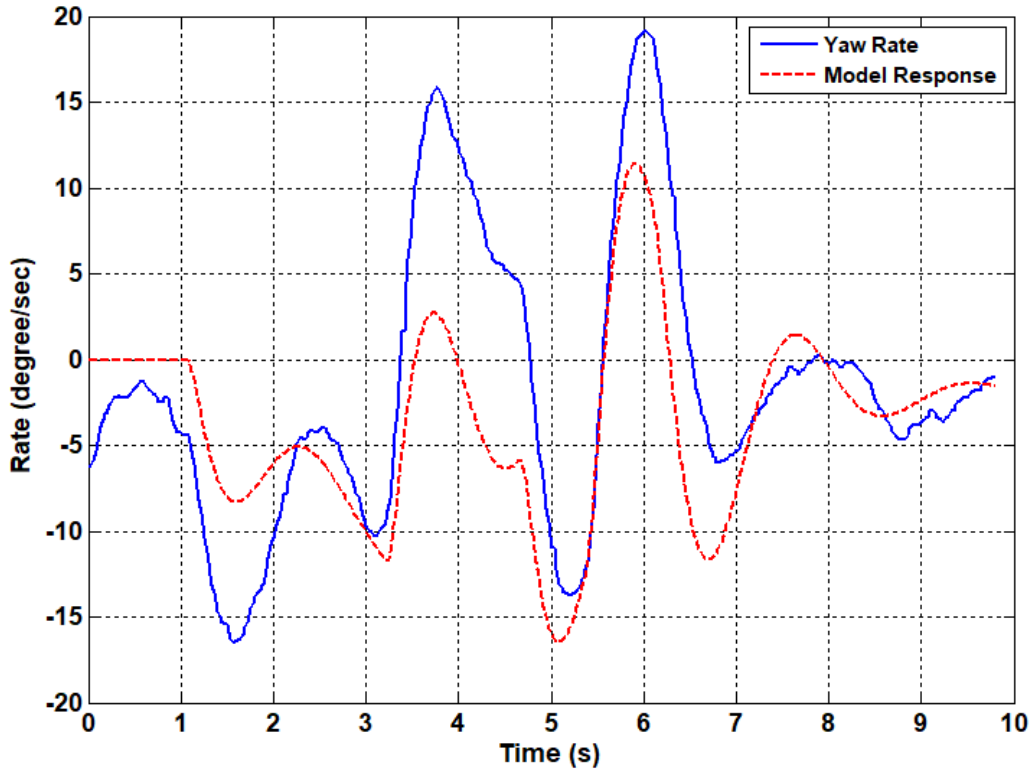


Figure 177: FLT04 - 3-2-1-1 Response

3. Select Model Responses

a. FLT 05: Aft CG Longitudinal Survey

Flight 05 was flown at cruise condition, but with weight added to the aft portion of the vehicle, to move the CG back and to create an off-nominal case.

The doublet excitation model response for MOI method 1 and 2 are shown in Figure 178 and Figure 181, respectively. The model response for both MOI methods exhibited a very close match to the excitation flight data. The only difference between the two models is the minor existence of an amplitude offset demonstrated in the MOI method 2 model response. The maneuver flight data exhibits one set of data drop out from the ~7-9 seconds region.

The pulse excitation model response for MOI method 1 and 2 in Figure 179 and Figure 182, respectively. The model response for both MOI methods exhibited a close match to the excitation flight data. Both models exhibit a minor amount of amplitude offset. The maneuver flight data exhibits one set of data drop out from the ~5-13 seconds region.

The 3-2-1-1 excitation model response for MOI method 1 and 2 in Figure 180 and Figure 183, respectively. The model response for both MOI methods exhibited a close match to the excitation flight data. Both models exhibit a minor amount of amplitude offset and a small time delay.

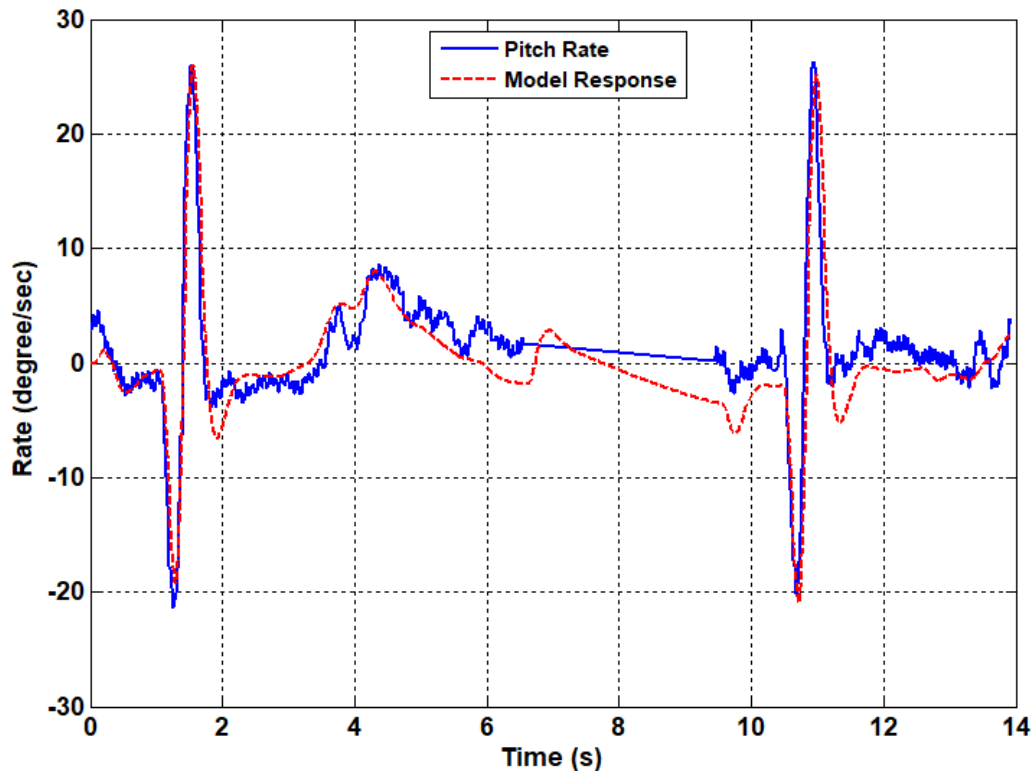


Figure 178: FLT05-MOI Method 1 - Doublet Response

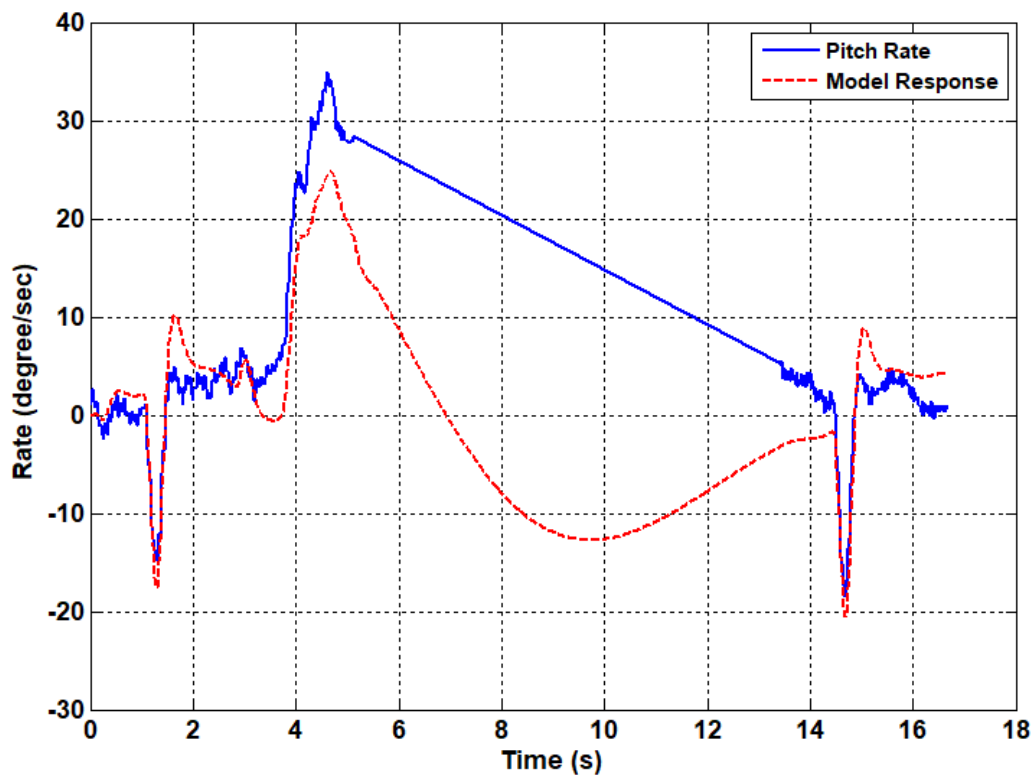


Figure 179: FLT05-MOI Method 1 - Pulse Response

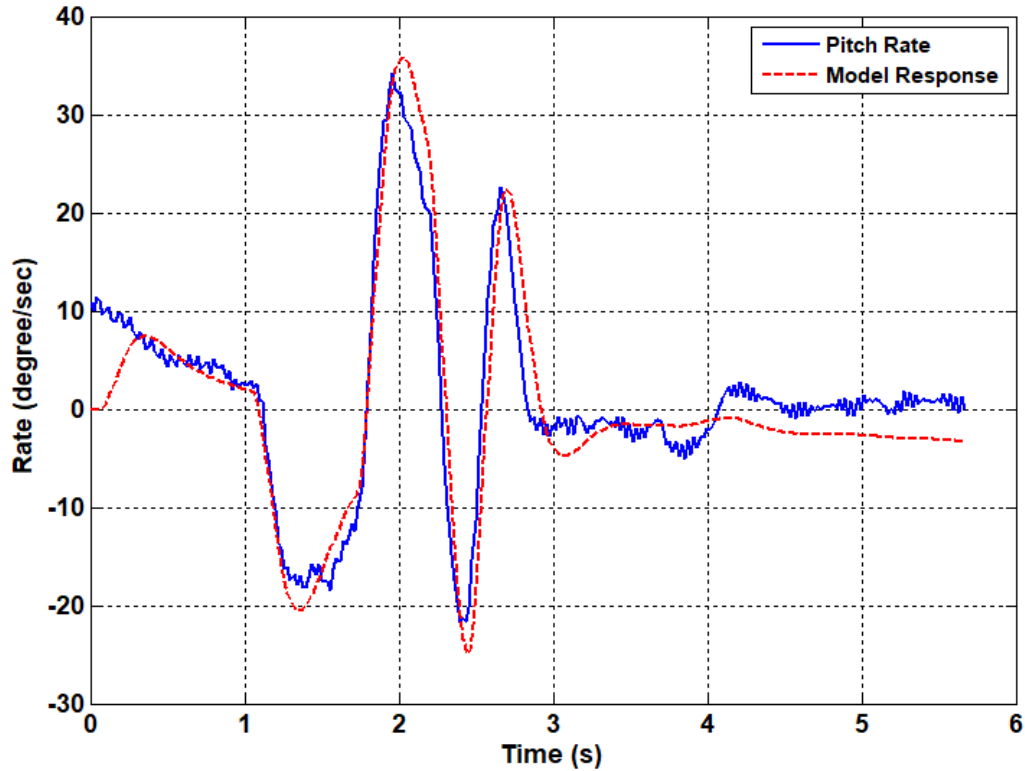


Figure 180: FLT05-MOI Method 1 - 3-2-1-1 Response

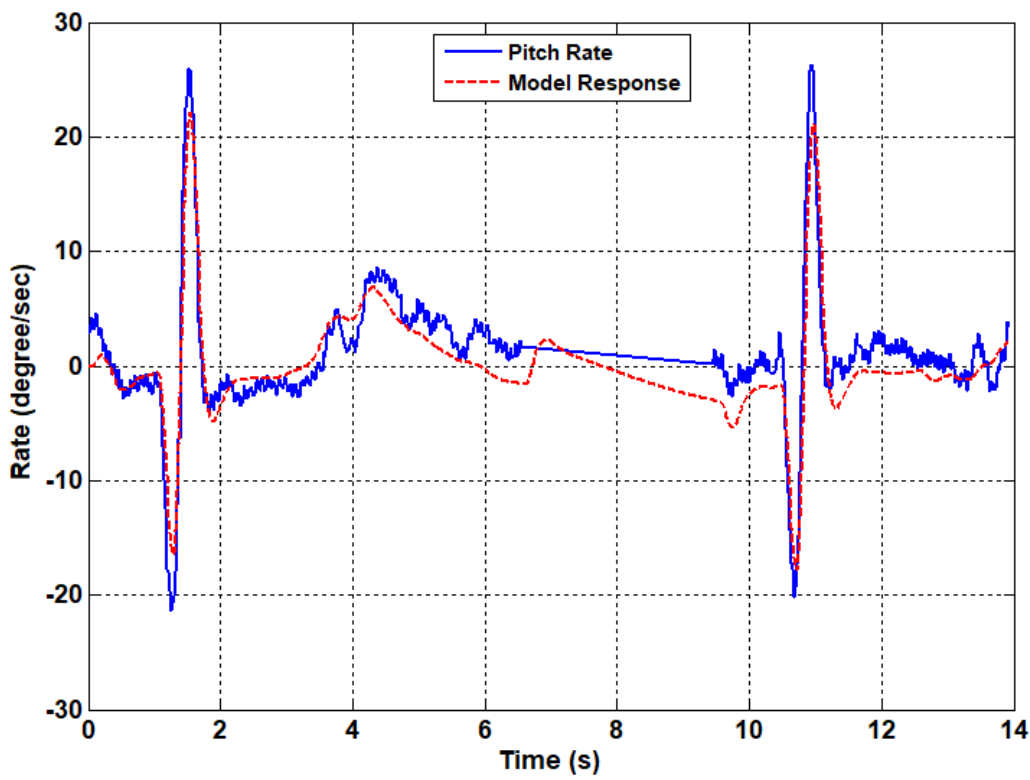


Figure 181: FLT05-MOI Method 2 - Doublet Response

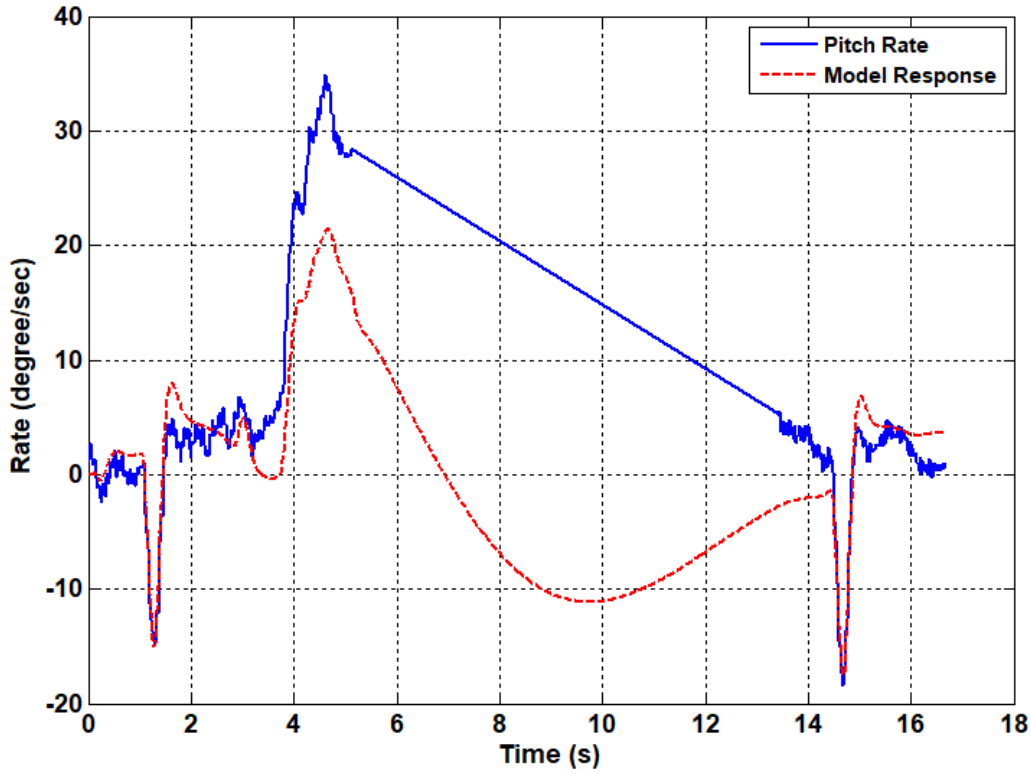


Figure 182: FLT05-MOI Method 2 - Pulse Response

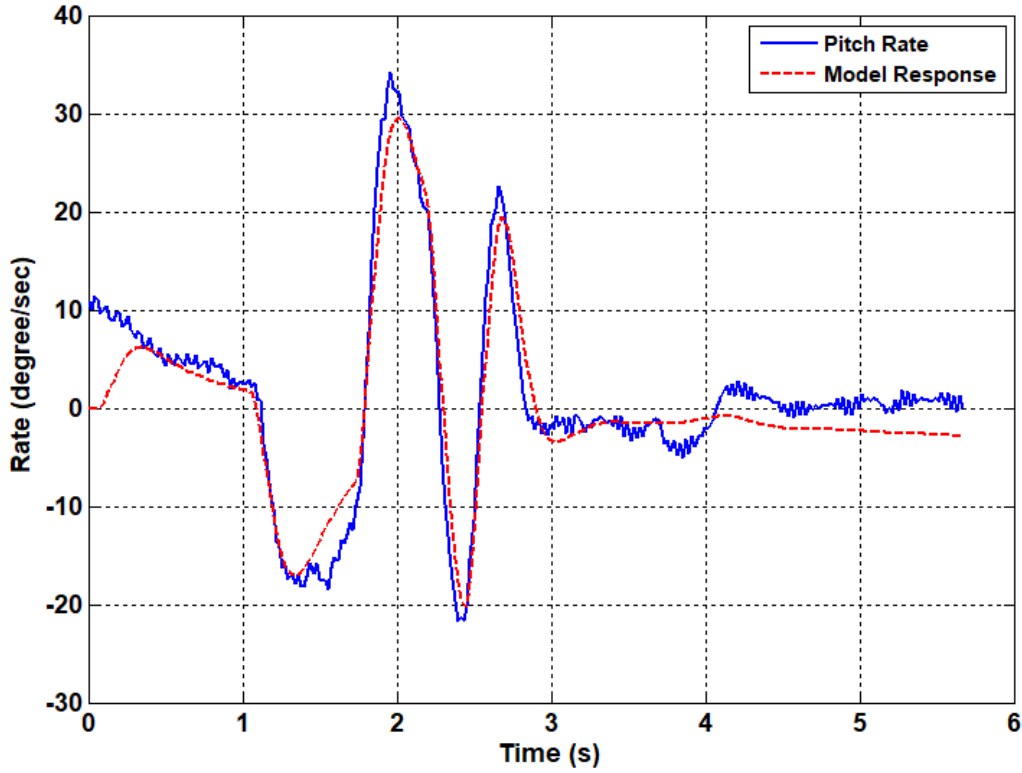


Figure 183: FLT05-MOI Method 2 - 3-2-1-1 Response

b. FLT 10: Time Delay Lateral Survey

Flight 10 was flown at cruise condition, straight and level flight, with computer generated inputs. An additional time delay of 80ms was added to the system for this flight.

The short duration 3-2-1-1 excitation model response for the lateral axis can be seen in Figure 187. The model response for exhibited a close match to the maneuver flight data with only a moderate amount amplitude offset demonstrated in the model response.

The short duration responses for the lateral axis can be seen in Figure 184, Figure 185, Figure 186, and Figure 187. The model response for the doublet and pulse input excitations exhibited a decent match to the excitation flight data and the wider pulse and 3-2-1-1 model responses exhibited close matches. There is a considerable amount of amplitude offset demonstrated in both the doublet and pulse responses and a moderate amplitude offset in the 3-2-1-1 response. The wider pulse response exhibits a minor time delay.

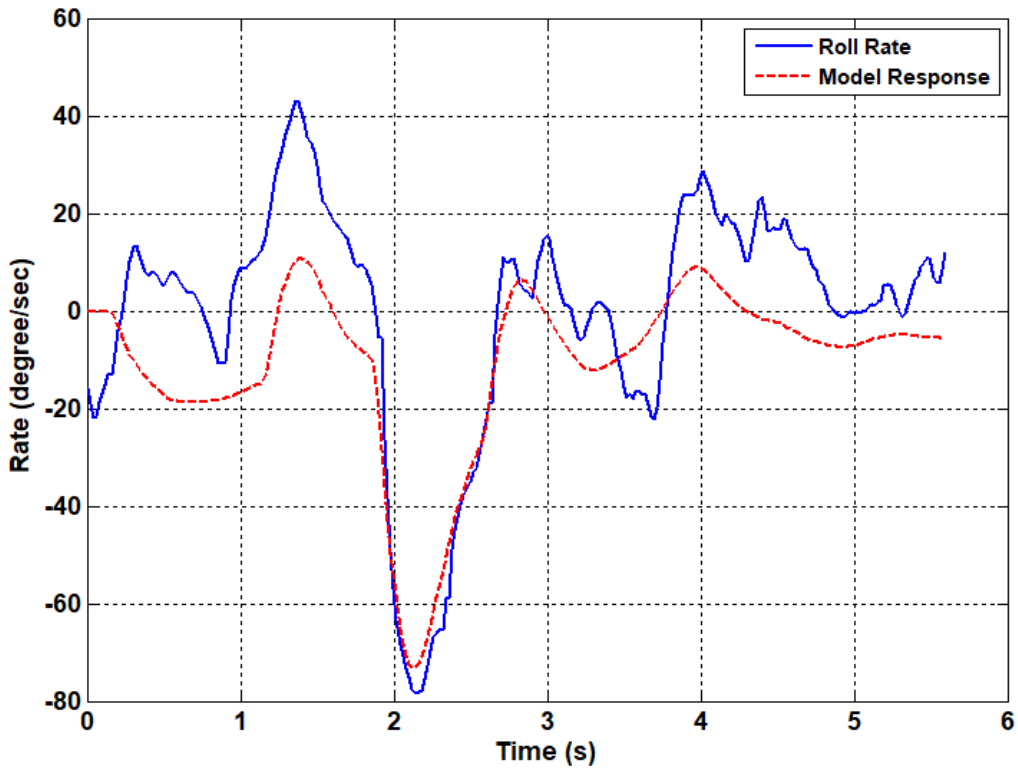


Figure 184: FLT10 - Doublet Response

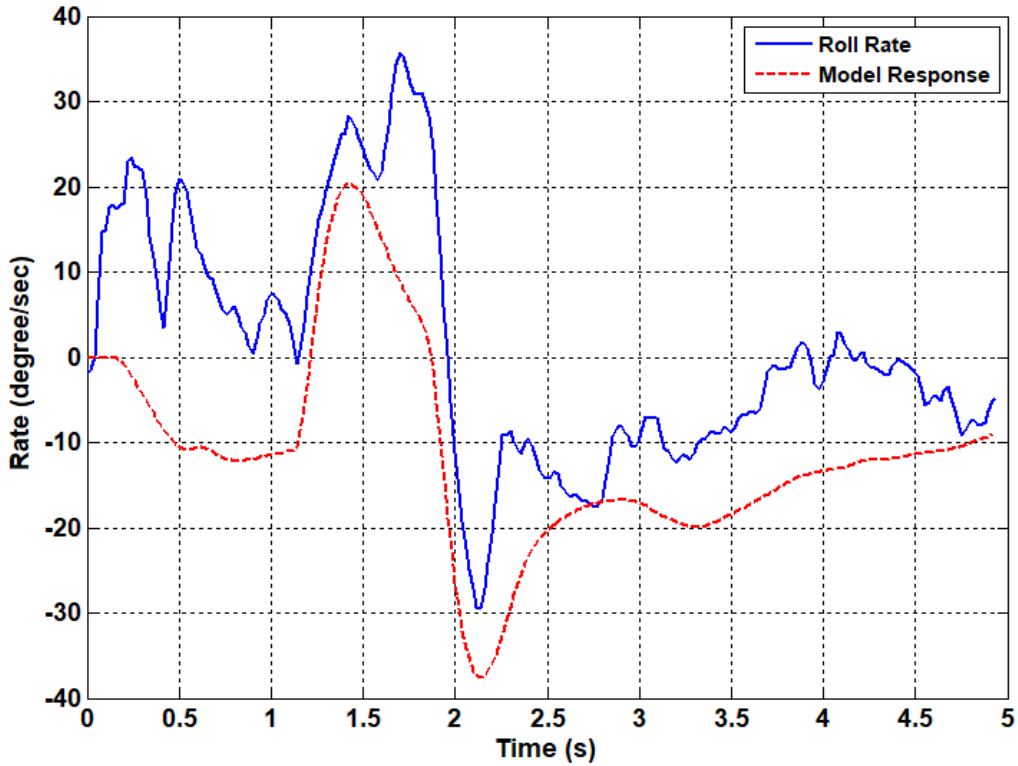


Figure 185: FLT10 - Pulse Response

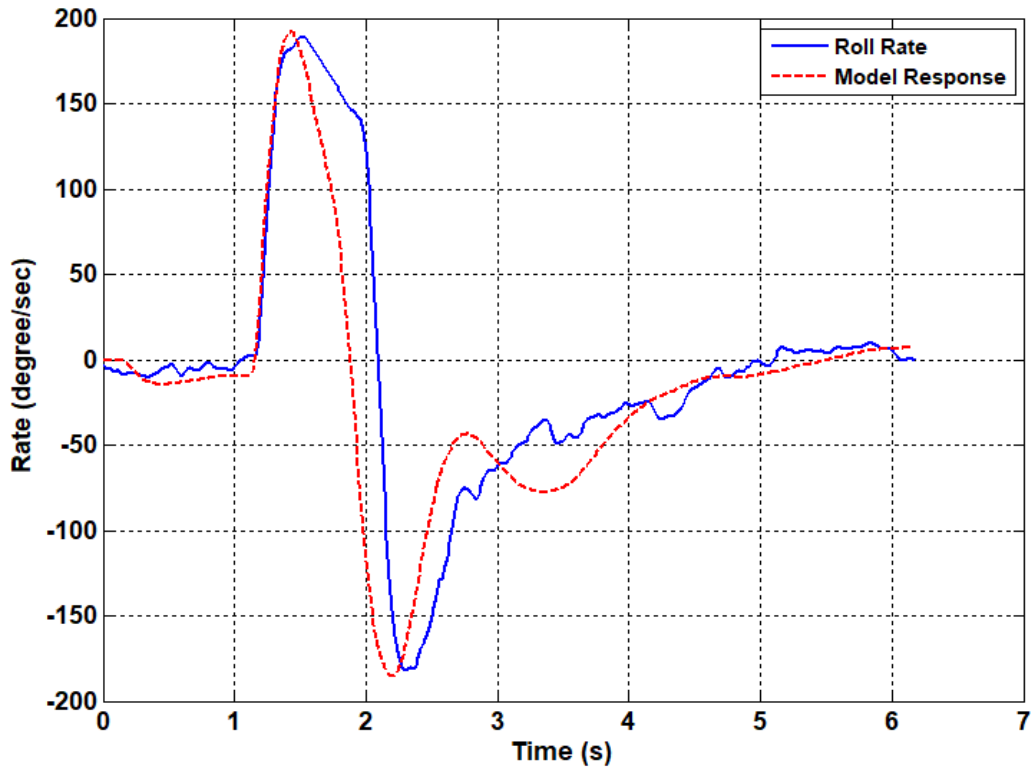


Figure 186: FLT10 - Wider Pulse Response

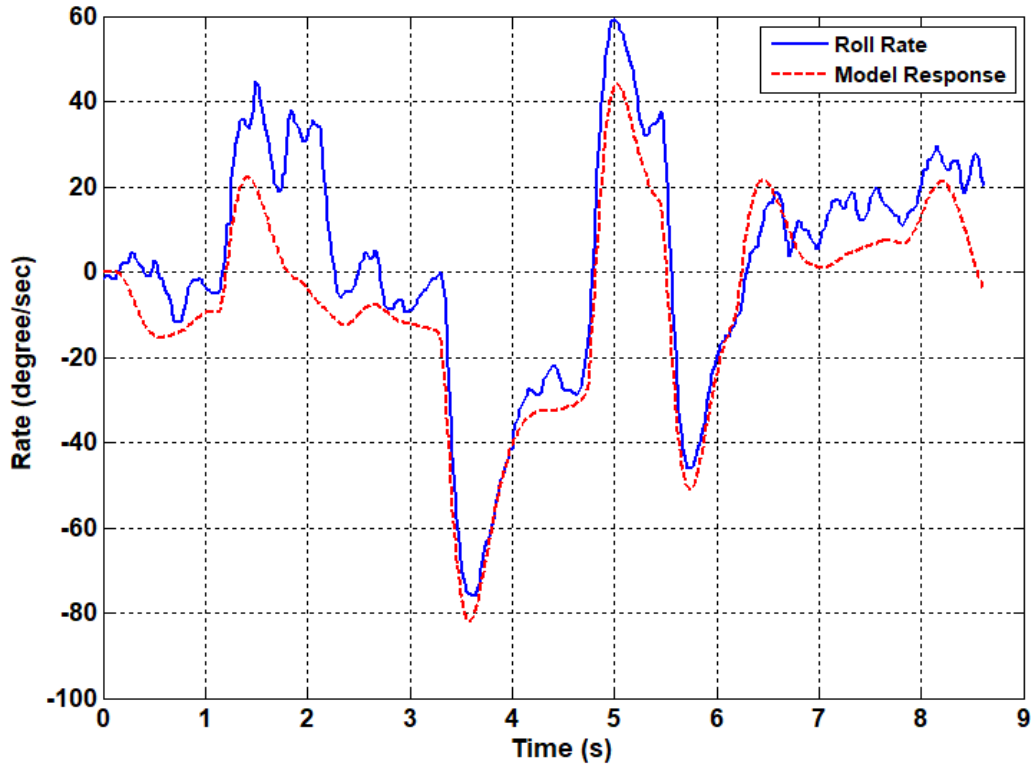


Figure 187: FLT10 - 3-2-1-1 Response

REFERENCES

46. Miller, J. P., D. H. Klyde, P. C. Schulze, B. P. Danowsky, and D. G. Mitchell, *Analysis of Longitudinal and Lateral Dynamics of the UltraStick120*, STI-WP-1456-3, Systems Technology, Inc., October 20, 2017.
47. Morelli, E.A., "Multiple Input Design for Real-Time Parameter Estimation in the Frequency Domain," Paper REG-360, *13th IFAC Symposium on System Identification*, Rotterdam, The Netherlands, August 2003.
48. Myers, T. T., B. L. Aponso, D. H. Klyde, T. J. Rosenthal, R. E Magdaleno, *FREDA, Frequency Domain Analysis Program User's Guide*, STI-WP-433-2, Systems Technology, Inc., 1988.

Appendix D – Multirotor Flight Test Data

A. INTRODUCTION

This appendix provides a review of the initial flight testing of multirotor aircraft as part of an effort to develop, test, and validate Mission Task Elements (MTEs) for sUAS. Specifically, the tasks included herein were defined for the common set of multirotor MTEs that were introduced in Ref. 49. It is intended that the evaluations described herein will serve to document nominal system performance of the selected vehicles. This performance will later be compared with results conducted in the presence of representative hazards (e.g., steady winds). The nominal system flight testing was conducted at the Autonomy Incubator (AI) at NASA Langley Research Center in April 2018. Follow-on testing was conducted in the 14-by 22-foot Subsonic Wind Tunnel (14 x 22) at NASA Langley Research Center in late March 2019. The MTEs were flown in the presence of steady winds up to 25 mph. It was beyond scope and period of performance to analyze and document the results of the wind tunnel evaluations for this program.

The data analysis in this appendix was conducted by two summer interns from California State Polytechnic University, Pomona, Eric Gonzalez and Joshua Klyde, under the direction of the STI Principal Investigator and Dr. Amanda Lampton of STI.

B. FLIGHT TEST SUMMARY

The test was conducted at the AI on a course defined by hover boards positioned according to each MTE description. Four low speed MTEs were tested: Precision Hover, Lateral Sidestep, Vertical Reposition, and Landing. Complete descriptions of the MTEs are provided in Appendix C. The checkout flights were flown by two pilots, and the checkout vehicle was the Tarot X6 hexacopter. The verification flights were flown by the same two pilots as well as a third pilot with a Tarot 650 Sport quadcopter as the test vehicle. The test vehicles are shown in Figure 188.



a) Tarot X6



b) Tarot 650 Sport

Figure 188: Multirotor Test Vehicles

Two sets of data and video were generated for each set of flight test evaluation runs. The video consists of a stationary video that captures the entire test range and an over-the-shoulder video of the pilot to capture pilot perception and line-of-sight. The AI is equipped with a Vicon system that provides precision position tracking of vehicles. Both multirotors were outfitted with Vicon tracking nodes. These data in concert with the over-the-shoulder video can and will be used to calculate performance metrics for these tests. In addition, the aircraft carry Pixhawk autopilots that record GPS, IMU, pilot command, and control deflection data. The GPS data are not accurate in the indoor AI environment and cannot be used for measuring performance, but the IMU, pilot command, and control deflection data will be valuable in understanding the pilot-vehicle system and how that affects performance.

C. FLIGHT TEST RESULTS

1. Run Logs

During a test session for a given vehicle, the pilot performed an MTE (e.g. Precision Hover) multiple times before landing, resetting, and proceeding to the next MTE. A Vicon data file was stored at the

completion of the final run of an MTE as the pilot landed the vehicle to reset such that only a single type of MTE was recorded in each file. Run logs for the Vicon data are included in Table 46. For each pilot and the vehicle flown, the time range over which an MTE or task was performed and recorded in their respective Vicon data files is listed in Table 46. The total number of a given MTE that was performed and the total run time is included. For the Vertical Reposition, the time range is recorded for both a “Vertical Up” maneuver from a 5 ft to 10 ft and a “Vertical Down” maneuver from 10 ft to 5 ft with the downward maneuver listed first as that was first step in the task. Similarly, for the Lateral Sidestep, runs were separated by the direction in which the vehicle stepped, as indicated by “Sidestep Left” or “Sidestep Right.” These were listed in the order in which the pilot performed the maneuver with all but Pilot 2 stepping to the right first.

If a set of MTE runs were recorded over two or more Vicon data files for a single pilot and vehicle rather than one, the time entries for each run are followed by an integer in parentheses (e.g., (1)) indicating in which file they are stored.

Table 46: Vicon Data Run Logs

Pilot	1					
Vehicle	Tarot 650 Sport					
Task	Vertical Down	Vertical Up	Landing	Hover	Sidestep Right	Sidestep Left
Number of Runs	6	5	4	2	4	4
Times of Runs (sec)	27.5-34.5 55.5-69.5 91-102 121.5-129.5 147-157.5 177.5-187	40-50 75-85 105.5-117 135.5-143.5 162-172.7	40-72 79-107 115-151 157-187	69-101 124.5-166	83.5-90.5 115-127 151-163 196-209.5	97.5-105 134.5-140 172-183.5 217.5-228
Total Runtime	206.2		204.6	184.1	258.6	

Pilot	2					
Vehicle	Tarot 650 Sport					
Task	Vertical Down	Vertical Up	Landing	Hover	Sidestep Left	Sidestep Right
Number of Runs	4	3	0	2+2	3+3	2+3
Times of Runs (sec)	26-36 55.5-65 85.5-98 114-122.5	41.5-51.5 67.5-81.5 100-110		63-93 (1) 110-148 (1) 46-83 (2) 98-126 (2)	46.5-72 (1) 109.5-124.5 (1) 164-178 (1) 68-86 (2) 125.5-137.5 (2) 189-196 (2)	84-102 (1) 134-154 (1) 98-113.5 (2) 146-163 (2) 206-214 (2)
Total Runtime	142			173.6 (1) 149.6 (2)	204.3 (1) 242.5 (2)	
Pilot	2					
Vehicle	Tarot X6-2					
Task	Vertical Down	Vertical Up	Landing	Hover	Sidestep Right	Sidestep Left
Number of Runs	4	3	3	1+2	3	2

Times of Runs (sec)	15-27 51.5-68.5 96.5-119.5 146-163	33.5-48 72.5-90 123-142	10-40 52-78 86-119	83.5-128.5 (1) 67-100 (2) 123-171 (2)	35-68 92.5-105.5 131.5-147.5	75.5-85 112-125
Total Runtime	203.9		135.5	143.8 (1) 192.3 (2)	173.8	

Pilot	3					
Vehicle	Tarot 650 Sport					
Task	Vertical Down	Vertical Up	Landing	Hover	Sidestep Right	Sidestep Left
Number of Runs	4	3	3	3+2	3	2
Times of Runs (sec)	30.5-43.5 65.5-76.5 93.5-103.5 120.5-128	49-59.5 80-89 106.5-115.5	24-58 66.5-101.5 109-144	66.5-78 (1) 98-125 (1) 162-187 (1) 88-101 (2) 128.5-162 (2)	34-36 69.5-81.5 111-122	44-61 88.5-100
Total Runtime	153.9		155	200.3 (1) 182.2 (2)	147.8	

Pilot	3					
Vehicle	Tarot X6-2					
Task	Vertical Down	Vertical Up	Landing	Hover	Sidestep Right	Sidestep Left
Number of Runs	3	2	1+2	0	3	2
Times of Runs (sec)	32.5-55 84.5-100 135-151	64-72 116-127	33.5-90.5 (1) 38-93.5 (2) 111-183 (2)		65.5-70.5 103.5-107.5 138-151	82.5-89.5 116-125.5
Total Runtime	177.4		106.7 (1) 203.1 (2)		182.4	

2. Performance Metrics

Based on the MTE definitions in Appendix C, performance metrics can be defined based on the vehicle's position (i.e., X, Y, and Z coordinates), attitude (i.e., roll, pitch and heading angles), and velocity. Since the Vicon data does not include velocity, it was derived by differentiating aircraft position. Performance metrics include % Desired performance and % Adequate performance. From this collection of data, it is possible to assess the performance of each MTE and determine if and how the MTEs should be improved.

To visualize these data with the desired and adequate regions and to calculate performance, ten separate plots were created for each MTE run. An example of these for a Precision Hover MTE run are shown in Figure 189 through Figure 192. Figure 189 shows aircraft position with respect to time; Figure 190 shows aircraft attitude with respect to time; Figure 191 shows aircraft velocity with respect to time; and Figure 192 shows the inertial position of the aircraft for the full set of runs, or batch, for the MTE.

In general, the subfigures in Figure 189 through Figure 191 follow the same pattern to show the desired and adequate regions. The desired performance region is defined by an opaque grey region outlined in solid black lines. The adequate performance region is defined by dashed lines. The flight data is shown in blue, and the performance test range for the run is defined by dashed red lines.

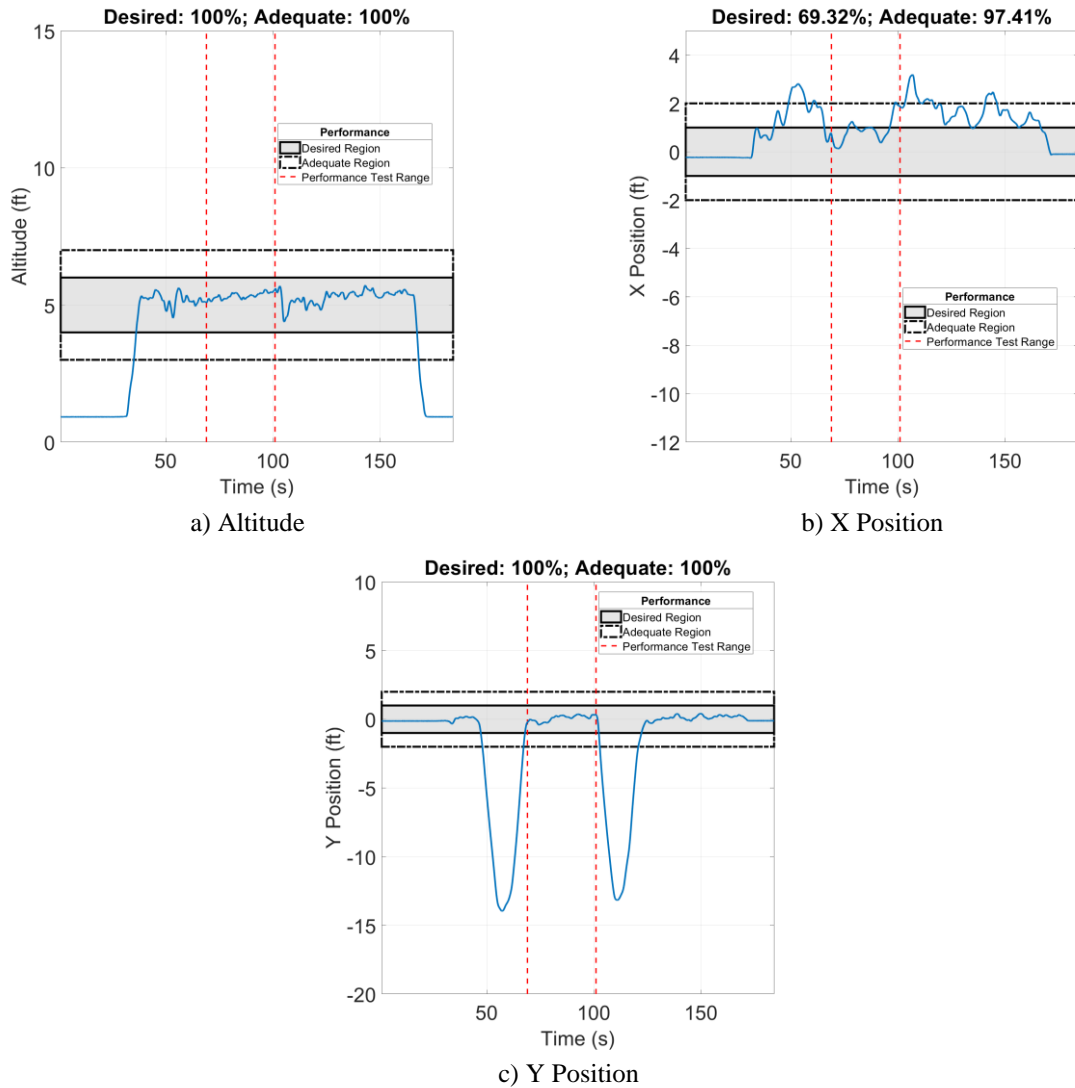
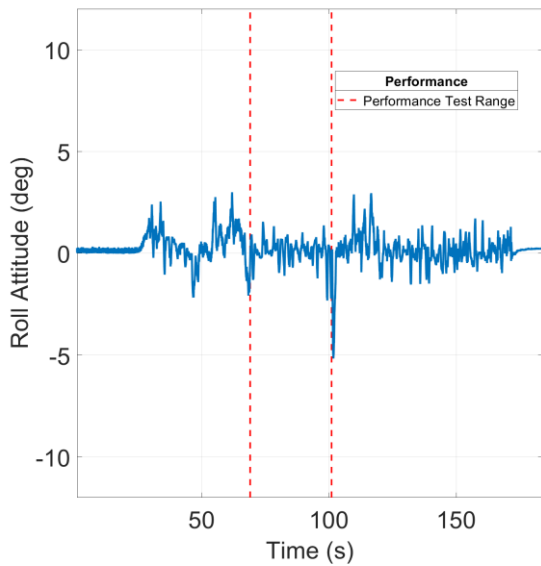
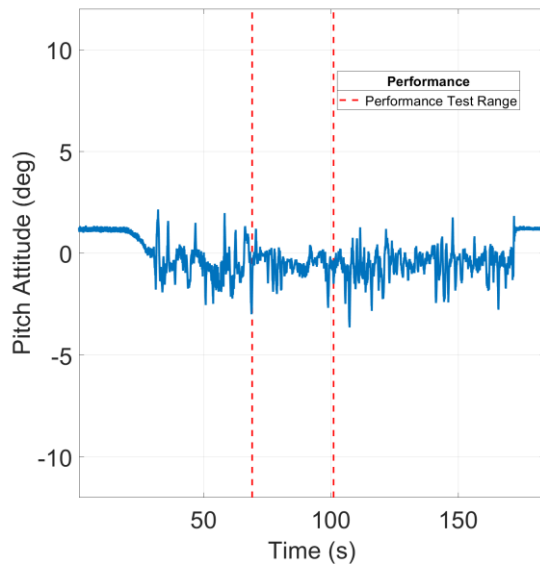


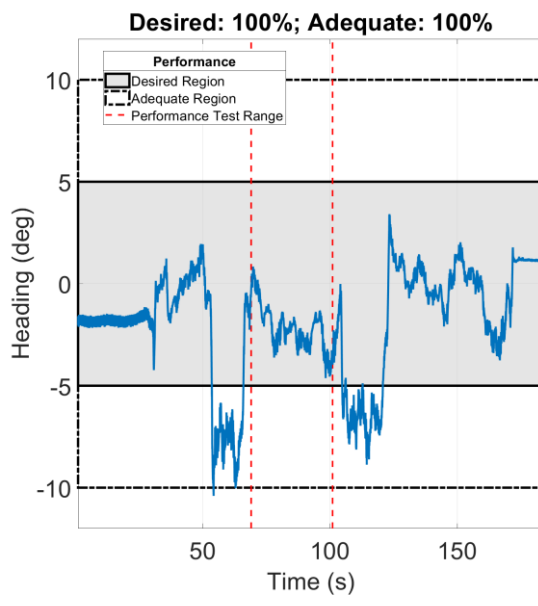
Figure 189: Tarot 650 Sport Precision Hover MTE, Pilot 1, Run 1 – Positions



a) Roll Attitude



b) Pitch Attitude



c) Heading Angle

Figure 190: Tarot 650 Sport Precision Hover MTE, Pilot 1, Run 1 – Attitudes

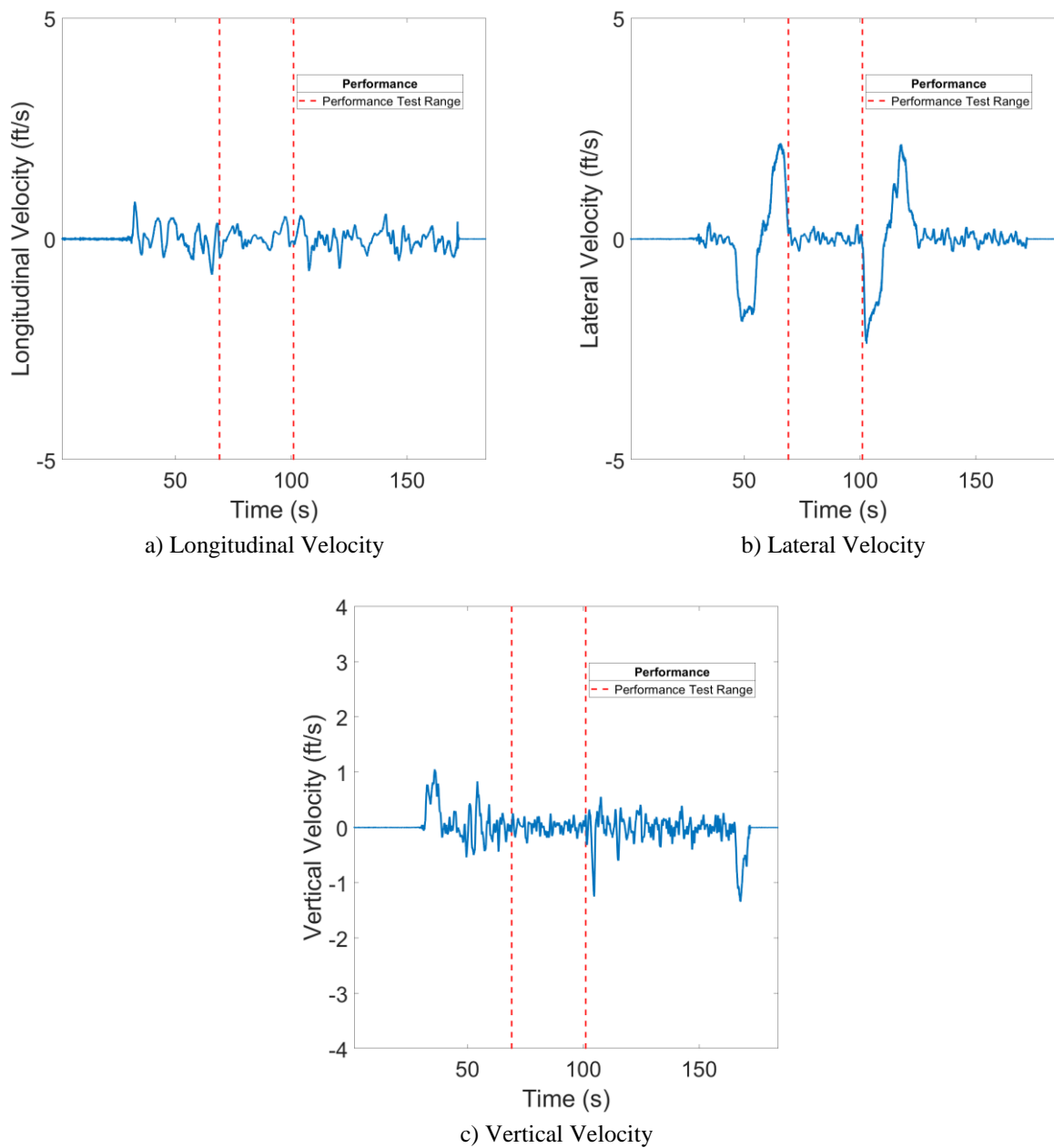


Figure 191: Tarot 650 Sport Precision Hover MTE, Pilot 1, Run 1 – Velocities

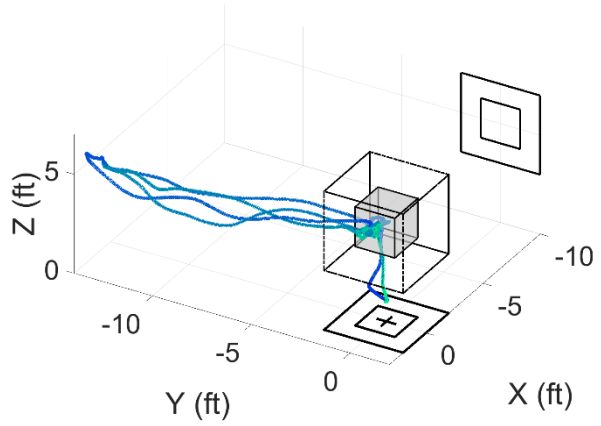


Figure 192: Tarot 650 Sport Precision Hover MTE, Pilot 1, Batch 1 – Inertial Position

Calculating the percentage of time spent within preset adequate and desired bounds for a given aircraft state is a standard method of determining task performance. This is calculated by assessing each data point over the test performance range to determine if it falls within the desired or adequate and dividing the number of points within each by the total number of data points. If the pilot keeps the aircraft within the desired bounds more than 50% of the time for the task, then the overall task performance is considered desired. If less than 50% is within the desired bounds, but more than 50% is within the adequate bounds, then task performance is adequate. If less than 50% is within the adequate bounds, then the pilot fails in task performance.

As a detailed example of this, consider the X position data in Figure 6b. These data show Pilot 1's first attempt at the Precision Hover MTE with the Tarot 650 Sport. The pilot's station-keeping biased in the negative X direction resulting in a desired performance of 69.32%, adequate performance of 97.41%, and thus an overall performance of Adequate.

3. Analysis

a. Precision Hover MTE

To execute the precision hover task, pilots were instructed to start the vehicle and begin hovering at 5 feet. The pilot then executed a step to the left while maintaining the longitudinal position and altitude. The pilot immediately stepped the vehicle back to the original lateral position and to hover above the origin for approximately thirty seconds. This MTE was repeated several times, and then the pilot landed the vehicle at its original position (see example in Figure 193).

From the complete set of runs, it is observed that the pilots were adept at minimizing lateral deviation during the hover task as seen in Y-position for each Hover MTE run. This is characterized by pilot maintaining the aircraft in hover close to the center of the desired region with few excursions beyond the desired bounds. Never did a pilot deviate beyond the adequate performance bounds.

However, secondary tasks proved to be challenging, especially that of maintaining longitudinal position. Due to the pilots' position behind the aircraft, accuracy was limited to the lateral and vertical directions. As such, deviations in longitudinal position either forward or aft were common and usually resulted in the pilot maintaining an incorrect longitudinal position for the duration of the maneuver. The pilots were skilled at keeping a constant altitude for the duration of each Hover MTE as seen in the relevant altitude figures. Most pilots have a continuously smooth and centered altitude within the desired region.

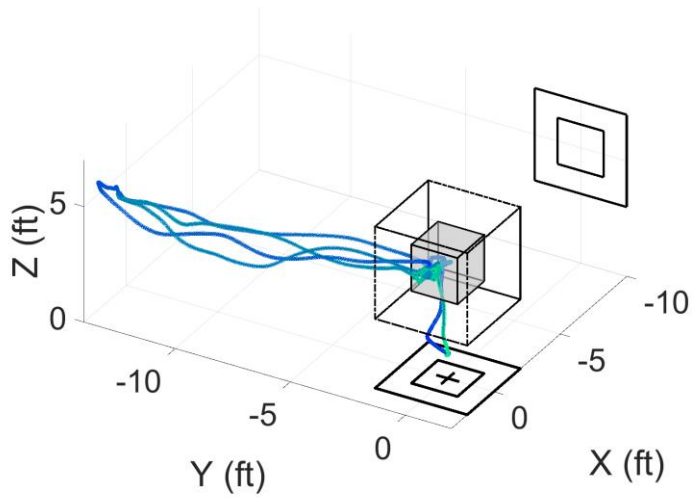


Figure 193: Tarot 650 Sport Precision Hover MTE, Pilot 1, Batch 1 – Inertial Position

1. Qualitative Individual Pilot Assessment

Pilot 1 was the most skilled of the three pilots in the Hover MTE, which can be confirmed by comparing his performance for each hover maneuver against the other two pilots. The data are noticeably smoother with fewer large deviations from the objective. For each run, Pilot 1 maintained the vehicle’s vertical and lateral position within the desired bounds. Although slight, a small perturbation in altitude often accompanied the lateral sidestep from the origin but was quickly corrected. A similar trend appeared in the longitudinal position of the vehicle. The left sidestep was accompanied by a forward deviation that was corrected by the time the aircraft returned to hover. Like the other pilots, he was susceptible to longitudinal deviations forward without correction until landing.

Pilot 2 was adept at the main task, executing a precision hover for each vehicle. He maintained the hover in the desired region for all but a second of the time performing the maneuver. The secondary tasks proved more difficult as there were many longitudinal excursions with a few altitude overcorrections. The most prominent such excursion was an inadvertent 7-ft aft deviation during the second hover run. These issues were amplified when piloting the Tarot X6-2, though this was to be expected considering the larger weight and higher difficulty in precisely maneuvering the vehicle.

Pilot 3 had some difficulty in performing the Hover MTE in his first flight. He was the only pilot to deviate outside the desired bounds for an extended period and had a few large excursions in longitudinal position. Additionally, during the last hover in the first flight, a large vertical deviation occurred without explanation as there is no coinciding video from which to glean such information. Unfortunately, though Pilot 3 completed the Hover MTE multiple times with the Tarot X6-2, very little data was recorded, and that which remained was heavily corrupted. The only significant data for Pilot 3 flying the Tarot X6-2 are from the video of each flight. This video shows the bulkier vehicle proved challenging for him to fly. There were many deviations in all directions with him able to maintain at least an adequate score for only the lateral position during the hover.

2. Performance

Tables of the pilots’ performance for the Precision Hover MTE are included in Table 47 through Table 51. The tables contain the desired and adequate scores for altitude, X-position, Y-position, and heading angle for each pilots’ individual run within each MTE. The pilots had high performance scores for altitude, lateral position, and heading angle. For these three performance measures, the percent values

never differed by more than 10%. The most difficult task was keeping the vehicle's longitudinal position in the desired region.

Table 51 lists the averages for the data in Table 47 through Table 50. The lowest average pilot performance score for the desired region is just 18.23% and the highest is 36.78%. However, the highest adequate score for the longitudinal performance measurement is 92.11% with a low of 29.91%. The pilots are consistent in which axis is easy or difficult to meet performance requirements. From the data herein, it is apparent that maintaining longitudinal position of the vehicle in a small region is a challenging task whereas maintaining altitude, lateral position, and heading is fairly easy.

The only pilot to fly both the Tarot 650 Sport and the Tarot X6-2 with data recorded was Pilot 2, thus making it difficult to make comparisons between the relative difficulty of performing the MTE with the vehicles. However, Pilot 2 kept the aircraft within the desired bounds for altitude, lateral position, and heading 7% more of the time with the Tarot 650 Sport than with the larger Tarot X6-2 and was 6% more successful at maintaining a desired longitudinal position.

Table 47: Precision Hover MTE Performance – Pilot 1, Tarot 650 Sport

Pilot: 1	Task: Hover	
Run: 1	Vehicle: Tarot 650 Sport	
	Desired (%)	Adequate (%)
Altitude	100.00	100.00
X Position	69.32	97.41
Y Position	100.00	100.00
Heading Angle	100.00	100.00

Pilot: 1	Task: Hover	
Run: 2	Vehicle: Tarot 650 Sport	
	Desired (%)	Adequate (%)
Altitude	100.00	100.00
X Position	4.23	86.81
Y Position	100.00	100.00
Heading Angle	100.00	100.00

Table 48: Precision Hover MTE Performance – Pilot 2, Tarot 650 Sport

Pilot: 2	Task: Hover	
Run: 1	Vehicle: Tarot 650 Sport	
	Desired (%)	Adequate (%)
Altitude	95.03	100.00
X Position	45.83	79.25
Y Position	100.00	100.00
Heading Angle	100.00	100.00

Pilot: 2	Task: Hover	
Run: 2	Vehicle: Tarot 650 Sport	
	Desired (%)	Adequate (%)
Altitude	90.54	100.00
X Position	13.02	64.87
Y Position	100.00	100.00
Heading Angle	100.00	100.00

Pilot: 2	Task: Hover	
Run: 3	Vehicle: Tarot 650 Sport	
	Desired (%)	Adequate (%)
Altitude	98.66	100.00
X Position	16.47	32.14
Y Position	100.00	100.00
Heading Angle	99.97	100.00

Pilot: 2	Task: Hover	
Run: 4	Vehicle: Tarot 650 Sport	
	Desired (%)	Adequate (%)
Altitude	88.70	100.00
X Position	9.13	27.13
Y Position	100.00	100.00
Heading Angle	95.32	100.00

Table 49: Precision Hover MTE Performance – Pilot 3, Tarot 650 Sport

Pilot: 3	Task: Hover	
Run: 1	Vehicle: Tarot 650 Sport	
	Desired (%)	Adequate (%)
Altitude	91.13	100.00
X Position	0.00	7.83
Y Position	61.91	100.00
Heading Angle	26.30	61.65

Pilot: 3	Task: Hover	
Run: 2	Vehicle: Tarot 650 Sport	
	Desired (%)	Adequate (%)
Altitude	98.20	100.00
X Position	0.00	0.00
Y Position	100.00	100.00
Heading Angle	85.69	100.00

Pilot: 3	Task: Hover	
Run: 3	Vehicle: Tarot 650 Sport	
	Desired (%)	Adequate (%)
Altitude	12.98	40.76
X Position	26.16	44.04
Y Position	82.90	100.00
Heading Angle	98.60	100.00

Pilot: 3	Task: Hover	
Run: 4	Vehicle: Tarot 650 Sport	
	Desired (%)	Adequate (%)
Altitude	100.00	100.00
X Position	81.58	100.00
Y Position	100.00	100.00
Heading Angle	100.00	100.00

Pilot: 3	Task: Hover	
Run: 5	Vehicle: Tarot 650 Sport	
	Desired (%)	Adequate (%)
Altitude	100.00	100.00
X Position	0.00	23.70
Y Position	100.00	100.00
Heading Angle	95.91	100.00

Table 50: Precision Hover MTE Performance – Pilot 2, Tarot X6-2

Pilot: 2	Task: Hover	
Run: 1	Vehicle: Tarot X6-2	
	Desired (%)	Adequate (%)
Altitude	94.06	100.00
X Position	11.90	26.08
Y Position	100.00	100.00
Heading Angle	96.02	100.00

Pilot: 2	Task: Hover	
Run: 2	Vehicle: Tarot X6-2	
	Desired (%)	Adequate (%)
Altitude	74.82	100.00
X Position	34.12	68.21
Y Position	99.03	100.00
Heading Angle	59.91	100.00

Pilot: 2	Task: Hover	
Run: 3	Vehicle: Tarot X6-2	
	Desired (%)	Adequate (%)
Altitude	88.52	100.00
X Position	0.00	10.66
Y Position	100.00	100.00
Heading Angle	97.68	100.00

Table 51: Precision Hover MTE Pilot Performance Averages

Average Pilot Performance for Vertical Reposition MTE								
	Altitude		Fore/Aft Position		Lateral Position		Heading Angle	
Pilot #	Desired	Adequate	Desired	Adequate	Desired	Adequate	Desired	Adequate
1	100.00	100.00	36.78	92.11	100.00	100.00	100.00	100.00
2	89.52	100.00	18.23	42.91	99.84	100.00	91.68	100.00
3	80.46	88.15	21.55	35.11	88.96	100.00	81.30	92.33
AVG	89.99	96.05	25.52	56.71	96.27	100.00	90.99	97.44

Average Pilot Performance for Vertical Reposition MTE Using Tarot 650 Sport								
	Altitude		Fore/Aft Position		Lateral Position		Heading Angle	
Pilot #	Desired	Adequate	Desired	Adequate	Desired	Adequate	Desired	Adequate
1	100.00	100.00	36.78	92.11	100.00	100.00	100.00	100.00
2	93.23	100.00	21.11	50.85	100.00	100.00	98.82	100.00
3	80.46	88.15	21.55	35.11	88.96	100.00	81.30	92.33
AVG	91.23	96.05	26.48	59.36	96.32	100.00	93.37	97.44

Average Pilot Performance for Vertical Reposition MTE Using Tarot 650 Sport w/o Pilot 1								
	Altitude		Fore/Aft Position		Lateral Position		Heading Angle	
Pilot #	Desired	Adequate	Desired	Adequate	Desired	Adequate	Desired	Adequate
1								
2	100.00	100.00	17.33	34.07	100.00	100.00	99.65	100.00
3	85.54	98.62	0.00	41.56	96.01	100.00	97.25	100.00
AVG	92.77	99.31	8.66	37.81	98.01	100.00	98.45	100.00

Average Pilot Performance for Vertical Reposition MTE Using Tarot X6-2								
	Altitude		Fore/Aft Position		Lateral Position		Heading Angle	
Pilot #	Desired	Adequate	Desired	Adequate	Desired	Adequate	Desired	Adequate
1								
2	85.80	100.00	15.34	34.98	99.68	100.00	84.54	100.00
3								
AVG	85.80	100.00	15.34	34.98	99.68	100.00	84.54	100.00

b. Lateral Sidestep MTE

For the Lateral Sidestep MTE, the pilots were instructed to fly the vehicle laterally in one direction, capture and hold a static position, then sidestep in the other direction to capture and hold the original position. In most cases, the pilot first flew the aircraft to a hover board approximately 6.5 feet to the right of the takeoff point and then sidestepped towards a hover board about 15 feet to the left of the takeoff point. The lateral sidestep was then repeated several times (see example in Figure 194). Most flights consisted of 5 or 6 sidesteps with Pilot 1 performing 8. The time spent hovering in position after completing the lateral movement was short, lasting 10-25 seconds depending on the preference of the pilot. In general, the pilots had a higher degree of success with the right sidestep.

The pilots were effective at maintaining desired performance during the right lateral maneuver. They also performed the left sidestep well, though they were prone to under- or overshooting the target. This under- and overshooting the target can be attributed to depth perception and line-of-sight issues. The right sidestep end position was much closer to the pilot making it easier to judge vehicle's position relative to the hover board and adequate/desired bounds. In terms of maintaining altitude, the pilots had moderate success with small dips when beginning the sidestep.

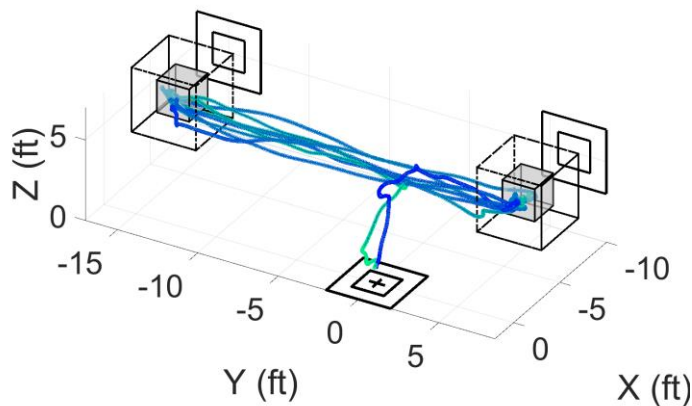


Figure 194: Tarot 650 Sport Lateral Sidestep MTE, Pilot 1, Batch 1 – Inertial Position

1. Qualitative Individual Pilot Assessment

Pilot 1 performed very well during each individual sidestep maneuver. He completed 8 different lateral repositions, starting by sidestepping to the right. Aside from the first left sidestep, he finished the entire run in the desired area. In the altitude portion of the task, he remained in the desired zone for the duration of the run but deviated by a few inches every time a lateral reposition was initiated. This deviation was then corrected during each quick hover at the sidestep point. For the longitudinal position, Pilot 1 was unable to complete the aft reposition 5 feet behind the origin, and instead held a very unsteady position 3-4 feet behind. He was, however, able to return the vehicle to landing zone at the conclusion of the task.

Pilot 2 faced some difficulty in performing sections of the sidestep maneuver. While piloting the Tarot 650 Sport he made multiple altitude overcorrections and was unable to achieve a steady hover during any left lateral repositions. He found more success in the right sidestep maneuver, consistently achieving a desired position. He also attempted to perform a 5 foot aft reposition that was unsuccessful and resulted in erratic longitudinal position changes between 2 and 5 feet behind the origin. While piloting the Tarot X6-2, he encountered many similar problems as he did with the Tarot 650 Sport, but with the additional

variable of increased air circulation. There was a glass panel near the right hoverboard which allowed the air circulation from the powerful hex rotors to bounce off it, disturbing the air around it causing fluctuations in altitude and lateral position.

Pilot 3 proved to be adept at maintaining lateral positioning of each of his vehicles. Additionally, unlike the other two pilots, he was able to successfully perform the aft reposition five feet behind the origin. Despite the correct repositioning of the vehicle, Pilot 3 still exhibited similar oscillatory behavior in the longitudinal axis to Pilot 2, although his perturbations mostly fell within the desired and adequate areas. His performance piloting the Tarot 650 Sport and the Tarot X6-2 were very comparable, but understandably, there were more jarring and frequent movements during the Tarot X6-2 runs due to its bulkier size.

2. Performance

Tables of the pilots' performance for the Lateral Sidestep MTE are included in Table 52 through Table 57. In addition to containing similar information to the Hover MTE, each pilot was scored on their ability to maintain a desired or adequate altitude position during the translation from one sidestep to the next. Altitude, longitudinal position, lateral position, and heading angle were more coupled in the Lateral Sidestep MTE than in any other MTE. Pilots' performance reflected more difficulty in precisely and accurately controlling the lateral position of the vehicle within the desired and adequate bounds, which is not seen in other the MTEs. They also had difficulty maintaining desired heading angle, another trend not seen in any other maneuver.

When performance scores are separated as shown in Table 57, pilots excelled at staying in the desired region for altitude with a desired performance of 94.33% and an adequate performance of 99.94%. Holding altitude between hover positions was an easy task for the pilots with an average of 87% desired performance score with a near 100% adequate score. Lateral position was relatively easy for the pilots to control with a desired performance of 85.21% and an adequate performance of 96.95%. Average heading angle performance was 65.52% desired and 97.47% adequate. Longitudinal position performance was just 39.08% desired and 70.87% adequate.

Comparing the two vehicles, there are small differences in performance measures. In altitude during hover, the Tarot 650 Sport has a desired performance over 12% higher at 97.64% than the Tarot X6-2 at 85.35%. In lateral position, the pilots achieved a higher desired performance with the Tarot X6-2 at 87.83%, 10% higher than with the Tarot 650 Sport. However, this can be explained by Pilot 2's poor performance flying the Tarot 650 Sport while Pilot 3 performed slightly worse with the Tarot X6-2. Heading angle performance was nearly identical between the two vehicles. This lack of consistency in one vehicle performing better than the other means that a claim cannot be made for an evidence-based difference in vehicle performance.

Table 52: Lateral Sidestep MTE Performance – Pilot 1, Tarot 650 Sport

Pilot: 1	Task: Sidestep	
Run: 1	Vehicle: Tarot 650 Sport	
	Desired (%)	Adequate (%)
Altitude	100.00	100.00
X Position	0.00	30.29
Y Position	100.00	100.00
Heading Angle	9.43	100.00

Pilot: 1	Task: Sidestep	
Run: 2	Vehicle: Tarot 650 Sport	
	Desired (%)	Adequate (%)
Altitude	100.00	100.00
X Position	0.00	19.32
Y Position	37.44	100.00
Heading Angle	51.50	100.00

Pilot: 1	Task: Sidestep	
Run: 3	Vehicle: Tarot 650 Sport	
	Desired (%)	Adequate (%)
Altitude	100.00	100.00
X Position	0.00	76.97
Y Position	89.30	94.71
Heading Angle	1.96	61.31

Pilot: 1	Task: Sidestep	
Run: 4	Vehicle: Tarot 650 Sport	
	Desired (%)	Adequate (%)
Altitude	100.00	100.00
X Position	74.45	100.00
Y Position	100.00	100.00
Heading Angle	34.45	100.00

Pilot: 1	Task: Sidestep	
Run: 5	Vehicle: Tarot 650 Sport	
	Desired (%)	Adequate (%)
Altitude	100.00	100.00
X Position	44.21	100.00
Y Position	100.00	100.00
Heading Angle	78.46	100.00

Pilot: 1	Task: Sidestep	
Run: 6	Vehicle: Tarot 650 Sport	
	Desired (%)	Adequate (%)
Altitude	100.00	100.00
X Position	100.00	100.00
Y Position	95.52	100.00
Heading Angle	0.00	95.35

Pilot: 1	Task: Sidestep	
Run: 7	Vehicle: Tarot 650 Sport	
	Desired (%)	Adequate (%)
Altitude	100.00	100.00
X Position	32.15	100.00
Y Position	100.00	100.00
Heading Angle	42.26	100.00

Pilot: 1	Task: Sidestep	
Run: 8	Vehicle: Tarot 650 Sport	
	Desired (%)	Adequate (%)
Altitude	100.00	100.00
X Position	100.00	100.00
Y Position	100.00	100.00
Heading Angle	0.00	100.00

Pilot: 1	Task: Sidestep	
Translation Alt. Hold	Vehicle: Tarot 650 Sport	
	Desired (%)	Adequate (%)
Altitude Run 1	100.00	100.00
Altitude Run 2	100.00	100.00
Altitude Run 3	100.00	100.00
Altitude Run 4	100.00	100.00
Altitude Run 5	100.00	100.00
Altitude Run 6	100.00	100.00
Altitude Run 7	100.00	100.00
Altitude Run 8	100.00	100.00
Altitude Run 9	100.00	100.00

Pilot 1 Lateral Sidestep Direction Comparison Tarot 650 Sport		
	Desired (%)	Adequate (%)
AVG Right	62.96	91.78
AVG Left	68.34	94.67

Table 53: Lateral Sidestep MTE Performance – Pilot 2, Tarot 650 Sport

Pilot: 2	Task: Sidestep	
Run: 1	Vehicle: Tarot 650 Sport	
	Desired (%)	Adequate (%)
Altitude	82.94	95.88
X Position	14.75	46.84
Y Position	45.02	83.96
Heading Angle	99.45	100.00

Pilot: 2	Task: Sidestep	
Run: 2	Vehicle: Tarot 650 Sport	
	Desired (%)	Adequate (%)
Altitude	100.00	100.00
X Position	13.97	48.92
Y Position	100.00	100.00
Heading Angle	63.64	100.00

Pilot: 2	Task: Sidestep	
Run: 3	Vehicle: Tarot 650 Sport	
	Desired (%)	Adequate (%)
Altitude	100.00	100.00
X Position	18.77	32.37
Y Position	38.97	95.73
Heading Angle	73.03	100.00

Pilot: 2	Task: Sidestep	
Run: 4	Vehicle: Tarot 650 Sport	
	Desired (%)	Adequate (%)
Altitude	100.00	100.00
X Position	0.00	19.15
Y Position	100.00	100.00
Heading Angle	47.08	93.20

Pilot: 2	Task: Sidestep	
Run: 5	Vehicle: Tarot 650 Sport	
	Desired (%)	Adequate (%)
Altitude	100.00	100.00
X Position	0.00	28.14
Y Position	29.46	99.64
Heading Angle	100.00	100.00

Pilot: 2	Task: Sidestep	
Run: 6	Vehicle: Tarot 650 Sport	
	Desired (%)	Adequate (%)
Altitude	98.42	100.00
X Position	21.14	45.22
Y Position	33.78	91.72
Heading Angle	99.94	100.00

Pilot: 2	Task: Sidestep	
Run: 7	Vehicle: Tarot 650 Sport	
	Desired (%)	Adequate (%)
Altitude	100.00	100.00
X Position	0.00	18.19
Y Position	73.29	100.00
Heading Angle	96.81	100.00

Pilot: 2	Task: Sidestep	
Run: 8	Vehicle: Tarot 650 Sport	
	Desired (%)	Adequate (%)
Altitude	100.00	100.00
X Position	0.00	0.00
Y Position	0.00	9.00
Heading Angle	100.00	100.00

Pilot: 2	Task: Sidestep	
Run: 9	Vehicle: Tarot 650 Sport	
	Desired (%)	Adequate (%)
Altitude	83.18	100.00
X Position	8.79	17.82
Y Position	98.15	100.00
Heading Angle	94.82	99.62

Pilot: 2	Task: Sidestep	
Run: 10	Vehicle: Tarot 650 Sport	
	Desired (%)	Adequate (%)
Altitude	100.00	100.00
X Position	0.00	0.00
Y Position	0.00	46.86
Heading Angle	100.00	100.00

Pilot: 2	Task: Sidestep	
Run: 11	Vehicle: Tarot 650 Sport	
	Desired (%)	Adequate (%)
Altitude	100.00	100.00
X Position	19.56	77.31
Y Position	100.00	100.00
Heading Angle	100.00	100.00

Pilot: 2	Task: Sidestep	
	Vehicle: Tarot 650 Sport	
Translation Alt. Hold	Desired (%)	Adequate (%)
Altitude Run 1	100.00	100.00
Altitude Run 2	76.18	100.00
Altitude Run 3	58.71	100.00
Altitude Run 4	63.87	100.00
Altitude Run 5	67.33	99.92
Altitude Run 6	100.00	100.00

Pilot: 2	Task: Sidestep	
	Vehicle: Tarot 650 Sport	
Translation Alt. Hold	Desired (%)	Adequate (%)
Altitude Run 7	100.00	100.00
Altitude Run 8	62.16	100.00
Altitude Run 9	85.71	100.00
Altitude Run 10	87.09	100.00
Altitude Run 11	100.00	100.00
Altitude Run 12	100.00	100.00
Altitude Run 13	40.97	100.00

Pilot 2 Lateral Sidestep Direction Comparison Tarot 650 Sport		
	Desired (%)	Adequate (%)
AVG Right	60.94	74.94
AVG Left	67.20	83.31

Table 54: Lateral Sidestep MTE Performance – Pilot 3, Tarot 650 Sport

Pilot: 3	Task: Sidestep	
Run: 1	Vehicle: Tarot 650 Sport	
	Desired (%)	Adequate (%)
Altitude	100.00	100.00
X Position	100.00	100.00
Y Position	100.00	100.00
Heading Angle	100.00	100.00

Pilot: 3	Task: Sidestep	
Run: 2	Vehicle: Tarot 650 Sport	
	Desired (%)	Adequate (%)
Altitude	92.56	100.00
X Position	54.97	94.32
Y Position	100.00	100.00
Heading Angle	62.85	100.00

Pilot: 3	Task: Sidestep	
Run: 3	Vehicle: Tarot 650 Sport	
	Desired (%)	Adequate (%)
Altitude	100.00	100.00
X Position	37.42	100.00
Y Position	100.00	100.00
Heading Angle	36.21	92.92

Pilot: 3	Task: Sidestep	
Run: 4	Vehicle: Tarot 650 Sport	
	Desired (%)	Adequate (%)
Altitude	100.00	100.00
X Position	85.79	100.00
Y Position	94.00	100.00
Heading Angle	100.00	100.00

Pilot: 3	Task: Sidestep	
Run: 5	Vehicle: Tarot 650 Sport	
	Desired (%)	Adequate (%)
Altitude	100.00	100.00
X Position	86.92	100.00
Y Position	100.00	100.00
Heading Angle	86.96	100.00

Pilot: 3	Task: Sidestep	
	Vehicle: Tarot 650 Sport	
Translation Alt. Hold	Desired (%)	Adequate (%)
Altitude Run 1	100.00	100.00
Altitude Run 2	71.38	100.00
Altitude Run 3	89.28	100.00
Altitude Run 4	63.87	100.00
Altitude Run 5	94.18	100.00
Altitude Run 6	93.83	100.00

Pilot 3 Lateral Sidestep Direction Comparison Tarot 650 Sport		
	Desired (%)	Adequate (%)
AVG Right	87.29	99.41
AVG Left	84.53	99.04

Table 55: Lateral Sidestep MTE Performance – Pilot 2, Tarot X6-2

Pilot: 2	Task: Sidestep	
Run: 1	Vehicle: Tarot X6-2	
	Desired (%)	Adequate (%)
Altitude	98.09	100.00
X Position	18.69	59.58
Y Position	91.82	100.00
Heading Angle	93.44	100.00

Pilot: 2	Task: Sidestep	
Run: 2	Vehicle: Tarot X6-2	
	Desired (%)	Adequate (%)
Altitude	100.00	100.00
X Position	0.00	22.42
Y Position	54.42	93.84
Heading Angle	100.00	100.00

Pilot: 2	Task: Sidestep	
Run: 3	Vehicle: Tarot X6-2	
	Desired (%)	Adequate (%)
Altitude	100.00	100.00
X Position	19.42	34.62
Y Position	100.00	100.00
Heading Angle	98.58	100.00

Pilot: 2	Task: Sidestep	
Run: 4	Vehicle: Tarot X6-2	
	Desired (%)	Adequate (%)
Altitude	100.00	100.00
X Position	36.42	80.23
Y Position	100.00	100.00
Heading Angle	100.00	100.00

Pilot: 2	Task: Sidestep	
Run: 5	Vehicle: Tarot X6-2	
	Desired (%)	Adequate (%)
Altitude	94.22	100.00
X Position	37.56	48.56
Y Position	100.00	100.00
Heading Angle	85.25	100.00

Pilot: 2	Task: Sidestep	
Translation Alt. Hold	Vehicle: Tarot X6-2	
	Desired (%)	Adequate (%)
Altitude Run 1	100.00	100.00
Altitude Run 2	100.00	100.00
Altitude Run 3	100.00	100.00
Altitude Run 4	100.00	100.00
Altitude Run 5	100.00	100.00
Altitude Run 6	100.00	100.00

Pilot 2 Lateral Sidestep Direction Comparison Tarot X6-2		
	Desired (%)	Adequate (%)
AVG Right	78.09	86.90
AVG Left	74.70	87.03

Table 56: Lateral Sidestep MTE Performance – Pilot 3, Tarot X6-2

Pilot: 3	Task: Sidestep	
Run: 1	Vehicle: Tarot X6-2	
	Desired (%)	Adequate (%)
Altitude	74.70	100.00
X Position	22.30	66.70
Y Position	100.00	100.00
Heading Angle	0.00	88.70

Pilot: 3	Task: Sidestep	
Run: 2	Vehicle: Tarot X6-2	
	Desired (%)	Adequate (%)
Altitude	60.07	100.00
X Position	50.93	100.00
Y Position	83.36	100.00
Heading Angle	94.79	100.00

Pilot: 3	Task: Sidestep	
Run: 3	Vehicle: Tarot X6-2	
	Desired (%)	Adequate (%)
Altitude	96.88	100.00
X Position	59.88	100.00
Y Position	100.00	100.00
Heading Angle	100.00	100.00

Pilot: 3	Task: Sidestep	
Run: 4	Vehicle: Tarot X6-2	
	Desired (%)	Adequate (%)
Altitude	29.56	100.00
X Position	0.00	86.11
Y Position	48.66	100.00
Heading Angle	97.95	100.00

Pilot: 3	Task: Sidestep	
Run: 5	Vehicle: Tarot X6-2	
	Desired (%)	Adequate (%)
Altitude	100.00	100.00
X Position	96.77	100.00
Y Position	100.00	100.00
Heading Angle	93.92	100.00

Pilot: 3	Task: Sidestep	
Translation Alt. Hold	Vehicle: Tarot X6-2	
	Desired (%)	Adequate (%)
Altitude Run 1	70.98	100.00
Altitude Run 2	80.73	100.00
Altitude Run 3	86.83	100.00
Altitude Run 4	24.22	98.92
Altitude Run 5	100.00	100.00
Altitude Run 6	63.33	100.00

Pilot 3 Lateral Sidestep Direction Comparison Tarot X6-2		
	Desired (%)	Adequate (%)
AVG Right	78.70	96.28
AVG Left	62.27	97.87

Table 57: Lateral Sidestep MTE Pilot Performance Averages

Average Pilot Performance for Lateral Sidestep MTE								
	Altitude		Fore/Aft Position		Lateral Position		Heading Angle	
Pilot #	Desired	Adequate	Desired	Adequate	Desired	Adequate	Desired	Adequate
1	100.00	100.00	43.85	78.32	90.28	99.34	27.26	94.58
2	97.62	99.81	15.62	39.72	72.75	91.52	92.03	99.67
3	85.38	100.00	57.76	94.57	92.60	100.00	77.27	98.16
AVG	94.33	99.94	39.08	70.87	85.21	96.95	65.52	97.47

Average Pilot Performance for Lateral Sidestep MTE Using Tarot 650 Sport								
	Altitude		Fore/Aft Position		Lateral Position		Heading Angle	
Pilot #	Desired	Adequate	Desired	Adequate	Desired	Adequate	Desired	Adequate
1	100.00	100.00	43.85	78.32	90.28	99.34	27.26	94.58
2	96.78	99.63	8.82	30.36	56.24	84.27	88.62	99.35
3	98.51	100.00	69.54	98.58	98.80	100.00	77.20	98.58
AVG	98.43	99.88	40.74	69.09	81.78	94.53	64.36	97.50

Average Pilot Performance for Lateral Sidestep MTE Using Tarot 650 Sport without Pilot 1								
	Altitude		Fore/Aft Position		Lateral Position		Heading Angle	
Pilot #	Desired	Adequate	Desired	Adequate	Desired	Adequate	Desired	Adequate
1								
2	96.78	99.63	8.82	30.36	56.24	84.27	88.62	99.35
3	98.51	100.00	69.54	98.58	98.80	100.00	77.20	98.58
AVG	97.64	99.81	39.18	64.47	77.52	92.13	82.91	98.97

Average Pilot Performance for Lateral Sidestep MTE Using Tarot X6-2								
	Altitude		Fore/Aft Position		Lateral Position		Heading Angle	
Pilot #	Desired	Adequate	Desired	Adequate	Desired	Adequate	Desired	Adequate
1								
2	98.46	100.00	22.42	49.08	89.25	98.77	95.45	100.00
3	72.24	100.00	45.97	90.56	86.40	100.00	77.33	97.74
AVG	85.35	100.00	34.20	69.82	87.83	99.38	86.39	98.87

Average Pilot Performance for Altitude Hold Translation		
Vehicle	Desired (%)	Adequate (%)
Tarot 650 Sport	87.66	100.00
Tarot X6-2	85.51	99.91
Average	87.02	99.97

3. Left/Right Hover Performance

When capturing and hovering at the left and right hover boards at the ends of the Lateral Sidestep MTE course, there is a noticeable difference in performance as listed in Table 58, though it is not consistent between aircraft. This is surprising since the left hover board is 15 ft from the pilot and the right hover board is only 5 ft from the pilot, which one would think would make the left more difficult to cue from. However, when flying the Tarot X6-2, there is a 10% difference in the average performance of hovering at the left hover board as compared to the right, which reflects the perceived difficulty in precisely capturing and hovering this aircraft at a distance. There is only a 3% difference when flying the Tarot 650 Sport with capturing and hovering near the left hover having higher performance. This could be due to visual feedback and the faster dynamics of the smaller vehicle at close range compared to long range, but more data for more multi-rotor vehicles are needed to draw a confident conclusion.

Table 58: Left/Right Hover Performance Averages

Pilot Lateral Sidestep Direction Comparison Tarot 650 Sport			Pilot Lateral Sidestep Direction Comparison Tarot X6-2		
	Desired (%)	Adequate (%)		Desired (%)	Adequate (%)
AVG Right	70.40	88.71	AVG Right	78.40	91.59
AVG Left	73.36	92.34	AVG Left	68.49	92.45

Pilot Lateral Sidestep Direction Comparison		
	Desired (%)	Adequate (%)
AVG Right	73.60	89.86
AVG Left	71.41	92.38

c. Vertical Reposition MTE

For the Vertical Reposition MTE, the pilots were instructed to takeoff and stabilize in a hover for 5 seconds relative to a hover board placed 5 ft above the ground. The pilots were then instructed to fly the vehicle \geq 10 feet higher in altitude from the ground, the visual landmark for which was the top of the white portion of the large projector screen at the back of the AI. Due to the perspective of the pilot, this placed the aircraft \sim 10 ft above the ground. As such the requirement for the MTE was modified to 10 ft above the ground from the original 15 ft. The desired and adequate performance bounds relative to this point was kept the same. However, the altitude of the vehicle was highly influenced by the longitudinal position of the vehicle and the pilot's line of sight. Once at this altitude the pilot stabilized the vehicle in a hover for 5 seconds and then descended back to the original hover position (see example in Figure 195).

In general, the pilots executed the vertical reposition correctly and were able to return to the correct position in front of the lower hover board. This task appeared more difficult when flying the Tarot X6-2. Each pilot maintained precise control of the aircraft in the lateral plane, rarely straying beyond the desired bounds and never exiting the adequate bounds. However, as with the other tasks, maintaining a steady, accurate longitudinal position proved to be difficult, more so while flying the Tarot X6-2.

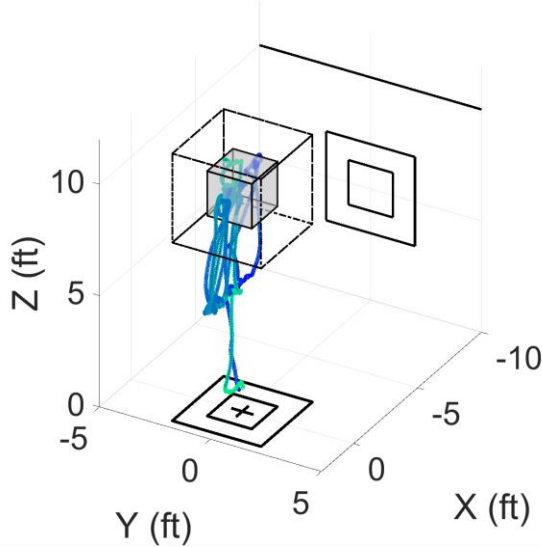


Figure 195: Tarot 650 Sport Vertical Reposition MTE, Pilot 1, Batch 1 – Inertial Position

1. Qualitative Individual Pilot Assessment

Pilot 1 consistently stayed within desired bounds for each Vertical Position MTE he performed. He had few lateral perturbations, barely moving to the left or right of the landing zone. He stabilized within the desired bounds during each of his 5 Vertical Reposition MTEs, although on his first and last runs, he overshot the peak altitude slightly. The ascent of the vehicle was usually accompanied by a slight forward movement, which was corrected during the descent of the vehicle.

Pilot 2 was generally unsteady while performing this MTE, though he did attain the desired altitudes. He had difficulty in maintaining the aircraft's longitudinal position with vertical movements often accompanied by an aft deviation and subsequent correction. The pilot had trouble capturing the peak altitude of 10 ft, often oscillating vertically about target point. This oscillation also occurred when capturing the lower altitude hover. However, he maintained lateral position precisely with only small deviations in either direction. Conversely, when flying the Tarot X6-2, the pilot precisely captured altitudes while exhibiting large aft deviations and maintaining a steady lateral position.

Pilot 3 performed 5 vertical repositions to varying degrees of success. With the Tarot 650 Sport, vertical maneuvers mostly remained within the desired bounds with some deviations into the adequate region. As with the other pilots, lateral motion was kept to a minimum. The two runs flown with the Tarot X6-2 showed very similar deviations in vertical and lateral position as compared to those flown with the Tarot 650 Sport. However, the vehicle deviated aft at takeoff and the pilot maintained the longitudinal position >5 ft behind the origin until landing. With both vehicles, Pilot 3 failed to attain the initial stabilized hover at 5 ft and instead steadily gained altitude. He also had difficulty capturing the hover at 5 ft, usually undershooting to hover above the desired bounds.

2. Performance

The performance metrics for each run are listed in Table 59 through Table 63 with the averages listed in Table 64. Odd numbered runs represent the hover at 5 feet, and even numbered runs represent the vertical reposition to 10 feet. Altitude performance was captured at each height. In general, the pilots were very capable at flying the vehicles within the desired bounds for altitude, latitude position, and heading angles with an average desired performance across all pilots and vehicles of 94.46% and 100% adequate performance. Two pilots were unable to meet desired longitudinal position with an average desired performance of 25.76% and adequate performance of 42.74%. However, these data are skewed by the excellent performance of Pilot 1. If Pilot 1's data are removed, the average desired performance is 0% and

the average adequate performance is 21.92%. This performance data is listed in Table 64. This maneuver overall seemed to have a larger impact on longitudinal position performance than the other maneuvers. For Pilots 2 and 3, this phenomenon occurred across the entire maneuver, both in the up and down vertical positions. Interestingly, for Pilot 1, aside from his first vertical reposition, was able to consistently maintain a desired longitudinal position in subsequent runs. However, during some of the repositions downward, he was unable or barely able maintain a desired position in the X direction. Much of the difficulty of the task for the pilots can be attributed to line of sight issues that worsen when flying a vehicle above eye level.

Table 59: Vertical Reposition MTE Performance – Pilot 1, Tarot 650 Sport

Pilot: 1	Task: Vertical	
Run: 1	Vehicle: Tarot 650 Sport	
	Desired (%)	Adequate (%)
Altitude	100.00	100.00
X Position	100.00	100.00
Y Position	100.00	100.00
Heading Angle	100.00	100.00

Pilot: 1	Task: Vertical	
Run: 2	Vehicle: Tarot 650 Sport	
	Desired (%)	Adequate (%)
Altitude	100.00	100.00
X Position	21.24	100.00
Y Position	100.00	100.00
Heading Angle	82.81	100.00

Pilot: 1	Task: Vertical	
Run: 3	Vehicle: Tarot 650 Sport	
	Desired (%)	Adequate (%)
Altitude	100.00	100.00
X Position	100.00	100.00
Y Position	100.00	100.00
Heading Angle	100.00	100.00

Pilot: 1	Task: Vertical	
Run: 4	Vehicle: Tarot 650 Sport	
	Desired (%)	Adequate (%)
Altitude	100.00	100.00
X Position	100.00	100.00
Y Position	100.00	100.00
Heading Angle	100.00	100.00

Pilot: 1	Task: Vertical	
Run: 5	Vehicle: Tarot 650 Sport	
	Desired (%)	Adequate (%)
Altitude	100.00	100.00
X Position	0.00	46.86
Y Position	100.00	100.00
Heading Angle	100.00	100.00

Pilot: 1	Task: Vertical	
Run: 6	Vehicle: Tarot 650 Sport	
	Desired (%)	Adequate (%)
Altitude	100.00	100.00
X Position	100.00	100.00
Y Position	100.00	100.00
Heading Angle	100.00	100.00

Pilot: 1	Task: Vertical	
Run: 7	Vehicle: Tarot 650 Sport	
	Desired (%)	Adequate (%)
Altitude	100.00	100.00
X Position	0.00	75.27
Y Position	100.00	100.00
Heading Angle	100.00	100.00

Pilot: 1	Task: Vertical	
Run: 8	Vehicle: Tarot 650 Sport	
	Desired (%)	Adequate (%)
Altitude	100.00	100.00
X Position	87.88	100.00
Y Position	100.00	100.00
Heading Angle	100.00	100.00

Pilot: 1	Task: Vertical	
Run: 9	Vehicle: Tarot 650 Sport	
	Desired (%)	Adequate (%)
Altitude	100.00	100.00
X Position	9.24	100.00
Y Position	100.00	100.00
Heading Angle	83.04	100.00

Pilot: 1	Task: Vertical	
Run: 10	Vehicle: Tarot 650 Sport	
	Desired (%)	Adequate (%)
Altitude	94.81	100.00
X Position	100.00	100.00
Y Position	100.00	100.00
Heading Angle	98.83	100.00

Pilot: 1	Task: Vertical	
Run: 11	Vehicle: Tarot 650 Sport	
	Desired (%)	Adequate (%)
Altitude	100.00	100.00
X Position	100.00	100.00
Y Position	100.00	100.00
Heading Angle	100.00	100.00

Table 60: Vertical Reposition MTE Performance – Pilot 2, Tarot 650 Sport

Pilot: 2	Task: Vertical	
Run: 1	Vehicle: Tarot 650 Sport	
	Desired (%)	Adequate (%)
Altitude	100.00	100.00
X Position	0.00	1.10
Y Position	100.00	100.00
Heading Angle	100.00	100.00

Pilot: 2	Task: Vertical	
Run: 2	Vehicle: Tarot 650 Sport	
	Desired (%)	Adequate (%)
Altitude	100.00	100.00
X Position	0.00	13.95
Y Position	100.00	100.00
Heading Angle	100.00	100.00

Pilot: 2	Task: Vertical	
Run: 3	Vehicle: Tarot 650 Sport	
	Desired (%)	Adequate (%)
Altitude	100.00	100.00
X Position	68.83	89.15
Y Position	100.00	100.00
Heading Angle	97.58	100.00

Pilot: 2	Task: Vertical	
Run: 4	Vehicle: Tarot 650 Sport	
	Desired (%)	Adequate (%)
Altitude	100.00	100.00
X Position	0.00	41.16
Y Position	100.00	100.00
Heading Angle	100.00	100.00

Pilot: 2	Task: Vertical	
Run: 5	Vehicle: Tarot 650 Sport	
	Desired (%)	Adequate (%)
Altitude	100.00	100.00
X Position	22.00	33.40
Y Position	100.00	100.00
Heading Angle	100.00	100.00

Pilot: 2	Task: Vertical	
Run: 6	Vehicle: Tarot 650 Sport	
	Desired (%)	Adequate (%)
Altitude	100.00	100.00
X Position	0.00	0.00
Y Position	100.00	100.00
Heading Angle	100.00	100.00

Pilot: 2	Task: Vertical	
Run: 7	Vehicle: Tarot 650 Sport	
	Desired (%)	Adequate (%)
Altitude	100.00	100.00
X Position	30.47	59.71
Y Position	100.00	100.00
Heading Angle	100.00	100.00

Table 61: Vertical Reposition MTE Performance – Pilot 3, Tarot 650 Sport

Pilot: 3	Task: Vertical	
Run: 1	Vehicle: Tarot 650 Sport	
	Desired (%)	Adequate (%)
Altitude	55.67	90.31
X Position	0.00	20.80
Y Position	100.00	100.00
Heading Angle	87.39	100.00

Pilot: 3	Task: Vertical	
Run: 2	Vehicle: Tarot 650 Sport	
	Desired (%)	Adequate (%)
Altitude	83.87	100.00
X Position	0.00	0.00
Y Position	72.09	100.00
Heading Angle	100.00	100.00

Pilot: 3	Task: Vertical	
Run: 3	Vehicle: Tarot 650 Sport	
	Desired (%)	Adequate (%)
Altitude	75.14	100.00
X Position	0.00	2.77
Y Position	100.00	100.00
Heading Angle	100.00	100.00

Pilot: 3	Task: Vertical	
Run: 4	Vehicle: Tarot 650 Sport	
	Desired (%)	Adequate (%)
Altitude	92.73	100.00
X Position	0.00	72.68
Y Position	100.00	100.00
Heading Angle	94.00	100.00

Pilot: 3	Task: Vertical	
Run: 5	Vehicle: Tarot 650 Sport	
	Desired (%)	Adequate (%)
Altitude	91.40	100.00
X Position	0.00	69.85
Y Position	100.00	100.00
Heading Angle	100.00	100.00

Pilot: 3	Task: Vertical	
Run: 6	Vehicle: Tarot 650 Sport	
	Desired (%)	Adequate (%)
Altitude	100.00	100.00
X Position	0.00	100.00
Y Position	100.00	100.00
Heading Angle	99.33	100.00

Pilot: 3	Task: Vertical	
Run: 7	Vehicle: Tarot 650 Sport	
	Desired (%)	Adequate (%)
Altitude	100.00	100.00
X Position	0.00	24.80
Y Position	100.00	100.00
Heading Angle	100.00	100.00

Table 62: Vertical Reposition MTE Performance – Pilot 2, Tarot X6-2

Pilot: 2	Task: Vertical	
Run: 1	Vehicle: Tarot X6-2	
	Desired (%)	Adequate (%)
Altitude	100.00	100.00
X Position	15.63	35.96
Y Position	100.00	100.00
Heading Angle	97.21	100.00

Pilot: 2	Task: Vertical	
Run: 2	Vehicle: Tarot X6-2	
	Desired (%)	Adequate (%)
Altitude	99.07	100.00
X Position	0.00	13.31
Y Position	100.00	100.00
Heading Angle	99.72	100.00

Pilot: 2	Task: Vertical	
Run: 3	Vehicle: Tarot X6-2	
	Desired (%)	Adequate (%)
Altitude	93.44	100.00
X Position	11.32	16.32
Y Position	100.00	100.00
Heading Angle	92.68	100.00

Pilot: 2	Task: Vertical	
Run: 4	Vehicle: Tarot X6-2	
	Desired (%)	Adequate (%)
Altitude	93.46	100.00
X Position	0.00	0.00
Y Position	100.00	100.00
Heading Angle	47.69	99.97

Pilot: 2	Task: Vertical	
Run: 5	Vehicle: Tarot X6-2	
	Desired (%)	Adequate (%)
Altitude	88.35	100.00
X Position	0.00	0.00
Y Position	100.00	100.00
Heading Angle	91.96	100.00

Pilot: 2	Task: Vertical	
Run: 6	Vehicle: Tarot X6-2	
	Desired (%)	Adequate (%)
Altitude	86.81	100.00
X Position	0.00	0.00
Y Position	90.66	100.00
Heading Angle	94.31	100.00

Pilot: 2	Task: Vertical	
Run: 7	Vehicle: Tarot X6-2	
	Desired (%)	Adequate (%)
Altitude	92.53	100.00
X Position	0.00	4.35
Y Position	81.79	100.00
Heading Angle	89.44	99.56

Table 63: Vertical Reposition MTE Performance – Pilot 3, Tarot X6-2

Pilot: 3	Task: Vertical	
Run: 1	Vehicle: Tarot X6-2	
	Desired (%)	Adequate (%)
Altitude	23.76	75.78
X Position	0.00	8.67
Y Position	100.00	100.00
Heading Angle	100.00	100.00

Pilot: 3	Task: Vertical	
Run: 2	Vehicle: Tarot X6-2	
	Desired (%)	Adequate (%)
Altitude	64.69	100.00
X Position	0.00	0.00
Y Position	100.00	100.00
Heading Angle	87.25	100.00

Pilot: 3	Task: Vertical	
Run: 3	Vehicle: Tarot X6-2	
	Desired (%)	Adequate (%)
Altitude	65.84	100.00
X Position	0.00	0.00
Y Position	75.94	100.00
Heading Angle	97.42	100.00

Pilot: 3	Task: Vertical	
Run: 4	Vehicle: Tarot X6-2	
	Desired (%)	Adequate (%)
Altitude	30.91	100.00
X Position	0.00	0.00
Y Position	100.00	100.00
Heading Angle	99.95	100.00

Pilot: 3	Task: Vertical	
Run: 5	Vehicle: Tarot X6-2	
	Desired (%)	Adequate (%)
Altitude	93.63	100.00
X Position	0.00	0.00
Y Position	100.00	100.00
Heading Angle	100.00	100.00

Table 64: Vertical Reposition MTE Pilot Performance Averages

Average Pilot Performance for Vertical Reposition MTE								
	Altitude		Fore/Aft Position		Lateral Position		Heading Angle	
Pilot #	Desired	Adequate	Desired	Adequate	Desired	Adequate	Desired	Adequate
1	99.53	100.00	65.31	92.92	100.00	100.00	96.79	100.00
2	96.69	100.00	10.59	22.03	98.03	100.00	93.61	99.97
3	70.65	99.31	0.00	20.78	95.60	100.00	97.09	100.00
AVG	88.96	99.77	25.30	45.24	97.88	100.00	95.83	99.99

Average Pilot Performance for Vertical Reposition MTE Using Tarot 650 Sport								
	Altitude		Fore/Aft Position		Lateral Position		Heading Angle	
Pilot #	Desired	Adequate	Desired	Adequate	Desired	Adequate	Desired	Adequate
1	99.53	100.00	65.31	92.92	100.00	100.00	96.79	100.00
2	100.00	100.00	17.33	34.07	100.00	100.00	99.65	100.00
3	85.54	98.62	0.00	41.56	96.01	100.00	97.25	100.00
AVG	95.02	99.54	27.54	56.18	98.67	100.00	97.90	100.00

Average Pilot Performance for Vertical Reposition MTE Using Tarot 650 Sport w/o Pilot 1								
	Altitude		Fore/Aft Position		Lateral Position		Heading Angle	
Pilot #	Desired	Adequate	Desired	Adequate	Desired	Adequate	Desired	Adequate
1								
2	100.00	100.00	17.33	34.07	100.00	100.00	99.65	100.00
3	85.54	98.62	0.00	41.56	96.01	100.00	97.25	100.00
AVG	92.77	99.31	8.66	37.81	98.01	100.00	98.45	100.00

Average Pilot Performance for Vertical Reposition MTE Using Tarot X6-2								
	Altitude		Fore/Aft Position		Lateral Position		Heading Angle	
Pilot #	Desired	Adequate	Desired	Adequate	Desired	Adequate	Desired	Adequate
1								
2	93.38	100.00	3.85	9.99	96.06	100.00	87.57	99.93
3	55.76	100.00	0.00	0.00	95.19	100.00	96.92	100.00
AVG	74.57	100.00	1.92	5.00	95.63	100.00	92.25	99.97

d. Landing MTE

To execute the Landing MTE, the pilots were instructed to fly the vehicle above 10 ft, then gently land the vehicle at the same spot from which they took off, minimizing lateral and longitudinal deviations (see example in Figure 196). They were also required to limit vertical velocity at touchdown to ≤ 2 ft/s. Each pilot executed this MTE three or four times per vehicle. There was no requirement to capture or maintain a certain altitude as the focus was on the landing position.

Each pilot had few or no problems maintaining lateral position with the vehicle, as expected considering the favorable line of sight. However, the pilots generally had issues maintaining the aircraft's longitudinal positions with many runs exhibiting large excursions upwards of 10 ft from the landing zone. Although

each individual run featured at least an adequate touchdown vertical velocity, the pilots did have some difficulty in touching down with a vertical velocity below 2 ft/s.

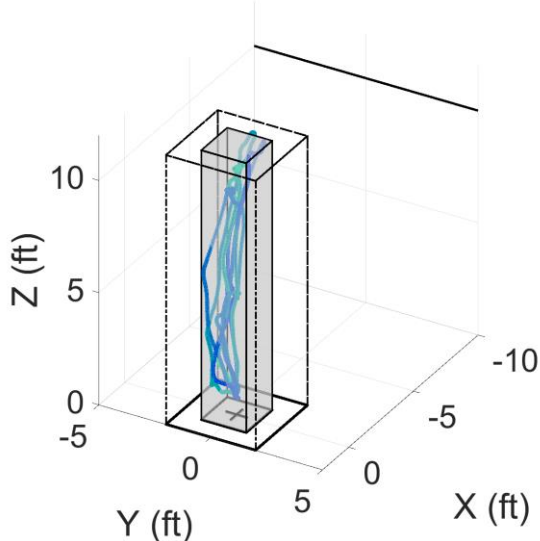


Figure 196: Tarot 650 Sport Landing MTE, Pilot 1, Batch 1 – Inertial Position

1. Qualitative Individual Pilot Assessment

Pilot 1 achieved at least adequate performance for each of his four landings. His only major excursion beyond the desired bounds was a touchdown vertical velocity that slightly exceeded 2 ft/s. For each individual Landing MTE, Pilot 1 flew the vehicle above the task definition recommendation of 10 ft before descending to land. He better maintained longitudinal position as compared to the other MTEs and never strayed more than 2 ft in any direction from the landing zone center. The only performance measure in any of the runs to not qualify as desired performance was the second landing that had a vertical velocity at touchdown just above 2 ft/s.

Pilot 2 performed three landings for each vehicle; however, no data was recorded for him flying this MTE with the Tarot 650 Sport. The video of the flight shows these maneuvers and gives some idea of his performance flying this MTE with the Tarot 650 Sport. There are signs of deviations in both lateral and longitudinal position, such as during the second landing in which the vehicle moved towards the camera and to the right landing outside of the front left corner of the landing zone. As the vehicle landed, it bounced multiple times, indicating that vertical velocity was not ideal. His performance improves with the Tarot X6-2 with all landings inside the landing zone. Pilot 2 maintained a consistent lateral position and tended to fly the vehicle aft while ascending before correcting for the landing with the occasional overcorrection forward.

Pilot 3 was competent flying the MTE with the Tarot 650 Sport but struggled with the Tarot X6-2. With the Tarot 650 Sport, he performed the Landing MTE three times with minimal lateral deviation and with longitudinal deviations after during the ascent that was corrected before landing. With the Tarot X6-2, this MTE proved to be a challenging task with the first run resulting in a longitudinal excursion aft over 15 ft and a failed correction attempt that culminated in a landing 7 ft from the landing zone center. Much improvement was shown in the next two runs with a still present but less severe longitudinal excursion aft of 10 ft. In these two runs the excursion was successfully corrected, and the pilot landed the vehicle close to the landing zone center. In the first two runs, touchdown vertical velocity exceeded 2 ft/s, but it was within the desired bounds in the final landing run.

2. Performance

The performance metrics for each run are listed in Table 65 through Table 68 with the averages listed in Table 69. For this maneuver, pilots had no altitude requirements but instead had to attempt to land with a touchdown of less than 2 fps. The pilots generally excelled in controlling lateral position and heading angle for both vehicles with high desired performance. The measure with the lowest and highest desired performance was lateral position with Tarot X6-2 of 70.43% and lateral position with the Tarot 650 Sport of 100%, respectively. The adequate performance for both vehicles in lateral position and heading angle was $\geq 95\%$. This high performance for lateral position and heading angle indicate that it was easy for the pilots to control these states performing this MTE.

Controlling the vertical velocity when landing was difficult for the pilots with both vehicles. Since the performance assessment of landing vertical velocity is a discrete metric in which the pilot had Desired, Adequate, or Failed performance, a performance between 0-100% is irrelevant. However, to keep a consistent format and to be more easily compared to the other MTE performance measures, a percent desired/adequate performance was assigned. If the landing vertical velocity was within the desired bounds, the metric was assigned a 100% desired performance and 100% adequate performance. If the landing vertical velocity was outside the desired bounds but within the adequate bounds, the metric was assigned a 0% desired performance and 100% adequate performance. Finally, if the landing vertical velocity was beyond the adequate bounds, the metric was assigned a 0% desired performance and 0% adequate performance. Averaging these assigned values results in the performance averages listed in Table 24.

On average across both vehicles, the pilots only met the desired landing vertical velocity requirements 36.11% of the time but were always able meet the adequate requirements. This low desired performance measure is a direct result of the complete failure of Pilot 2 and Pilot 3 meeting the desired requirement when flying this MTE with the Tarot X6-2. There was no data recorded for Pilot 2 flying this MTE with the Tarot 650 Sport, but Pilot 3's data for the two aircraft can be compared. Pilot 3 met the desired requirements when flying the Tarot 650 Sport 66.67% of the time, suggesting the Tarot X6-2 was more difficult than the Tarot 650 Sport to land slowly.

Longitudinal position once again showed poor performance. The Tarot X6-2 had the lowest average for desired longitudinal position at just 20.74% while the Tarot 650 Sport had a still low desired performance of 53.85%. This implies that maintaining longitudinal position was easier for the Tarot 650 Sport than the Tarot X6-2, but there is not enough data to draw a meaningful conclusion.

Table 65: Landing MTE Performance – Pilot 1, Tarot 650 Sport

Pilot: 1	Task: Landing	
Run: 1	Vehicle: Tarot 650 Sport	
	Desired (%)	Adequate (%)
Landing Speed	100.00	100.00
X Position	79.31	100.00
Y Position	100.00	100.00
Heading Angle	95.45	100.00

Pilot: 1	Task: Landing	
Run: 2	Vehicle: Tarot 650 Sport	
	Desired (%)	Adequate (%)
Landing Speed	0.00	100.00
X Position	87.39	100.00
Y Position	100.00	100.00
Heading Angle	91.32	100.00

Pilot: 1	Task: Landing	
Run: 3	Vehicle: Tarot 650 Sport	
	Desired (%)	Adequate (%)
Landing Speed	100.00	100.00
X Position	69.69	100.00
Y Position	100.00	100.00
Heading Angle	97.92	100.00

Pilot: 1	Task: Landing	
Run: 4	Vehicle: Tarot 650 Sport	
	Desired (%)	Adequate (%)
Landing Speed	100.00	100.00
X Position	100.00	100.00
Y Position	100.00	100.00
Heading Angle	93.78	100.00

Table 66: Landing MTE Performance – Pilot 3, Tarot 650 Sport

Pilot: 3	Task: Landing	
Run: 1	Vehicle: Tarot 650 Sport	
	Desired (%)	Adequate (%)
Landing Speed	100.00	100.00
X Position	28.10	49.90
Y Position	100.00	100.00
Heading Angle	91.43	98.28

Pilot: 3	Task: Landing	
Run: 2	Vehicle: Tarot 650 Sport	
	Desired (%)	Adequate (%)
Landing Speed	0.00	100.00
X Position	25.96	42.64
Y Position	100.00	100.00
Heading Angle	64.97	94.67

Pilot: 3	Task: Landing	
Run: 3	Vehicle: Tarot 650 Sport	
	Desired (%)	Adequate (%)
Landing Speed	100.00	100.00
X Position	16.76	43.04
Y Position	100.00	100.00
Heading Angle	76.23	96.86

Table 67: Landing MTE Performance – Pilot 2, Tarot X6-2

Pilot: 2	Task: Landing	
Run: 1	Vehicle: Tarot X6-2	
	Desired (%)	Adequate (%)
Landing Speed	0.00	100.00
X Position	34.93	47.47
Y Position	78.08	100.00
Heading Angle	100.00	100.00

Pilot: 2	Task: Landing	
Run: 2	Vehicle: Tarot X6-2	
	Desired (%)	Adequate (%)
Landing Speed	0.00	100.00
X Position	34.00	49.79
Y Position	91.69	100.00
Heading Angle	83.15	100.00

Pilot: 2	Task: Landing	
Run: 3	Vehicle: Tarot X6-2	
	Desired (%)	Adequate (%)
Landing Speed	0.00	100.00
X Position	24.95	38.89
Y Position	84.89	100.00
Heading Angle	73.27	98.06

Table 68: Landing MTE Performance – Pilot 3, Tarot X6-2

Pilot: 3	Task: Landing	
Run: 1	Vehicle: Tarot X6-2	
	Desired (%)	Adequate (%)
Landing Speed	0.00	100.00
X Position	5.78	6.59
Y Position	47.14	84.63
Heading Angle	83.01	98.43

Pilot: 3	Task: Landing	
Run: 2	Vehicle: Tarot X6-2	
	Desired (%)	Adequate (%)
Landing Speed	100.00	100.00
X Position	13.77	21.11
Y Position	64.29	96.05
Heading Angle	91.25	100.00

Pilot: 3	Task: Landing	
Run: 3	Vehicle: Tarot X6-2	
	Desired (%)	Adequate (%)
Landing Speed	100.00	100.00
X Position	11.02	19.25
Y Position	56.49	89.51
Heading Angle	66.85	86.49

Table 69: Landing MTE Pilot Performance Average

Average Pilot Performance for Landing MTE									
	Landing Speed		Fore/Aft Position		Lateral Position		Heading Angle		
Pilot #	Desired	Adequate	Desired	Adequate	Desired	Adequate	Desired	Adequate	
1	75.00	100.00	84.10	100.00	100.00	100.00	94.62	100.00	
2	0.00	100.00	31.30	45.38	84.89	100.00	85.48	99.35	
3	33.33	100.00	16.90	30.42	77.99	95.03	78.96	95.79	
AVG	36.11	100.00	44.10	58.60	87.63	98.34	86.35	98.38	

Average Pilot Performance for Landing MTE Using Tarot 650 Sport									
	Landing Speed		Fore/Aft Position		Lateral Position		Heading Angle		
Pilot #	Desired	Adequate	Desired	Adequate	Desired	Adequate	Desired	Adequate	
1	75.00	100.00	84.10	100.00	100.00	100.00	94.62	100.00	
2									
3	66.67	100.00	23.61	45.19	100.00	100.00	77.54	96.60	
AVG	70.83	100.00	53.85	72.60	100.00	100.00	86.08	98.30	

Average Pilot Performance for Landing MTE Using Tarot X6-2									
	Landing Speed		Fore/Aft Position		Lateral Position		Heading Angle		
Pilot #	Desired	Adequate	Desired	Adequate	Desired	Adequate	Desired	Adequate	
1									
2	0.00	100.00	31.30	45.38	84.89	100.00	85.48	99.35	
3	0.00	100.00	10.19	15.65	55.97	90.06	80.37	94.97	
AVG	0.00	100.00	20.74	30.52	70.43	95.03	82.92	97.16	

e. Heading Performance

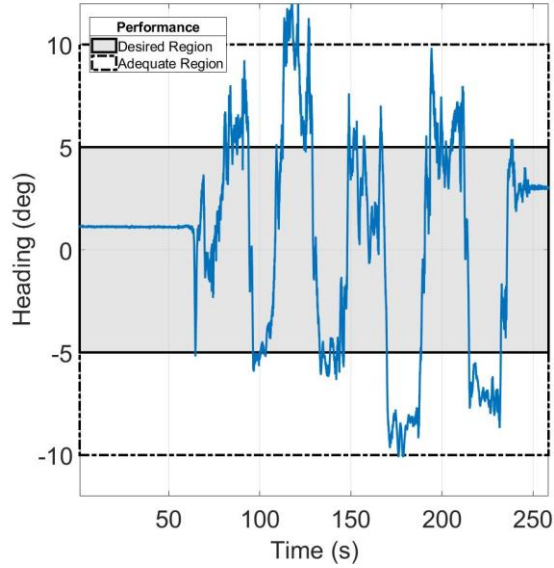
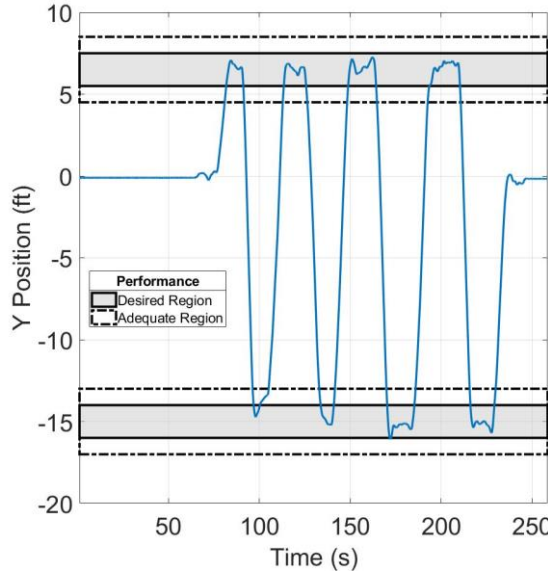
As listed in Table 70, heading angle performance during the Lateral Sidestep MTE were lower than any other maneuvers with a desired performance a full 13% lower than the next lowest performance, that for the Landing MTE.

Table 70: Heading Angle Performance Averages

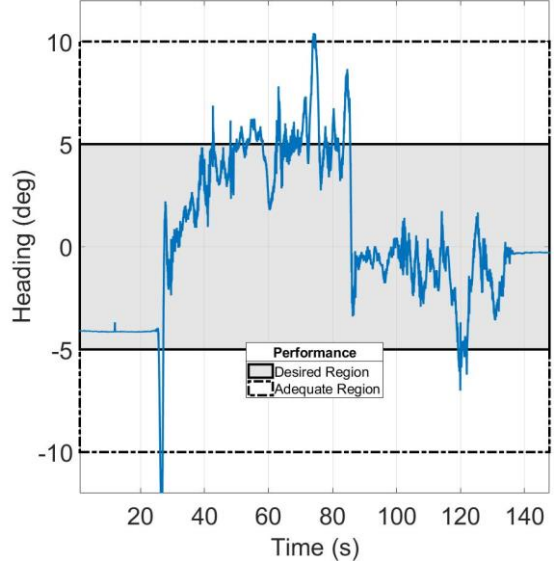
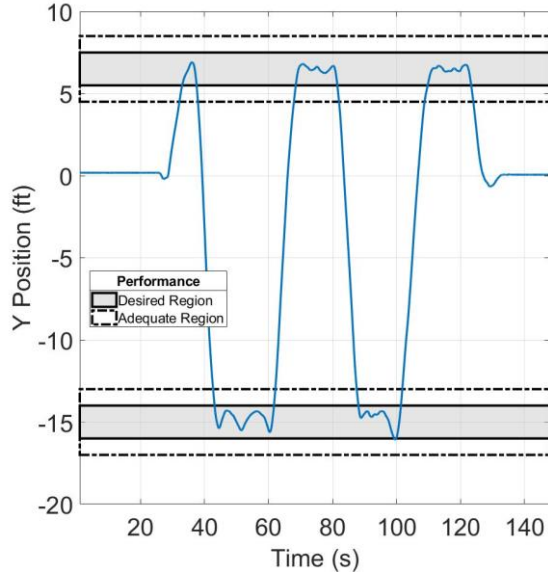
	Desired	Adequate
Precision Hover	88.33	96.97
Lateral Sidestep	72.09	97.95
Vertical Reposition	93.83	100.00
Landing	85.12	97.95

This large difference was largely caused by Pilot 1's performance of the Lateral Sidestep MTE. Pilot 1's average desired performance for heading angle was 27.26% while the combined average of Pilot 2 and Pilot 3 was 82.91%, as shown in Table 12. Pilot 1 consistently performs better than the other two pilots

for all other performance measures across all the MTEs. This failure at maintaining heading angle is an anomaly if just comparing the quantitative performance of the pilots. However, investigating qualitative performance through the correlation of lateral position and heading angle for Pilot 1 for the Lateral Sidestep MTE (see Figure 197) sheds some light this anomaly.



a) Pilot 1



b) Pilot 3

Figure 197: Juxtaposition of Heading Angle and Lateral Position

As shown in Figure 197a, Pilot 1 has a clear tendency of skewing the heading angle of the vehicle during the lateral travel of the vehicle and holding that angle during the hover. In Figure 197b, Pilot 3 shows no piloting tendency and maintains the vehicle heading relatively constant throughout. This correlation suggests Pilot 1 either did not understand the requirements and actively maneuvered in this manner to perform the MTE or he was skewing the heading unconsciously and did not realize that he needed to correct for heading.

4. Pilot Responses

After completing all four MTEs with the checkout vehicle, each piloted answered a debrief questionnaire the results of which are presented in Figure 198. The three pilots all agreed or strongly agreed that the MTEs were representative of an operational task element, well defined, and repeatable and easy to perform. They also agreed or strongly agreed that the MTEs had entry/exit conditions that were easy to establish and had course markers that were easy to follow. All agreed or strongly agreed that the MTEs effectively exposed aircraft characteristics and that the MTEs were valid for defining nominal performance. Note that one exception was that Pilot 3 neither agreed nor disagreed that the precision hover task was valid for defining nominal performance.

D. CONCLUSIONS

The purpose of this flight test was to determine the effectiveness of the mission task element (MTE) approach as a means to define sUAS nominal performance. The MTEs evaluated in the test program were precision hover, lateral sidestep, vertical reposition, and landing. From the qualitative results that included video recordings of each maneuver and pilot debrief questionnaires and the quantitative task performance results from the Vicon data, it was clearly demonstrated that the MTEs met the defined objectives. The main improvement necessary based on pilot feedback and evidence from the Vicon data is a visual marker to make it easier for pilots to determine their longitudinal fore/aft position. Otherwise the pilots proved capable of performing each task at least adequately, with less than adequate results caused mainly by pilot error, not the MTE requirements.

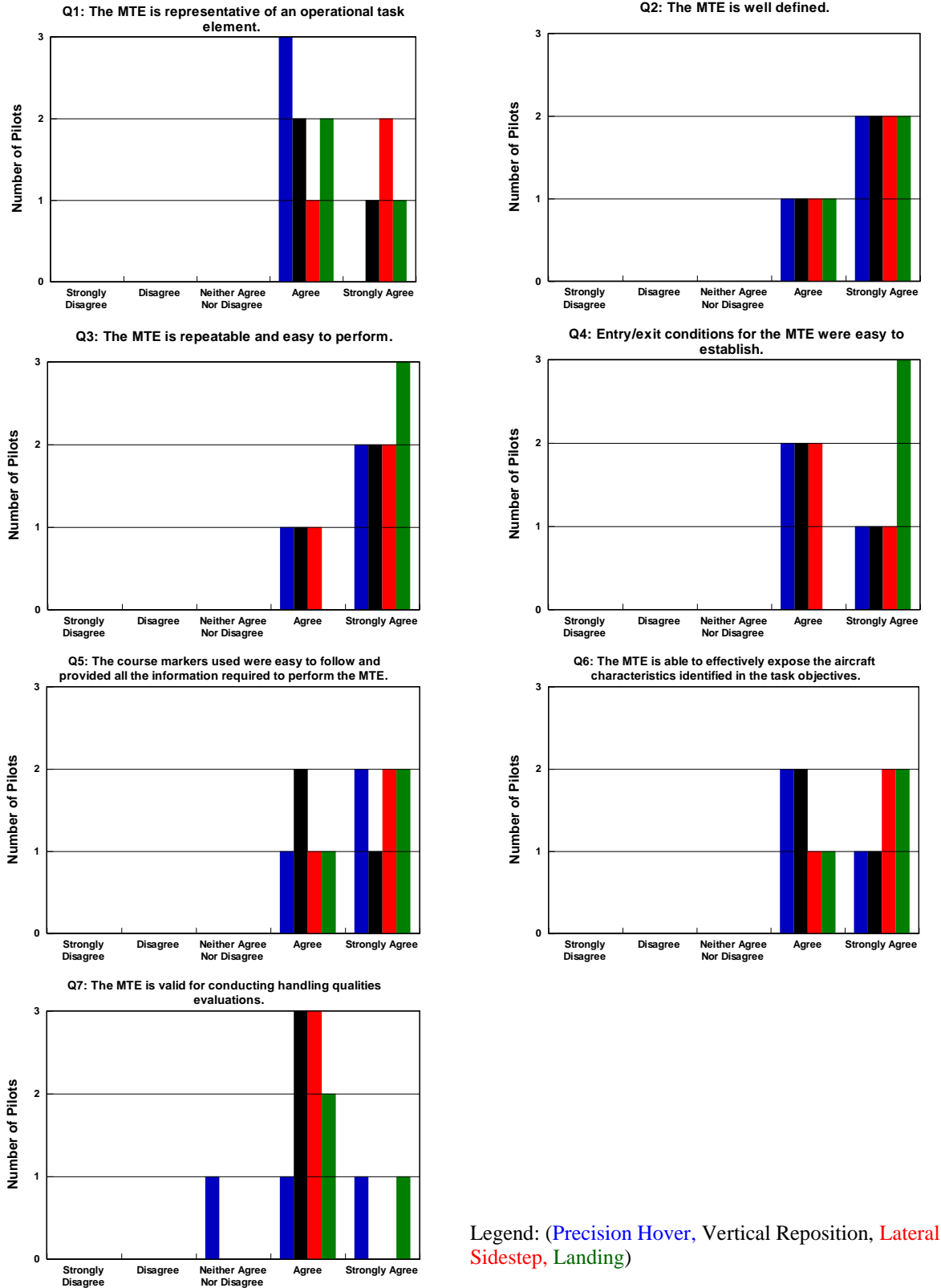


Figure 198: Debrief Questionnaire Results

REFERENCES

49. Belcastro, C. M., D. H. Klyde, M. J. Logan, R. L. Newman, and J. V. Foster, "Experimental Aircraft Testing for Assessing the Safety of Unmanned Aircraft System Safety-Critical Operations," AIAA-2017-3274 presented at the *AIAA Aviation Forum: 17th AIAA Aviation Technology, Integration, and Operations Conference*, Denver, CO, 5-9 June 2017.

Appendix E – Exploration of Dynamic Scaling

A. INTRODUCTION

For piloted vehicles, there is decades of work to draw upon when assessing handling qualities (Ref. 50). It would be beneficial to the definition of handling qualities for UAS if elements of the piloted vehicle work could be transitioned to UAS, especially the sUAS that are of interest in this program. To this end, this working paper provides a way to compare dynamic modes of standard fixed wing, manned aircraft to that of small UAS. The comparison is done by scaling down a given manned aircraft using techniques that have been developed to carry out scaled model test flights for different aircraft designs (Refs. 51 and 52). This comparison supplements the work done in the area of UAS handling qualities as part of this NASA program. Furthermore, the scaling up of the sUAS dynamic characteristics was also explored.

Handling qualities quantities including the Control Anticipation Parameter (CAP) and Aircraft Bandwidth are computed for the longitudinal dynamics and Aircraft Bandwidth for the lateral-directional dynamics for the UltraStick120 UAS belonging to UAV laboratory at the University of Minnesota (UMN). The dynamic model was provided by UMN, and modal requirements were computed for the open-loop, Aircraft Bandwidth parameters were computed for the closed-loop. For definitions of these parameters, see the above-referenced working paper.

Since there is no database or compendium available that provides an acceptable range within which these parameters should fall for small UAS (sUAS), it is difficult to evaluate the handling qualities in terms of these traditional parameters. Therefore, in an effort to assess the handling qualities of UltraStick120, this working paper attempts to ‘scale down’ the parameters corresponding to a full-scale aircraft – the Cessna 172. The model for the Cessna 172 is taken from Ref. 53. The dynamics of the Cessna 172 are considered a benchmark for this analysis, and therefore the dynamics of its scaled version may therefore be compared to UltraStick120. As shown in later sections, the UltraStick120 is determined at 22% scale of the Cessna 172. Since the size, mass properties and flight conditions for the large-scale aircraft is very different from that of the UltraStick120, dynamic scaling has to be carried out as described in the sections ahead.

Besides comparing the dynamics of UltraStick120 to that of the scaled version of Cessna 172, a comparison is also made within the UltraStick family of sUAS. UMN also provides the dynamic model for the UltraStick25e, which is a 66% scaled model of the UltraStick120. Thus, the availability of this model is used to provide a validation or ‘sanity check’ for this analysis. The logic here is that if the scaled Cessna dynamics do not compare favorably with UltraStick120, but the 120 and 25e compare well within themselves, it may be concluded that the differences between the Cessna and UltraStick platforms are due to different dynamics rather than flawed scaling process. To summarize, dynamics of Cessna 172 are scaled down to 22% of the original values and compared to those of UltraStick120; separately, UltraStick120 dynamics are scaled down 60% and compared to UltraStick25e as a validation/sanity check step.

An alternate approach for evaluating the handling qualities of the UltraStick120 and 25e is also presented, where instead of scaling down the Cessna 172, dynamics of the UltraStick UAVs are scaled up. This is done to take advantage of existing handling qualities performance standards and requirements that have been established for Cessna-class aircraft. By scaling up different modal quantities of the UltraStick UAVs, a direct evaluation using the established standards is possible. This analysis is also presented in the following sections.

B. FROUDE SCALING FOR DYNAMIC SIMILITUDE

Since small-scaled models are often used to test different aircraft designs, they need to be built specifically to ensure so-called dynamic similitude. Dynamic similitude essentially means similar angular displacement and relative movement of different components after proportional amount of time between the scaled and actual aircraft. Unless scaled properly, test results from a scaled model does not provide any meaningful insights into the expected performance of the large-scale model. The scaling technique used for this purpose is called the Froude scaling.

Since the motion of an aircraft is dependent on its mass properties as well as flight conditions, the scaled models must feature properly scaled mass properties and must be flown in appropriate flight conditions. Assuming the linear scaling factor between an aircraft and its scaled model to be n ($n < 1$), Table 71 provides the scaling factors of relevant quantities at sea-level. Here, σ stands for the ratio of air density at flight condition to that of sea level.

Table 71: Froude Scaling Factors for Scaled Models

Property	Scaling Factor
Linear Dimension	n
Area	n^2
Weight/Mass	n^3/σ
Moment of Inertia	n^5/σ
Linear Velocity	$n^{1/2}$
Relative Density ($m/\rho L^3$)	1
Time	$n^{1/2}$

Before comparing the dynamics of the UltraStick120 and the scaled version of the Cessna 172, validity of this exercise is checked by looking at the mass properties of the two aircraft. A good match between the mass properties of the UltraStick120 and scaled Cessna 172 indicates that Froude-scaled dynamics of the Cessna 172 will provide a reasonable benchmark for the UltraStick120.

Since aspect ratios of the Cessna 172 differs from that of the UltraStick120, wingspan comparison of the two aircraft reveals a scaling factor of $n_s = 0.176$, while the mean chord-based comparison gives a scaling factor of $n_c = 0.27$. For this analysis, the scaling factor is assumed to be the average of these two values, i.e., $n = 0.22$. Furthermore, the Cessna 172 model available is for straight and level flight at an altitude of 5000 ft (i.e., $\sigma = 0.85$) and an airspeed of 219 ft/s. These flight conditions are kept in mind for scaling purposes. The scaled mass properties of the Cessna 172 to the UltraStick120 are compared in Table 72 to see how close the Froude-scaled Cessna 172 is to the UltraStick120.

Table 72: Comparison of UltraStick120 to the Froude-Scaled Cessna 172

Property	Cessna 172	22% Scaled Cessna 172	UltraStick120	Difference
Mass (Kg)	1150.72	10.66	6-10 (nominal 7.411)	43.84%
I_{xx} (Kg m ²)	1285.3	0.768	0.857	10.4%
I_{yy} (Kg m ²)	1824.9	1.092	1.01	7.33%
I_{zz} (Kg m ²)	2666.9	1.594	1.701	6.24%

From Table 72 we can see that although the Froude-scaled mass of Cessna 172 is substantially more than that of the nominal mass of UltraStick120, the inertia properties match up very well. However, the maximum allowable mass of UltraStick120 matches closely to that of the Cessna 172 scaled value, which is encouraging. A number of factors such as payloads, absence of passenger weight, etc. can account for variations in overall mass.

To further validate this scaling method for comparing the dynamics of different-sized aircraft the dynamics of the UltraStick25e, which is a 60% scaled model of UltraStick120 and whose models are available from UMN, was compared to the scaled-down values obtained from the UltraStick120. The comparison of mass properties is shown in Table 73 below.

Table 73: Mass properties comparison between UltraStick120 and 25e

Property	UltraStick120 Scaled 60%	UltraStick25e
Mass (Kg)	1.87	1.96
I _{xx} (Kg m ²)	0.0777	0.0715
I _{yy} (Kg m ²)	0.0916	0.864
I _{zz} (Kg m ²)	0.154	0.153

The mass properties for the 60% scaled UltraStick120 model align very well with those of UltraStick25e. Therefore, when comparing the dynamics of the Cessna 172 and UltraStick120, a comparison between 120 and 25e will also be made to check whether the dynamics scale properly. This serves as an additional verification of the scaling procedure working as expected.

From Table 71, time is scaled by a multiplication factor of $n^{1/2}$. Consequently, frequency associated with any dynamic motion has to be scaled by $n^{-1/2}$. This is the key factor used to obtain Froude-scaled frequencies for different modes for the Cessna 172 aircraft.

C. FROUDE-SCALED DYNAMICS

The dynamics of UltraStick120 is compared with the Cessna 172 aircraft, after scaling down the Cessna 172 to the scale of the UltraStick120. For the Froude scaling to be satisfied, equivalent flight conditions must be ensured. Since the Cessna 172 model is available at straight and level flight, altitude 5000 ft and airspeed 219 ft/s, the airspeed for the scaled model at sea-level has to be computed according to Table 71, which works out to be 31.3 m/s. For a proper comparison, the bandwidth values for the UltraStick120 must be recomputed at this airspeed.

In addition, to compare the scaled down dynamics of UltraStick120 at 31.3 m/s to that of 25e, the scaled down airspeed of UltraStick25e comes out to be 24.25 m/s. Both longitudinal and lateral-directional dynamics are discussed in the following sub-sections.

1. Longitudinal Dynamics

The transfer function from elevator (δ_e) to pitch angle (θ) for the Cessna 172 is given as,

$$\frac{\theta}{\delta_e} = \frac{-39.42(0.0597)(2.044)}{[0.116, 0.181][0.685, 6.03]} \quad (4)$$

a. Longitudinal Modes Comparison

We also compare the damping and frequencies of phugoid and short period modes for the Cessna 172 scaled model and the UltraStick120.

Table 74: Modal Frequencies and Damping Comparison (Long.)

Aircraft	Phugoid		Short Period	
	Damping	Frequency	Damping	Frequency
Cessna 172	0.116	0.181	0.685	6.03
Cessna 172 scaled 22%	0.116	0.386	0.685	12.85
UltraStick120	0.246	0.396	0.76	12.8

We can see from Table 74 that the frequencies match very well between the scaled values of Cessna 172 and the UltraStick120. The damping for Phugoid mode does not match as closely as that for the short

period mode. Nevertheless, it may be concluded that the longitudinal dynamics of the UltraStick120 meets the benchmark values set by the scaled Cessna 172 aircraft.

In addition, we also compare the longitudinal modes of 60% scaled UltraStick120 and the UltraStick25e, as shown in Table 75. The comparison is very close, which is encouraging.

Table 75: Modal Frequencies and Damping Comparison (Long.), 120 & 25e

Aircraft	Phugoid		Short Period	
	Damping	Frequency	Damping	Frequency
UltraStick120, scaled 60%	0.246	0.511	0.76	21.33
UltraStick25e	0.428	0.514	0.759	21.95

Table 75 shows that the excellent agreement in modal frequencies between the scaled Cessna 172 and UltraStick120 is not a one-off.

2. Modal Flying Qualities Requirements (CAP)

The Control Anticipation Parameter (CAP) represents the ability of the pilot to anticipate long-term changes in vertical accelerations based on his/her sense of initial pitch angular acceleration. It is defined as,

$$CAP = \frac{\omega_{sp}^2}{N_{z_\alpha}} \quad (5)$$

where ω_{sp} is the short period mode frequency and,

$$N_{z_\alpha} = n/\alpha = \frac{C_{L\alpha}qS}{W} \quad (6)$$

CAP as well as scaled CAP are computed for the Cessna 172 and the UltraStick120. The scaling factor, as mentioned earlier, is $n^{-1/2}$. The results are shown in Table 76.

Table 76: CAP Value Comparison

Aircraft	ω_{sp} (rad/s)	CAP (rad ³ /s ² /g)
Cessna 172	6.03	2.35
Cessna 172 scaled 22%	12.85	10.68
UltraStick120	12.8	5.98

As can be seen, the UltraStick120 has ~60% of the CAP corresponding to a scaled Cessna 172 flying straight and level at 31.3 m/s. The 60% scaled value for UltraStick120 was also compared with the UltraStick25e, shown in Table 77.

Table 77: CAP Value Comparison (120 & 25e)

Aircraft	ω_{sp} (rad/s)	CAP (rad ³ /s ² /g)
UltraStick120 scaled 60%	21.33	9.96
UltraStick25e	21.95	18.1

Again, the CAP does not scale well, even though the short period mode frequency matches very well. This is in line with what was seen in Table 76 between the UltraStick120 and the scaled Cessna 172. Therefore, it cannot readily be concluded that the CAP for UltraStick120 is better/worse compared to that of the benchmark set by Cessna 172.

3. Lateral-Directional Dynamics

We compare spiral, Dutch roll and roll subsidence modes for the UltraStick120 and the Cessna 172.

Table 78: Modal Frequencies and Damping Comparison (Lateral-Directional)

Aircraft	Roll		Spiral		Dutch Roll	
	Damping	Frequency	Damping	Frequency	Damping	Frequency
Cessna 172	-	12.4	-	0.011	0.203	3.38
Cessna 172 scaled 22%	-	26.44	-	0.0235	0.203	7.21
UltraStick120	-	12.2	-	0.0304	0.292	5.44

From Table 78 we see that though roll subsidence frequency does not match between UltraStick120 and Cessna 172, there is reasonable agreement between the other two modes. We also check for this in the comparison between UltraStick120 and 25e, shown in Table 79.

Table 79: Modal Frequencies and Damping Comparison (Lateral-Directional), 120 & 25e

Aircraft	Roll		Spiral		Dutch Roll	
	Damping	Frequency	Damping	Frequency	Damping	Frequency
UltraStick120 scaled 60%		15.75		0.0392	0.292	7.02
UltraStick25e	-	23	-	0.026	0.328	7.85

We can see that the roll subsidence frequency does not match well between UltraStick25e and the scaled 120 values either. However, the Dutch roll modes between the two aircraft are very close. This is again, in line with what is seen in Table 78.

D. SCALING UP ANALYSIS FOR ULTRASTICK AIRCRAFT

Froude scaling can also be used to scale up the modal quantities of the UltraStick120 and 25e to the scale of a small, lightweight aircraft similar to the Cessna 172. The advantage of scaling up these quantities is that standard performance requirements in terms of these quantities are available for the class of small, light aircraft (so called Class I), see Ref. 54. Therefore, by computing modal quantities of interest such as short period frequency and damping for the UltraStick aircraft and then scaling them up to the dimension of the Cessna 172, the handling qualities of the UltraStick series may be evaluated against the standard requirements.

For the analysis presented in this section, nominal flight conditions are assumed for both UltraStick aircraft, as opposed to the ‘scaled down’ flight conditions considered in the previous sections. The intention is to evaluate the UAVs under their nominal flying conditions. For UltraStick120, steady level flight at 23 m/s and altitude of 100m is considered, while an airspeed of 17m/s is considered for UltraStick 25. Modal quantities for both UAVs are scaled up using scaling factors $n_{120} = 4.54$ and $n_{25} = 6.88$ respectively that match the dimensions of Cessna 172.

Data associated with Cessna 172 is also presented along with the scaled up results for the UltraStick aircraft. Since the Cessna 172 is considered to be a ‘well behaved’ design, it is used here for demonstrating how an actual Class I aircraft measures up with respect to the specifications. A direct comparison between Cessna 172 and the scaled up UAVs is not carried out, since the flight conditions do not scale appropriately. However, the Cessna 172 data serves as a useful ‘sanity check’, providing suitable context to the scaled-up data obtained for the UltraStick aircraft.

In Ref. 54, classification of different aircraft, flight phases and performance levels are as follows:

1. Aircraft types: 4 classes of aircraft are defined:
 - a. Class I: Small light aircraft (utility, observation etc.)
 - b. Class II: Medium weight, low-to-medium maneuverability aircraft (search and rescue, light/medium transporter etc.)
 - c. Class III: Large, heavy, low-to-medium maneuverability aircraft (heavy transporter, heavy bomber etc.)
 - d. Class IV: High-maneuverability aircraft (Fighters, tactical reconnaissance, trainers)
2. Three Flight phases are defined:
 - a. Category A: Nonterminal flight phases that require maneuvering, precision tracking, or precise flight-path control (air-to-air combat, terrain following etc)
 - b. Category B: Nonterminal flight phases accomplished using gradual maneuvers (climbing, cruise, loiter etc.)
 - c. Category C: Terminal flight phases accomplished using gradual maneuvers, require accurate flight-path control (take-off, landing etc.)
3. Three levels of performance defined:
 - a. Level I: Satisfactory (flying qualities adequate for mission with minimal pilot compensation)
 - b. Level II: Acceptable (flying qualities adequate for mission with increase in pilot load or decrease in mission effectiveness)
 - c. Level III: Controllable (flying qualities such that aircraft can be controlled in context of the mission Flight Phase with excessive pilot load, degradation of mission effectiveness)

For this analysis, we seek to compare the scaled up modal quantities of the UltraStick UAVs to the standards provided for a Class I aircraft under Category B flight phase. The desired level of performance is of course, Level I.

1. Longitudinal Dynamics

Both phugoid and short period modes are evaluated for the UltraStick120 and 25e at their nominal flight conditions. The nominal, as well as scaled up values of damping and frequencies are provided in Table 80 along with those for Cessna 172.

Table 80: Longitudinal Modal Damping and Frequencies

Aircraft	Phugoid	Short Period
----------	---------	--------------

	Damping	Freq.	Damping	Freq.
UltraStick120 (23m/s)	0.21	0.48	0.75	9.48
UltraStick25e (17m/s)	0.24	0.66	0.76	15.38
Scaled UltraStick120	0.21	0.22	0.75	4.45
Scaled UltraStick25e	0.24	0.25	0.76	7.21
Cessna 172	0.11	0.18	0.68	6.03

For phugoid mode, Ref. 54 states that the minimum requirements for phugoid damping (ζ_p) are:

- Level I: $\zeta_p > 0.04$
- Level II: $\zeta_p > 0$
- Unstable phugoid acceptable, as long as time for amplitude to double (T_2) > 55 seconds

We can see that all the phugoid damping values listed in Table 80 satisfy the Level I criteria. For the short period mode, the frequency-related specifications are conveniently provided in terms of ω_{sp} vs (n/α) graphs, where ω_{sp} stands for short period mode frequency, n is the load factor and α is the angle of attack. The quantity (n/α) is computed as,

$$\frac{n}{\alpha} = \frac{V}{g} \left(\frac{1}{T_{02}} \right) \quad (7)$$

Where $(1/T_{02})$ is a zero in the $(\theta/\delta e)$ transfer function. Figure 199 shows the graph for scaled UltraStick UAVs as well as Cessna 172.

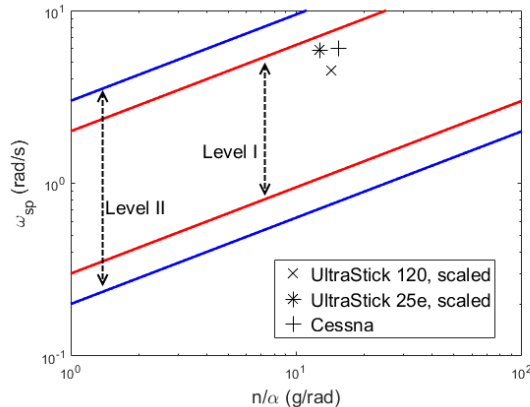


Figure 199: Short period frequency specifications

Figure 199 shows that the scaled up short period mode dynamics for both UltraStick aircraft fall within the Level I performance limits, therefore indicating satisfactory handling qualities. Short period damping requirements are shown in the next section along with flying qualities parameter CAP requirements.

2. CAP Specifications

Ref. 54 provides specifications for short period damping and CAP in terms of CAP vs ζ_{sp} graphs, where ζ_{sp} represents short period damping. The graph for the scaled UltraStick aircraft and Cessna 172 are shown in Figure 200.

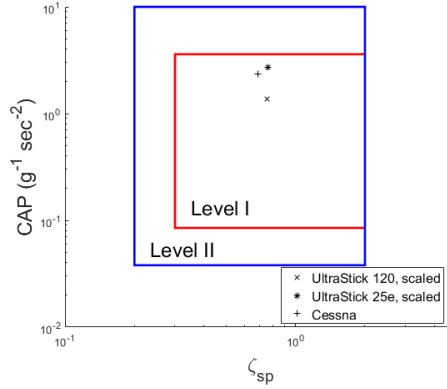


Figure 200: CAP vs ζ_{sp} requirements short period mode

As seen from Figure 200, the short period damping as well as CAP for all three aircraft (scaled UltraStick120, 25e and Cessna 172) lie within the Level I specifications.

3. Lateral-Directional Dynamics

Roll subsidence, spiral and Dutch roll modes are analyzed for both UltraStick aircraft and evaluated against the standards provided in Ref. 54. We also look at the Cessna 172 lateral-directional dynamics for validation purposes, as done in the previous subsections.

a. Roll Subsidence

For roll subsidence, the most convenient form of establishing performance requirements is by fixing an upper limit on the roll time constant (T_r) which is essentially the inverse of the frequency associated with roll subsidence mode. The maximum upper limits for Level 1 and Level 2 specifications are:

- Level 1: $T_r \leq 1.4$
- Level 2: $T_r \leq 3$

Keeping these limits in mind, the roll time constants computed for UltraStick120 and 25e, their scaled-up values and Cessna 172 are presented in Table 81.

Table 81: Roll Time Constant

Aircraft	Roll Time Constant (seconds)
UltraStick120	0.109
UltraStick25e	0.063
Scaled UltraStick120	0.232
Scaled UltraStick25e	0.164
Cessna 172	0.08

From Table 81, it can be seen that the roll time constants for all aircraft are significantly below the desired upper limit for Level 1 performance. This provides confidence in the ability of a UAV pilot to carry out precision roll commands in both of the UltraStick aircraft in a satisfactory manner.

b. Spiral Mode

For the spiral mode, we consider time to double the amplitude (T_{2s}) for evaluation purposes. Since it is required for T_{2s} to be as high as possible, a lower limit for Levels 1, 2 and 3 is provided in Ref. 54 for T_{2s} as:

- Level 1: $T_{2s} \geq 20$
- Level 2: $T_{2s} \geq 8$
- Level 3: $T_{2s} \geq 4$

The spiral mode is stable for the UltraStick and Cessna 172 cases. Thus, both of the UltraStick aircraft meet the required specifications for spiral mode, by definition, when scaled up to the dimensions of Cessna 172.

c. Dutch Roll Mode

The Dutch roll mode damping and frequencies are obtained for both UltraStick aircraft and scaled up appropriately. Ref. 54 provides lower limits for both these quantities for performance Levels 1 and 2.

Table 82: Dutch Roll Mode Damping and Frequencies

Aircraft	Damping	Frequency (rad/s)
UltraStick120	0.29	3.99
UltraStick25e	0.33	5.59
Scaled UltraStick120	0.29	1.87
Scaled UltraStick25e	0.33	2.13
Cessna 172	0.21	3.38

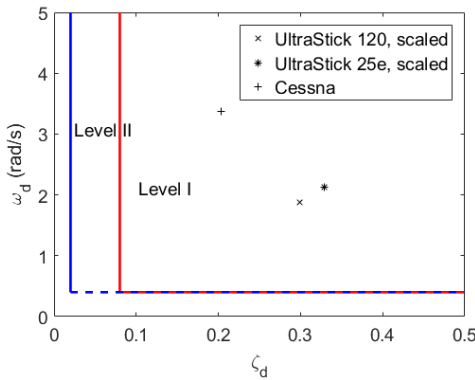


Figure 201: Dutch Roll Mode Damping and Frequency Specifications

From Table 82 and Figure 201, it can be seen that all the aircraft configurations clearly exceed the required specifications for Level I performance.

4. Aircraft Bandwidth Specifications

The scaled up values for pitch attitude bandwidth as well as roll attitude bandwidth for UltraStick120 and 25 are also computed at the standard flight conditions. We also compute the phase delay τ_p for both UAVs, using elevator to pitch angle and aileron to bank angle transfer functions respectively. Using the

specifications for levels 1 & 2 provided in Ref. 55 for these parameters, the bandwidth properties of UltraStick UAVs can be evaluated. Figure 202 and Figure 203 show the scaled bandwidth properties of the UltraStick UAVs along with the specifications.

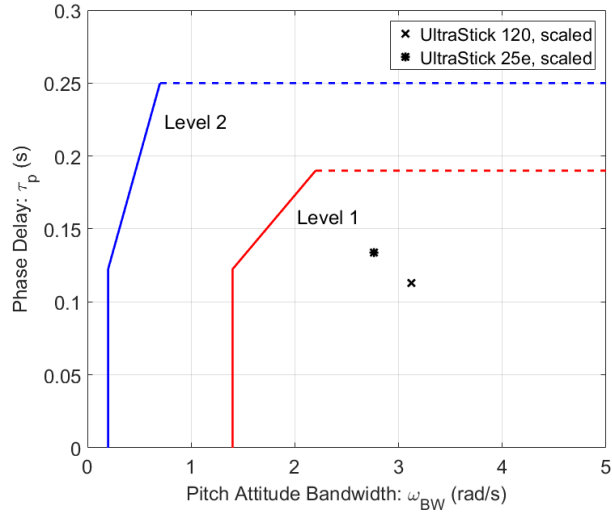


Figure 202: Pitch Attitude Bandwidth and Phase Delay Specifications

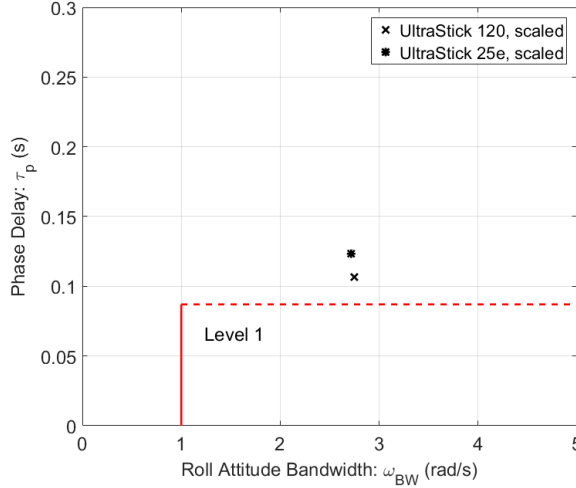


Figure 203: Roll Attitude Bandwidth and Phase Delay Specifications

It can be seen that for both pitch and roll bandwidth properties (scaled), the UltraStick UAVs meet or exceed the specifications for level 1 performance, though the roll phase delay falls outside the level 1 requirements.

E. CONCLUSIONS / FUTURE WORK

The overall conclusion from these analyses is that the dynamics of UltraStick family of UAS is qualitatively very similar to the Cessna 172 aircraft. The mass properties scale well between the aircraft, and subsequently, modal frequencies and damping are shown to be qualitatively close under appropriate flight conditions. The Froude scaling process is also validated by scaling the UltraStick120 down by 66% and compared to the known dynamics of UltraStick25e.

The second part of the analysis involves scaling in the opposite direction, where the dynamics of both UltraStick UAVs are scaled up to the dimensions of the Cessna 172 aircraft. This analysis is primarily carried out in order to evaluate the flying/handling qualities of UltraStick120 and 25e using standards and requirements established for Cessna-sized (Class I) aircraft. The analysis shows that the UltraStick UAVs meet or exceed all specifications in longitudinal as well as lateral-directional handling qualities.

In near future, this analysis (carried out for cruise – Category B) can be extended to Category C flight conditions that include landing and take-off procedures as well. Further research using data from different UAVs and manned aircraft can help establish Froude-scaling based analysis as an important step for evaluating handling qualities for small UAS.

REFERENCES

50. Mitchell, D. G., D. B. Doman, D. L. Key, D. H. Klyde, D. B. Leggett, D. J. Moorhouse, D. H. Mason, D. L. Raney, and D. K. Schmidt, "Evolution, Revolution, and Challenges of Handling Qualities," *J. Guidance, Control, and Dynamics*, Vol. 27, No. 1, Jan.-Feb. 2004, pp. 12-28.
51. Chambers, J. R., *Modeling Flight: The Role of Dynamically Scaled Free-Flight Models in Support of NASA's Aerospace Programs*, NASA SP-2009-575, 2009.
52. Wolowicz, C. H., J. S. Bowman, Jr., and W. P. Gilbert, *Similitude Requirements and Scaling Relationships as Applied to Model Testing*, NASA TP-1435, 1979.
53. Roskam, J., Airplane Flight Dynamics and Automatic Flight Controls, Roskam Aviation and Engineering Corporation, Ottawa, KS, 1979.
54. Mitchell, D. G., R. H. Hoh, B. L. Aponso, and D. H. Klyde, *Proposed Incorporation of Mission-Oriented Flying Qualities into MIL-STD-1797A*, WL-TR-94-3162, Oct. 1994.
55. Mitchell, D.G., and Hoh, R.H., *Development of Methods and Devices to Predict and Prevent Pilot-Induced Oscillations*, AFRL-VA-WP-TR-2000-3046, Jan. 2000.

REPORT DOCUMENTATION PAGE					Form Approved OMB No. 0704-0188
<p>The public reporting burden for this collection of information is estimated to average 1 hour per response, including the time for reviewing instructions, searching existing data sources, gathering and maintaining the data needed, and completing and reviewing the collection of information. Send comments regarding this burden estimate or any other aspect of this collection of information, including suggestions for reducing this burden, to Department of Defense, Washington Headquarters Services, Directorate for Information Operations and Reports (0704-0188), 1215 Jefferson Davis Highway, Suite 1204, Arlington, VA 22202-4302. Respondents should be aware that notwithstanding any other provision of law, no person shall be subject to any penalty for failing to comply with a collection of information if it does not display a currently valid OMB control number.</p> <p>PLEASE DO NOT RETURN YOUR FORM TO THE ABOVE ADDRESS.</p>					
1. REPORT DATE (DD-MM-YYYY) 01-02-2020		2. REPORT TYPE Contractor Report		3. DATES COVERED (From - To)	
4. TITLE AND SUBTITLE Defining Handling Qualities of Unmanned Aerial Systems: Phase II Final Report			5a. CONTRACT NUMBER		
			5b. GRANT NUMBER NNX117CL13C		
			5c. PROGRAM ELEMENT NUMBER		
6. AUTHOR(S) David H. Klyde, Chase P. Schulze, Justin P. Miller, Jose A. Manriquez, Aditya Kotikalpudi, David G. Mitchell, Peter J. Seiler, Christopher Regan, Brian Taylor, Curt Olson			5d. PROJECT NUMBER		
			5e. TASK NUMBER		
			5f. WORK UNIT NUMBER 533127.02.18.07.02		
7. PERFORMING ORGANIZATION NAME(S) AND ADDRESS(ES) NASA Langley Research Center Hampton, Virginia 23681-2199			8. PERFORMING ORGANIZATION REPORT NUMBER		
9. SPONSORING/MONITORING AGENCY NAME(S) AND ADDRESS(ES) National Aeronautics and Space Administration Washington, DC 20546-0001			10. SPONSOR/MONITOR'S ACRONYM(S) NASA		
			11. SPONSOR/MONITOR'S REPORT NUMBER(S) NASA/CR-2020-220564		
12. DISTRIBUTION/AVAILABILITY STATEMENT Unclassified- Subject Category 08 Availability: NASA STI Program (757) 864-9658					
13. SUPPLEMENTARY NOTES Langley Technical Monitor: Natalia Alexandrov					
14. ABSTRACT A myriad of issues slows the development of verification, validation, and certification methods that will enable the safe introduction of Unmanned Air Systems (UAS) to the National Airspace System. The issues include the lack of consensus in UAS categorization process and quantitative certification requirements, including the definition of handling qualities. Because of the wide variety of UAS types, there cannot be a one-size-fits-all set of requirements. To address these issues, Systems Technology Inc. (STI) has developed the UAS Handling Qualities Assessment process and corresponding draft specification that will guide UAS stakeholders through a systematic evaluation process.					
15. SUBJECT TERMS Handling qualities; UAS; sUAS					
16. SECURITY CLASSIFICATION OF: a. REPORT b. ABSTRACT c. THIS PAGE U U U			17. LIMITATION OF ABSTRACT UU	18. NUMBER OF PAGES 277	19a. NAME OF RESPONSIBLE PERSON STI Help Desk (email: help@sti.nasa.gov) 19b. TELEPHONE NUMBER (Include area code) (757) 864-9658